

Development of Chemical Probes for non-BET Bromodomains

PhD Thesis

Natalie Theodoulou

March 2016

Supervisors: Dr. Philip Humphreys and Professor Nicholas Tomkinson

Department of Pure & Applied Chemistry, University of Strathclyde, 295
Cathedral Street, Glasgow G1 1XL

GSK Medicines Research Centre, Gunnels Wood Road, Stevenage,
Hertfordshire, SG1 2NY

This thesis is the result of the author's original research. It has been composed by the author and has not been previously submitted for examination which has led to the award of a degree.

The copyright of this thesis belongs to the author under the terms of the United Kingdom Copyright Acts as qualified by University of Strathclyde Regulation 3.50. Due acknowledgement must always be made of the use of any material contained in, or derived from, this thesis.

Signed:

Date:

Acknowledgements

Firstly, I would like to thank my two supervisors, Dr. Phil Humphreys and Professor Nick Tomkinson for their guidance and support throughout my PhD studies. Thank you to Nick for providing encouragement and welcoming me so warmly at Strathclyde. Your constant positivity has helped to motivate me throughout my studies.

I am hugely grateful to Phil for welcoming me into his team at GSK and for providing me with so many opportunities during this time. Thank you for always having my best interests at heart, guiding me in the right direction and helping me to get to where I want to be. None of this would have been possible without your help.

I would thank the Epinova DPU for having me and particularly Rab for supporting my PhD. Additional thanks to Professors Harry Kelly and William Kerr for accepting me on to the PhD program and for their continued support and encouragement.

I would like to thank all of those who have helped me with the science. To Chun-wa and Paul for their help with X-ray crystallography and modeling and to Mel and Laurie for training me to run the TR-FRET assays. I have appreciated your willingness to help and always making the time to answer my many questions!

I would like to thank the other members of my team: Tom, Tracy and Helen. Your support in the bay has been fantastic and I have loved working with you all. Extra thanks to Tom for answering all of my stupid questions and always being so patient!

Thank you to the other PhD students: Rob, Craig, Ben, Sam, Aymeric and Jonathan. You've made my time at GSK so much fun.

Thank you to my boyfriend, Liam, for all of the support and encouragement over the last 4 years. Without his understanding and patience, this would not have been possible.

Finally, thank you to Mum, Dad and Rach. Particularly Mum who always encouraged me to be the best that I can be.

Table of Contents

1	Introduction.....	1
1.1	DNA structure and function.....	1
1.2	Epigenetics and the histone code	3
1.3	Bromodomain structure and acetyl lysine recognition	7
1.4	Bromodomains as therapeutic targets	9
1.4.1	Oncology	10
1.4.2	Neurological disorders	11
1.4.3	Metabolic disease.....	11
1.4.4	Inflammation.....	12
1.4.5	Infectious disease.....	13
1.4.6	Therapeutic potential of BCPs	13
1.5	Chemical probes.....	14
1.5.1	Chemical probes as tool molecules	14
1.5.2	Chemical probes for the BET family of bromodomains	16
1.5.3	Chemical probes for non-BET bromodomains	26
1.6	Aims	39
2	The development of I-BRD9 , a chemical probe for Brd9.....	41
2.1	Introduction.....	41
2.1.1	Identification of Brd9 as a novel bromodomain target	41
2.1.2	Compound screening in Brd9	43
2.1.3	Physico-chemical property requirements of a chemical probe	53
2.1.4	Aims for Brd9 chemical probe discovery	54
2.2	Results and discussion for Brd9 chemical probe discovery.....	57
2.2.1	X-ray crystallography of Brd9 and Brd4 BD1	57
2.2.2	Design and synthesis of amides	59
2.2.3	Design and synthesis of amide array	69
2.2.4	Design and synthesis of alternative cores.....	75

2.3	Modifications at the 2-position of the TP core	82
2.3.1	Alkyl and alcohol derivatives	82
2.3.2	Amine derivatives	88
2.3.3	Design and synthesis of amidine derivatives	93
2.3.4	Square array.....	99
2.3.5	Optimisation of amidine 2.071d	110
2.3.6	Amidine Array.....	113
2.3.7	Optimisation of 2.081q	121
2.3.8	Further profiling of 2.081q and 2.082	123
2.3.9	Comparison of I-BRD9 to other Brd9 chemical probes	135
2.4	Conclusion.....	136
3	Studies towards the development of a chemical probe for TAF1 BD2.....	138
3.1	Introduction.....	138
3.1.1	Identification of TAF1 as a target	138
3.1.2	TAF1 Structure and function	138
3.1.3	Small molecule inhibitors of TAF1	141
3.1.4	Aims	142
3.2	Results and discussion for TAF1 chemical probe discovery.....	143
3.2.1	Identification of a start point for chemical probe discovery	143
3.2.2	Initial SAR investigation at the 5-position	149
3.2.3	5-Position SAR: pyridine vs. phenyl	155
3.2.4	SAR investigation at the 8-position	158
3.2.5	Determination of TAF1 BD2 activity by <i>BROMOscan</i>	172
3.2.6	Further investigations at the 8-position	173
3.2.7	5-Position array	180
3.2.8	Further optimisation of 3.002a	186
3.3	Conclusions.....	196
3.4	Future work	198

4	Experimental.....	199
4.1	General experimental	199
4.2	Experimental procedures.....	203
5	Appendix	335
5.1	TR-FRET assay protocol	335
	Brd9 TR-FRET assay	335
	Ligand preparation.....	335
5.2	Thermal shift analysis	336
5.3	Isothermal titration calorimetry.....	337
5.4	Brd9 Amide array.....	339
	5.4.1 General experimental procedure	339
	5.4.2 Amide array TR-FRET data	339
5.5	Brd9 Amidine array TR-FRET data.....	341
5.6	BROMOscan bromodomain profiling.....	342
	5.6.1 Full data for compound 2.081q	343
	5.6.2 Full data for compound 2.082 (I-BRD9)	343
5.7	TAF1 8-Position array 1.....	344
5.8	TAF1 8-Position array 2.....	346
5.9	TAF1 5-Position array.....	348
6	References	350

Abbreviations

Å	Angstrom
A	Adenine
AAA	ATPases Associated with diverse cellular Activities
Ac	Acetyl
AchE	Acetylcholine esterase
AhR	Aryl hydrocarbon receptor
AIDS	Acquired immunodeficiency syndrome
AMP	Artificial membrane permeability
AP	Amino-pyridazine
ApoA1	Apolipoprotein A1
Ar	Aromatic group
Arg	Arginine
Asn	Asparagine
ATAD2	ATPase family, AAA domain containing 2
AUC	Area under curve
Aq.	Aqueous
BAF	BRG1/brm-associated factor
BAZ1B	Bromodomain adjacent to zinc finger domain, 1B
BAZ2A	Bromodomain adjacent to zinc finger domain protein 2A
BPTF	Bromodomain PHD finger transcription factor
BCP	Bromodomain containing protein
BD	Bromodomain
BET	Bromodomain and Extra Terminal domain
BLI	Biolayer interferometry
Boc	<i>N-tert</i> -Butoxycarbonyl
Bn	Benzyl
Brd2	Bromodomain containing protein 2
Brd3	Bromodomain containing protein 3

Brd4	Bromodomain containing protein 4
Brd7	Bromodomain containing protein 7
Brd9	Bromodomain containing protein 9
BrdT	Bromodomain containing protein, testis-specific
BRPF1	Bromodomain and PHD Finger containing protein 1
BRPF2	Bromodomain and PHD Finger containing protein 2
BRPF3	Bromodomain and PHD Finger containing protein 3
Bu	Butyl
^t Bu	Tertiary butyl
C	Cytosine
cat.	Catalyst
CAT	Compound Array Team
CDI	Carbonyldiimidazole
CECR2	Cat eye syndrome chromosome region, candidate 2
CHAPS	3-[(3-Cholamidopropyl)dimethylammonio]-1-propanesulfonate
CLND sol.	Chemiluminescent nitrogen detection solubility
C _{max}	Maximum concentration of a drug observed after its administration
Conc.	Concentrated
COX2	Cytochrome c oxidase subunit II
CREBBP	cAMP response element-binding protein binding protein
Cr	Crotyl
CTK	C terminal kinase domain
DBU	1,8-Diazabicyclo[5.4.0]undec-7-ene
DCM	Dichloromethane
Decomp.	Decomposition
DIPEA	<i>N,N</i> -Diisopropylethylamine
DME	1,2-Dimethoxyethane
DMF	<i>N,N</i> -Dimethylformamide
DMSO	Dimethylsulfoxide
DNA	Deoxyribonucleic acid

DPPA	Diphenylphosphoryl azide
DPU	Discovery Performance Unit
DTT	Dithiothreitol
DUF	Domain of unknown function
EBV	Epstein-Barr virus
EDC	1-Ethyl-3-(3-dimethylaminopropyl)carbodiimide
EPL1	Enhancer of polycomb-like
EP300	E1A binding protein p300
Et	Ethyl
ET	Extra terminal
eq.	Equivalent
eXP	Enhanced cross panel
F	Bioavailability
FDA	Food and Drug Administration
FP	Furan pyridone
FRAP	Ferric reducing ability of plasma
FRET	Time-resolved Forster (fluorescence) resonance energy transfer
G	Guanine
GCN5	General control of amino acid synthesis protein 5-like 2
GPCR	G protein-coupled receptor
GSK	GlaxoSmithKline
h	Hour(s)
HAC	Heavy atom count
HAT	Histone acetyltransferase
HATU	<i>O</i> -(7-Azabenzotriazol-1-yl)- <i>N,N,N',N'</i> -tetramethyluronium hexafluorophosphate
HBA	Hydrogen-bond acceptor
HBD	Hydrogen-bond donor
HDAC	Histone deacetylase
HEPG2	Human hepatocellular liver carcinoma cell line

hERG	Human Ether-à-go-go-Related Gene
His	Histidine
HIV	Human immunodeficiency virus
HPV	Human papiloma viurs
HRMS	High resolution mass spectrometry
HTS	High throughput screen
H2A	Histone 2A
H2B	Histone 2B
H3	Histone 3
H3K4Me ₃	Histone 3 acetyl-lysine 4 trimethyl
H3K14	Histone 3 acetyl-lysine 14
H3K27Me ₃	Histone 3 acetyl-lysine 27 trimethyl
H4	Histone 4
Ile	Isoleucine
IL-6	Interleukin 6
IP	Imidazole pyridone
IPA	Isopropyl alcohol
ITC	Isothermal titration calorimetry
IV	Intravenous
KAc	Acetyl-lysine
KBu	Butyrl-lysine
KCr	Crotonyl-lysine
KPr	Propyl-lysine
LBF	Liver blood flow
LCMS	Liquid column mass spectrometry
LE	Ligand efficiency
LG	Leaving group
Lit.	Literature
LPS	Lipopolysaccharide
Lys	Lysine

M	Molar, moles/decimetre ³
MDAP	Mass directed autopreparation
Me	Methyl
MeCN	Acetonitrile
MeOH	Methanol
min	Minute
mmol	Millimol
MOZ	Monocytic leukemia zinc finger protein
MORF	Multiple organellar RNA editing factor
m.p.	Melting point
mRNA	Messenger ribonucleic acid
MS	Mass spectrometry
m/z	mass/charge ratio
NaHMDS	Sodium bis(trimethylsilyl)amide
NCT	National clinical trial
NBS	<i>N</i> -Bromosuccinimide
nFκB	Nuclear factor kappa-light-chain-enhancer of activated B cells
NHC	<i>N</i> -Heterocyclic Carbene
NIS	<i>N</i> -Iodosuccinimide
nm	Nanometre
nM	Nanomolar
NMC	NUT midline carcinoma
NMP	<i>N</i> -Methyl-2-pyrrolidone
NMR	Nuclear magnetic resonance
NTK	N terminal kinase domain
NUT	Nuclear protein in testis
PBMC	Peripheral blood mononucleated cell
PBRM1(5)	Polybromodomain containing protein 1 (5)
PCAF	P300/CREBBP-associated factor
PDE3A	Phosphodiesterase 3A

PDE4B	Phosphodiesterase 4B
PEPPSI	Palladium-enhanced Precatalyst Preparation Stabilisation and Initiation
PFI	Property forecast index
Ph	Phenyl
PHD	Plant Homeo Domain
PHIP	Pleckstrin homology domain interacting protein
PI3K γ	Phosphatidylinositide 3-kinase γ
PK	Pharmacokinetic
Pr	Propyl
PTM	Post-translational modification
P-TEFb	Positive transcription elongation factor b
quant.	Quantitative
qPCR	Quantitative polymerase chain reaction
RNA	Ribonucleic acid
Rt	Room temperature
R _t	Retention time
sat.	Saturated
SAR	Structure activity relationship
SEM	2-(Trimethylsilyl)ethoxymethyl
SGC	Structural Genomics Consortium
SiRNA	Small interfering RNA
SMARCA2	SWI/SNF related, matrix associated, actin dependent regulator of chromatin, subfamily A, member 2
SMARCA4	SWI/SNF related, matrix associated, actin dependent regulator of chromatin, subfamily A, member 4
Sol.	Solubility
SPR	Surface plasmon resonance
SP140	SP140 nuclear body protein
STD	Saturation transfer difference
SWI/SNF	Switch/sucrose nonfermentable

T	Thymine
$t_{1/2}$	Half-life
TAF1	Transcription initiation factor TFIID subunit 1
TAF1L	TAF1 RNA polymerase II, TATA box binding protein (TBP)-associated factor, 210kDa-like
TBP	TATA-binding protein
TEA	Triethanolamine
TFA	Trifluoroacetic acid
THF	Tetrahydrofuran
THP	Tetrahydropyran
TFIID	Transcription Factor IID
T_{max}	Time at which C_{max} is observed
TMEDA	Tetramethylethylenediamine
TP	Thieno-pyridinone
TR-FRET	Time-resolved Forster (fluorescence) resonance energy transfer
tRNA	Transfer ribonucleic acid
TRIM24	Tripartite motif-containing 24
TRIM28	Tripartite motif-containing 28
ΔT_m	Thermal shift
V_{ss}	Apparent volume of distribution
vs.	Versus
wt.	Weight
w/v	Weight by volume
μ wave	Microwave

Abstract

This thesis describes the development and discovery of chemical probe molecules for non-BET bromodomains.

Studies have demonstrated that inhibitors of the BET family of bromodomains show profound anti-cancer and anti-inflammatory properties, with several molecules entering clinical trials. However, the BET family represents just 8 of the 56 human bromodomains identified, leaving the majority of this intriguing target class yet to be investigated. Chemical probes are an essential component of the biological tool set required to delineate the function of bromodomains for both target validation and invalidation. Therefore, this thesis describes the studies towards the identification of chemical probes for non-BET bromodomains to facilitate elucidation of their biological roles.

Firstly, the development of **I-BRD9**, the first selective cellular probe for Bromodomain Containing Protein 9 (Brd9) is presented. **I-BRD9** was identified through iterative medicinal chemistry, starting from a potent but unselective amide. Structure-based design was used to guide modifications to the scaffold to deliver excellent activity (Brd9 pK_d : 8.7) and greater than 70-fold selectivity for Brd9 over every other bromodomain tested. **I-BRD9** shows good selectivity over 49 pharmacologically relevant targets, and evidence of Brd9 cellular target engagement. The compound is now freely available to the scientific community through the Structural Genomics Consortium or for purchase *via* commercial suppliers. Therefore, the biological effect of Brd9 bromodomain inhibition can be investigated for the first time.

Secondly, focus was placed on the development of a chemical probe for Transcription initiation factor TFIID subunit 1 (TAF1). Starting from a hit identified in a cross-screen, work was carried out to optimise the activity, selectivity and physico-chemical properties of the chemotype. A compound with excellent TAF1 BD2 activity ($pI_{C_{50}}$: 7.2) and ≥ 80 -fold selectivity over every bromodomain tested was identified. However, the compound shows poor permeability, therefore, further work to optimise the physico-chemical properties of the template is required.

1 Introduction

1.1 DNA structure and function

DNA, the carrier of genetic information, which can be passed on from one generation to the next, is pivotal to the existence of life. As the blueprint for creating living organisms, it codes for the highly specific synthesis of proteins from a series of amino acids.

The 3-dimensional structure of DNA was first investigated by Wilkins and Franklin in 1953 using X-ray diffraction.^{1, 2} The characteristic diffraction pattern indicated that DNA was formed of two chains, assembled in a regular helical structure. From these discoveries, Watson and Crick provided a structural model of DNA,³ for which they were awarded the Nobel Prize in Medicine in 1962. These findings led to the discovery that DNA consists of chains of nucleotides, each composed of a sugar, a phosphate and a base. The sugar-phosphate backbone serves a structural role, whilst the specific sequence of bases provides the genetic code.⁴ The double helical structure consists of two anti-parallel but complementary nucleic acid strands, which interact through a series of hydrogen-bonds. Although relatively weak, these interactions provide support to the helical structure, tethering the two chains together (**Figure 1**).

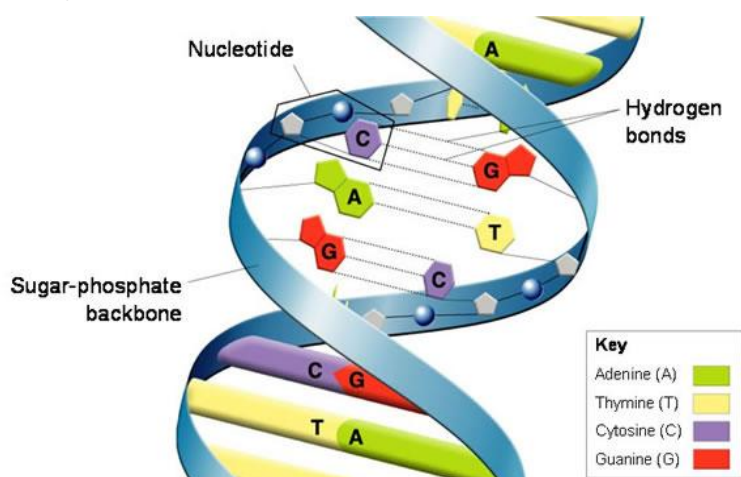


Figure 1: 3-Dimensional structure of DNA.⁵

There are four DNA bases, namely adenine (A), guanine (G), cytosine (C) and thymine (T), which form two sets of complementary pairs. G is always paired with C and A with T, which determines the sequence of the newly formed DNA strand during the replication process (**Figure 2**).

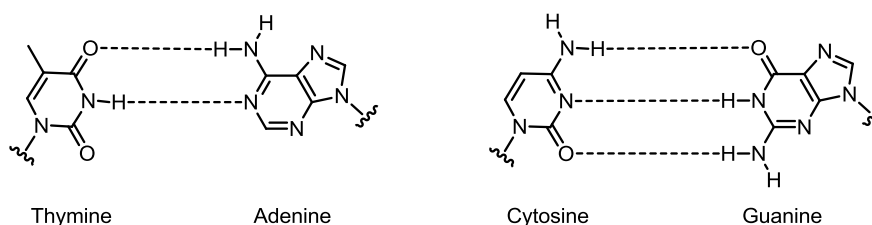


Figure 2: Complementary pairs of DNA bases.

Although genes are composed of sections of DNA, the DNA itself is not the direct template for protein synthesis. The process of transcription describes the copying of DNA into RNA, the complementary nucleic acid strand. This RNA, namely messenger RNA (mRNA), provides a set of instructions for subsequent translation, the process by which cellular ribosomes synthesise proteins. A sequence of three base pairs in mRNA, defined as a codon, interacts with the anti-codon located on transfer RNA (tRNA), *via* hydrogen-bonds. As each tRNA molecule carries a specific amino acid defined by its anti-codon, this determines the sequence of residues in the growing polypeptide chain.⁶

The flow of genetic information from DNA to RNA, eventually to form proteins, is described by the central dogma of molecular biology, stated by Francis Crick in 1970 (Figure 3).⁷

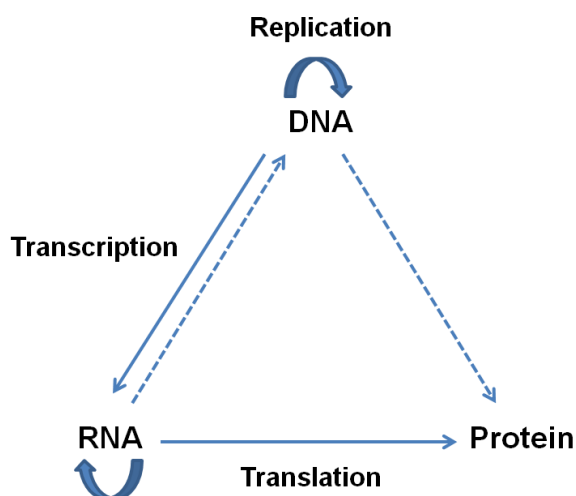


Figure 3: Schematic representing the central dogma of molecular biology as described by Francis Crick.

DNA directs its own replication through transcription to yield RNA, which is translated to form proteins. The solid lines indicate the transfers of genetic information that occur in all cells and dotted lines represent special transfers known to occur, but only under specific conditions. These transfers could be observed in

the case of viruses or in a laboratory. Finally, according to the central dogma, transfers such as protein to DNA or protein to RNA are postulated to never occur.

1.2 Epigenetics and the histone code

The decoding of the human genome in 2003 revealed the specific sequence of chemical base pairs which make up DNA. This genetic blueprint allowed individual protein encoding genes to be identified of which there are approximately 30,000 in humans.⁸ Chromosomes, located inside the nucleus of every cell, carry this genetic information, which serves as a template for the regulation of gene expression and subsequent transcription.⁹ A comparison of the number of genes identified by the human genome project with the many phenotypes recognised in human development, suggests that there are far fewer genes than originally considered. One hypothesis is that this could be due to epigenetics, defined as heritable changes in gene expression caused by mechanisms other than those facilitated by changes to the underlying DNA sequence.^{10, 11} Simplistically, epigenetic processes control patterns of gene expression, which in turn, are governed by the structure of chromatin and therefore the accessibility of DNA.

Chromosomes contain a large amount of DNA relative to their condensed length. Each chromosome consists of a single double helix, which in humans, averages approximately 2×10^8 nucleotide pairs. If extended, this would measure 6 cm in length, 10,000 times longer than the diameter of a cell nucleus (6 μm).⁶ This DNA, including that of the 45 other human chromosomes, must be compacted into the nucleus of each cell. To aid this organisation, DNA is wrapped around an octameric core of small protein modules known as histones (H2A, H2B, H3 and H4). These structural subunits are termed nucleosomes, which bundle together to form chromatin fibre (**Figure 4**).¹²

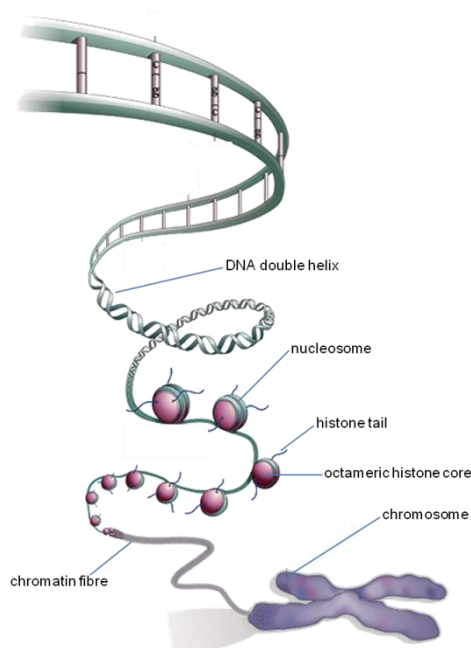


Figure 4: Structure of a chromosome. DNA is compacted around histone proteins (shown as purple spheres) to form nucleosomes, which bundle together to form chromatin fibre.¹³

Importantly, the packing of genetic material is dynamic, changing size and position to allow transcriptional enzymes to move along the DNA. The regulation of DNA packing to form open and closed states of chromatin is mediated by epigenetic proteins through a series of post-translational modifications (PTMs). The termini of histone tails, which protrude out from the nucleosome surface, are susceptible to various PTMs, including acetylation, methylation and phosphorylation.¹⁴ These site specific modifications act in a combinatorial fashion to form the ‘histone code’, which aids the regulation of chromatin cellular activity and, in particular, gene expression.¹⁵

Lysine acetylation is one of the most abundant and extensively studied histone modifications, regulated by the opposing action of histone acetyltransferases (HATs) and histone deacetylases (HDACs), which ‘write’ and ‘erase’ acetylation marks, respectively (**Figure 5**).¹²

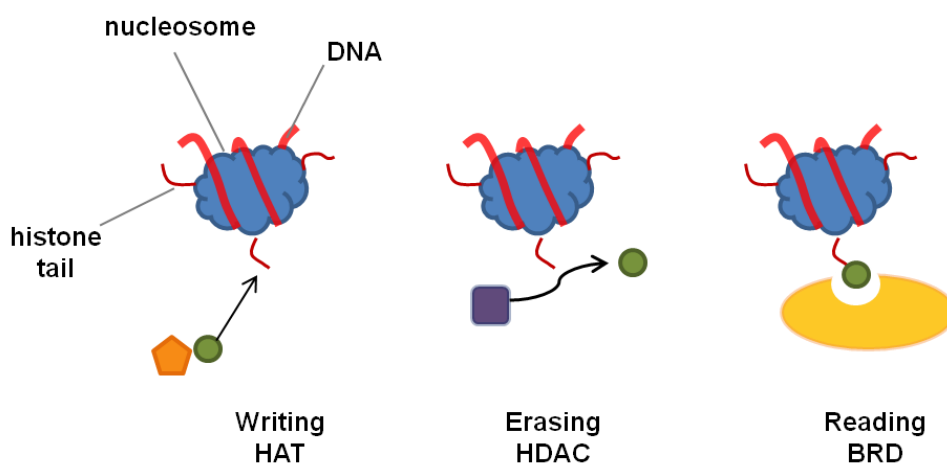


Figure 5: Nucleosomes are subject to the activity of chromatin modifying enzymes. Writers (left) introduce modifications to histone tails, erasers (centre) delete and the reader proteins (right) recognise.

Approximately 25% of the residues present in histone proteins are positively charged lysine and arginine residues,⁶ which attract the negatively charged phosphate backbone in DNA. Acetylation of the lysine ϵ -amino group, mediated by HAT enzymes (writers), leads to charge neutralisation, and therefore reduces the strength of these electrostatic interactions. Simplistically, this creates a more open and relaxed state of chromatin (euchromatin), increasing the accessibility of DNA to the binding of transcriptase enzymes. This in turn, leads to transcriptional activation and subsequent gene expression. In contrast, HDACs (erasers) oppose the activity of HATs and reverse lysine acetylation levels. Consequently, the positive charge on the lysine residue is restored, creating a compact, deactivated state of chromatin (heterochromatin).¹⁶ However, this theory is now considered to be an over simplification, as it is believed that the recruitment of multiple chromatin remodelling complexes is required for transcriptional activation.¹⁷ For example, methylation of lysine residues does not lead to neutralisation of positive charge, and therefore does not affect chromatin structure directly. Interestingly, like bromodomain binding, lysine methylation can be associated with either transcriptional activation or repression. For example, H3K4Me₃ represents a marker for transcriptionally active genes, whereas H3K27Me₃ is associated with silenced genes.¹¹

Chromatin modifying enzymes have been the focus of much research in drug development, leading to the discovery of novel inhibitors for these domains.¹⁸ Associated with this, there are currently two Food and Drug Administration (FDA) approved drugs, namely Vorinostat (**1.001**)¹⁹ and Romidepsin (**1.002**),²⁰ which are in use for the treatment of T-cell lymphoma (**Figure 6**).

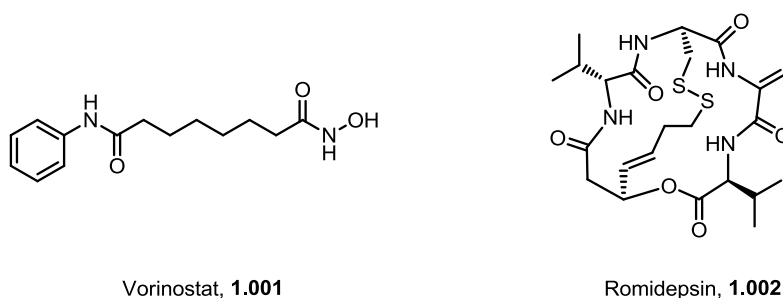


Figure 6: Chemical structures of HDAC inhibitors Vorinostat (1.001) and Romidepsin (1.002).

Vorinostat (**1.001**) and Romidepsin (**1.002**) act as class I HDAC inhibitors and aim to rebalance abnormal lysine acetylation levels.

The discovery of potent inhibitors for HDAC enzymes has generated considerable pharmaceutical interest in targeting HAT complexes for drug development. However, the majority of HAT inhibitors identified to date are promiscuous, binding to multiple classes of proteins. The large bi-substrate inhibitor, Lys-CoA (**1.003**) shows 0.5 μM and 200 μM activities against HAT-containing proteins p300 and PCAF, respectively.²¹ Subsequently, Lys-CoA (**1.003**) was used to probe the enzymatic function of these proteins, serving as a useful tool to evaluate the cellular role of HATs. More recently, C646 (**1.004**), was reported as an inhibitor of p300.²² Discovered by virtual screening, C646 (**1.004**) displays $K_i = 400$ nM against p300, with selectivity over 6 other HAT complexes (**Figure 7**).

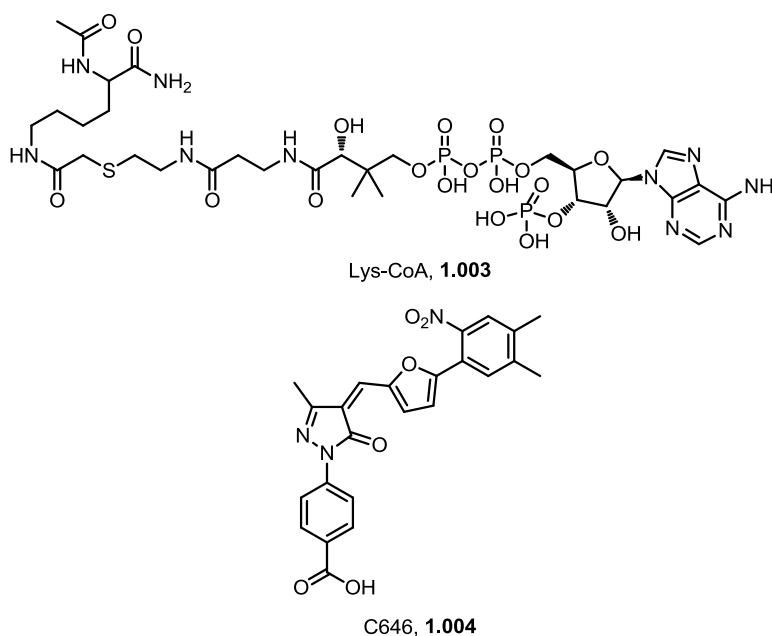


Figure 7: Chemical structures of Lys-CoA (1.003) and C646 (1.004).

Until recently, significantly less attention had been paid to the ‘reader’ proteins known as bromodomains, which along with other epi-reader modules act to decipher the ‘histone code’. These domains often form part of far larger chromatin associated proteins, containing other catalytic domains such as HATs and HDACs.²³ As such, bromodomain-containing-proteins (BCPs) aid the recruitment of the cellular transcriptional machinery, helping to localise the relevant effector protein to a certain histone mark.

1.3 Bromodomain structure and acetyl lysine recognition

Bromodomains, named after the *Drosophila* gene *brahma*, where they were first identified,²⁴ are the only protein modules known to selectively target and bind to acetylated lysine residues.²³ To date, at least 42 human BCPs are known, each of which contains between 1 and 6 individual bromodomains. In total, this amounts to 56 unique bromodomains, which are classified into 8 distinct subgroups based on their sequence homology (**Figure 8**).^{25, 26}

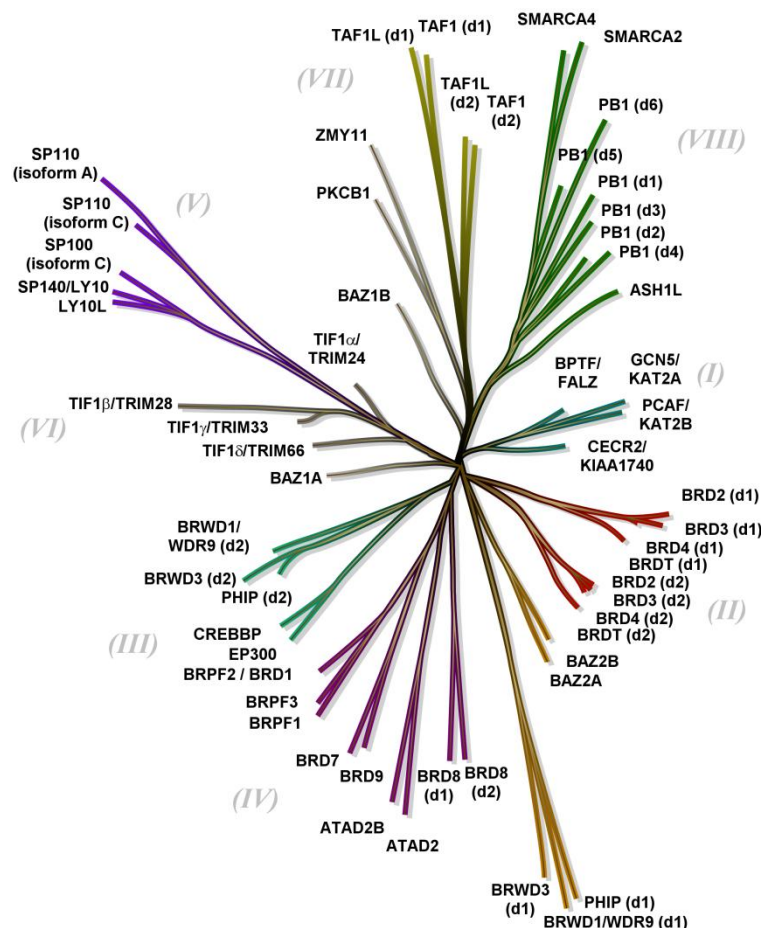


Figure 8: Human bromodomain phylogenetic tree. The 56 bromodomains are placed into 8 subfamilies according to their sequence homology.

Bromodomains found within the same protein often exhibit no greater similarity to each other than bromodomains located within different proteins, suggesting that each individual domain serves a unique and distinct function.²⁷ The first bromodomain structure resolved was that of PCAF in 1999 by solution NMR.²⁸ Since then, the 3-dimensional structures of over half of these domains have been determined, mostly by X-ray crystallography. These structural discoveries have revealed that bromodomains possess a highly conserved structure, consisting of approximately 110 amino acids. The majority are characterised by 4 α helices (α_A , α_B , α_C , α_Z), linked by two flexible loop regions (**Figure 9**).²⁹

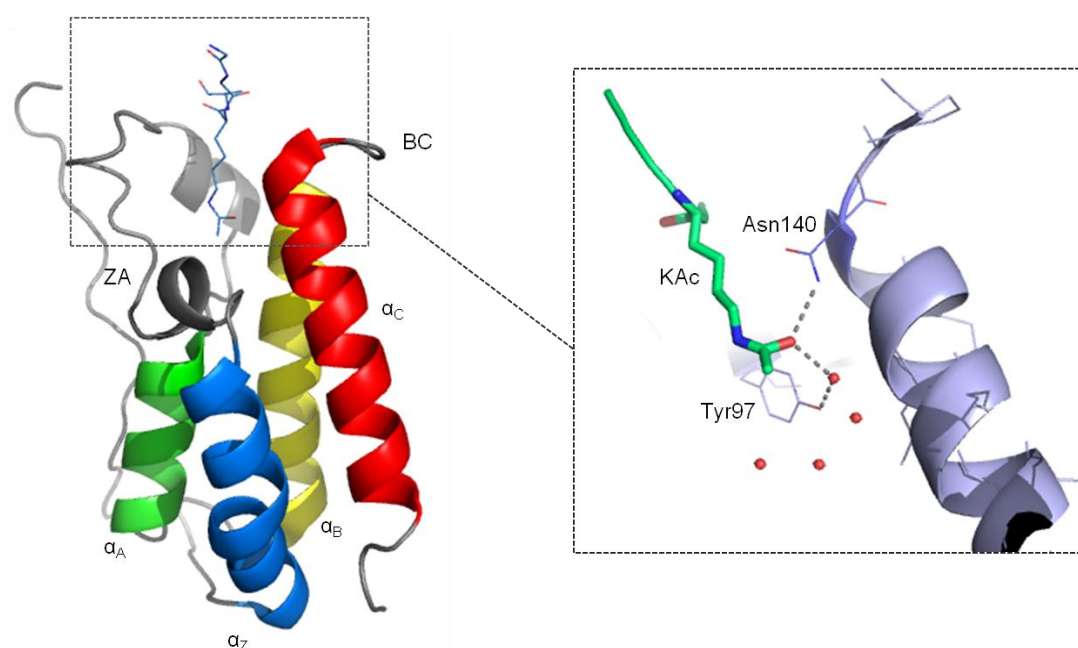


Figure 9: X-ray crystal structure of Brd4 BD1 in complex with H3K14 (PDB code = 3UVW). Grey dashed lines represent hydrogen-bonds and water molecules are shown as red spheres. Highlighted in grey are the ZA and BC loops, which form the basis of the hydrophobic binding pocket. The expanded area displays the conserved asparagine (Asn140) and tyrosine (Tyr97) residues. Asn140 forms the key hydrogen-bond to the carbonyl moiety of KAc, whilst Tyr97 participates in a water-mediated interaction.

Two highly conserved amino acids located within the hydrophobic binding pocket are known to be essential for acetyl-lysine (KAc) recognition in typical bromodomains. The acetyl carbonyl group forms a direct hydrogen-bond to the side chain amide nitrogen of an asparagine residue (Asn140, Brd4 BD1 numbering), as well as a water-mediated interaction to a tyrosine (Tyr97, Brd4 BD1 numbering).^{23,25,30} In addition, the methyl group of the acetyl moiety sits in a small hydrophobic cavity, surrounded by four crystallographically ordered water molecules. Interestingly, these waters are conserved in the majority of bromodomains. Despite being situated in a hydrophobic region, research has shown

that these water molecules are difficult to displace, suggesting a key role in the assembly of the binding site.³¹ Additional studies have shown that the larger propyl (KPr), butyl (KBU) and crotonyl (KCr) moieties can be accommodated in this hydrophobic cavity.^{32,33} The biological significance of this remains unclear, however, histones containing both propionylated and butyrylated residues have been found in both yeast and mammals.²⁷

Although the hydrogen-bond interactions described are essential for KAc recognition, binding affinity to the bromodomain itself is inherently weak.^{29, 34} In the case of the histone specifically, binding affinity arises from interactions between the histone peptide tail and the entrance to the KAc binding pocket. In the BET family of bromodomains, this region corresponds to a small lipophilic cleft known as the WPF shelf. This area is defined by 3 amino acids (Brd4 BD1 numbering), namely, Trp81 (W), Pro82 (P) and Phe83 (F). Numerous studies have shown that interactions with this lipophilic region are important for the binding of synthetic ligands.¹⁷

The overall organisation of typical bromodomains is largely conserved, however, sequence variations occur within the ZA and BC loops, due to numerous amino acid insertions and deletions. These regions exhibit the greatest sequence variation, accounting for the ability of bromodomains to discriminate between KAc residues in different peptide sequences.²⁴

1.4 Bromodomains as therapeutic targets

Of the 42 human BCPs identified to date, very few have well-characterised biological roles. However, the BCPs that have been identified have been implicated in a variety of diseases including cancer, inflammation and viral replication.^{17, 35, 36, 37} BCPs are often multi-component complexes, but, in very few cases has the bromodomain within the BCP been specifically linked to a disease. In fewer still has inhibition of the bromodomain-KAc interaction been shown to be functionally relevant. As a result of this, the therapeutic potential of bromodomain inhibition is not well understood.³⁸ The diseases for which human BCPs have been implicated can be classified into 5 distinct areas: oncology, neurological disorders, metabolic disease, inflammation, and infectious disease, each of which will be discussed in turn. It is of note that the majority of these disease indications are supported by protein knock-down experiments, and those that have been identified by selective bromodomain inhibition will be referred to specifically.

1.4.1 Oncology

BCPs have been found to play a significant role in the cell cycle, apoptosis, metastasis and proliferation, suggesting that there is a convincing rationale for targeting these domains within oncology.³⁹ Furthermore, research has shown that the expression levels of several bromodomains have been associated with various forms of cancer. In a subset of BCPs, siRNA protein knock-down studies have shown that decreased BCP expression inhibits tumour cell growth and/or enhances survival. These BCPs include ATAD2, BPTF, EP300, SMARCA2, SMARCA4, TRIM24 and TRIM28.³⁸ Furthermore, ATAD2 is over expressed in more than 70% of breast cancers and high protein levels correlate with poor survival and disease reoccurrence.⁴⁰ Abnormal expression of TRIM24 has also been reported in breast cancer and high expression levels have been shown to negatively correlate with patient survival rates.⁴¹ The human transcriptional co-activator CREBBP has been implicated in tumour initiation, progression and metastasis. Furthermore, elevated expression levels of CREBBP are observed in patients with prostate, breast and lung cancers, as well as acute leukaemia.^{42, 43}

The Bromodomain and Extra Terminal domain (BET) family of bromodomains, including Brd2, Brd3, Brd4 and BrdT, are the most extensively studied family, providing the most compelling evidence that bromodomain inhibition may be relevant in oncology. For example, the use of (+)-JQ1⁴⁴ (**1.005a, Figure 10**), a high affinity BET family selective chemical probe, demonstrated that the chromosomal translocation of Brd4 (and more rarely Brd3) with the NUT gene results in a rare but fatal condition known as NUT midline carcinoma (NMC). This translocation leads to the expression of the Brd4-NUT onco-protein, a leading cause of aggressive tumour growth.^{45, 46} The structurally related BET bromodomain inhibitor, I-BET762 (**1.006a, Figure 10**), identified by GSK is currently undergoing phase I/II clinical trials for the treatment of NMC and other haematological malignancies (NCT01587703).⁴⁷

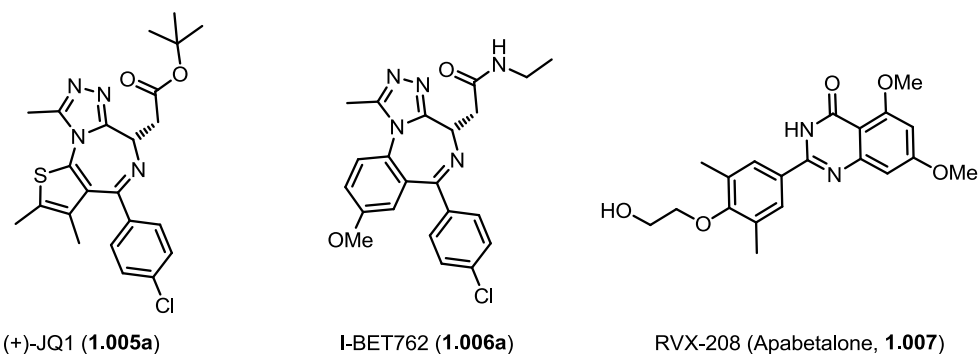


Figure 10: Chemical structures for BET bromodomain inhibitors (+)-JQ1 (1.005a), I-BET762 (1.006a) and RVX-208 (Apabetalone, 1.007).

Further studies have shown that the BET proteins act as regulatory cofactors for c-Myc, a master regulatory factor of cell proliferation. Activation of the c-Myc oncoprotein is known to significantly affect cell division and survival, playing a key role in the development of cancer.⁴⁸

More recently, Brd9 and SMARCA4 have been identified as part of the human BAF-Type SWI/SNF multi-protein domain, a chromatin remodelling complex involved in transcription and DNA repair.^{49, 50} This complex has been found to play a key role in the development of synovial sarcomas, an aggressive soft tissue tumour accounting for approximately 10% of all human soft-tissue sarcomas.⁵¹

1.4.2 Neurological disorders

There is increasing evidence to suggest that epigenetic proteins play a significant part in the development of various neurological conditions such as schizophrenia and bipolar disorder (Brd1 and SMARCA2),^{52,53} William's syndrome (BAZ1B),⁵⁴ Rubinstein-Taybi syndrome (CREBBP, EP300)⁵⁵ and epilepsy (Brd2).⁵⁶ In these cases, genetic studies have shown that reduced protein expression and/or reduction or loss of function is associated with disease. Therefore, therapeutic agents which up-regulate or activate the appropriate BCP could provide a method for treatment. However, no study has addressed bromodomain specific effects in this context. Therefore, the positive or negative effects of bromodomain inhibition remain unknown.³⁸

1.4.3 Metabolic disease

Several BCPs have been implicated in various metabolic diseases. This has been observed for BAZ1B, with links to plasma protein C concentrations,⁵⁷ type 2 diabetes⁵⁸ and serum lipid cholesterol,⁵⁹ for SMARCA4, with links to total plasma cholesterol,⁶⁰ and for PCAF with links to vascular morbidity and mortality.⁶¹ In

addition, the BET family of bromodomains, in particular Brd2, have been found to play a role in the development of obesity and type 2 diabetes.⁶² More specifically, Brd2 is known to be involved in promoting insulin resistance. The BET family selective chemical probe, I-BET762 (**1.006a**, **Figure 10**) has been shown to upregulate Apolipoprotein A1 (ApoA1), a protein involved in anti-inflammatory and metabolic processes.⁴⁷ As ApoA1 plays a crucial role in lipid transport, metabolism and protection against cardiovascular disease, inhibition of these bromodomains may represent an effective treatment for these conditions.

1.4.4 Inflammation

Genetic links to autoimmune and inflammatory conditions have been reported for several BCPs. For example, Brd2 has been implicated in rheumatoid arthritis⁶³ and SP140 in Crohn's disease.⁶⁴ Furthermore, links to other disease indications have been reported for bromodomain containing HATs including CREBBP and EP300, which were proposed therapeutic targets for the treatment of asthma and lung inflammation.⁶⁵ EP300 and PCAF regulate inflammatory responses through the regulation of COX2, a key enzyme of prostaglandin synthesis and a clinically successful target for the development of anti-inflammatory drugs.⁶⁶ SMARCA4, a crucial component of the previously mentioned SWI/SNF BAF type complex has been implicated in various immune functions. This complex is required for T cell differentiation and development, and for the induction of a subset of cell signalling proteins known as cytokines.⁶⁷

The BET family of bromodomains are the most well-validated targets for autoimmune and inflammatory disease. Early evidence for the role of BET proteins came from experiments in which Brd2 was over-expressed in transgenic mice. Results from this study showed development of splenic follicular B cell lymphoma.⁶⁸ The protein for which there is most evidence for targeting bromodomains within this context is Brd4. This bromodomain has been shown to play an important role in lipopolysaccharide (LPS)⁶⁹ stimulated, NF- κ B⁷⁰ dependent gene expression in macrophage immune cells.⁴⁷

The most recent studies in this area utilise the BET bromodomain inhibitor, I-BET762 (**1.006a**), providing an indication that there is therapeutic potential in targeting the bromodomain within the BCP.⁴⁷ Studies have shown that I-BET762 (**1.006a**) suppresses the expression of key inflammatory genes in LPS stimulated macrophages. The translation of these *in vitro* observations to an *in vivo* mouse

model of endotoxic shock provided exciting results. Dosing of I-BET762 (**1.006a**) suppressed cytokine expression and promoted survival in mice administered with lethal doses of LPS.^{47,71}

Further evidence for the role of the BET family of bromodomains in inflammatory disease is provided by RVX-208 (Apabetalone, **1.007**, **Figure 10**), developed by Resverlogix.⁷² Although not developed as a BET bromodomain ligand, RVX-208 (**1.007**) was the first BET inhibitor to enter clinical trials for the treatment of atherosclerosis (currently in phase III; NCT01067820). This compound acts by increasing expression levels of the high density lipoprotein ApoA1, which has emerged as a promising strategy for the treatment of this disease. ApoA1 expression is regulated by BET BCPs and inhibition of these bromodomains has been associated with ApoA1 up-regulation on both transcriptional and protein levels.^{73, 74}

1.4.5 Infectious disease

Several BCPs are known to be involved in modulating responses to viral or bacterial infection. For example, protein knock-down experiments suggest that BET proteins play a role in the life cycle of HIV, herpes and papilloma viruses.⁷⁵ In addition, a number of studies suggest that the bromodomain of PCAF plays a fundamental role in HIV replication, through an association with the viral Tat protein.⁷⁶ Small molecule inhibitors which block this association could present an opportunity to suppress HIV progression.

1.4.6 Therapeutic potential of BCPs

Given the increasing weight of evidence to support BCP association with disease, there is now a convincing rationale for targeting these proteins as a therapeutic strategy. However, across the entire BCP family, relatively few sub-micromolar affinity, selective bromodomain ligands are known. Therefore, the development of high quality chemical probes is essential to enable effective target validation and subsequent drug discovery.

1.5 Chemical probes

1.5.1 Chemical probes as tool molecules

Chemical probes are tool molecules, which can be used to interrogate the biology of a target protein. The use of these compounds aims to bridge the gap between chemical biology and drug discovery, enabling target validation (or invalidation, see Section 1.5.3.8, page 36) before the launch of a full drug discovery programme. However, the understanding of what constitutes a high quality probe is a topic of debate. Recent reviews^{77, 78, 79} in this area suggest that a chemical probe should be a potent and selective inhibitor of protein function at the site of action, which should satisfy a short list of guidelines: (i) *in vitro* potency versus the target and selectivity against other molecular targets that could potentially interfere with the biological read-out of interest; (ii) *in vitro* evidence of the mechanism of action in the target protein; (iii) sufficient chemical and physical property data to interpret results as due to its intact structure or a well-characterised derivative; and (iv) cellular activity data to address a hypothesis about the role of the molecular target in a cell's response to its environment (**Figure 11**).



Figure 11: The 4 principles which should apply in order to generate high quality chemical probes to enable target validation.

It is important to understand the key difference between a drug molecule and a chemical probe: drugs must be safe and effective, whereas chemical probes are used to ask a specific biological question. As such, drug molecules and chemical probes can be very different in their characteristics. For example, unlike a chemical probe, a drug does not need to have a selective activity profile. Indeed, polypharmacology may be a desirable property to drive efficacy in a disease state. In addition, drug candidates should display excellent physico-chemical properties and pharmacokinetics (PK). Chemical probes do not need to meet the same requirements as a successful medicine, as their purpose is entirely different. Whilst physico-chemical properties and PK can be important and useful for probe molecules, these qualities are not essential for their use. However, it is essential that chemical probes display high potency and excellent selectivity in order to confidently assign a given phenotype to the protein of interest. To build further confidence in the

biological phenotype observed, further validation experiments should be conducted.⁸⁰ For example, a structurally orthogonal probe molecule with equal affinity and selectivity should be developed and tested against the target of interest. If the two probes show an identical biological read-out, the link between inhibition of the target and phenotype is confirmed. In addition, the development of a structurally similar negative control compound is recommended. If a similar phenotype is observed through the use of both active and inactive compounds, the link between the target and phenotype is called into question.

The use of chemical probes to dissect the biology of epigenetic protein targets is an area of intense interest. The field of epigenetics offers over 400 domains available for study across a range of ‘reader’, ‘writer’ and ‘eraser’ modules.⁸¹ Protein knock-down experiments, which block the action of an entire complex offer a method for probing protein function. However, bromodomains often exist as part of far larger complexes, which contain multiple domains of different function. For example, BRPF1 contains 2 PHD domains, an EPL1 domain as well as a bromodomain (Figure 12).²⁶

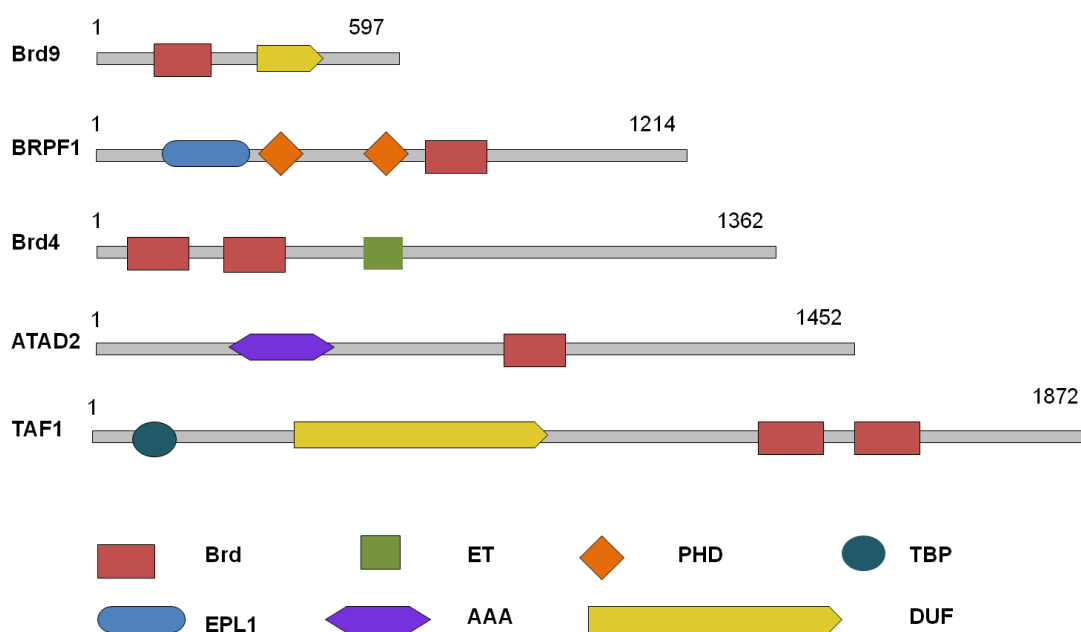


Figure 12: Domain organisation of Brd9, BRPF1, Brd4, ATAD2 and TAF1 BCPs. The numbers represent the number of amino acid residues present in each BCP and the locations of the individual domains are indicated by the relative positions of the blocks. Bromodomains (Brd) are shown in red.

A chemical probe approach, which aims to inhibit the action of a specific domain may show different effects to protein knock-down experiments. As mediators of protein-protein interactions, bromodomains were considered to be less tractable

points of intervention. However, the recent development of high affinity, selective, BET family chemical probes challenges this perception.³⁸ The bromodomain within the BCP has pre-organised architecture brought about by 4 α -helices and 2 loop regions, which form the basis of the binding site (**Figure 9**, page 8).²³ Within the bromodomain recognition pocket, the KAc residue forms a series of specific hydrogen-bonds. It is proposed that the defined nature of the binding site enables small molecules to mimic this interaction, leading to high affinity association with the bromodomain. The development of BET family chemical probes highlights the unique nature of the bromodomain, as targeting alternative protein-protein interactions, which are generally large, flat and featureless, poses major challenges.^{82,83}

Although there have been major advances in the field of chemical probes for the BET bromodomains, there has been comparatively little reported outside of this family. Considering this, Vidler and co-workers⁸⁴ investigated the tractability of non-BET bromodomains to small molecule intervention. A selection of 33 bromodomains were analysed and grouped according to common binding site features. Results from these investigations indicated that bromodomains were more tractable than other protein-protein interactions, supporting the previous discussion. Of the 33 bromodomains considered, 13 were classed as druggable, meaning that they are able to (or predicted to be able to) bind to drug-like molecules. The 13 bromodomains identified included the BET family (excluding BrdT), PCAF, CECR2, BRPF1, GCN5, TAF1 BD2, BPTF and PHIP. Furthermore, Brd9, Brd1, CREBBP, PB1 BD2 and PB1 BD5 were viewed as intermediate, whilst the remainder were classified as difficult to drug. However, as this ranking is based on knowledge of current X-ray crystal structures, it is likely to change as a greater number of non-BET bromodomain inhibitors are developed.

1.5.2 Chemical probes for the BET family of bromodomains

This majority of research in the field of epigenetic reader modules has focused on the development of inhibitors for the human BET family, resulting from their potential as anticancer, anti-inflammatory and antiviral agents.⁸⁵ With the exception of BrdT, which is solely expressed in the testes, the BET BCPs are ubiquitously expressed in humans. The BET family of bromodomains, of which there are 4 members: Brd2, Brd3, Brd4 and BrdT contain 2 bromodomains each, as well as an extra terminal domain (**Figure 12**, page 15). In total, this amounts to 8 bromodomains, with the first

and second domain of each BET protein defined as BD1 and BD2, respectively. Although they are located in the same protein, the BD1 domains do not possess identical structures to their BD2 counterparts. However, the BD1 and BD2 domains are highly homologous within their individual groups.

The majority of BET bromodomain ligands reported to date are pan-BET inhibitors, which target all 8 bromodomains of this family. These molecules show little selectivity between individual members of the BET family or between the first and second bromodomains of each protein. It is believed that the development of molecules which selectively inhibit a single BET BCP or one of the two tandem bromodomains would be extremely challenging, due to the high sequence similarity of these proteins. In the absence of selective ligands, it would be very difficult to determine which of the 8 bromodomains targeted is driving the phenotypic response. However, the therapeutic potential arising from more selective BET inhibitors has not yet been reported. Indeed, it may be that a greater level of discrimination provides little improvement on the biological profiles observed through the use of pan-BET inhibitors.

To date, several distinct chemotypes have been identified as inhibitors of the KAc-BET bromodomain interaction, the first of which were based on the triazolodiazepine scaffold (**Figure 13**).

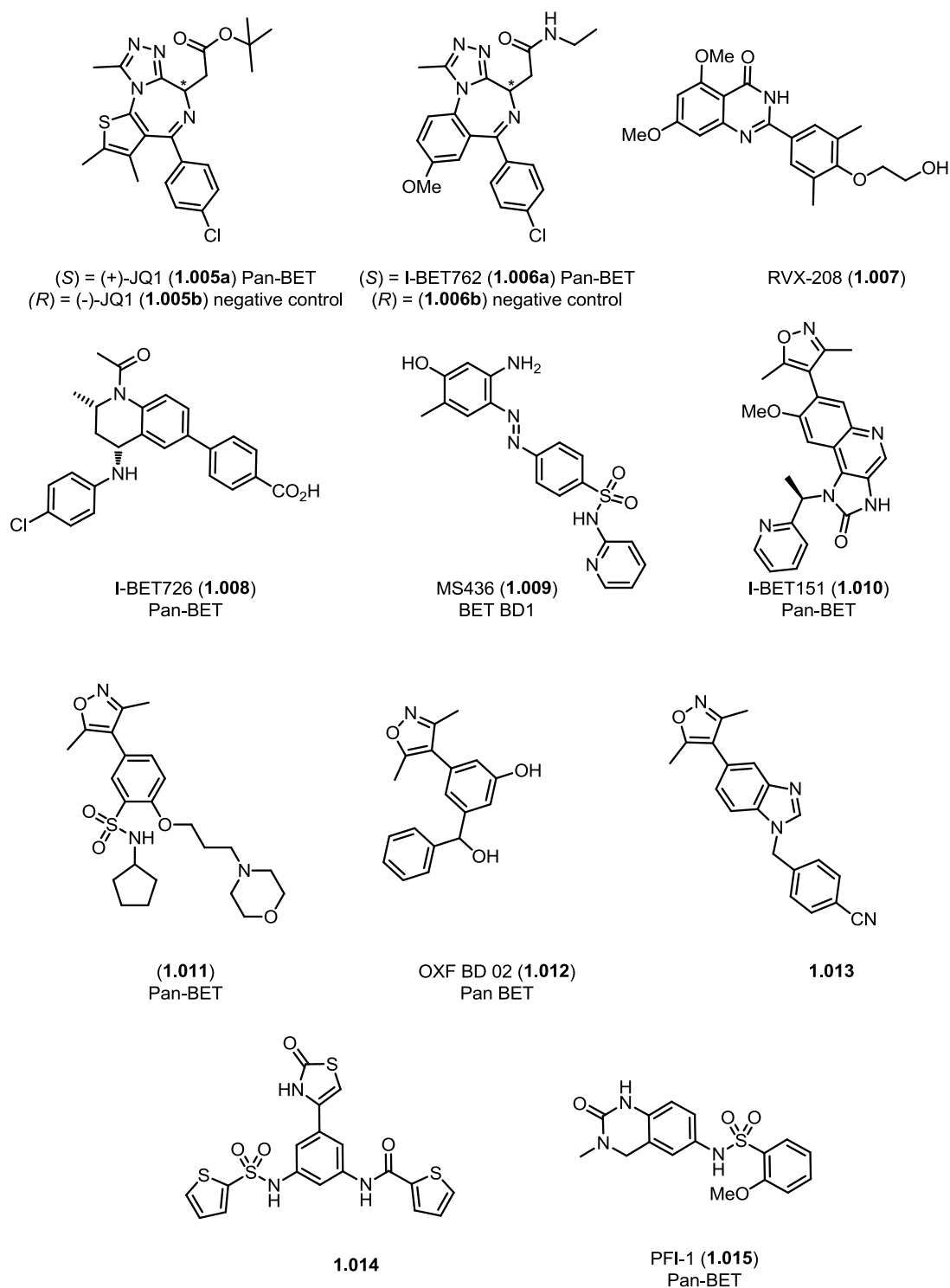


Figure 13: Chemical structures for a selection of BET bromodomain inhibitors.

Potent and selective inhibitors derived from this template were published simultaneously by Fillipakopoulos and co-workers⁴⁴ and Nicodeme and co-workers,⁴⁷ who detail the discovery of (+)-JQ1 (**1.005a**) and I-BET762 (**1.006a**), respectively. (+)-JQ1 (**1.005a**) was developed from compounds disclosed in a patent

by Mitsubishi Pharmaceuticals.⁸⁶ Initially synthesised as a racemate, it was discovered that only a single enantiomer of JQ1 was active, with (+)-JQ1 (**1.005a**) exhibiting IC₅₀ values of 77 and 33 nM in Brd4 BD1 and BD2, respectively (AlphaScreen). The IC₅₀ value for the (-)-enantiomer (**1.005b**) was estimated to be above 10,000 nM in Brd4 BD1, providing a negative control compound to support biological studies. Broader bromodomain selectivity profiling revealed that the enantiomers of JQ1 showed little or no detectable binding to 33 other bromodomains tested, as determined by thermal shift (ΔT_m).

The studies of Nicodeme and co-workers⁴⁷ detail the discovery of I-BET762 (**1.006a**), a BET bromodomain inhibitor identified by a phenotypic screen for small molecule upregulators of ApoA1. As previously discussed (Section 1.4.3, page 11), ApoA1 up-regulation is linked with protection from atherosclerosis and anti-inflammatory effects. However, no molecular mechanism for modulating ApoA1 had been reported at this time. In this case, a human HepG2 hepatocyte⁸⁷ cell line with an ApoA1 luciferase reporter was used to screen a library of compounds. This cellular phenotypic screen led to the discovery of **1.016**, which showed potent induction of the ApoA1 reporter gene, with an EC₁₇₀ value of 440 nM (**Figure 14**).

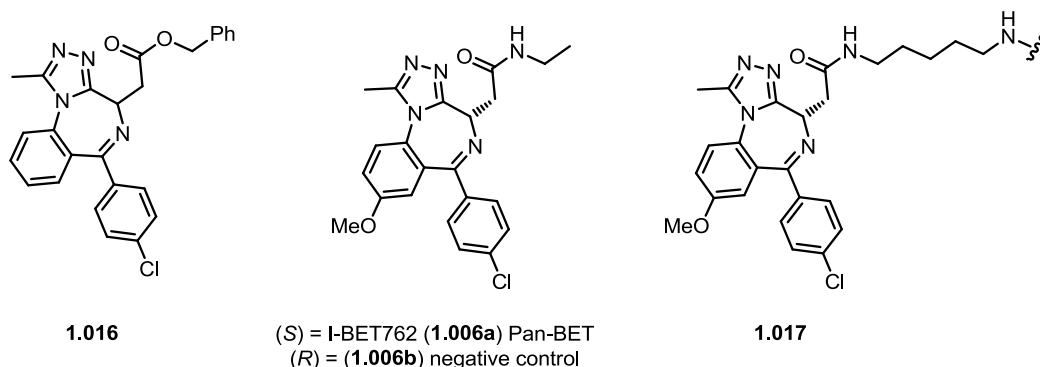


Figure 14: Chemical structures of compounds 1.016, I-BET762 (1.006a) and 1.017. Compound 1.016 was identified by a phenotypic screen for small molecule up-regulators of ApoA1 and 1.017 is a derivative of I-BET762 (1.006a), which was attached to a bead for chemoproteomics experiments.

Given this result, compound **1.016** was progressed for lead optimisation. A programme of medicinal chemistry was initiated in order to optimise potency against the ApoA1 up-regulation assay, as well as the physico-chemical and PK properties of the molecule.⁸⁸ These studies revealed that the triazolodiazepine core was essential for activity and the 6-position aryl ring was common to all active analogues screened. SAR exploration at the 4-position led to the discovery of I-BET762 (**1.006a**), which displayed an EC₁₇₀ of 700 nM in the ApoA1 reporter assay. The

stereochemistry at the 4-position was found to be important for activity, suggesting that this template was interacting with a particular molecular target. In order to investigate the mode of action of I-BET762 (**1.006a**), a chemoproteomics approach was utilised. In these experiments, compound **1.017**, a derivative of I-BET762 (**1.006a**) was attached to an affinity matrix *via* a flexible amine linker. In addition, the inactive enantiomer (**1.006b**) of I-BET762 (**1.006a**) was prepared, providing the ideal control matrix for non-specific activity. Using these solid-supported compounds, affinity chromatography was conducted with HepG2 cell lysates in order to determine possible protein binding partners.⁸⁸ Results from this experiment showed that several proteins were bound to active compound **1.017**. Interestingly, these proteins were not associated with the inactive control (**1.006b**), suggesting a selective interaction by compound **1.017**. Furthermore, a competition experiment in which compound **1.016** was introduced showed dissociation of these proteins, suggesting that they were the specific targets of compound **1.017**. Using LC-MS/MS, the protein binding partners were identified as Brd2, Brd3 and Brd4, 3 members of the BET family of BCPs. As BrdT is only expressed in testes and not present in HepG2 cells, no binding was detected. Importantly, only the BET proteins were identified as binding partners, suggesting that this family may be the molecular targets of the triazolodiazepine scaffold.

In order to determine specificity, that is to say, which region of the BET BCPs compound **1.017** was binding to, biophysical and structural methods were employed. Through cloning and expression of the isolated bromodomains, isothermal titration calorimetry (ITC) and surface plasmon resonance (SPR) confirmed direct, high affinity binding to the BET bromodomains. Furthermore, a time-resolved fluorescence resonance energy transfer (TR-FRET) assay was employed to determine dose-dependent inhibition of peptide binding. I-BET762 (**1.006a**) displayed IC₅₀ values in the range of 32.5–42.5 nM, confirming inhibition of the BET bromodomain-histone interaction.

To validate the utility of I-BET762 (**1.006a**) as a BET bromodomain chemical probe, broader pharmacological screening was conducted.⁸⁸ These experiments indicated negligible activity outside of the BET family, providing confidence in the selectivity of this molecule.

Importantly, extensive SAR analysis of this scaffold showed that BET bromodomain inhibition correlated with whole-cell potency for ApoA1 expression, further supporting this phenotype in cells. Finally, siRNA knock-down experiments were conducted as an orthogonal method for target validation.⁸⁸ Progressive knock-down of Brd4 was found to induce up-regulation of ApoA1 in HepG2 cells. However, knock-down of Brd2 and Brd3 had no effect on ApoA1 expression, suggesting that inhibition of Brd4 alone was responsible for the observed phenotype. Through this medicinal chemistry programme, I-BET762 (**1.006a**) was confirmed as a high quality cellular chemical probe for the BET family of bromodomains. This compound is currently undergoing phase I/II clinical trials for the treatment of NUT midline carcinoma and other hematological malignancies (NCT01587703).⁸⁸

Compound **1.007**, (RVX-208, Apabetalone), developed by Resverlogix, is the most advanced BET bromodomain inhibitor currently undergoing phase III clinical trials for the treatment of atherosclerosis (NCT01067820).⁷² Using a similar approach to Nicodeme and co-workers,⁴⁷ RVX-208 (**1.007**) was identified from a phenotypic screen for up-regulators of ApoA1. RVX-208 (**1.007**) increased the thermal shift of all BET bromodomains but did not bind to CREBBP, p300, BAZ2B, GCN5, PHIP or SMARCA2, suggesting selectivity for the BET family. RVX-208 (**1.007**) showed a bias for the BD2 domain of Brd4, with IC₅₀ values of 0.04 µM and 1.8 µM against BD1 and BD2, respectively (TR-FRET).^{73,74}

Compound **1.008**, I-BET726⁸⁹ developed by GSK, contains the 1-acyl tetrahydroquinoline KAc mimetic. I-BET726 (**1.008**) interacts with the tandem bromodomains of Brd4 with an IC₅₀ of 22 nM (TR-FRET) and K_d of 4 nM (ITC). Compound **1.008** shows excellent selectivity against the closely related bromodomain of CREBBP with a K_d of 6.3 µM (ITC) and no significant activity against a panel of other bromodomains.

Zhou and co-workers⁹⁰ developed MS436 (**1.009**), a BD1 biased BET bromodomain inhibitor. MS436 (**1.009**) shows <50 nM activity against Brd4 BD1, with 10 fold selectivity over Brd4 BD2. The compound also displays activity against the bromodomains of CREBBP, PCAF, Brd7, BPTF, BAZ2B and SMARCA4, as determined by a fluorescence anisotropy binding assay.

The 3,5-dimethylisoxazole moiety is an KAc mimetic for the BET family of bromodomains, as shown by Dawson and co-workers,⁹¹ Bamborough and co-

workers,⁹² Hewings and co-workers,^{93,94} and Hay and co-workers.⁹⁵ Dawson and co-workers reported the discovery of I-BET151 (**1.010**) from molecules identified in a high throughput screen for up-regulators of ApoA1.^{91,96} Developed in parallel to I-BET762 (**1.006a**), I-BET151 (**1.010**) is also selective for the BET bromodomains, with IC₅₀ values between 0.25 and 0.79 μM for Brd2, Brd3 and Brd4 [Fluorescence polarization (FP) assay]. Importantly, only a small change in ΔT_m was seen for CREBBP and no change for the 19 other bromodomains tested, confirming selectivity for the BET family.⁹⁷

Further work reported by Bamborough and co-workers has identified phenyl dimethylisoxazole derivatives from a focused fragment screen.⁹² Sulfonamide compound **1.011** was identified as a lead, displaying IC₅₀ values of 1.5, 1.1 and 2.6 μM for Brd2, Brd3 and Brd4, respectively (TR-FRET). Selectivity was assessed by thermal shift, although this method does not allow for precise quantification. Compound **1.011** stabilised the melting temperature for the BET bromodomains, with ΔT_m: >5 °C. In contrast, shifts of ≤1.5 °C were seen for the other bromodomains tested, suggesting selectivity for the BET family.

Hewings and co-workers have reported a small, ligand efficient 3,5-dimethylisoxazole derivative, OXF BD 02 (**1.012**), which shows an IC₅₀ value of 382 nM against Brd4 BD1.^{93,94} Following this, Hay and co-workers⁹⁵ reported the discovery of 5- and 6-isoxazolylbenzimidazoles as selective BET bromodomain inhibitors. Lead compound **1.013** displays an IC₅₀ of 200 nM against Brd4 BD1 and at least 100-fold selectivity over CREBBP, as determined by AlphaScreen. The broader selectivity of compound **1.013** was assessed by thermal shift, with ΔT_m: 3.2 °C against Brd4 BD1, 1.1 °C against CREBBP and ≤ 0.1 °C against a panel of phylogenetically diverse bromodomains.

More recently, Zhao and co-workers⁹⁸ identified a new KAc mimetic from a fragment-based approach. Initially, a collection of 487 fragments were selected on the basis of various parameters including LogP, molecular weight and number of rotatable bonds. Docking of these compounds using the published X-ray crystal structure of (+)-JQ1 (**1.005a**) in complex with Brd4 BD1 narrowed this compound set to 41. These molecules were progressed for X-ray crystallography in Brd4 BD1, providing 9 compounds, with several chemotypes identified as KAc mimetics. The 2-thiazolidinone template was selected for further optimisation, leading to the

development of compound **1.014**. This molecule shows an IC₅₀ value of 230 nM against Brd4 BD1 as determined by FP analysis.

Finally, dihydroquinazolinone compound **1.015**, PFI-1, reported by Fish and co-workers^{99,100} is a BET bromodomain selective chemical probe. Identified from a fragment-based screen, PFI (**1.015**) displays an IC₅₀ value of 220 nM against the Brd4 BD1, with good selectivity over a panel of non-BET bromodomains, as determined by thermal shift. Furthermore, PFI-1 (**1.015**) shows good selectivity beyond the bromodomain family, with less than 50% inhibition seen across a panel of kinases, GPCRs and ion channels.

1.5.2.1 KAc mimetics of the BET family of bromodomains

As discussed in the previous section, there are several chemotypes known to act as KAc mimetics for the BET family of bromodomains. The binding modes of each scaffold have been determined by X-ray crystallography, with all warheads exhibiting common interactions: a direct hydrogen-bond to the NH₂ moiety of Asn140; and a water-mediated interaction to Tyr97 (Brd4 BD1 numbering, **Figure 15**).

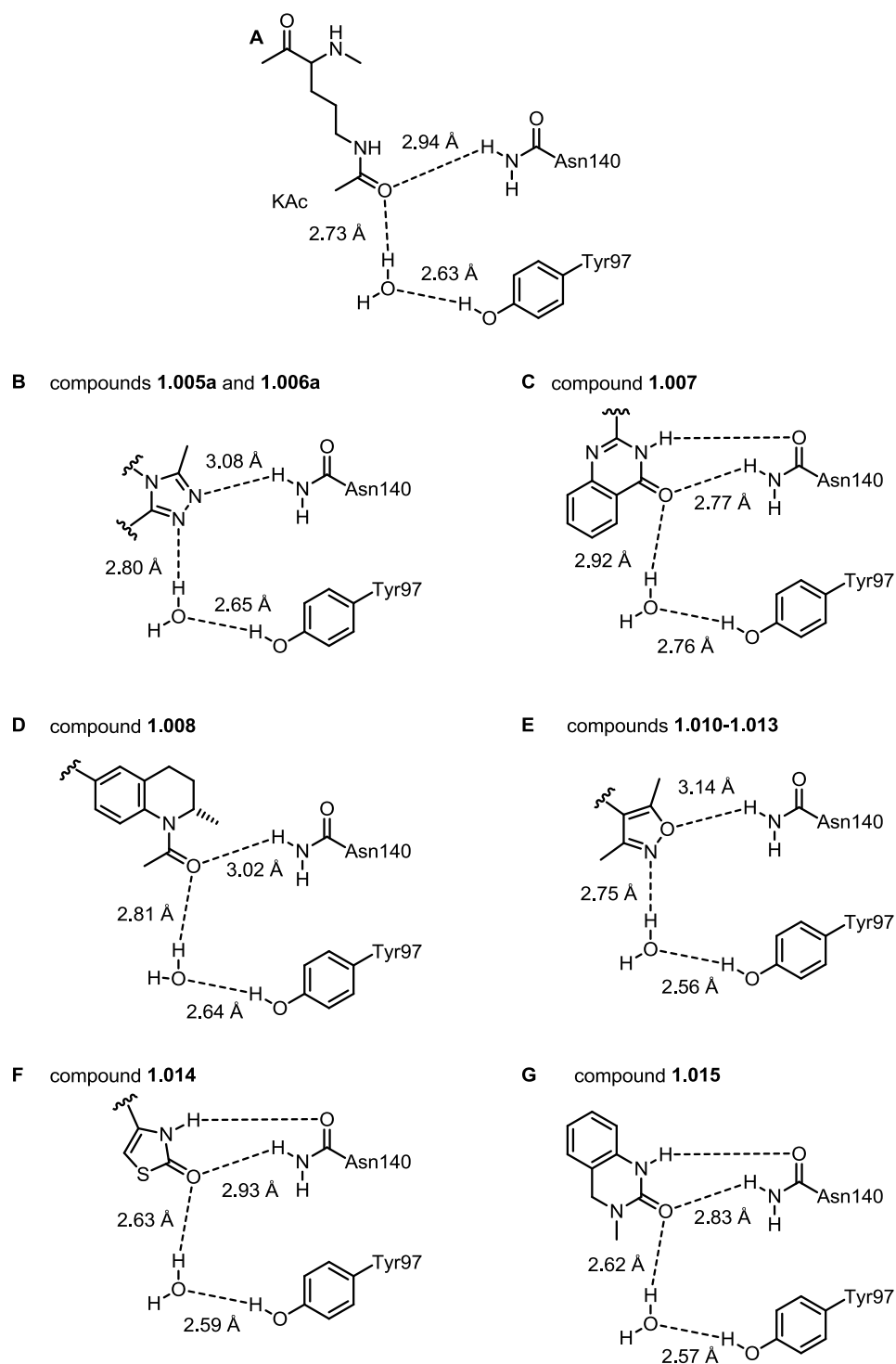


Figure 15: Schematic representations of bromodomain binding to various KAc mimetic motifs (Brd4 BD1 numbering). KAc has been included for direct comparison (A).

As a direct structural mimetic of KAc (**Figure 15, A**), the triazole unit of compounds **1.005a** and **1.006a** forms the key hydrogen-bonds to Asn140 and Tyr97 (**Figure 15, B**). One of the triazole N atoms forms a direct interaction to the NH₂ moiety of Asn140, whilst another participates in a water-mediated hydrogen-bond to Tyr97.

The methyl substituent is placed in a small hydrophobic cavity, in a similar orientation to that of KAc.^{44,71}

The quinazolin-4-one core of RVX-208 (**1.007**) acts as the KAc mimetic (**Figure 15, C**). The carbonyl group forms a direct hydrogen-bond to the NH₂ moiety of Asn140, as well as a water-mediated interaction to the hydroxyl of Tyr97. In addition, the quinazolin-4-one NH forms a hydrogen-bond to the carbonyl of Asn140, creating a bidentate interaction with the amide moiety.⁷⁴

The *N*-acetyl moiety of the tetrahydroquinoline scaffold in compound **1.008** acts as the KAc mimetic. The carbonyl group forms a direct hydrogen-bond to Asn140 and a through-water interaction to Tyr97 (**Figure 15, D**).

The 3,5-dimethylisoxazole moiety is the KAc mimetic in compounds **1.010–1.013**, forming similar interactions to the triazole ring (**Figure 15, E**). The isoxazole oxygen forms a hydrogen bond to the NH₂ group of Asn140, whilst the nitrogen forms a water-mediated interaction to Tyr97.^{92,94,95,97}

The 2-thiazolidinone scaffold of compound **1.014** forms a bidentate interaction to Asn140 (**Figure 15, F**). The NH and carbonyl moieties of **1.014** interact with the carbonyl and NH₂ groups of Asn140, respectively. Furthermore, the carbonyl moiety of **1.015** forms a through water hydrogen-bond to the hydroxyl group of Tyr97.⁹⁸

The cyclic urea motif of the dihydroquinazolinone scaffold in PFI-1 (**1.015**) acts as the KAc mimetic (**Figure 15, G**). The NH and carbonyl moieties form a bidentate interaction to Asn140, interacting with the carbonyl and NH₂ groups, respectively. In addition, the carbonyl moiety of compound **1.016** forms a water-mediated interaction to Tyr97.⁹⁹

All of the templates discussed act as direct structural analogues of KAc, forming hydrogen bonds to Asn140 and Tyr97 (Brd4 BD1 numbering). Interestingly, in the majority of cases, the water mediated hydrogen-bond to Tyr97 is the strongest, as indicated by the distances between interacting atoms. Whilst these interactions are important for potency, further elaboration of these scaffolds is required to confer additional potency and selectivity for the BET bromodomains. This is usually achieved through interactions with the WPF shelf region of this family (Section 1.3, page 9).

1.5.3 Chemical probes for non-BET bromodomains

The profound biology associated with the BET BCPs suggests that there may be therapeutic potential in targeting other members of the bromodomain family for the treatment of disease. To date, there has been comparatively little reported outside the BET family, leaving the majority of a new and exciting target class yet to be investigated. Therefore, the development of high quality, selective chemical probes for non-BET bromodomains will facilitate validation of these proteins as therapeutic targets and potentially lead to the development of new medicines. In recent years, there has been significant progress towards this goal, with influential contributions from academic and industrial laboratories, as well as public-private partnerships such as the Structural Genomics Consortium (SGC). These efforts have resulted in the publication of a growing number of chemical probes for non-BET bromodomains, highlighting the intense interest in this area of epigenetic research.

1.5.3.1 Multi-Bromodomain chemical probes

It remains unclear whether multi-bromodomain pharmacology or more selective inhibition is necessary to deliver a relevant phenotype within the context of human disease. Therefore, the development of both selective chemical probes and multi-bromodomain inhibitors will help to answer this question. To this end, the SGC and their collaborators have reported a series of multi-bromodomain inhibitors.

Bromosporine (**1.018**) is a non-selective ligand, which shows $\Delta T_m \geq 3.0$ °C in the bromodomains of CECR2, TAF1 BD2, Brd9 and CREBBP, as reported on the SGC website (**Figure 16**).¹⁰¹ Structurally related compound **1.019**, also exhibits multi-bromodomain activity.¹⁰² As these compounds are not selective for a single bromodomain, they are unsuitable for use as chemical probes. However, they may be enabling as start points towards chemical probes as well as for use in assay development.

1.5.3.2 ATAD2

The ATAD2 BCP is highly expressed in many diverse cancer types and expression levels have been strongly correlated with short patient survival and disease progression.¹⁰³ Although the bromodomain of ATAD2 has been reported as difficult to drug,⁸⁴ some progress had been made towards the development of chemical probes, which could represent a useful start point for cancer therapy. In order to target this challenging protein, Fesik and co-workers employed a fragment based screen to identify novel inhibitors.¹⁰⁴ Using NMR spectroscopy, compound **1.020**

was identified and showed the greatest potency against ATAD2 with a K_d value of 350 μ M (**Figure 16**).

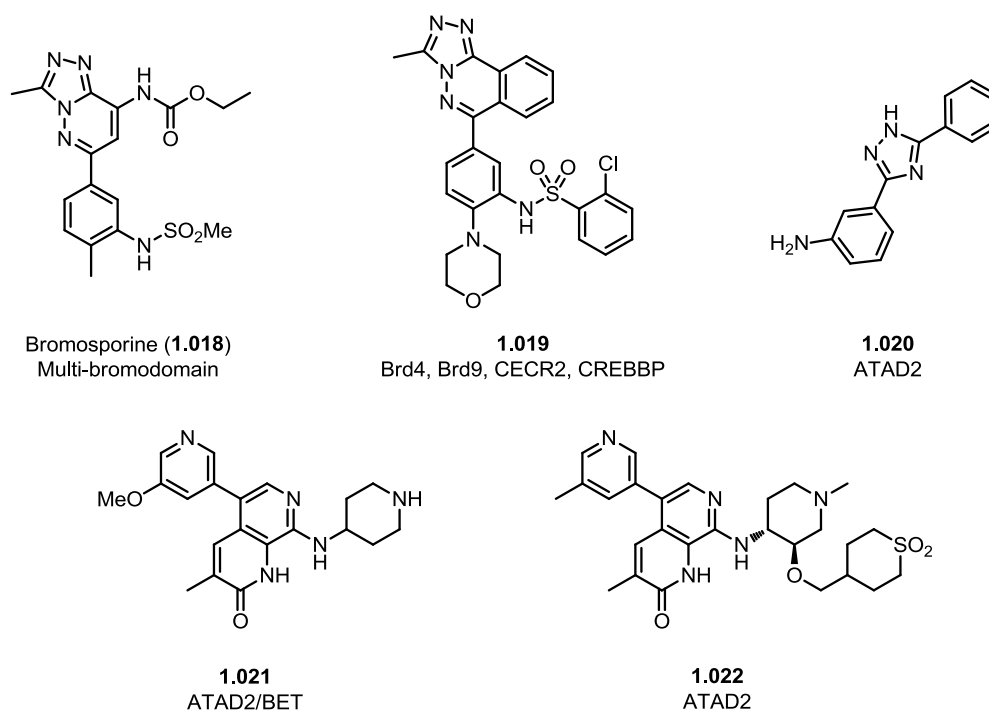


Figure 16: Chemical structures for selected non-BET bromodomain inhibitors.

More recently, GSK reported compound **1.021** as an ATAD2 inhibitor.¹⁰⁵ **1.021** was optimised from a hit identified in a fragment-based targeted array and represents the first known micromolar inhibitor of ATAD2 ($pI_{C_{50}}$: 5.9, TR-FRET), albeit not cell permeable or selective over the BET family. Optimisation of **1.021** delivered compound **1.022**, which is potent against ATAD2 ($pI_{C_{50}}$: 6.5, TR-FRET) and 160 fold selective over the BET family.¹⁰⁶ However, broader bromodomain profiling revealed that **1.022** is also active against TAF1 BD2 and TAF1L BD2. The authors state that future work on this series will focus on optimisation of this template to deliver a more selective molecule.

1.5.3.3 BAZ

The highly homologous bromodomains of BAZ2A/B belong to the BAZ family of proteins, which are ubiquitously expressed. As very little is known about the biological roles of the BAZ family, the development of chemical probes will help to elucidate their function. Although the BAZ2A/B BCPs have low predicted druggability,⁸⁴ multiple inhibitors of these domains have been reported. For example, Ciulli and co-workers used a fragment based screening approach to analyse a library of 1300 compounds.¹⁰⁷ Of these, 10 fragment hits were identified and

crystallised in the bromodomain of BAZ2B. A tetrahydro- γ -carboline fragment showed the greatest potency and was optimised to deliver compound **1.023** (Figure 17), which showed an IC₅₀ value of 9 μ M against BAZ2B (AlphaLISA).

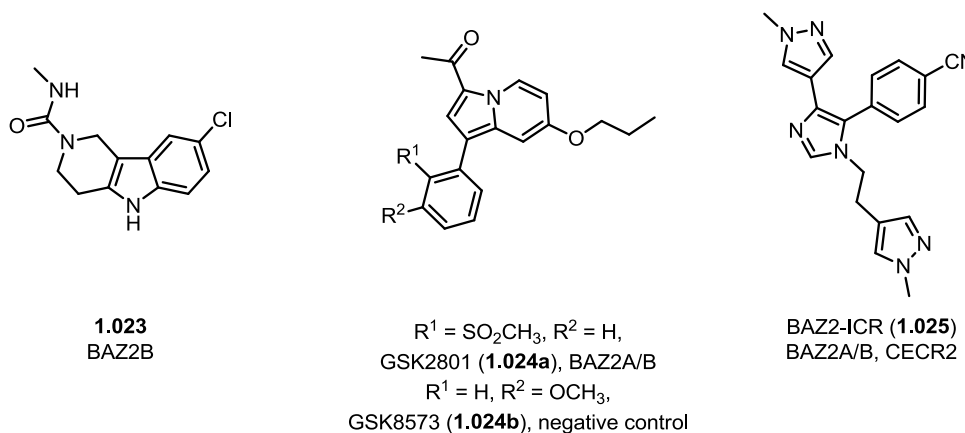


Figure 17: Chemical structures for BAZ inhibitors **1.023**–**1.025**.

GSK and the SGC collaborated to develop GSK2801 (**1.024a**), the first chemical probe reported to be selective for BAZ2A/B.¹⁰⁸ The indolizine template was identified from screening the BAZ2A bromodomain against a set of molecules that contained KAc mimetics. Following this, an iterative medicinal chemistry design strategy was employed to deliver GSK2801 (**1.024a**), which displays K_d values of 257 and 136 nM (ITC) against BAZ2A and BAZ2B, respectively. In order to investigate broader selectivity across a panel of 46 bromodomains, thermal shift analysis was employed. At 10 μ M, GSK2801 (**1.024a**) showed a Δ T_m of 4.1 and 2.7 °C for BAZ2A and BAZ2B, respectively. Significant shifts were also observed for TAF1L BD2 (3.4 °C) and Brd9 (2.3 °C). Moving forward, a chemoproteomic competition binding assay was utilised to investigate whether GSK2801 (**1.024a**), would bind to endogenous BAZ2 proteins. To this end, a linkable analogue of GSK2801 (**1.024a**), was immobilized on to a solid-support and incubated with nuclear and chromatin enriched HuT78 extracts. Of the 18 endogenous full-length bromodomain proteins that bound to the immobilised compound, only BAZ2A and BAZ2B displayed a dose-dependent reduction in the presence of GSK2801 (**1.024a**). Evidence of cellular target engagement was provided by a FRAP assay in which GSK2801 (**1.024a**) displaced BAZ2A/B from chromatin in U2OS cells. Finally, in order to determine the suitability of GSK2801 (**1.024a**) as an *in vivo* tool, PK parameters were measured after intraperitoneal and oral dosing to male CD1 mice. GSK2801 (**1.024a**) had reasonable *in vivo* exposure after oral dosing, modest clearance and plasma stability, which should allow the compound to be used as a BAZ2A/B bromodomain

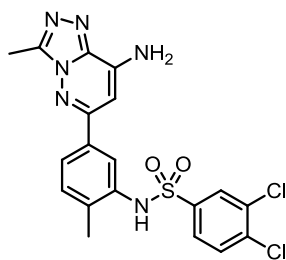
inhibitor *in vivo*. In addition, structurally similar negative control compound **1.024b** was developed to help inform biological investigations.

More recently, the SGC have collaborated with the Institute of Cancer Research to develop BAZ2-ICR (**1.025**) as a chemical probe for BAZ2A/B.¹⁰⁹ A single hit was identified from a screen of putative bromodomain inhibitors and subsequently optimised to deliver BAZ2-ICR (**1.025**). This compound shows K_d values of 109 and 170 nM against BAZ2A and BAZ2B respectively, as determined by ITC. In agreement with the ITC data, BAZ2-ICR (**1.025**) showed ΔT_m : 5.2 and 3.8 °C for BAZ2A and BAZ2B, with no significant shifts against all other bromodomains, except CECR2 (ΔT_m : 2.0 °C). Further ITC experiments revealed a K_d : 1.55 μ M at CECR2, showing 15-fold selectivity relative to BAZ2A/B. A chromatin displacement FRAP assay was used to provide evidence of cellular target engagement. Mouse PK data indicated that BAZ2-ICR (**1.025**) is suitable for use *in vivo*, with 70% bioavailability and moderate clearance (~50% of mouse liver blood flow) and volume of distribution (1.09 L/Kg).

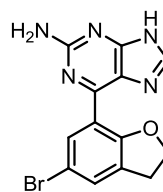
The progress made to date towards chemical probes for the BAZ bromodomains is significant, with molecules from a diverse range of chemotypes identified. In the case of GSK2801 (**1.024a**), a structurally analogous negative control compound has been developed, providing further support for biological investigations. In addition, compounds **1.024a** and **1.025** are suitable for use *in vivo*, allowing the biological role of BAZ to be studied in animals.

1.5.3.4 Brd9

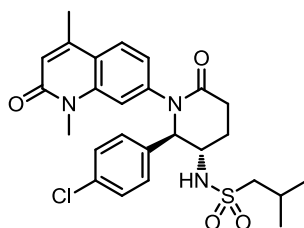
At the outset of this project, there was very little in the literature concerning the Brd9 protein. However, in the last year there have been several inhibitors reported, highlighting intense interest in this area. The first binder of Brd9 was reported by Ley and co-workers, who used flow chemistry to identify a series of compounds based on the structure of Bromosporine (**1.018**, **Figure 16**).¹¹⁰ Initially, binding to Brd9 was assessed in flow by frontal affinity chromatography coupled with mass spectrometry. Subsequent analysis by means of thermal shift confirmed the initial binding data generated. Of the compounds tested, compound **1.026** (**Figure 18**) showed the greatest thermal shift against Brd9 (ΔT_m : 4.3 °C). However, significant shifts were also seen for Brd4 (6.7 °C), BRPF1 (5.4 °C), BRPF3 (3.1 °C), CECR2 (5.6 °C), CREBBP (4.3 °C), EP300 (8.0 °C), and TRIM24 (1.8 °C), demonstrating a lack of selectivity.



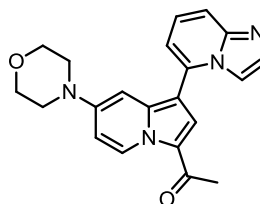
1.026
Brd9, Brd4, CECR2, CREBBP,
BRPF1, BRPF3, EP300 and TIF1
Published March 2014



1.027
Brd9
Published March 2015



LP99 (**1.028**)
Brd9/Brd7
Published May 2015



1.029
Brd9/Brd7
Published June 2015

Figure 18: Chemical structures for Brd9 bromodomain inhibitors.

Filippakopoulos and co-workers used iterative structure based design to identify compound **1.027** as a ligand for Brd9.¹¹¹ Compound **1.027** shows a K_d value of 0.28 μM against Brd9 (ITC), with some Brd4 BD1 activity (K_d : 1.4 μM). In order to understand the binding mode of compound **1.027** in complex with Brd9, attempts were made to obtain an X-ray crystal structure. Although these attempts were unsuccessful, X-ray crystallography of a structurally related analogue indicated occupation of the KAc binding site. In addition, the analogue was found to induce a structural rearrangement in the Brd9 binding pocket, resulting in an unprecedented cavity shape. Subsequent docking studies suggested that **1.027** elicits the same structural rearrangement as observed for the analogue. Cellular target engagement for compound **1.027** was demonstrated using a NanoBRET assay¹¹² in which **1.027** was found to displace Brd9 from chromatin with an IC_{50} value of 477 nM.

More recently, the SGC and the University of Oxford reported LP99 (**1.028**) as a dual Brd9/Brd7 chemical probe.¹¹³ LP99 (**1.028**) was developed from a fragment to deliver good Brd9 (K_d : 99 nM) and Brd7 (K_d : 909 nM) activities (ITC). Broader activity against a panel of 48 bromodomains was investigated by thermal shift. LP99 (**1.028**) showed <1 $^{\circ}\text{C}$ stabilization of all bromodomains except Brd9 and Brd7, suggesting good selectivity. Cellular target engagement was assessed by a NanoBRET assay,¹¹² confirming the ability of LP99 (**1.028**) to disrupt binding of Brd9

and Brd7 to chromatin in cells. To investigate the effect of Brd9/7 inhibition on the expression of proinflammatory cytokines, a human THP-1 monocytic cell line was stimulated with LPS. LP99 (**1.028**) was found to inhibit production of interleukin 6 (IL-6) in a dose dependent manner, demonstrating that Brd9/7 may be potential targets for anti-inflammatory treatment.

The SGC also report BI-9564 as a Brd9/7 selective chemical probe, developed in collaboration with Boehringer Ingelheim.¹¹⁴ Although the structure and details regarding development have not yet been reported, ITC data are available on the SGC website. BI-9564 shows excellent activity, with K_d values of 14 and 239 nM, against Brd9 and Brd7 respectively. Selectivity over the BET family of bromodomains was assessed by AlphaScreen with $IC_{50} >100 \mu\text{M}$. BI-9564 shows off-target activity against CECR2 *in vitro* (K_d : 258 nM, ITC), but not in cells (at 1 μM , FRAP).

Most recently, the SGC and the University of Oxford report compound **1.029** as a dual Brd9/7 inhibitor.¹¹⁵ Using BAZ2A/B chemical probe **1.024a** (Figure 17) as a start point, **1.029** was developed *via* a series of optimisations. Compound **1.029** is potent at Brd9 (K_d : 68 nM) and Brd7 (K_d : 368 nM), with good selectivity over Brd4 BD1 (K_d : 15 μM), as determined by ITC. Although not a quantitative method, thermal shift analysis was used to determine broader selectivity. Compound **1.029** showed ΔT_m : 5.6 °C against Brd7, with weak affinity for the bromodomains of CBP, p300 and BPTF (ΔT_m : 1.8, 2.0, and 1.1 °C respectively).

Although there has been significant progress towards the development of chemical probes for Brd9, all inhibitors discussed in this section target at least two bromodomains. Therefore, confidently assigning any observed phenotype to Brd9 inhibition specifically remains challenging. The requirement for a Brd9 selective chemical probe remains essential in order to fully elucidate the biology of this bromodomain.

1.5.3.5 BRPF

The BRPF family consists of BRPF1B/2/3, which are important scaffolding proteins for the assembly of HAT complexes of the MOZ/MORF family of transcriptional coactivators. It is reported that translocations of MOZ are associated with aggressive subtypes of leukemia.¹¹⁶ Therefore, chemical probes for the BRPF family

could potentially represent a start point towards cancer therapy. Towards this goal, the SGC have disclosed several BRPF chemical probes.

The SGC website reports OF-1 (**1.030**) as a BRPF1B/2/3 chemical probe, which displays K_d values of 100 nM, 500 nM and 2400 nM, respectively (**Figure 19**).¹¹⁷ Selectivity against other bromodomains is good, in general >100 fold, with the closest off-target activity being Brd4 (39 fold selectivity), although the SGC does not report what this is against.

NI-57 (**1.031**) is a BRPF family selective chemical probe developed by the SGC in collaboration with University College London.¹¹⁸ As reported on the SGC website, NI-57 (**1.031**) binds to BRPF1B (K_d : 31 nM), BRPF2 (K_d : 108 nM) and BRPF3 (K_d : 408 nM), with nanomolar affinity, as determined by ITC. NI-57 (**1.031**) is very selective against the BET family and the closest off-target effects are against BRD9 (32 fold).

The SGC website also reports PFI-4 (**1.032**) as a chemical probe for BRPF1B, which was developed in collaboration with Pfizer.¹¹⁹ Full details of the discovery PFI-4 (**1.032**) have not yet been published, but the SGC report a BRPF1B K_d : 13 nM, as determined by ITC. At this stage, the broader selectivity profile of this compound has not been described.

GSK have reported compound **1.033a** as the first BRPF1B selective inhibitor, which shares the same benzimidazolone core as OF-1 (**1.030**).¹²⁰ Compound **1.033a** was identified from a cross-screen of analogues from a fragment hit identified in a Brd4 STD-NMR screen. Excellent BRPF1B activity was observed with an IC_{50} value of 80 nM (TR-FRET), with 100 and >1000 fold selectivity over BRPF2 and BRPF3, respectively. Following this, compound **1.033a** was progressed for further selectivity profiling by means of BROMOscan.¹²¹ In a panel of 35 bromodomains, **1.033a** showed a BRPF1B K_d : 7.9 nM, with a good window of selectivity over the BET family and BRPF2/3. Evidence of cellular target engagement was achieved using a cellular chromatin displacement assay in which **1.033a** showed disruption of chromatin with an IC_{50} value of 1 μ M. In addition, compound **1.033b** was reported as a structurally analogous negative control, which will facilitate biological investigations.

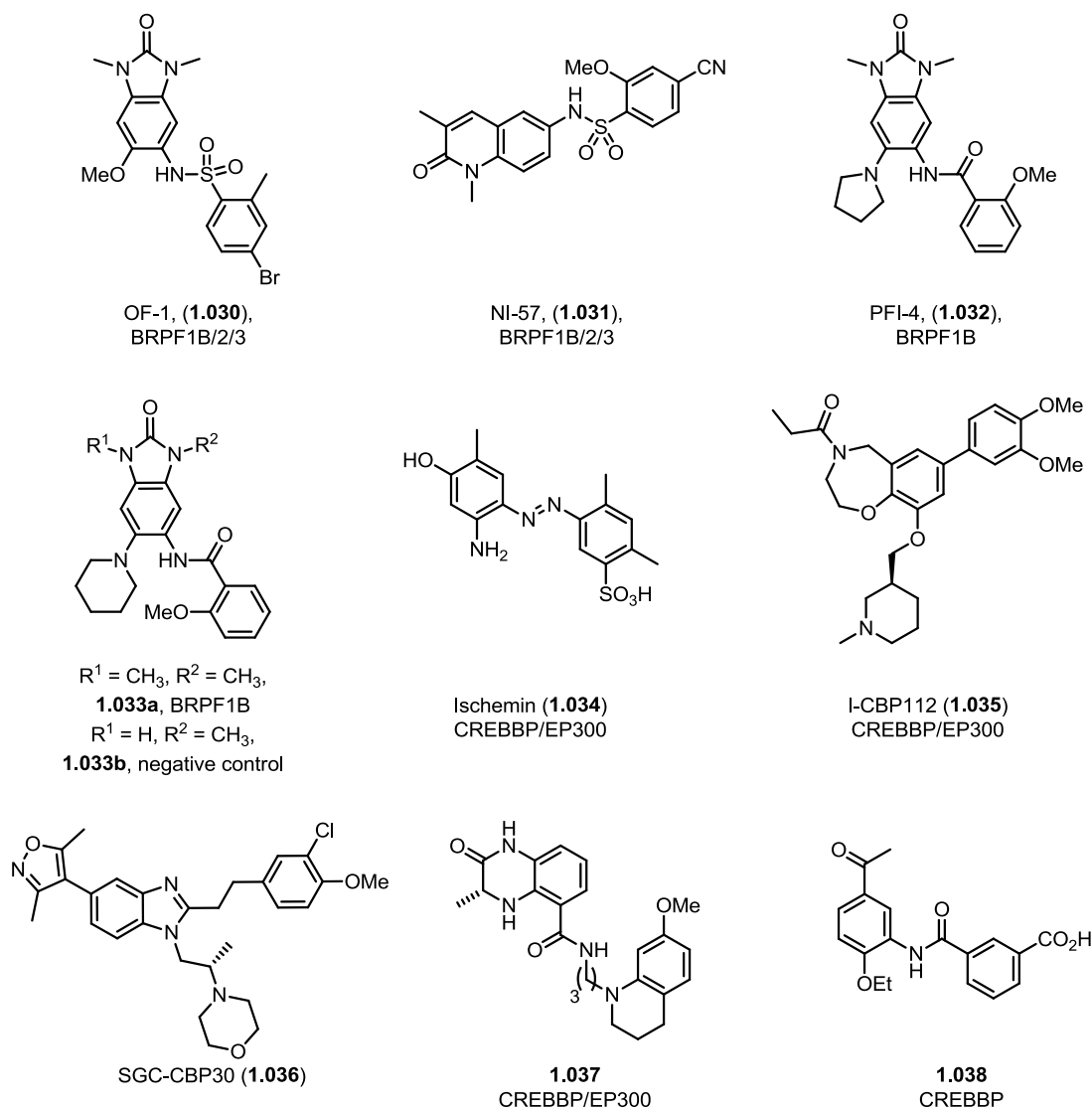


Figure 19: Chemical structures for BRPF and CREBBP inhibitors.

There are now a significant number of BRPF family chemical probes reported in the literature. These tool molecules will facilitate biological investigations with the aim to fully understand the role of these proteins in human disease. However, the chemical probes for which the structures have been reported share the same benzimidazolone core. In the future, biological validation experiments would benefit from BRPF family chemical probes from a variety of structural scaffolds.

1.5.3.6 CREBBP

Outside of the BET family, much of the focus in chemical probe discovery has been with the structurally related bromodomains of CREBBP and EP300. This may be due to the fact that many unselective BET bromodomain binders also interact with the bromodomain of CREBBP (see compound **1.012**, **Figure 13**). Research

conducted by Zhou and co-workers¹²² led to the discovery that the bromodomain of CREBBP binds to KAc382 of p53.¹²³ In order to develop small molecule binders of the CREBBP bromodomain specifically, several groups aimed to inhibit the CREBBP-p53 interaction.

Zhou co-workers conducted an NMR screen of a diverse library of 3000 compounds, with the aim to identify novel inhibitors for CREBBP.¹²⁴ Of the 3000 compounds tested, 10 hits were generated and optimised to deliver Ischemin (**1.034**, **Figure 19**), which contains the azobenzene moiety. Ischemin (**1.034**) inhibits the CREBBP bromodomain-p53 interaction with an IC₅₀ value of 5 µM, as determined by a cell-based assay. Selectivity over other bromodomains was investigated using a fluorescence displacement assay in which Ischemin (**1.034**) was up to 5-fold selective over the bromodomains of PCAF, Brd4 BD1 and BAZ2B. **1.034** prevents apoptosis in ischemic cardiomyocytes (hence the name Ischemin), suggesting that inhibition of the CREBBP bromodomain or the other targets that bind to this compound with similar affinity may provide an effective treatment for diseases such as myocardial ischemia.

I-CBP112 (**1.035**) is a CREBBP/EP300 chemical probe developed by GSK in collaboration with the SGC (**Figure 19**).¹²⁵ Further details regarding the development of I-CBP112 (**1.035**) have not yet been published, but the SGC website provides limited data. I-CBP112 (**1.035**) shows K_d values of 151 and 625 nM against CREBBP and EP300, respectively (ITC). Selectivity over a range of bromodomains was established including ATAD2, BAZ2B, Brd2 BD2, Brd4 BD1, PB1 BD5, PCAF, PHIP BD2 and TRIM24, as determined by bio-layer interferometry (BLI).

The SGC and the University of Oxford collaborated to develop SGC-CBP30 (**1.036**), a chemical probe for CREBBP and EP300.¹²⁶ SGC-CBP30 (**1.036**) shows K_d values of 21 and 38 nM against CREBBP and EP300, respectively (ITC). In addition, compound **1.036** is 40 fold selective over BET family member, Brd4 BD1. Broader bromodomain selectivity was assessed by thermal shift, in which compound **1.036** was tested against 10 targets. No ΔT_m above 2 °C was observed against any other bromodomains apart from BET family members Brd2 BD1, Brd3 BD1, and Brd4 BD1, with ΔT_m between 1 and 2 °C. Evidence of cellular target engagement was obtained using a FRAP assay, in which **1.036** was shown to disrupt the CREBBP bromodomain-chromatin complex in HeLa cells. Moving forward, compound **1.036**

was tested in cells in order to investigate its effect on the CREBBP bromodomain-p53 interaction. Compound **1.036** inhibited doxorubicin induced p53 activity with an IC_{50} value of 1.5 μ M, as determined by a luciferase reporter assay for p53 induction. Limited PK studies were then conducted to understand the utility of **1.036** as an *in vivo* probe. In a human liver microsome stability assay, no compound was detected after 1 hour, suggesting rapid metabolism. Although **1.036** may not be suitable as an *in vivo* tool, this compound is likely to be valuable in understanding the biological function of both CREBBP and EP300 *in vitro*.

Conway and coworkers subsequently reported compound **1.037** as a ligand for the CREBBP bromodomain.¹²⁷ **1.037** displays a K_d value of 390 nM against CREBBP (ITC), with modest selectivity over Brd4 BD1 (K_d : 1.4 μ M). A FRAP assay was used to evaluate **1.037** in a cellular setting. Compound **1.037** was found to displace the CREBBP bromodomain from chromatin in U2OS cells in a dose dependent manner. Although not selective over the BET family, **1.037** is a valuable addition to the CREBBP tool set to help validate this protein as a target for the treatment of disease.

Most recently, Unzue and co-workers reported the development of compound **1.038** as an inhibitor of CREBBP.¹²⁸ Fragment-based docking into the structure of the CREBBP bromodomain was used to identify a start point for ligand discovery. Of the 17 compounds initially selected for *in vitro* validation, the acetyl benzene scaffold was selected for further investigation to deliver a series of CREBBP inhibitors. Compound **1.038** showed the best combination of potency and selectivity with a CREBBP K_d value of 2.0 μ M and Brd4 BD1 K_d value of >50 μ M (ITC). As the authors report that **1.038** shows low cell permeability, its utility as a chemical probe is limited. This is most likely due to the charged nature of the carboxylic acid moiety at physiological pH.

Although there has been significant progress towards a CREBBP chemical probe from multiple groups, there has yet to be a potent and selective molecule developed. Given the high sequence homology with the BET family of bromodomains, it is unsurprising that the molecules identified to date do not show appropriate selectivity over this family. Therefore, future work in this area should focus on the development of an appropriate selectivity profile to aid investigations into the precise role of the CREBBP bromodomain.

1.5.3.7 PCAF

Zhou and co-workers were the first to report a small molecule ligand for a bromodomain, namely PCAF.¹²⁹ This group showed that the bromodomain of PCAF binds specifically to KAc50 of the HIV-Tat protein complex, a critical interaction for viral replication.¹³⁰ Moving forward, NMR screening was used to discover small molecule inhibitors of this interaction. These efforts led to the discovery of several inhibitors including compound **1.039 (Figure 20)**, which displays an IC₅₀ value of 1.6 μM against PCAF (peptide competition assay). Despite efforts to optimise compound **1.039**, no increase in potency was reported.

1.5.3.8 SMARCA4

SMARCA4 is part of the SNF/SWI complex, which plays a key role in chromatin remodelling and transcription control. Loss of function of SMARCA4 and other components of SWI/SNF has been linked to cancer development.¹³¹ PFI-3 (**1.040**) is an inhibitor for the bromodomain of SMARCA4 developed by Pfizer in collaboration with the SGC (**Figure 20**).^{132,133} This novel chemotype shows K_d values of 89 nM against SMARCA4, as well as 48 nM against the homologous PB1(5) bromodomain (ITC), as reported on the SGC website. Broader bromodomain selectivity was assessed by thermal shift with binding confirmed at SMARCA4 (ΔT_m : 5.1), SMARCA2 (ΔT_m : 6.4) and PB1 BD5 (ΔT_m : 7.5). No interaction was observed with PB1(BD2–4), and there was no cross-reactivity in a panel of 36 kinases. X-ray crystallography of PFI-3 (**1.040**) has not yet been reported, therefore, the precise binding mode of the molecule remains unknown. However, it is believed that the vinylogous amide moiety may act as the KAc mimetic.

Interestingly, Pfizer and their collaborators recently reported that PFI-3 (**1.040**) has been used to probe the biological function of SMARCA2/4 bromodomains.¹³³ Although PFI-3 (**1.040**) is capable of displacing the SMARCA2 bromodomain from chromatin, it fails to display the antiproliferative phenotype observed through protein knock-down studies. Therefore, this chemical probe approach has invalidated the SMARCA2 bromodomain, and instead, helped to identify the ATPase domain as the relevant therapeutic target. These studies further highlight the power of chemical probes for both target validation and invalidation, particularly in combination with protein knock-down experiments.

1.5.3.9 Others

There are a growing number of inhibitors that are broadly selective, showing activity against a small number of bromodomains. For example, Bradner and coworkers used fluororous tagged multi-component reactions to develop a library of 3,5-dimethylisoxazole containing bromodomain inhibitors.¹³⁴ Subsequent optimization of the scaffold delivered lead compound **1.041**, which binds to Brd4 BD1 with a K_d value of 550 nM as determined by ITC (**Figure 20**). Broader bromodomain screening by means of BROMOscan¹²¹ confirmed binding to Brd4 (K_d : 80 nM) but revealed activity against TAF1 BD2 (K_d : 560 nM) and TAF1L BD2 (K_d : 1.3 μ M). Although the binding to TAF1 BD2 is relatively weak, compound **1.041** could represent a starting point for the development of a selective TAF1 chemical probe.

The SGC have reported benzimidazolone **1.042** as an inhibitor of BRPF1B/2 and TRIM24 (**Figure 20**).¹³⁵ In order to develop a TRIM24 specific inhibitor, commercially available 1,3-benzimidazolone compounds were tested using AlphaScreen technology. Several compounds were identified to be active against TRIM24 but were also active against BRPF1B/2. Subsequently, the template was modified to deliver compound **1.042**, which shows a K_d value of 222 and 137 nM against TRIM24 and BRPF1B respectively (ITC). Thermal shift technology was used to evaluate the selectivity of compound **1.042**. In a panel of 45 bromodomains, significant shifts were observed for BRPF1B/2 and TRIM24, supporting the ITC data generated. Cellular activity was determined using a FRAP assay in which **1.042** displaced full-length TRIM24 from chromatin.

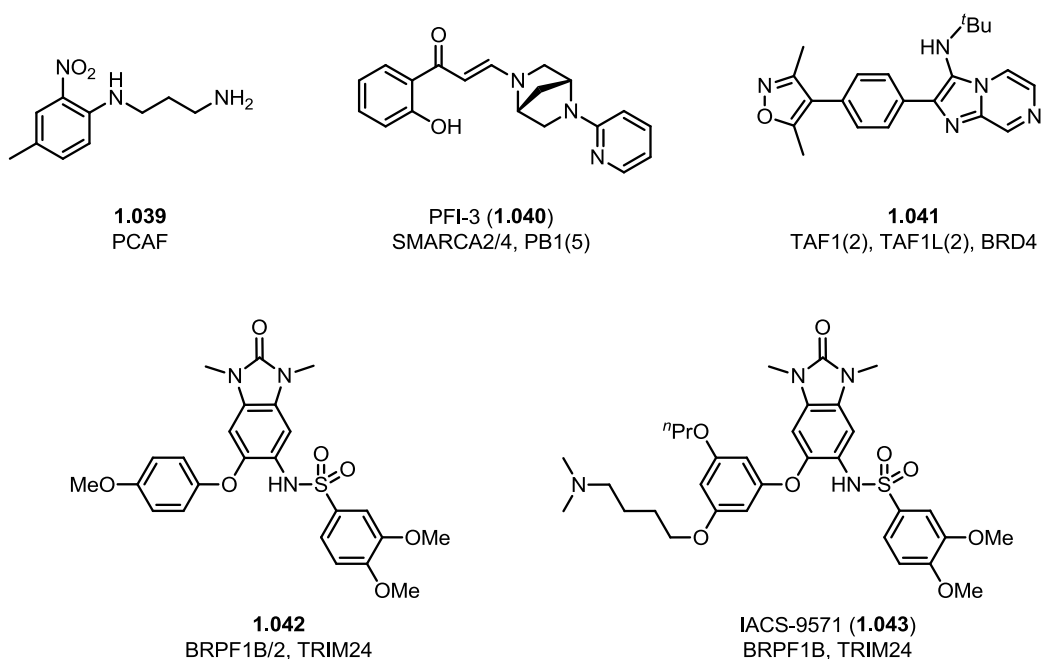


Figure 20: Chemical structures for selected non-BET bromodomain inhibitors.

Independently, Palmer and co-workers used a structure guided approach to develop compound **1.043** as a TRIM24 inhibitor.¹³⁶ Like the SGC, their aim was to develop a selective TRIM24 inhibitor by first intent. To this end, three hit identification approaches were explored: virtual *in silico* high-throughput screening (HTS), construction of a focused KAc mimetic library, and a traditional small molecule HTS. Three different chemotypes were indentified, but the benzimidazolone template was selected for further optimisation. SAR evaluation around this core provided IACS-9571 (**1.043**), which showed a TRIM24 IC₅₀ value of 7.6 nM (AlphaScreen). BROMOscan¹²¹ technology was used to investigate broader selectivity against 32 bromodomains. Results from this screen indicated off target activity against the BRPF family and subsequent dose-response determinations demonstrated **1.043** to be a dual TRIM24/BRPF1B inhibitor (K_d: 1.3/2.1 nM), with 9 and 21 fold selectivity over BRPF2 and BRPF3 respectively. Compound **1.043** displays greater than 7700 fold selectivity versus Brd4 BD1/2 relative to TRIM24. Moving forward, compound **1.043** was progressed to understand its utility as an *in vivo* tool in rodent. After IV administration of a 1 mg/kg dose in female CD1 mice, moderate clearance (43 mL/min/kg) was observed and terminal half-life was 0.7 h. After oral dosing of 10 mg/kg, bioavailability of **1.043** was 29%, suggesting that this molecule could be useful for *in vivo* studies.

1.5.3.10 Summary

Although each of the ligands discovered for the non-BET bromodomains are hugely important, only two compounds, albeit with the same chemotype (**1.032** and **1.033a**, **Figure 19**) are selective for a single bromodomain. Therefore, linking inhibition of a particular bromodomain to a given phenotype would be extremely challenging. Consequently, development of non-BET family chemical probes, which selectively target a single bromodomain remains important in order to validate these proteins as therapeutic targets. Of the non-BET chemical probes discussed, only GSK2801 (**1.024a**), BAZ-ICR (**1.025**) and IACS-9571 (**1.043**) are reported to be suitable for use as *in vivo* tools. It is not clear whether the other inhibitors reported would be suitable for *in vivo* experiments, which may highlight a limitation in the discoveries made to date. Therefore, future effort should be placed on the development of *in vivo* tools to fully understand the role of bromodomains in preclinical models, to provide further insight into their function in human disease.

1.6 Aims

Considering the biological implications of the bromodomains which have been successfully investigated to date, there is now convincing rationale for using small molecule chemical probes to help validate bromodomains as therapeutic targets. However, despite the important advances within the BET family, the pharmacological potential of the remaining families is far less explored, leaving a vast area of research yet to be investigated. As non-BET bromodomains have been implicated in various diseases such as cancer and HIV, the identification of high quality chemical probes could serve as a start point towards the development of a novel class of therapeutics.

The aim of this PhD research was to develop high quality chemical probes for non-BET bromodomains Brd9 and TAF1 BD2. Inspired by Bunnage and co-workers,⁷⁷ we envisaged these probe molecules would satisfy the following criteria:

1. $pIC_{50} \geq 7$ against the target of interest.
2. ≥ 100 fold selectivity over the BET family of bromodomains, given the profound biology associated with these proteins (Brd4 will be used as a representative member of the family).
3. ≥ 30 fold selectivity over other non-BET bromodomains.

4. ≥ 100 fold selectivity over broader pharmacological targets outside of the bromodomain family.
5. Evidence of cellular target engagement.

The specific details regarding probe development for Brd9 and TAF1 BD2 will be discussed in turn.

2 The development of I-BRD9, a chemical probe for Brd9

2.1 Introduction

2.1.1 Identification of Brd9 as a novel bromodomain target

At the outset of this project, there were no Brd9 chemical probes reported in the literature. Therefore, the development of a high quality chemical probe for this bromodomain was deemed essential in order to delineate its function within human disease.

The current GSK BET-family selective probes, I-BET762 (**1.006a**)⁴⁷ and I-BET151 (**1.010**)⁹¹ target all 8 bromodomains of this family (Section 1.5.2, pages 16–18). Therefore, significant resource within our laboratories has been placed on narrowing this profile from 8 bromodomains to 4, to investigate whether more selective inhibition delivers a different phenotype. To this end, each domain selective programme aims to target either BD1 or BD2 of the BET family. Thieno-pyridinone (TP) compound **2.001** was identified as part of the BD1 domain selective project (**Figure 21**).¹³⁷ As there is very little selectivity shown amongst the individual BET proteins, this molecule is termed a pan-BD1 inhibitor.

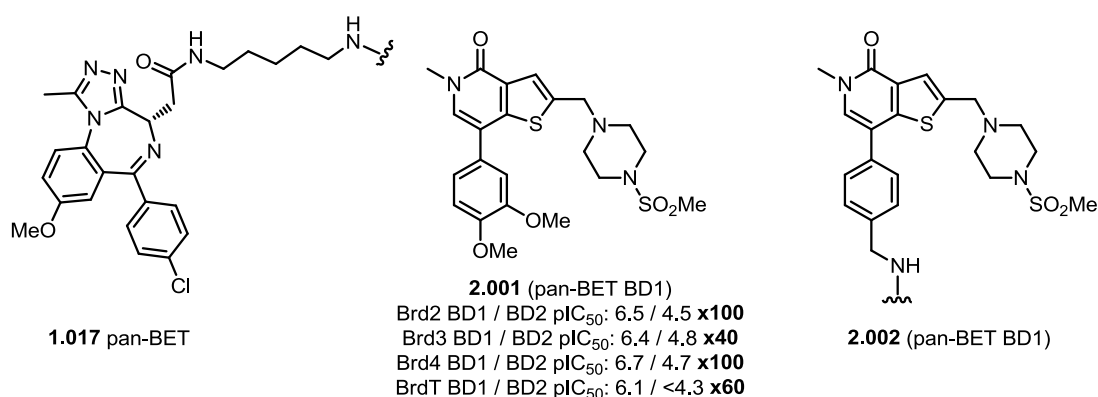


Figure 21: Chemical structures of compounds 1.017 and 2.002, which were attached to a solid-support for use in a chemoproteomics experiment; BET bromodomain pIC₅₀ values for pan BD1 compound 2.001,¹³⁸ as determined by TR-FRET analysis. Data are n≥3.

In order to determine whether or not a pan-BD1 inhibitor was capable of delivering a different phenotype to a pan-BET molecule, a chemoproteomics experiment was utilised¹³⁹ (as discussed in Section 1.5.2, page 19 and **Figure 22**).

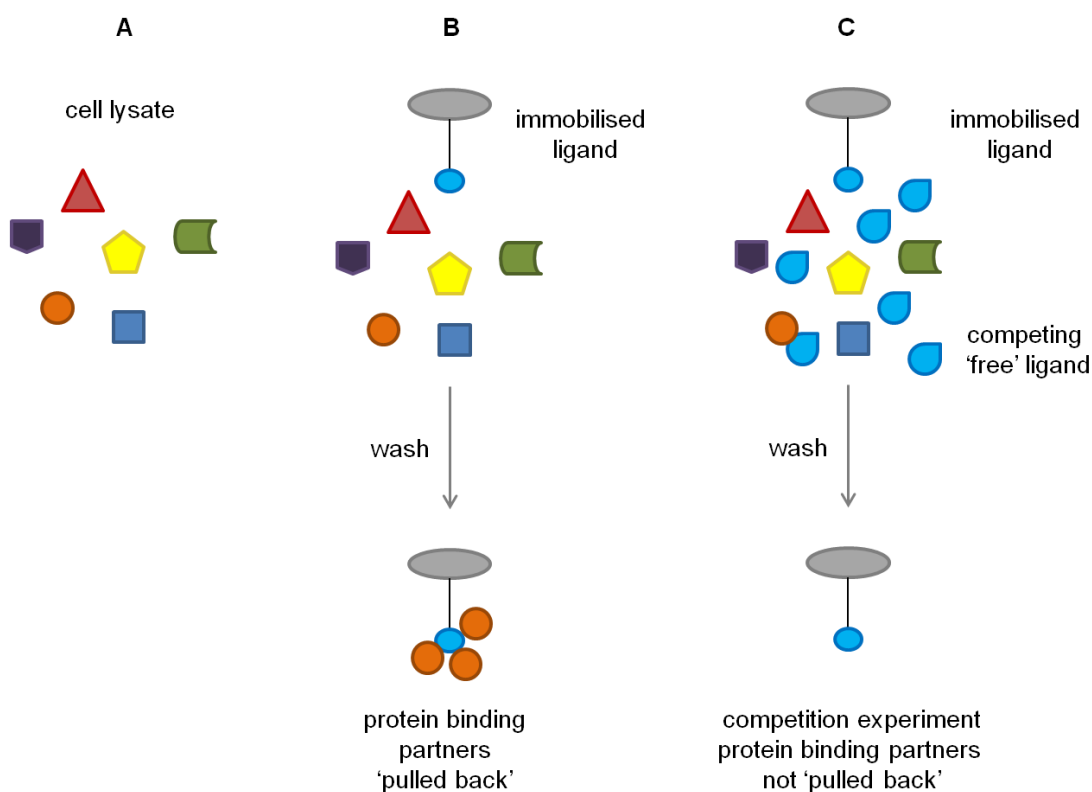


Figure 22: (A) Cell lysate containing possible protein targets; (B) The immobilised ligand is incubated with the cell lysate. The target proteins are identified after the un-complexed proteins are washed away; (C) A competing 'free ligand' is pre-incubated with the cell lysate. The binding sites of the target proteins are blocked by the 'free compound' so they cannot interact with the immobilised molecule. The target proteins are removed on washing and is absent from analysis.

These investigations aimed to investigate the potential protein binding partners of I-BET762 (**1.006a**) and compound **2.001** in leukemic cell line, HL-60. Initially, a linkable version of I-BET762 (**1.006a**) was immobilised on to a solid-support (compound **1.017**, **Figure 21**). Incubation of immobilised **1.017** with the cell lysate followed by analysis of the proteins, which were 'pulled back', indicated that Brd2, Brd3 and Brd4 were the preferred binding partners, as determined by mass spectrometry (**Figure 22B**). The remaining member of the BET family, BrdT was not detected as it is not expressed in HL-60 cells. Although **Figure 22** depicts few protein binding partners being 'pulled back', it is likely that other proteins would form part of this complex, *via* an association with the BET proteins. In order to confirm the BET family as binding partners for I-BET762 (**1.006a**), a competition experiment was conducted. In this case, HL-60 cell lysate was pre-incubated with 'free' I-BET762 (**1.006a**), allowing it to bind to particular proteins. As such, the active sites of these proteins were blocked and therefore not 'pulled back' upon treatment with compound **1.017** (**Figure 22C**). Indeed, Brd2, Brd3 and Brd4 were competed away

with **1.006a**, indicating that the BET family of bromodomains were the preferred protein targets.

Following these results, an identical experiment was conducted, this time, with pan-BD1-inhibitor, **2.002** immobilised onto a solid-support. Analysis of the binding partners which were 'pulled back' indicated that other proteins, as well as the BET family were present. This collection of proteins included Brd9, suggesting that pan-BD1 compound **2.002** was associated with this protein. To confirm these proteins as binding partners, a competition experiment was conducted. HL-60 cell lysate was pre-incubated with pan-BD1 inhibitor, **2.001**, as described previously. The BET family of bromodomains and Brd9 were not 'pulled back' upon treatment with immobilised **2.002**, suggesting that they were interacting with compound **2.001**.

Importantly, I-BET762 (**1.006a**) and compound **2.001** showed different binding profiles as only **2.001** was associated with Brd9. However, at this stage, it was not clear how compound **2.001** interacted with this bromodomain. It was hypothesised that this could be *via* a direct interaction with the bromodomain or through complexation with the BET family. In order to investigate the former, a TR-FRET assay was enabled, utilising Brd9 protein truncate. Results from this experiment confirmed direct Brd9 bromodomain binding by pan-BET BD1 inhibitor, **2.001**, with a pIC₅₀ value of 6.6.

2.1.2 Compound screening in Brd9

2.1.2.1 TR-FRET assay

As compound **2.001** was found to bind to Brd9 directly, other compounds from this series were profiled by colleagues in the bromodomains of Brd9 and Brd4 (BD1/2). This was achieved by means of TR-FRET, a competitive displacement assay which relies on the energy transfer between donor and acceptor molecules. In this case, a fluoroligand of known binding affinity interacts with the bromodomain, forming the acceptor species. To detect this interaction, the His-tagged bromodomain recognises an anti-His tagged europium chelate complex, which acts as the donor in the FRET pair. The binding of the fluoroligand to the bromodomain is detected upon laser excitation of the europium. This causes an energy transfer from the donor to the acceptor, leading to emission of light. However, when a competing ligand is introduced, this can potentially inhibit the bromodomain-fluoroligand interaction, leading to a decrease in luminescence. The amount of luminescence produced is

measured by a detector to quantify the strength of binding (**Figure 23**; for full details see Appendix 5.1).

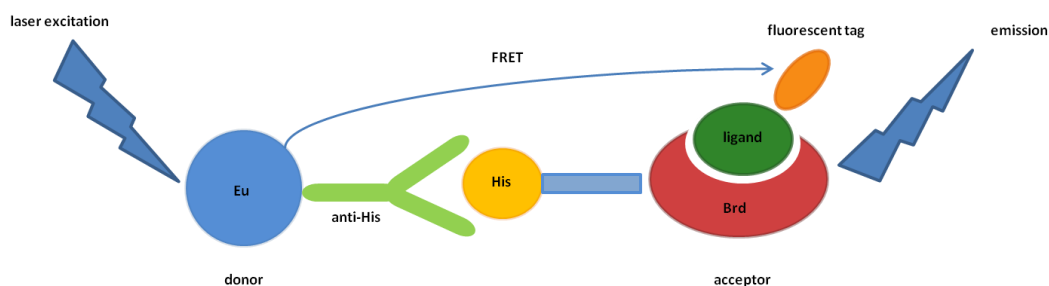


Figure 23: Schematic representation of a TR-FRET assay.

Typically, these measurements of binding are quoted as IC_{50} values, defined as the half maximal inhibitory concentration. This value specifies the concentration of competing ligand required to reduce fluorescence by 50%, indicating displacement of the fluoroligand. When calculated from a competition binding assay, the biological target is exposed to the competing ligand at a variety of concentrations, whilst the concentration of fluoroligand is kept constant. Typically, measurements are recorded between a set of controls in which: (i) the competing ligand is absent; and (ii) a standard ligand of known binding affinity is present at a single concentration, representing 100% displacement of the fluoroligand. Analysis of the resulting dose-response curve allows the concentration at which the competing ligand displaces 50% of the fluoroligand to be identified (**Figure 24**, example curve). This value is the IC_{50} , and is often converted to pIC_{50} , the equivalent on a negative logarithmic scale [$IC_{50} = -\log(pIC_{50})$].

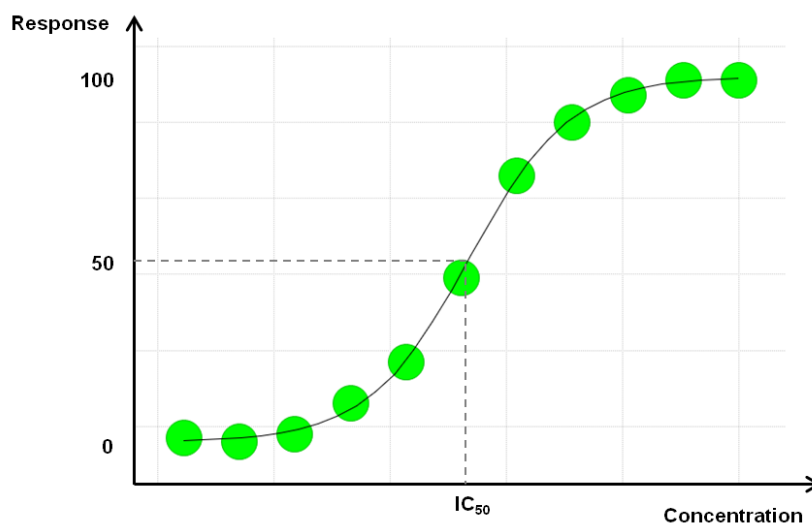


Figure 24: Example dose-response curve from which an IC_{50} value can be calculated.

As discussed above, an IC_{50} value represents the concentration of test compound required to displace 50% of the fluoroligand. In contrast, the K_i value is the concentration of competing ligand, which would occupy 50% of the receptors if no fluoroligand were present. Unlike IC_{50} values, K_i is absolute and can be calculated using the Cheng-Prusoff equation (**Equation 1**).¹⁴⁰

$$K_i = IC_{50} / [1 + ([L]/K_d)]$$

[L] = concentration of fluoroligand used in the assay, K_d = dissociation constant of the fluoroligand for the receptor.

Equation 1: Cheng-Prusoff equation.

In the case of Brd9 and Brd4 TR-FRET assays, the concentration of the fluoroligands is K_d , the concentration at which, at equilibrium, 50% of protein receptor sites are occupied (**Figure 25**).

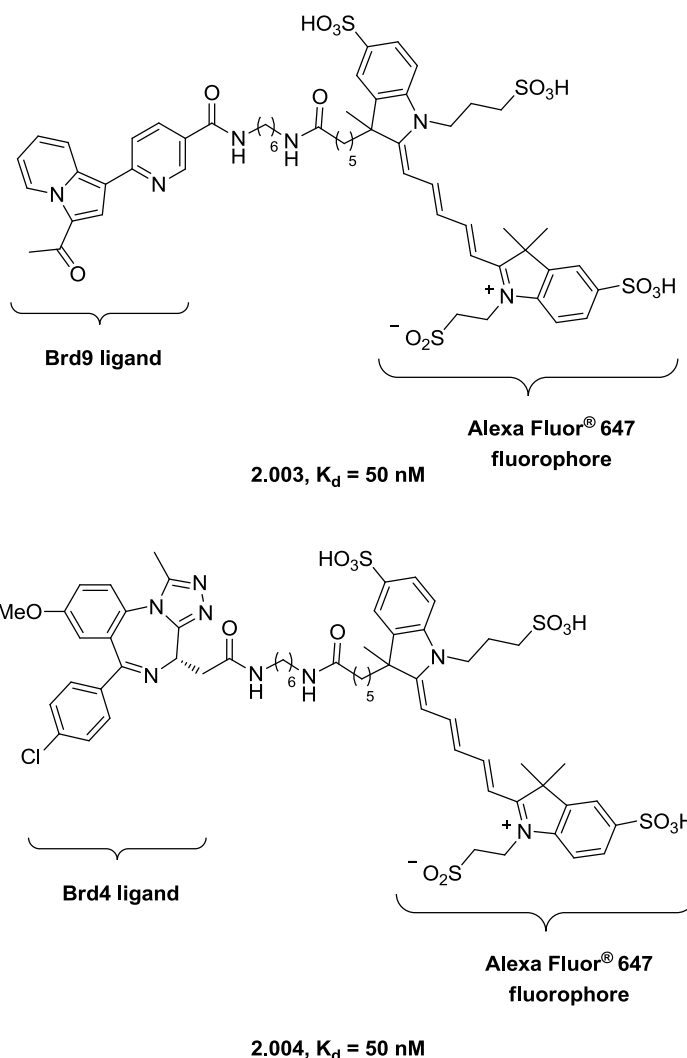


Figure 25: Chemical structures of Brd9 and Brd4 TR-FRET assay fluoroligands 2.003 and 2.004, respectively.

As the concentration of the fluoroligand in both Brd9 and Brd4 assays is K_d , the pIC_{50} values generated can be compared directly. This can be rationalised using the Cheng-Prusoff equation (**Calculation 1**).¹⁴⁰

$$K_i = IC_{50} / [1 + ([L]/K_d)]$$

[L] = concentration of fluoroligand used in the assay, K_d = dissociation constant of the fluoroligand for the receptor.

$$pK_i = pIC_{50} + \log[1 + ([L]/K_d)]$$

For Brd9:

$$pK_i = pIC_{50} + \log[1 + (50 \text{ nM}/50 \text{ nM})]$$

$$pK_i = pIC_{50} + \log[1 + 1]$$

$$pK_i = pIC_{50} + \log[2]$$

$$pK_i = pIC_{50} + 0.3$$

For Brd4:

$$pK_i = pIC_{50} + \log[1 + (50 \text{ nM}/50 \text{ nM})]$$

$$pK_i = pIC_{50} + \log[1 + 1]$$

$$pK_i = pIC_{50} + \log[2]$$

$$pK_i = pIC_{50} + 0.3$$

Calculation 1: Cheng-Prusoff equation applied to Brd9 and Brd4 TR-FRET assays.

However, not all assays use fluoroligands at their K_d values. For example, if the K_d of a ligand is high then the assay may be conducted below this value in order to save reagent; or, if there is limited signal from the fluoroligand, the assay may be run above K_d to increase luminescence. Therefore, in order to compare the binding affinities of a particular compound in two different assays, the inhibition constant, K_i must be used. For example, K_i values are used to compare the results from the Brd9 and Brd7 assays, as the Brd7 experiment is run below K_d . This can be rationalised using the Cheng-Prusoff equation (**Calculation 2**).¹⁴⁰

$$K_i = IC_{50} / [1 + ([L]/K_d)]$$

[L] = concentration of fluoroligand used in the assay, K_d = dissociation constant of the fluoroligand for the receptor.

$$pK_i = pIC_{50} + \log[1 + ([L]/K_d)]$$

For Brd9:

$$pK_i = pIC_{50} + \log[1 + (50 \text{ nM}/50 \text{ nM})]$$

$$pK_i = pIC_{50} + \log[1 + 1]$$

$$pK_i = pIC_{50} + \log[2]$$

$$pK_i = pIC_{50} + 0.3$$

For Brd7:

$$pK_i = pIC_{50} + \log[1 + (100 \text{ nM}/400 \text{ nM})]$$

$$pK_i = pIC_{50} + \log[1 + 1/4]$$

$$pK_i = pIC_{50} + \log[1.25]$$

$$pK_i = pIC_{50} + 0.1$$

Calculation 2: Cheng-Prusoff equation applied to Brd9 and Brd7 assays.

Selectivity for the bromodomain Brd9 over BrdX (bromodomain of choice) is calculated using **Equation 2**.

$$\text{Fold Selectivity for Brd9} = 10^{(\text{pKi Brd9} - \text{pKi BrdX})}$$

Equation 2: Fold selectivity for Brd9 over BrdX.

Importantly, fluoroligand **2.004** (**Figure 25**) binds to both bromodomains of Brd4 with equal affinity. Therefore, in order to measure the binding affinity of a test compound against a single bromodomain, a mutated version of the protein is used. For example, for determination of ligand binding at BD1, the BD2 bromodomain is mutated causing **2.004** to display 1000 fold selectivity for BD1.

2.1.2.2 Compound profiling in Brd9 and Brd4

In addition to the compounds from the TP template, a second series, originally designed for the PCAF programme were tested by colleagues as part of a cross screening strategy to identify potential off target liabilities.¹⁴¹ In total, 246 compounds were screened in the bromodomains of Brd9 and Brd4. Selectivity over the BET bromodomains was considered, with Brd4 used as a representative member of the family. The results from this initial cross-screen are displayed in **Figure 26**. The line of unity in the centre of the plot indicates which compounds are equipotent in both Brd9 and Brd4 BD1. The dashed lines on either side represent 10 fold selectivity for Brd4 BD1 and Brd9 at the top and bottom, respectively. The Amino-Pyridazine (AP) series, identified from the PCAF programme, is shown in red and the TP series, from the BET BD1 domain selective programme, in blue.

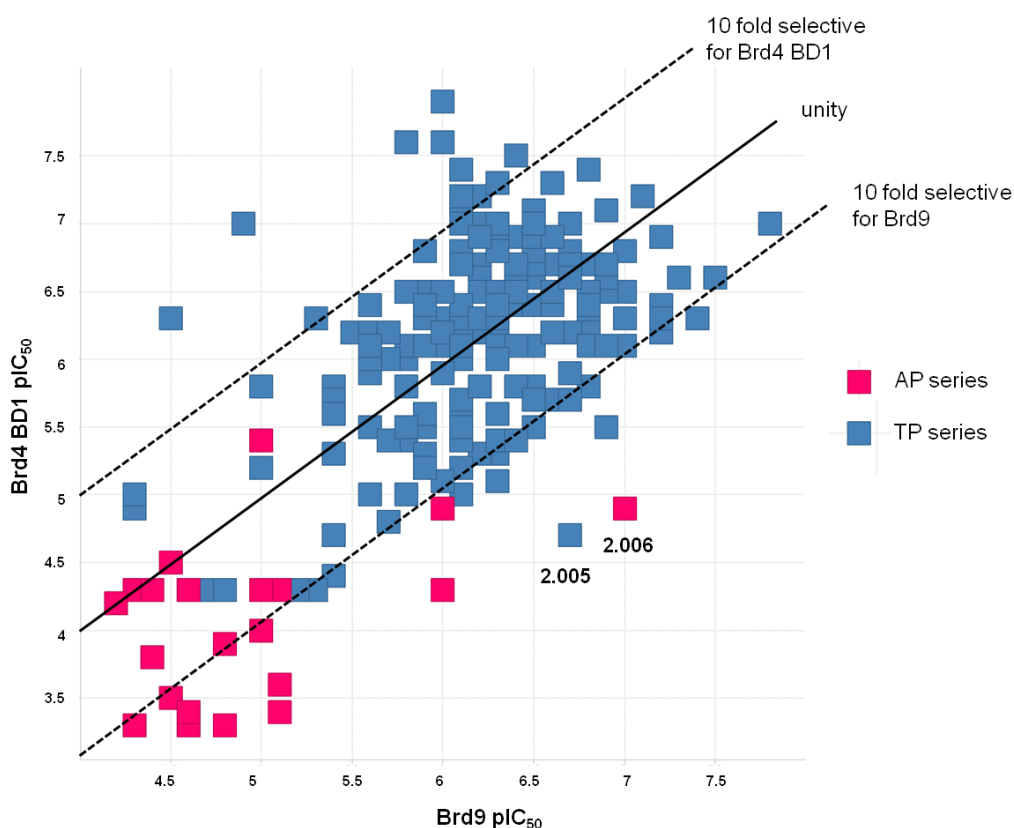


Figure 26: Graphical representation of the data for the 246 compounds screened in Brd9 and Brd4 BD1 (TR-FRET). The AP series is highlighted in red and the TP in blue. Brd9 pIC_{50} values are represented on the x-axis and Brd4 BD1 on the y-axis.

Results from this compound screen led to identification of two chemically distinct chemotypes, as potent and selective inhibitors of Brd9. These compounds showed good Brd9 potency and ligand efficiency, as well as acceptable selectivity over the bromodomains of Brd4 (**Figure 27**).

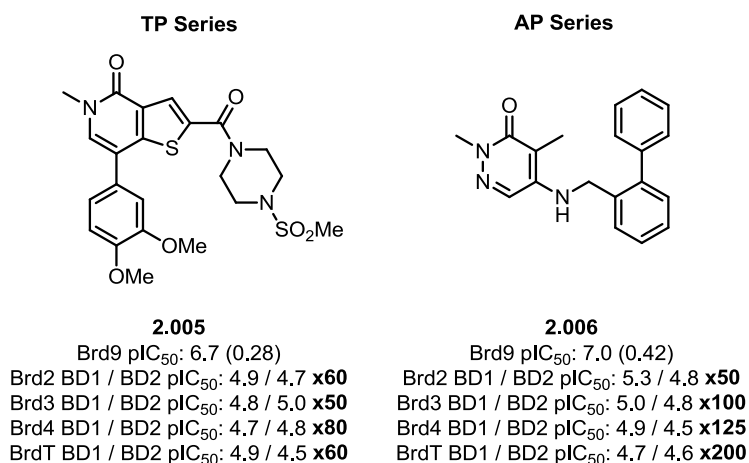


Figure 27: pIC_{50} values for compounds 2.005¹⁴² and 2.006¹⁴³ in the bromodomains of the BET family and Brd9 (TR-FRET). Brd9 ligand efficiency values are shown in parentheses. Selectivity over the BET family of bromodomains is calculated relative to the maximum value. Data are $n \geq 2$.

Compound **2.005** showed good Brd9 activity with a pIC_{50} value of 6.7 and 80 fold selectivity over Brd4. Similarly, compound **2.006** from the AP series showed a Brd9 pIC_{50} value of 7.0, with 125 fold selectivity window over Brd4. Moving forward with these encouraging results, further investigations were conducted to probe the potential of the TP series to deliver a Brd9 selective chemical probe. Follow up investigations on the AP series were prosecuted by colleagues, primarily *via* outsourcing.

2.1.2.3 Further profiling of compound 2.005

Further profiling of compound **2.005** was conducted by colleagues in order to confirm direct Brd9 binding. These experiments provided an orthogonal determination of ligand-bromodomain binding to investigate a potential correlation with the TR-FRET data. Initially, compound **2.005** was tested in a thermal shift experiment,¹⁴⁴ using a Brd9 protein truncate (see Appendix 5.2 for details). Results from this assay showed a Brd9 ΔT_m : 10.4 °C, with no significant shifts seen for Brd4 BD1/2, PCAF or ATAD2. Although not a quantitative method, these results suggest that **2.005** may show some selectivity over the bromodomains of PCAF, ATAD2, and Brd4. These data provided good evidence for Brd9 specific binding, providing further confidence in the data generated by the TR-FRET assay (**Figure 28**).

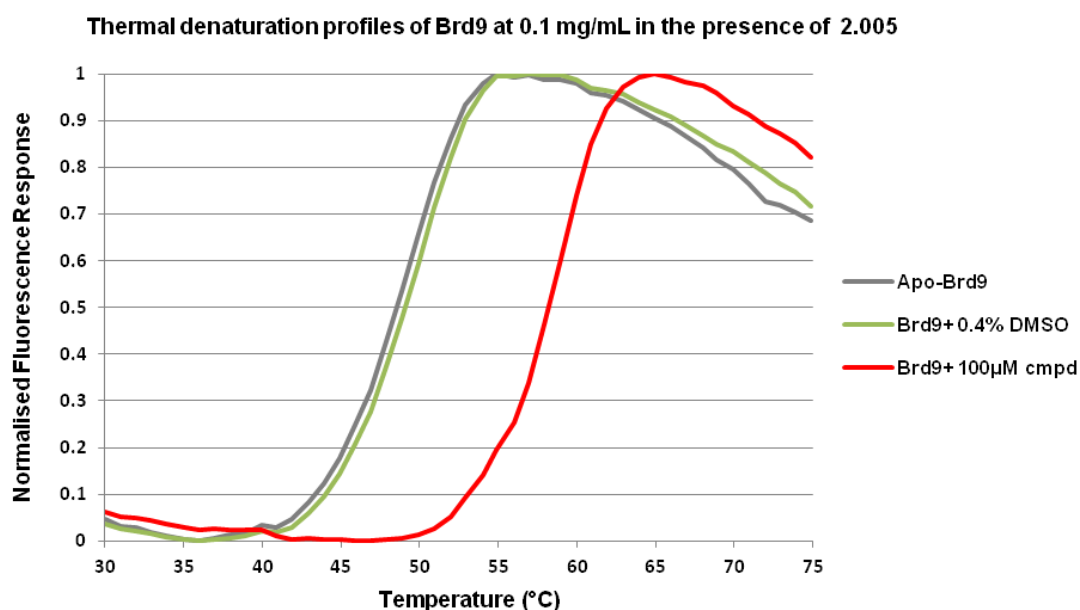


Figure 28: Thermal shift results for compound 2.005 against Brd9.

Further investigations into the thermodynamics of ligand interactions were conducted in the form of ITC.¹⁴⁴ More specifically, this experiment provided an evaluation of the Gibbs free energy change (ΔG) and its components: ΔH , the

change in enthalpy; ΔS , the change in entropy; and K_d , the dissociation constant (Equation 3).

$$\Delta G = \Delta H - T\Delta S$$

$$\Delta G = -RT\ln K_d$$

Equation 3: Definition of Gibbs free energy (ΔG).

The enthalpy change, ΔH represents the net change in the number and/or strength of non-covalent bonds moving from the free to bound state; and ΔS represents the change in entropy upon ligand binding, accounting for solvation effects, as well as changes in conformational degrees of freedom.¹⁴⁵ These studies provided a third, orthogonal determination of ligand-protein binding, building confidence in the data generated by both the TR-FRET and thermal shift assays. Pleasingly, compound **2.005** showed a Brd9 pK_d : 6.9, correlating well with pIC_{50} : 6.7, as determined by TR-FRET (Table 1, see Appendix 5.3 for further details).

Compound	ITC pK_d	TR-FRET pIC_{50}	ΔH	ΔS
2.005	6.9	6.7	-6738 cal/mol	8.23 cal/mol/deg

Table 1: TR-FRET and ITC data for compound **2.005** in the bromodomain of Brd9.

Despite encouraging results for Brd9 bromodomain binding, there was still no evidence to suggest that compound **2.005** targeted the Brd9 protein in a cellular environment. As TR-FRET, thermal shift and ITC use truncated Brd9 with only the bromodomain present, they do not assess the ability of the compound to bind to endogenous protein. Therefore, a chemoproteomics experiment was conducted by colleagues to assess binding to full length Brd9.¹³⁹ In this case, several compounds known to bind to a variety of bromodomains were immobilised onto solid-supports, including pan-BET BD1 compound **2.002**, BAZ2B ligand **2.007** and a mixture of synthetic histone tails, each containing KAc. Although the bromodomain binding affinity of the synthetic peptides was weaker than the ligands, they were included to provide a potential binding partner for bromodomains that were not known to interact with **2.002** or **2.007** (Figure 29). Given that the KAc-bromodomain interaction is inherently weak,^{29,34} synthetic ligands are often used in displacement assays.

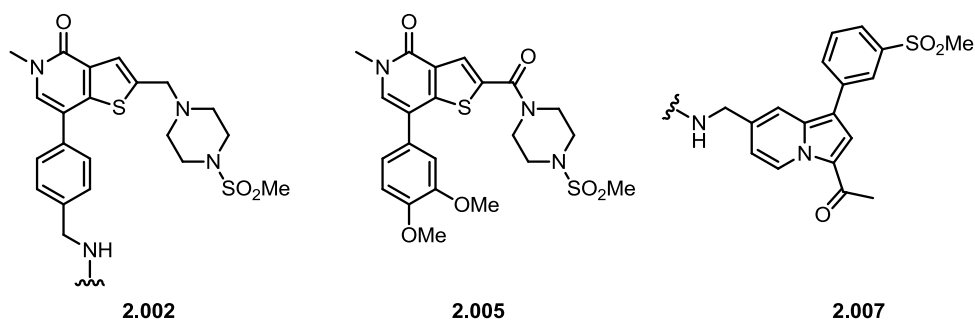


Figure 29: Chemical structures for compounds 2.002, 2.005 and 2.007. Compounds 2.002 and 2.007 were attached to a solid-support via an amine linker for use in a chemoproteomics experiment.

Initially, the synthetic histone combination and immobilised compounds **2.002** and **2.007** were incubated with T-cell lymphoma and leukaemia cell lysate, HUT-78. Following ‘pull-back’ of these compounds and extensive washing, the proteins which were bound were analysed by mass spectrometry. In a separate experiment, compound **2.005** was pre-incubated with the cell lysate, allowing it to interact with its preferred protein binding partners, thereby blocking their binding sites. The cell lysate was then treated with immobilised compounds **2.002**, **2.007** and the synthetic histone combination. Upon ‘pull-back’ and washing, only the proteins which were bound to the immobilised compounds were removed, leaving compound **2.005** and its protein binding partners behind. Comparison of the proteins bound to the immobilised compounds in the presence and absence of compound **2.005** revealed the protein binding partners. This was experiment was performed by dose-response to give pK_d values (**Figure 30**).

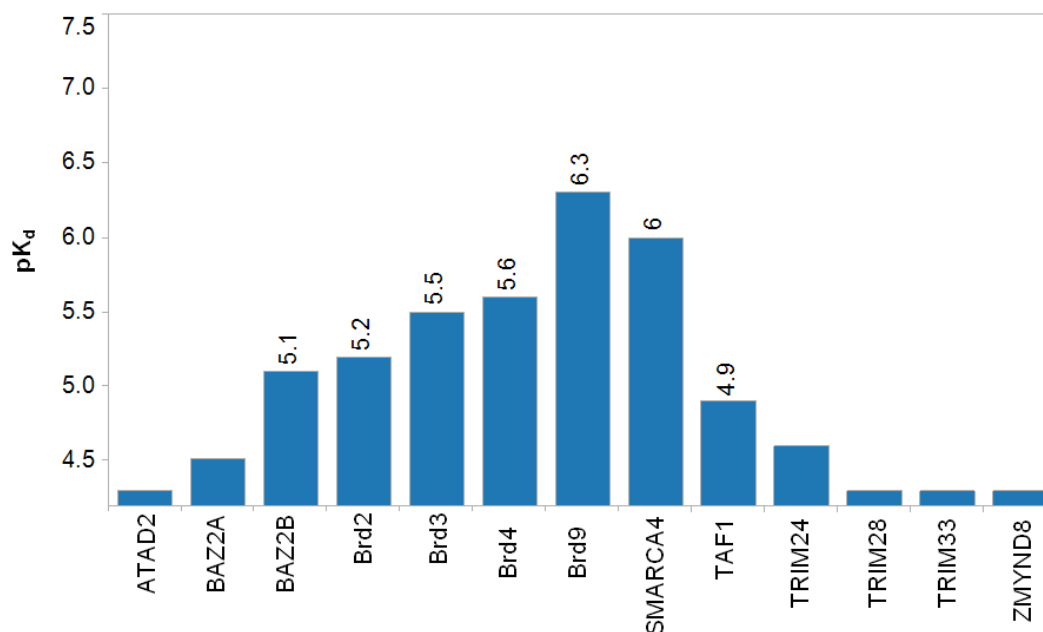


Figure 30: Chemoproteomics results for compound 2.005, showing associated bromodomains.

It is important to note that proteins which were not identified by an association with **2.005** may still be potential binding partners. Some bromodomains may not be expressed in this cell line or their relative concentration may be too low to detect. Pleasingly, the highest affinity association detected was with Brd9 (pK_d : 6.3), indicating that compound **2.005** interacted with the endogenous form of the protein. However, significant binding was also seen to the BET family (Brd4 pK_d : 5.6), and SMARCA4 (pK_d : 6.0), suggesting a lack of selectivity. These results provide no indication of how a particular BCP interacts with a ligand, only that they are associated in some way. Therefore, these proteins could have interacted with compound **2.005** *via* a direct binding, or through complexation to known partner, Brd9. It is reported that both Brd9 and SMARCA4 are components of the chromatin remodelling SWI/SNF BAF complex,^{49,50,51} suggesting that SMARCA4 could be associated with Brd9 rather than *via* a direct interaction with compound **2.005**.

With high affinity binding confirmed to both truncated and full length Brd9, compound **2.005** was progressed for further investigation to assess its utility as a chemical probe. These experiments included a broader pharmacological selectivity screen [enhanced cross screen panel (eXP)], consisting of *in vitro* assays designed to measure the effect of compound **2.005** on various receptor sites, ion channels, transporters and enzymes (**Table 2**).

eXP Targets	Compound 2.005 pIC_{50}
PDE3A	5.1
PDE4B	6.0
PI3Ky	6.0

Table 2: pIC_{50} values for selected pharmacological targets identified in eXP screen.

Several off target effects were identified for compound **2.005** including activity against PDE3A and PDE4B phosphodiesterase enzymes, as well as PI3Ky kinase. These results suggested that the broader pharmacological selectivity of compound **2.005** was poor. Indeed, these results highlighted the promiscuous nature of **2.005**, as the eXP targets are from different families with inherently different binding sites.

Given the importance of exquisite selectivity for high quality chemical probes,⁷⁷ compound **2.005** was considered unsuitable for use. The lack of selectivity shown by compound **2.005** in both the eXP screen and chemoproteomics experiment would make it very difficult to trust any phenotype observed through the use of this compound. In particular, the disconnect observed between the TR-FRET data (80 fold selective for Brd9 over Brd4) and cellular data (5 fold selective for Brd9 over

Brd4) was a cause for concern. Therefore, a medicinal chemistry program was initiated in order to develop a potent and highly selective Brd9 chemical probe.

2.1.3 Physico-chemical property requirements of a chemical probe

When evaluating the potential of a compound as a chemical probe, it is important to consider its physico-chemical properties in line with the recommendations for drug-like molecules. For example, ligand efficiency (LE) is a measurement of the binding energy per non-hydrogen atom to its binding partner. Formally, this value is defined as the negative of the Gibbs free energy of binding per 'heavy' atom.^{146,147,148} With some thermodynamic manipulation this approximately equates to that shown in **Equation 4**.

$$\begin{aligned} \text{LE} &= -\Delta G/\text{HAC} \rightarrow \text{LE} = RT\ln(K_d)/\text{HAC} \rightarrow \text{LE} \approx RT\ln(\text{IC}_{50})/\text{HAC} \\ &\rightarrow \text{LE} = (1.37 \times \text{pIC}_{50})/\text{HAC} \end{aligned}$$

Equation 4: Definition of ligand efficiency.

LE considers both the potency and size of the molecule, and thus enables determination whether or not an initial hit is likely to be optimisable to a potent, drug-like lead. ΔG is the Gibbs free energy of binding, with dissociation constant K_d (or half the maximal inhibitory concentration, IC_{50}), and HAC represents the number of 'heavy' non-hydrogen atoms in the molecule. Typically, this drug-like endpoint is taken to be a molecule that has 36 heavy atoms (corresponding to Lipinski's maximum molecular weight of 500),¹⁴⁹ with a potency of 10 nM. This profile would provide a $\text{LE} = 0.3 \text{ kcal mol}^{-1}$ per heavy atom. Therefore, in general, LE values of 0.3 and above are considered acceptable.

The lipophilicity of a given molecule influences factors such as selectivity, solubility and binding affinity. This measurement can be accounted for by the property forecast index (PFI), the sum of hydrophobicity plus aromatic ring count (**Equation 5**).¹⁵⁰

$$\text{PFI} = \text{ChromLogD}_{7.4} + \text{aromatic ring count}$$

Equation 5: Definition of PFI.

ChromLogD is the effective hydrophobicity of a molecule at a given pH, accounting for its lipophilicity. This property is of paramount importance in drug discovery since compounds which exhibit high *ChromLogD* values can often exhibit a range of associated problems.¹⁵¹ Such issues include reduced aqueous solubility, and poor selectivity, leading to a greater number of off-target interactions.^{152,153} In addition, high plasma protein binding is often observed, meaning there is little of the drug

available to exert its action. The aromatic ring count of a given molecule contributes to lipophilicity, which if high, can be detrimental to the PK profile. It is of note that too much aromatic character provides fewer opportunities to introduce diversity for a given molecular weight and results in a lack of 3-dimensional structure. It is proposed that increased aromatic character can decrease ligand-receptor complementarity, resulting in lower binding affinities.¹⁵⁴ Within our laboratories it has been shown that PFI values of 7 and below are considered optimal and within the recommended guidelines for the design of drug-like molecules (compound **2.005** PFI = 6).

2.1.4 Aims for Brd9 chemical probe discovery

Following the identification of compound **2.005** as a bromodomain binder by colleagues,¹³⁷ the aim of this PhD research was to build upon these findings. More specifically, the aim was to explore the potential of the TP template, to deliver a potent and selective Brd9 chemical probe. As discussed previously (Section 1.6, page 39), the Brd9 chemical probe should satisfy the following criteria:

1. Brd9 pIC₅₀ ≥ 7, as determined by TR-FRET assay.
2. ≥100 fold selectivity over the BET family, Brd4 used as a representative member.
3. ≥30 fold selectivity over other non-BET bromodomains.
4. ≥100 fold selectivity over broader pharmacological targets outside of the bromodomain family, as determined by eXP.
5. Evidence of cellular target engagement.

Since the TP series remained completely unexplored from a Brd9 perspective, this would be achieved through structure driven design, guided, in part, by X-ray crystallography (**Figure 31**).

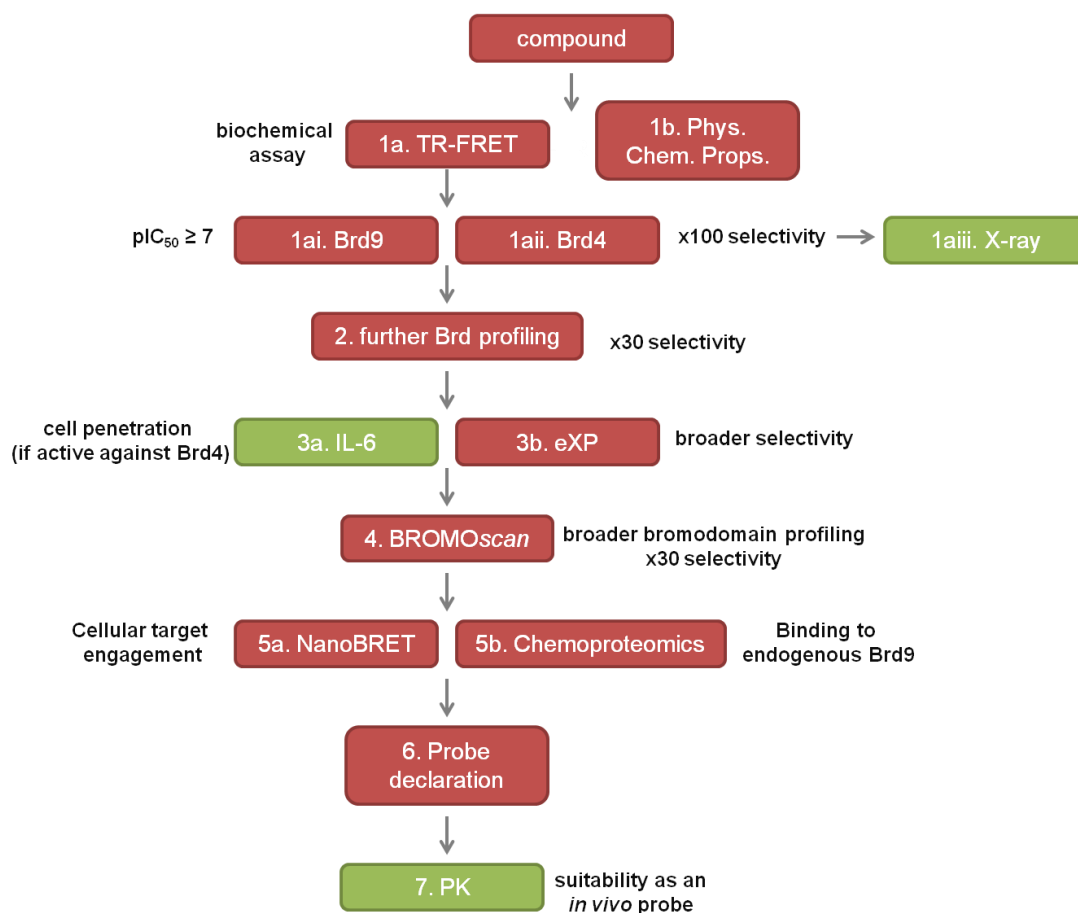


Figure 31: Screening cascade for the development of a Brd9 selective chemical probe. Red boxes indicate critical components on the pathway and green non-critical.

Initially, compounds would be tested in TR-FRET assays to determine Brd9 potency and selectivity over the BET family, using Brd4 as a surrogate (step 1a). Simultaneously, physico-chemical properties such as *ChromLogD*, solubility and permeability would be measured (step 1b). If acceptable potency and BET selectivity were achieved, X-ray crystallography would be used to analyse the binding mode and guide structural modifications to the scaffold (step 1aiii). Following this, the compound would be profiled in non-BET bromodomain assays to understand the broader selectivity (step 2). If the compound displayed ≥ 30 fold selectivity it would be progressed for determination of cellular target engagement (step 3a). Previous work in our laboratories has shown that inhibition of the BET family of bromodomains can lead to inhibition of proinflammatory cytokine production.^{47,88,97,92} Furthermore, it has been reported that there is correlation between inhibition of IL-6 and BET bromodomain activity, as demonstrated for multiple chemotypes. Therefore, as proof of cellular target engagement at Brd4 (given the compound shows Brd4 activity), the compound would be tested for

inhibition of IL-6. For example, compound **2.005** showed IL-6 inhibition with a pIC_{50} value of 4.9, correlating well with its Brd4 BD1 activity ($pIC_{50} = 4.7$).

In parallel, eXP profiling would be conducted to assess broader pharmacological selectivity (step 3b). If these milestones were achieved, the compound would be progressed for further bromodomain profiling by means of BROMOscan (step 4).¹²¹ In this experiment, the compound would be tested against a panel of 34 bromodomains, providing selectivity data across a panel of phylogenetically diverse proteins. If the compound satisfied the 30 fold selectivity criteria as outlined above, it would be progressed for determination of cellular target engagement using a NanoBRET chromatin displacement assay (Step 5a).¹¹⁶ Simultaneously, binding to endogenous Brd9 would be determined by a chemoproteomics experiment conducted by colleagues at Cellzome (Step 5b). If all these criteria were satisfied, the compound would be declared as the Brd9 chemical probe (step 6). Following this, the probe would be progressed for mouse PK studies to determine its suitability as an *in vivo* tool (step 7).

With the Brd9 chemical probe identified, the aim would be to share it with the scientific community through publication of the research, presentations at external conferences and making it available through the SGC. With the compound freely available to the scientific community, the biological effects of Brd9 bromodomain inhibition can be investigated.

2.2 Results and discussion for Brd9 chemical probe discovery

2.2.1 X-ray crystallography of Brd9 and Brd4 BD1

In order to design molecules which displayed selectivity for Brd9 over Brd4, the binding pockets of the respective bromodomains were examined. This was achieved using X-ray crystallography, allowing regions of structural diversity to be identified and therefore exploited in the design of potent and selective compounds (**Table 3**).

	BRD9	BRD4 BD1	
1	GLY43	TRP81	WPF motif
2	PHE44	PRO82	WPF motif
3	PHE45	PHE83	WPF motif
4	ALA46	GLN84	ZA channel
5	PHE47	GLN85	ZA channel
6	PRO48	PRO86	ZA channel
7	VAL49	VAL87	ZA channel
8	THR50	ASP88	ZA loop
9	ASP51	ALA89	ZA loop
10	INS53	LYS91	ZA loop
11	INS53	LEU92	ZA loop
12	ILE53	ASN93	ZA loop
13	ALA54	LEU94	ZA loop
14	TYR57	TYR97	Water-binding Tyr
15	SER58	TYR98	
16	ILE61	ILE101	
17	MET92	MET132	
18	ASN95	ASN135	
19	ALA96	CYS136	Conserved Ala
20	TYR99	TYR139	Conserved Tyr
21	ASN100	ASN140	Conserved Asn
22	THR104	ASP144	
23	VAL105	ASP145	
24	TYR106	ILE146	Gatekeeper
25	TYR107	VAL147	
26	LEU109	MET149	
27	ALA110	ALA150	

Table 3: Sequence similarity for the KAc binding site of the bromodomains of Brd9 and Brd4 BD1. Identical residues are highlighted in green and different in red. Grey boxes represent amino acid insertions.

Most notably, Brd9 and Brd4 BD1 possess different lipophilic shelves, leading to a distinct contrast in the architecture of their ZA channels (**Table 3**, residues 1–7). The respective shelves are defined by 3 amino acid residues, namely Gly43, Phe44 and Phe45 (GFF) in Brd9 and Trp81, Pro82 and Phe83 (WPF) in Brd4 BD1. Numerous studies have shown that interactions with the WPF shelf in Brd4 are important for the binding of synthetic ligands e.g. I-BET762 [**1.006a (Figure 32)**].⁸⁵

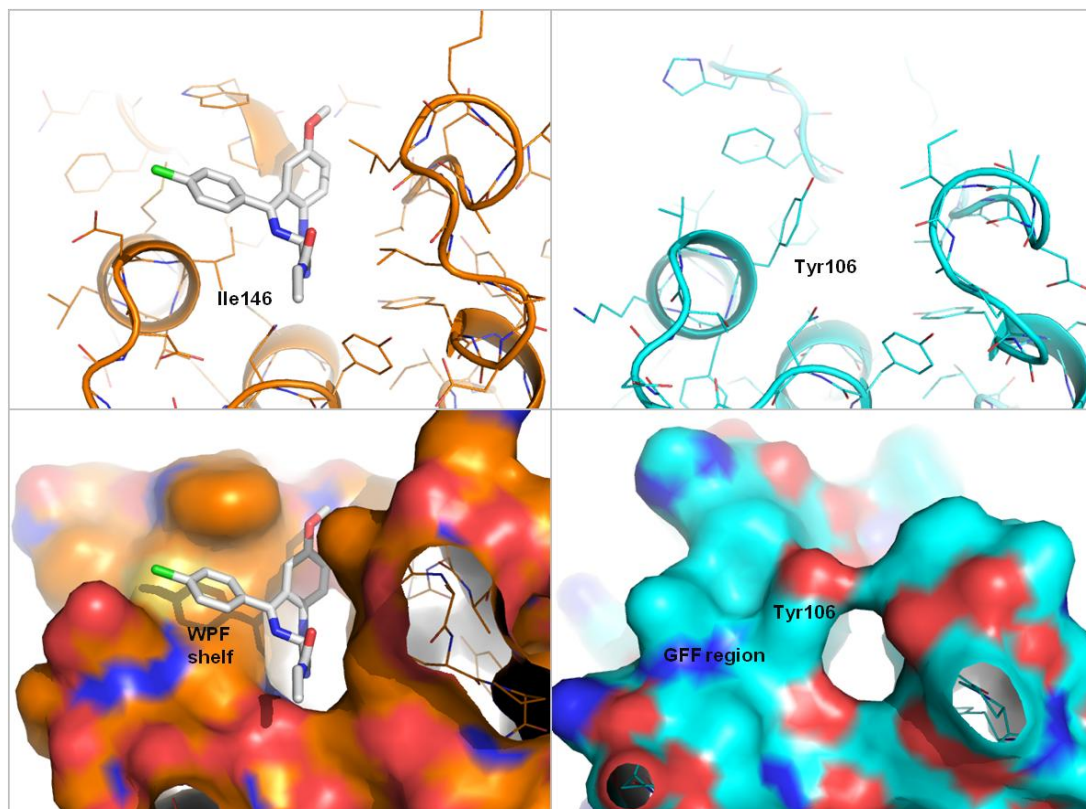


Figure 32: X-Ray crystallography of I-BET762 (1.006a) in complex with the bromodomain of Brd4 BD1 (orange, left, PDB code = 3P50) and apo Brd9 (blue, right).

Importantly, Brd9 and Brd4 possess different gate keeper residues, located towards the entrance of the lipophilic shelf. In Brd9 this corresponds to Tyr106, which completely blocks access to this area of the binding pocket. In contrast, Brd4 BD1 contains a smaller Ile146 gate keeper, leading to greater accessibility to the shelf. X-Ray crystallography of I-BET762 (**1.006a**) modelled in the bromodomain of Brd9 indicates that the phenyl ring which occupies the WPF shelf in Brd4 BD1 would undergo a steric clash with Tyr106 in Brd9 (**Figure 33**).

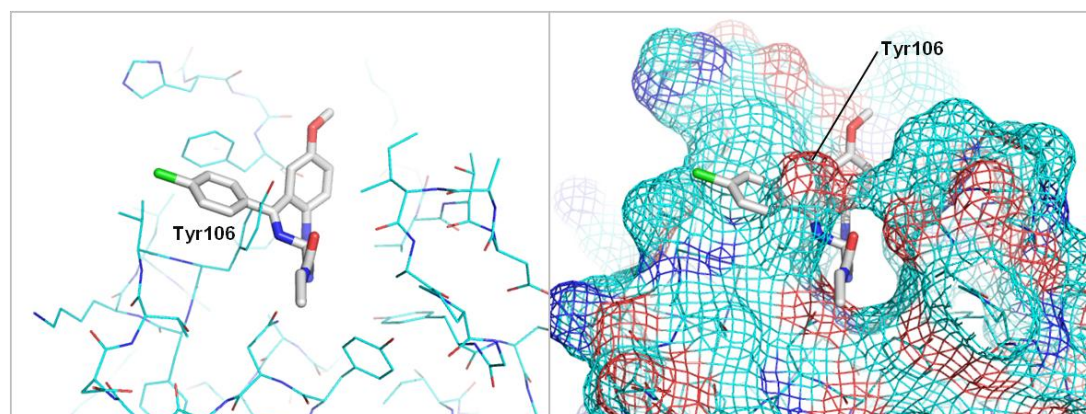


Figure 33: X-Ray crystallography of I-BET762 (1.006a, PDB code = 3P50) modelled in the bromodomain of Brd9.

2.2.2 Design and synthesis of amides

2.2.2.1 Identification of target compounds

Analysis of the data generated by the cross-screen previously described (**Figure 26**, page 48) revealed an example in which the introduction of the carbonyl functionality, transforming amine **2.001** into its amide analogue, **2.005**, significantly increased selectivity over Brd4 BD1. More specifically, amide **2.005** displayed 80 fold selectivity over Brd4 BD1, whilst amine **2.001** was not selective. The selectivity window shown by **2.005** was achieved whilst maintaining Brd9 potency, with both compounds exhibiting pIC₅₀ values of approximately 6.7 (**Figure 34**).

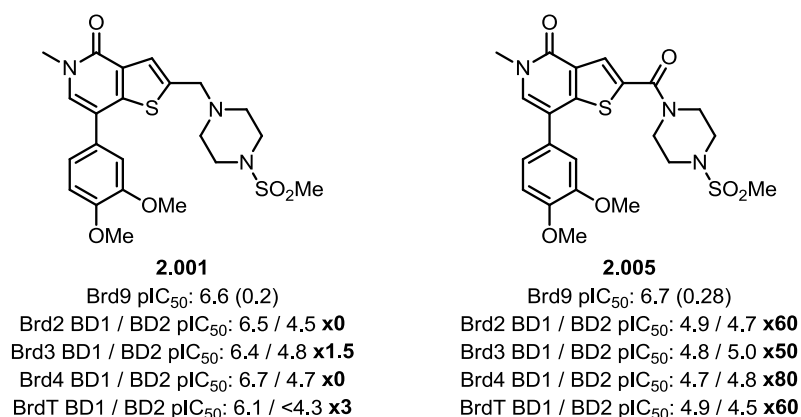


Figure 34: pIC₅₀ values for compounds **2.001** and **2.005** in the bromodomains of Brd9 and Brd4 (BD1 and BD2), as determined by TR-FRET analysis. Brd9 ligand efficiency values are shown in parentheses. Selectivity over the BET proteins is calculated relative to the maximum value, either BD1 or BD2. Data are n≥2.

In order to determine the binding mode of compound **2.005** and to further investigate its SAR, X-ray crystallographic analysis was utilised. A co-crystal structure of **2.005** in the bromodomains of Brd9 (left, green) and Brd4 BD1 (right, blue) provided good evidence for the specific interactions responsible for its activity (**Figure 35**).

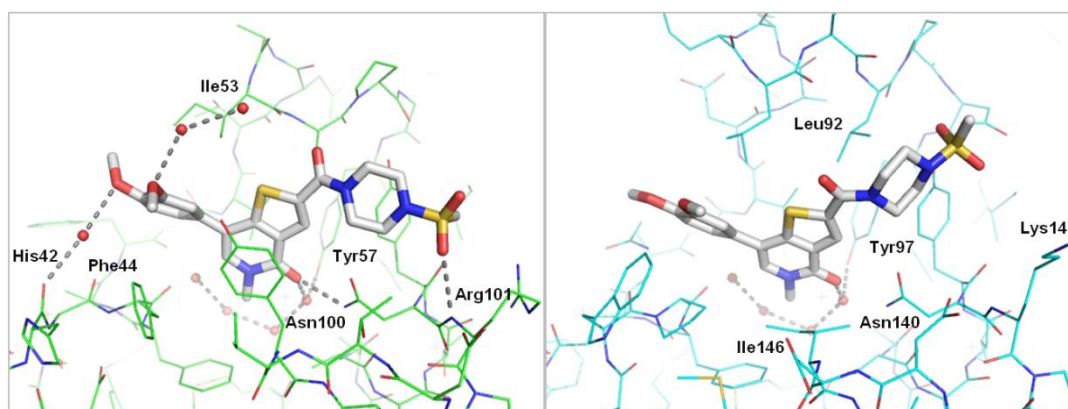


Figure 35: X-Ray crystallography of **2.005** in complex with the bromodomains of Brd9 (left, green, PDB code = 4UIT) and Brd4 BD1 (right, blue, PDB code = 4UIZ). Hydrogen-bonds are shown as grey dashed lines and water molecules as red spheres.

In both Brd9 and Brd4 BD1, the *N*-methyl pyridone moiety of the ligand acts as a direct structural analogue of KAc. The carbonyl group forms a direct hydrogen-bond to the NH₂ moiety of the conserved Asn residue (Asn100, Brd9; Asn140, Brd4 BD1) and a water-mediated interaction with the Tyr (Tyr57, Brd9; Tyr94, Brd4 BD1).

In Brd9, the 7-dimethoxyphenyl substituent protrudes into the ZA channel, in close contact with Phe44 and Ile53 on either side. The dimethoxy group participates in a series of through-water interactions, with the 4-methoxy substituent forming a water-mediated hydrogen-bond to the backbone carbonyl of His42. At the other end of the molecule, the 2-position amide forms multiple interactions, however, not all are favourable. For example, the amide carbonyl sits 2.7 Å from the carbonyl oxygen of Ile53, located in the peptide backbone. This is a close interaction for two carbonyl moieties, potentially leading to unfavourable electrostatics. In compensation, the piperazine amide is conformationally restricted, directing the methyl sulfonamide to a position where it can accept a hydrogen-bond from the backbone NH of Arg101.

In general, compound **2.005** exhibits a similar binding mode in Brd4 BD1. However, more detailed interactions of the compound differ. One difference arises from the double substitution of Brd9 Ala54/Tyr106 for Brd4 Leu94/Leu146 on either side of the thieno-pyridinone ring, leading to a differently shaped pocket (**Figure 36**).

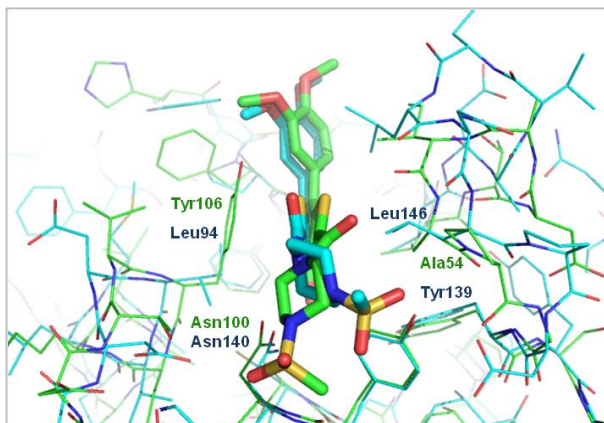


Figure 36: X-Ray crystallography of **2.005** in complex with the bromodomain of Brd9 (green, PDB code = 4UIT) overlaid with **2.005** in complex with Brd4 BD1 (blue, PDB code = 4UIZ).

These substitutions result in a tilt of the thieno-pyridinone ring by approximately 10° away from Leu94 in Brd4. The close proximity of Leu94 in Brd4 forces the thiophene 2-position carbonyl bond torsion into an almost planar, unfavourable conformation, in contrast to the ~30° angle seen in Brd9. Consequently, the piperidinyl sulfonamide is forced to adopt a different position, and as a result, the sulfonamide is unable to hydrogen-bond to the backbone of Lys141 (the equivalent of Arg101 in

Brd9). Instead, the sulfonamide is predicted to sit near the side-chain oxygen of Tyr139, an electrostatically unfavourable region. These observations are consistent with the lower potency of **2.005** for Brd4 compared to Brd9.

X-Ray crystallography¹⁵⁵ was also used to rationalise the difference in Brd4 activities shown for amine **2.001** (blue) compared to its amide analogue **2.005** (green). Conversion of amine to amide, transforming the hybridisation of the 2-position carbon atom from sp^3 to sp^2 causes a conformational change of the ligand (**Figure 37**).

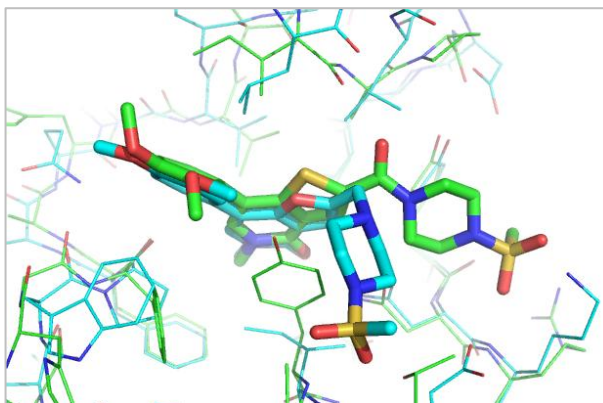


Figure 37: X-Ray crystallography of amide **2.005** (green, PDB code = 4UIT) in complex with the bromodomain of Brd9 overlaid with amine **2.001** (blue) in complex with the Brd4 BD1.

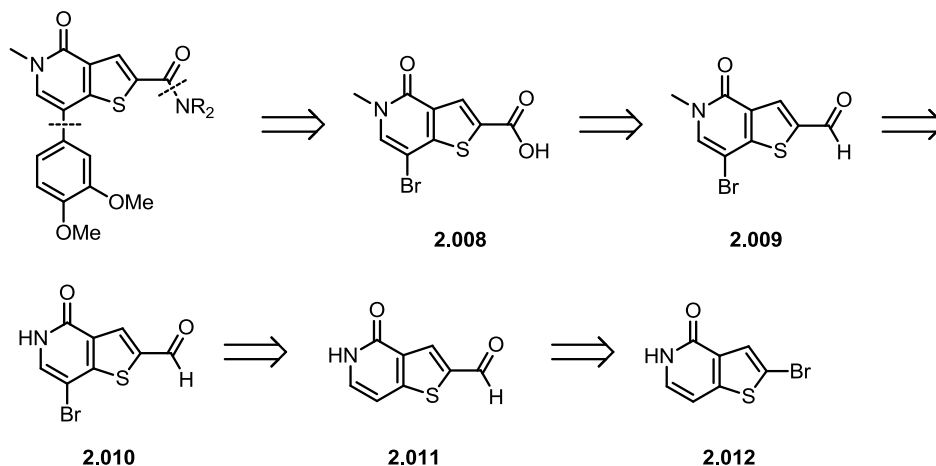
In Brd9, amide **2.005** moiety adopts $\sim 30^\circ$ degree torsion angle as discussed previously, allowing the sulfonamide moiety to interact with the backbone NH group of Arg101 (**Figure 35**). In contrast, the sp^3 linker of amine **2.001** causes the piperazine sulfonamide to occupy a different position, which is presumably identical in both Brd9 and Brd4 BD1.

Given the selectivity of compound **2.005**, potentially driven by the amide linker, a series of amides were synthesised to explore this hypothesis.

2.2.2.2 Preparation of various amide derivatives

2.2.2.2.1 Retrosynthesis of amide derivatives

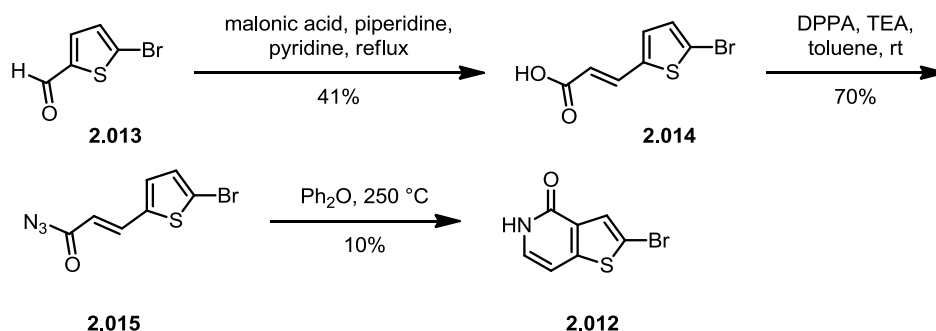
In order to access the various 2-position amides, the following retrosynthetic analysis was proposed (**Scheme 1**).



Scheme 1: Retrosynthetic analysis of 2-position amides from known starting material 2.012.

It was believed that the 7-position dimethoxyphenyl motif could be installed *via* a Suzuki-Miyaura coupling using the appropriate boronic acid. The 2-position amide moiety could be derived from the corresponding acid, providing intermediate **2.008**, which could be functionalised at both the 2 and 7-positions. The carboxylic acid group of **2.008** could be accessed by oxidation of aldehyde **2.009**, which in turn, could be derived from *N*-methylation of **2.010**. Selective bromination at the 7-position of compound **2.011** would provide intermediate **2.010**. Finally, installation of the 2-position formyl moiety could be achieved by lithium-halogen exchange of known compound **2.012**,¹⁵⁶ followed by the addition of DMF.

Starting material **2.012** was made available on scale *via* outsourcing. However, the synthesis has previously been reported by Gentile and co-workers¹⁵⁶ from the commercially available aldehyde **2.013** (**Scheme 2**).

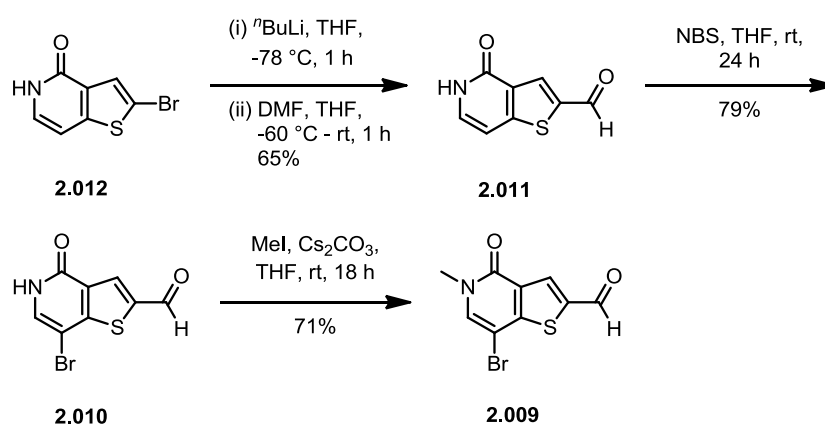


Scheme 2: Synthesis of known compound 2.012 as reported by Gentile and co-workers.¹⁵⁶

A Knoevenagel condensation of aldehyde **2.013** with malonic acid provided α,β -unsaturated carboxylic acid, **2.014** in a 41% yield. Subsequent addition of DPPA with TEA in toluene afforded the acyl azide **2.015**, which underwent a Curtius rearrangement and subsequent cyclisation to provide compound **2.012** in a 10% yield.

2.2.2.2.2 Synthesis of the Thieno-Pyridinone (TP) core

Previous work conducted by co-workers¹⁵⁷ led to the successful synthesis of key intermediate **2.009**, which allowed for the introduction of structural diversity at both the 2- and 7-positions. Preparation of **2.009** was achieved *via* a 3-step procedure from known thieno-pyridinone **2.012** (Scheme 3).¹⁵⁶

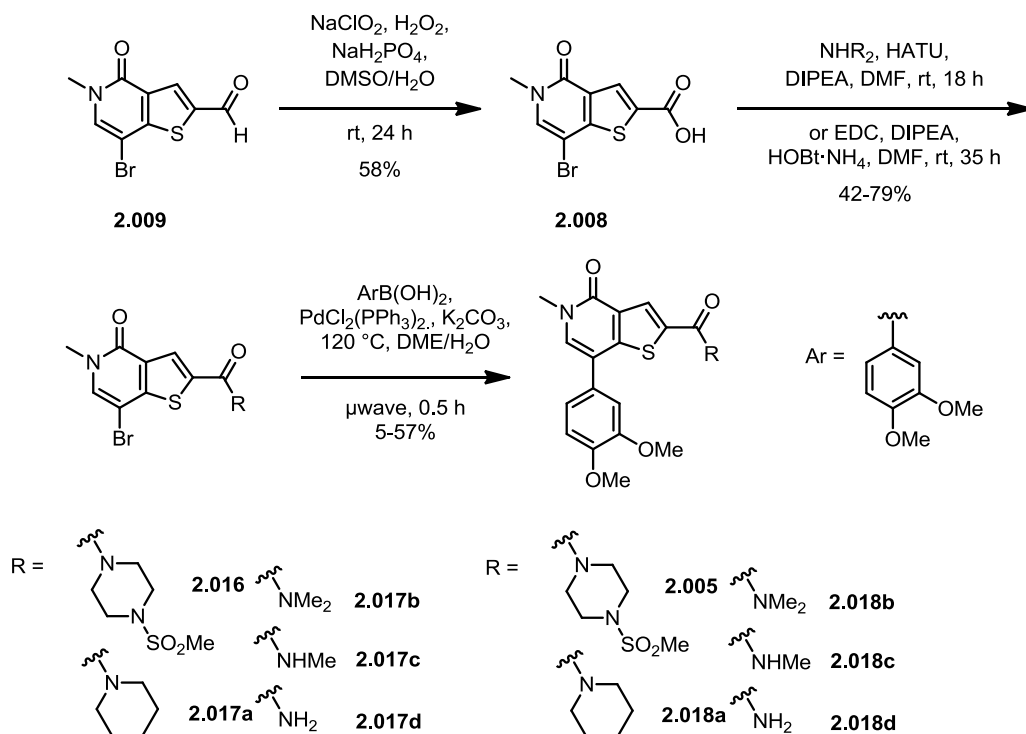


Scheme 3: Synthesis of aldehyde **2.009**.

Initial treatment of compound **2.012** with ⁿBuLi at -78 °C, followed by the drop-wise addition of DMF at -60 °C and warming to room temperature¹⁵⁸ afforded aldehyde **2.011** in a 65% yield. Subsequent selective bromination at the 7-position, employing NBS in THF provided **2.010** in a 79% yield. Following this, *N*-methylation with MeI and Cs₂CO₃¹⁵⁹ furnished compound **2.009** in a 71% yield. Pleasingly, this route proved to be highly scalable, providing over 30 g of aldehyde **2.009**.

2.2.2.3 Functionalisation of 2.008

With intermediate **2.009** in hand, initial focus was placed on installation of the amide functionality followed by a Suzuki-Miyaura coupling to introduce the aryl motif (**Scheme 4**).



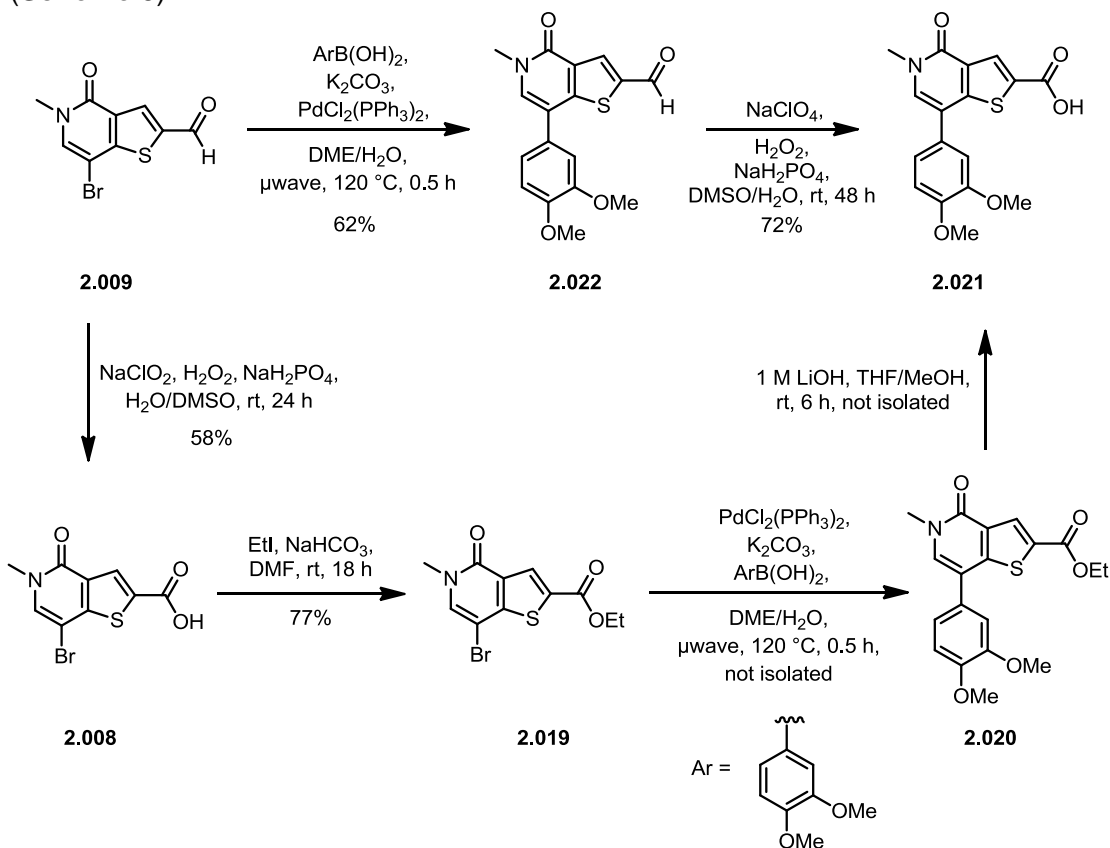
Scheme 4: Synthesis of amides 2.005 and 2.018a–d.

The synthesis of acid **2.008** was achieved *via* a Pinnick oxidation,¹⁶⁰ employing NaClO_2 , NaH_2PO_4 and H_2O_2 as a scavenger. Following this, standard peptide coupling conditions using HATU and DIPEA in DMF ¹⁶¹ yielded amides **2.016** and **2.017a–c** in modest to high yields. Primary amide **2.017d** was synthesised using different coupling reagents: EDC and 1-hydroxybenzotriazole ammonium salt.¹⁶² These conditions were favoured over the use of ammonia and a coupling reagent as 1-hydroxybenzotriazole ammonium salt provided an efficient, weighable source of ammonia. Final compounds **2.005** and **2.018a–d** were synthesised by a Suzuki-Miyaura coupling,¹⁶³ employing $\text{PdCl}_2(\text{PPh}_3)_2$ as a precatalyst.

Despite the successful synthesis of compounds **2.005** and **2.018a–d**, the above route was lengthy, and as such, did not provide an attractive method for further SAR exploration at the 2-position. With this in mind, an alternative, shorter pathway, in which structural diversity could be introduced at a later stage was devised.

2.2.2.4 Preparation of key intermediate **2.021**

In order to access a series of amide coupled derivatives *via* a route in which the final step allows for the introduction of structural diversity, focus was placed on a larger scale preparation of key intermediate **2.021** *via* two different synthetic strategies (**Scheme 5**).



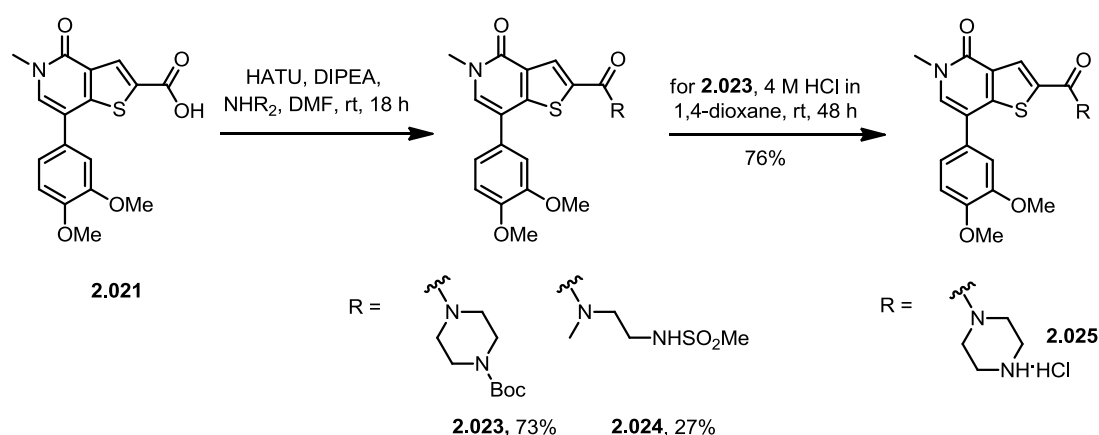
Scheme 5: Synthetic route to late stage intermediate **2.021.**

In an attempt to synthesise acid **2.021** directly, a Suzuki-Miyaura coupling¹⁶³ with acid **2.008** was undertaken. LCMS analysis of the crude reaction mixture indicated a complex mixture of products with no desired product (**2.021**) observed. Considering this result, an identical coupling was attempted with the acid functionality protected as ethyl ester **2.019**, which was synthesised in a 77% yield from acid **2.008**.¹⁶⁴ Analysis of the subsequent Suzuki-Miyaura coupling¹⁶³ indicated product formation by LCMS. Consequently, the crude mixture was taken forward to attempt a deprotection by hydrolysis. Treatment of crude ethyl ester **2.020** with 1 M LiOH in THF/MeOH¹⁶⁵ furnished free acid **2.021** (not isolated). However, in order to avoid the introduction of two additional steps in the overall synthetic plan, an alternative route was explored *via* a Suzuki-Miyaura coupling¹⁶³ with aldehyde **2.009**. Pleasingly, aldehyde **2.022** was isolated in a 62% yield using identical conditions as

previously described. Subsequently a Pinnick oxidation¹⁶⁰ using NaClO₂, NaH₂PO₄ and H₂O₂ as a scavenger furnished carboxylic acid **2.021** in a 72% yield. Indeed, this route proved to be scalable, providing over 5 g of **2.021**. With a successful scale-up route to this key intermediate established, further functionalisation of acid **2.021** was explored.

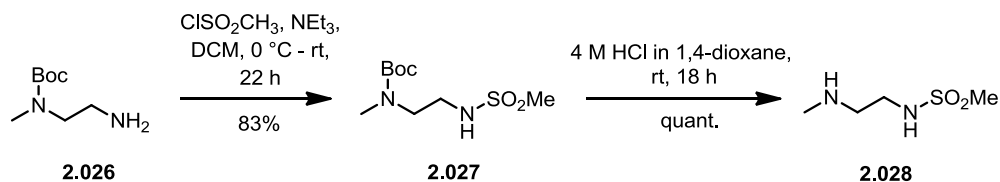
2.2.2.5 Preparation of various amides from key intermediate 2.021

With intermediate **2.021** in hand, a simple amide coupling employing HATU and DIPEA with the appropriate amine afforded compounds **2.023** and **2.024** (Scheme 6). Compound **2.023** was synthesised from the commercially available Boc protected piperazine. Following this, deprotection, employing 4 M HCl in 1,4-dioxane furnished amide **2.025** in a 76% yield.



Scheme 6: Synthesis of amides **2.024** and **2.025** from intermediate acid **2.021**.

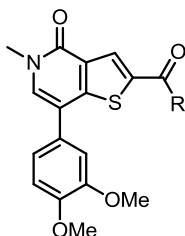
The amine required for the synthesis of compound **2.024** was accessed *via* a 2-step procedure from the commercially available methyl diamine derivative, **2.026** (Scheme 7). Mesylation of carbamate **2.026** employing methane sulfonyl chloride and NEt₃ in DCM¹⁶⁶ provided **2.027** in an 83% yield. Following this, Boc deprotection employing 4 M HCl in 1,4-dioxane furnished amine **2.028** in a quantitative yield.



Scheme 7: Synthesis of amine **2.028** from commercially available carbamate **2.026**.

2.2.2.6 SAR discussion of amide derivatives

In order to determine the binding affinity of these amides against the bromodomains of Brd9 and Brd4 (BD1 and BD2), a competitive displacement assay was utilised (**Figure 31**, step 1a). Each compound was screened in an *in vitro* TR-FRET assay from which pIC₅₀ values were calculated. Fold selectivity for Brd9 is shown relative to the maximum Brd4 value [typically BD1 (**Table 4**)].



Entry	Compound	R =	Brd9 pIC ₅₀	Brd9 LE	Brd4 BD1 pIC ₅₀	Brd4 BD2 pIC ₅₀	Selectivity
1	2.005		6.7	0.28	4.7	4.8	x80
2	2.025 ¹⁶⁷		5.6	0.26	5.0	4.4	x4
3	2.018a ¹⁶⁸		5.4	0.26	4.8	4.3	x4
4	2.018b ¹⁶⁹		5.3	0.28	4.9	4.7	x3
5	2.018c		6.9	0.38	6.7	6.9	x1
6	2.018d		7.0	0.40	6.9	6.8	x1
7	2.029 ¹⁷⁰		7.0	0.31	7.0	6.6	x1
8	2.024		5.2	0.22	5.0	4.6	x2

Table 4: pIC₅₀ values for selected amides in the bromodomains of Brd9 and Brd4 (BD1 and BD2) as determined by TR-FRET analysis. Selectivity is calculated relative to the maximum Brd4 value. Data are n≥3.

All compounds showed ~5 μM or greater affinity for Brd9 with pIC₅₀ values of 5.2 and above. Analysis of the data compared to compound **2.005**, the original start point for this project, indicated that the methylsulfonamide moiety was important for both potency and selectivity. Truncation of the piperazine methylsulfonamide functionality of **2.005** to give unfunctionalised piperazine **2.025**, piperidine **2.018a** and dimethyl amide **2.018b**, reduced Brd9 potency, with little effect on Brd4 activity (entries 1–4). It was presumed that the reduction in Brd9 activity was due to the loss

of a hydrogen-bond upon removal of the methylsulfonamide group in **2.005**. This hypothesis is consistent with X-ray crystallography¹⁵⁵ of piperazine **2.025** (right) in complex with the bromodomain of Brd9 [Figure 38, amide **2.005** (left) shown for comparison].

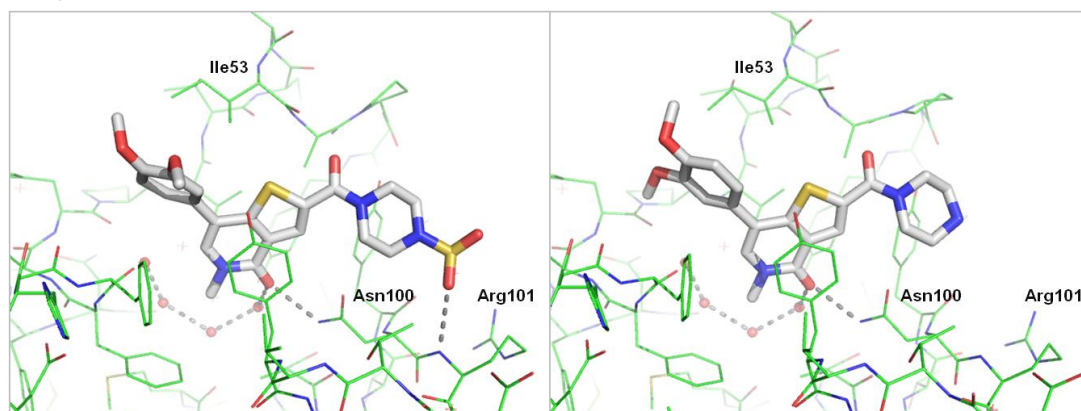


Figure 38: X-Ray crystallography of amides **2.005** (left, PDB code = 4UIT) and **2.025** (right) in complex with the bromodomain of Brd9. Hydrogen-bonds are shown as grey dashed lines and water molecules as red spheres.

Interestingly, although not selective over Brd4, secondary amides **2.018c**, **2.018d** and **2.029** restored the Brd9 activity observed for **2.005** (entries 1 and 5–7). It was presumed that the amide NH was forming an additional interaction in both Brd9 and Brd4, accounting for the increase in activity. This exciting result demonstrated that high potency could be achieved without extension beyond the amide moiety, providing molecules with improved ligand efficiencies (compare entries 1 and 6). Analysis of the X-ray crystal structure¹⁵⁵ **2.018c** in complex with the bromodomain of Brd9 (right) indicated that the amide carbonyl had rotated by approximately 110° relative to compound **2.005** (left). As such, the NH moiety was able to form a direct hydrogen-bond to the carbonyl group of Ile53 (Figure 39).

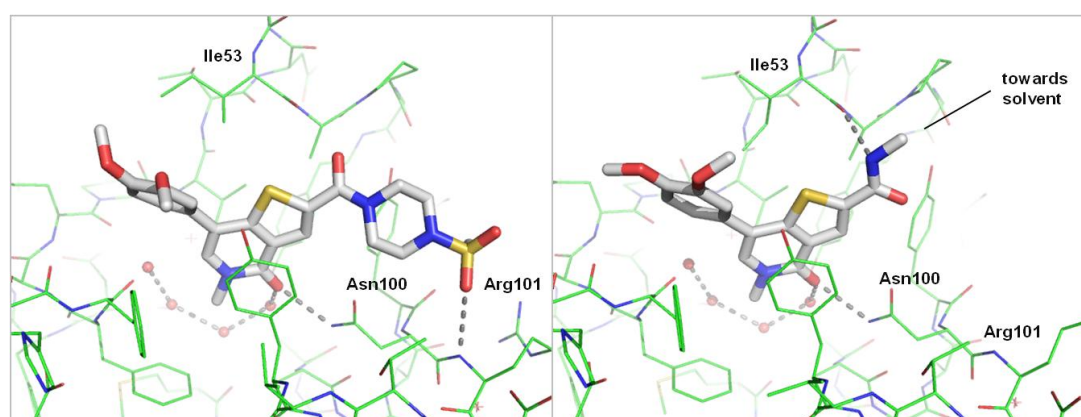


Figure 39: X-Ray crystallography of amides **2.005** (left, PDB code = 4UIT) and **2.018c** (right) in complex with the bromodomain of Brd9. Hydrogen-bonds are shown as grey dashed lines and water molecules as red spheres.

Interestingly, secondary amide **2.029** was equipotent to amides **2.018c** and **2.018d** despite the presence of an additional hydrogen-bond acceptor at the terminal end of the alkyl chain. The sulfonamide moiety was expected to participate in a hydrogen-bond interaction, increasing potency relative to **2.018c** and **2.018d**. However, X-ray crystallography of compound **2.018c** (**Figure 39**, page 68) indicated that the amide methyl substituent was directed towards solvent. Presumably, extension beyond a methyl group to give sulfonamide **2.029** could result in a similar binding mode. Therefore, the terminal sulfonamide group would be unable to participate in any hydrogen-bond interactions within the bromodomain binding pocket. Methylated variant **2.024** exhibited a similar activity profile to that of the other tertiary amides, despite its more flexible nature relative to the conformationally restrained ring systems (compare entries 3 and 8).

In summary, the methyl sulfonamide group of compound **2.005** was found to be essential for Brd9 activity and selectivity over Brd4. However, an increase in Brd9 potency was achieved by secondary amides **2.018c**, **2.018d** and **2.029** via an interaction with Ile53 (**Figure 39**, page 68). Although these amides showed little to no selectivity over Brd4, the improvement in Brd9 potency and ligand efficiency represented a significant advance in the project, leading to further investigations around the amide series.

2.2.3 Design and synthesis of amide array

2.2.3.1 Identification of array compounds

Having established limited SAR around the TP amide series, compound **2.005** continued to display the best combination of potency and selectivity. With a route to the precursor of lead compound **2.005** established, and an intermediate in which structural diversity could be introduced at the final stage, an array of amides was designed. This was achieved through the use of a GSK database of commercially available and in-house monomers, which can be filtered based on various parameters such as: functional group; molecular weight; cLogP; number of aromatic rings; and number of hydrogen-bond acceptors (HBA) or donors (HBD). Data from the previous compound set (**Table 4**, page 67) in combination with X-ray crystallographic analysis, aided the design of a series of secondary and tertiary amides. These data indicated that the sulfonamide moiety of **2.005** acted as a HBA, specifically orienting the amide carbonyl group to deliver selectivity. In contrast, secondary amide **2.018c** provided high Brd9 activity through the HBD ability of the

amide NH. Considering this result, focus was placed on combining the HBA methane sulfonamide group with the HBD amide NH, in order to provide compounds that were both potent and selective (**Figure 40**).

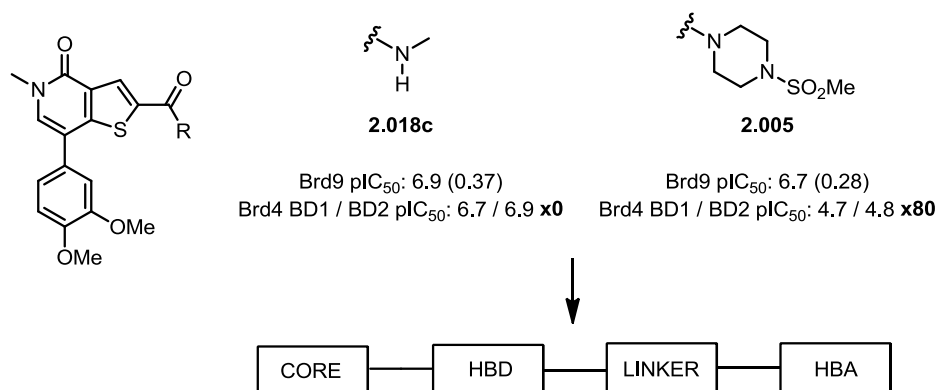


Figure 40: Rationale behind the design of amide array. Brd9 ligand efficiency values are shown in parentheses and selectivity is calculated relative to the maximum Brd4 value. Data are n≥3.

This concept was employed in the design of several conformationally restricted secondary amides, which combine these two features *via* various linkers. By means of locking the HBA functionality in various ring systems and substituted chains in order to induce torsional strain, it was hypothesised that this key selectivity inducing group would no longer be capable of protruding into the solvent.

As well as the secondary amide set, a collection of tertiary amides were designed with the aim to explore the optimum position of the HBA functionality. This series of compounds included various substitution patterns, ring sizes and alternative HBA moieties (**Figure 41**).

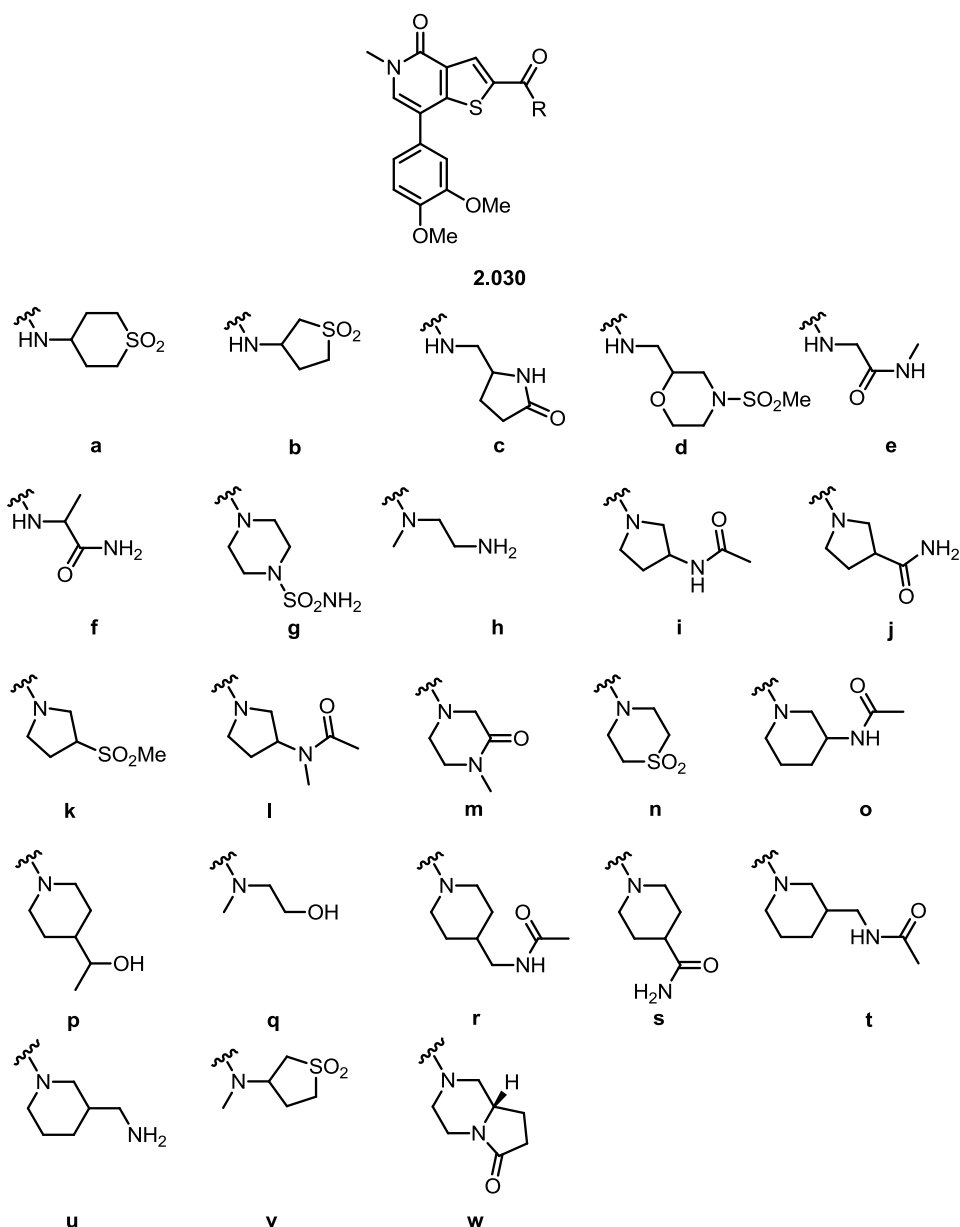
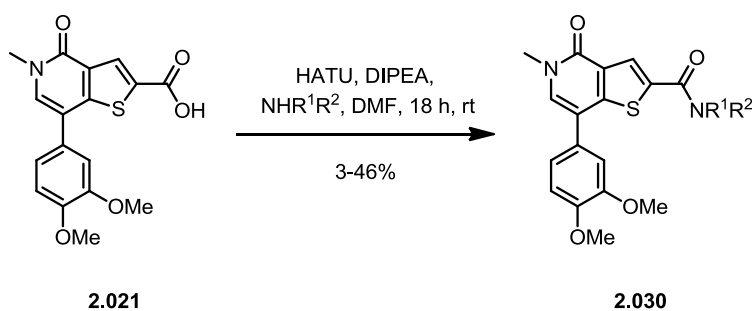


Figure 41: Chemical structures for amides synthesised in the amide array.

Preparation of these compounds was carried out by colleagues within the GSK Compound Array Team,¹⁷¹ a group specialising in the small-scale synthesis of target compounds for biological test and evaluation. This hugely enabling resource utilised a pre-prepared intermediate, delivering the desired series within a 10 day time frame. The contribution from the Compound Array Team proved extremely valuable as the sequential synthesis of these compounds would be far less efficient. Although 23 amides were designed, the Compound Array Team were able to successfully deliver 20 compounds for biological test and evaluation. This was achieved *via* a

peptide coupling on advanced intermediate **2.021**, employing HATU and DIPEA in DMF (**Scheme 8**, for experimental detail see Appendix 5.4.1).



Scheme 8: Synthesis of amides by the Compound Array Team.

The synthesis of the remaining compounds was attempted but unsuccessful, providing only starting material as judged by LCMS analysis. It has been reported that reactions that succeed in synthetic arrays tend to be more lipophilic, reflecting the propensity to use organic work-up procedures that favour these molecules.¹⁵³ In an attempt to investigate this correlation on the array compounds, the LogP values of the successful and unsuccessfully synthesised amides were analysed. Unfortunately, no such trend was observed.

2.2.3.2 SAR discussion of amide array

As with the original set of amides, the array compounds were tested in an *in vitro* TR-FRET assay, in order to determine binding affinity against the bromodomains of Brd9 and Brd4 (Figure 31, step 1a). Figure 42 displays a graphical representation of the array data (for full data set see Appendix 5.4.2). The line of unity indicates which compounds were equipotent in the bromodomains of Brd4 (maximum value quoted, either BD1 or BD2) and Brd9, whilst the dashed lines represent 10 fold selectivity for Brd4 (top) and Brd9 (bottom). Tertiary amide compounds are highlighted in orange and secondary in green.

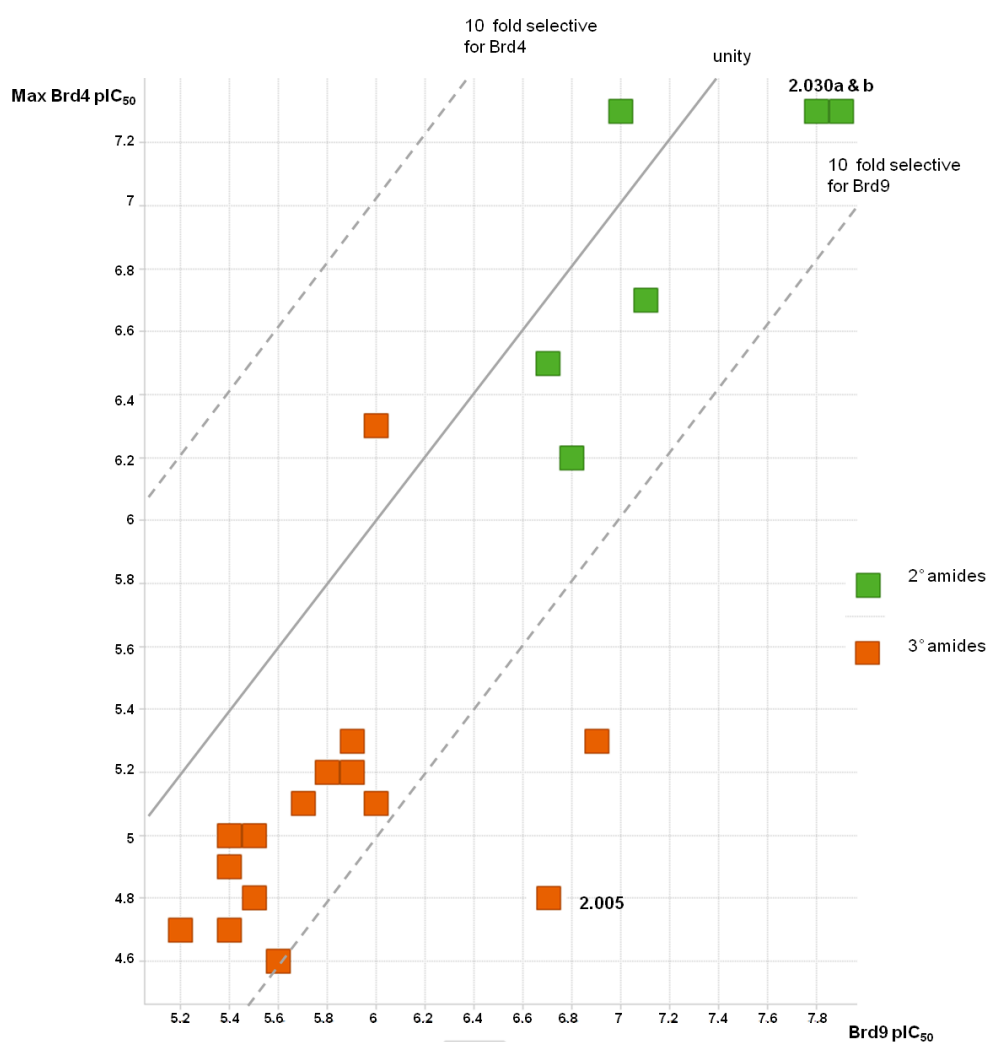


Figure 42: Graphical representation of TR-FRET assay results from the amide array. Brd9 pIC₅₀ values are shown on the x-axis and maximum Brd4 (BD1 or BD2) on the y-axis. Secondary amides are highlighted in green and tertiary in orange.

In general, the secondary amides displayed much greater activity in both Brd9 and Brd4 than the tertiary compounds, presumably due to their ability to form an

additional hydrogen-bond (**Figure 39**, page 68). Cyclic sulfones **2.030a** and **b** are highlighted as they delivered over 10 fold increase in Brd9 potency relative to compound **2.005**, albeit with reduced selectivity over Brd4 (**Figure 43**).

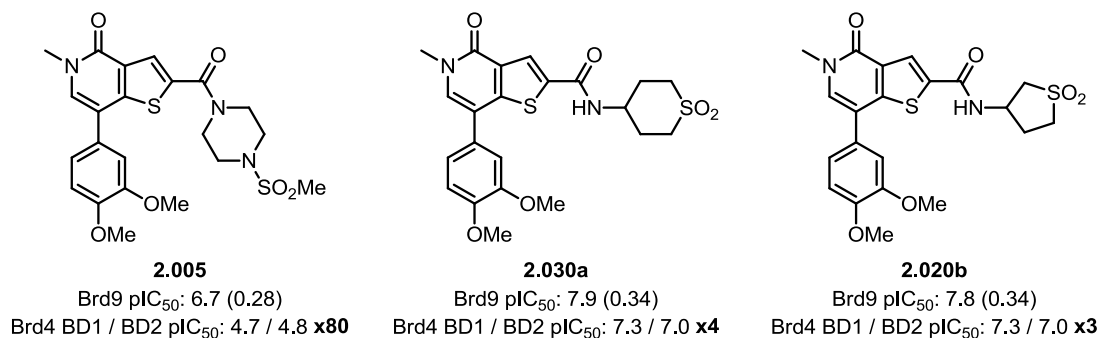


Figure 43: pIC₅₀ values for compounds 2.005, 2.030a and 2.030b in the bromodomains of Brd9 and Brd4 (BD1 and BD2), as determined by TR-FRET analysis. Brd9 ligand efficiency values are shown in parentheses. Brd4 selectivity is calculated relative to the maximum Brd4 activity. Data are n≥3.

X-Ray crystallography¹⁵⁵ of amide **2.030a** in complex with the bromodomains of Brd9 (left, green) and Brd4 BD1 (right, blue) provided good evidence for the interactions responsible for the observed potency (**Figure 44**).

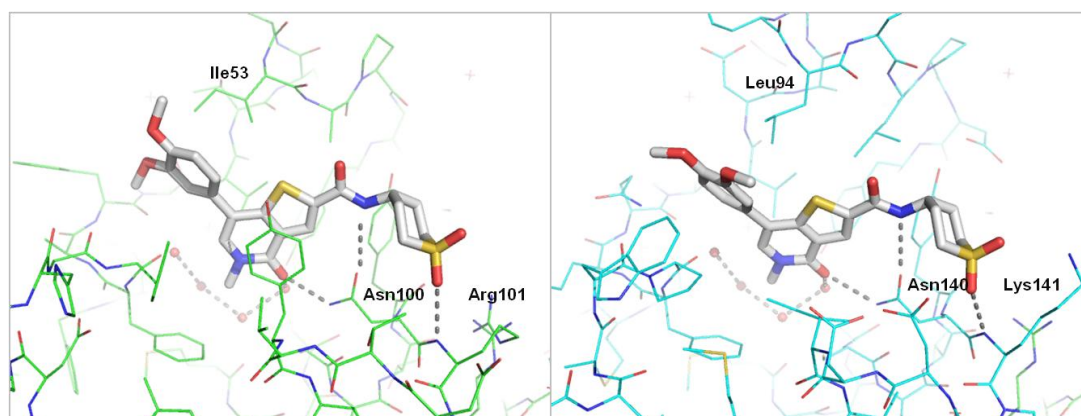


Figure 44: X-Ray crystallography of amide 2.030a in complex with the bromodomain of Brd9 (left, green, PDB code = 4UIU) and Brd4 BD1 (right, blue, PDB code = 4UIX). Hydrogen-bonds are shown as grey dashed lines and water molecules as red spheres.

Analysis of the X-ray crystal structures indicated that amide **2.030a** forms identical interactions in Brd9 and Brd4 BD1. The amide NH moiety forms a direct hydrogen-bond to the conserved Asn (Asn100, Brd9; Asn140, Brd4 BD1) creating a bidentate interaction in combination with the TP core KAc mimetic. Furthermore, these structures suggest that the increased potency of amide **2.030a** compared to **2.028c** (**Table 4**, page 67) is likely due to the cyclic sulfone. Surprisingly, this ring bound such that the amide NH moiety was in the axial position, placing the sulfone group within hydrogen-bonding range of the backbone NH of Arg101 in Brd9. The

conformation of this group was very similar in Brd4 BD1, with the sulfone forming a hydrogen-bond to the backbone NH of Lys141 (the equivalent of Arg101 in Brd9). As **2.030a** forms very similar interactions in both Brd9 and Brd4, there was very little selectivity (4 fold) shown between these bromodomains.

As 5-membered sulfone **2.030b** was originally synthesised as a racemate, the single enantiomers were prepared¹⁷² and tested to determine their individual activities. Results from the TR-FRET assay indicated that both the (*R*)- and (*S*)-enantiomers were equipotent to the racemate, indicating that the stereochemical configuration of the chiral centre made no difference to the interactions between the ligand and bromodomain.

No significant results were obtained from the tertiary amide array, as most compounds exhibited pIC₅₀ values in the region of 5.5, with minor selectivity over Brd4. Alternative HBA functionalities and their locations around the ring had little effect on activity, which suggested an inability to mimic the hydrogen-bond interaction made by the sulfonamide moiety in **2.005**. The data set provided by these tertiary amides (see Appendix 5.4) highlighted the intriguing nature of compound **2.005** and its ability to deliver both potency and selectivity in the 2-position of the template. Indeed, this activity profile proved extremely difficult to replicate or improve upon through further exploration of alternative amide substituents. However, the compounds delivered by the Compound Array Team provided a 10 fold increase in Brd9 potency relative to compound **2.005** and consequently highlighted the benefit of forming a bidentate interaction to Asn100.

2.2.4 Design and synthesis of alternative cores

2.2.4.1 Identification of target compounds

Considering the SAR generated around the various 2-position amides, it was believed that an increase in Brd9 activity and ligand efficiency could be gained through changes to the central core. Replacement of the lipophilic thiophene ring for a more polar imidazole would not only reduce the inherent lipophilicity of the template but could also provide an increase in potency. As discussed in Section 2.2.2.6 (page 67) the formation of a bidentate interaction to Asn100 causes Brd9 activity to increase by 30 fold for compounds **2.018b** and **c**, respectively. Moving forward, it was hypothesised that an imidazole NH could be capable of mimicking this interaction, leading to greater Brd9 ligand efficiency (**Figure 45**). If successful,

further elaboration at the 2-position of the scaffold could be conducted, providing opportunities to explore alternative parts of the protein.

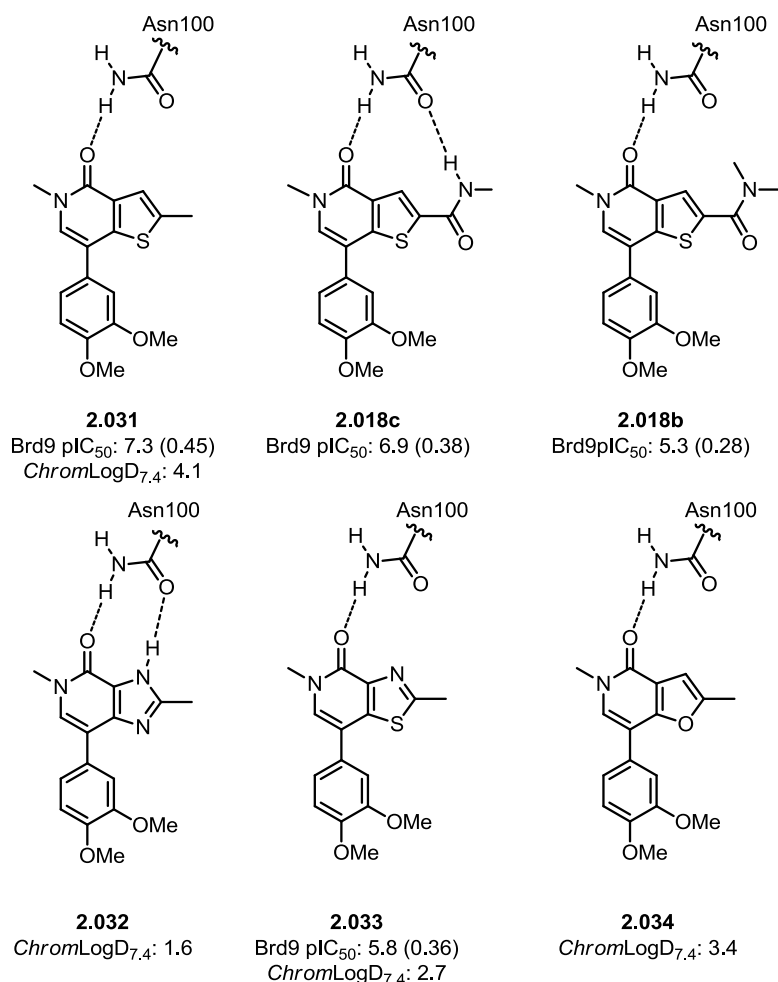


Figure 45: Representation of bidentate interactions to Asn100 for modified TP compounds. Brd9 ligand efficiency values are shown in parentheses.

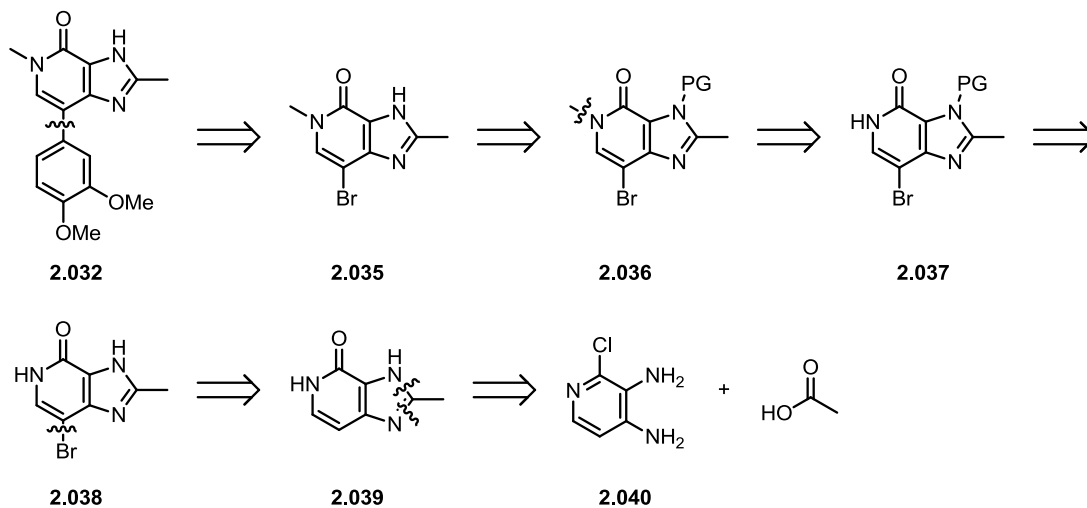
Imidazole pyridinone (IP) core **2.032** was selected for the basis of this investigation, proving an ideal comparison to TP analogue **2.031** and thiazole **2.033** previously synthesised by colleagues.¹⁷³ Although not able to form a bidentate interaction, Furan Pyridinone (FP) analogue **2.034** was included as an additional comparator, due to its reduced lipophilicity relative to TP compound **2.031**.

As previously discussed (Section 2.1.3, page 53) *ChromLogD* is used to assess the lipophilicity of a compound and therefore gives an indication of drug-like properties. As shown in **Figure 45**, IP (**2.032**, *ChromLogD*_{7.4}: 1.6), thiazole (**2.033**, *ChromLogD*_{7.4}: 2.7) and FP (**2.034**, *ChromLogD*_{7.4}: 3.4) compounds have reduced lipophilicity compared to TP compound (**2.031**, *ChromLogD*_{7.4}: 4.1).

2.2.4.2 Synthesis of the IP core

2.2.4.2.1 Retrosynthetic analysis

In order to access IP core compound **2.032** the following retrosynthetic analysis was proposed (**Scheme 9**).

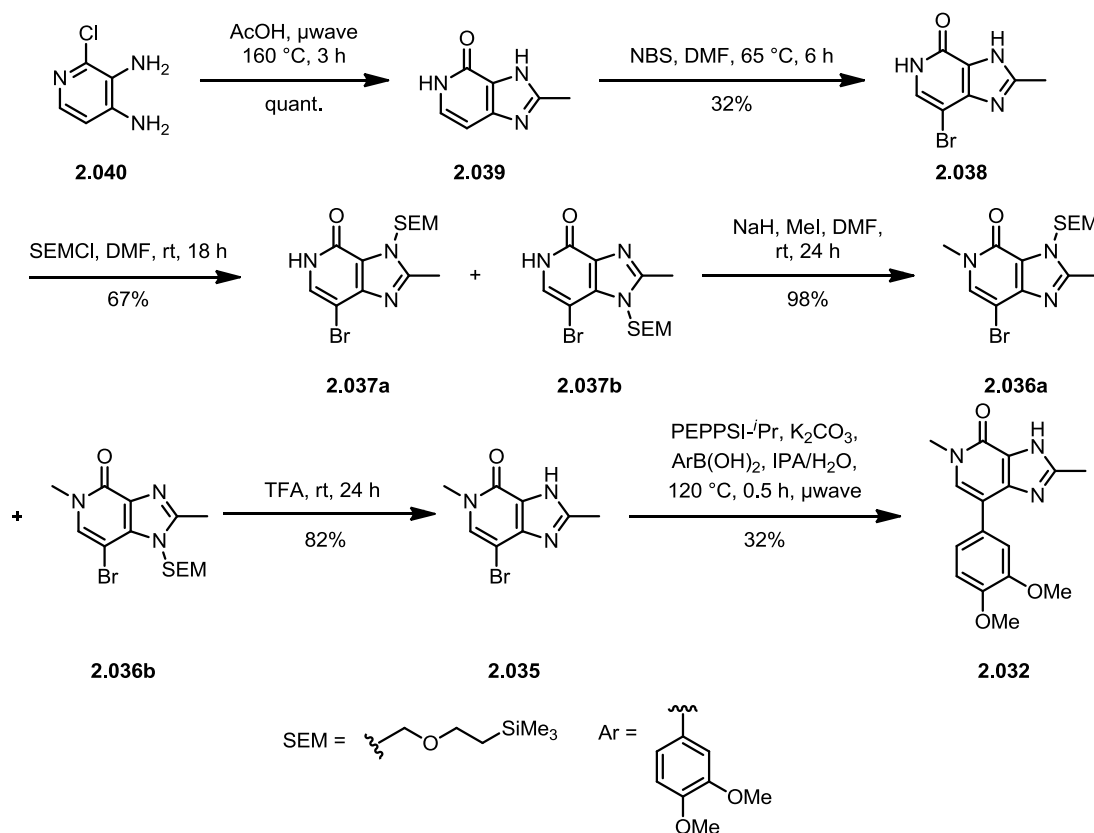


Scheme 9: Retrosynthetic analysis of compound 2.032.

A disconnection at C-7 would provide intermediate **2.035**, a suitable Suzuki-Miyaura coupling partner, to which the dimethoxyphenyl group could be installed. This, in turn, could be derived from protected **2.036**, accessed *via* a methylation of **2.037**. It was believed that protection of the imidazole NH was necessary in order to achieve selective pyridone N-5 methylation. Intermediate **2.038** could be accessed by a selective 7-position bromination of unfunctionalised core **2.039**. Finally, construction of IP scaffold **2.039** could be achieved *via* cyclisation of commercially available chloro-pyridine derivative **2.040** with acetic acid.

2.2.4.2.2 Preparation of the IP core

Synthesis of the IP core was successfully achieved *via* a 6-step route from commercially available pyridine **2.040** (Scheme 10).



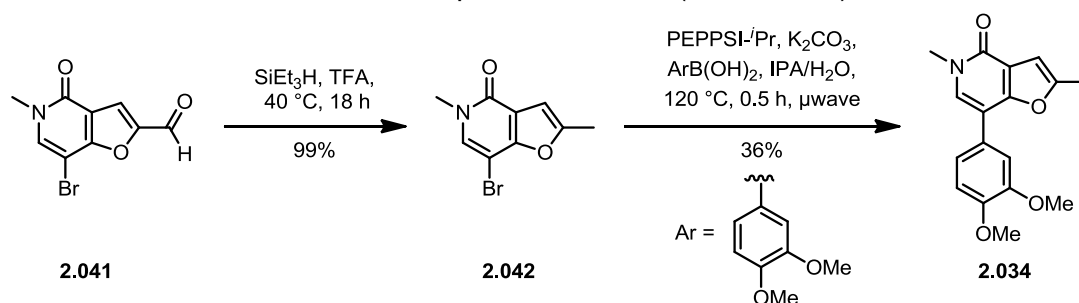
Scheme 10: Synthesis of IP core compound **2.032**.

Exploration of in-house GSK databases revealed conditions for the synthesis of **2.039**: heating pyridine **2.040** in AcOH.¹⁷⁴ Initially, this reaction was performed under thermal heating at 160 °C for 24 hours. However, with some optimisation, the reaction time was shortened to 3 hours under microwave irradiation at 160 °C. Pleasingly, these conditions provided unfunctionalised core **2.039** in quantitative yield. Subsequent electrophilic bromination employing NBS in DMF provided bromide **2.038** in a 32% yield. The low yield for this reaction was attributed to difficulties during purification by silica gel chromatography due to the high polarity of the compound. To improve this result, crude **2.038** could be taken on to the subsequent step without purification. Interestingly, no brominated product was observed using DCM or THF as solvents, even when heated to reflux. This was presumably due to lack of solubility of **2.039** under these conditions. In order to selectively methylate the pyridone nitrogen, it was necessary to protect the imidazole

NH. Previous studies within GSK¹⁷⁴ had shown that the SEM group was optimal for this pathway given the synthetic ease of installation and orthogonal conditions required for deprotection, leaving the N-5 methyl substitution intact. Treatment of bromide **2.038** with SEMCl in DMF provided **2.037a** and **b** in a 67% yield as a 5:1 mixture of regioisomers. This structural assignment was confirmed by ¹H NMR spectroscopy through observation of a 3-bond coupling between NCH₂OR and C-8 of the ring junction by HMBC. Reasons behind the observed selectivity of N-3 protection over N-1 can be rationalised through steric considerations. Addition of the SEM group at N-1 would be less favoured since it would sit in close proximity to the bulky Br substituent. Therefore, selective addition to the sterically less encumbered N-3 was observed. Following protection, methylation at N-5 employing MeI in DMF at room temperature proved successful, providing a 5:1 mixture of regioisomers, with the major component shown as **2.036a**. This was confirmed by ¹H NMR spectroscopy as described for regioisomers **2.037a** and **b**. Following this, SEM deprotection in neat TFA at room temperature furnished key intermediate **2.035** in an 82% yield. Finally, a Suzuki-Miyaura coupling¹⁶³ using the PEPPSI-*i*Pr pre-catalyst system¹⁷⁵ was employed to install the dimethoxyphenyl motif.

2.2.4.3 Synthesis of the FP core

The synthesis of the FP core molecule **2.034** was achieved in 2-steps from aldehyde **2.041**, available from the GSK compound collection (**Scheme 11**).

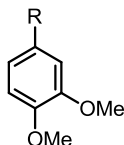


Scheme 11: Synthesis of FP compound 2.034.

Aldehyde **2.041** was successfully reduced to methyl-substituted compound **2.042** in excellent yield using triethylsilane in TFA at 40 °C.¹⁷⁶ Following this, a Suzuki-Miyaura coupling¹⁶³ with PEPPSI-*i*Pr¹⁷⁵ furnished final compound **2.034** in 36% yield.

2.2.4.4 SAR discussion of alternative core compounds

Alternative core compounds **2.031–2.034** were tested in a TR-FRET assay against the bromodomains of Brd9 and Brd4 (BD1 and BD2), in order to determine binding affinity (**Figure 31**, step 1a). Fold selectivity for Brd9 is shown relative to the maximum Brd4 value (**Table 5**).



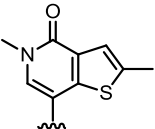
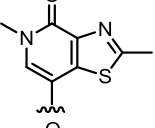
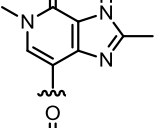
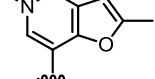
Entry	Compound Number	R	Brd9 pIC ₅₀	Brd9 LE	Brd4 BD1 pIC ₅₀	Brd4 BD2 pIC ₅₀	Selectivity
1	2.031		7.3	0.45	6.3	5.9	x10
2	2.033 ¹⁷³		5.8	0.40	5.7	5.4	x1
3	2.032		6.5	0.40	6.4	6.1	x2
4	2.034		7.1	0.44	6.3	6.0	x6

Table 5: pIC₅₀ values for compounds **2.031–2.034** in the bromodomains of Brd9 and Brd4 (BD1 and BD2) as determined by TR-FRET analysis. Selectivity is calculated relative to the maximum Brd4 value. Data are n≥3.

Pleasingly, Brd9 ligand efficiencies of all alternative core compounds were uniformly high. However, incorporation of additional heteroatoms into the 5-membered ring caused Brd9 potency to decrease. For example, moving from TP **2.031** to thiazole **2.033** caused Brd9 potency to decrease by 30 fold, as well as selectivity over Brd4 (entries 1 and 2). It was proposed that this reduction in activity was due to the nitrogen lone pair of the thiazole ring causing a unfavourable electrostatic interaction with the carbonyl moiety of Asn100. Pleasingly IP compound **2.032** provided a 5 fold improvement in Brd9 potency relative to thiazole **2.033**, albeit with no selectivity over Brd4. However, IP compound **2.032** provided no improvement in Brd9 potency or selectivity compared to TP **2.031** (entries 1 and 3). X-Ray crystallography¹⁵⁵ of TP

2.031 (left) and IP core **2.032** (right) was obtained in order to assess their binding modes in Brd9 (**Figure 46**).

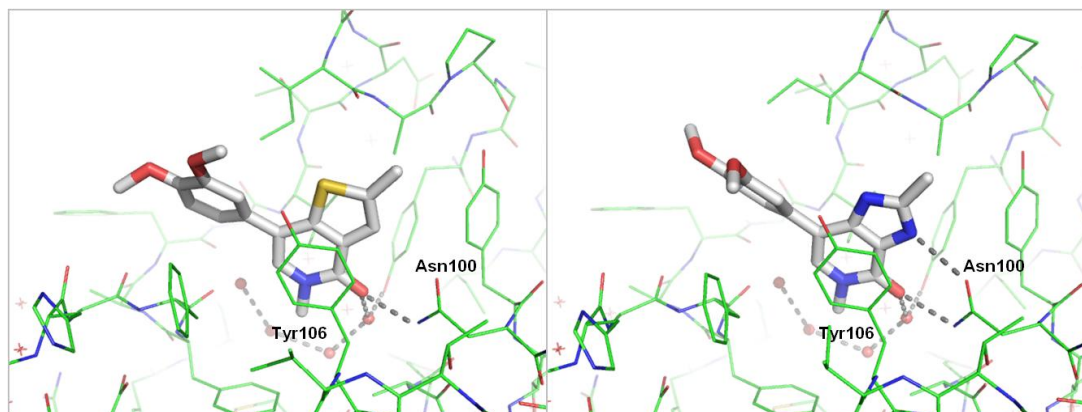


Figure 46: X-Ray crystallography of TP **2.031** (left) and IP **2.032** (right) in complex with the bromodomain of Brd9. Hydrogen-bonds are shown as grey dashed lines and water molecules as red spheres.

Analysis of the X-ray crystal structures indicates that both the TP and IP compounds, **2.031** and **2.032**, respectively adopt very similar binding modes in Brd9. As expected, the pyridone moiety acts as the KAc mimetic, forming a hydrogen-bond to Asn100. In the case of IP compound **2.032**, the imidazole NH also forms an interaction to the NH₂ group of Asn100. In the absence of X-ray crystallography of these compounds in complex with Brd4 BD1, it was presumed that they would adopt a similar conformation in this bromodomain, accounting for the relatively small selectivity window observed.

Despite the formation of an additional hydrogen-bond, IP compound **2.032** showed decreased Brd9 potency and selectivity compared to TP **2.031**. The reasoning behind this observation remains uncertain, however, it was hypothesised that the electronics of the different ring systems may play a part. Transformation of TP **2.031** to IP **2.032** had no effect on Brd4 activity, suggesting that the electronic effect was Brd9 specific. As discussed previously (Section 2.2.1, page 57), a key difference between the bromodomains of Brd9 and Brd4 is the presence of a Tyr106 gate keeper, present in Brd9 only. It was hypothesised that the electronics of the different core compounds could have affected their ability to undergo a π - π stacking interaction with this residue, leading to different activity.

Finally, furan analogue **2.034** displayed the most similar activity profile to TP **2.031**, displaying almost identical results. However, due the availability of large quantities of intermediate, the TP scaffold was progressed for further optimisation.

2.3 Modifications at the 2-position of the TP core

Having established the TP core as the optimal template for Brd9, focus was placed on the exploration of non-amide containing 2-position substituents. The high Brd9 potency and ligand efficiency shown by methyl substituted compound **2.031** (Table 5, page 80), suggested that the 2-position could represent an appropriate vector for further elaboration. At this point in the project, acceptable levels of Brd9 potency had been achieved, therefore, further studies would focus on improving selectivity over Brd4. Initial investigations would examine the effect of alternative functional groups including alkyl, alcohol, amine and amidine.

2.3.1 Alkyl and alcohol derivatives

2.3.1.1 Identification of target compounds

As discussed previously (Section 2.2.2.6, page 67), truncation of the piperazine sulfonamide to the simple methyl amide increased both Brd9 activity and ligand efficiency, albeit with no selectivity over Brd4 (Figure 47).

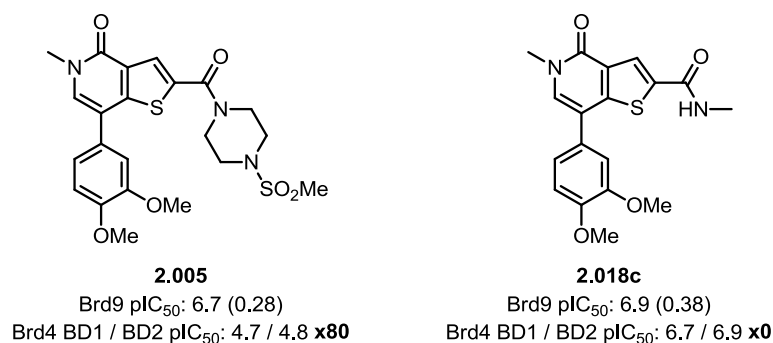


Figure 47: pIC₅₀ values for compounds 2.005 and 2.018c in the bromodomains of Brd9 and Brd4 (BD1 and BD2) as determined by TR-FRET analysis. Brd9 ligand efficiency values are shown in parentheses. Selectivity is calculated relative to the maximum Brd4 value. Data are n≥3.

Considering the increased ligand efficiency of **2.018c**, focus was placed on enhancing Brd4 selectivity through the introduction of various 2-position substituents. Initially, it was envisaged that installation of alkyl groups could have the potential to induce a steric clash in Brd4, whilst maintaining acceptable levels of Brd9 activity and increased ligand efficiency. To this end, 2-position substituted H (**2.043**), methyl (**2.031**), ethyl (**2.044**) and isopropyl (**2.045**) compounds were accessed in order to investigate the possibility of alkyl branching to deliver selectivity over Brd4 (Figure 48).

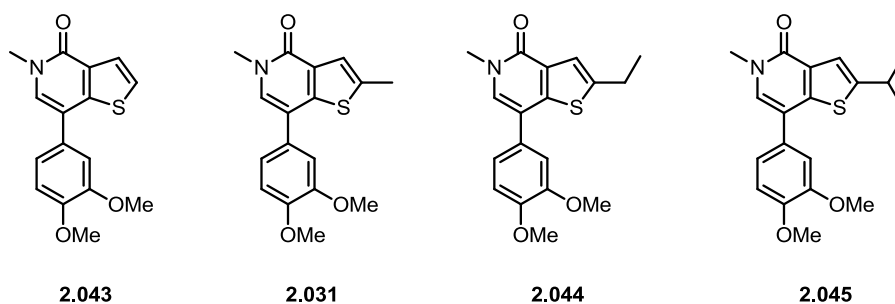
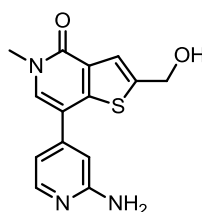


Figure 48: Chemical structures for the various 2-alkyl substituted compounds.

Primary alcohol **2.046**, available from the GSK compound collection,¹⁷³ displayed a Brd9 pIC₅₀ value of 6.7 with 10 fold selectivity over Brd4 (Figure 49).



2.046
 Brd9 pIC₅₀: 6.7 (0.46)
 Brd4 BD1 / BD2 pIC₅₀: 5.7 / 5.3 x10

Figure 49: pIC₅₀ values for compound **2.046** in the bromodomains of Brd9 and Brd4 (BD1 and BD2) as determined by TR-FRET analysis. Brd9 ligand efficiency is shown in parentheses. Selectivity over Brd9 is calculated relative to the maximum value. Data are n≥3.

Despite a different aryl group in the 7-position, making direct SAR comparison difficult, X-ray crystallography¹⁵⁵ of this compound in complex with the bromodomain of Brd9 highlighted an interesting interaction (Figure 50).

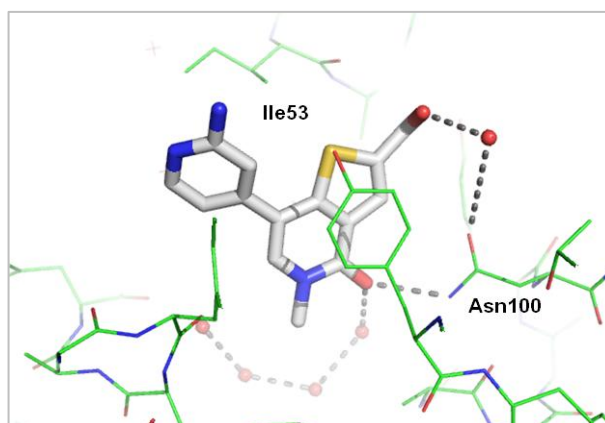


Figure 50: X-Ray crystal structure of compound **2.046** in complex with the bromodomain of Brd9. Grey dashed lines represent the hydrogen-bonds and water molecules are shown as red spheres.

Analysis of the X-ray crystal structure of compound **2.046** indicated that the primary alcohol moiety participates in a water-mediated hydrogen-bond to Asn100. Moving forward with this observation, it was hypothesised that substitution at the C(2) centre

could lead to rotation of the C(2)-CH₂OH bond, potentially placing the hydroxyl group in close proximity to the carbonyl group of Ile53. If successful, the alcohol moiety could form a hydrogen-bond interaction to this carbonyl group, leading to an increase in Brd9 potency and therefore a greater selectivity window over Brd4. In the absence of an X-ray crystal structure of compound **2.046** in Brd4, reasons behind the observed selectivity remain unclear.

In line with the proposed 2-position alkyl substituted compounds, the synthesis and evaluation of primary (**2.047**), secondary (**2.048**)¹⁷³ and tertiary alcohols (**2.049**) would aid investigations into the amount of branching tolerated in the bromodomains of both Brd4 and Brd9 (**Figure 51**).

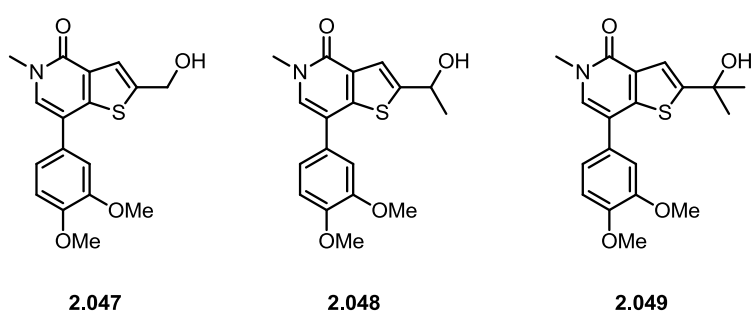
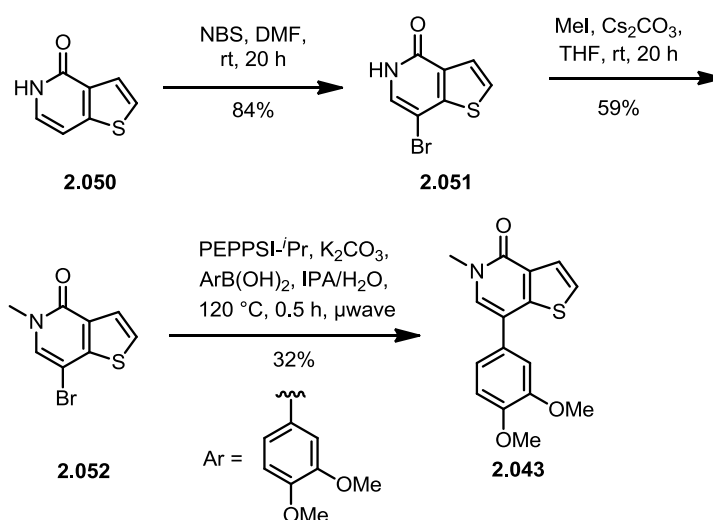


Figure 51: Chemical structures for the various alcohol substituted compounds.

2.3.1.2 Preparation of a truncated TP core and alkyl derivatives

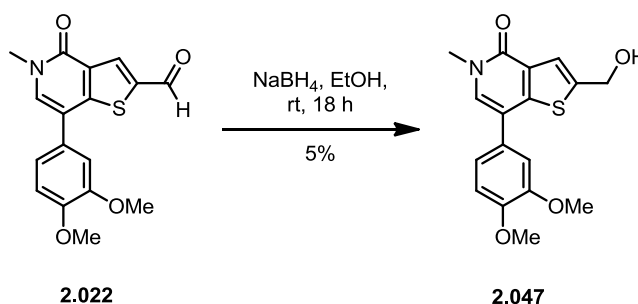
Initial work focused on the synthesis of unfunctionalised TP core **2.043**, which was accessed *via* a 3-step route from the commercially available starting material, **2.050** (**Scheme 12**).



Scheme 12: Synthesis of unfunctionalised TP core **2.043**.

Bromination of **2.050** employing NBS in DMF provided intermediate bromide **2.051** in an 84% yield. Subsequent pyridinone *N*-methylation with MeI and Cs₂CO₃ in THF furnished compound **2.052** in 59% yield. Finally, a Suzuki-Miyaura coupling¹⁶³ using the PEPPSI-*i*Pr precatalyst system¹⁷⁵ provided access to final compound **2.043** in 32% yield.

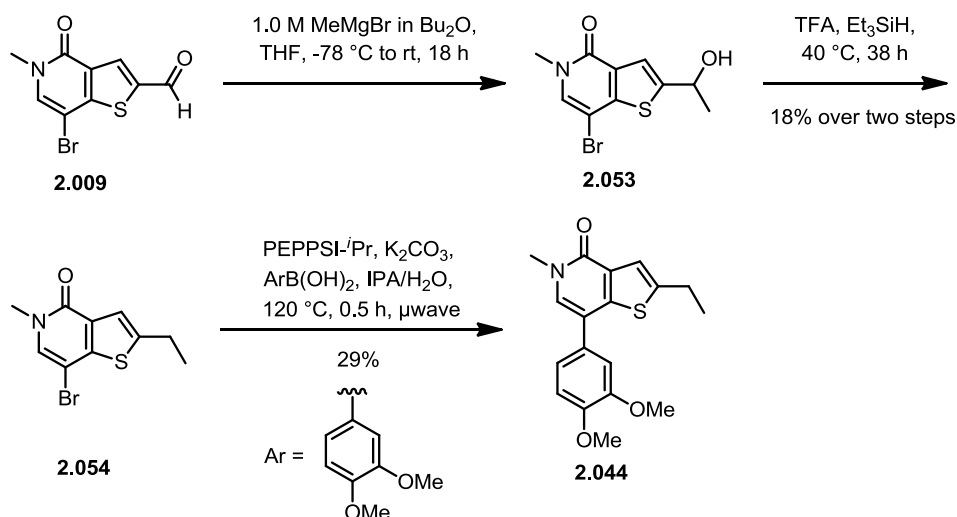
Primary alcohol **2.047** was prepared by reduction of late stage intermediate **2.022** with NaBH₄ in EtOH at room temperature (**Scheme 13**).



Scheme 13: Synthesis of primary alcohol 2.047 from aldehyde 2.022.

A disappointingly low yield was seen under these conditions, due to the poor solubility of aldehyde **2.022**. However, sufficient quantities of material were isolated, and as such, this transformation was not investigated further.

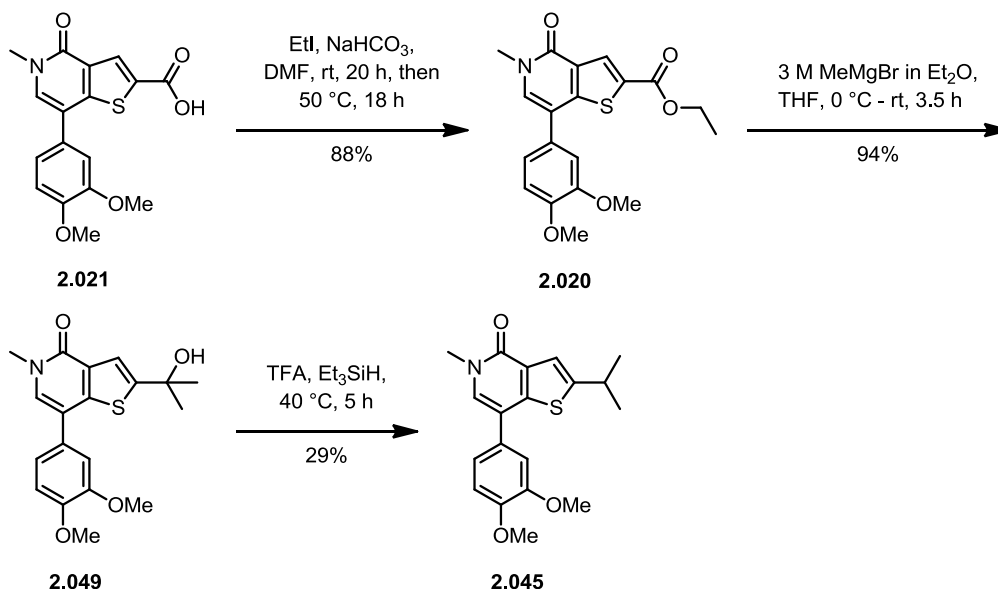
Given the poor solubility of aldehyde **2.022** as discussed above, subsequent chemistry utilised early stage intermediate **2.009**. Ethyl substituted compound **2.044** was accessed *via* Grignard chemistry followed by reduction of the resulting alcohol (**Scheme 14**).



Scheme 14: Synthesis of ethyl substituted TP compound 2.044.

Addition of MeMgBr to aldehyde **2.009** provided secondary alcohol **2.053**, which was subsequently reduced, employing triethylsilane in TFA¹⁷⁶ to give intermediate **2.054**. Finally, a Suzuki-Miyaura¹⁶³ coupling employing PEPPSI-Pr¹⁷⁵ afforded ethyl substituted compound **2.044** in a 29% yield.

Having established a successful route to ethyl substituted compound **2.044**, isopropyl variant **2.045** was prepared using a similar approach (**Scheme 15**).



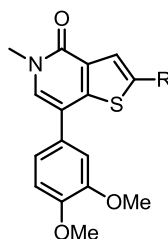
Scheme 15: Synthesis of isopropyl substituted TP core 2.045.

Although successful (88% yield), esterification of acid **2.021** using EtI and NaHCO₃ in DMF proved sluggish, requiring additional EtI and NaHCO₃ after 20 h at room temperature, followed by heating at 50 °C. Following this, addition of excess MeMgBr to ester **2.020** in THF at 0 °C furnished tertiary alcohol **2.049** in a 94% yield. Finally, reduction of the tertiary alcohol moiety using the previously described triethylsilane in TFA conditions¹⁷⁶ furnished isopropyl compound **2.045** in a 29% yield.

Overall, this chemistry provided straight forward access to a range of alkyl and alcohol substituted compounds to explore the steric requirements associated with the 2-position.

2.3.1.3 SAR discussion of alkyl and alcohol modifications

Both the alkyl and alcohol substituted compounds were taken forward for test in an *in vitro* TR-FRET assay from which pIC₅₀ values were calculated (**Figure 31**, step 1a). Fold selectivity for Brd9 is shown relative to the maximum Brd4 pIC₅₀ (**Table 6**).



Entry	Compound Number	R =	Brd9 pIC ₅₀	Brd9 LE	Brd4 BD1 pIC ₅₀	Brd4 BD2 pIC ₅₀	Selectivity
1	2.043	H	7.1	0.46	6.1	5.6	x10
2	2.031	Me	7.3	0.45	6.3	5.9	x10
3	2.044	Et	7.1	0.42	6.2	5.6	x8
4	2.045	<i>i</i> Pr	6.3	0.36	5.8	4.9	x3
5	2.047		6.7	0.40	5.8	5.3	x8
6	2.048 ¹⁷³		6.3	0.36	5.4	4.9	x8
7	2.049		5.4	0.30	5.3	4.5	x1

Table 6: pIC₅₀ values for 2-position alkyl and alcohol derivatives in the bromodomains of Brd9 and Brd4 (BD1 and BD2) as determined by TR-FRET analysis. Selectivity is calculated relative to the maximum Brd4 value. Data are n≥3.

Analysis of the resulting data indicated that increasing the 2-position chain length from H to ethyl had little effect on Brd9 activity and selectivity over Brd4 (entries 1–3). However, increasing alkyl branching from ethyl to isopropyl caused both Brd9 and Brd4 potencies to decrease, suggesting that sterically demanding substituents are not well tolerated in either of these bromodomains (entries 3 and 4). Although the selectivity profiles of compounds **2.031** and **2.044** were not optimal for a chemical probe, they showed high Brd9 activity and ligand efficiency, making them attractive for further modification (entries 2 and 3). An identical SAR pattern was observed for the primary, secondary and tertiary alcohols tested, with both Brd9 and Brd4 potency decreasing with increasing steric demand of the 2-position substituent (entries 5–7).

Comparison of alkyl compounds **2.031**, **2.044** and **2.045** with their alcohol analogues **2.047–2.049** indicated that unfunctionalised alkyl groups were preferred (compare entries 2 and 5, 3 and 6, 4 and 7). The alkyl compounds displayed greater Brd9 potency, ligand efficiency and selectivity over Brd4 compared to the analogous alcohols, suggesting that the hydrogen-bond made by primary alcohol **2.047** (**Figure 50**, page 83) was not necessary for potency.

Given the poor activity and selectivity profile of the 2-position alcohol compounds, no further optimisation was conducted. However, due to the high ligand efficiency of methyl compound **2.031**, extensive SAR exploration was undertaken by colleagues.

2.3.2 Amine derivatives

2.3.2.1 Identification of target compounds

In line with plans to investigate alternative functional groups at the 2-position to optimise selectivity against Brd4, a series of amines were designed for direct comparison with their amide analogues. In particular, these investigations focused on secondary amines, as SAR data for numerous tertiary amines was already available as part of the studies conducted by the BET BD1 programme. To this end, amines **2.055a–d** were accessed (**Figure 52**).

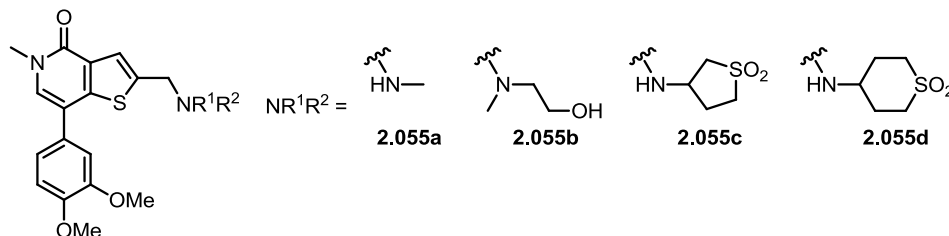
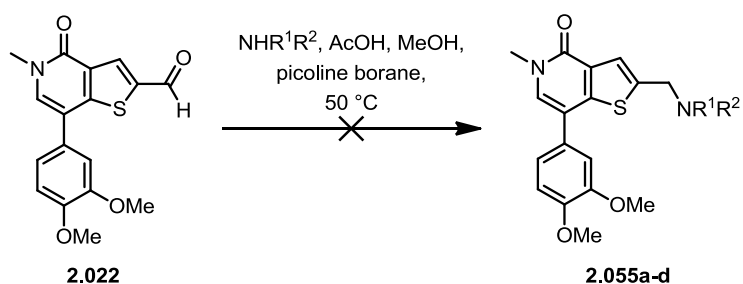


Figure 52: Chemical structures for amines 2.055a–d.

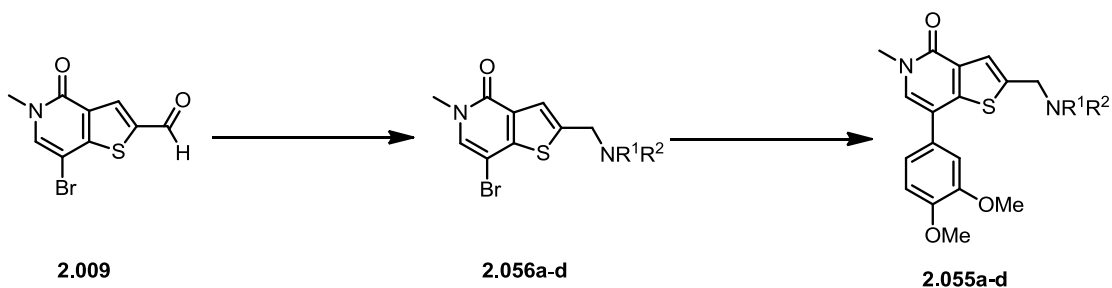
2.3.2.2 Preparation of various amines

Initially, a reductive amination reaction was attempted with aldehyde **2.022**, as this method was more applicable for the introduction of late stage diversity. However, these reactions were unsuccessful providing only starting material as judged by LCMS analysis. As discussed previously (Section 2.3.1.2, page 84), the insolubility of aldehyde **2.022** under the reaction conditions proved problematic (**Scheme 16**).



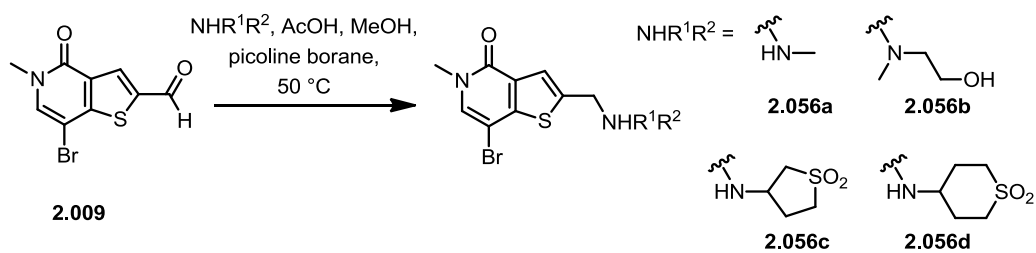
Scheme 16: Attempted synthesis of amines 2.055a–d from aldehyde 2.022.

Therefore, it was expected that synthesis of amines **2.055a–d** could be achieved via a reductive amination of aldehyde **2.009**, followed by a Suzuki-Miyaura¹⁶³ reaction to install the 7-position aryl motif (**Scheme 17**).



Scheme 17: Synthesis of amines 2.055a–d.

Treatment of **2.009** with methylamine hydrochloride, followed by the addition of $\text{NaBH}(\text{OAc})_3$ ¹⁷⁷ resulted in little amine formation, with reduction of the aldehyde to the corresponding alcohol observed as the major product by LCMS (**Table 7**, entry 1).

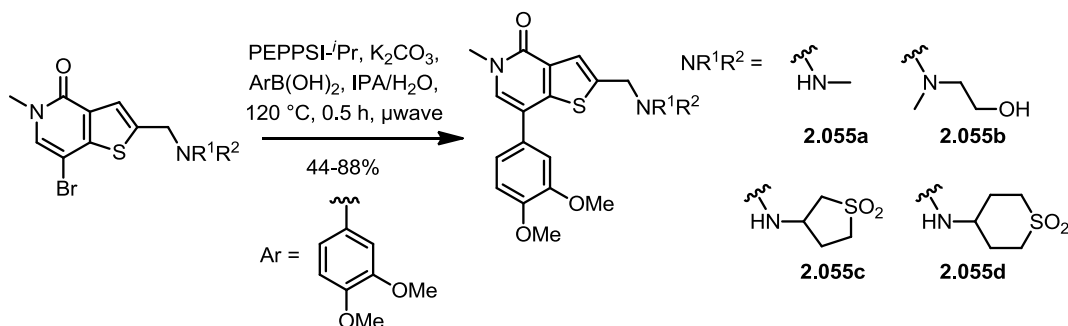


Entry	NHR ¹ R ²	Reagents and Conditions	Result (LCMS peak area)
1		AcOH, rt, 30 min then NaHB(OAc) ₃ , rt, 48 h	17% product 2.056a , 32% reduction by LCMS
2		AcOH, 50 °C, 4 h then picoline borane, 50 °C, 20 h	48% product 2.056a isolated
3		AcOH, rt, 20 min then picoline borane, 50 °C, 18 h	22% product 2.056b isolated
4		AcOH, 50 °C, 3 h then picoline borane, 50 °C, 4 h	95% product 2.056c isolated
5		AcOH, 50 °C, 4 h then picoline borane, 50 °C, 20 h	56% product 2.056d isolated

Table 7: Reagents and conditions for amide coupling of aldehyde 2.009.

In order to drive iminium ion formation and preferential reduction of this intermediate, an alternative reducing agent was investigated. Treatment of aldehyde **2.009** with methylamine hydrochloride in AcOH and MeOH at 50 °C, followed by the addition of picoline borane¹⁷⁸ provided amine **2.056a** in a 48% isolated yield (entry 2). Pleasingly, these conditions also proved successful for the synthesis of amines **2.056b–d**, indicating that picoline borane reacted preferentially with the iminium ion rather than aldehyde **2.009** (entries 3–5).

Subsequent Suzuki-Miyaura coupling¹⁶³ using the PEPPSI-*i*-Pr precatalyst system¹⁷⁵ provided final compounds **2.055a–d** in moderate to good yields (**Scheme 18**).

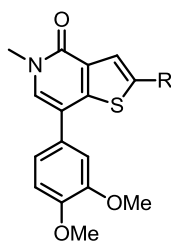


Scheme 18: Synthesis of amines 2.055a–d.

In summary, amines **2.055a–d** were synthesised by reductive amination of early stage aldehyde **2.009** followed by a Suzuki-Miyaura coupling. These amines were taken forward for test to directly compare their activity with their amide analogues.

2.3.2.3 SAR discussion of amines vs amide analogues

Amine derivatives **2.055a–d** were submitted for test in TR-FRET assays against Brd9 and Brd4 from which pIC_{50} values were calculated (**Figure 31**, step 1a). The activity profiles of the various amines and their amide analogues were compared in the bromodomains of Brd9 and Brd4. Fold selectivity for Brd9 is calculated relative to the maximum Brd4 pIC_{50} (**Table 8**).



Entry	Compound Number	R =	Brd9 pIC_{50}	Brd9 LE	Brd4 BD1 pIC_{50}	Brd4 BD2 pIC_{50}	Selectivity
1	2.055a		6.2	0.35	5.9	4.7	x2.5
2	2.018c		6.9	0.38	6.7	6.9	x1
3	2.055b		6.2	0.31	5.9	4.7	x3
4	2.030q		5.4	0.26	5.0	4.5	x3
5	2.055c		6.7	0.31	6.7	5.0	x1
6	2.030b		7.8	0.34	7.3	7.0	x3
7	2.055d		6.9	0.30	6.1	4.8	x6
8	2.030a		7.9	0.34	7.3	7.0	x4

Table 8: pIC_{50} values for selected amides and amines in the bromodomains of Brd9 and Brd4 (BD1 and BD2) as determined by TR-FRET analysis. Selectivity is calculated relative to the maximum Brd4 value. Data are $n \geq 3$.

In general, Brd9 ligand efficiency values were uniformly high, with the exception of tertiary amide **2.030q**. All secondary amines tested were less active in Brd9 than their amide analogues. However, tertiary amine **2.055b** displayed a 6 fold increase in both Brd9 and Brd4 BD1 potencies relative to amide **2.030q** (compare entries 3 and 4). In contrast, secondary amines **2.055a**, **c** and **d** showed approximately 10 fold reduction in Brd9 potency compared to the corresponding amides (entries 1 and 2 and 5–8). This suggested that the amine substituent occupied a different region of space compared to the analogous amide, and therefore could not form a bidentate interaction to Asn100. X-Ray crystallography¹⁵⁵ of amide **2.030a** (left) and amine **2.055d** (right) in complex with Brd9 supports this hypothesis. The different conformations of the sulfone moiety observed for amide **2.030a** and amine **2.055d** was attributed to the change in hybridisation of the linker C atom from sp^2 to sp^3 , respectively (**Figure 53**).

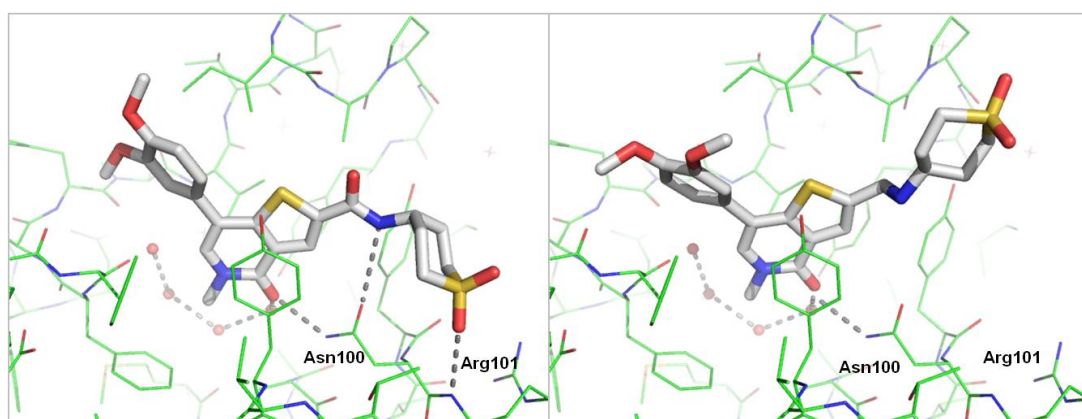


Figure 53: X-Ray crystallography of amide **2.030a** (left, PDB code = 4UIU) and amine **2.055d** (right) in complex with the bromodomain of Brd9. Hydrogen-bonds are shown as grey dashed lines and water molecules as red spheres.

The secondary amines provided little selectivity over Brd4, with no significant difference compared to their amide analogues. This suggested that the amines adopted similar conformations in both bromodomains, accounting for the reduction in both Brd9 and Brd4 potency upon conversion of amide to the analogous amine.

It is of note that the amines displayed good levels of selectivity over Brd4 BD2, whilst the amides were almost equipotent. The basis for this selectivity can be rationalised through the use of X-ray crystallography¹⁵⁵ of compound **2.055d** in complex with Brd4 BD1 (left) and modelled in BD2 (right) (**Figure 54**).

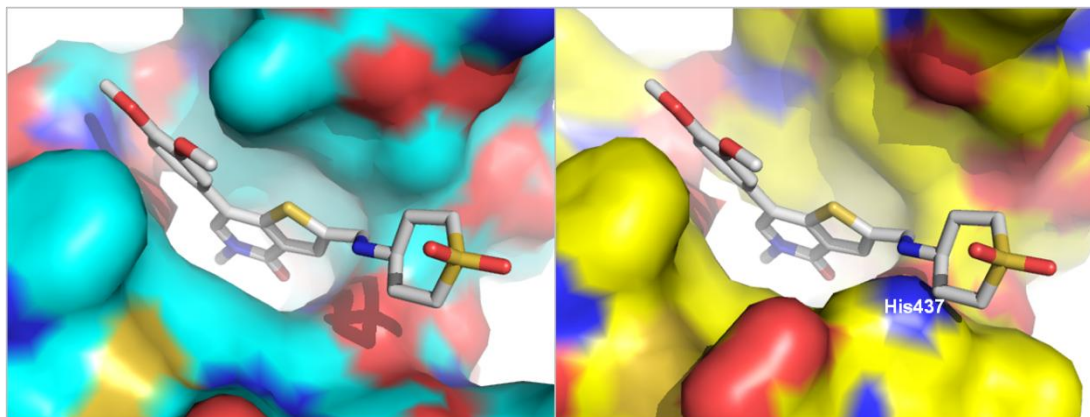


Figure 54: X-Ray crystallography of amine **2.055d** in complex with Brd4 BD1 (left) and modelled in Brd4 BD2 (right).

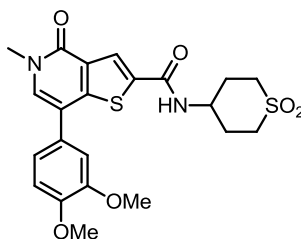
These X-ray crystal structures indicate that the 6-membered sulfone substituent of **2.055d** sits unhindered in Brd4 BD1, displaying good shape complementarity with the binding pocket. In contrast, the cyclic sulfone appears to clash with His437, present in Brd4 BD2 only, presumably leading to a less favourable binding mode.

Although the amines tested were found to be more selective for Brd9, their activity was reduced compared to the amide analogues. Considering this result, no further investigations were conducted with this series.

2.3.3 Design and synthesis of amidine derivatives

2.3.3.1 Identification of target compounds

In line with efforts to investigate alternative functional groups at the 2-position, focus was directed towards optimisation of secondary amide **2.030a**, the most potent compound synthesised to date (**Figure 55**).



2.030a
 Brd9 pIC₅₀: 7.9 (0.36)
 Brd4 BD1 / BD2 pIC₅₀: 7.3 / 7.0 x4

Figure 55: pIC₅₀ values for compound **2.030a** in the bromodomains of Brd9 and Brd4 (BD1 and BD2) as determined by TR-FRET analysis. Brd9 ligand efficiency is shown in parentheses. Selectivity is calculated relative to the maximum Brd4 value. Data are n≥3.

Analysis of the X-ray crystal structure¹⁵⁵ of amide **2.030a** in complex with Brd9 indicated that the amide carbonyl group sat within 4 Å of the carbonyl of Ile53, located in the peptide backbone (**Figure 44**, page 74). Although the vectors appeared challenging, it was hypothesised that replacement of the amide carbonyl group with a HBD moiety could increase activity. This could be achieved either through a direct hydrogen-bond to the backbone carbonyl of Ile53 or *via* a through-water interaction. Furthermore, it was believed that the alternative linker should be capable of maintaining the bidentate interaction to Asn100 as observed for amide **2.030a**.

Further analysis of the X-ray crystal structure of **2.030a** in complex with Brd9 (green) overlaid with apo Brd4 BD1 (blue) revealed a key residue change in close proximity to the amide moiety of the ligand (**Figure 56**).

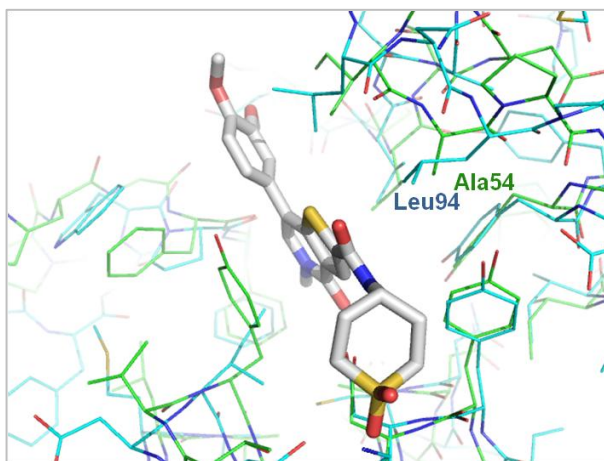
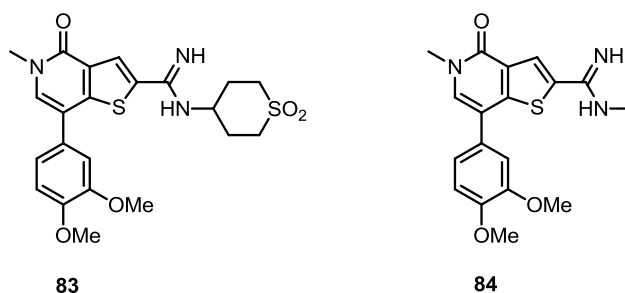


Figure 56: X-Ray crystal structure of amide **2.030a** in complex with Brd9 (green, PDB code = 4UIU) overlaid with apo Brd4 BD1 (blue, PDB code = 4UIZ).

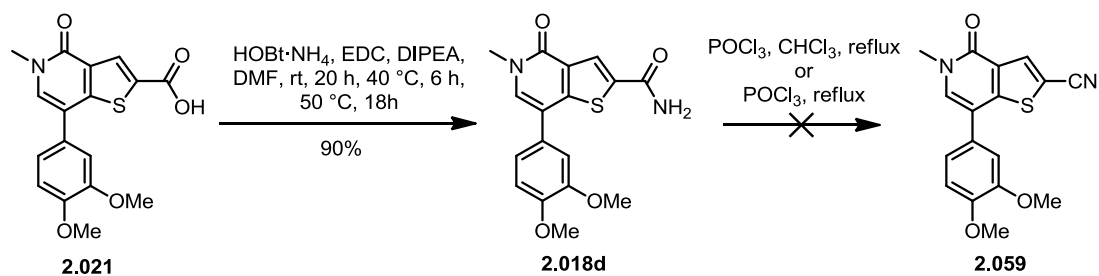
It was proposed that selectivity for Brd9 could be gained through exploitation of a key residue change moving from Brd9 to Brd4 BD1. The region of the binding pocket in which the amidine moiety was proposed to sit, is more hydrophobic in Brd4 BD1 (Leu94) compared to Brd9 (Ala54). Taking these factors into consideration, it was proposed that the amide moiety should be replaced by the corresponding amidine. Given the basic nature of the amidine group, it was hypothesised that when protonated and therefore charged, it would sit less favourably in the more hydrophobic environment of Brd4 BD1.

In order to explore this hypothesis further, amidines **2.057** and **2.058** were selected for direct comparison to their amide analogues **2.030a** and **2.018c**, respectively (**Figure 57**).

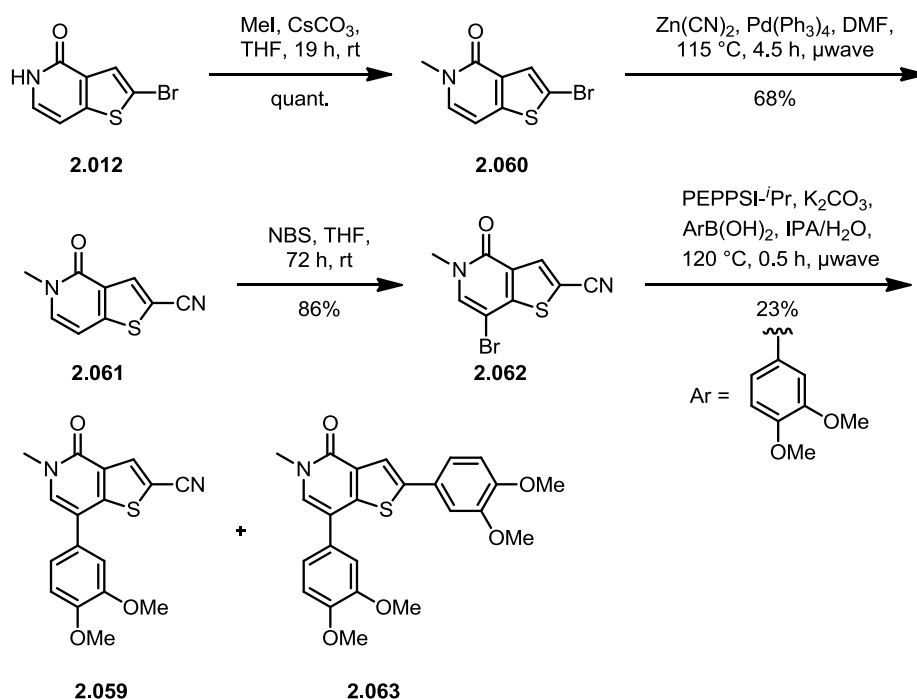
Figure 57: Amidines **2.057** and **2.058** selected for synthesis.

2.3.3.2 Synthesis of amidine compounds

It was envisaged that the amidine functionality could be accessed *via* a Pinner reaction¹⁷⁹ from the corresponding nitrile precursor. Initially, the aim was to preinstall the dimethoxyphenyl motif so that a series of Pinner reactions to afford the various amidines could be explored. To start with, focus was placed on accessing nitrile intermediate **2.059** from acid **2.021** (Scheme 19).

Scheme 19: Attempted synthesis of nitrile intermediate **2.059**.

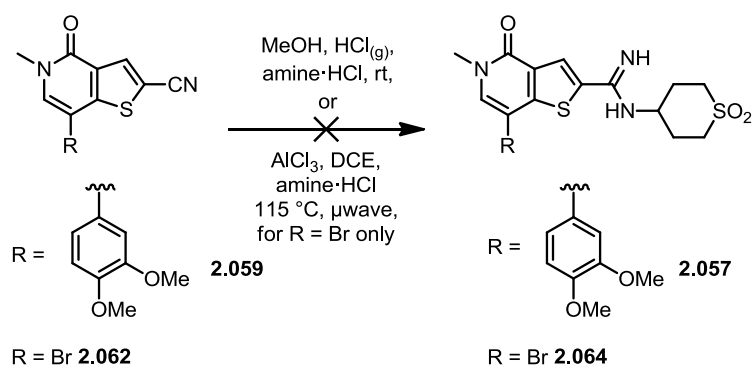
Acid **2.021** was treated with HOBT·NH₄ under standard peptide coupling conditions, employing EDC and DIPEA in DMF.¹⁶² This afforded primary carboxamide **2.018d** in a 90% yield. However, attempts to dehydrate **2.018d** to give nitrile **2.059** proved unsuccessful despite treatment with 3 equivalents of POCl₃ in CHCl₃ at reflux and neat POCl₃.¹⁸⁰ It was believed that solubility issues under these conditions prevented reaction. Given this result, an alternative route was investigated (Scheme 20).



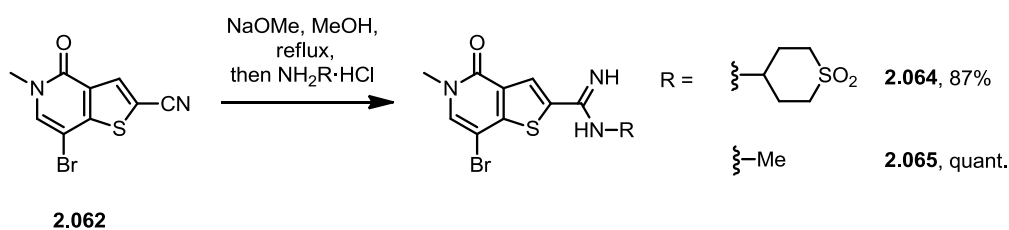
Scheme 20: Synthesis of nitrile intermediate 2.059.

Considering the unreactive nature of amide **2.018d** under the reported conditions, attempts were made to access compound **2.059** via a Negishi cyanation¹⁸¹ reaction utilising early stage intermediate **2.060**. Alkylation of known compound **2.012**¹⁵⁶ using MeI and Cs₂CO₃ proved straight forward, providing **2.060** in quantitative yields. Following this, installation of the nitrile moiety was achieved using Zn(CN)₂ and Pd(PPh₃)₄ under microwave irradiation.¹⁸¹ Pleasingly, these conditions afforded intermediate **2.061** in a 68% yield. Subsequent electrophilic bromination with NBS in THF gave compound **2.062**, to which the dimethoxyphenyl motif was installed via a Suzuki-Miyaura coupling.¹⁶³ Employing the PEPPSI-*i*Pr precatalyst conditions previously described, nitrile **2.059** was obtained in a 23% yield. Although key intermediate **2.059** was synthesised successfully, it was not the major product of the reaction. ¹H NMR spectroscopy and LCMS analysis indicated that the dimethoxyphenyl motif had also been introduced at the 2-position to deliver compound **2.063**. As this reaction was not productive for the synthesis of nitrile intermediate **2.059**, no further studies were conducted. It was proposed that formation of by-product **2.063** could have proceeded via a decarboxylation mechanism. However, literature in this area reports the requirement for copper or silver additives to facilitate this reaction.^{182,183,184}

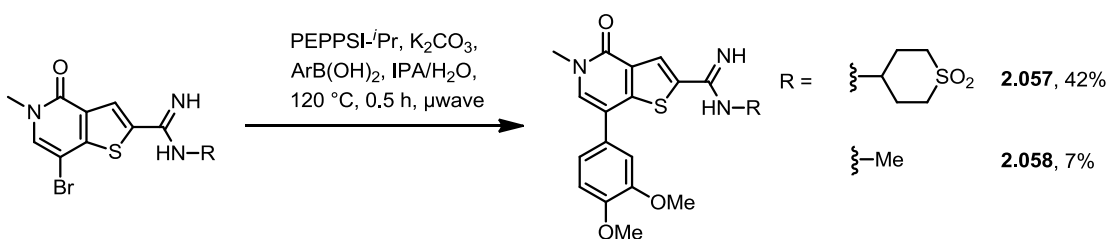
Nonetheless, the poor yield for the final step of this sequence (Suzuki-Miyaura coupling, 23%) made it less attractive for SAR exploration, as it would be difficult to synthesise high quantities of this final intermediate. However, 60 mg of nitrile **2.059** was prepared to attempt installation of the amidine functionality. Initially, HCl was bubbled through MeOH, followed by the addition of nitrile **2.059** and the appropriate amine¹⁷⁹ (**Scheme 21**).



No product was observed under these conditions as judged by LCMS analysis. It was hypothesised that the limited solubility of **2.059** in MeOH could be affecting reactivity; therefore, early stage nitrile compound **2.062** was reacted under identical conditions. Despite the improved solubility of **2.062** no desired product was observed by LCMS analysis. With this in mind, nitrile **2.062** was heated in the presence of AlCl_3 ,¹⁸⁵ in an attempt to form amidine **2.064**. However, only starting material was observed by LCMS, therefore an alternative synthetic strategy was employed (**Scheme 22**).



Pleasingly, treatment of nitrile **2.062** with NaOMe solution in MeOH, followed by the addition of the appropriate amine hydrochloride¹⁸⁶ gave amidines **2.064** and **2.065** in excellent yields. With these intermediates in hand, the dimethoxyphenyl motif was installed *via* a Suzuki-Miyaura coupling¹⁶³ with the PEPPSI-*i*Pr precatalyst¹⁷⁵ (**Scheme 23**).

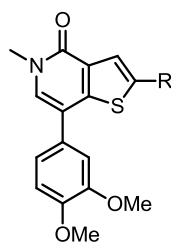


Scheme 23: Synthesis of amidines **2.057** and **2.058** from compounds **2.064** and **2.065**, respectively.

This chemistry provided easy access to the desired amidines *via* a Pinner reaction utilising NaOMe solution in MeOH. Following this, compounds **2.057** and **2.058** were progressed for testing to investigate the effect of the amidine linker on Brd9 activity and selectivity over Brd4.

2.3.3.3 SAR discussion of amidines and their amide analogues

Amidines **2.057** and **2.058** were submitted for test in a TR-FRET assay from which pIC_{50} values were calculated (**Figure 31**, step 1a). The activity profiles of these amidines and their amide analogues were compared in the bromodomains of Brd9 and Brd4. As before, fold selectivity for Brd9 is calculated relative to the maximum Brd4 value (**Table 9**).



Entry	Compound Number	R =	Brd9 pIC_{50}	Brd9 LE	Brd4 BD1 pIC_{50}	Brd4 BD2 pIC_{50}	Selectivity
1	2.018c		6.9	0.38	6.7	6.9	x1
2	2.030a		7.9	0.34	7.3	7.0	x4
3	2.058		7.1	0.40	5.9	5.9	x16
4	2.057		8.1	0.35	6.4	5.4	x50

Table 9: pIC_{50} values for compounds **2.018c**, **2.030a**, **2.057** and **2.058** in the bromodomains of Brd9 and Brd4 (BD1 and BD2) as determined by TR-FRET analysis. Selectivity is calculated relative to the maximum Brd4 value. Data are $n \geq 3$.

Critically, both amidines **2.057** and **2.058** retained the Brd9 activity of their amide analogues with improved levels of selectivity over Brd4. For example, transformation of methyl amide **2.018c** into its amidine analogue **2.058** caused selectivity to increase to 16 fold (compare entries 1 and 3). Furthermore, amidine **2.057** was 50 fold selective over Brd4, a significant improvement on the 4 fold selectivity seen for amide **2.030a** (entries 2 and 4). In agreement with the amide data, amidine **2.058** was 10 fold more active in Brd9 than the methyl amidine analogue, **2.018c** (compare entries 3 and 4). This suggested that like amide **2.030a**, the sulfone moiety of **2.057** was forming a hydrogen-bond in Brd9, providing an increase in potency (**Figure 44**, page 74).

With the exception of tertiary amide **2.005**, the amidines represented the first 2-position substituents to deliver significant selectivity over Brd4, providing confidence in the idea that this functional group sits less favourably in a more hydrophobic environment (Ala54 in Brd9 vs. Leu94 in Brd4 BD1). Considering the excellent Brd9 potency and selectivity provided by amidine **2.057**, this compound was taken forward for further optimisation.

2.3.4 Square array

2.3.4.1 Design of array

At this point in the project, additional assays became available in order to assess selectivity over a broader range of bromodomains (**Figure 31**, step 2). As such, a series of compounds from the TP series were screened in Brd7 and BRPF1 TR-FRET assays from which valuable SAR was generated. An understanding of selectivity over these bromodomains was of particular importance as they belong to the same family as Brd9, indicating high sequence similarity (**Figure 8**, page 7). The compound set tested included molecules synthesised by colleagues as part of attempts to improve the selectivity of secondary amide **2.030a**. It was discovered that exchange of the 7-position dimethoxyphenyl group for saturated ring systems¹⁸⁷ significantly improved selectivity over Brd4 (**Figure 58**).

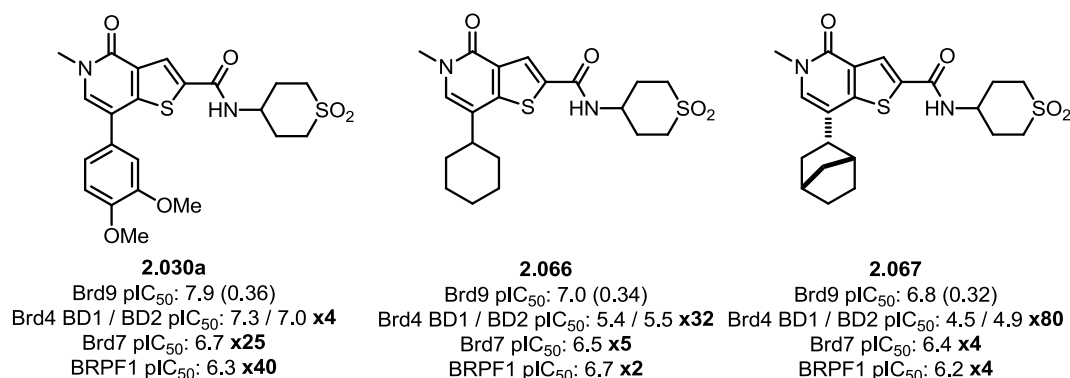


Figure 58: pIC₅₀ values for compounds **2.030a**, **2.066** and **2.067**¹⁸⁸ in the bromodomains of Brd9, Brd4 (BD1 and BD2), Brd7 and BRPF1 as determined by TR-FRET analysis. Brd9 ligand efficiency values are shown in parentheses. Brd9 selectivity is calculated based on pK_i values (see Section 2.1.2.1, page 45) and selectivity over Brd4 relative to the maximum value. Data are n≥3.

It was proposed that the 3-dimensional structure provided by the saturated 7-position substituents caused a steric clash in the narrower ZA channel of Brd4, leading to a less favourable binding mode (**Figure 32**, page 58). For example, exchange of the dimethoxyphenyl group in compound **2.030a** for a cyclohexyl ring as in **2.066** caused selectivity over Brd4 to increase from 4 to 32 fold. Furthermore, the introduction of a bridged ring system, provided additional selectivity, with compound **2.067** delivering 80 fold selectivity over Brd4. However, the introduction of saturated ring systems caused both Brd9 and Brd4 activities to decrease, whilst Brd7 and BRPF1 activities remained approximately constant. Examination of the additional Brd7 and BRPF1 data indicated that exchange of aryl rings for saturated systems had a detrimental effect on selectivity over these bromodomains. As Brd9 activity decreased and Brd7 and BRPF1 potencies remained constant, the selectivity windows for compounds **2.066** and **2.067** were reduced. For example, dimethoxyphenyl substituted compound **2.030a** showed 25 and 40 fold selectivity over Brd7 and BRPF1, respectively, whilst cyclohexyl compound **2.066** displayed little selectivity over these bromodomains (≤5 fold). These data indicated that a 7-position aryl ring was required for Brd9 potency as well as selectivity over Brd7 and BRPF1. However, saturated ring systems provided improved selectivity over Brd4.

The observed selectivity with **2.030a** over the highly homologous Brd7 was particularly surprising given its proximity to Brd9 on the phylogenetic tree (**Figure 8**, page 7). These bromodomains share 85% sequence similarity across the residues present within the KAc binding pocket (**Table 10**).

	BRD9	BRD4 BD1	BRD7	BRPF1	
1	GLY43	TRP81	ALA154	ASN633	WPF motif
2	PHE44	PRO82	PHE155	ILE634	WPF motif
3	PHE45	PHE83	PHE156	PHE635	WPF motif
4	ALA46	GLN84	SER157	SER636	ZA channel
5	PHE47	GLN85	PHE158	GLU637	ZA channel
6	PRO48	PRO86	PRO159	PRO638	ZA channel
7	VAL49	VAL87	VAL160	VAL639	ZA channel
8	THR50	ASP88	THR161	PRO640	ZA loop
9	ASP51	ALA89	ASP162	LEU641	ZA loop
10	INS53	LYS91	INS164	INS643	ZA loop
11	INS53	LEU92	INS164	INS643	ZA loop
12	ILE53	ASN93	ILE164	GLU643	ZA loop
13	ALA54	LEU94	ALA165	VAL644	ZA loop
14	TYR57	TYR97	TYR168	TYR647	Water-binding Tyr
15	SER58	TYR98	SER169	LEU648	
16	ILE61	ILE101	ILE172	ILE651	
17	MET92	MET132	MET203	ILE682	
18	ASN95	ASN135	ASN206	ASN685	
19	ALA96	CYS136	ALA207	CYS686	Conserved Ala
20	TYR99	TYR139	TYR210	TYR689	Conserved Tyr
21	ASN100	ASN140	ASN211	ASN690	Conserved Asn
22	THR104	ASP144	THR215	THR694	
23	VAL105	ASP145	ILE216	ILE695	
24	TYR106	ILE146	TYR217	PHE696	Gatekeeper
25	TYR107	VAL147	TYR218	TYR697	
26	LEU109	MET149	ALA220	ALA699	
27	ALA110	ALA150	ALA221	ALA700	

Table 10: Sequence similarity of Brd4 BD1, Brd9, Brd7 and BRPF1 across the KAc binding pocket. Residues which are identical to those in Brd9 are shown in green; residues which are similar to those in Brd9 are shown in orange; residues which are different to those in Brd9 are shown in red. Grey boxes indicate an amino acid insertion.

Although there is an NMR derived structure reported for Brd7, there is no crystal structure published to date.¹⁸⁹ Therefore, reasons behind the observed selectivity over this bromodomain remain unclear. Potentially, selectivity arose from the differences in the constituent amino acids of the WPF shelf (residues 1–3, Brd4 nomenclature) and ZA channels (residues 4–7) of these bromodomains. In Brd9, Gly43 is replaced by Ala154 in the WPF region of Brd7 and Ala46 by Ser157 in the ZA channel. These key changes could have provided a difference in the architecture of these binding regions, potentially altering the conformation of other residues in the ZA channel.

Pleasingly, X-ray crystallography¹⁵⁵ of BRPF1 was available, aiding investigations into the selectivity shown by amide **2.030a** (Figure 59).

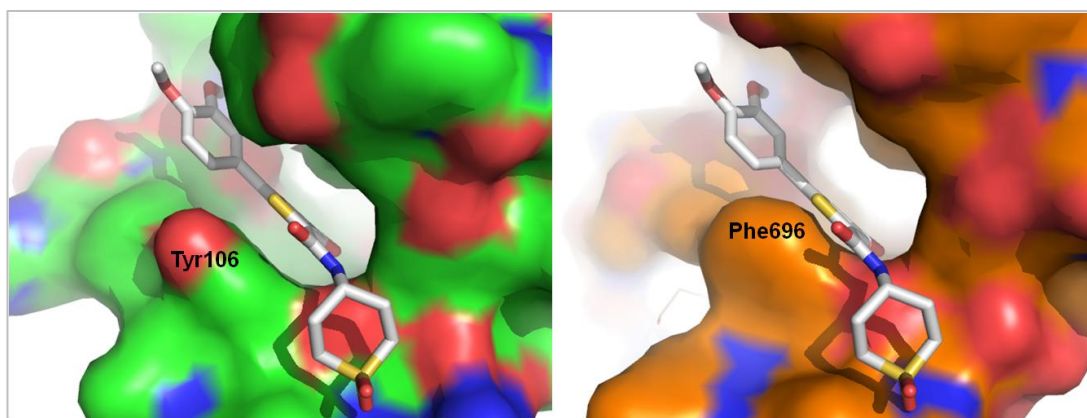


Figure 59: X-Ray crystallography of amide **2.030a** in complex with the bromodomain of Brd9 (PDB code = 4UIU, left) and modelled in BRPF1 (orange, right).

X-Ray crystallography of amide **2.030a** in complex with Brd9 (left, green) compared to that of **2.030a** modelled in BRPF1 (right, orange) provides good evidence for the observed selectivity. The TP core of **2.030a** sits in close proximity to the gate keeper residues present in each bromodomain. In Brd9, this is Tyr106, which is replaced by Phe696 in BRPF1. The above structures indicate that the Phe696 gatekeeper of BRPF1 sits much closer to the ligand than the equivalent residue in Brd9, presumably leading to a steric clash and less favourable binding mode.

Given this exciting result, a square array was designed to explore the potential to deliver selectivity over Brd4 and the additional non-BET bromodomains. This array would provide multiple data points, quantifying the affect of a particular group on the SAR. As 7-position aryl rings delivered high Brd9 potency and selectivity over Brd7 and BRPF1, the array aimed to incorporate various aromatic rings into this region. The design of the array was aided by a Free-Wilson analysis of the data from all the compounds tested in Brd9 to date.

Free-Wilson analysis¹⁹⁰ is a useful method for investigating the SAR of a particular chemotype with multiple regions of structural diversity. This mathematical model splits a template into its constituent parts quantifying their contribution, based on their activities (**Figure 60**).

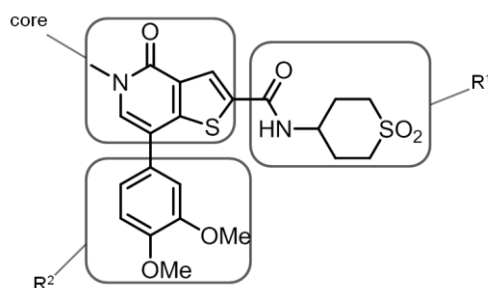


Figure 60: Compound 2.030a split into its constituent parts according to the Free-Wilson model. The total response observed (pIC_{50} value) is equivalent to the sum of the constituent parts (**Equation 6**).

Response = effect of core + effect of R^1 substituent + effect of R^2 substituent

Equation 6: Free-Wilson analysis of activity, based on the constituent parts of a molecule.

The effect of each substituent is quantified based on the following assumptions:

1. The core makes a constant contribution
2. All contributions are additive
3. There are no interactions between the core and substituents
4. There are no interactions between the substituents

This calculation was performed on a 553 compound set to provide a set of scores for individual substituents, with the 2-position of the TP core representing R^1 and the 7-position R^2 . With the idea that maximum knowledge could be gained from varying both the 2 and 7-positions of the core, a 6 (2-position) \times 4 (7-position) array was designed.

2.3.4.1.1 2-Position substituents (R^1)

As the majority of work on this template had focused on the 2-position, there was a greater variety of substituents from which to select 6 different groups for the square array (**Figure 61**).

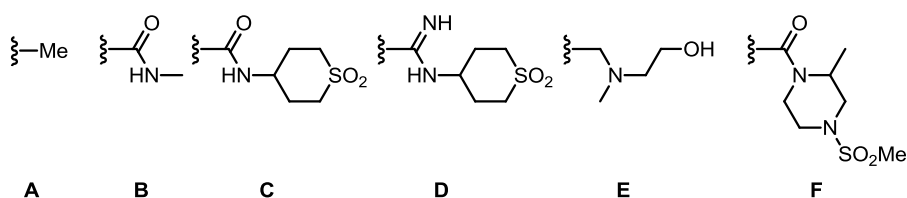


Figure 61: 2-Position substituents selected for square array.

In addition to the scores provided by the Free-Wilson analysis, substituents were selected in order to provide variety in terms of both size and functional group. For

example, groups **A–C** were included to represent small, medium and large substituents, respectively. When in combination with a 7-position dimethoxyphenyl moiety, groups **A–C** showed high Brd9 potency with improved ligand efficiency **A** and **B** (Brd9 $pI_{C_{50}}$ values of 7.4, 6.9 and 7.9, respectively). Amide **C** was also ranked highly by the Free-Wilson model for selectivity over Brd4, on the basis of 5 data points. Amidine **D** was selected due to its high Brd9 potency and selectivity over Brd4 as discussed in the previous section (Section 2.3.3, page 93). Amine **E** was included for the purposes of variety and tertiary amide **F** was ranked highest by the Free-Wilson model for selectivity over Brd4, albeit on the basis of a single data point.

2.3.4.1.2 7-Position substituents (R^2)

Four aryl rings were selected for installation at the 7-position of the TP template (**Figure 62**).

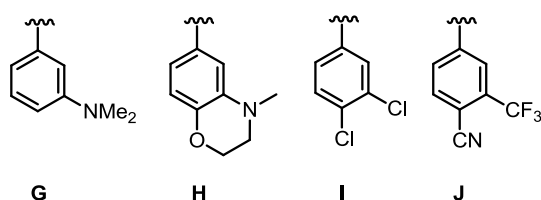
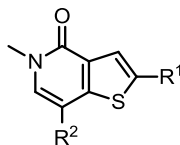


Figure 62: 7-Position substituents selected for square array.

The Free-Wilson Model indicated that substituent **G** was the most selective aryl ring, closely followed by **J**. Substituent **H** was identified as the ring which displayed the best combination of potency and selectivity as judged by the model. Aryl rings **I** and **J** were ranked highly in terms of selectivity but were also included for variety. Substituents **G** and **H** both contain electron-donating substituents, whereas **I** and **J** contain electron-withdrawing groups, providing insights into electronic requirements for selectivity.

These substituents, along with those in the 2-position have been included in **Table 11**, giving the 24 possible combinations of these groups.

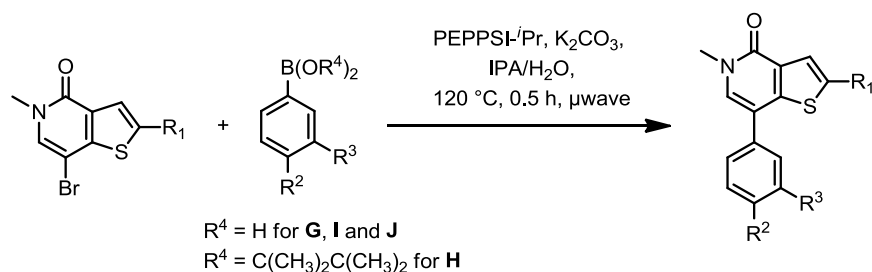


		R ¹					
R ²		2.068a	2.069a	2.070a	2.071a	2.072a	2.073a
		2.068b	2.069b	2.070b	2.071b	2.072b	2.073b
		2.068c	2.069c	2.070c	2.071c	2.072c	2.073c
		2.068d	2.069d	2.070d	2.071d	2.072d	2.073d

Table 11: The 24 possible combinations from 2- and 7-position substituents included in the square array.

2.3.4.2 Synthesis of square array

It was envisioned that the 24 compounds could be synthesised in parallel *via* a Suzuki-Miyaura coupling¹⁶³ with the 2-substituted TP bromide and the appropriate commercially available boronic acid/ester (**Scheme 24**).



Scheme 24: General scheme for the synthesis of square array compounds *via* a Suzuki-Miyaura coupling.

Compounds **2.074** and **2.075** were available from the GSK compound collection and the synthesis of **2.017c** (**Scheme 4**, page 64), **2.064** (**Scheme 22**, page 97), **2.056b** (**Scheme 17**, page 89) was conducted using previously reported chemistry (**Figure 63**).

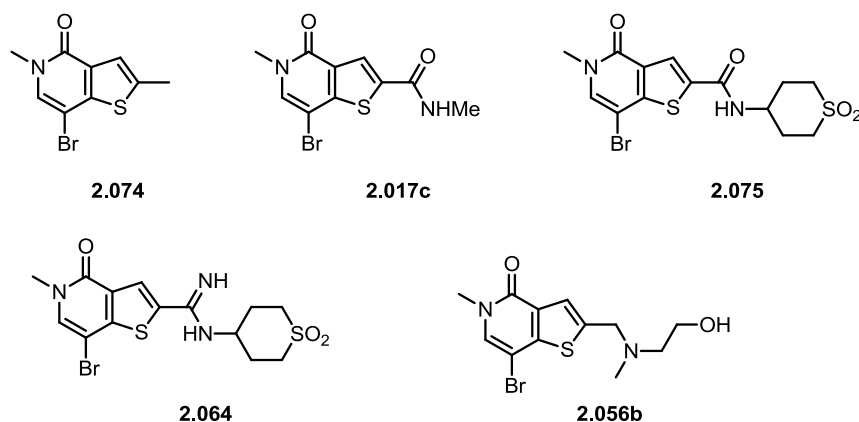
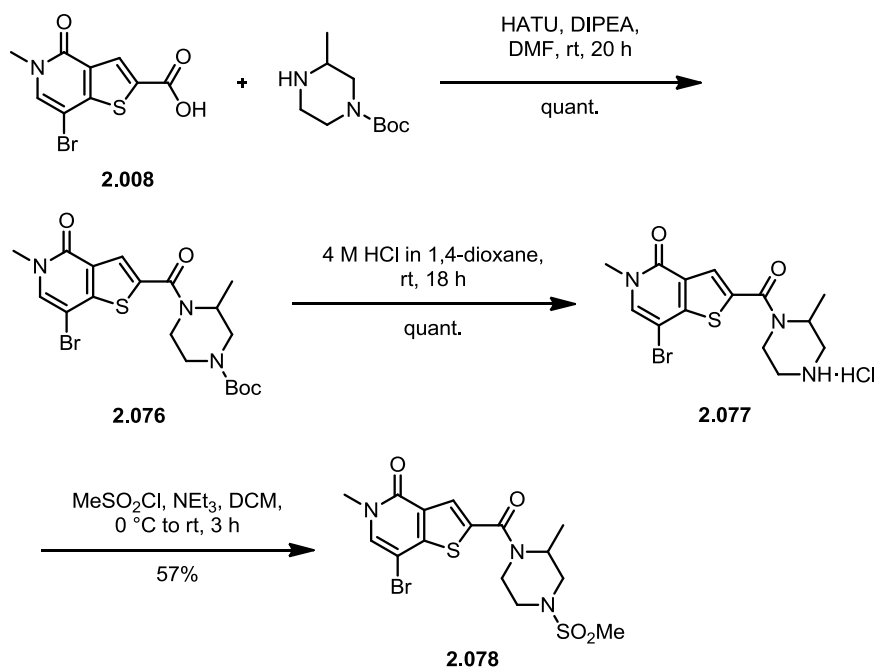


Figure 63: Compounds 2.074 and 2.075 available from the GSK compound collection. Compounds 2.017c, 2.056b and 2.064, synthesised using previously reported chemistry.

Tertiary amide **2.078** was accessed *via* an amide coupling using the commercially available Boc protected 3-methyl piperazine (**Scheme 25**).

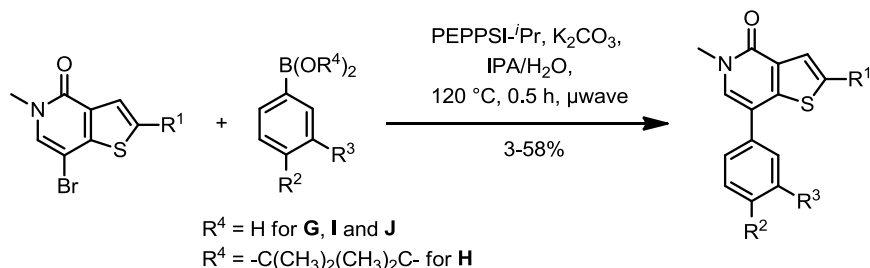


Scheme 25: Synthesis of amide 2.078 from acid 2.008.

An amide coupling of acid **2.008** using HATU and DIPEA in DMF provided intermediate **2.076** in quantitative yield. Following this, 4 M HCl in 1,4-dioxane was

employed for removal of the Boc protecting group, affording **2.077** in a quantitative yield. Subsequent mesylation with methane sulfonyl chloride furnished desired amide **2.078** in a 57% yield.

With the substituted cores **2.017c**, **2.056b**, **2.064**, **2.074** and **2.075** in hand, a series of Suzuki-Miyaura couplings¹⁶³ were conducted in parallel to install the 7-position aryl motif (**Scheme 26**).

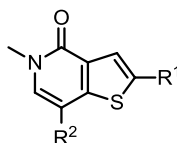


Scheme 26: General scheme for the synthesis of square array compounds *via* a Suzuki-Miyaura coupling.

Each reaction was performed on 0.15 mmol scale using the PEPPSI-*Pr* precatalyst¹⁷⁵ system as previously described. Of the 24 reactions carried out, 7 proved unsuccessful, due to difficulties in obtaining suitably pure compound for test. Five of these compounds were synthesised independently to provide a complete data set. Attempts to re-synthesise compounds **2.073a** and **c** were unsuccessful due to further difficulties during purification. Therefore, these compounds are not included in the results chart (**Table 12**).

2.3.4.3 SAR discussion of square array compounds

The square array compounds were submitted for test in a TR-FRET assay to determine their affinities for Brd9, Brd4 (BD1 and BD2), Brd7 and BRPF1 (**Figure 31**, steps 1a and 3, **Table 12**).



		R ²			
R ¹		2.068a Brd9: 6.9 Brd4: 6.1, 5.6 Brd7: 5.9 BRPF1: 5.4	2.068b Brd9: 7.0 Brd4: 6.4, 5.8 Brd7: 6.0 BRPF1: 5.4	2.068c ¹⁹¹ Brd9: 6.5 Brd4: <4.3, <4.3 Brd7: 4.8 BRPF1: <4.0	2.068d ¹⁹² Brd9: 6.9 Brd4: <4.3, <4.3 Brd7: 5.7 BRPF1: <4.0
		2.069a Brd9: 6.4 Brd4: 6.5, 6.6 Brd7: 5.5 BRPF1: 5.5	2.069b Brd9: 6.6 Brd4: 6.7, 6.9 Brd7: 5.6 BRPF1: 5.7	2.069c * ¹⁹³ Brd9: 5.9 Brd4: 5.8, 6.0 Brd7: 5.0 BRPF1: <4.0	2.069d ¹⁹⁴ Brd9: 6.1 Brd4: 4.5, <4.3 Brd7: 4.5 BRPF1: <4.0
		2.070a Brd9: 7.7 Brd4: 7.2, 6.8 Brd7: 6.7 BRPF1: 6.5	2.070b Brd9: 7.9 Brd4: 7.3, 6.9 Brd7: 6.8 BRPF1: 6.4	2.070c ¹⁹⁵ Brd9: 7.4 Brd4: 6.8, 4.3 Brd7: 5.6 BRPF1: 6.1	2.070d * Brd9: 7.4 Brd4: 5.5, 5.5 Brd7: 5.9 BRPF1: 5.6
		2.071a Brd9: 8.0 Brd4: 6.3, 5.4 Brd7: 6.8 BRPF1: 6.1	2.071b Brd9: 8.0 Brd4: 6.5, 5.6 Brd7: 6.8 BRPF1: 6.0	2.071c ** Brd9: 7.8 Brd4: 6.0, 5.0 Brd7: 6.7 BRPF1: 5.7	2.071d ¹⁹⁶ Brd9: 7.4 Brd4: 5.1, 4.7 Brd7: 6.1 BRPF1: 5.1
		2.072a Brd9: 5.8 Brd4: 5.9, 4.5 Brd7: 4.9 BRPF1: 4.5	2.072b Brd9: 6.0 Brd4: 6.0, 4.8 Brd7: 5.0 BRPF1: 4.7	2.072c Brd9: 6.1 Brd4: 5.8, 4.6 Brd7: 5.2 BRPF1: 4.7	2.072d * Brd9: 5.8 Brd4: 5.0, <4.3 Brd7: 4.7 BRPF1: <4.0
		2.073a	2.073b Brd9: 6.2 Brd4: 4.9, 4.7 Brd7: 5.1 BRPF1: 4.8	2.073c	2.073d ¹⁹⁷ Brd9: 5.9 Brd4: <4.3, <4.3 Brd7: 4.7 BRPF1: <4.0

*Synthesised independently; ** Synthesised in amidine array (page 112)

Table 12: pIC₅₀ values for square array compounds in the bromodomains of Brd9, Brd4 (BD1 and BD2), Brd7 and BRPF1 as determined by TR-FRET analysis. Data are n≥2. Green boxes show compounds with ≥ 50 fold selectivity for Brd9 over Brd4; orange 3≥ fold <50; and red with no selectivity.

Pleasingly, analysis of the resulting data indicated that acceptable levels of selectivity over Brd4 could be achieved with 7-position aryl groups. In general, the

electron-deficient aromatic rings provided a greater degree of selectivity over Brd4, Brd7 and BRPF1. For example, methyl substituted compounds **2.068a** and **d** displayed the same Brd9 activity. However, upon exchange of the electron-rich dimethylamino ring (**2.068a**) for the electron poor cyano trifluoromethyl substituted compound (**2.068d**), Brd4 selectivity increased from 6 fold to 400 fold; Brd7 from 16 fold to 25 fold; and BRPF1 from 32 fold to 800 fold. Methyl amide substituted compounds showed a similar trend, with improved selectivity observed with an electron-deficient aryl ring, albeit with a reduction in Brd9 activity. The cyclic sulfone compounds showed high Brd9 potencies but with little selectivity over the other bromodomains. Amidine substituted compounds also showed high Brd9 potencies, with improved levels of selectivity compared to their amide analogues. For example, amidine **2.071d** displayed excellent levels of selectivity, with 200 fold over Brd4, 32 fold over Brd7 and 200 fold over BRPF1. In contrast, its amide analogue **2.070d** was only 80 fold selective over Brd4, 50 fold over Brd7, and 60 fold over BRPF1. Both tertiary amine and amide substituted compounds showed modest Brd9 activity, with little selectivity over Brd4 compared to their amidine analogues.

Of the 22 compounds tested, two were highlighted as they displayed greater than 100 fold selectivity over Brd4 and BRPF1, with surprising selectivity over the highly homologous Brd7 (**Figure 64**).

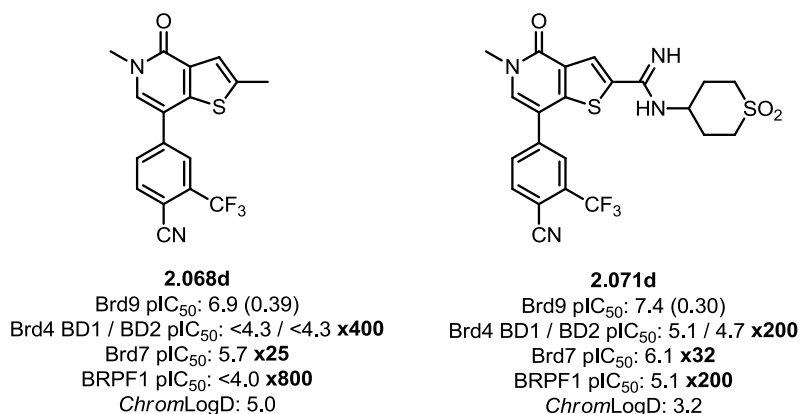


Figure 64: pIC₅₀ values for compounds **2.068d** and **2.071d** in the bromodomains of Brd9, Brd4 (BD1 and BD2), Brd7 and BRPF1 as determined by TR-FRET analysis. Brd9 ligand efficiency values are shown in parentheses. Brd9 selectivity is calculated based on pK_i values and selectivity over Brd4 relative to the maximum value. Data are n≥2.

Although methyl compound **2.068d** showed improved selectivity compared to amidine analogue **2.071d**, this compound was dismissed due to its lower Brd9 activity and high *ChromLogD* value (5.0). The increased lipophilicity of this molecule indicated that its physico-chemical properties would sit outside the recommended guidelines for drug-like molecules.¹⁵⁰ Furthermore, **2.068d** has a lower number of

sp^3 C centres (3 in **2.068d** vs. 7 in **2.071d**), which can lead to increased promiscuity due to fewer specific interactions with the preferred binding partner.¹⁵⁴ With this in mind, amidine **2.071d** was taken forward for further optimisation.

2.3.5 Optimisation of amidine **2.071d**

2.3.5.1 Identification of target compounds

With amidine **2.071d** representing the new lead compound from this series, further investigations were conducted to determine the requirement for a 6-membered sulfone as the amidine substituent. It was believed that the synthesis and evaluation of the 5-membered sulfone analogues **2.079a** and **b** would provide insights into the potency and selectivity shown by **2.071d** (Figure 65).

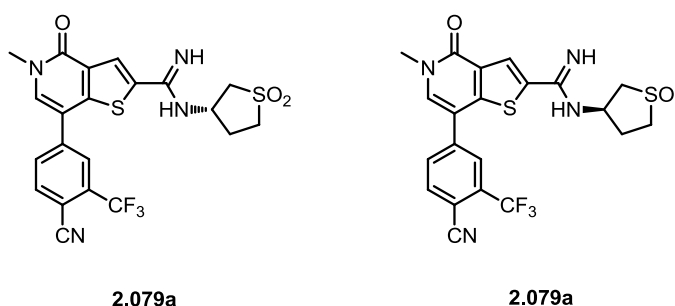
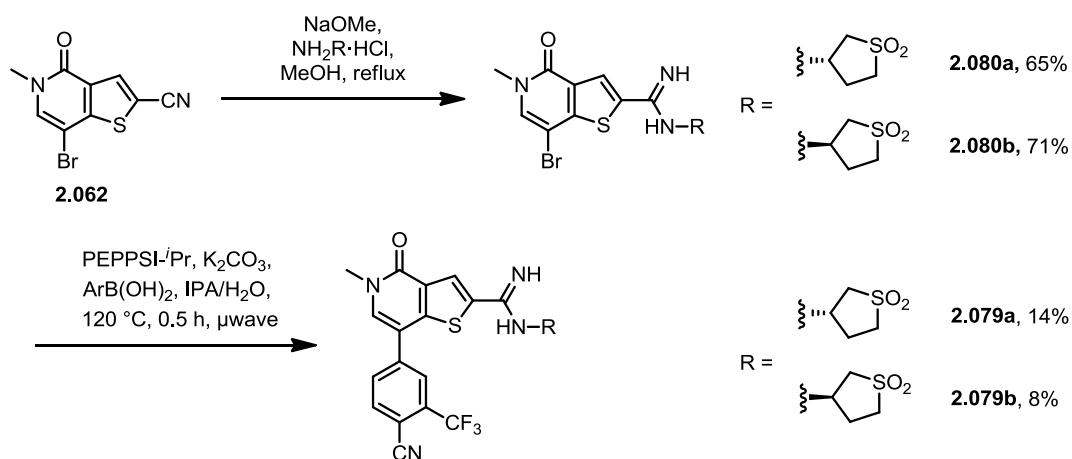


Figure 65: Chemical structures for 5-membered sulfone enantiomers **2.079a** and **2.079b**.

2.3.5.2 Synthesis of enantiomers **2.079a** and **b**

The synthesis of enantiomers **2.079a** and **b** proved straight forward using previously reported chemistry (Section 2.3.3.2, page 97; Scheme 27).

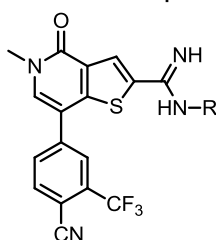


Scheme 27: Synthesis of enantiomers **2.079a** and **b** from nitrile **2.062**.

Treatment of nitrile **2.062** with NaOMe solution in MeOH followed by the addition of the appropriate amine hydrochloride furnished intermediates **2.080a** and **b** in acceptable yields (65–71%). Following this, a Suzuki-Miyaura coupling¹⁶³ was employed to install the aryl motif using the PEPPSI-*i*-Pr precatalyst¹⁷⁵ system previously discussed.

2.3.5.3 SAR discussion of amidines **2.071d**, **2.079a** and **b**

Amidine compounds **2.079a** and **b** were submitted for test in a TR-FRET assay against Brd9, Brd4 (BD1 and BD2), Brd7 and BRPF1. Six-membered sulfone compound **2.071d** was included for direct comparison (**Table 13**).



Entry	Compound Number	R =	Brd9 pIC ₅₀	Brd4 BD1 pIC ₅₀	Brd4 BD2 pIC ₅₀	Brd7 pIC ₅₀	BRPF1 pIC ₅₀
1	2.071d		7.4	5.1 (x200)	4.7 (x500)	6.1 (x32)	5.1 (x200)
2	2.079a ¹⁹⁸		7.4	5.4 (x100)	5.1 (x200)	5.9 (x50)	<4.0 (x2500)
3	2.079b ¹⁹⁹		7.4	5.4 (x100)	4.7 (x500)	5.9 (x50)	4.4 (x1000)

Table 13: pIC₅₀ values for amidines **2.071d**, **2.079a** and **b** in the bromodomains of Brd9, Brd4 (BD1 and BD2), Brd7 and BRPF1 as determined by TR-FRET analysis. Brd9 selectivity (shown in parentheses) is calculated based on pK_i values and selectivity over Brd4 relative to the maximum Brd4 value. Data are n≥2.

Pleasingly, all amidines showed significant selectivity over Brd4 and BRPF1, with some selectivity over the highly homologous bromodomain of Brd7. This was rationalised through consideration of the respective bromodomain binding sites (**Figure 66**).

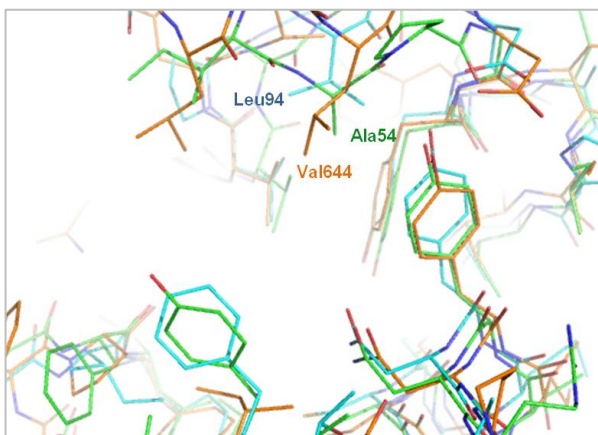


Figure 66: X-Ray crystal structures of apo Brd9 (green), Brd4 BD1 (blue) and BRPF1 (orange).

As previously discussed (Section 2.3.3.1, page 94), the region of the binding pocket where the amidine moiety is expected to sit is different in Brd9 (green), Brd4 BD1 (blue) and BRPF1 (orange). In Brd9, the residue in closest proximity to the amidine group is Ala54 in contrast to the more hydrophobic Leu94 and Val644 in Brd4 BD1 and BRPF1, respectively. Given the basic nature of the amidine functionality (compound **2.071d**, measured $pK_a = 8.4$), it was proposed that when protonated and therefore charged, it would sit less favourably in the more hydrophobic environment provided by Brd4 BD1 and BRPF1.

Further analysis of the resulting data indicated that the 6-membered sulfone **2.071d** provided an optimum selectivity profile compared to its 5-membered analogues. Compound **2.071d** was 200 fold selective over Brd4, whereas enantiomers **2.079a** and **b** showed only 100 fold. Interestingly, enantiomers **2.079a** and **b** displayed approximately identical activities, indicating that the stereochemistry of the chiral centre was not important for binding. Both **2.079a** and **b** showed improved selectivity over BRPF1 compared to 6-membered analogue **2.071d**. For example, 5-membered sulfone **2.079a** displayed 2500 fold selectivity, whereas **2.071d** showed only 200 fold. In the absence of X-ray crystallography of either of these compounds in the bromodomain of BRPF1, the reasons behind the observed selectivity remained unclear.

Although **2.079a** and **b** satisfied the requirements for a Brd9 chemical probe, improved selectivity over Brd4 took priority, given the profound biology associated with the BET proteins. Therefore, compound **2.071d** was taken forward for further optimisation.

2.3.6 Amidine Array

2.3.6.1 Identification of target compounds

As the lead compound for the TP series, satisfying the Brd9 probe criteria defined at the start of the project, amidine **2.071d** was taken forward for further development (Figure 67).

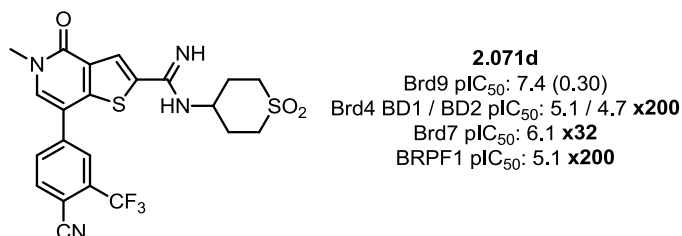
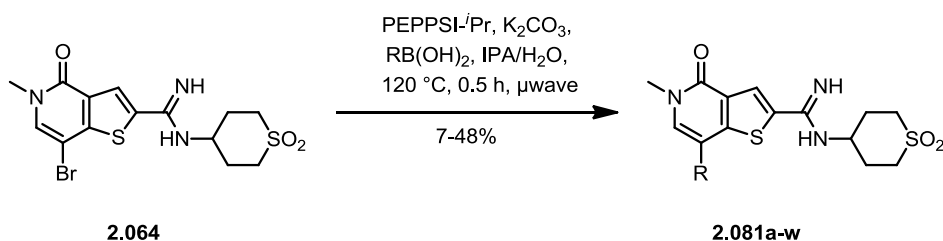


Figure 67: pIC₅₀ values for compound **2.071d** in the bromodomains of Brd9, Brd4 (BD1 and BD2), Brd7 and BRPF1 as determined by TR-FRET analysis. Brd9 ligand efficiency is shown in parentheses. Brd9 selectivity is calculated based on pK_i values and selectivity over Brd4 relative to the maximum Brd4 value. Data are n≥3.

Although **2.071d** satisfied the chemical probe criteria, with respect to bromodomain activity and selectivity (Section 2.1.4, page 54), it was believed that further selectivity could be gained through modifications at the 7-position. As very little focus had been placed in this region of the molecule, a 24 compound amidine array was designed to explore this position more thoroughly. Previous studies conducted in the 7-position were limited, focusing primarily on the analysis of 6-membered rings with a narrow range of substitution patterns. Therefore, this array would include: rings of various sizes; rings which contained substituents of both electron-withdrawing and -donating character; heteroaromatic rings; and rings with a range of substitution patterns.

2.3.6.2 Synthesis of amidine array compounds

Given the success of the previous 24 compound square array, identical chemistry was used to access the range of 7-position functionalised compounds shown in Figure 67. A Suzuki-Miyaura reaction¹⁶³ was used to couple bromide **2.064** to a series of commercially available boronic acids (Scheme 28).



Scheme 28: Synthesis of amidine array compounds from bromide **2.064**.

Each reaction was performed on a 0.15 mmol scale in parallel, providing 11 out of the 24 compounds shown in **Figure 68**. The remainder of the reactions were unsuccessful due to purification issues or the reaction was so low yielding that there was not enough material isolated to meet the requirements for test (9 μ M). The reactions which were unsuccessful were repeated independently providing the appropriate quantity of material for *in vitro* evaluation.

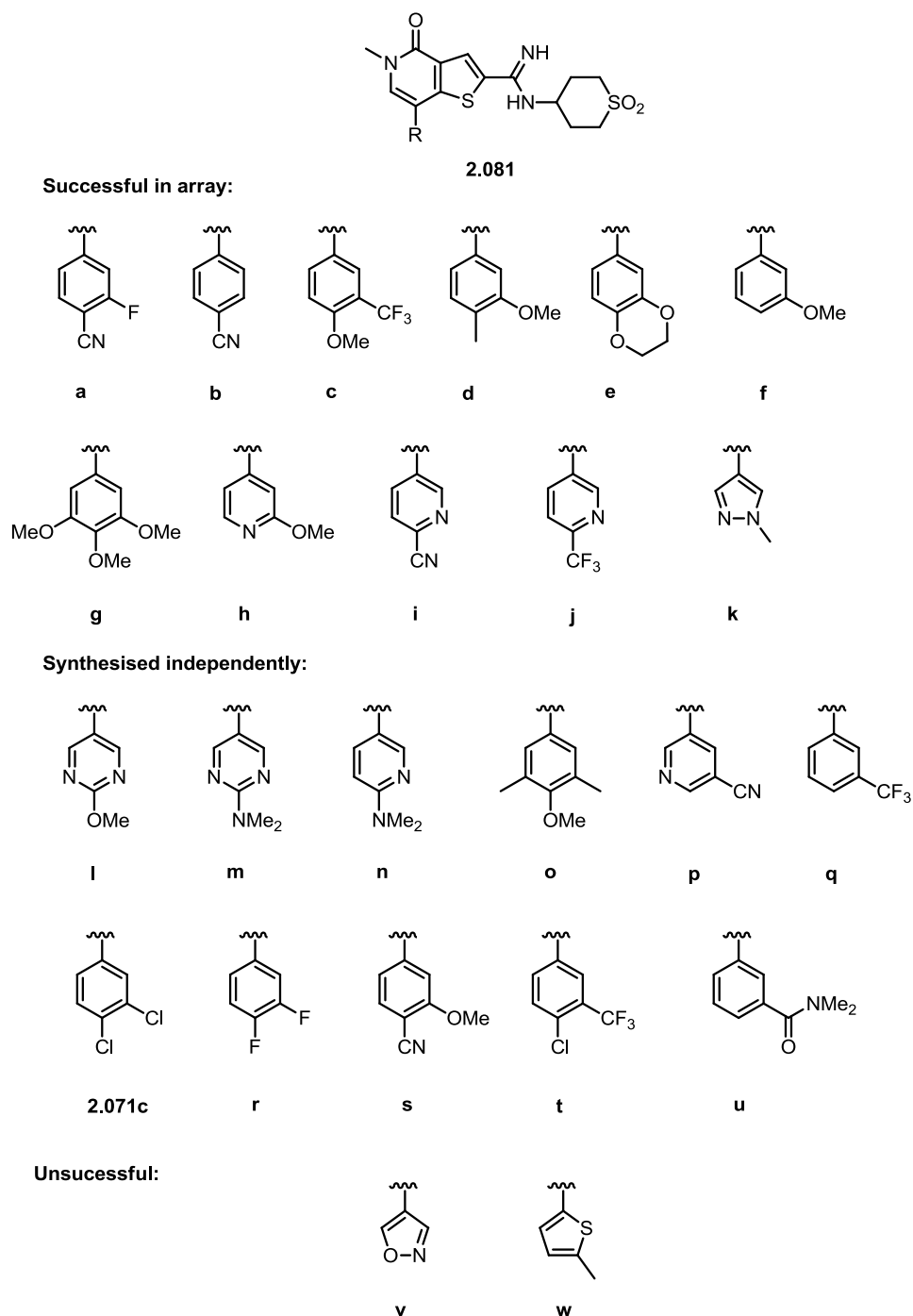
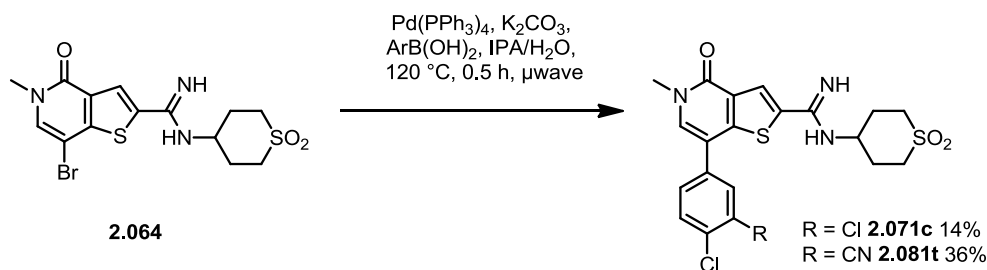


Figure 68: Synthesis of amidine array compounds.

The reactions performed to access compounds **2.071c** (originally designed for the square array) and **2.081t** were unsuccessful when repeated. LCMS analysis of the crude reaction mixtures indicated protodehalogenation resulting from oxidative insertion of Pd in the C-Cl bond of the aryl ring. With this in mind, an alternative, less active catalyst was employed for the Suzuki-Miyaura coupling (**Scheme 29**).¹⁶³



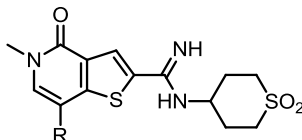
Scheme 29: Synthesis of compounds 2.071c and 2.081t.

Pleasingly, treatment of bromide **2.064** with the appropriate boronic acid and $\text{Pd(PPh}_3)_4$ under standard conditions provided compounds **2.071c** and **2.081t**, albeit in poor yields (14% and 36%, respectively).

The reactions to access 5-membered heterocycles **2.081v** and **w** were repeated but abandoned. LCMS analysis of the crude reaction mixture indicated very little product had formed, making isolation of the desired product challenging, even by preparative reverse phase HPLC. It was hypothesised that the electron-rich nature of the 5-membered heterocycles could have affected their reactivity under the Suzuki-Miyaura conditions described. However, as 22 analogues were successfully prepared, it was believed that sufficient data around the 7-position would be generated in the absence of compounds **2.081v** and **w**. Therefore, no further work was conducted on this series.

2.3.6.3 SAR discussion of amidine array compounds

The amidine array compounds were submitted for test in a TR-FRET assay against Brd9, Brd4 (BD1 and BD2), Brd7 and BRPF1 (**Figure 31**, steps 1a and 3). Of the 22 compounds tested, 6 satisfied the Brd9 probe criteria defined at the outset of the project (**Table 14**, see Appendix 5.5 for full data).



Entry	Compound Number	R =	Brd9 pIC ₅₀	Brd4 BD1 pIC ₅₀	Brd4 BD2 pIC ₅₀	Brd7 pIC ₅₀	BRPF1 pIC ₅₀
1	2.081c		7.9	5.8 (x125)	4.9 (x1000)	6.6 (x32)	5.7 (x160)
2	2.081d		8.1	6.1 (x100)	5.2 (x800)	6.8 (x32)	5.8 (x200)
3	2.081g		8.3	6.0 (x200)	5.3 (x1000)	7.1 (x25)	5.9 (x250)
4	2.081o		8.1	6.1 (x100)	5.1 (x1000)	6.8 (x32)	6.1 (x100)
5	2.081q		7.8	5.6 (x160)	4.8 (x1000)	6.6 (x25)	5.6 (x160)
6	2.081t		7.7	5.5 (x160)	4.7 (x1000)	6.4 (x32)	5.4 (x200)

Table 14: pIC₅₀ values for selected amidine array compounds in the bromodomains of Brd9, Brd4 (BD1 and BD2), Brd7 and BRPF1 as determined by TR-FRET analysis. Brd9 selectivity (shown in parentheses) is calculated based on pK_i values and selectivity over Brd4 relative to the maximum Brd4 value. Data are n≥2.

Pleasingly, all of the above compounds showed sub 20 nM activity against Brd9, with greater than 100 fold selectivity over Brd4. X-Ray crystallography¹⁵⁵ of compound **2.081q** in complex with Brd9 (green, left) and Brd4 BD1 (orange, right) was obtained to investigate the interactions responsible for the observed potency (**Figure 69**).

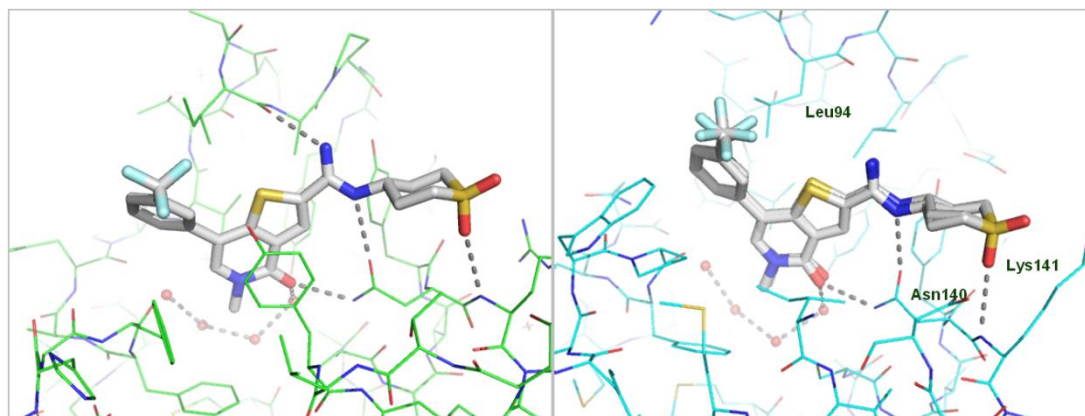


Figure 69: X-Ray crystallography of compound **2.081q** in complex with Brd9 (left, green, PDB code = 4UIV) and Brd4 BD1 (right, blue, PDB code = 4UIY). Two ligands are shown in the Brd4 BD1 structure as the CF₃ group can be modelled in two orientations, indicating that it will probably sit in both. Hydrogen-bonds are shown as grey dashed lines and water molecules as red spheres.

Analysis of the X-ray crystal structures indicated that compound **2.081q** adopts a similar conformation in both Brd9 and Brd4 BD1. As hypothesised, the amidine moiety forms a bidentate interaction to the conserved Asn (Asn100, Brd9; Asn140, Brd4 BD1), placing the sulfone group within hydrogen-bonding range ($\sim 3\text{\AA}$) of a backbone NH. In Brd9, this residue corresponds to Arg101 and Lys141 in Brd4 BD1. However, there is an additional interaction present in Brd9, accounting for the greater potency compared to that seen for Brd4. The amidine moiety acts as a hydrogen-bond donor, forming a direct interaction with the backbone carbonyl of Ile53. Furthermore, the amidine sits in close proximity to a key residue change moving from Brd9 (Ile53) to Brd4 BD1 (Leu94). Given the basic nature of the amidine moiety (measured $pK_a = 8.4$), it was proposed to sit less favourably in the more hydrophobic environment provided by Brd4 BD1, accounting for the observed selectivity over this bromodomain.

Although highly homologous to Brd9, some selectivity was gained over Brd7. Furthermore, excellent selectivity over BRPF1 was observed, with compounds ranging from 250 fold (compound **2.081g**, **Table 14**, entry 3) to 100 fold (compound **2.081o**, **Table 14**, entry 4).

As all compounds discussed met the initial requirements for a Brd9 chemical probe (Section 2.1.4, page 54), further profiling was conducted to assess their selectivity over the bromodomain of CECR2 (step 3, **Figure 31**), as this assay only became available at this stage of the project (**Table 15**).

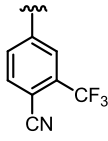
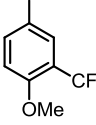
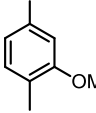
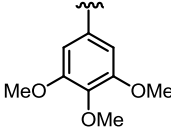
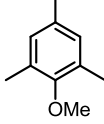
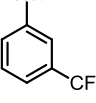
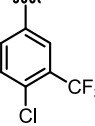
Entry	Compound Number	R =	Brd9 pIC ₅₀	CECR2 pIC ₅₀	Selectivity
1	2.071d		7.4	6.6	x10
2	2.081c		7.9	7.5	x4
3	2.081d		8.1	7.1	x16
4	2.081g		8.3	7.5	x10
5	2.081o		8.1	7.4	x8
6	2.081q		7.8	6.4	x40
7	2.081t		7.7	6.6	x20

Table 15: pIC₅₀ values for selected amidines in the bromodomains of Brd9 and CECR2 as determined by TR-FRET analysis. Selectivity for Brd9 is calculated based on pK_i values. Data are n≥2.

Of the 7 compounds listed, only **2.081q** showed significant selectivity over the bromodomain of CECR2. The data indicated that *meta*-substitution was favoured with all other di- and tri-substituted compounds providing little to no selectivity. For example, removal of the *para*-methoxy substituent in compound **2.081c** to give **2.081q** caused selectivity to increase from 4 to 40 fold, respectively (compare entries 2 and 6). In the absence of X-ray crystallography of any of these compounds in CECR2 it was difficult to account for this result. However, analysis of the peptide sequence of the respective bromodomain binding sites highlighted key residue changes (**Figure 70**).

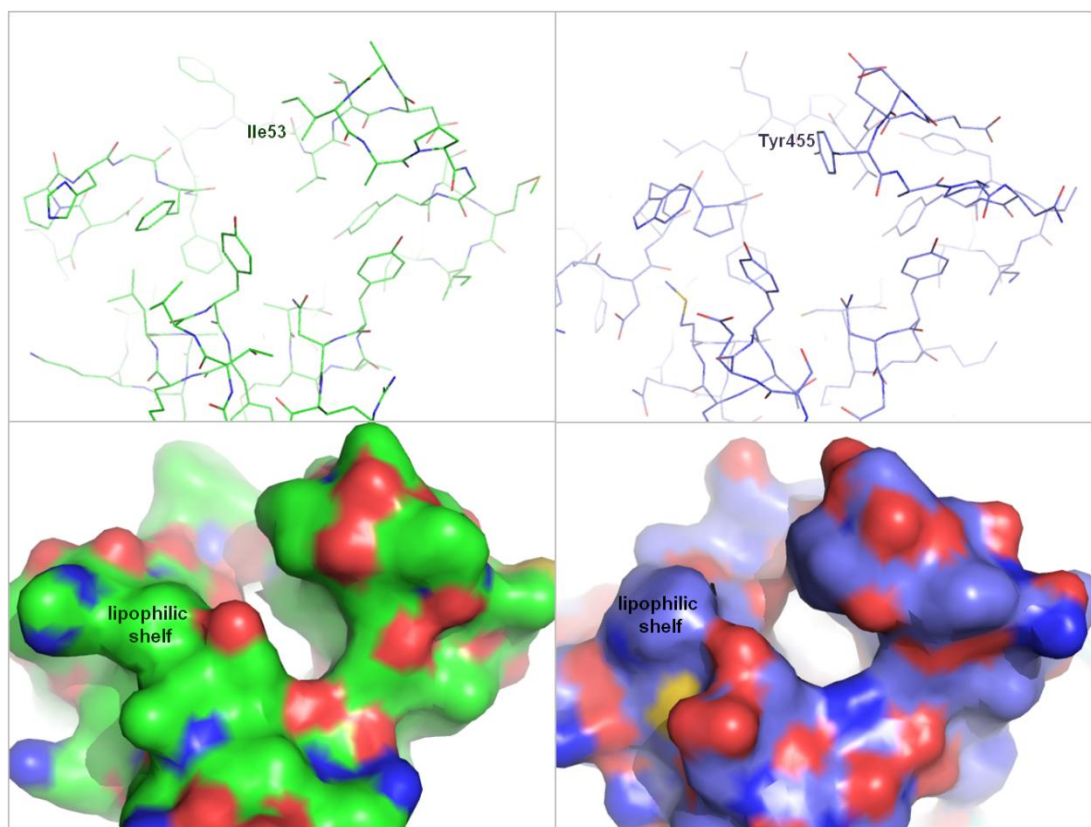


Figure 70: X-Ray crystallography of apo Brd9 (left, green) and CECR2 (right, purple).

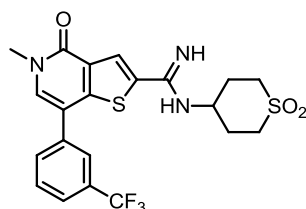
The X-ray crystal structures indicated that exchange of Ile53 in Brd9 (left, green) for Tyr455 in CECR2 (right, purple) delivers a contrast in the architecture of the binding grooves. In addition, the constituent amino acids, which form the lipophilic shelves are different in these bromodomains. In Brd9, Gly43 is replaced by Trp445 and Phe44 for Pro446, potentially causing the shape of the ZA channel to change (**Table 16**, identical residues are highlighted in green and different in red). Presumably, it is these structural differences, which account for selectivity observed for compound **2.081q**.

Although compound **2.081q** showed selectivity over the bromodomain of CECR2, all other compounds tested displayed relatively high levels of CECR2 activity (pIC_{50} values ranging from 6.6–7.5). These data indicate that the bromodomains of CECR2 and Brd9 must show some similarities. Both Brd9 and CECR2 contain a Tyr gate keeper residue (**Table 16**), a key feature which determines the shape of the KAc binding site. Recent studies³³ concerning bromodomain binding to a broad range of modified lysines has shown that both Brd9 and CECR2 recognise butyrlated lysine. These results support the conclusions made and further highlight the similarities of these two bromodomains.

BRD9	CECR2	
GLY43	TRP445	WPF motif
PHE44	PRO446	WPF motif
PHE45	PHE447	WPF motif
ALA46	LEU448	ZA channel
PHE47	GLU449	ZA channel
PRO48	PRO450	ZA channel
VAL49	VAL451	ZA channel
THR50	ASP452	ZA loop
ASP51	GLU453	ZA loop
ILE53	TYR455	ZA loop
ALA54	ALA456	ZA loop
TYR57	TYR459	Water-binding Tyr
SER58	TYR460	
ILE61	ILE463	
MET92	MET494	
ASN95	ASN497	
ALA96	CYS498	Conserved Ala
TYR99	TYR501	Conserved Tyr
ASN100	ASN502	Conserved Asn
THR104	SER506	
VAL105	GLU507	
TYR106	TYR508	Gatekeeper
TYR107	THR509	
LEU109	MET511	
ALA110	SER512	

Table 16: Sequence similarity across the bromodomain binding sites of Brd9 and CECR2. Identical residues are highlighted in green; similar residues in orange and different in red.

As *meta*-substituted compound **2.081q** displayed the greatest selectivity profile observed to date, along with acceptable physico-chemical properties, this compound was progressed for further investigations (**Figure 71**).



2.081q
 Brd9 pIC₅₀: 7.8 (0.33)
 Brd4 BD1 / BD2 pIC₅₀: 5.6 / 4.8 **x160**
 Brd7 pIC₅₀: 6.6 **x25**
 BRPF1 pIC₅₀: 5.6 **x160**
 CECR2 pIC₅₀: 6.4 **x40**
 MW: 484
 PFI: 6.3

Figure 71: pIC₅₀ values for compound **2.081q** in the bromodomains of Brd9, Brd4 (BD1 and BD2), Brd7, BRPF1 and CECR2 as determined by TR-FRET analysis. Brd9 ligand efficiency is shown in parentheses. Brd9 selectivity is calculated based on pK_i values and selectivity over Brd4 relative to the maximum Brd4 value. Data are n≥2.

2.3.7 Optimisation of 2.081q

2.3.7.1 Identification of target compounds

As the new lead compound for the TP series, compound **2.081q** was progressed for further optimisation. It has previously been reported that KAc mimetics containing alkyl groups larger than a methyl can be accommodated in the bromodomain binding pocket.^{32,33} With the aim to improve selectivity further, alternative KAc mimetic alkyl groups were investigated. To this end, *N*-ethyl and *N*-isopropyl compounds **2.082** and **2.083**, respectively were accessed (**Figure 72**).

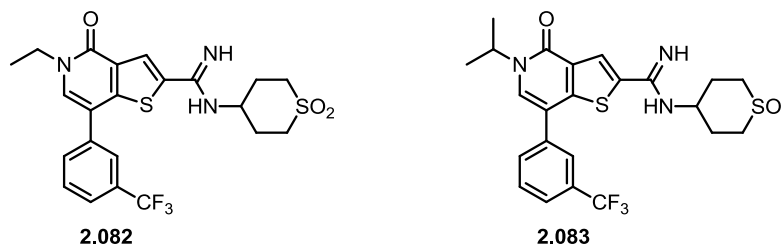
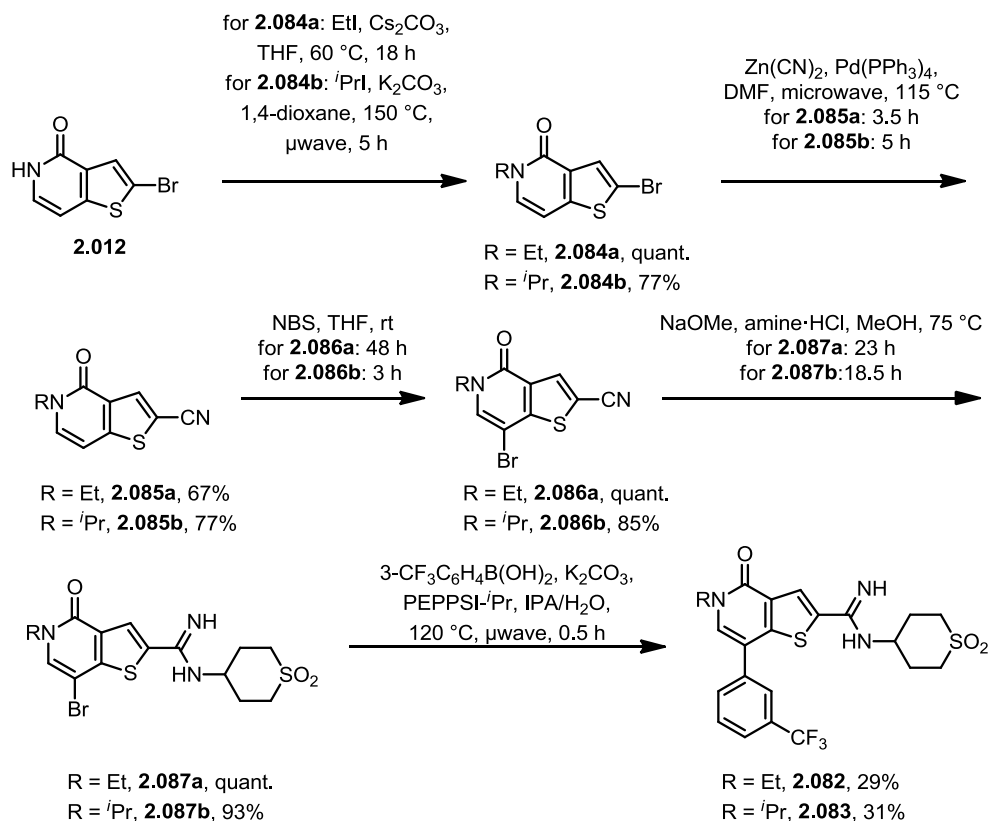


Figure 72: Alternative KAc mimetic compounds **2.082** and **2.083**.

2.3.7.2 Synthesis of alternative KAc mimetics 2.082 and 2.083

Alternative KAc mimetic compounds **2.082** and **2.083** were prepared by a similar route to that described previously (**Scheme 30**).



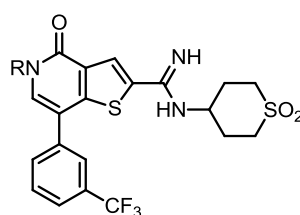
Scheme 30: Synthesis of *N*-ethyl and *N*-isopropyl compounds **2.082** and **2.083**.

Selective *N*-alkylation of known compound **2.012**¹⁵⁶ was successful for both *N*-ethyl and *N*-isopropyl variants, providing compounds **12.084a** (quant.) and **b** (77%) in excellent yields. Following this, the nitrile moiety was installed *via* a Negishi cyanation¹⁸¹ reaction, affording **2.085a** and **b**. Subsequent electrophilic bromination using NBS in THF followed by conversion of the nitrile to the amidine provided **2.087a** (67%) and **b** (77%) in excellent yields. Finally, the 3-trifluoromethylphenyl ring was installed by a Suzuki-Miyaura reaction¹⁶³ employing the PEPSSI-*i*Pr precatalyst system.¹⁷⁵

Using this robust chemistry previously developed (Section 2.3.3.2, page 97), alternative KAc mimetic compounds **2.082** and **2.083** were rapidly accessed. These compounds were progressed for investigations to determine the steric boundaries of the KAc alkyl group.

2.3.7.3 SAR discussion of alternative KAc mimetics 2.082 and 2.083

Compounds **2.082** and **2.083** were tested in a TR-FRET assay to determine their activity against the bromodomains of Brd9, Brd4 (BD1 and BD2), Brd7 and BRPF1 (**Figure 31**, steps 1a and 3, **Table 17**).



Entry	Compound Number	R =	Brd9 pIC ₅₀	Brd4 BD1 pIC ₅₀	Brd4 BD2 pIC ₅₀	Brd7 pIC ₅₀	BRPF1 pIC ₅₀
1	2.081q	Me	7.8	5.6 (x160)	4.8 (x1000)	6.6 (x25)	5.6 (x160)
2	2.082	Et	7.3	5.3 (x100)	4.4 (x800)	6.0 (x32)	4.6 (x500)
3	2.083	<i>i</i> Pr	5.5	<4.3 (x16)	<4.3 (x16)	4.6 (x8)	<4.0 (x32)

Table 17: pIC₅₀ values for selected amidines in the bromodomains of Brd9, Brd4 (BD1 and BD2), Brd7 and BRPF1 as determined by TR-FRET analysis. Brd9 selectivity (shown in parentheses) is calculated based on pK_i values and selectivity over Brd4 relative to the maximum Brd4 value. Data are n≥2.

Pleasingly, increasing the KAc chain length from *N*-methyl to *N*-ethyl maintained greater than 100 fold selectivity over Brd4 (entries 1 and 2). Furthermore, selectivity over the highly homologous Brd7 increased from 25 to 32 fold. These effects were most pronounced for BRPF1 where the selectivity window increased from 160 fold for **2.081q** to 500 fold for **2.082**. However, the introduction of the more sterically

demanding *N*-isopropyl substituent, as in compound **2.083**, significantly reduced activities in all of the bromodomains tested, indicating that branching was not well tolerated (entry 3).

As compounds **2.081q** and **2.082** both satisfied the initial requirements for a Brd9 chemical probe (Section 2.1.4, page 54), they were progressed for further profiling (**Figure 31**, step 4) to assess their utility as cellular tool molecules (**Figure 73**).

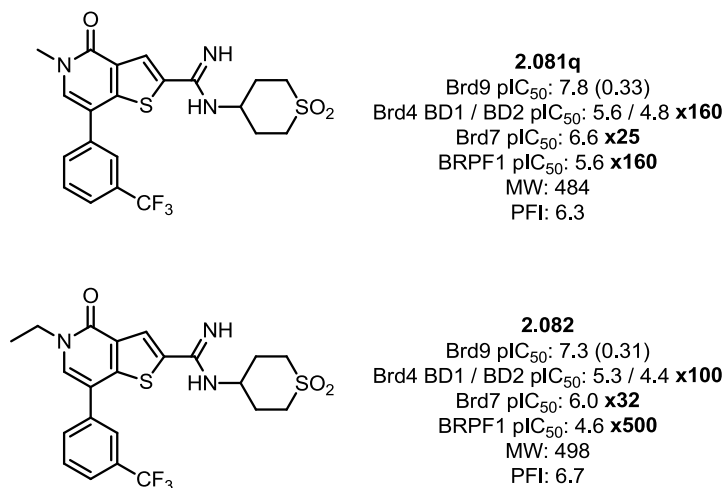


Figure 73: pIC₅₀ values for compounds **2.081q** and **2.082** in the bromodomains of Brd9, Brd4 (BD1 and BD2), Brd7 and BRPF1. Brd9 ligand efficiency values are shown in parentheses. Brd9 selectivity is calculated based on pK_i values and selectivity over Brd4 relative to the maximum Brd4 value. Data are n≥2.

2.3.8 Further profiling of **2.081q** and **2.082**

2.3.8.1 Proof of cellular target engagement

In order to validate compounds **2.081q** and **2.082** as cellular chemical probes, it was necessary to determine cellular target engagement (**Figure 31**, step 3a). Although there is no cellular phenotype described for Brd9, it has been reported that inhibition of the BET family of bromodomains correlates with inhibition of pro-inflammatory cytokine, IL-6. This has been shown for multiple chemotypes across a range of pan-BET bromodomain ligands. As compounds **2.081q** and **2.082** showed low levels of Brd4 BD1 activity, with pIC₅₀ values of 5.6 and 5.3, respectively, it was possible to determine cellular target engagement at Brd4. Therefore, compounds **2.081q** and **2.082** were tested in an LPS challenge assay.

In this experiment, human peripheral mononuclear blood cells (PBMCs) were treated with LPS in order to induce an immune response and expression of IL-6. Upon treatment with compounds **2.081q** and **2.082**, dose-dependent inhibition of IL-

6 was observed with pIC₅₀ values of 5.8 and 5.3, respectively, correlating well with inhibition of Brd4 BD1 (pIC₅₀: 5.6 and 5.3 respectively). As such, it was concluded that compounds **2.081q** and **2.082** were capable of entering into the cell and interacting with the bromodomains of Brd4. This result provided confidence in cellular target engagement at Brd9 and further validated compounds **2.081q** and **2.082** as potential cellular chemical probes.

2.3.8.2 Selectivity profiling against broader pharmacological targets

Although compounds **2.081q** and **2.082** showed acceptable levels of bromodomain selectivity, as determined by internal TR-FRET assays, it was necessary to determine selectivity over a broader range of pharmacological targets (**Figure 31**, step 3b). This was achieved by means of eXP, a series of *in vitro* assays used to measure the effect of the test compound on a range of ion channels, enzymes, receptors and transporters.

Compounds **2.081q** and **2.082** were submitted for testing against a panel of 49 pharmacologically diverse targets. Pleasingly, both compounds showed excellent profiles, with only minor activity seen at the hERG ion channel and AchE enzyme (**Table 18**).

eXP target pXC ₅₀	2.081q	2.082
hERG	5.1	4.8
AchE	5.1	5.3

Table 18: Off-target liabilities identified for compounds 2.081q and 2.082 in eXP.

Given that the Brd9 pIC₅₀ values of these compounds were 7.8 and 7.3 for **2.081q** and **2.082**, respectively, at least 100 fold selectivity over hERG and AchE was observed. The hERG activity is only a problematic for a drug molecule in which it would enter humans. As chemical probes are not dosed to humans, this activity is less of a concern.

Importantly, compounds **2.081q** and **2.082** show much improved eXP profiles compared to the original start point for the project, compound **2.005** (**Table 2**, page 52). No significant off-target liabilities were indentified, building confidence in the selectivity profiles of these compounds.

2.3.8.3 Broader bromodomain profiling

As the most selective compounds synthesised, **2.081q** and **2.082** were progressed for further profiling (**Figure 31**, Step 4). These investigations aimed to assess their selectivity over a panel of 34 phylogenetically diverse bromodomains (**Figure 31**, step 5). This was achieved by means of BROMOscan,¹²¹ an assay which quantifies the strength of bromodomain-ligand binding by measuring the amount of protein captured on a solid-support. In this case, the bromodomain is attached to a DNA tag for the purposes of identification. In the absence of a test compound, the bromodomain binds to a ligand, which is immobilised on a solid support (**Figure 74A**).

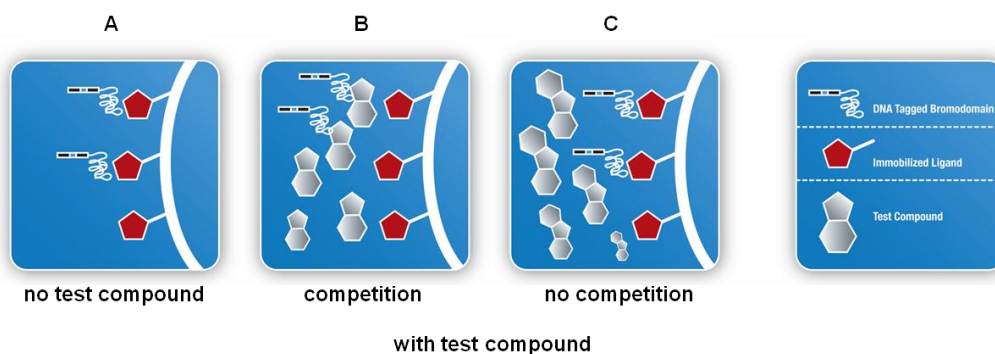


Figure 74: BROMOscan assay principle.²⁰⁰

Test compounds which bind to the bromodomain prevent it from interacting with the immobilised ligand. Therefore, the amount of protein captured on the solid-support is reduced (**B**). In contrast, test compounds which do not bind to the bromodomain have no effect on the amount of protein captured (**C**). Active test compounds are identified by measuring the amount of protein captured versus a control sample by qPCR, which detects the DNA label of the bromodomain. The dissociation constant (K_d) for bromodomain-ligand binding is then calculated by measuring the amount of bromodomain captured on the solid-support as a function of test compound concentration. In this manner, K_d values for bromodomain-ligand binding were calculated for compounds **2.081q** and **2.082** across a range of 34 proteins. The results for these experiments are shown as tree spot diagrams (**Figure 75**, **Table 19**). The size of the spot is directly proportional to strength of binding i.e. the larger the spot, the higher the affinity for that particular bromodomain. Only bromodomains for which binding was measured to be within 1000 fold of that for Brd9 are shown (For full data, see Appendix 5.6).

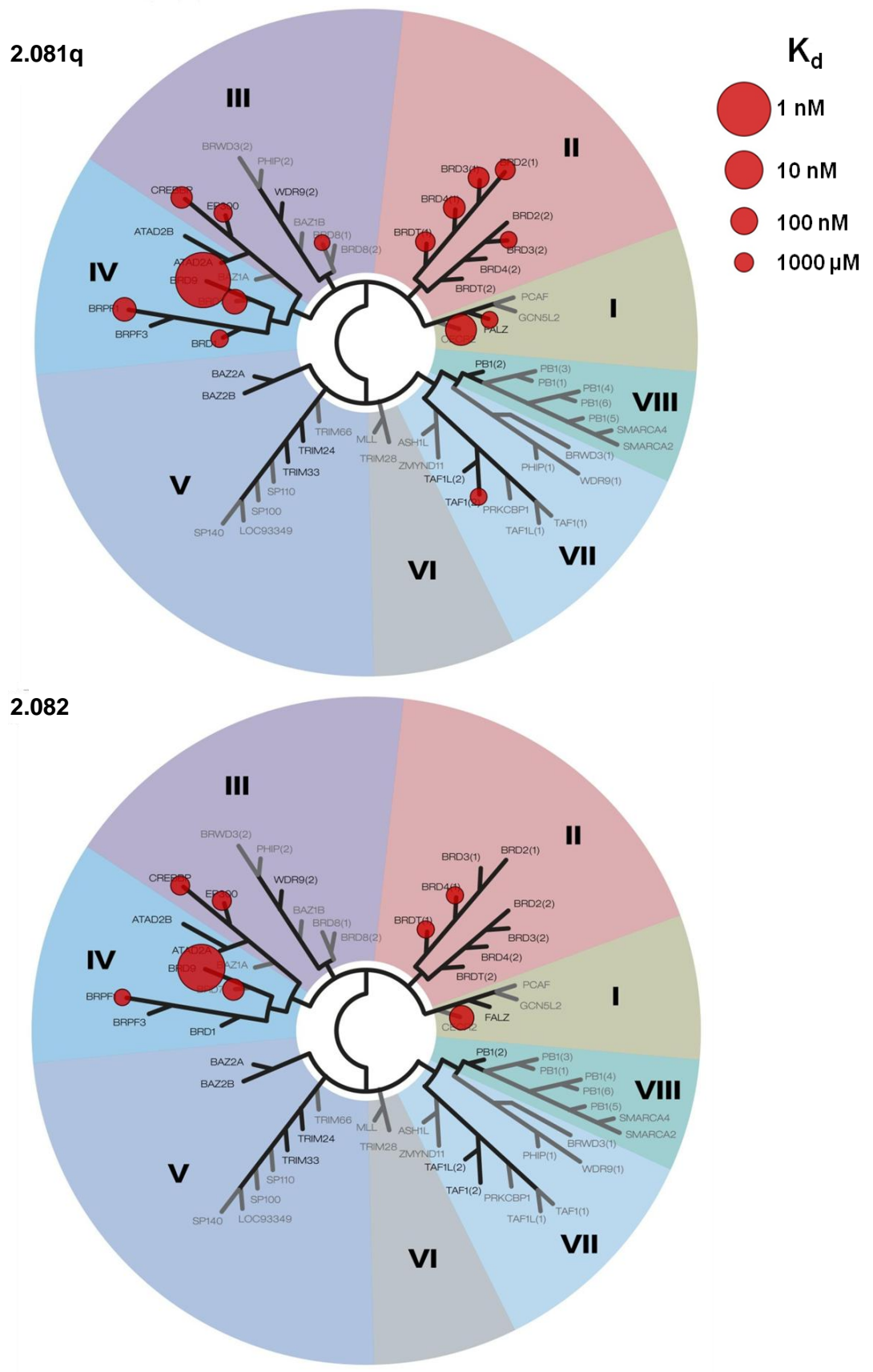


Figure 75: BROMOscan data for compounds 2.081q (top) and 2.082 (bottom).

	Brd9 pK _d	Brd4 BD1pK _d	Brd7 pK _d	CECR2 pK _d
2.081q	9.2	6.5 (x500)	6.9 (x200)	7.5 (x50)
2.082	8.7	5.8 (x800)	6.4 (x200)	6.8 (x80)

Table 19: pK_d values determined by BROMOscan for compounds **2.071q** and **2.082** against the bromodomains of Brd9, Brd4 (BD1), Brd7 and CECR2. Selectivity is shown in parentheses.

Pleasingly, both compounds **2.081q** and **2.082** showed nanomolar affinity for Brd9 with pK_d values of 9.2 (0.63 nM) and 8.7 (2 nM), respectively. Ethyl substituted compound **2.082** displayed greater selectivity overall with 800 fold over the BET family, 200 fold over the highly homologous Brd7 and 70 fold over every other bromodomain tested. Methyl compound **2.081q** was slightly less selective, showing 500 fold over the BET family and 180 fold over Brd7, but only 50 fold selective over the other bromodomains tested. The data suggested that the *N*-ethyl KAc mimetic was less well tolerated in all other bromodomains tested except Brd9, providing the greatest selectivity profile observed to date.

It is of note that the next highest affinity binding after Brd9, is against CECR2, further highlighting the similarities between these two bromodomains, brought about by their gatekeeper residues.

X-Ray crystallography¹⁵⁵ of compounds **2.081q** (left) and **2.082** (right) in complex with the Brd9 provided insights into the observed potencies against this bromodomain (**Figure 76**).

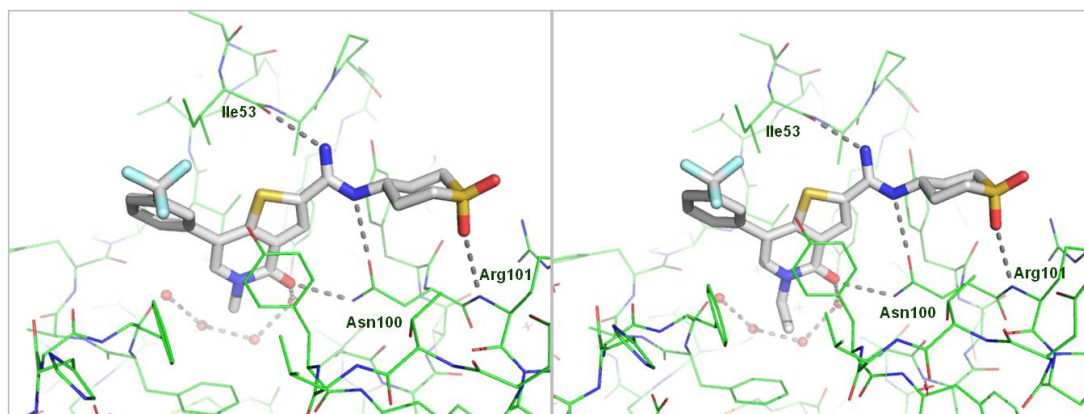


Figure 76: X-Ray crystallography of compounds **2.081q** (left, PDB code = 4UIV) and **2.082** (right, PDB code = 4UIW) in complex with Brd9. Hydrogen bonds are shown as grey dashed lines and water molecules as red spheres.

Both compounds adopt identical binding modes, indicating that the larger *N*-ethyl KAc mimetic has little effect on the overall conformation of the molecule. As previously seen for compound **2.081q** (**Figure 69**, page 117), *N*-ethyl variant **2.082** forms identical interactions to Asn100, Ile53 and Arg101.

Based on the high Brd9 affinity and excellent bromodomain selectivity, *N*-ethyl compound **2.082**, was progressed for further analysis.

2.3.8.4 Physico-chemical properties of 2.082

Compound **2.082** shows good physico-chemical properties, sitting within the recommended guidelines for the design of drug-like molecules (Table 20).

2.082	
Molecular Weight	497
ChromLogD _{7.4} , PFI	3.7, 6.7
Brd9 ligand efficiency	0.36 (pK _d = 8.7, BROMOscan)
CLND solubility	179 µg/mL (pH = 7.4)

Table 20: Physico-chemical properties of 2.082

Compound **2.082** has a molecular weight less than 500 and acceptable lipophilicity with a ChromLogD_{7.4} value of 3.7. Furthermore, Brd9 ligand efficiency was 0.36 based on the data provided by the BROMOscan assay. Finally, CLND solubility, determined at pH 7.4 was 179 µg/mL.

2.3.8.5 Further evidence of cellular target engagement at Brd9

In order to determine cellular target engagement at Brd9 specifically (Figure 31, step 5a), compound **2.082** was tested in a NanoBRET assay,¹¹² which measured displacement of NanoLuc-tagged Brd9 bromodomain from Halo-tagged histone H3.3 (Figure 77). Pleasingly, **2.082** displaced Brd9 from the histone with a pIC₅₀ value of 6.8, correlating well with the TR-FRET data generated (pIC₅₀: 7.3).

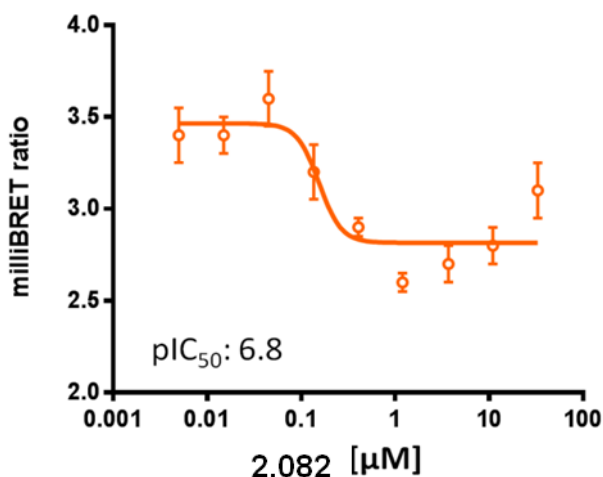


Figure 77: Brd9 bromodomain cellular NanoBRET dose-response curve of compound 2.082.

2.3.8.6 Binding to endogenous Brd9

Up until this point in the project, all determinations of Brd9 binding affinity had been conducted with protein truncate. Since bromodomains exist as part of BCPs, it was believed that a more biologically relevant experiment would be to determine whether **2.082** was capable of binding to full length, endogenous Brd9 (**Figure 31**, step 5b). In order to investigate this further, a chemoproteomic competition binding assay was conducted by colleagues at Cellzome. In this case, linkable compound **2.007** was attached to a solid-support and treated with HUT-78cell lysate (**Figure 78**).

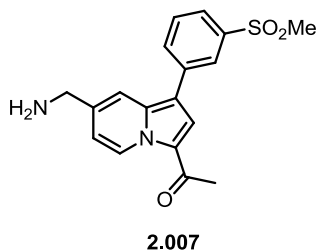


Figure 78: Chemical structure for linkable compound **2.007**, which was attached to a solid support for use in a chemoproteomic binding assay.

Following this, **2.082** was spiked into the mixture at a variety of concentrations. The bromodomains to which **2.007** were bound were identified by mass spectrometry following 'pull back' of the solid-support. Pleasingly, **2.082** showed dose dependent binding to Brd9 with a pIC_{50} value of 7.1 (**Figure 79**). As **2.082** interacted with Brd9, this protein was not 'pulled back' by linkable compound **2.007**. Importantly, **2.082** displayed >625 fold selectivity for Brd9 over BET family member Brd3. These data confirm excellent potency at Brd9 in a cellular context and selectivity over the BET family was maintained with endogenous proteins.

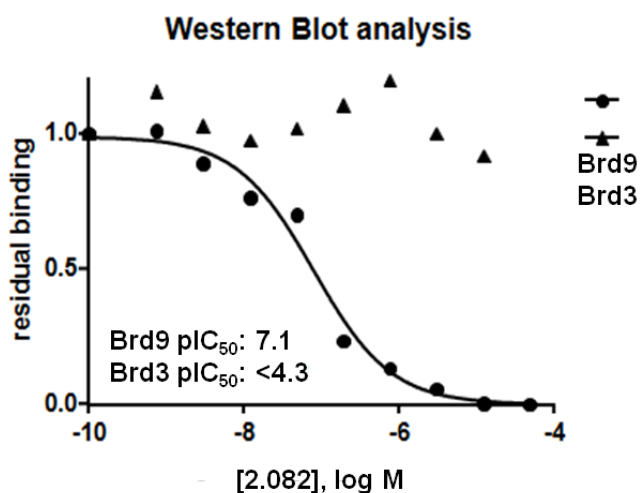


Figure 79: Dose–response binding of **2.082** with endogenous Brd9 and Brd3 from HuT-78 cell lysates, measured in a chemoproteomic competition binding assay.

These data are in contrast to that obtained for compound **2.005**, the original start point for this project. Selectivity for Brd9 over the BET family was not observed endogenously for **2.005**, meaning it was not suitable for use as a chemical probe. Therefore, the excellent selectivity shown by **2.082** both biochemically and endogenously, builds confidence in the quality of this molecule.

2.3.8.7 Brd9 chemical probe declaration

Compound **2.082** satisfied the probe criteria defined at the outset of this project (Section 2.1.4, page 54), and was therefore selected as the Brd9 chemical probe, known as **I-BRD9** henceforth (**Figure 31**, step 6). With greater than 70 fold selectivity over a panel of 34 bromodomains tested, **I-BRD9** represents the first selective chemical probe for Brd9 and one of only three chemical probes known to be selective for a single bromodomain. Brd9 chemical probes reported^{113,114} following the publication of **I-BRD9** are also active against Brd7.

2.3.8.8 PK profiling of I-BRD9

In order to assess the utility of **I-BRD9** as an *in vivo* tool compound, it was progressed for rodent PK studies (**Figure 31**, step 7). These experiments aimed to investigate the systemic exposure of **I-BRD9** in mouse. The mouse was selected for the basis of these investigations given its prevalence in immuno-inflammation animal studies. Furthermore, considering that **I-BRD9** was to be released into the broader scientific community, it was believed that the data generated from these studies would be in keeping with the mouse models currently favoured by academics for *in vivo* experimentation.

Initially *in vitro* clearance was determined in mouse liver microsomes, providing an indication of how quickly the compound would be eliminated by phase I metabolism. In this case, the clearance was 0.56 mL/min/g, scaling to 23% of liver blood flow (LBF). With this encouraging result, **I-BRD9** was taken forward for *in vivo* studies.²⁰¹

Following intravenous (IV) infusion of **I-BRD9** (1.3 mg/Kg) over 1 hour, C_{max} , the maximum concentration of compound observed in the blood was 194 ng/mL or 0.4 μ M (**Figure 80**, **Table 21**). This concentration was significantly above the IC_{50} of **I-BRD9** (50 μ M as determined by TR-FRET assay), but decreased rapidly due to high clearance.

Blood concentration time profile of I-BRD9 following 1.3 mg/Kg 1 hour IV infusion to the male CD1 mouse

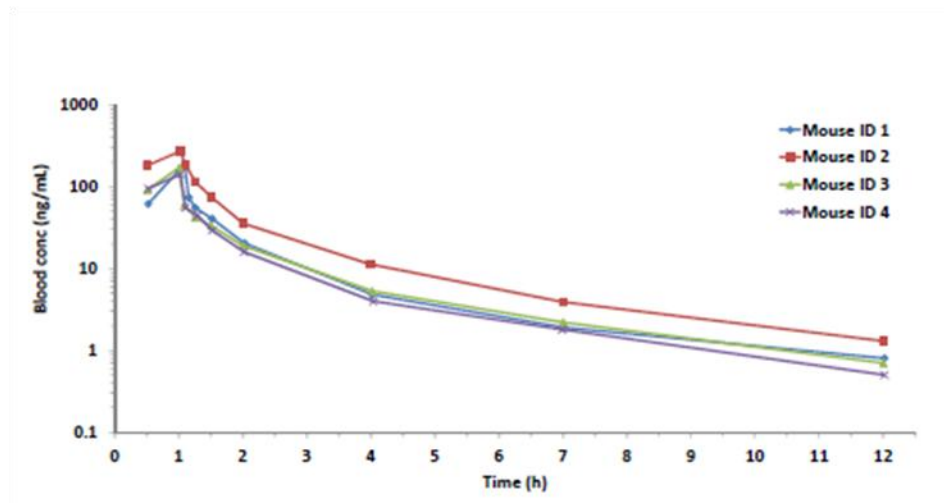


Figure 80: Blood concentration time profile for I-BRD9 following 1.3 mg/kg 1 h IV infusion.

IV PK Parameters	Mean (n = 4)
C_{max} (ng/mL)	194
C_{max} (μ M)	0.4
CL_b (mL/min/Kg)	112
%LBF	93
V_{ss} (L/Kg)	9.8
$t_{1/2}$ (h)	2.8
AUC/ D_{∞} (min.Kg/L)	10

Table 21: IV PK parameters for I-BRD9.

In contrast to the clearance of 23% LBF predicted by mouse microsomes, **I-BRD9** was rapidly cleared at 112 mL/min/Kg (93% LBF) *in vivo*. Since both phase I modification (e.g. oxidation or reduction) and phase II metabolism (active metabolites are conjugated to charged species) were possible in mouse, this *in vivo* result could suggest that the rapid clearance was due to phase II effects. In addition, **I-BRD9** showed a high volume of distribution (9.8 L/Kg) and a moderate half life of 2.8 hours, indicating distribution to the tissues.

In parallel, **I-BRD9** was administered orally at 3 mg/kg (Figure 81, Table 22).

Blood concentration time profile of I-BRD9 following 3 mg/Kg oral administration to the male CD1 mouse.

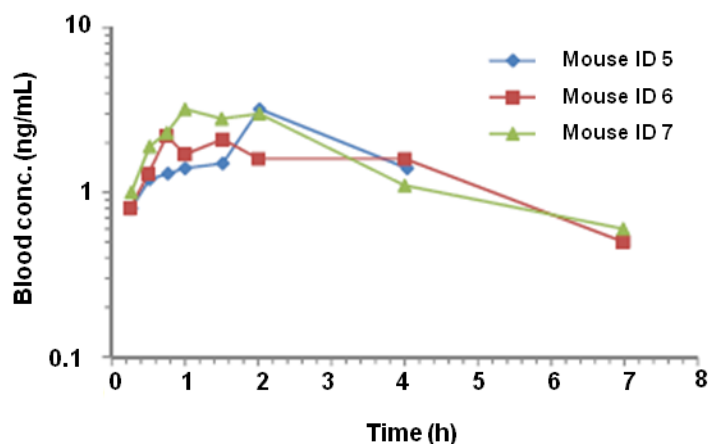


Figure 81: Blood concentration time profile of I-BRD9 following 3 mg/kg oral administration.

Oral PK Parameters	Mean (n = 3)
C_{max} (ng/mL)	2.9
C_{max} (μ M)	0.01
T_{max} (h)	1.00
F%	2
V_{ss} (L/Kg)	9.8
$t_{1/2}$ (h)	2.6
AUC/ D_{∞} (min.Kg/L)	0.2

Table 22: Oral PK parameters for I-BRD9.

I-BRD9 showed a low systemic exposure of 0.2 min.Kg/L, following oral administration. This was most likely due to poor absorption through the gut membrane and into the blood. In addition, poor bioavailability (F), the fraction of the administered dose reaching the systemic circulation was observed at 2%.

Following the poor PK results from both oral and IV administration, **I-BRD9** was administered *via* subcutaneous and intraperitoneal injection. Pleasingly, results from these experiments showed improved C_{max} and systemic exposure compared to oral administration (**Figure 82, Table 23**).

Blood concentration time profile of I-BRD9 following 3 mg/kg subcutaneous administration (top) and intraperitoneal administration (bottom) to the male CD1 mouse.

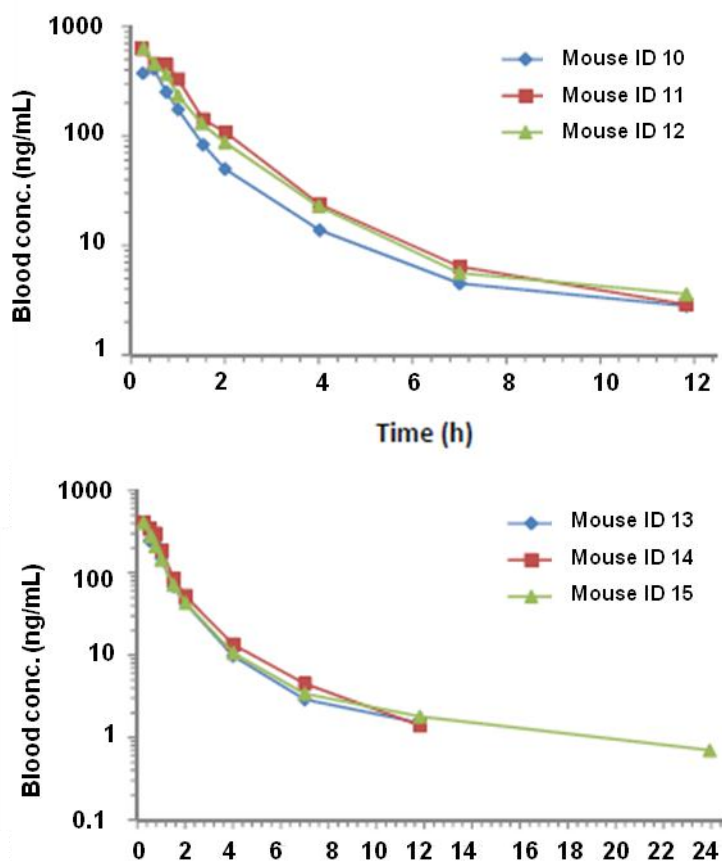


Figure 82: Blood concentration time profile of I-BRD9 following 3 mg/kg subcutaneous administration (top) and intraperitoneal injection (bottom).

PK Parameters	Subcutaneous Mean (n = 3)	Intraperitoneal Mean (n = 3)
C_{max} (ng/mL)	555	405
C_{max} (μ M)	1.12	0.81
T_{max} (h)	0.27	0.25
F%	129	86
$t_{1/2}$ (h)	3.1	2.9
AUC/ D_{∞} (min.Kg/L)	12.4	8.3

Table 23: PK parameters following subcutaneous administration of I-BRD9 (left); PK parameters following intraperitoneal administration of I-BRD9.

For example, systemic exposure was 0.2 min.Kg/L following oral administration (Table 22), whereas subcutaneous and intraperitoneal injection (Table 23) provided 12.4 and 8.3 min.kg/L, respectively. Furthermore, C_{max} was 555 ng/mL for subcutaneous injection and 405 ng/mL for intraperitoneal, leading to bioavailabilities of 129% and 86%, respectively. Although subcutaneous and intraperitoneal injection provided an improvement on oral administration, only subcutaneous injection gave

an improvement on the systemic exposure observed for IV injection (IV: 10 min.Kg/L, subcutaneous: 12.4 min.Kg/L).

Considering the improved C_{max} and systemic exposure provided by subcutaneous injection, **I-BRD9** was progressed for further studies in order to assess its utility as an *in vivo* tool compound. The fraction of unbound **I-BRD9** in mouse blood was determined, providing an indication of how much compound would be available to bind to Brd9 at any one time. Results from this experiment showed that only 4% of **I-BRD9** was available. As a result of this, a dose of 500 mg/kg would be required to achieve exposure greater than the TR-FRET IC_{50} (50 μ M) over a period of 24 hours. Although this dose is not excessively high, delivering this quantity of compound *via* subcutaneous injection is expected to be extremely challenging. Given these data, **I-BRD9** was deemed unsuitable for use as an *in vivo* tool compound in mouse.

Although **I-BRD9** was not suitable for use *in vivo*, as an *in vitro* tool molecule, it exceeded the initial criteria outlined at the start of this project. PK data on **I-BRD9** was generated after probe declaration, meaning no optimisation against these parameters was conducted. In order to improve these results, optimised compounds could be tested in hepatocytes (liver cells in which both phase I and II metabolism are possible), providing a better prediction of *in vivo* PK. Through these studies, it would be possible to investigate a correlation between both *in vitro* and *in vivo* PK in order to guide lead optimisation.

One approach to optimise the PK data would be to improve the Brd9 potency of the probe molecule. This in turn, would reduce the quantity of compound required for efficacy, resulting in a lower dose. An alternative path would be to decrease the rate of clearance, thereby increasing systemic exposure and half life. Finally, in order to improve the predicted dose, optimisation against plasma protein binding could be conducted. Increasing the fraction of unbound compound would mean more would be available to interact with the target of interest. However, this is considered a difficult strategy as a higher free-drug fraction could result in higher clearance. Therefore, as reported by Smith and co-workers²⁰² a better approach may be to optimise against clearance and absorption, thereby increasing the free-drug concentration at the site of action.

2.3.9 Comparison of I-BRD9 to other Brd9 chemical probes

Following the publication of **I-BRD9**,²⁰³ two Brd9/Brd7 dual chemical probes were reported by the SGC and their collaborators at the University of Oxford and Boehringer Ingelheim. LP-99¹¹³ (**1.030**, **Figure 83**) and BI-9564¹¹⁴ (structure not yet disclosed) were obtained from the SGC and tested in Brd9 and Brd4 (BD1/2) TR-FRET assays in our laboratories. Results from these experiments confirm that these compounds are active against Brd9, with selectivity over Brd4.

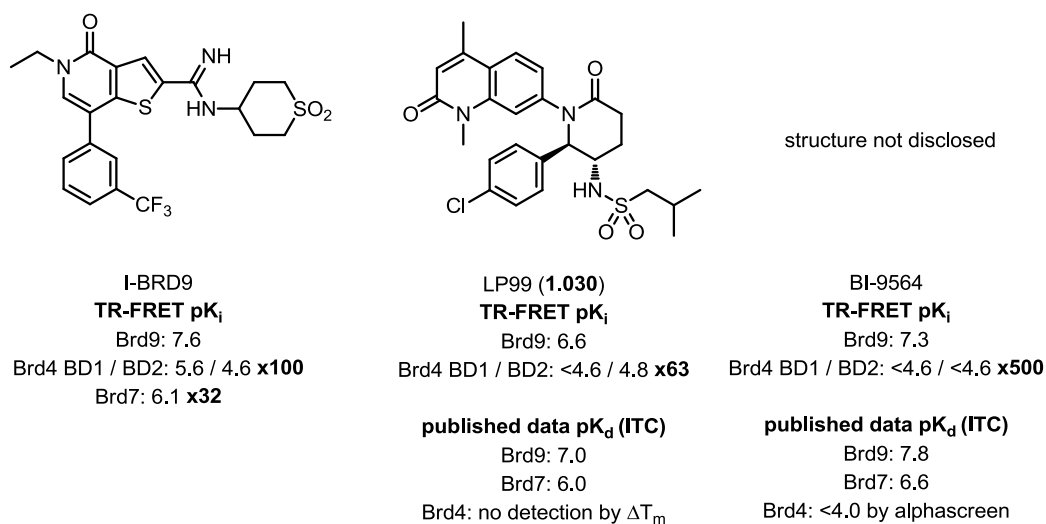


Figure 83: Brd9/7/4 data for I-BRD9, LP99 and BI-9564. Data are n≥2.

The data generated by the TR-FRET assays is in good agreement with the published results. LP99 (**1.030**) showed a pK_i value of 6.6 against Brd9, with 63 fold selectivity over Brd4 (TR-FRET). These results correlate well with the ITC data published (Brd9 pK_d: 7.0). Although not a quantitative method, selectivity over Brd4 was determined by thermal shift analysis. Therefore, direct comparison of the TR-FRET and published data is not possible.

BI-9564 also showed data in good agreement with literature values. The Brd9 pK_i value was 7.3, with 500 fold selectivity over Brd4 (TR-FRET). The SGC website reports a Brd9 pK_d value of 7.8, as determined by ITC. Selectivity over Brd4 was determined by alphascreen in which BI-9564 tested as inactive. Indeed this result correlates with the TR-FRET data, which showed Brd4 pK_i values of <4.6.

Overall, these data correlate with that reported in the literature, providing further confidence in the assays run within our laboratories. Comparison of the TR-FRET data for **I-BRD9** to the other probe molecules indicates that the potency of the compound is excellent. Although **I-BRD9** is slightly less selective over Brd4 than BI-

9564, the 100 fold window displayed is acceptable. Importantly, **I-BRD9** differs from the other tool molecules in that it is selective over Brd7. Both LP99 (**1.030**) and BI-9564 are dual probes, showing significant activity against the highly homologous Brd7. As a result of this, **I-BRD9** is the first and only selective Brd9 chemical probe reported to date.

2.4 Conclusion

Through several iterations of structure-based design starting from tertiary amide **2.005**, **I-BRD9** was identified as the first and only selective chemical probe for Brd9. During the course of these studies, all areas of the TP template were investigated. Primarily, array chemistry was used in order to explore the chemical space in a timely and efficient manner. Ultimately, the highly potent amidine moiety was critical to the success of **I-BRD9**, providing excellent selectivity over the BET family. Following the identification of this group at the 2-position of the template, selectively over non-BET bromodomains was gained through modifications to the 7-position and the *N*-alkyl KAc mimetic.

Overall, **I-BRD9** displays an excellent profile, with nanomolar activity against Brd9 ($pK_d: 8.7$, BROMOscan¹²¹), as well as excellent selectivity across a panel of 34 bromodomains. The compound is 800 fold selective over the BET family, 200 fold over the highly homologous Brd7 and 70 fold over every other bromodomain tested. Due to the exquisite profile shown by **I-BRD9**, it represents one of only three chemical probes known to target a single bromodomain selectively.

The broader pharmacological selectivity of **I-BRD9** was demonstrated *via* eXP, with no activity seen at less than 5 μ M against a panel of 49 diverse targets. **I-BRD9** is cellularly penetrant with proof of target engagement shown through a NanoBRET chromatin displacement assay¹¹² (pIC_{50} : 6.8). **I-BRD9** was shown to interact with endogenous Brd9 with good activity (pIC_{50} : 7.1) and excellent selectivity ($\times >625$) over the BET family, as shown by a chemoproteomic binding assay. With drug-like physico-chemical properties, **I-BRD9** meets and exceeded the chemical probe criteria defined at the outset of this project, and as such, was declared as a Brd9 selective chemical probe.

Following publication of this research,²⁰³ **I-BRD9** was presented to the SGC. The compound was fully endorsed and has been made freely available to the scientific community as part of the SGC epigenetic chemical probe set.²⁰⁴ In addition, the compound is available to purchase via several commercial suppliers (**Figure 84**). As **I-BRD9** is now published and available for use, the biological effects of Brd9 bromodomain inhibition can be explored for the first time.

The figure consists of two screenshots of websites advertising I-BRD9.

Top Screenshot (SGC Website): The page title is "I-BRD9 A chemical probe for BRD9". It features the SGC logo and logos of partner institutions: University of Oxford, UNICAMP, and Goethe University Frankfurt am Main. A search bar is present in the top right. Below the title, a green banner states "This probe is available from Tocris and Cayman". A navigation menu includes "Overview", "Properties", "Selectivity Profile", "Cellbased Assay Data", "Co-crystal structures", "References", and "Materials and Methods". A section titled "Biology of the BRD9 Bromodomains" contains a brief description: "BRD9 is a bromodomain containing protein that form a small sub-branch of the bromodomain family tree [1]. Human BRD9 contains a single bromodomain and has five isoforms that are produced by alternative splicing. Little is known about BRD9 function but it has been implicated in chromatin remodelling as part of the SWI/SNF complex."

Bottom Screenshot (Tocris Website): The page title is "I-BRD9". It features the Tocris logo and a "Quick Search" bar. A navigation menu includes "Home", "About Tocris", "Support", "Resources", "Literature", and "Special O". A left sidebar lists categories: "Pharmacology" (All Targets, 7-TM Receptors, Ion Channels, Nuclear Receptors, Enzyme-Linked Receptors, Transporters, Enzymes, Other Pharmacology) and "Cell Biology" (Angiogenesis, Apoptosis, Cell Cycle, Cell Metabolism). The main content area shows the chemical structure of I-BRD9, its catalog number "Cat. No. 5591", and a "New" badge. The chemical name is: "5-Ethyl-4,5-dihydro-4-oxo-N-(tetrahydro-1,1-dioxido-2H-thiopyran-4-yl)-7-[3-(trifluoromethyl)phenyl]thieno[3,2-c]pyridine-2-carboximidamide". A "Price and Availability" section includes a country selection dropdown and a "Submit" button. A note states: "By clicking submit you agree to accept a cookie from Tocris Bioscience. For details, please read our [privacy and cookie policy](#)."

Figure 84: I-BRD9 advertisements on the SGC (top) and Tocris (bottom) websites.

3 Studies towards the development of a chemical probe for TAF1 BD2

3.1 Introduction

3.1.1 Identification of TAF1 as a target

Following the successful identification of **I-BRD9**, focus was placed on the development of a chemical probe for Transcription initiation factor TFIID subunit 1 (TAF1), a BCP for which the biological role is currently unknown. To date, there are no chemical probes reported for TAF1. Therefore, the identification of an appropriate tool molecule was essential in order to elucidate its biological function.

3.1.2 TAF1 Structure and function

Transcription of genes requires the assembly of a large multi-protein complex to transcriptional start sites. A major component required is Transcription Factor IID (TFIID), a multi-subunit complex that initiates the assembly of the cellular transcriptional machinery.²⁰⁵ TFIID binds to the promoter region on DNA and serves as a scaffold for the assembly of approximately 70 proteins that constitute the transcription initiation complex. TFIID is composed of the TATA Binding Protein (TBP) and 14 TBP-Associated Factors (TAFs or TAF_{II}s).²⁰⁶ TAF1 or TAF_{II}250, the largest subunit of TFIID mediates promoter region and DNA binding, alteration of chromatin structure, and post-translational modification of general transcription factors. As such, TAF1 facilitates transcriptional activation.²⁰⁷

The TAF1 protein is reasonably well studied and it has been reported that dysfunction of TAF1 is associated with various disease states. For example, increased TAF1 expression is correlated with progression of human prostate cancers,²⁰⁸ and TAF1 has been found to modulate the Human Papillomavirus (HPV), the main factor in the development of cervical cancer.²⁰⁹ In addition, it has been reported that reduced expression of the TAF1 gene is associated with X-Linked Dystonia-Parkinsonism; a condition characterised by sustained muscle contractions, causing twisting and repetitive movements or abnormal postures.²¹⁰

The TAF1 protein is made up of approximately 2000 amino acid residues and consists of various domains, which are responsible for its role in transcriptional activation. More specifically, TAF1 contains: a HAT domain; two atypical protein

kinase domains; and a tandem pair of bromodomains, namely BD1 and BD2 (Figure 85).^{207,211}



Figure 85: Schematic representation of the TAF1 protein complex, which contains: NTK, N-terminal kinase domain; HAT, histone acetyltransferase; BD1, bromodomain 1; BD2, bromodomain 2; and CTK, C-terminal kinase domain.

There is literature evidence to suggest that TAF1 is a protein kinase in its own right. However, as TAF1 does not possess classical kinase architecture, it is more likely that this activity is due to an association with protein kinase CK2. It is believed that this association may play a role in the phosphorylation and function of Mdm2, a critical regulator of the p53 tumour suppressor.²¹²

TAF1 contains a tandem pair of bromodomains for which a crystal structure has been reported. The individual bromodomains are connected *via* a linking helix, creating a separation of approximately 25 Å between each KAc binding site (Figure 86).²¹³

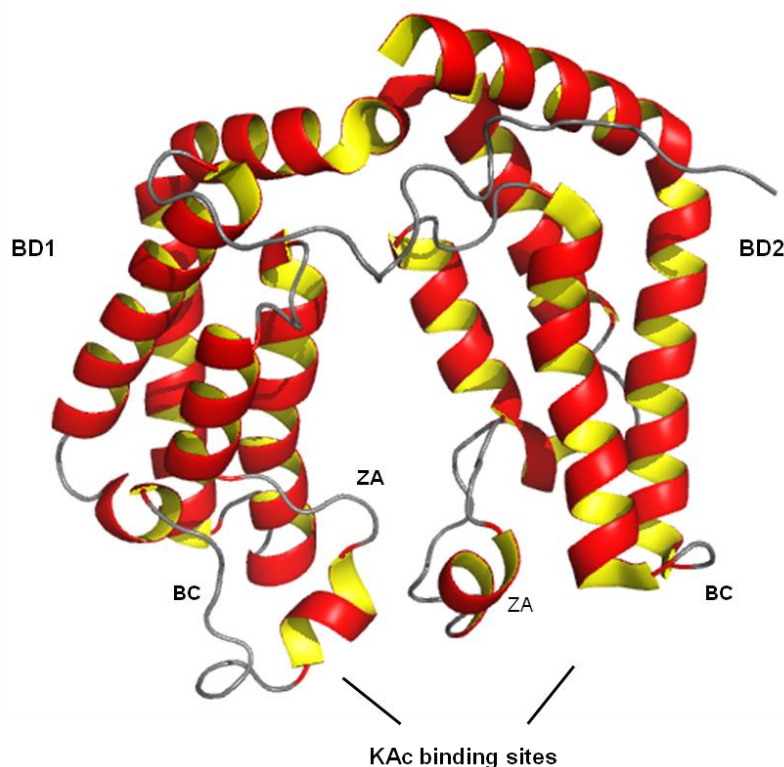


Figure 86: X-Ray crystallography of the TAF1 bromodomains, BD1 and BD2 (PDB code = 1EQF).

The connectivity of the two bromodomains of TAF1 makes them ideally positioned to recognise histone tails containing two KAc residues separated by 7 or 8 amino

acids. It has been reported that the tandem bromodomains of TAF1 bind with greater affinity to diacetylated histone tails than to monoacetylated due a cooperative effect.²¹⁴ As a result of this, the bromodomains of TAF1 recognise a specific combination of acetyl marks on histone tails.

TAF1 is a member of family 7 of the bromodomain phylogenetic tree (**Figure 8**, page 7), along with Transcription initiation factor TFIID subunit 1-like (TAF1L), a highly homologous tandem bromodomain (**Table 24**).

TAF1L BD1	TAF1 BD1		TAF1L BD2	TAF1 BD2	Comment
HIS1399	TYR1380		TRP1522	TRP1503	WPF motif
PRO1400	PRO1381		PRO1523	PRO1504	WPF motif
PHE1401	PHE1382		PHE1524	PHE1505	WPF motif
HIS1402	HIS1383		HIS1525	HIS1506	ZA channel
THR1403	THR1384		HIS1526	HIS1507	ZA channel
PRO1404	PRO1385		PRO1527	PRO1508	ZA channel
VAL1405	VAL1386		VAL1528	VAL1509	ZA channel
ASN1406	ASN1387		ASN1529	ASN1510	ZA loop
ALA1407	ALA1388		LYS1530	LYS1511	ZA loop
INS1409	INS1390		INS1532	INS1513	ZA loop
INS1409	INS1390		INS1532	INS1513	ZA loop
VAL1409	VAL1390		PHE1532	PHE1513	ZA loop
VAL1410	VAL1391		VAL1533	VAL1514	ZA loop
TYR1413	TYR1394		TYR1536	TYR1517	Water-binding Tyr
TYR1414	TYR1395		TYR1537	TYR1518	
ILE1417	ILE1398		ILE1540	ILE1521	
ILE1448	ILE1429		ILE1571	ILE1552	
ASN1451	ASN1432		ASN1574	ASN1555	
SER1452	SER1433		SER1575	SER1556	
TYR1455	TYR1436		TYR1578	TYR1559	Conserved Tyr
ASN1456	ASN1437		ASN1579	ASN1560	Conserved Asn
HIS1460	HIS1441		SER1583	SER1564	
SER1461	SER1442		GLN1584	GLN1565	
LEU1462	LEU1443		TYR1585	TYR1566	Gatekeeper
THR1463	THR1444		THR1586	THR1567	
ILE1465	ILE1446		THR1588	THR1569	
SER1466	SER1447		ALA1589	ALA1570	

Table 24: Sequence similarity across the KAc binding sites of TAF1 (BD1 and BD2) and TAF1L (BD1 and BD2). Identical residues are highlighted in green and different in red. Amino acid insertions are shown in grey.

The KAc binding sites of TAF1 and TAF1L share high sequence similarity: the BD1 domains differ by one amino acid residue and the BD2 domains are identical. Given their high homology, it is likely that compounds which are active against TAF1 will also be active against TAF1L.

As previously discussed (Section 2.3.6.3, page 119), recent studies³³ have confirmed the ability of Brd9 and CECR2 to bind to butyrylated lysine residues but not the crotonylated variant. These results were extended to TAF1 BD2 and TAF1L BD2, which were found to bind to butyryllysine. However, unlike Brd9 and CECR2,

TAF1 BD2 and TAF1L BD2 also bound crotonyllysine and were the only bromodomains screened to do so. X-Ray crystallography of the crotonyl lysine in complex with TAF1 BD2 shows displacement of two of the conserved water molecules from their usual positions, allowing the crotonyl double bond to adopt an almost coplanar conformation with the amide bond (**Figure 87**).

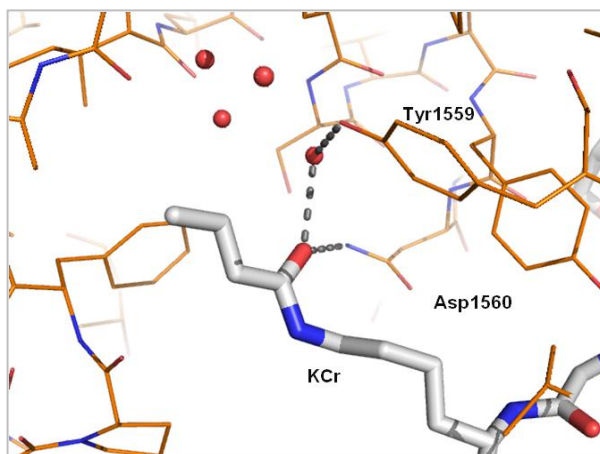


Figure 87: X-Ray crystallography of KCr in complex with TAF1 BD2 (PDB code = 4YYN). Hydrogen-bonds are shown as grey dashed lines and water molecules as red spheres.

The fact that only the BD2 domains of TAF1 and TAF1L bind butyl and crotonyl lysines further confirms their sequence similarity and their differences to the equivalent BD1 domains.

3.1.3 Small molecule inhibitors of TAF1

Although the TAF1 protein is associated with various disease states, the biological roles of the individual domains are yet to be determined. A chemical probe approach offers a method to investigate protein function *via* selective inhibition of an individual domain. Towards this goal, McKeown and co-workers¹³⁴ developed multi-component reactions to access novel bromodomain inhibitors. Although not selective over the BET family, compound **1.041** shows activity against TAF1 BD2 and the highly homologous TAF1L, with pK_d values of 6.3 and 5.9, respectively (**Figure 88**).

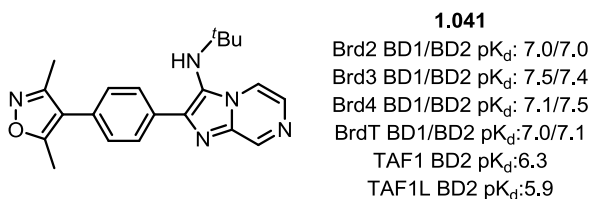


Figure 88: Compound **1.041** developed by McKeown and co-workers.¹³⁴

It is important to note that only TAF1 BD2 activity is reported for compound **1.041**, presumably because there was no assay available for BD1. Compound **1.041** has not been used for biological investigation and therefore does not provide any indication of TAF1 bromodomain function. As **1.041** shows multi-bromodomain pharmacology, it would be difficult to assign any phenotype observed to inhibition of a particular bromodomain. As such, compound **1.041** is not suitable for use as a chemical probe.

McKeown and co-workers¹³⁴ report an X-ray crystal structure of compound **1.041** in complex with Brd4 BD1 (**Figure 89**).

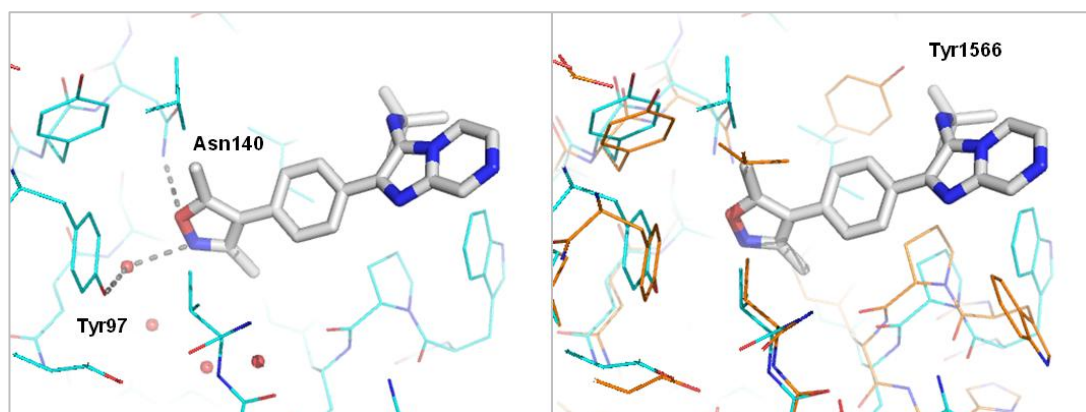


Figure 89: (A) X-Ray crystallography of compound **1.041** in complex with Brd4 BD1 (left, blue; PDB code = 4WIV); (B) X-Ray crystallography of compound **1.041** in complex with Brd4 BD1 (right, blue; PDB code = 4WIV) overlaid with apo TAF1 BD2 (right, orange). Hydrogen-bonds are shown as grey dashed lines and water molecules as red spheres.

The 3,5-dimethylisoxazole moiety acts as the KAc mimetic, forming hydrogen-bonds to Asn140, as well as a water mediated interaction to Tyr97. This binding motif is consistent with that described for compounds **1.010–1.013**, which share the same KAc mimetic (Section 1.5.2, page 18). The remainder of the molecule occupies the ZA channel and the ^tBu group rests in a groove located close to the WPF shelf region.

3.1.4 Aims

There is very little in the literature concerning TAF1 bromodomain biology, which, in part, is due to the lack of potent and selective chemical probes. Therefore, the development of a high quality chemical probe, which is selective for TAF1 is essential to elucidate its biological function. Accordingly, the aim of this research was to develop a potent and selective chemical probe for TAF1, which, as discussed previously (Section 1.6, page 39), should satisfy the following criteria:

1. $pIC_{50} \geq 7$ against TAF1, as determined by TR-FRET assay.
2. ≥ 100 fold selectivity over the BET family of bromodomains (Brd4 will be used as a representative member of the family).
3. ≥ 30 fold selectivity over other non-BET bromodomains, as determined by BROMOscan.
4. ≥ 100 fold selectivity over broader pharmacological targets outside of the bromodomain family.
5. Evidence of cellular target engagement.

It is important to note that any compound shown to be active against TAF1 will also be active against TAF1L, given their high homology (**Figure 8**, page 7). However, this hypothesis would only be confirmed by BROMOscan analysis. Therefore, if a compound was found to be active against TAF1L, it could be possible to tag this compound to a fluorescent probe in order to develop a TR-FRET assay. In addition, suitable biophysical experiments could be utilised in order to confirm direct binding.

3.2 Results and discussion for TAF1 chemical probe discovery

3.2.1 Identification of a start point for chemical probe discovery

In order to identify compounds to provide a start point for the TAF1 chemical probe effort, a cross-screening strategy was conducted. In total, 946 compounds were tested against TAF1 BD2 by means of a TR-FRET assay. The ligand (**3.001**, **Figure 90**) used to configure this assay has greater affinity for BD2 (~150 nM) than BD1 (~3 μ M).

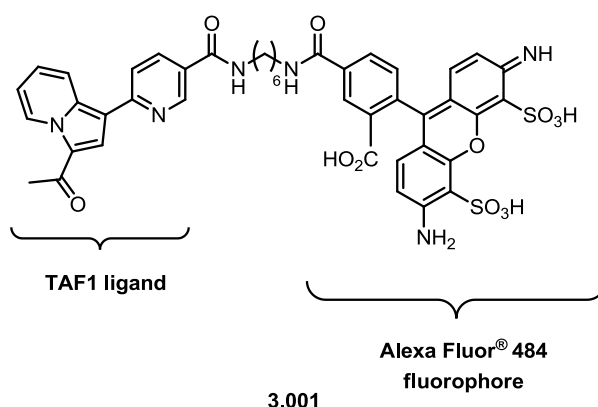


Figure 90: Chemical structure for TAF1 TR-FRET assay ligand, 3.001.

During the development of the TR-FRET assay, a ligand with equal affinity in both BD1 and BD2 could not be identified and no ligand tested showed greater affinity for BD1. Therefore, although the TAF1 protein contains two bromodomains, binding

affinity was measured at BD2 only. This is consistent with the commercial bromodomain assays that are available such as BROMOscan by DiscoverX,¹²¹ suggesting that identifying potent binders of BD1 is extremely challenging. In addition, analysis of bromodomain druggability conducted by Vidler and co-workers³¹ indicates that unlike TAF1 BD1, the BD2 domain is tractable to inhibition by small molecules.

The KAc binding regions of the TAF1 bromodomains show 66% sequence similarity (Table 25).

TAF1 HUMAN 1	TAF1 HUMAN 2	Comment
TYR1380	TRP1503	WPF motif
PRO1381	PRO1504	WPF motif
PHE1382	PHE1505	WPF motif
HIS1383	HIS1506	ZA channel
THR1384	HIS1507	ZA channel
PRO1385	PRO1508	ZA channel
VAL1386	VAL1509	ZA channel
ASN1387	ASN1510	ZA loop
ALA1388	LYS1511	ZA loop
INS1390	INS1513	ZA loop
INS1390	INS1513	ZA loop
VAL1390	PHE1513	ZA loop
VAL1391	VAL1514	ZA loop
TYR1394	TYR1517	Water-binding Tyr
TYR1395	TYR1518	
ILE1398	ILE1521	
ILE1429	ILE1552	
ASN1432	ASN1555	
SER1433	SER1556	
TYR1436	TYR1559	Conserved Tyr
ASN1437	ASN1560	Conserved Asn
HIS1441	SER1564	
SER1442	GLN1565	
LEU1443	TYR1566	Gatekeeper
THR1444	THR1567	
ILE1446	THR1569	
SER1447	ALA1570	

Table 25: Sequence similarity of TAF1 BD1 and BD2 across the KAc binding pocket. Residues which are identical are shown in green; residues which are similar in orange; and residues which are different in red. Grey boxes indicate an amino acid insertion.

Presumably, the differences in the amino acid residues which constitute the KAc binding pockets of TAF1 BD1 and BD2 deliver different protein architectures, which may account for the selectivity of the assay ligand for BD2. However, without an X-ray crystal structure, it is difficult to form a solid hypothesis.

The results from the cross-screen identified several compounds which showed high TAF1 BD2 potency, with some selectivity over Brd4 (Figure 91, potent and selective compounds shown in green).

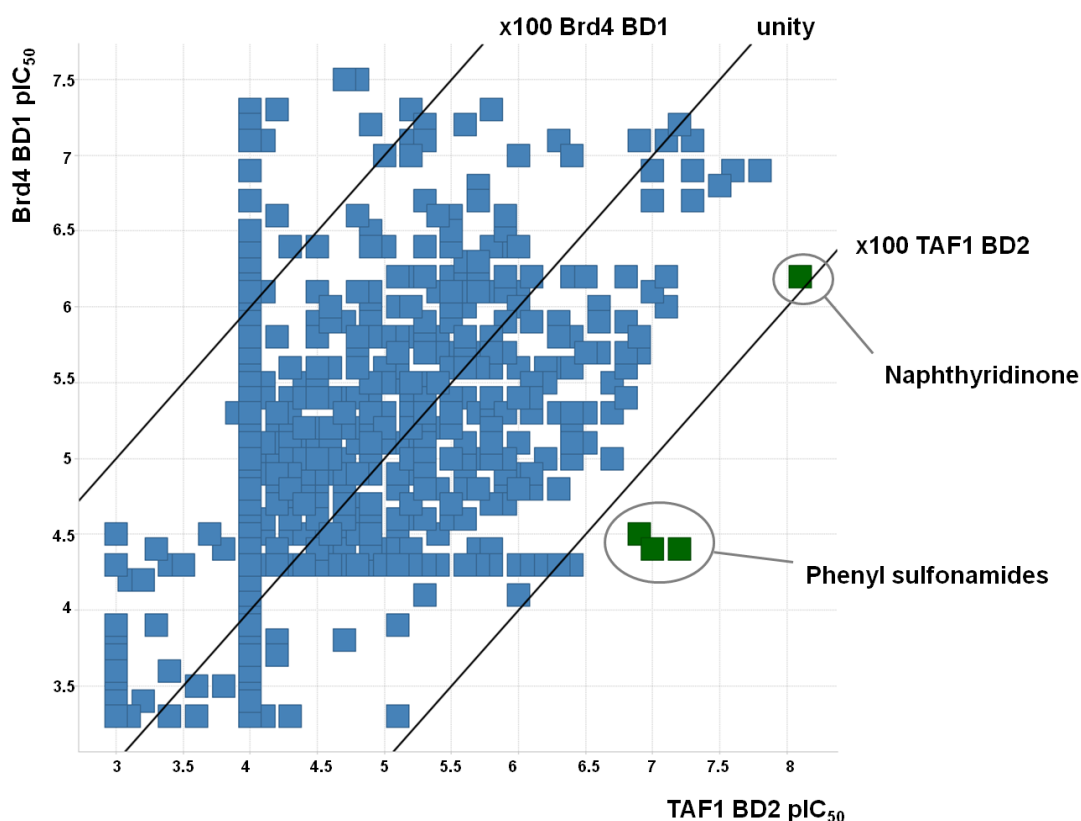
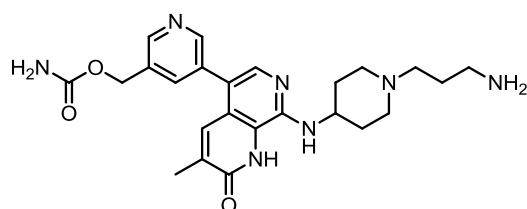


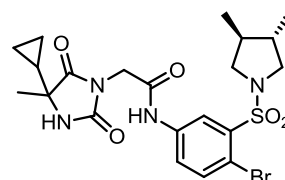
Figure 91: Graph to show data from initial TAF1 BD2 screen, in which 946 compounds were screened. TAF1 BD2 activity is shown on the x-axis and Brd4 BD1 on the y-axis.

The compounds highlighted correspond to naphthyridinone **3.002a** and three phenylsulfonamides, for which **3.003** is shown as a representative example (Figure 92).



3.002a

TAF1 BD2 pIC₅₀: 8.1 (0.33)
 Brd4 BD1 / BD2 pIC₅₀: 6.2 / 5.3 **x80**
 ATAD2 pIC₅₀: 6.2 **x125**



3.003

TAF1 BD2 pIC₅₀: 7.2 (0.31)
 Brd4 BD1 / BD2 pIC₅₀: 4.4 / 5.2 **x100**
 ATAD2 pIC₅₀: 7.6 **x0**

Figure 92: pIC₅₀ values for compounds **3.002a** and **3.003** against TAF1 BD2 and Brd4 BD1, BD2 and ATAD2, as determined by TR-FRET analysis. Selectivity over Brd4 is calculated relative to the maximum value and selectivity over ATAD2 is calculated based on pK_i values. Data are n≥2.

Further research into the development of these compounds revealed that they were designed and synthesised in an effort to deliver a chemical probe for the bromodomain of ATAD2. In particular, compound **3.002a** shares the same chemotype as published ATAD2 inhibitors **1.021** and **1.022** (Figure 16, page 27).^{105,106} It has been reported that compound **3.002a** was attached to a fluorescent

ligand for use in the ATAD2 TR-FRET assay.^{105,106} For this reason, TAF1 BD2 and ATAD2 data were compared (**Figure 93**).

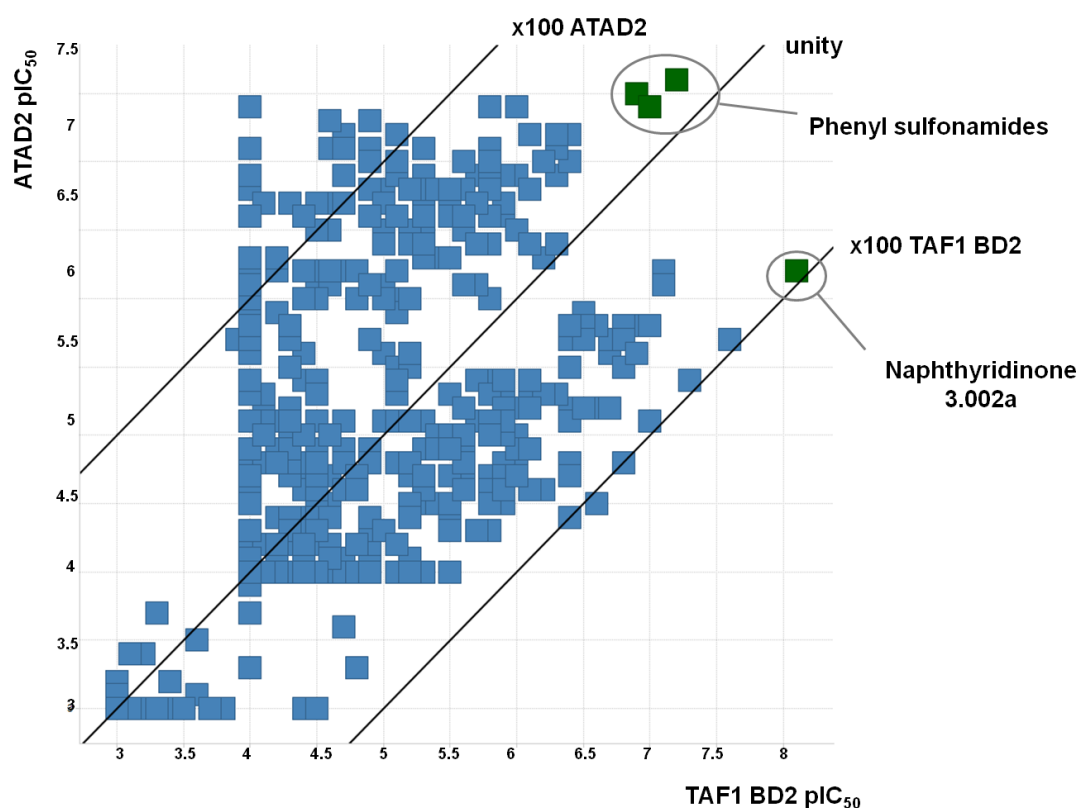


Figure 93: Graph to show data from initial TAF1 BD2 screen, in which 946 compounds were screened. TAF1 BD2 activity is shown on the x-axis and ATAD2 on the y-axis.

As indicated in **Figure 92**, naphthyridinone **3.002a** shows high TAF1 BD2 activity, with ~ 100 fold selectivity against ATAD2. In contrast, the phenylsulfonamides showed high TAF1 BD2 activity with no selectivity over ATAD2. For this reason, compound **3.002a** was progressed for further profiling (**Table 26**).

Compound 3.002a	
TAF1 BD2 pIC ₅₀ (LE)	8.1 (0.33)
Brd4 BD1 / BD2 pIC ₅₀	6.2 / 5.3 x80
Brd7 pIC ₅₀	5.5 x400
Brd9 pIC ₅₀	7.2 x8
BRPF1 pIC ₅₀	5.1 x1000
ATAD2 pIC ₅₀	6.2 x125
MW, <i>ChromLogD</i> _{7.4}	466, 0.44
CLND sol., AMP	39 µg/mL, 16.5 nm/s
IL-6 pIC ₅₀	4.9

Table 26: Summary of compound 3.002a. Selectivity over Brd4 is calculated relative to the maximum value and selectivity over ATAD2 is calculated based on pK_i values. Data are n≥2.

Compound **3.002a** showed high TAF1 BD2 activity with a pIC_{50} of 8.1, acceptable ligand efficiency of 0.33, and good selectivity over Brd4 (80 fold) and ATAD2 (125 fold). Furthermore, **3.002a** showed excellent selectivity over the bromodomains of BRPF1 (1000 fold) and Brd7 (400 fold). Although Brd9 is highly homologous to Brd7, activity against this bromodomain was high (Brd9 pIC_{50} of 7.2), providing little selectivity.

Although the bromodomain activity and selectivity data was encouraging, **3.002a** showed undesirable physico-chemical properties, such as high polarity (*ChromLogD*_{7.4} 0.44) and poor solubility [CLND sol.: 39 μ g/mL (determined by precipitation of 10 mM DMSO solution at pH 7.4)]. Following biological evaluation of **3.002a**, the compound was found to precipitate from DMSO solution at 10 mM concentration. As such, **3.002a** was deemed too insoluble to conduct further tests. It was believed that the poor solubility shown by compound **3.002a**, was a result of several factors. For example, **3.002a** contains 10 HBAs and 4 HBDs, meaning that individual molecules can interact with each other through hydrogen-bonding. In addition, **3.002a** contains 3 directly fused aromatic rings, creating a planar structure, with minimal 3D character. A combination of these two features can result in poor solubility and is consistent with that reported in the literature.^{154,215,216,217}

Compound **3.002a** showed limited cellular penetration as demonstrated by the artificial membrane permeability (AMP: 16.5 nm/s) and IL-6 inhibition (pIC_{50} : 4.9) data. As discussed previously (Section 2.3.8.1, page 123), the IL-6 biomarker can be used to provide an indication of cellular target engagement at Brd4 BD1. When tested for IL-6 inhibition, **3.002a** showed a pIC_{50} value of 4.9, providing poor correlation to Brd4 BD1 activity (pIC_{50} : 6.2). The disconnect observed between the biochemical and cellular data suggested that the compound did not reach the site of action. It was hypothesised that the highly polar (*ChromLogD*_{7.4} 0.44) and charged nature of **3.002a** meant that it had limited ability to pass through the phospholipid bilayer of the cell membrane.

Moving forward with the naphthyridinone series, compound **3.002a** was broken down into its constituent parts for analysis. A model of a truncated version of this compound allowed the key interactions to be examined (**Figure 94**).²¹⁸

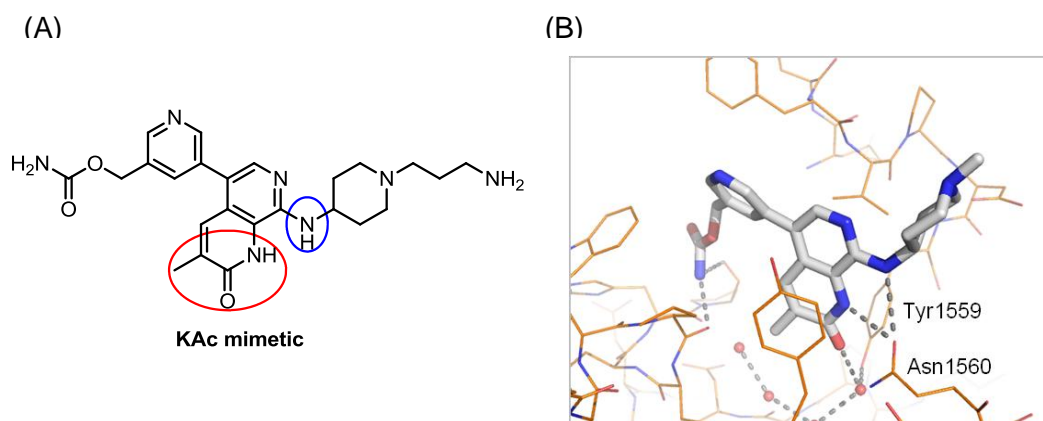


Figure 94: (A) Chemical structure of compound 3.002a with the KAc mimetic and amine NH groups highlighted; (B) Truncated compound 3.002a modelled in TAF1 BD2. Hydrogen-bonds are shown as grey dashed lines and water molecules as red spheres.

The pyridinone moiety of **3.002a** (highlighted in red) acts as the KAc mimetic. The carbonyl group forms a hydrogen-bond to the NH₂ moiety of Asn1560, as well as a water mediated interaction with Tyr1559. In addition, the amine NH (highlighted in blue) forms a hydrogen-bond to the carbonyl of Asn1560, creating a tridentate interaction. As such, it was believed that these groups should be maintained in future structures.

Moving to the 8-position of the scaffold, the modelling studies predicted that any functionalisation of the piperidine ring would protrude into solvent (**Figure 95**).

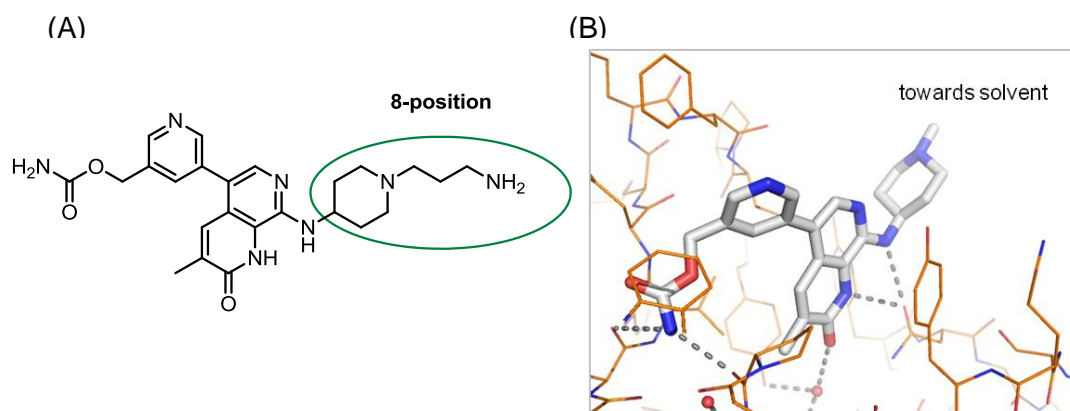


Figure 95: (A) Chemical structure of compound 3.002a with the 8-position highlighted; (B) Truncated compound 3.002a modelled in TAF1 BD2. Hydrogen-bonds are shown as grey dashed lines and water molecules as red spheres.

At the 5-position of the molecule, the docking studies predicted that the NH₂ of the carbamate group forms interactions to the backbone carbonyl moieties of Pro1548 and 1552 (**Figure 96**).

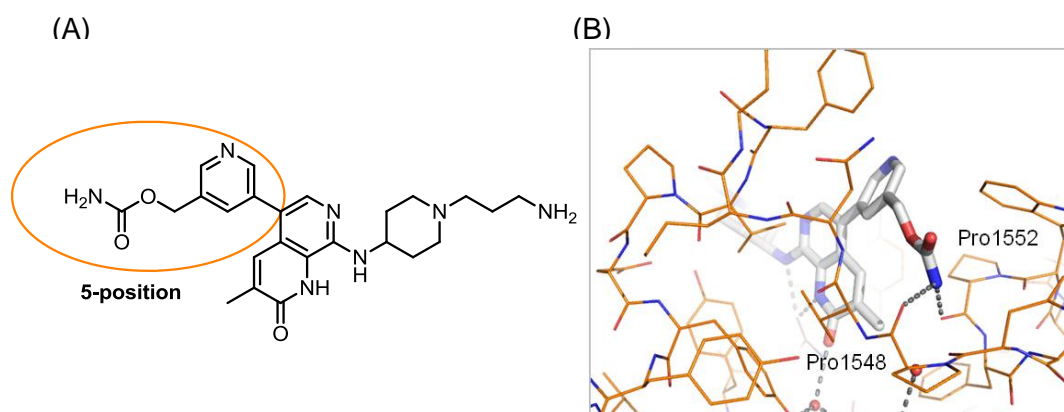


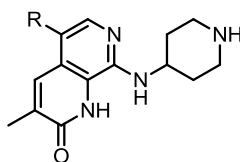
Figure 96: (A) Chemical structure of compound **3.002a** with the 5-position highlighted; (B) Truncated compound **3.002a** modelled in TAF1 BD2. Hydrogen-bonds are shown as grey dashed lines and water molecules as red spheres.

Considering the proposed interactions of compound **3.002a**, as predicted by the docking studies, initial focus was placed on the 5-position in order to investigate the value of the carbamate group.

3.2.2 Initial SAR investigation at the 5-position

3.2.2.1 Identification of target compounds

Initial investigations focused on the 5-position due to the polar nature of the carbamate moiety, which was thought to contribute to high polarity, poor solubility and permeability. In order to explore the SAR at this position, several groups were identified as possible alternatives based previously generated data. Although these data were from the unfunctionalised amino piperidine scaffold, 3 compounds²¹⁹ were noted as maintaining high TAF1 BD2 activity with improved selectivity over Brd4. Along with physico-chemical properties, selectivity over Brd4 was considered in the first instance (**Table 27**).



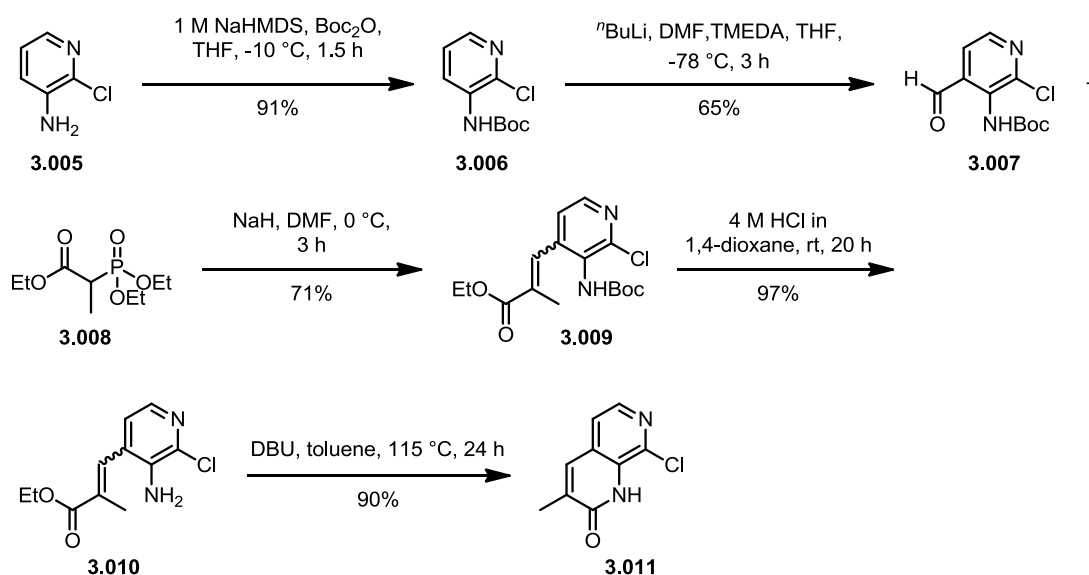
Entry	Compound number	R =	TAF1 BD2 pIC ₅₀	Brd4 BD1 pIC ₅₀	Brd4 BD2 pIC ₅₀	Selectivity
1	3.004a		6.8	5.9	4.8	x8
2	3.004b		6.8	5.4	4.7	x25
3	3.004c		6.7	5.6	4.8	x13
4	3.004d		6.8	5.3	4.9	x32

Table 27: pIC₅₀ values for compounds 3.004a–d in the bromodomains of TAF1 BD2 and Brd4 BD1 and BD2 as determined by TR-FRET analysis. Selectivity over Brd4 is calculated relative to the maximum value. Data are n≥2.

Truncation of carbamate, **3.004a** to alcohol, **3.004b** and methyl compound **3.004c** maintained TAF1 BD2 activity at 6.8, with improved selectivity over Brd4. Furthermore, pyridinone, **3.004d** showed identical TAF1 BD2 activity, with much improved selectivity (compare entries 1 and 4). In order to understand if this SAR was transferable to the propylamine functionalised scaffold and to investigate the true effect of this substituent, these 5-position groups were installed onto the corresponding intermediate.

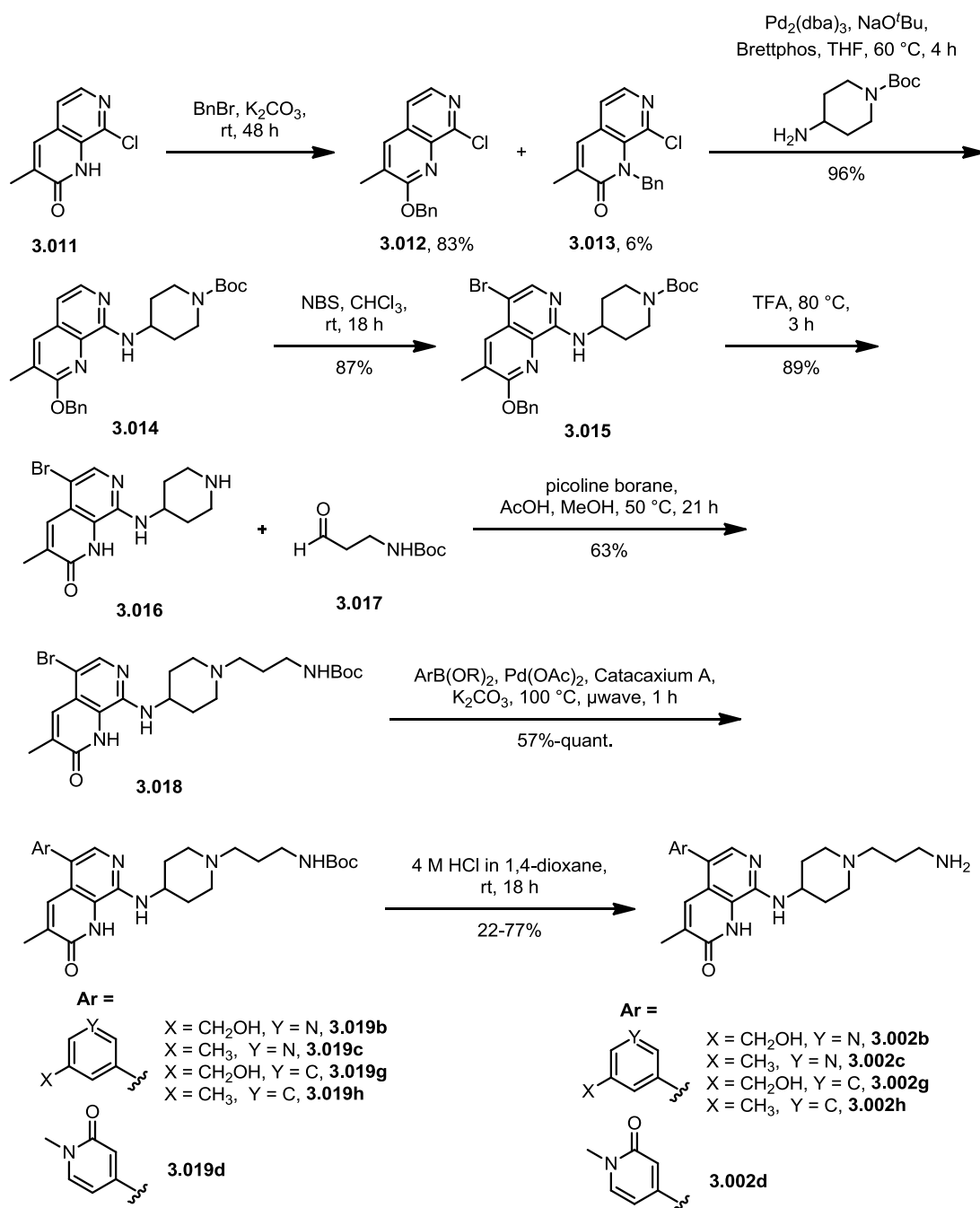
3.2.2.2 Synthesis of 5-position analogues

In order to efficiently explore the SAR at the 5-position, the aim was to access an intermediate from which structural diversity could be introduced in the final step. To this end, compounds **3.002b–d** were synthesised *via* an 11-step route. The first portion of this synthesis was conducted using previously reported chemistry¹⁰⁵ on a 50 g scale to provide key intermediate **3.011** (Scheme 31).



Scheme 31: Synthetic route to access intermediate 3.011 on 50 g scale.

Commercially available pyridine **3.005** was Boc protected in 91% yield using NaHMDS and Boc₂O²²⁰ to deliver compound **3.006**. Following this, formylation with ⁿBuLi, then careful addition of DMF at –78 °C²²¹ furnished aldehyde **3.007**. A Horner-Wadsworth-Emmons reaction²²² was employed using commercially available phosphonate **3.008** to deliver compound **3.009**. Boc deprotection was achieved using 4 M HCl in 1,4-dioxane, followed by cyclisation with DBU. With an efficient and high yielding route to access compound **3.011** investigated, functionalisation of the 5-position was examined (**Scheme 32**).

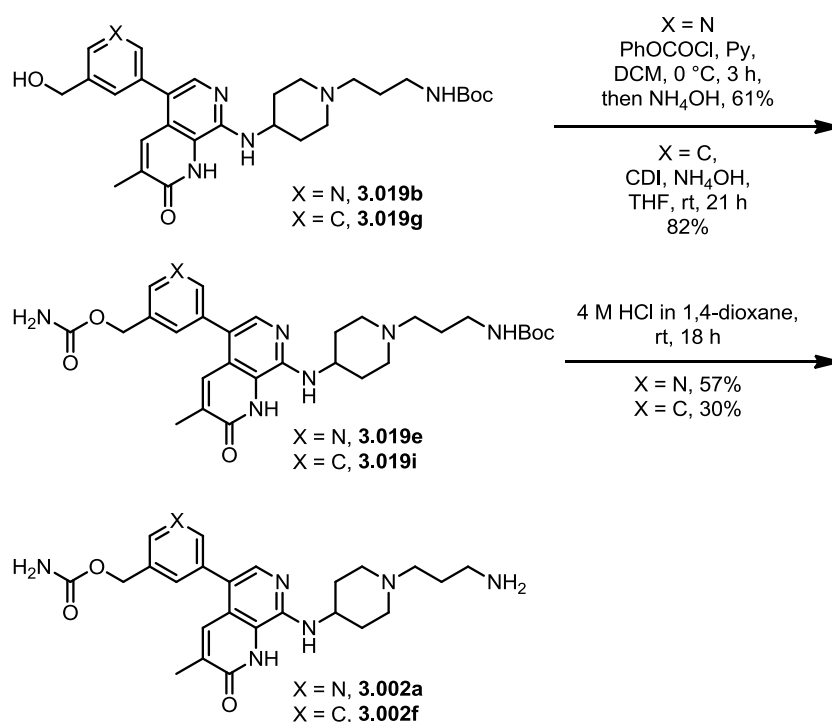


Scheme 32: Synthesis of compounds 3.002b, c, g and h from key intermediate 3.011.

During these investigations, it was found that protection of the pyridinone moiety of intermediate **3.011** as the O-benzyl was necessary for the subsequent Buchwald-Hartwig coupling.^{223,224} In the absence of this protecting group, the reaction did not proceed, with starting material observed by LCMS analysis. It was postulated that the Pd catalyst may have coordinated to the naphthyridinone moiety, preventing oxidative addition. As such, **3.011** was benzylated using benzyl bromide and K₂CO₃ at room temperature. These conditions delivered O-benzyl compound, **3.012** as the

major product (83%), although a small amount of the *N*-benzyl analogue, **3.013** was observed (6%). Presumably, the *O*-benzylated product was favoured due to the greater steric encumbrance surrounding the pyridone nitrogen. Following this, a Buchwald-Hartwig amination was conducted using the Pd₂(dba)₃ and Brettphos catalyst system¹⁰⁵ to deliver compound **3.014** in 96% yield. The newly installed amino piperidine served as a directing group for electrophilic bromination with NBS, which proceeded in good yield (87%). The Boc and benzyl groups were simultaneously cleaved by heating in TFA to provide intermediate **3.016**. Previously conducted chemistry on this series had shown that stoichiometric TFA did not remove the benzyl group at room temperature or at reflux. Reductive amination²²⁵ chemistry was utilised to functionalise the amino piperidine. Aldehyde **3.017** was accessed from the corresponding alcohol *via* an oxidation with Dess Martin periodane.²²⁶ Compound **3.018** served as the key intermediate to which the various aryl groups were installed *via* a Suzuki-Miyaura coupling,²²⁷ with Pd(OAc)₂ and bulky phosphine ligand, Catacaxium A. Finally, deprotection of the Boc group was achieved with 4 M HCl in 1,4-dioxane to furnish final compounds **3.002b, c, g** and **h**.

To access the original hit molecule **3.002a**, intermediate **3.019b** was taken forward for further functionalisation (**Scheme 33**).

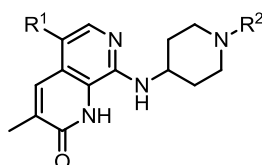


Scheme 33: Synthesis of compounds 3.002a and 3.002f.

The carbamate moiety was installed on compound **3.019b** by treatment with phenyl chloroformate and pyridine in DCM at 0 °C. This furnished compound **3.019e** in 61% yield. Subsequent Boc deprotection using 4 M HCl in 1,4-dioxane delivered final compound **3.002a** in reasonable yield (57%). The all carbon analogue, **3.002f** was prepared in a similar fashion.

3.2.2.3 SAR discussion of 5-position analogues

In order to determine the binding affinity of compounds **3.002** and **3.004a–d** in TAF1 BD2 and Brd4 BD1 and BD2, a TR-FRET assay was utilised. The data are shown in **Table 28** and selectivity is calculated relative to the maximum Brd4 value. In contrast to the Brd9 chemical probe efforts in which the TP template was most active at BD1, the naphthyridinone scaffold showed activity at both BD1 and BD2.



Entry Compound Number	1 3.004 a	2 3.002 a	3 3.004 b	4 3.002 b	5 3.004 c	6 3.002 c	7 3.004 d	8 3.002 d
R ¹ =								
R ² =	H		H		H		H	
TAF1 BD2 pIC ₅₀	6.8	8.1	6.8	7.5	6.7	7.3	6.8	7.3
Brd4 BD1 pIC ₅₀	5.9	6.2	5.4	5.6	5.5	5.6	5.3	5.5
Brd4 BD2 pIC ₅₀	4.9	5.3	4.7	5.0	4.8	4.7	4.9	5.2
Selectivity	x8	x80	x25	x80	x16	x50	x32	x63
CLND sol. (µg/mL)	144	-	137	34	72	29	31	45
AMP (nm/s)	<3	16.5	<3	8	<3	11	<3	7.4

Table 28: pIC₅₀ values for compounds **3.002a–d** and **3.004a–d** in the bromodomains of TAF1 BD2 and Brd4 (BD1 and BD2) as determined by TR-FRET analysis. Selectivity is calculated relative to the maximum Brd4 value. Data are n≥2.

Analysis of the data indicated that the nature of R¹ made very little difference to both TAF1 BD2 and Brd4 activities when R² was H or propylamine. For example, truncation of carbamate **3.004a** to methyl substituted compound, **3.004c** maintained

TAF1 activity, with minor improvement in selectivity over Brd4 (compare entries 1 and 5). An identical trend was seen for compounds **3.004b** and **c** (compare entries 4 and 6). Transformation of R¹ from H to propylamine caused a significant increase in TAF1 BD2 activity, with little effect on Brd4 (compare entries 5 and 6). Despite X-ray crystallography indicating that this substituent would protrude into solvent (**Figure 95**, page 148), the data suggested that the propylamine chain could be making specific interactions in TAF1 BD2 but not in Brd4. The disconnect observed between the TR-FRET data and the structural modelling suggested that this result may be an assay artefact, resulting from a possible interference with the fluoroligand. In order to investigate this hypothesis further, a selection of compounds were progressed for test in an orthogonal screen (Section 3.2.5, page 172).

Pyridinone **3.002d** showed an acceptable profile with a TAF1 BD2 pIC₅₀ of 7.3 and 63 fold selectivity over Brd4. Although very encouraging, the pyridinone moiety was not progressed due to limited solubility (CLND sol. = 45 µg/mL) and artificial membrane permeability (AMP: 7.4 nm/s).

Overall, these data have demonstrated the profound effect of the propylamine chain on TAF1 activity, providing >10 fold increase in potency relative to the corresponding piperidine. Furthermore, the 5-pyridyl substituent had very little effect on potency or selectivity, with methyl and alcohol groups showing an identical profile.

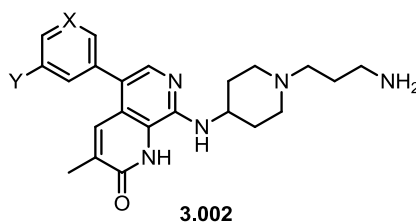
3.2.3 5-Position SAR: pyridine vs. phenyl

To gain a deeper understanding of the SAR at the 5-position, the phenyl analogues of compounds **3.002f–h** were synthesised for direct pair-wise comparison to the corresponding pyridine. It was believed that exchanging a more polar pyridyl moiety for a phenyl group could reduce the inherent polarity of the template as well as HBA count. This, in turn, could provide greater permeability and solubility. In addition, these investigations aimed to investigate whether the pyridyl nitrogen was forming specific interactions in TAF1 BD2.

The synthesis of compounds **3.002g** and **3.002h** is shown in **Scheme 32** (page 152) and in **Scheme 33** (page 153) for carbamate **3.002f**.

3.2.3.1 SAR discussion of 5-position pyridyl vs. phenyl

Compounds **3.002f–h** were tested in the bromodomains of TAF1 BD2 and Brd4 BD1 and BD2 by means of a TR-FRET assay. Selectivity is calculated relative to the maximum Brd4 value (**Table 29**).



Entry Compound Number	1	2	3	4	5	6
X =	N	C	N	C	N	C
Y =						
TAF1 BD2 pIC ₅₀	8.1	7.0	7.5	7.4	7.3	6.0
Brd4 BD1 pIC ₅₀	6.2	6.4	5.6	6.1	5.6	5.7
Brd4 BD2 pIC ₅₀	5.3	5.5	5.0	5.4	4.7	5.3
Selectivity	x80	x4	x80	x20	x50	x5
ChromLogD _{7.4}	0.44	1.31	0.30	1.01	1.08	2.84
CLND sol. (µg/mL)	-	23	34	42	29	22
AMP (nm/s)	16.5	9.2	8	9.2	11	13

Table 29: pIC₅₀ values for compounds **3.003a–c** and **f–h** in the bromodomains of TAF1 BD2 and Brd4 (BD1 and BD2) as determined by TR-FRET analysis. Selectivity over Brd4 is calculated relative to the maximum value. Data are n≥2.

Analysis of the data indicated that for all 3 pair-wise comparisons, the pyridyl motif provided increased TAF1 BD2 activity with little effect on Brd4. For example, pyridyl **3.002c** showed a TAF1 BD2 pIC₅₀ of 7.3, whereas phenyl analogue **3.002h** was 6.0 (compare entries 5 and 6). Modelling of compound **3.002c** in TAF BD2 supports this hypothesis, as the pyridyl nitrogen is predicted to form an interaction (dihedral angle: 86°) with a back-bone NH of Asn1554 (**Figure 97**).²¹⁸

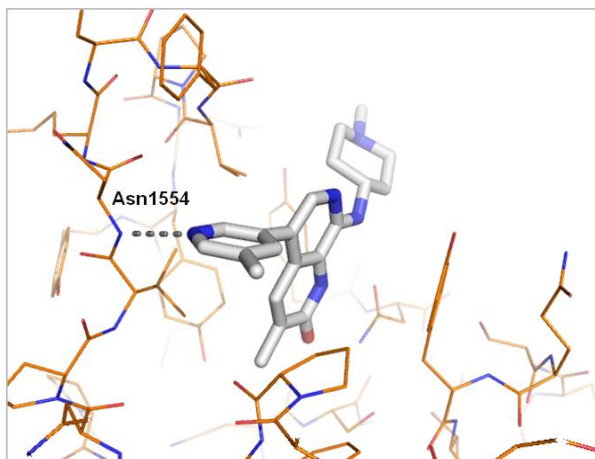


Figure 97: X-Ray crystallography of 3.002c modelled in TAF1 BD2. Hydrogen-bonds are shown as grey dashed lines.

Although the phenyl compounds showed a less desirable activity and selectivity profile, they were less polar as hypothesised. The removal of the pyridyl nitrogen provided higher *ChromLogD*_{7.4} values, which in some cases led to higher solubility (compare entries 1 and 2; and 3 and 4) and AMP (compare entries 5 and 6). Despite phenyl compounds **3.002f–h** showing a minor improvement in physico-chemical properties, the data generated were considered poor and not within the acceptable range for a drug-like molecule.

Carbamate **3.002a** showed the highest TAF1 BD2 activity, with 80 fold selectivity over Brd4. However, due to high polarity and poor solubility, **3.002a** could not be progressed for further profiling. Although compounds **3.002b** and **c** showed very similar profiles, **3.002c** was selected for further optimisation due to synthetic tractability.

3.2.4 SAR investigation at the 8-position

Having established the 5-methylpyridyl motif as an appropriate 5-position group, focus was placed on exploration of the 8-position. Initial investigations aimed to understand the contribution of the functionalised amino piperidine to TAF1 activity. In addition, the solubility issues were to be addressed through the introduction of substituents with fewer hydrogen-bond donor and acceptor motifs. To this end, a series of amine substituents was installed onto the 5-position of the naphthyridinone template *via* array chemistry (**Figure 98**).

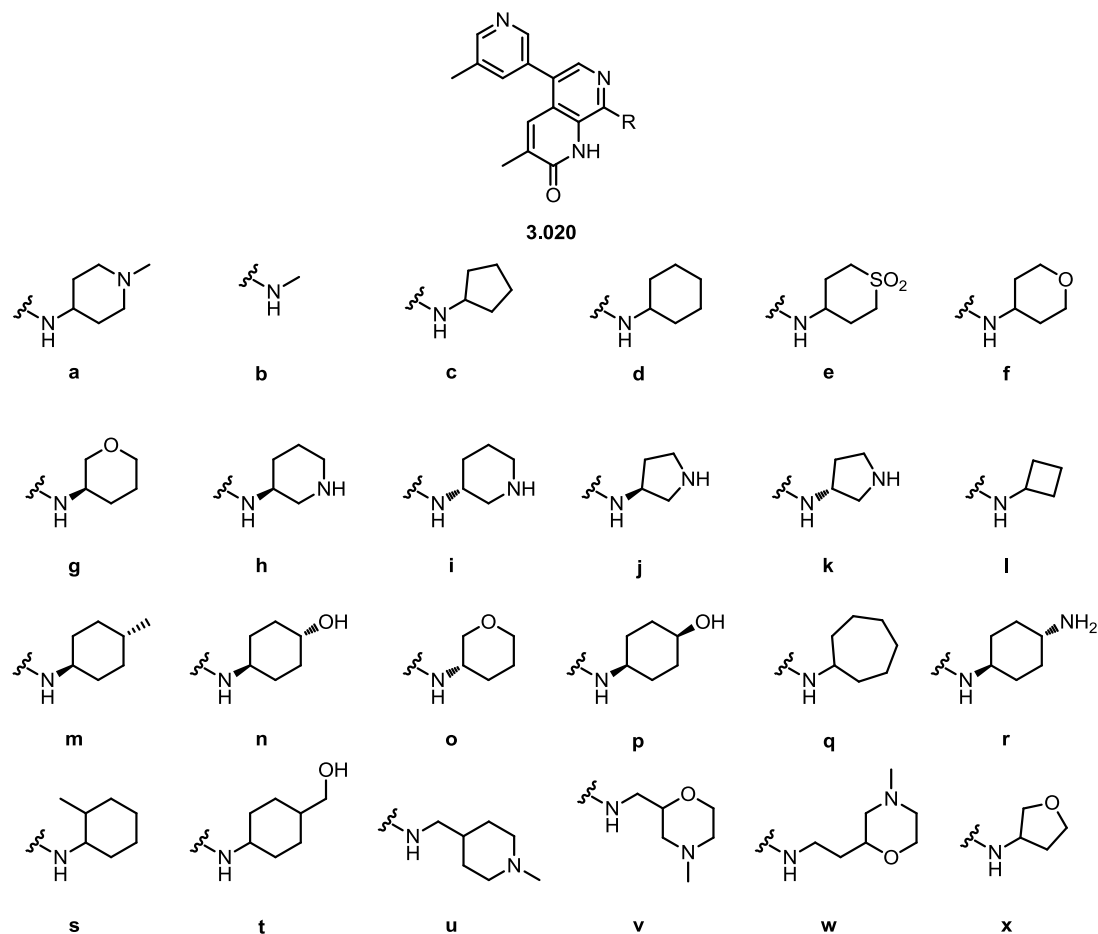
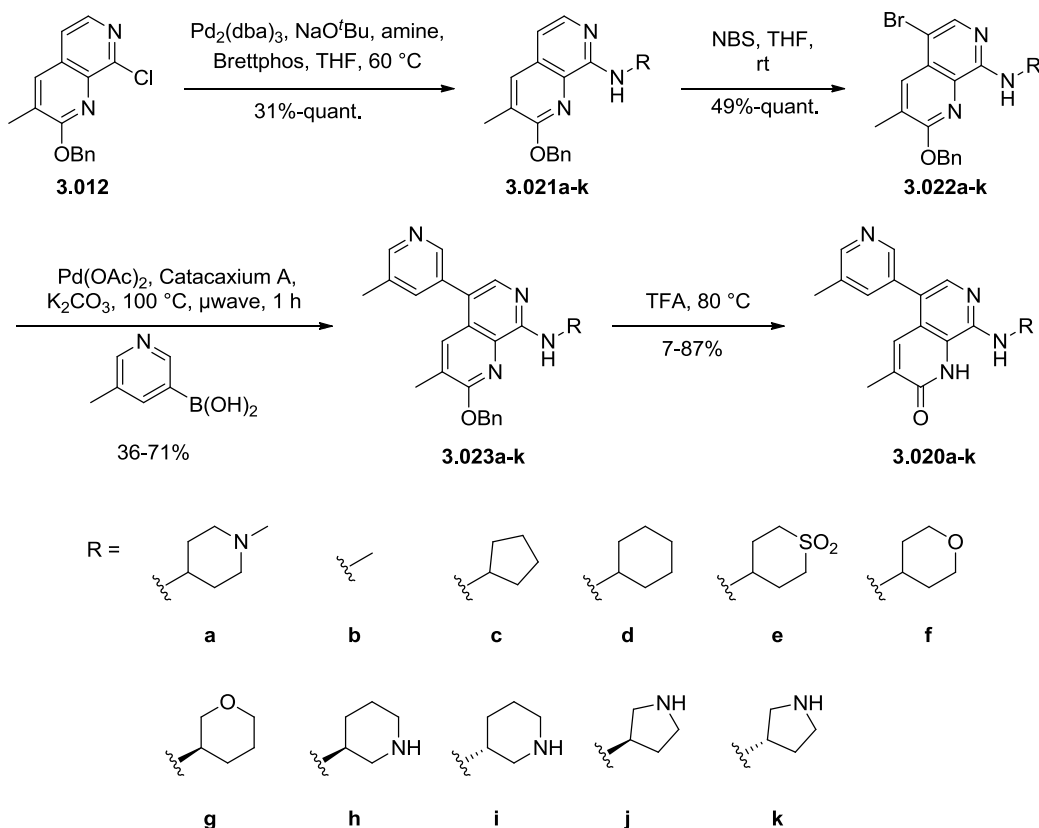


Figure 98: 8-Position array compounds 3.020a–x.

3.2.4.1 Synthesis of 8-position analogues

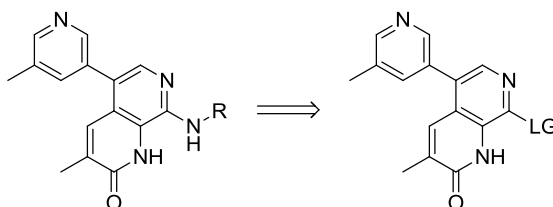
Initial investigations to access 8-position analogues **3.020a–k** made use of a reliable but lengthy route (**Scheme 34**).^{105,106}



Scheme 34: Synthetic route to access 5-position amines **3.020a–k** from intermediate **3.012**.

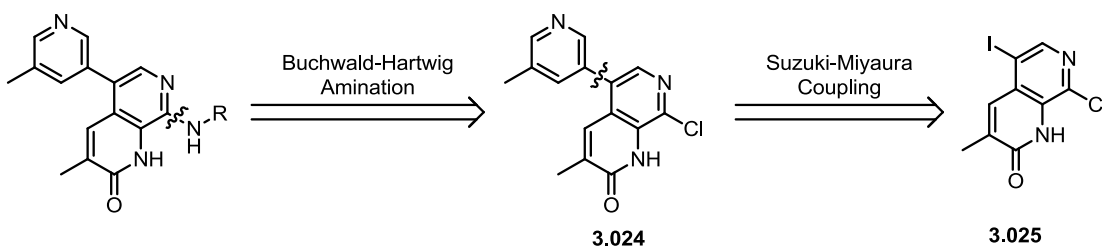
Each amine was installed onto intermediate **3.012** via a Buchwald-Hartwig coupling, which provided a directing group for the subsequent electrophilic bromination with NBS. Following this, the 5-methyl pyridine motif was installed by a Suzuki-Miyaura coupling. Finally, the *O*-benzyl protecting group was cleaved by heating in TFA to deliver the final compounds. In the case of compounds **3.020h–k**, the amine was installed as the Boc protected compound. Therefore, the Boc groups were also removed in the final step of this synthesis.

Although this route provided final compounds successfully, it was not suitable for array chemistry. Ideally, structural diversity should be introduced in the final step of a synthesis to ensure efficient access to a range of analogues. Therefore, in order to synthesise the 8-position compounds in a single step, a late-stage intermediate containing a leaving group (LG) at C-8 was required (**Scheme 35**).

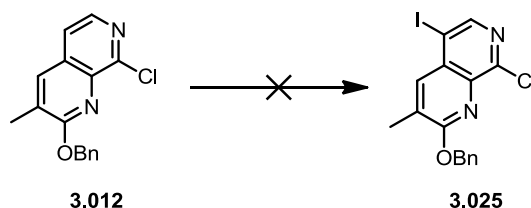


Scheme 35: Retrosynthesis of 8-position amine.

Early investigations focussed on the synthesis of a late stage intermediate, which could be functionalised at both the 5- and 8-positions. It was believed that the appropriate amines would be installed *via* a Buchwald-Hartwig coupling with compound **3.024**, which in turn, would be accessed from a selective Suzuki-Miyaura coupling at the 5-position of **3.025** (Scheme 36).

Scheme 36: Retrosynthesis of 8-position amine to the corresponding intermediates **3.024** and **3.025**.

In an attempt to access compound **3.025**, several iodination reactions were conducted (Table 30).

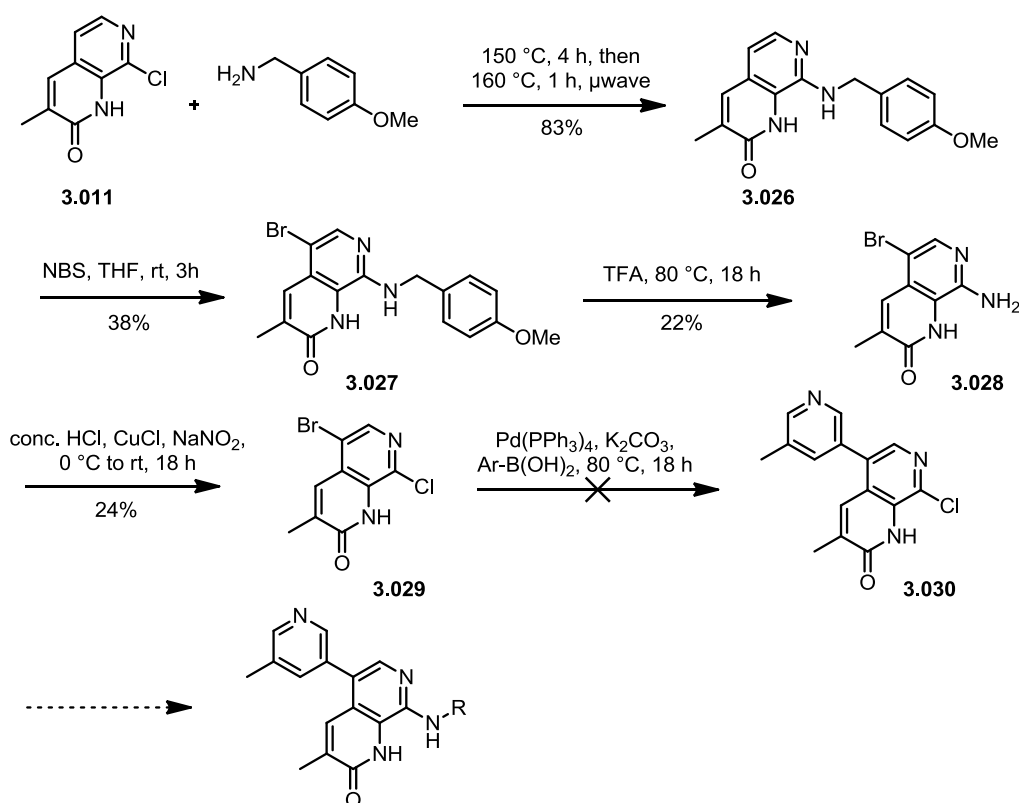


Entry	Starting material	Reagents	Temperature, Time	Observation (LCMS)
1	3.012	NIS, THF	rt, 2 h 65 °C, 2 h	No reaction
2	3.012	NIS, DMF	rt, 48 h 80 °C, 3 h	No reaction
3	3.012	NIS, MeCN	rt, 2 h 80 °C, 2 h	No reaction
4	3.012	NIS, TFA cat., MeCN	rt, 1h 80 °C, 2 h	No reaction
5	3.012	ICl, KOAc, AcOH	80 °C, 20 h	No reaction
6	3.012	Benzoyl peroxide, NIS, EtOAc	90 °C, 0.5 h, μwave	Mixture of products
7	3.011 (Scheme 32)	NIS, TFA cat., MeCN	rt, 1h 80 °C, 2 h	No reaction

Table 30: Reagents and conditions for attempted iodination chemistry.

Several attempts were made to iodinate compound **3.012** using NIS with a range of solvents and temperatures (entries 1–3). As no product was observed by LCMS analysis, conditions using catalytic TFA^{229, 230} were investigated, but this delivered only starting material (entry 4). Subsequently, ICl²³¹ was utilised as a more reactive iodinating agent but again no reaction was seen by LCMS analysis (entry 5). A radical iodination reaction with benzoyl peroxide and NIS in the microwave also proved unsuccessful (entry 6). In addition, unprotected compound **3.011** (**Scheme 32**, page 152) was subjected to reaction with NIS and TFA but no reaction was observed (entry 7). A bromination reaction with NBS at both room temperature and reflux also failed to deliver the corresponding bromide. As all attempts to functionalise the 5-position were unsuccessful, an alternative strategy was investigated.

It was believed that in order for the naphthyridinone scaffold to undergo an electrophilic aromatic substitution reaction, it would require a more effective activating group than Br or Cl. Having already proved that the template can undergo bromination with NBS in the presence of an amine directing group (**Scheme 34**, step 2, page 159), this strategy was investigated (**Scheme 37**).

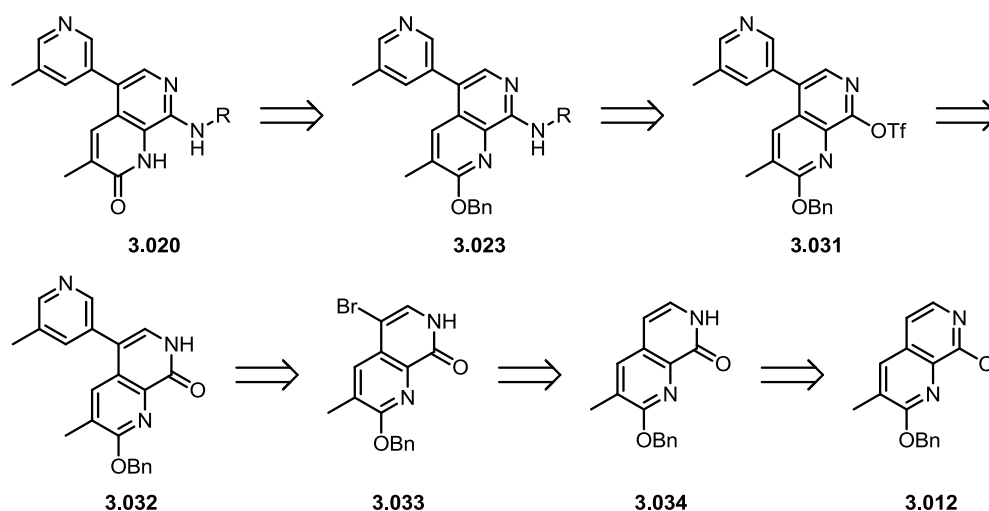


Scheme 37: Attempted synthesis of intermediate 3.030.

As previous chemistry efforts had suggested that the naphthyridinone scaffold required activation for successful electrophilic aromatic substitution, a PMB protected amine was installed at the 8-position of compound **3.011** via an S_NAr reaction. This proceeded in 83% yield to deliver intermediate **3.026**. An iodination reaction with NIS was attempted but proved unsuccessful, with only starting material observed by LCMS analysis. As an alternative, **3.026** was subjected to a bromination reaction with NBS, which delivered compound **3.027** in 38% yield. Following this, the PMB group was removed by heating in TFA to afford compound **3.028** (22%). Both the bromination and deprotection reactions were low yielding due to difficulties during purification caused by the insolubility of the corresponding products. However, 73 mg of **3.028** was isolated and progressed in a Sandmeyer reaction.²³² These conditions furnished intermediate **3.029**, which had the potential for functionalisation at both the 5- and 8-positions. A Suzuki-Miyaura coupling¹⁶³ was then employed in an attempt to selectively install the aryl motif at the 5-position, exploiting the greater potential for C-Br to undergo oxidative addition with Pd(0). Despite several attempts, the reaction failed to provide any indication of desired product as judged by LCMS analysis.

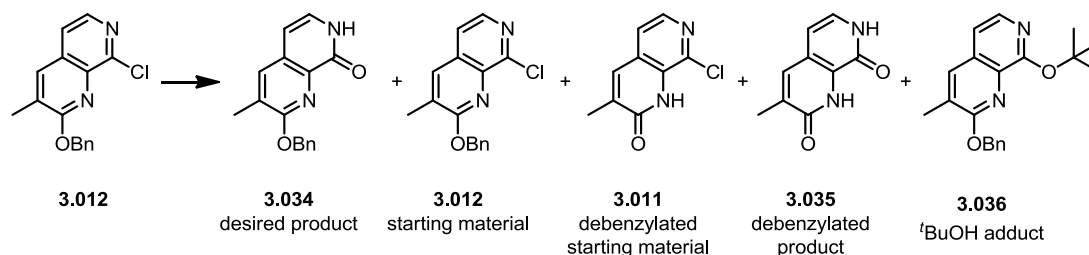
Critical analysis of this route revealed several issues. The yields for steps 2–4 were low as a result of difficulties experienced during purification. The highly polar nature and consequent insolubility of these molecules made isolation challenging. It is of note that the bromination chemistry was attempted with *O*-benzylated variant of **3.026**, as it was believed that the benzyl moiety would aid purification. However, the benzyl group was cleaved under bromination conditions, offering no improvement. It was also envisioned that considerable effort would be required in order to identify the appropriate Suzuki-Miyaura coupling¹⁶³ conditions to selectively install the aryl group at the 5-position. Given that the route to intermediate **3.029** was low yielding and lengthy, this chemistry was considered unacceptable for both scale-up and late-stage diversification of compound **3.030**. Therefore, an alternative strategy was investigated.

It was believed that the appropriate amine could be installed onto the naphthyridinone scaffold using pyridyl triflate **3.031**. This, in turn, would be accessed from pyridinone **3.032**, which would act as a directing group for the electrophilic bromination of compound **3.034** (**Scheme 38**).



Scheme 38: Retrosynthesis of 8-position amine.

With the idea that the pyridinone moiety could act as both a directing group and a masked leaving group, the synthesis of pyridinone **3.034** was attempted. Conversion of 2-chloro pyridine derivative, **3.012** into the corresponding pyridinone proved challenging as there was a risk of O-benzyl cleavage. However, this protecting group was required to differentiate between the two pyridinones. As such, several attempts were made to access compound **3.034** (Table 31).



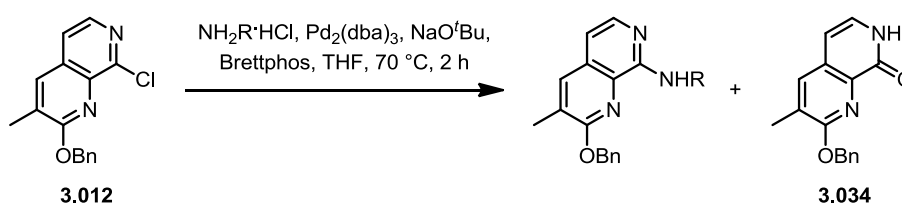
Entry	Reagents	Temperature / Time	Observation (LCMS peak area)
1	AcOH, μ wave	100 °C, 1 h	10% 3.034 ; 23% 3.012 ; 20% 3.011 ; 41% 3.035
2	KO ^t Bu, ^t BuOH, μ wave	80 °C, 1 h	42% 3.034 ; 21% 3.011 , 11% 3.036
3	Pd ₂ (dba) ₃ , CsOH, Bipyphos, 1,4-dioxane, μ wave	100 °C, 1 h,	33% isolated product 3.034

Table 31: Reagents and conditions for attempted synthesis of pyridinone **3.034**.

Heating compound **3.012** in AcOH²³³ in the microwave resulted in formation of the desired product as judged by LCMS analysis. However, multiple side-products were also observed, the major corresponding to debenzylated compound **3.035** (entry 1). Treatment of **3.012** with KO^tBu, in ^tBuOH at 80 °C in the microwave also provided the desired product along with debenzylated starting material **3.011** (entry 2).²³⁴

Following these results, a literature search revealed conditions for a Pd catalysed pyridinone formation.²³⁵ As such, compound **3.012** was treated with Pd₂(dba)₃, bipyphos and CsOH and heated at 100 °C in the microwave. Pleasingly, desired product, with no debenzoylation of starting material, was observed. However, purification of **3.034** proved extremely challenging by both silica gel chromatography and trituration, resulting in poor yields. Although desired product was isolated (33% yield), the Pd catalysed reaction was not suitable for a scale-up route.

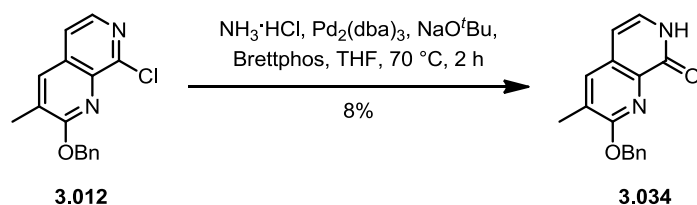
The very minor success achieved with the Pd catalysed chemistry highlighted an observation that had been noted during previous chemistry (**Table 32**).



Entry	R =	Result (LCMS peak area)
1		Product 37%; 3.034 18%; other 45%
2		Product 30%; 3.034 60%; other 10%
3		Product 0%; 3.034 80%; other 20%; 70% isolated yield of 3.034

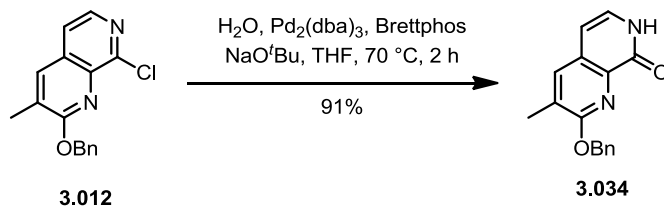
Table 32: Reagents and conditions for the attempted Buchwald-Hartwig couplings.

During investigations involving Buchwald-Hartwig amination chemistry^{105,106} to install various amines at the 5-position of the template, it was noted that pyridinone **3.034** was produced as a side-product when the amine was employed as the HCl salt. In particular, the use of ammonium chloride as the nucleophile (entry 3) showed 80% conversion to pyridone **3.034** as judged by LCMS analysis. Following work-up and purification, **3.034** was isolated in 70% yield. Although not productive for the Buchwald-Hartwig chemistry, this observation proved useful for pyridinone formation. Therefore, the reaction with ammonium chloride was repeated in order to confirm this result (**Scheme 39**).



Scheme 39: Attempted synthesis of pyridinone 3.034.

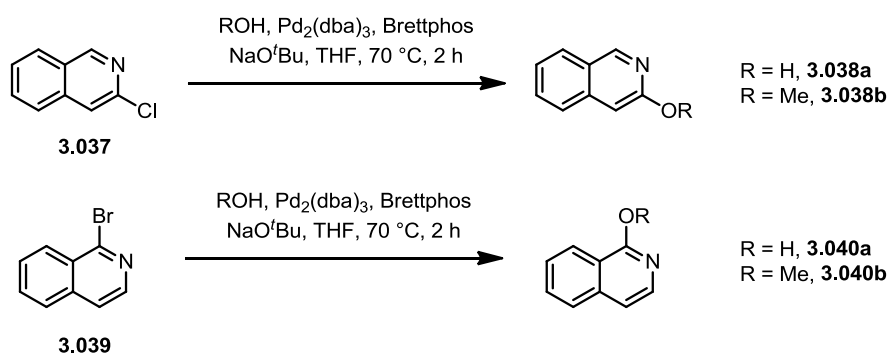
Disappointingly, the repeat reaction did not provide pyridinone **3.034** in comparable yields (8%), indicating that ammonium chloride was not solely responsible for the activity described in **Table 32**, entry 3. It was hypothesised that in HCl salt form, the amine contained traces of water, which could have driven reactivity. Therefore, the reaction was repeated, this time, replacing ammonium chloride with water (**Scheme 40**).



Scheme 40: Successful synthesis of pyridinone 3.034.

Pleasingly, pyridinone **3.034** was successfully synthesised in 91% yield, confirming that residual water was responsible for product formation as shown in **Table 32**. To investigate this reaction further, the chemistry was attempted in the absence of each reagent in turn. Results from this screen showed that all components were required for the reaction to progress. Although this chemistry using these reagents is not described in the literature, both Beller and co-workers²³⁶ and Buchwald and co-workers²³⁷ have reported Pd catalysed coupling reactions of aryl halides to synthesise phenols and aromatic ethers.

To investigate whether this chemistry would be amenable to the synthesis of both pyridines and pyridyl ethers on alternative substrates, further investigations were conducted. Isoquinoline compounds **3.037** and **3.039** were selected for test reactions (**Table 33**).

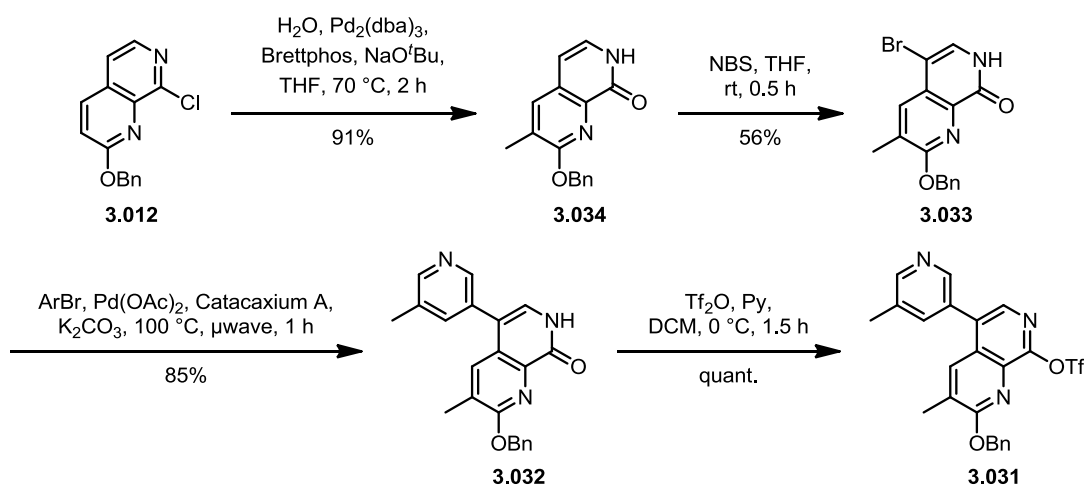


Entry	R =	Result (LCMS peak area)
1	H	100%
2	Me	83%
3	H	95%
4	Me	88%

Table 33: LCMS results for pyridinone and pyridyl ether formation.

Pleasingly, this chemistry proved successful when applied to alternative substrates. Both chloro- and bromo-substituted isoquinolines reacted to form the corresponding pyridinones, as judged by LCMS analysis of the crude reaction mixture (entries 1 and 3). Furthermore, LCMS analysis indicated that this reaction could be used to synthesise methyl ethers **3.038b** and **3.040b** (entries 2 and 3). Therefore, this chemistry may provide an option for the selective synthesis of *O*- rather than *N*-alkylated pyridones, particularly when these compounds cannot be accessed by S_NAr chemistry.

With a method to synthesise pyridinone **3.034** in excellent yield, the remainder of the chemistry to access key intermediate **3.031** was conducted (**Scheme 41**).

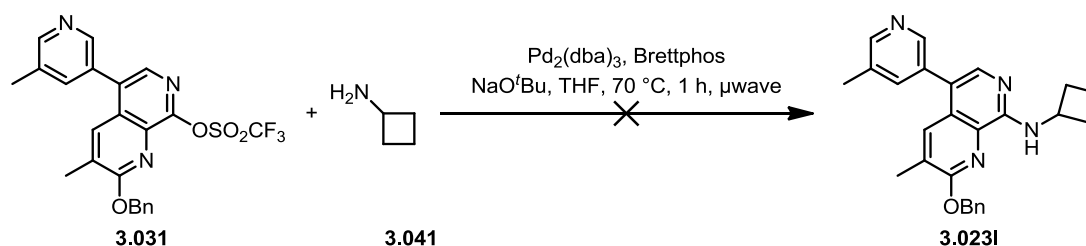


Scheme 41: Synthetic route to access key intermediate 3.031.

An electrophilic aromatic substitution reaction with NBS in THF, afforded intermediate **3.033** in reasonable yield (56%). Subsequently, a Suzuki-Miyaura

coupling was used to install the aryl motif. Pleasingly, this reaction proceeded in 85% yield to provide intermediate **3.032**. Following this, the pyridinone moiety was transformed into the corresponding pyridyl triflate, **3.031** in quantitative yield.²³⁸ This chemistry was performed on scale, providing ~2 g of triflate **3.031** in 4-steps in 44% overall yield.

With a stock of key intermediate **3.031** in hand, focus was placed on installation of the amine functionality. Initially, amine **3.041** was used for test reactions, the first of which was a Buchwald-Hartwig coupling (**Scheme 42**).



Scheme 42: Attempted Buchwald-Hartwig coupling to install amine 3.042.

The Buchwald-Hartwig conditions used for the synthesis of **3.034** were applied to triflate **3.031**. LCMS analysis of the crude reaction mixture indicated conversion to the corresponding pyridinone with no desired product observed. As such, an alternative strategy was investigated. It was hypothesised that the amine functionality could be installed by an S_NAr reaction (**Table 34**).²³⁹

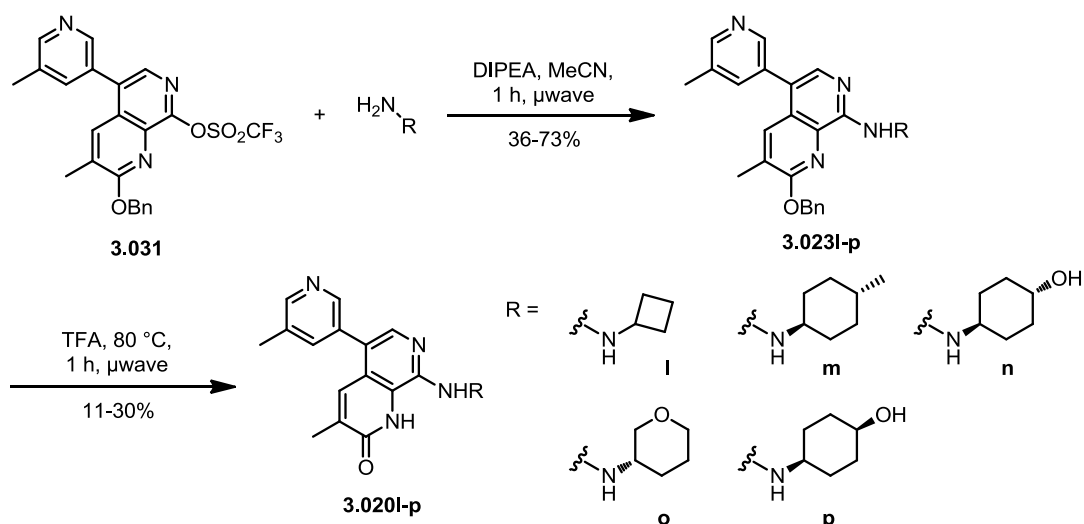


Entry	Solvent	Temperature/Time	Result (LCMS peak area)
1	NMP	150 °C, 1h then 200 °C, 1 h	48% 3.023I
2	Trifluorobenzene	150 °C, 1 h	26% 3.023I
3	DMF	150 °C, 1 h	44% 3.023I
4	MeCN	150 °C, 1 h	52% 3.023I
5	MeCN	140 °C, 1 h	67% 3.023I isolated yield

Table 34: Reagents and conditions used for the synthesis of compound 3.023I via S_NAr chemistry.

In order to investigate the potential of an S_NAr reaction to deliver the desired product, several high boiling, polar solvents were examined. Pleasingly, all solvent systems provided an indication of desired product as judged by LCMS analysis of

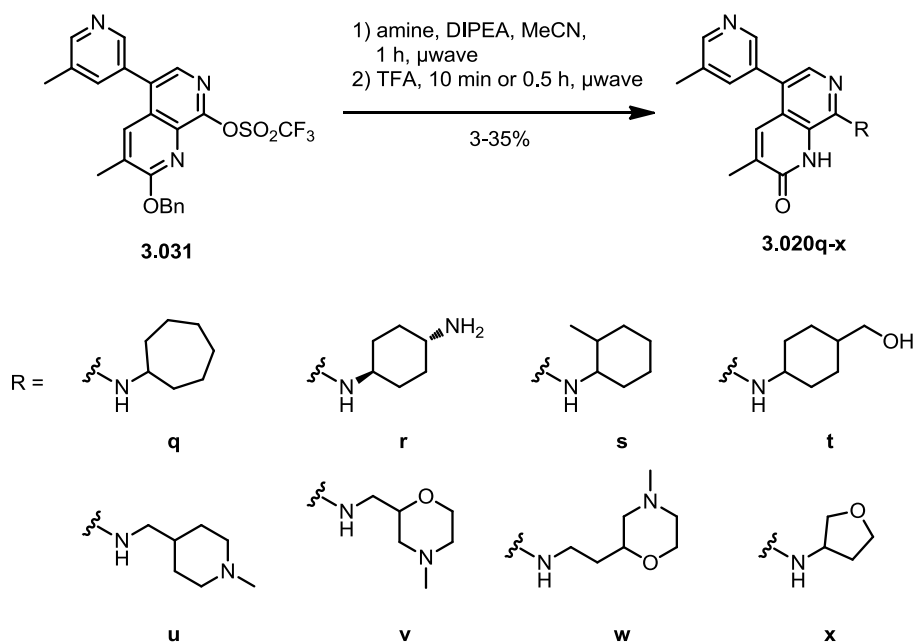
the crude reaction mixture. Both NMP and DMF showed reasonable results with 18% and 44% product observed respectively (entries 1 and 3). Trifluorobenzene proved less useful with only 26% product seen (entry 2). The use of MeCN at 150 °C provided a cleaner LCMS trace, with 52% **3.023I** observed. Taking MeCN forward and attempting the reaction at lower temperature afforded compound **3.023I** in 67% isolated yield (**Scheme 43**).



Scheme 43: Synthesis of compounds 3.020I-p via $\text{S}_{\text{N}}\text{Ar}$ chemistry

Following installation of the amine functionality, intermediate **3.023I** was taken forward through deprotection of the O-benzyl moiety. This was achieved by heating in TFA at 80 °C to furnish final compound **3.020I**. This synthetic route was also used for the synthesis of compounds **3.020m-p**.

As the 8-position investigations required the use of array chemistry, it was important to use chemistry which introduced structural diversity in the final-step from a common intermediate. Therefore, the synthesis of the remaining compounds **3.020q-x**, used triflate **3.031** but did not involve the isolation of intermediate **3.023**. Instead, **3.023** was telescoped through into the deprotection step (**Scheme 44**).

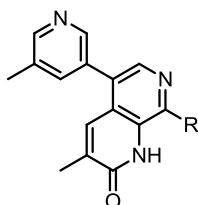


Scheme 44: Synthesis of compounds 3.020q-x.

Although the yields for this reaction were low due to the purification method used (reverse phase preparative HPLC), this chemistry allowed access to final compounds **3.020q-x** in a single flask.

3.2.4.2 SAR discussion for 8-position array 1

Compounds **3.020a–x** were tested in the bromodomains of TAF1 BD2 and Brd4 BD1 and BD2 by means of a TR-FRET assay. Selectivity is calculated relative to the maximum Brd4 value (for full data see Appendix 5.7). A small number of compounds has been selected for SAR discussion (**Table 35**).



Entry Compound Number	1 3.002a	2 3.020a	3 3.020d ²⁴⁰	4 3.020l	5 3.020b	6 3.020u
R =						
TAF1 BD2 pIC ₅₀	7.4	6.5	6.3	6.0	5.5	6.4
Brd4 BD1 pIC ₅₀	5.6	5.7	4.6	<4.3	<4.3	4.8
Brd4 BD2 pIC ₅₀	4.7	4.6	4.9	<4.3	<4.3	4.8
Selectivity	x63	x6	x25	x50	x16	x40
CLND sol. (µg/mL)	29	117	6	3	22	179
AMP (nm/s)	11	<3	6	3	310	<3

Table 35: pIC₅₀ values for compounds **3.002a** and **3.020a, d, l, b** and **u** in the bromodomains of TAF1 BD2 and Brd4 (BD1 and BD2) as determined by TR-FRET analysis. Selectivity over Brd4 is calculated relative to the maximum value. Data are n≥2.

Analysis of the data generated from the TR-FRET assay indicated that truncation of **3.002a** to deliver methyl substituted compound **3.020a** led to a reduction in TAF1 activity, whilst Brd4 potency was maintained (compare entries 1 and 2). Despite the X-ray crystallographic docking studies predicting that the propylamine chain of **3.002a** would protrude into solvent (**Figure 95**, page 148), these data suggest that this group was making specific interactions in TAF1 BD2. As previously discussed (Section 3.2.2.3, page 154) the disconnect between the modelling studies and the TR-FRET data generated were a cause for concern and suggested that the activity observed by compound **3.002a** may be a result of an assay artefact. Therefore, an orthogonal determination of binding affinity was required in order to build confidence in these results (Section 3.2.5, page 172).

Further truncation to provide compounds **3.020d** and **3.020i** delivered an increase in selectivity over Brd4, with TAF1 BD2 pIC₅₀ values in the region of 6 (compare entries 2–4). However, compounds **3.020d** and **3.020i** were found to be poorly soluble and permeable. Methyl substituted compound **3.020b** provided selectivity but at the cost of TAF1 BD2 activity and solubility (entry 5). Extension at the 8-position to give compound **3.020u** showed an increase in TAF1 BD2 activity, with reasonable selectivity over Brd4. In addition, **3.020u** displayed much improved solubility (CLND: 179 µg/mL), albeit not cell permeable [AMP: <3 nm/s (entry 6)].

Comparison of compounds **3.020a** and **3.020u** highlights an interesting trend (compare entries 2 and 6). The addition of a methylene unit to give **3.020u** maintains TAF1 BD2 activity with pIC₅₀ values ~6.5, with an improvement in selectivity over Brd4 (from 6 to 40 fold) and solubility (from 117 to 179 µg/mL). Further analysis of the full data set from this array indicates that compounds **3.020v** and **w** exhibited a similar trend (**Figure 99**).

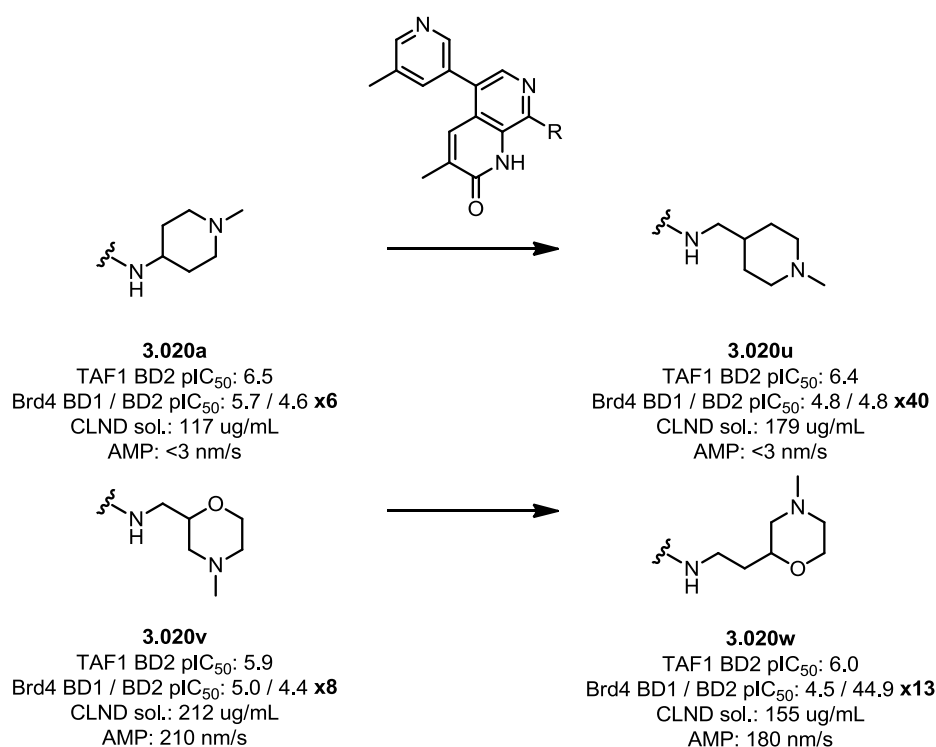


Figure 99: TR-FRET assay, solubility and permeability data for compounds 3.020a and u–w. Data are n≥2.²⁴¹

Analysis of these data indicates that increasing the chain length of the 8-position amine substituent provides an increase in selectivity over Brd4, whilst TAF1 BD2 potency is maintained. In the case of compounds **3.020a** and **u**, selectivity increased from 6 to 40 fold, respectively. This effect is not as pronounced for compounds

3.020v and **w**, but importantly these compounds show much improved physico-chemical properties. Compounds **3.020v** and **u** provide evidence that excellent solubility and permeability can be achieved with this template. However, the improvement in physico-chemical properties appears to be at the cost of TAF1 BD2 activity.

Moving forward with the hypothesis that increasing the chain length of the 8-position amine substituent delivers an increase in selectivity, with no effect on TAF1 BD2 activity, a second array was designed to investigate further.

Before additional studies could be conducted, it was important to build confidence in the TR-FRET data generated. In particular, compounds **3.002a–d** had shown TAF1 BD2 pIC₅₀ values which were not consistent with X-ray crystallographic modelling. Therefore, a series of compounds were examined in an orthogonal TAF1 BD2 assay.

3.2.5 Determination of TAF1 BD2 activity by BROMOscan

To investigate whether the data generated by compounds **3.002a–d** was a result of an assay artefact, a series of compounds from the naphthyridinone template was selected for test in an orthogonal BROMOscan assay.¹²¹ The compounds selected showed a range of TAF1 BD2 activities, as determined by TR-FRET (**Figure 100**).

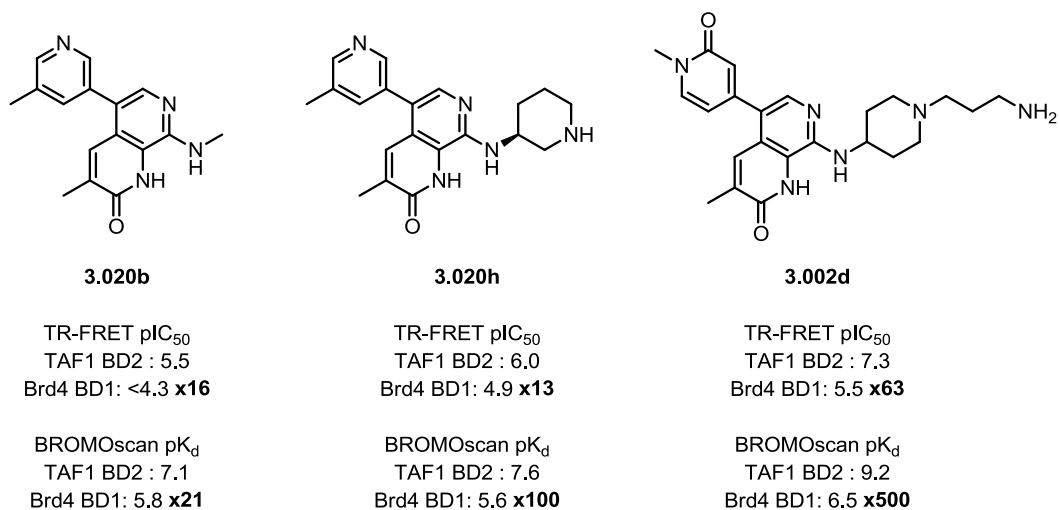


Figure 100: Compounds selected for test by BROMOscan.

Pleasingly, results from the BROMOscan¹²¹ screen indicated that the trend in TAF1 BD2 and Brd4 BD1 activities shown by TR-FRET was maintained. It is this second, orthogonal determination of binding affinity which helps to build confidence in the TR-FRET data. However, the BROMOscan results show a consistent improvement

in both TAF1 BD2 potency and selectivity. Although the precise reason for this is unknown, it may be due to the alternative detection system, protein construct and sample preparation methods used for these assays.

3.2.6 Further investigations at the 8-position

With confidence in the TAF1 BD2 TR-FRET assay confirmed by orthogonal screening by means of BROMOscan,¹²¹ the effect of the 8-position amine chain length on TAF1 activity and selectivity was examined. These investigations were conducted using array chemistry. As such, a series of compounds were designed to explore this hypothesis (**Figure 101**).

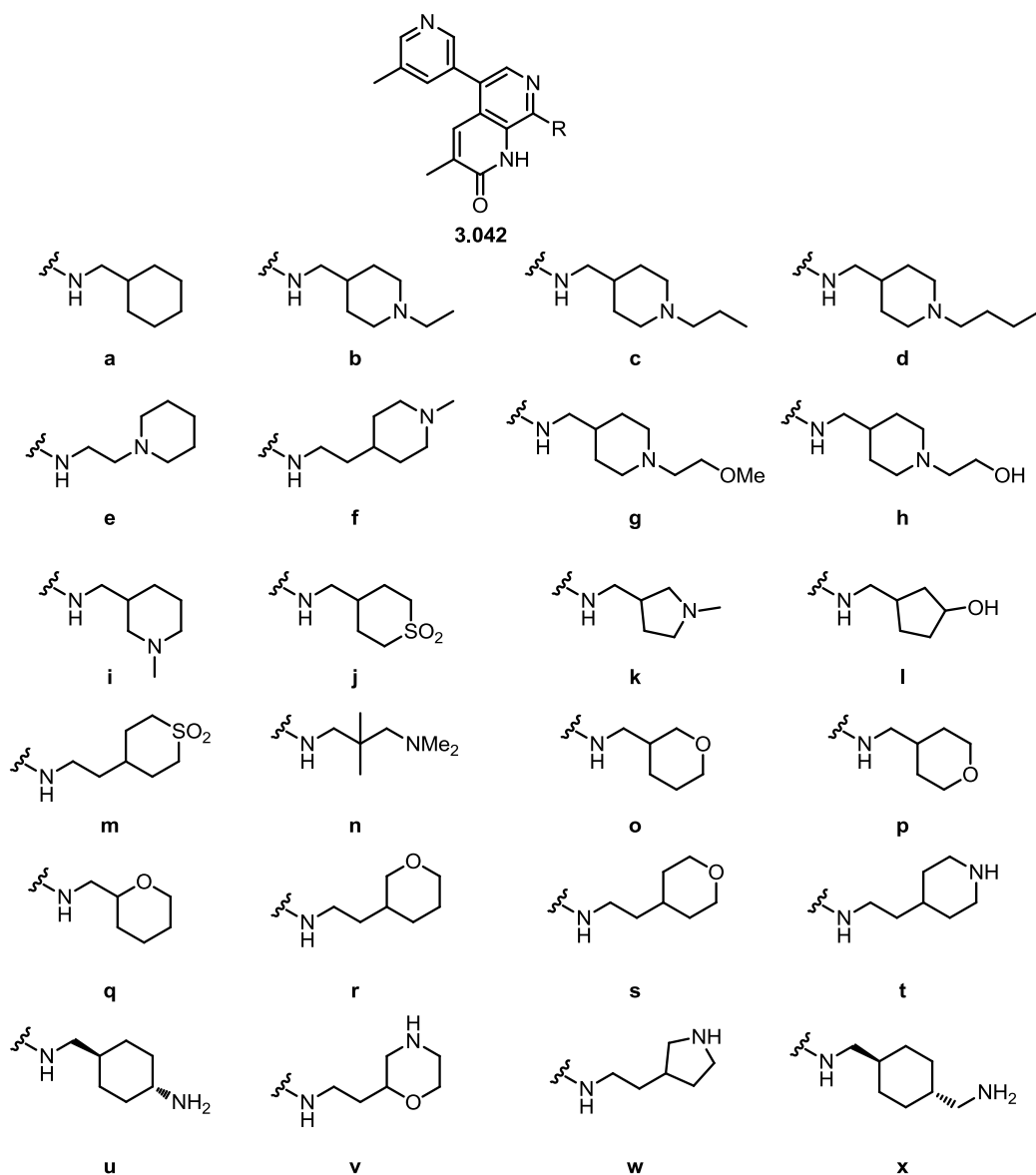
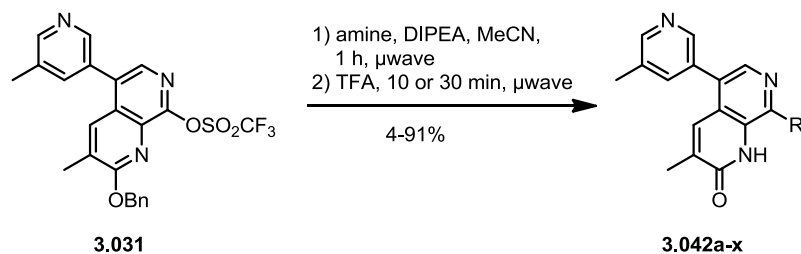


Figure 101: Second 8-position array.

3.2.6.1 Synthesis of second 8-position array compounds

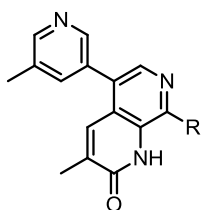
The synthesis of compounds **3.042a–x** was conducted using an identical method to that previously described. The chemistry worked well, delivering all final compounds in a range of yields (4–91%; **Scheme 45**).

Scheme 45: Synthesis of compounds **3.042a–x**.

3.2.6.2 SAR discussion for 8-position array 2

Compounds **3.042a–x** were tested in the bromodomains of TAF1 BD2 and Brd4 BD1 and BD2 by means of a TR-FRET assay. Selectivity is calculated relative to the maximum Brd4 value.

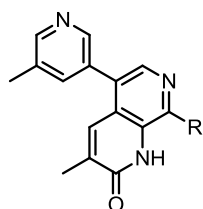
The majority of compounds tested showed reasonable TAF1 BD2 activity, with some selectivity over Brd4 (for full data see Appendix 5.8). Several compounds showed excellent physico-chemical properties, with good solubility and permeability. However, this improvement was at the expense of TAF1 BD2 potency and selectivity. Examples of such compounds are shown in **Table 36**.



Entry Compound Number	1 3.042c	2 3.042g	3 3.042k
R =			
TAF1 BD2 pIC ₅₀	6.3	6.1	6.6
Brd4 BD1 pIC ₅₀	4.5	4.4	5.2
Brd4 BD2 pIC ₅₀	4.7	4.6	5.0
Selectivity	x40	x32	x25
CLND sol. (µg/mL)	170	135	170
AMP (nm/s)	140	100	260

Table 36: pIC₅₀ values for compounds **3.042c, g** and **k** in the bromodomains of TAF1 BD2 and Brd4 (BD1 and BD2) as determined by TR-FRET analysis. Selectivity over Brd4 is calculated relative to the maximum value. Data are n≥2.

As hypothesised, there were compounds from this array which demonstrated the effect of 8-position amine chain length on TAF1 activity and selectivity. Compounds **3.020g/o** and **3.042o** show an interesting trend (**Table 37**).



Entry Compound Number	1 3.020g	2 3.020o	3 3.042o
R =			
TAF1 BD2 pIC ₅₀	5.9	6.4	6.2
Brd4 BD1 pIC ₅₀	<4.3	4.4	<4.3
Brd4 BD2 pIC ₅₀	<4.3	5.1	<4.3
Selectivity	x40	x20	x80
CLND sol. (µg/mL)	53	39	22
AMP (nm/s)	490	560	330

Table 37: pIC₅₀ values for compounds 3.020g/o and 3.042o in the bromodomains of TAF1 BD2 and Brd4 (BD1 and BD2) as determined by TR-FRET analysis. Selectivity over Brd4 is calculated relative to the maximum value. Data are n≥2.

Analysis of this data indicates that extending the amine chain length causes a significant increase in selectivity over Brd4, whilst TAF1 BD2 activity is maintained (compare entries 1 and 3). Compound **3.042o** shows acceptable TAF1 BD2 activity with a pIC₅₀ value of 6.2 and 80 fold selectivity over Brd4. In order to rationalise this selectivity, X-ray modelling²¹⁸ was utilised (**Figure 102**).

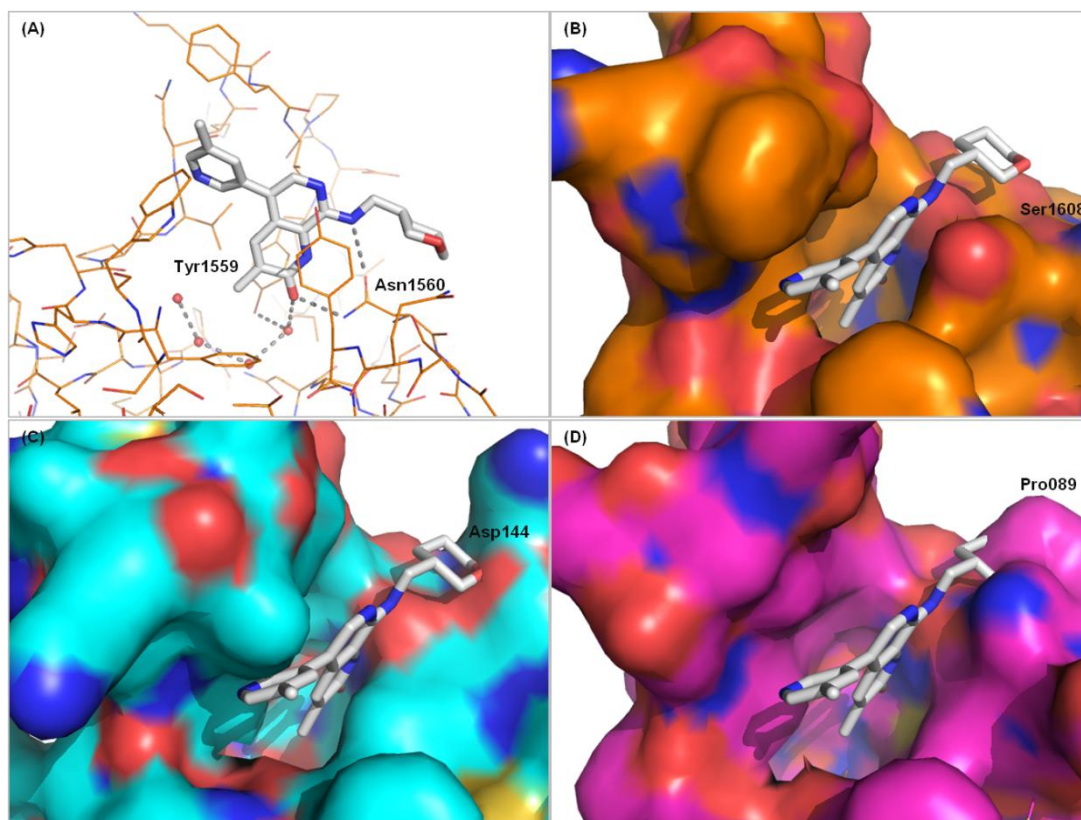


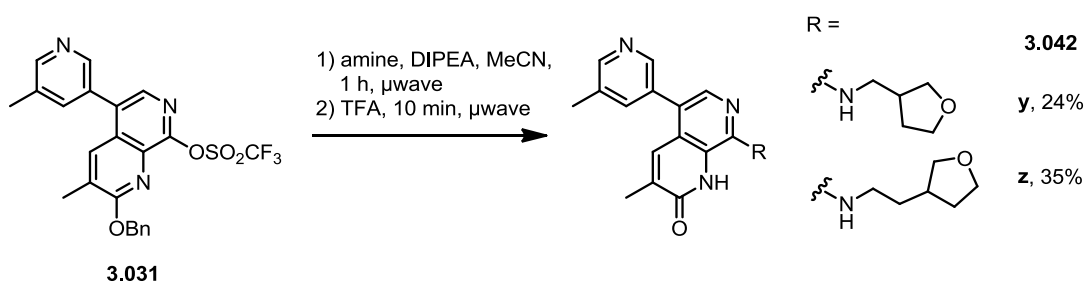
Figure 102: (A) Modelling of compound **3.042o** in complex with TAF1 BD2. Hydrogen-bonds are shown as grey dashed lines and water molecules as red spheres; (B) Modelling of compound **3.042o** in complex with TAF1 BD2 (bromodomain surface shown in orange); (C) Modelling of compound **3.042o** overlaid with apo Brd4 BD1 (bromodomain surface shown in blue); (D) Modelling of compound **3.042o** overlaid with apo Brd4 BD2 (bromodomain surface shown in pink).

Modelling of compound **3.042o** in complex with TAF1 BD2 (**Figure 102A** and **B**) suggests that the molecule occupies the KAc binding site with good shape complementarity. However, when this structure is overlaid with apo Brd4 BD1 (**Figure 102C**) and Brd4 BD2 (**Figure 102D**), the tetrahydropyran motif is predicted to clash with Asp144 and Pro089 in Brd4 BD1 and BD2 respectively. It was hypothesised that this steric clash could provide selectivity over Brd4.

Moving forward with this hypothesis, alternative substituents which had the potential to induce a clash in Brd4 were investigated.

3.2.6.3 Attempts to induce a clash in Brd4

In order to induce a clash with Asp144 and Pro089 in Brd4 BD1 and BD2 respectively, alternative substituents were installed in the 8-position of the naphthyridinone template. As such, compounds **3.042y** and **z** were synthesised using previously reported chemistry (**Scheme 46**).

Scheme 46: Synthesis of compounds **3.042y** and **z**.

Compounds **3.042y** and **z** were synthesised in 24 and 35% yields respectively, by S_NAr chemistry using late stage intermediate **3.031**.

3.2.6.3.1 SAR discussion for additional 8-position array compounds

Compounds **3.042y** and **z** were tested in the bromodomains of TAF1 BD2 and Brd4 BD1 and BD2 by means of a TR-FRET assay. Selectivity was calculated relative to the maximum Brd4 value. Compounds **3.020w** and **3.042o** are included for direct comparison (**Table 38**).

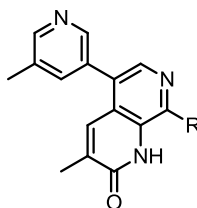
Entry Compound Number	1 3.042o	2 3.020w	3 3.042y ²⁴²	4 3.042z
R =				
TAF1 BD2 pIC ₅₀	6.2	6.2	6.1	6.1
Brd4 BD1 pIC ₅₀	<4.3	<4.3	4.5	<4.3
Brd4 BD2 pIC ₅₀	<4.3	5.0	5.0	<4.3
Selectivity	x80	x16	x13	x63
CLND sol. (μg/mL)	22	25	23	10
AMP (nm/s)	330	370	360	350

Table 38: pIC₅₀ values for compounds **3.020w** and **3.042o, y** and **z** in the bromodomains of TAF1 BD2 and Brd4 (BD1 and BD2) as determined by TR-FRET analysis. Selectivity over Brd4 is calculated relative to the maximum value. Data are n≥2.

Comparison of compound **3.042z** to shorter chain analogue **3.020w** indicates that increasing chain length has no effect on TAF1 BD2 activity but provides an increase in selectivity over Brd4 (compare entries 2 and 4). This trend is consistent with that

discussed in **Tables 35** (page 170) and **37** (page 176). Compound **3.045o** has similar TAF1 BD2 activity and selectivity as compound **3.045z**, suggesting that **z** also clashes with Asp144 and Pro089 in Brd4 BD1 and BD2 respectively (compare entries 1 and 4). As these compounds showed broadly similar solubility and AMP, they were progressed for further analysis.

Compounds **3.042o** and **z** were taken forward in order to understand their broader bromodomain selectivity. As such, **3.042o** and **z** were tested against the bromodomains of CREBBP, PCAF, BPTF and BRPF1 (**Table 39**).



Entry	Compound Number	R =	TAF1 BD2 pIC ₅₀	PCAF pIC ₅₀	BPTF pIC ₅₀	BRPF1 pIC ₅₀	CREBBP pIC ₅₀
1	3.042o ²⁴³		6.2	<5.0 (x16)	<4.0 (x250)	5.2 (x10)	<4.0 (x100)
2	3.042z		6.1	<4.0 (x125)	<4.0 (x125)	<4.0 (x125)	<4.0 (x80)

Table 39: pIC₅₀ values for compounds 3.042o and z in the bromodomains of TAF1 BD2, PCAF, BPTF, BRPF1 and CREBBP, as determined by TR-FRET analysis. Selectivity for TAF1 BD2 over other bromodomains is shown in parentheses and calculated based on pK_i values. Data are n≥2.

Analysis of the data generated from the wider bromodomain screen indicated that compounds **3.042o** and **z** showed good broader selectivity. Both compounds displayed excellent selectivity over BPTF and CREBBP (≥80 fold). However, compound **3.042z** showed greater selectivity over PCAF (x125 **z** vs. x16 **o**) and BRPF1 (x125 **z** vs. x10 **o**).

Despite its poor solubility (CLND sol.: 10 µg/mL) and relatively modest TAF1 BD2 activity (pIC₅₀: 6.1) compound **3.042z** was selected for further development due to the encouraging bromodomain selectivity profile. It was believed that improvements to both TAF1 BD2 activity as well as solubility could be made through modifications to the 5-position of the template, a vector that had not been investigated in detail previously.

3.2.7 5-Position array

To investigate the potential of the 5-position of the naphthyridinone template to deliver an increase in TAF1 BD2 activity and solubility, array chemistry was utilised. The compounds included in this array were designed to investigate the following:

1. Alternative substitution patterns around the pyridyl ring to engineer a twist at the 5-position to facilitate H-bond formation (**Figure 103**).
2. Alternative substitution patterns around the pyridyl ring to engineer a twist to reduce the planarity of the scaffold, aiding solubility (**Figure 103**).

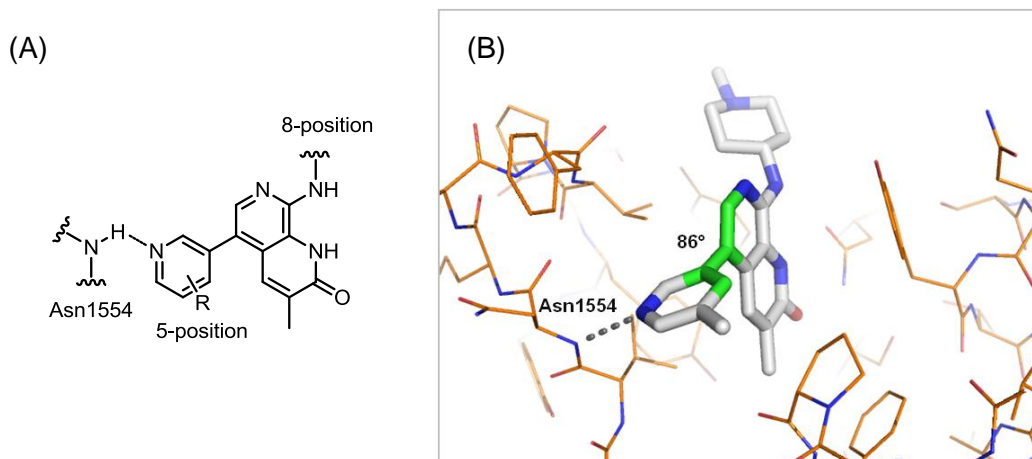


Figure 103: (A) General chemical structure of 5-position analogues designed to facilitate H-bond formation to Asn1554 in TAF1 BD2 and solubility; (B) X-Ray crystallography of truncated 3.002c modelled in TAF1 BD2. Hydrogen-bonds are shown as grey dashed lines. Dihedral angle highlighted in green.

3. Electronics, sterics and substitution patterns around the pyridyl ring.
4. Effect of 5-membered heterocycles (**Figure 104**).
5. Effect of fused ring systems (**Figure 104**).
6. Alternative HBA motifs on phenyl ring to replace the pyridyl group (**Figure 104**).

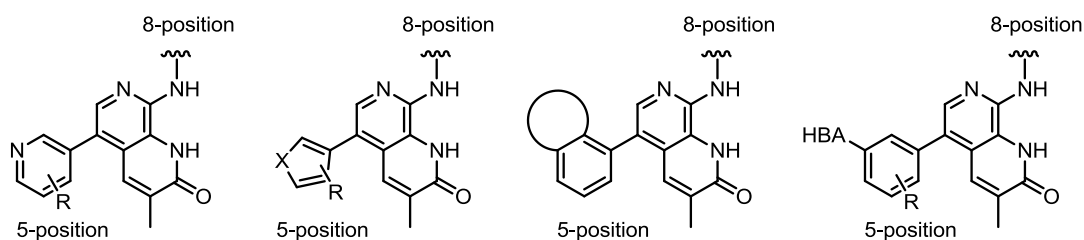


Figure 104: General chemical structures for 5-position analogues.

The 24 compounds included in the 5-position array are shown in **Figure 105**.

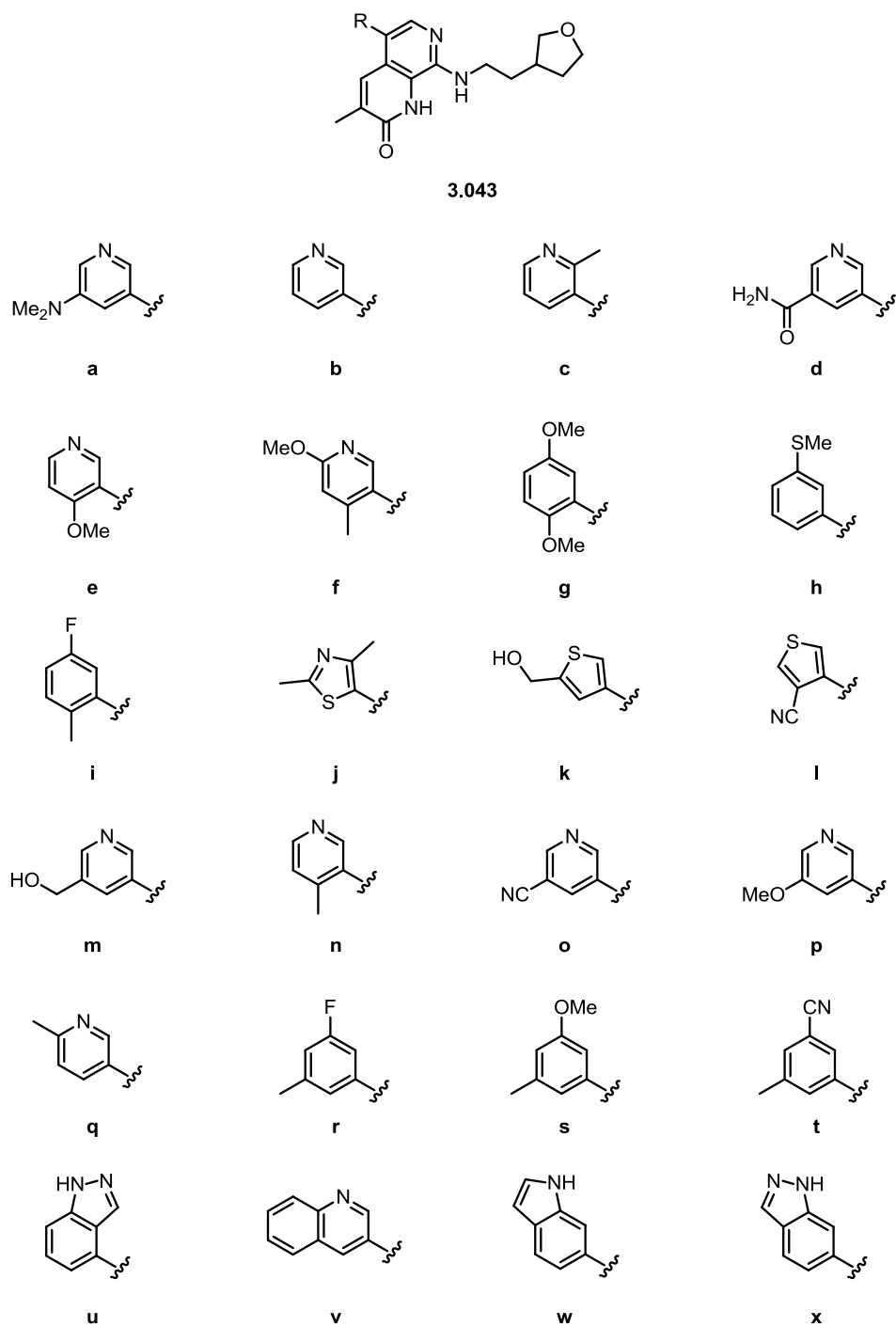
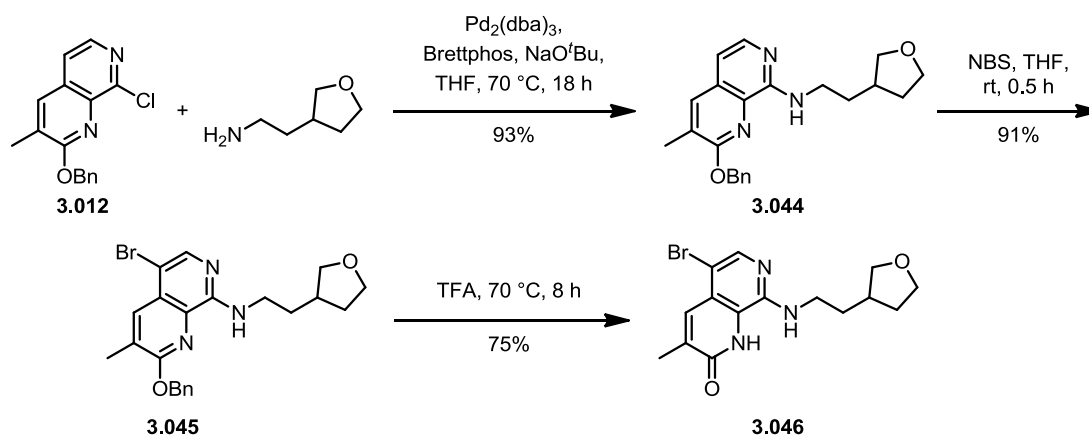


Figure 105: Compounds included in 5-position array.

3.2.7.1 Chemistry for 5-position array

As the 5-position of the naphthyridinone scaffold was to be investigated *via* array chemistry, it was important to deliver a key intermediate in which structural diversity

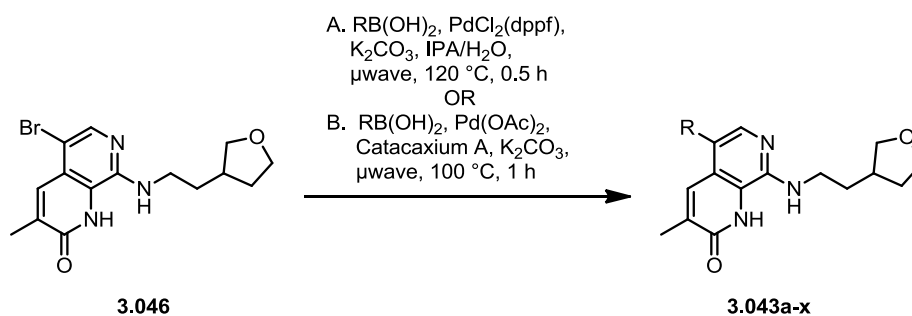
could be installed in the final step of the synthesis. Therefore, a 3-step route starting from *O*-benzyl protected compound **3.012** was identified (**Scheme 47**).



Scheme 47: Synthesis of intermediate 3.046 for use in 5-position array chemistry.

Using the Buchwald-Hartwig conditions previously described,^{105,106} the desired amine was installed at the 8-position of compound **3.012** in excellent yield (93%). The amine moiety then acted as a directing group to facilitate electrophilic bromination with NBS to deliver intermediate **3.045** in 91% yield. Finally, the *O*-benzyl moiety was removed by heating in TFA to furnish compound **3.046** (75%). This route proved efficient and high yielding, affording multiple grams of **3.046** in 63% overall yield.

With a stock of key intermediate **3.046** in hand, a Suzuki-Miyaura coupling was used to install the desired aryl motif (**Scheme 48**).



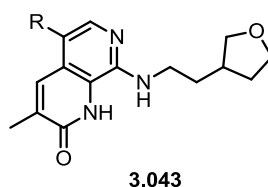
Scheme 48: Synthesis of 5-position array compounds using Suzuki-Miyaura chemistry.

Compounds **3.043a–l** were synthesised by colleagues in the Compound Array Team²⁴⁴ using conditions A. The remainder of the compounds, **3.043m–x** were synthesised sequentially using conditions B.^{105,106}

3.2.7.2 SAR discussion for 5-position array

Compounds **3.043a–x** were tested in the bromodomains of TAF1 BD2 and Brd4 BD1 and BD2 by means of a TR-FRET assay. Selectivity is calculated relative to the maximum Brd4 value.

The majority of compounds tested showed no improvement in TAF1 BD2 potency or selectivity, with many found to be inactive against TAF1 BD2 (for full data see Appendix 5.9). However, clear SAR trends were observed (**Table 40**).



Entry Compound Number	1 b	2 c	3 q	4 3.042z	5 n
R =					
TAF1 BD2 pIC ₅₀	5.9	<5.0	6.4	6.1	6.2
Brd4 BD1 pIC ₅₀	<4.3	<4.3	5.2	<4.3	4.7
Brd4 BD2 pIC ₅₀	5.2	<4.3	5.3	<4.3	5.2
Selectivity	x5	x<1	x13	x63	x10
CLND sol. (µg/mL)	25	52	17	10	186
AMP (nm/s)	390	330	300	350	350

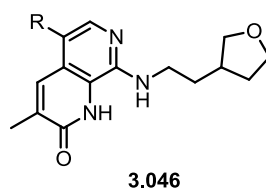
Table 40: pIC₅₀ values for compounds **3.042z** and **3.043b, c, n** and **q** in the bromodomains of TAF1 BD2 and Brd4 (BD1 and BD2) as determined by TR-FRET analysis. Selectivity over Brd4 is calculated relative to the maximum value. Data are n≥2.

Analysis of the data indicated that substitution around the pyridyl ring can deliver an increase in TAF1 BD2 activity and selectivity, with the exception of compound **3.043c**, which was not tolerated (entry 2). Presumably, the methyl group of compound **3.043c** induced a steric clash in both Brd4 and TAF1 BD2, causing the compound to test as inactive against both bromodomains. Compounds **3.043q, n** and **3.042z** (entries 3–5) showed TAF1 BD2 pIC₅₀ values in the region of 6.2, a minor improvement on unsubstituted compound **3.043b**. However, the position of

the methyl substituent was found to play an important role in determining selectivity over Brd4. Compounds **3.043q** and **n** were only 13 and 10 fold selective over Brd4 respectively, whilst compound **3.042z** was 63 fold (compare entries 3–5).

Despite a poor selectivity profile, compound **3.042z** showed much improved physico-chemical properties with good solubility and permeability data observed (entry 5). This result may suggest that the dihedral angle brought about by the methyl substituent in compound **3.043n** reduced the planarity of the scaffold as hypothesised.

As substitution at the 5-position of the pyridyl ring continued to provide the best combination of potency and selectivity, alternative groups with a variety of electronic characteristics were analysed (**Table 41**).



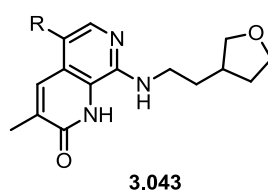
Entry Compound Number	1 d	2 o ²⁴⁵	3 3.042z	4 a	5 p
R =					
TAF1 BD2 pIC ₅₀	6.4	<5.0	6.2	6.5	6.4
Brd4 BD1 pIC ₅₀	<4.3	<4.3	<4.3	4.9	4.7
Brd4 BD2 pIC ₅₀	4.9	<4.3	<4.3	5.1	4.9
Selectivity	×32	×<1	×63	×25	×32
CLND sol. (µg/mL)	15	12	10	13	16
AMP (nm/s)	<10	390	350	460	410

Table 41: pIC₅₀ values for compounds **3.042z** and **3.043a, d, o** and **p** in the bromodomains of TAF1 BD2 and Brd4 (BD1 and BD2) as determined by TR-FRET analysis. Selectivity over Brd4 is calculated relative to the maximum value. Data are n≥2.

Analysis of the data revealed that all substituents apart from the nitrile group (compound **3.043o**, entry 2) provided a minor increase in TAF1 BD2 activity relative to methyl compound **3.042z**. However, this increase in TAF1 BD2 potency was at the expense of selectivity over Brd4, with a maximum of 32 fold selectivity observed

(compare entries 1, 4 and 5). In general, the substituent on the pyridyl ring made little difference to the physico-chemical properties of the scaffold with compounds **3.042z** and **3.043a, o** and **p** showing very similar solubility and permeability profiles. In contrast, compound **3.043d** displayed a significant reduction in permeability, brought about by the high polarity of this compound (*ChromLogD*_{7.4}: 1.56, entry 1)

In order to understand whether alternative groups at the 5-position of the naphthyridinone template would be tolerated in TAF1 BD2, a range of heterocycles and bicycles were introduced. These alternative ring systems were not well tolerated, often providing low TAF1 BD2 activity with poor selectivity over Brd4 (**Table 42**, entries 1 and 2).



Entry Compound Number	1 j ²⁴⁶	2 k	3 v ²⁴⁷	4 w ²⁴⁸	6 t ²⁴⁹
R =					
TAF1 BD2 pIC ₅₀	5.1	5.5	6.2	<5.0	<5.0
Brd4 BD1 pIC ₅₀	<4.3	5.3	5.4	5.3	4.4
Brd4 BD2 pIC ₅₀	<4.3	5.8	5.3	5.9	4.6
Selectivity	x6	x<1	x6	x<1	x1
CLND sol. (µg/mL)	18	16	7	4	4
AMP (nm/s)	470	470	830	-	<3

Table 42: pIC₅₀ values for compounds **3.043j, k, t, v** and **w** in the bromodomains of TAF1 BD2 and Brd4 (BD1 and BD2) as determined by TR-FRET analysis. Selectivity over Brd4 is calculated relative to the maximum value. Data are n≥2.

Fused bicyclic substituents also provided no improvement in potency or selectivity compared to compound **3.042z**. For example, compound **3.043v** showed acceptable TAF1 BD2 activity, but this was accompanied by an increase in Brd4 activity, leading to poor selectivity (entry 3).

Alternative HBA motifs on the phenyl ring were installed in an attempt to replace the pyridyl group. Compound **3.043t** was not tolerated in TAF1 BD2, testing as inactive (entry 5).

Although this array provided very clear SAR with respect to TAF1 BD2, the data revealed that the potency and selectivity profile of compound **3.042z** could not be matched or improved. The majority of modifications made to compound **3.042z** provided compounds which were inactive against TAF1 BD2, with very little, if any, selectivity over Brd4.

3.2.8 Further optimisation of 3.002a

3.2.8.1 Identification of target compounds

As the 5-position array chemistry had failed to deliver any improvement on the activity and selectivity profile shown by **3.042z**, focus was placed back on compound **3.002a**, the original start point for the project. X-Ray crystallography¹⁵⁵ of analogue **3.002b** had been obtained in an attempt to gain a better understanding of the role of the propyl amine chain in TAF1 BD2 activity (**Figure 106**).

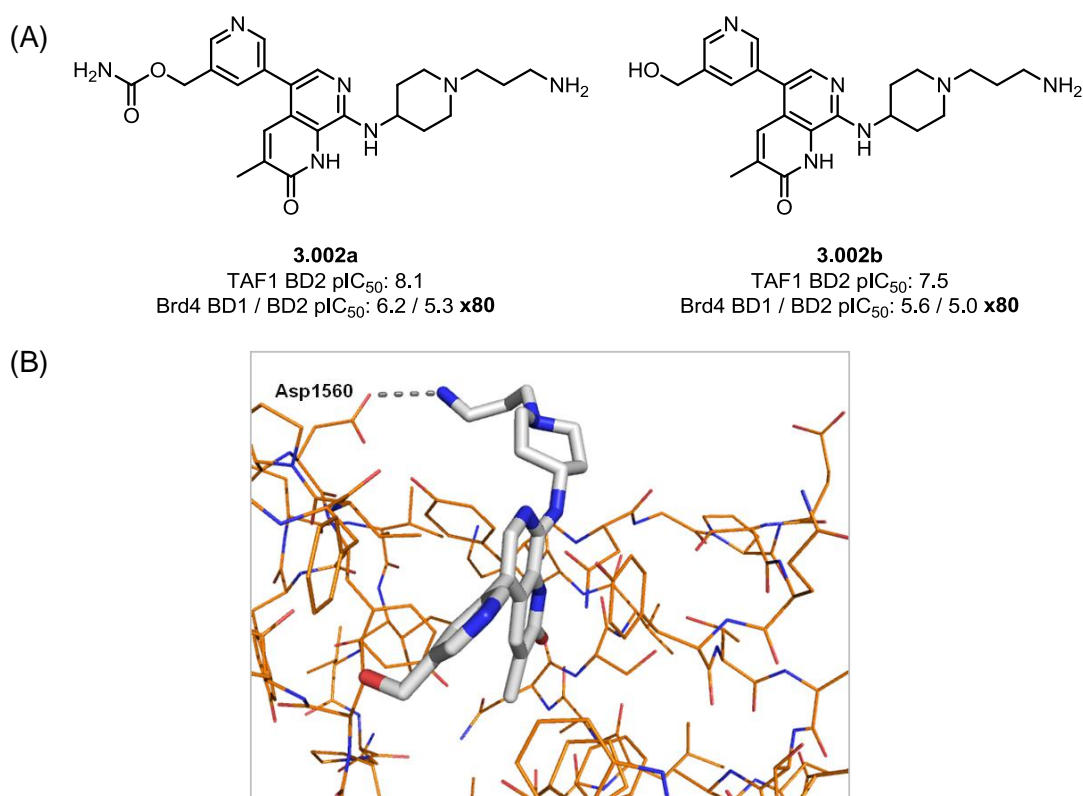


Figure 106: (A) pIC₅₀ values for compounds **3.002a** and **b** in the bromodomains of TAF1 BD2 and Brd4. Data are n≥2. Selectivity over Brd4 is calculated relative to the maximum Brd4 value; (B) X-Ray crystallography of compound **3.002b** in complex with TAF1 BD2. The hydrogen-bond is shown as a grey dashed line.

The X-ray crystal structure indicates that the propylamine chain does form an interaction in TAF1 BD2. The amine moiety picks up a hydrogen-bond to Asp1560, which may account for the increase in TAF1 BD2 activity that this group provides (**Table 28**, page 154).

As the interaction with Asp1560 appeared to deliver an increase in TAF1 BD2 potency and selectivity, efforts were placed on the synthesis of compounds which could form this interaction in an alternative, more efficient manner. As such, a series of compounds, which contained HBD motifs were designed. These investigations would be carried out on the scaffold shown below for direct comparison to the other 8-position compounds synthesised (**Figure 107**).

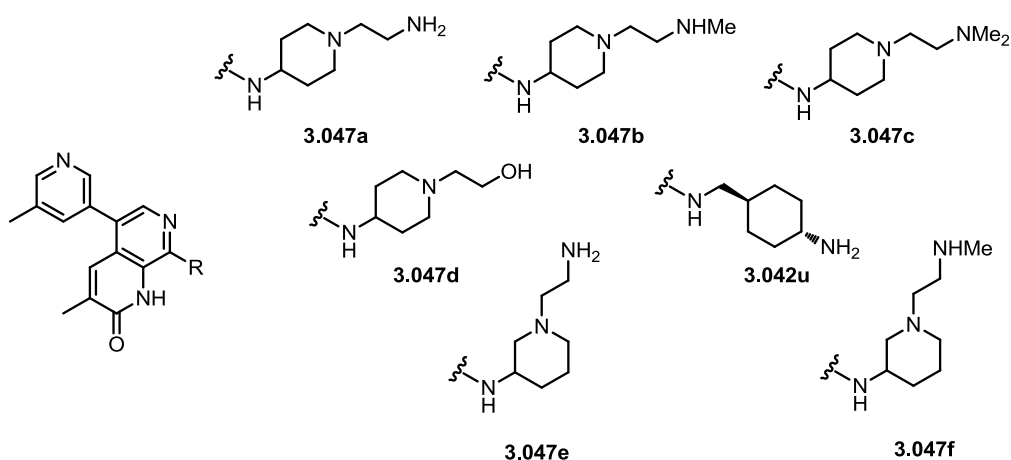


Figure 107: Chemical structures for compounds designed to form an interaction with Asp1560 in TAF1 BD2.

Docking studies²¹⁸ indicated that both compounds **3.042u** and **3.047e** would form a hydrogen-bond with Asp1560 in TAF1 BD2 (**Figure 108**).²¹⁸ Therefore, it was envisioned that the remaining compounds may be capable of forming the same interaction.

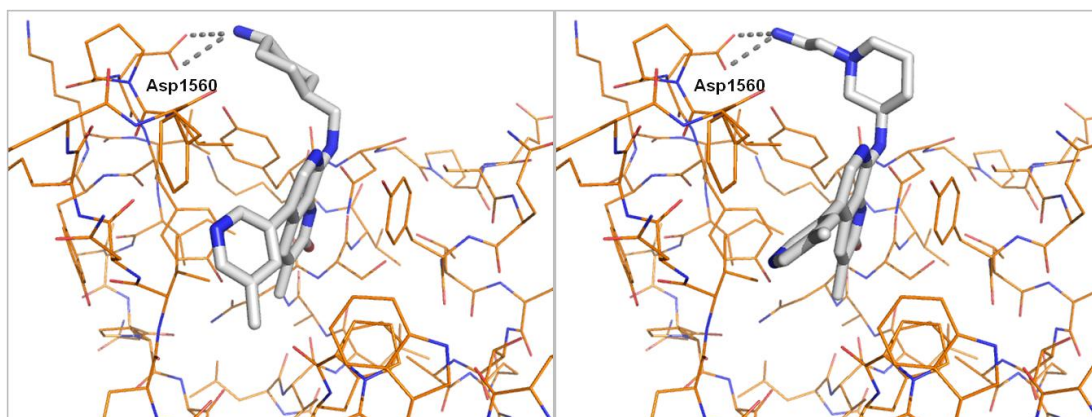
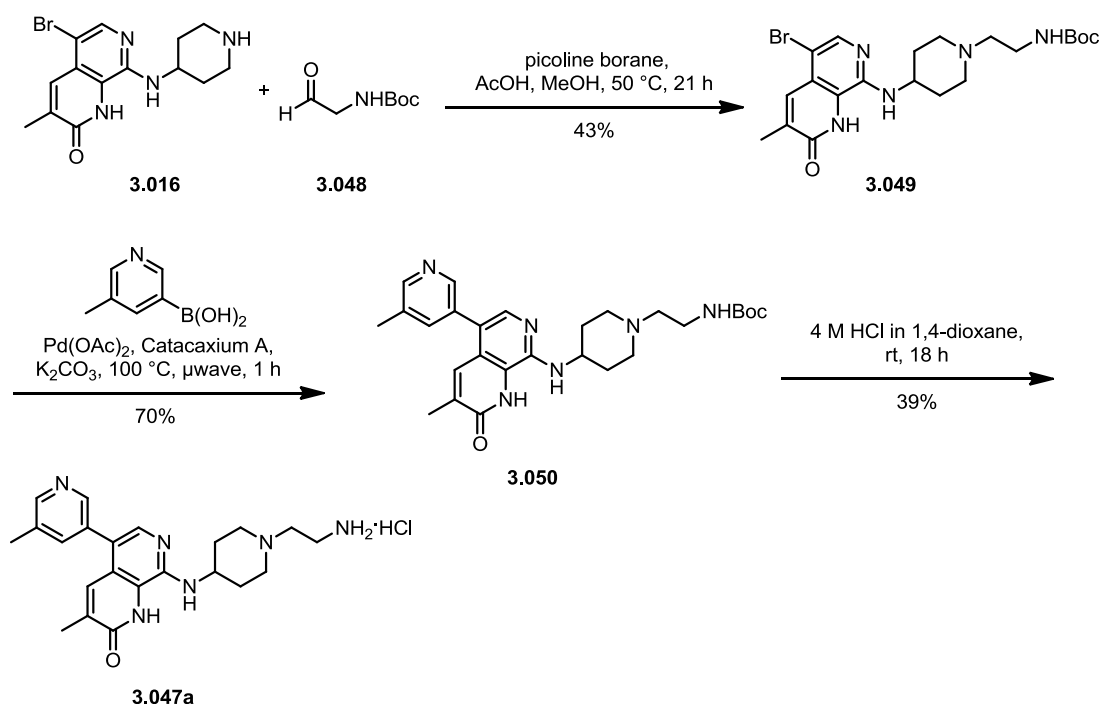


Figure 108: Modelling of compound **3.042u** (left) and **3.050e** (right) in complex with TAF1 BD2. Hydrogen-bonds are shown as grey dashed lines.

3.2.8.2 Synthesis of 3.002a analogues

Compound **3.042u** was synthesised as part of the second 5-position array chemistry (**Scheme 45**, page 174). The remaining compounds **3.047a–g** were synthesised using a variety of methods, making use of pre-synthesised intermediates. Compounds **3.047a** and **b** was accessed *via* lengthy but reliable routes (**Schemes 49** and **50**)

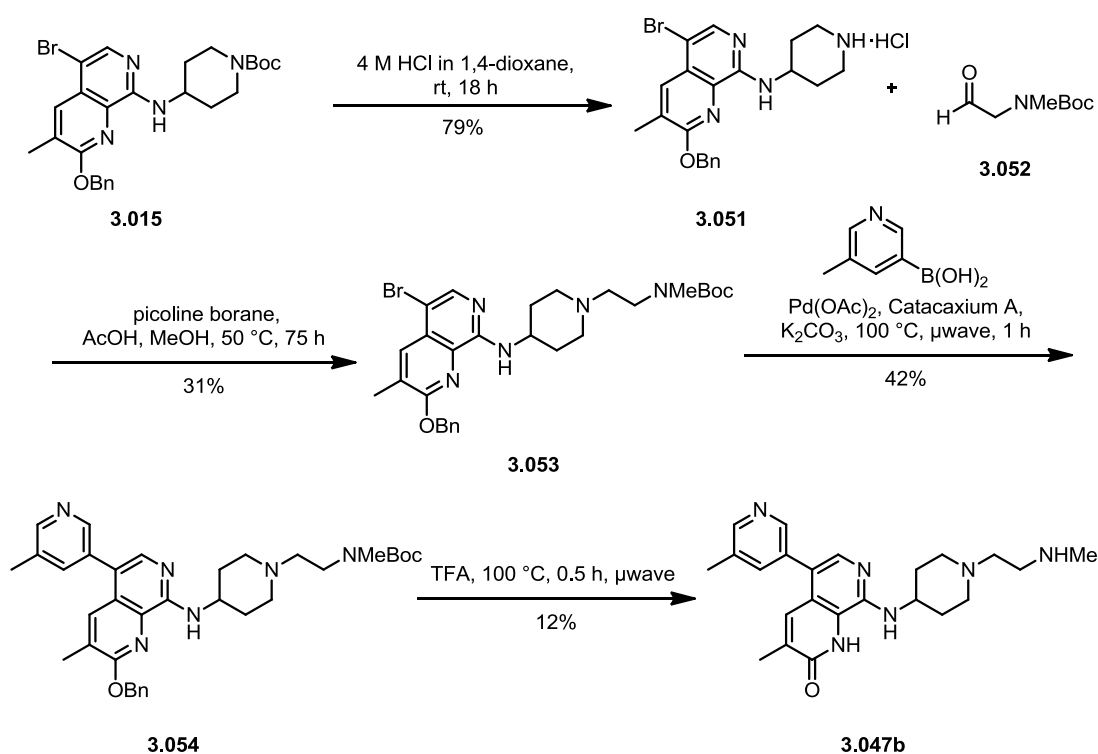


Scheme 49: Synthesis of compound **3.047a**

Utilising intermediate **3.016**, commercially available aldehyde **3.048** was employed in a reductive amination reaction²²⁵ to furnish amine **3.049** in 43% yield. A Suzuki-Miyaura coupling^{105,106} was then used to install the pyridyl motif in 70% yield.

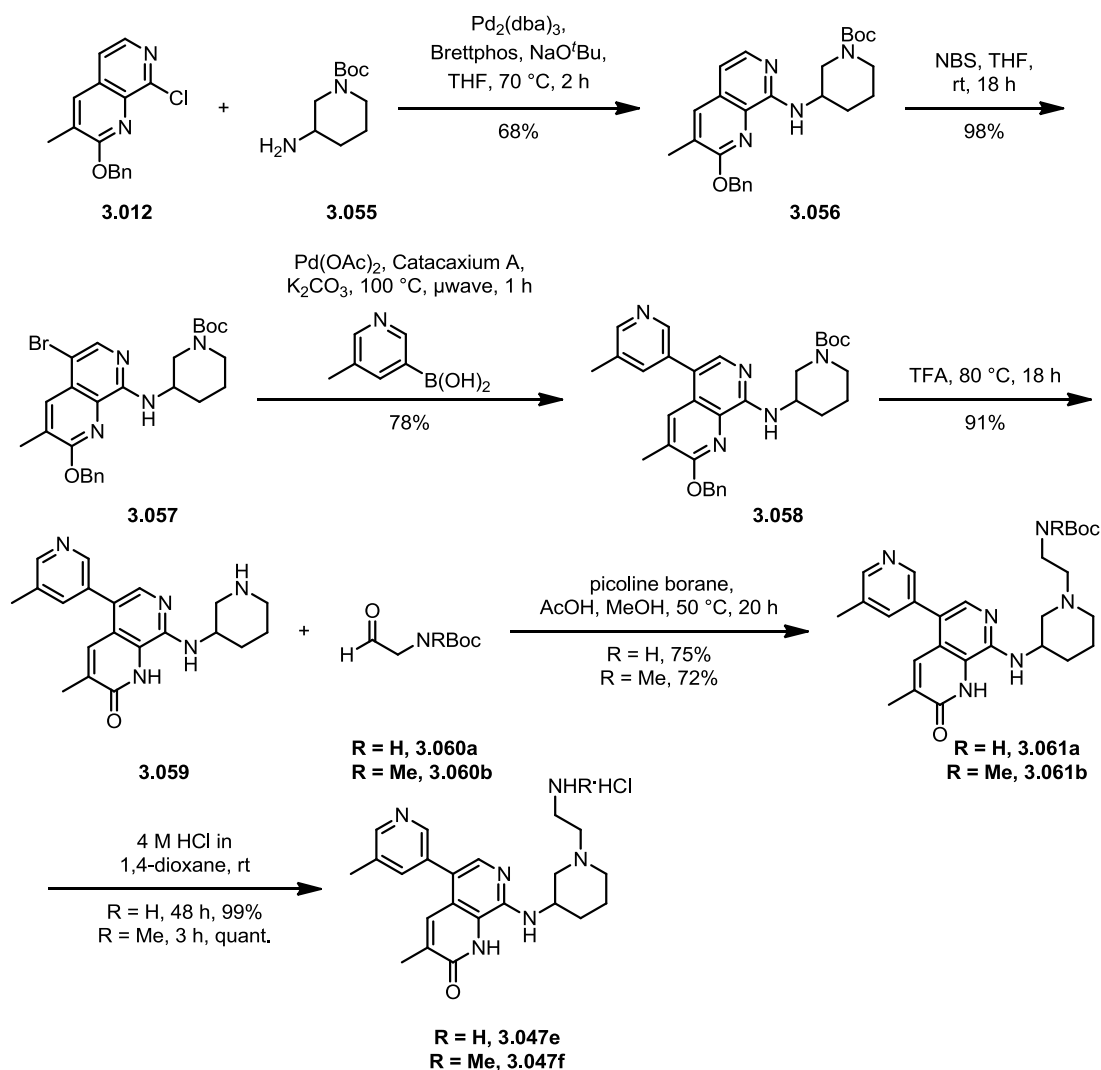
Following this, intermediate **3.050** was deprotected using 4 M HCl in 1,4-dioxane to deliver final compound **3.047a** (39% yield).

Compound **3.047b** was synthesised using a similar route, making use of intermediate **3.015**, which was prepared previously. Intermediate **3.015** was Boc deprotected using 4 M HCl in 1,4-dioxane, to deliver **3.051** in 79% yield. Intermediate **3.051** was then used in a reductive amination reaction²²⁵ with commercially available aldehyde **3.052**, which gave amine **3.053** (31% yield). Subsequently, a Suzuki-Miyaura coupling^{105,106} was used to install the pyridyl group in 42% yield, followed by deprotection with TFA to deliver final compound **3.047b** (12% yield, **Scheme 50**).



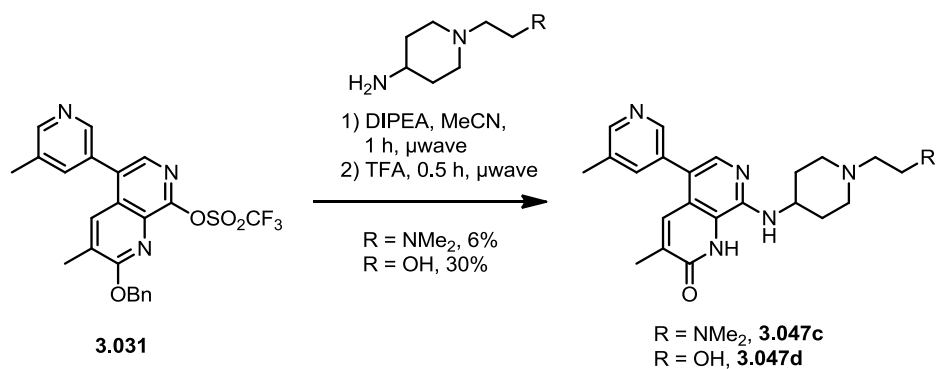
Compounds **3.047f** and **g** were synthesised using previously reported chemistry.^{105,106} Commercially available amine **3.055** was installed *via* a Buchwald Hartwig coupling to furnish intermediate **3.056** in 68% yield. Electrophilic bromination with NBS gave **3.057** in 98% yield. Following this, a Suzuki-Miyaura coupling was used to install the pyridyl motif in 78% yield. The Boc and *O*-benzyl groups were cleaved simultaneously by heating **3.058** in TFA over-night to provide late-stage intermediate **3.059** in excellent yield (91%). Aldehydes **3.060a** and **b** were used in reductive amination chemistry, followed by Boc deprotection to give final

compounds **3.047e** and **f** in excellent yields (99% and quant. respectively, **Scheme 51**).



Scheme 51: Synthesis of compounds 3.047e and g.

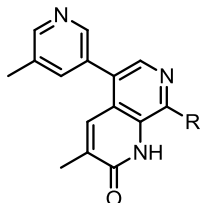
Compounds **3.047c** and **d** were synthesised using triflate **3.031** via $\text{S}_{\text{N}}\text{Ar}$ chemistry with commercially available amines (**Scheme 52**).



Scheme 52: Synthesis of compounds 3.047c and d via $\text{S}_{\text{N}}\text{Ar}$ chemistry.

3.2.8.3 SAR discussion of 3.002a analogues

Compounds **3.047a–f** and **3.045u** were tested in the bromodomains of TAF1 BD2 and Brd4 BD1 and BD2 by means of a TR-FRET assay. Selectivity is calculated relative to the maximum Brd4 value. Compound **3.002b** has been included in the data set for comparison (**Table 43**).



Entry	Compound number	R =	TAF1 BD2 pIC ₅₀	Brd4 BD1 pIC ₅₀	Brd4 BD2 pIC ₅₀	Selectivity
1	3.002b		7.3	5.6	4.7	x50
2	3.047a		7.1	5.2	5.2	x80
3	3.047b ²⁵⁰		6.7	5.2	5.5	x16
4	3.047c ²⁵⁰		6.4	5.2	5.3	x13
5	3.047d ²⁵⁰		6.3	5.6	4.8	x5
6	3.042u		6.6	4.9	5.4	x16
7	3.047e		6.1	4.7	5.2	x8
8	3.047f		6.2	4.7	5.2	x10

Table 43: pIC₅₀ values for compounds **3.002b**, **3.047a–f** and **3.042u** in the bromodomains of TAF1 BD2 and Brd4 (BD1 and BD2) as determined by TR-FRET analysis. Selectivity over Brd4 is calculated relative to the maximum value. Data are n≥2 unless stated otherwise.

Analysis of the data generated from the TR-FRET assay indicates that reducing the length of the propylamine chain (**3.002b**) to the ethyl variant (**3.047a**) makes little difference to TAF1 BD2 activity, but causes a reduction in Brd4 potency, providing

80 fold selectivity (compare entries 1 and 2). However, exchanging the primary amine (**3.047a**) for the secondary (**3.047b**) and tertiary (**3.047c**) analogues causes a reduction in both TAF1 BD2 potency and selectivity, suggesting that these molecules may not be capable of forming the hydrogen-bond to Asp1560 (compare entry 2 to 3 and 4). Furthermore, exchange of the amine for the primary alcohol causes further reduction in TAF1 BD2 activity and selectivity (entry 5). Despite docking studies predicting that compound **3.042u** would form an interaction to Asp1560 in TAF1 BD2 (**Figure 108**, page 188), this compound shows only moderate activity, with little selectivity over Brd4 (entry 6). Finally, 3-substituted amino piperidines **3.047e** and **f** also show reduced TAF1 BD2 activity compared to **3.047a**, suggesting a disconnect between the modelling and the data generated by the TR-FRET assay (compare entry 2 to 7 and 8).

Although, for the most part, attempts to improve the profile of **3.002b** proved unsuccessful, shorter chain compound **3.047a** showed acceptable TAF1 BD2 potency with 80 fold selectivity over Brd4. However, the physico-chemical properties shown by this compound were poor (CLND sol.: 58 µg/mL; AMP: <3 nm/s).

At this stage in the project, all attempts to improve TAF1 BD2 potency and selectivity whilst maintaining good physico-chemical properties were unsuccessful. Although many compounds were synthesised with much improved physico-chemical properties, which satisfied the guidelines for drug-like molecules, this was at the expense of TAF1 BD2 activity.

Therefore, in an attempt to improve the physico-chemical properties of **3.002a**, whilst maintaining good activity, saturated ring systems were introduced at the 5-position of the template. It is widely reported¹⁵⁴ that increasing the fraction of sp³ hybridised C atoms improves solubility of compounds.

3.2.8.4 Introduction of saturated substituents at the 5-position

In line with attempts to maintain high TAF1 BD2 activity along with acceptable physico-chemical properties, saturated substituents were introduced onto the 5-position of the naphthyridinone core. As discussed previously (Section 3.2.1, page 147), reducing the aromatic character can improve solubility. Therefore a selection of saturated ring systems were introduced, with the aim to investigate this hypothesis (**Figure 109**).

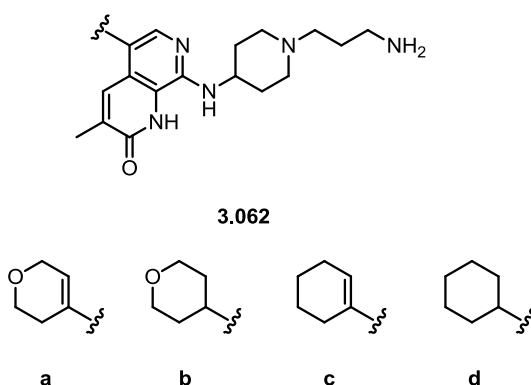
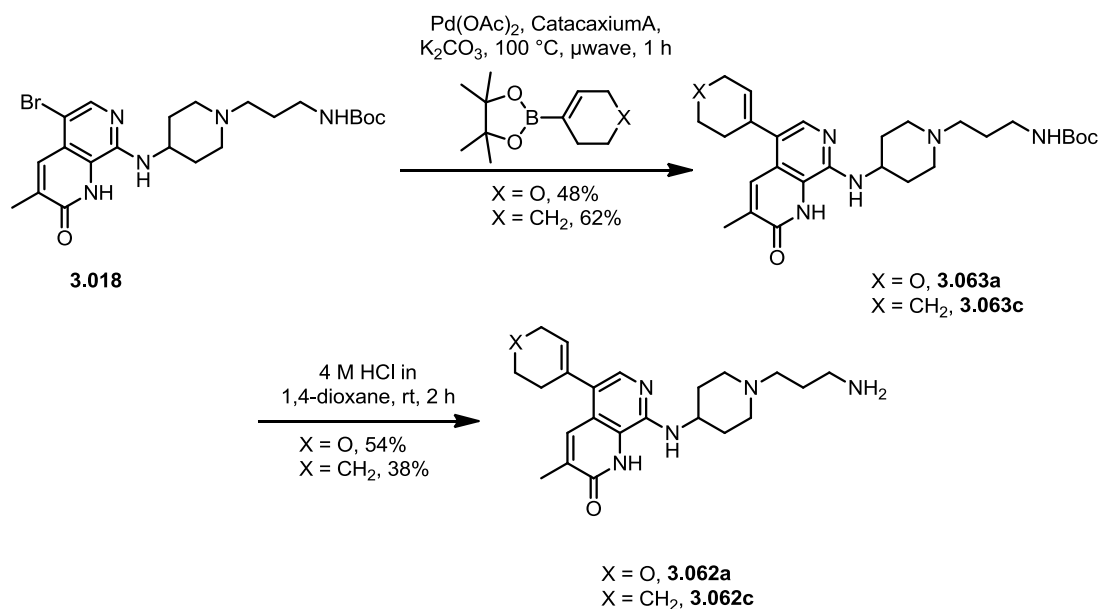


Figure 109: Saturated 5-position compounds 3.062a–d.

3.2.8.5 Synthesis of 5-position saturated analogues

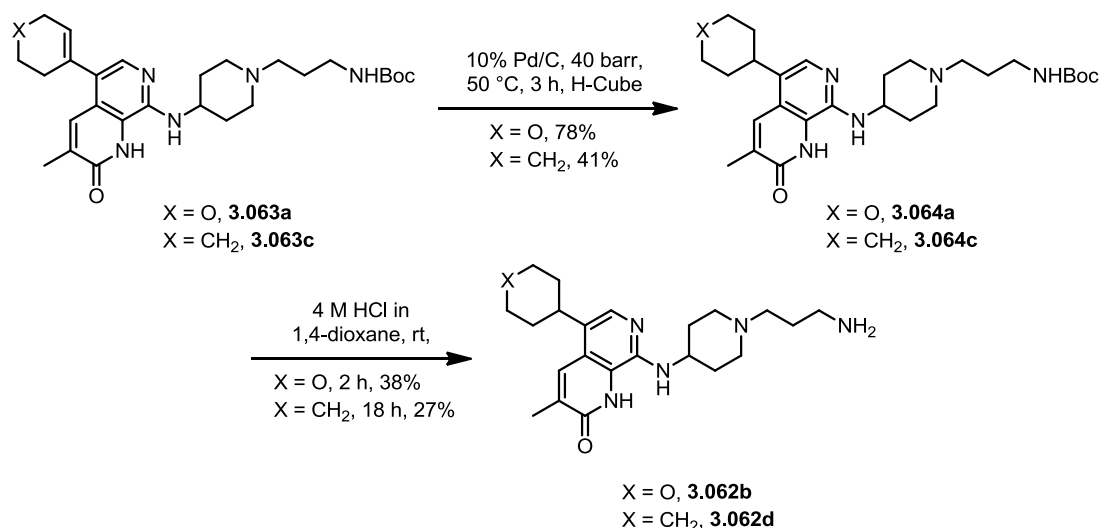
The synthesis of compounds **3.062a–d** was carried out using late-stage intermediate **3.018** (Scheme 53).



Scheme 53: Synthesis of compounds 3.062a and c.

A Suzuki-Miyaura coupling^{105,106} was used to install the ring systems at the 5-position of the scaffold in acceptable yields (48% and 62%). Following this, Boc deprotection was achieved using 4 M HCl in 1,4-dioxane to deliver compounds **3.062a** and **c** in 54% and 38% yields respectively.

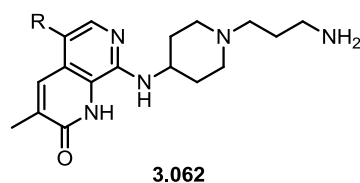
In order to synthesis fully saturated compounds **3.062b** and **d**, intermediates **3.063a** and **c** were used in hydrogenation chemistry in the H-Cube to deliver compounds **3.064d** and **d**. Subsequently, the Boc groups were cleaved under acidic conditions (Scheme 54).



Scheme 54: Synthesis of compounds 3.062b and d.

3.2.8.6 SAR discussion for 5-position saturated analogues

Compounds **3.062a–d** were tested in the bromodomains of TAF1 BD2 and Brd4 BD1 and BD2 by means of a TR-FRET assay. Selectivity was calculated relative to the maximum Brd4 value (**Table 44**).

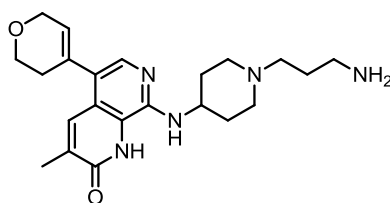


Entry	Compound number	R =	TAF1 BD2 pIC ₅₀	Brd4 BD1 pIC ₅₀	Brd4 BD2 pIC ₅₀	Selectivity
1	a		7.2	5.2	5.0	×100
2	b		6.4	4.8	4.9	×32
3	c		6.3	5.4	5.4	×8
4	d		6.2	4.9	5.3	×8

Table 44: pIC₅₀ values for compounds **3.062a–d** in the bromodomains of TAF1 BD2 and Brd4 (BD1 and BD2) as determined by TR-FRET analysis. Selectivity over Brd4 is calculated relative to the maximum value. Data are n≥2.

Analysis of the data from the TR-FRET assay indicates that, in general, compared to aryl substituted analogues, saturated ring systems deliver a reduction in TAF1 BD2

activity, with little effect on Brd4. Comparison of compounds **3.062c** and **d** shows that both sp^2 and sp^3 linker atoms at the 5-position provide almost identical activity and selectivity data (compare entries 3 and 4). However, THP compounds **3.062a** and **b** show a different trend. Increasing the saturation of the 5-position linker from sp^2 to sp^3 leads to a decrease in both TAF1 BD2 and Brd4 activities, although this is more pronounced for the former (compare entries 1 and 2). In addition, the data for compounds **3.062a** and **c** indicates that addition of the THP analogue delivers a 10 fold increase in activity against TAF1 BD2 (compare entries 1 and 3). Compound **3.062a** displays the best profile, with a TAF1 BD2 pIC_{50} : 7.2 and 100 fold selectivity over Brd4. In the absence of X-ray crystallography of compound **3.062a** in complex with TAF1 BD2, it was difficult account for this increase in activity. Nevertheless, **3.062a** showed good activity and selectivity, therefore, further analysis of the compound was conducted (**Figure 110**).

**3.062a**

TAF1 BD2 pIC_{50} : 7.2
 Brd4 BD1 / BD2 pIC_{50} : 5.2 / 5.0 **x100**
 Brd9 pIC_{50} : 5.3 **x80**
 CREBBP pIC_{50} : <4 **x1600**
 PCAF pIC_{50} : 4.0 **x1600**
 BAZ2A pIC_{50} : 4.6 **x400**
 CLND sol.: 87 μ g/mL
 AMP: <10 nm/s
 ChromLogD_{7.4}: 1.08

Figure 110: Summary of data for compound 3.062a. Data are $n \geq 2$.²⁵¹

Pleasingly, the **3.062a** was found to be 80 fold selective over the bromodomain of Brd9. This result was particularly surprising, as Brd9 has remained a close off-target for this series. In addition, **3.062a** tested as inactive against the bromodomains of PCAF and CREBBP and was 400 fold selective over BAZ2A. Since these bromodomains belong to different families of the phylogenetic tree (**Figure 8**, page 7), indicating sequence variation, this result may suggest good broader selectivity.

The solubility of **3.062a** compared to its aryl substituted analogues was much improved, with CLND sol.: 87 μ g/mL. However, permeability for this compound was poor (AMP: <10 nm/s) due to high polarity as shown by the ChromLogD_{7.4} value (1.08).

Although the bromodomain data shown by compound **3.062a** was very encouraging, the poor permeability data highlighted the physico-chemical property issues with this template in general. Nevertheless, compound **3.062a** represents a promising point on the path to TAF1 BD2 chemical probe discovery.

3.3 Conclusions

Throughout the course of the investigations to develop a TAF1 BD2 chemical probe from the naphthyridinone template, it proved very difficult to achieve high TAF1 activity in combination with good physico-chemical properties. Excellent TAF1 BD2 activity has been delivered, with reasonable to good selectivity over Brd4. However, this has never been obtained alongside good solubility and permeability, highlighting the difficulty of achieving the correct balance within this series (**Figure 111**).

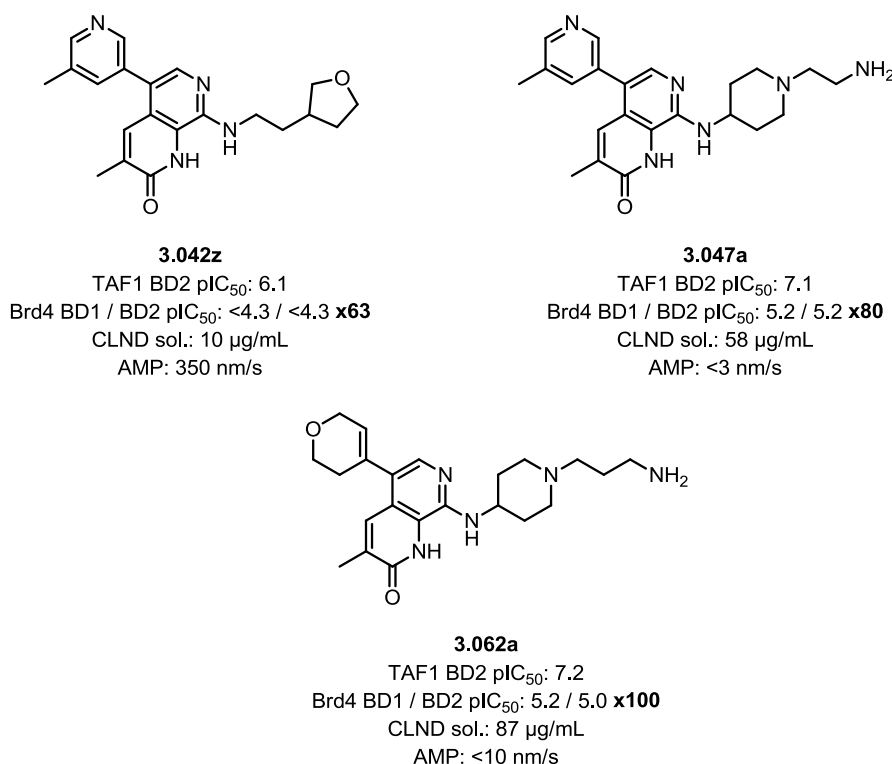
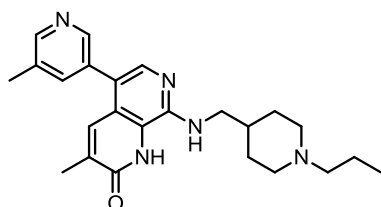
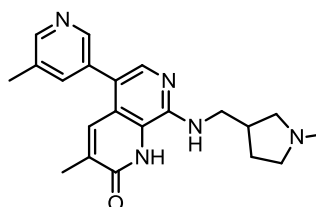


Figure 111: Data for compounds 3.042z, 3.047a and 3.062a. Data are n≥2.

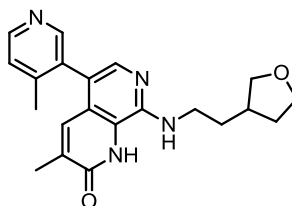
Several compounds were prepared with excellent physico-chemical properties showing good solubility and permeability profiles. However, this was at the expense of TAF1 BD2 activity and selectivity over Brd4 (**Figure 121**).

**3.042c**

TAF1 BD2 pIC₅₀: 6.3
 Brd4 BD1 / BD2 pIC₅₀: 4.5 / 4.7 **x40**
 CLND sol.: 170 µg/mL
 AMP: 140 nm/s
 PFI: 4.7

**3.042k**

TAF1 BD2 pIC₅₀: 6.3
 Brd4 BD1 / BD2 pIC₅₀: 5.2 / 5.0 **x13**
 CLND sol.: 170 µg/mL
 AMP: 260 nm/s
 PFI: 4.3

**3.043n**

TAF1 BD2 pIC₅₀: 6.2
 Brd4 BD1 / BD2 pIC₅₀: 4.7 / 5.2 **x10**
 CLND sol.: 186 µg/mL
 AMP: 350 nm/s
 PFI: 6.2

Figure 112: Data for compounds 3.042c and k and 3.043n. Data are n≥2.

Given the difficulty in achieving good physico-chemical properties and excellent bromodomain activity, it was not possible to deliver a compound, which satisfied the probe criteria outlined at the outset of this project (Section 3.1.4, page 143). However, this work delivered compound **3.062a**, which displays a very encouraging profile (**Figure 110**, page 195).

Compound **3.062a** shows excellent TAF1 BD2 activity (pIC₅₀: 7.2), 100 fold selectivity over Brd4, 80 fold over Brd9, >1500 fold over PCAF and CREBBP and 400 fold over BAZ2A. Given the difference in sequence homology between these bromodomains as indicated by their positions on the phylogenetic tree, it is believed that the broader selectivity of this compound would be within the 30 fold desired (Section 3.1.4, page 143). Therefore, **3.062a** represents the first compound reported to be selective for TAF1 BD2. Although the solubility of **3.062a** is acceptable (CLND sol.: 87 µg/mL), the permeability is poor (AMP: <10 nm/s), meaning that its utility as a cellular probe is limited. Therefore, in order to improve the profile of **3.062a**, future work could focus on improving the permeability of this compound, thus satisfying the probe criteria.

3.4 Future work

As previously described, investigations on the naphthyridinone template have delivered compound **3.062a**, which shows great potential as a TAF1 BD2 chemical probe. The compound shows excellent activity (TAF1 BD2 pIC₅₀: 7.2) and ≥80 fold selectivity over every other bromodomain tested. However, **3.062a** shows poor permeability (AMP: <10 nm/s), therefore limiting its utility as a cellular chemical probe. Future work on this series could focus on improving the permeability of **3.062a** so that it can be used to investigate the cellular role of TAF1 BD2.

Given that the poor permeability of **3.062a** is due to its high polarity (*ChromLogD*_{7.4}:1.08), future work could focus on functionalisation the piperidine ring to include lipophilic groups (**Figure 113**, left). This strategy would allow for investigation of a previously unexplored vector and deliver an increase in LogD, thereby increasing the permeability of the template.

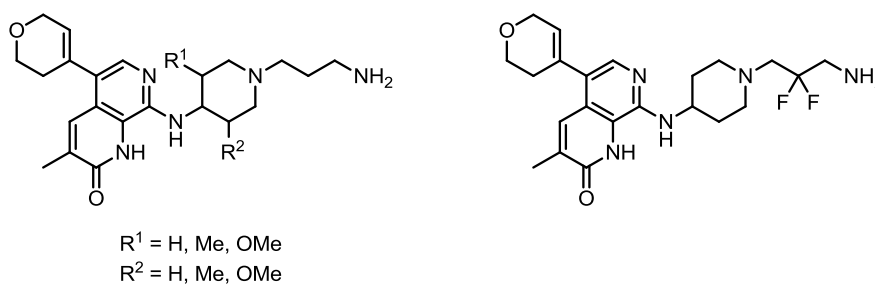


Figure 113: Proposed modifications to compound 3.062a.

An alternative approach could be to modulate the basicity of the pendant amine. It has been reported²⁵² that the introduction of F into piperidine rings decreases the basicity of the N centre due to the inductive effect of F (**Figure 113**, right). This, in turn, leads to an increase in LogD and therefore permeability.

In addition to increasing the permeability of compound **3.062a**, future work could focus on the delivery of a compound which contains the *N*-Crotyl KAc mimetic. As discussed previously (Section 3.1.2, page 140) recent studies have shown that TAF1 BD2 is capable of binding to this motif with good selectivity across the bromodomain family.³³ Therefore, future efforts could focus on the installation of the KCr mimetic on to a known bromodomain scaffold. Due to synthetic tractability, the TP core of **I-BRD9** could represent a start point for these investigations.

4 Experimental

4.1 General experimental

The names of the following compounds have been obtained using ChemDraw Ultra 12.0.

LCMS Methodology

Method using formic acid modifier – LCMS (formic acid)

LC conditions:

The UPLC analysis was conducted on an Acquity UPLC BEH C₁₈ column (50 mm x 2.1 mm, i.d. 1.7 µm packing diameter) at 40 °C. The solvents employed were: A = 0.1% v/v solution of formic acid in water; B = 0.1% v/v solution of formic acid in acetonitrile. The gradient (A:B) employed was from 97:3 to 3:97 over 2 min. The UV detection was a summed signal from wavelength of 210 nm to 350 nm.

MS conditions:

The mass spectrometry was conducted on a Waters ZQ mass spectrometer, with an ionisation mode of alternate–scan positive and negative electrospray. The scan range was 100 to 1000 AMU, the scan time was 0.27 seconds and the inter–scan delay was 0.10 seconds.

Method using ammonium bicarbonate modifier – LCMS (high pH)

LC conditions:

The UPLC analysis was conducted on an Acquity UPLC BEH C₁₈ column (50 mm x 2.1 mm, i.d. 1.7 µm packing diameter) at 40 °C. The solvents employed were: A = ammonium hydrogen carbonate in water adjusted to pH 10 with ammonia solution; B = acetonitrile. The gradient (A:B) employed was from 99:1 to 0:100 over 2 min. The UV detection was a summed signal from wavelength of 210 nm to 350 nm.

MS conditions:

The mass spectrometry was conducted on a Waters ZQ mass spectrometer, with an ionisation mode of alternate–scan positive and negative electrospray. The scan

range was 100 to 1000 AMU, the scan time was 0.27 seconds and the inter-scan delay was 0.10 seconds.

High Resolution Mass Spectrometry (HRMS)

Chromatography and analysis conditions:

An Agilent 1100 Liquid Chromatograph equipped with a model G1367A autosampler, a model G1312A binary pump and a HP1100 model G1315B diode array detector was used. The method used was generic for all experiments. All separations were achieved using a C₁₈ reversed phase column (100 x 2.1 mm, 3 μm particle size) or equivalent. Gradient elution was carried out with the mobile phases as (A) water containing 0.1% (v/v) TFA and (B) acetonitrile containing 0.1% (v/v) TFA. The conditions for the gradient elution were initially 0% B, increasing linearly to 95% B over 8 min, remaining at 95% B for 0.5 min then decreasing linearly to 0% B over 0.1 min followed by an equilibration period of 1.49 min prior to the next injection. The flow rate was 1 mL/min, split to source and the temperature controlled at 40 °C with an injection volume of between 2 to 5 μL.

Mass Spectrometry conditions:

Positive ion mass spectra were acquired using a Thermo LTQ–Orbitrap FT mass spectrometer, equipped with a ESI interface, over a mass range of 100 – 1100 Da, with a scan time of 1 second. The elemental composition was calculated using Xcalibur software and processed using RemoteAnalyzer (Spectral Works Ltd) for the [M+H]⁺ and the mass error quoted as ppm.

NMR Spectroscopy

NMR spectra were recorded on Bruker AV-400 (¹H = 400 MHz, ¹³C = 101 MHz), Bruker AV-500 (¹H = 500 MHz, ¹³C = 125 MHz) and Bruker AV-500 (¹H = 600 MHz, ¹³C = 151 MHz)

¹H NMR spectra: The chemical shift data for each signal are given as δ_H in units of parts per million (ppm) relative to tetramethylsilane (TMS) where δ (TMS) = 0.00 ppm. The multiplicity of each signal is indicated by: s (singlet); br.s (broad singlet); d (doublet); t (triplet); q (quartet); dd (doublet of doublets); ddd (double doublet of doublets), m (multiplet). The number of protons (n) for a given resonance signal is indicated by nH. Coupling constants (J) are quoted in Hz and

are recorded to the nearest 0.1 Hz. Identical proton coupling constants (J) are averaged in each spectrum and reported to the nearest 0.1 Hz.

^{13}C NMR spectra: Recorded with broadband proton decoupling. The chemical shift data for each signal are given as δ_{C} in units of parts per million (ppm) relative to tetramethylsilane (TMS) where δ_{C} (TMS) = 0.00 ppm.

NMR spectra were recorded at room temperature.

Flash column chromatography

Purification was performed on a Biotage SP4 System using KP-Sil™ cartridges eluting with solvents as supplied, under a positive pressure of compressed air.

MDAP Methodology

Method using formic acid modifier – MDAP (formic acid)

LC conditions:

The HPLC analysis was conducted on either a Sunfire C_{18} column (100 mm x 19 mm, i.d. 5 μm packing diameter) or a Sunfire C_{18} column (150 mm x 30 mm, i.d. 5 μm packing diameter) at ambient temperature. The solvents employed were: A = 0.1% v/v solution of formic acid in water; B = 0.1% v/v solution of formic acid in acetonitrile. The purification was run as a gradient (A:B) over either 15 or 25 minutes, with a flow rate of 20 mL/min (100 mm x 19 mm, i.d. 5 μm packing diameter) or 40 mL/min (150 mm x 30 mm, i.d. 5 μm packing diameter). The UV detection was a summed signal from wavelength of 210 nm to 350 nm.

MS conditions:

The mass spectrometry was conducted on a Waters ZQ mass spectrometer, with an ionisation mode of alternate-scan positive and negative electrospray. The scan range was 100 to 1000 AMU, the scan time was 0.50 secs and the inter-scan delay was 0.20 sec.

Method using ammonium bicarbonate modifier – MDAP (high pH)

LC conditions:

The HPLC analysis was conducted on either an Xbridge C_{18} column (100 mm x 19 mm, i.d. 5 μm packing diameter) or an Xbridge C_{18} column (100 mm x 30 mm, i.d.

5 μm packing diameter) at ambient temperature. The solvents employed were: A = 10 mM ammonium bicarbonate in water, adjusted to pH 10 with ammonia solution; B = acetonitrile. The purification was run as a gradient (A:B) over either 15 min or 25 min, with a flow rate of 20 mL/min (100 mm x 19 mm, i.d 5 μm packing diameter) or 40 mL/min (150 mm x 30 mm, i.d. 5 μm packing diameter). The UV detection was a summed signal from wavelength of 210 nm to 350 nm.

MS conditions:

The mass spectrometry was conducted on a Waters ZQ mass spectrometer, with an ionisation mode of alternate-scan positive and negative electrospray. The scan range was 100 to 1000 AMU, the scan time was 0.50 seconds and the inter-scan delay was 0.20 seconds.

Microwave Reactor

Reactions heated under microwave conditions were heated in a Biotage Initiator microwave. The initial absorption was set as 'very high'.

Compound Purity

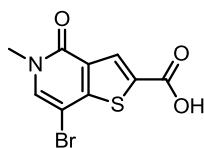
The purity of compounds tested in *in vitro* assays was of greater than 95% using interpretation of a combination of LCMS and ^1H NMR data.

Reagents and solvents

Reagents and solvents were purchased from Acros UK, Sigma Aldrich UK, Alfa Aesar UK or Fisher UK. Anhydrous DMF, THF and DCM were purchased from SigmaAldrich UK in a SureSeal™ bottle. All other solvents were used as supplied (analytical or HPLC grade). *In vacuo* refers to the use of a rotary evaporator attached to a diaphragm pump. Brine refers to a saturated aqueous solution of sodium chloride.

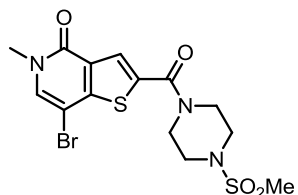
4.2 Experimental procedures

7-Bromo-5-methyl 4-oxo-4,5-dihydrothieno[3,2-c]pyridine-2-carboxylic acid (2.008)

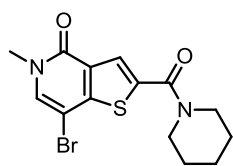


To a mixture of **2.009** (300 mg, 1.10 mmol) in H₂O (5.5 mL) and DMSO (5.5 mL), sodium chlorite (598 mg, 6.61 mmol), sodium dihydrogen phosphate (794 mg, 6.61 mmol) and hydrogen peroxide (35% wt in H₂O, 0.2 mL, 6.61 mmol) were added. The mixture was left to stir at rt for 24 h. The reaction mixture was acidified to pH 1 with glacial acetic acid (5 mL) and concentrated *in vacuo*. The residue was suspended in H₂O (20 mL) and acidified to pH 1 with glacial AcOH (5 mL). The aqueous phase was extracted with EtOAc (3 × 20 mL) and the combined organic layers were washed with brine (20 mL), dried (MgSO₄), filtered and concentrated *in vacuo* to give **2.008** as a light brown solid (184 mg, 58%); ¹H NMR (400 MHz, DMSO-d₆) 13.69 (s, 1H), 8.14 (s, 1H), 8.06 (s, 1H), 3.52 (s, 3H); LCMS (formic acid): R_t = 0.67 min (89%), MH⁺ = 287.0, 289.0.

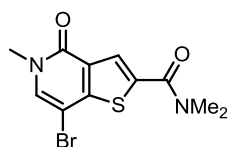
7-Bromo-5-methyl-2-(4-(methylsulfonyl)piperazine-1-carbonyl)thieno[3,2-c]pyridin-4(5H)-one (2.016)



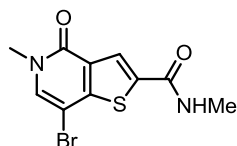
A mixture of **2.008** (183 mg, 0.64 mmol), 1-(methylsulfonyl)piperazine (128 mg, 0.78 mmol), HATU (290 mg, 0.76 mmol) and DIPEA (0.2 mL, 1.27 mmol) in DMF (5 mL) was left to stir at rt for 18 h. The volatile components were removed *in vacuo* and the resulting residue was dissolved in EtOAc (10 mL), washed with aq. citric acid (1 M, 3 × 10 mL), sat. aq. NaHCO₃ (3 × 10 mL), H₂O (10 mL) and brine (10 mL). The organic layer was passed through a hydrophobic frit and concentrated *in vacuo* to give **2.016** (150 mg, 54%) as a brown solid; ¹H NMR (400 MHz, CDCl₃) δ ppm 7.87 (s, 1H), 7.41 (s, 1H), 3.93 (t, *J* = 5.1, 4H), 3.65 (s, 3H), 3.35 (t, *J* = 5.1, 4H), 2.85 (s, 3H); LCMS (formic acid) R_t = 0.73 min (85%), MH⁺ = 434.1, 436.1.

7-Bromo-5-methyl-2-(piperidine-1-carbonyl)thieno[3,2-c]pyridin-4(5H)-one**(2.017a)**

A mixture of **2.008** (250 mg, 0.87 mmol), piperidine (0.11 mL, 1.13 mmol), HATU (396 mg, 1.04 mmol), and DIPEA (0.3 mL, 1.74 mmol) in DMF (7.5 mL) was stirred at rt for 18 h. The volatile components were removed *in vacuo*. The resulting residue was dissolved in EtOAc (25 mL) and washed with aq. citric acid (10% w/v, 3 × 25 mL), sat. aq. NaHCO₃ (3 × 25 mL), H₂O (25 mL) and brine (25 mL). The organic layer was passed through a hydrophobic frit and concentrated *in vacuo* to give **2.017a** (244 mg, 79%) as a light brown solid; ¹H NMR (400 MHz, CDCl₃) δ ppm 7.83 (s, 1H), 7.37 (s, 1H), 3.75–3.71 (m, 4H), 3.64 (s, 3H), 1.77–1.65 (m, 6H); LCMS (formic acid), R_t = 0.89 min (100%), MH⁺ = 355.2, 357.2.

7-Bromo-N,N,5-trimethyl-4-oxo-4,5-dihydrothieno[3,2-c]pyridine-2-carboxamide (2.017b)

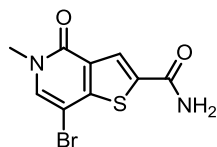
A mixture of **2.008** (150 mg, 0.52 mmol), dimethylamine hydrochloride (55 mg, 0.68 mmol), HATU (238 mg, 0.63 mmol), and DIPEA (0.18 mL, 1.04 mmol) in DMF (4.5 mL) was left to stir at rt for 18 h. The volatile components were removed *in vacuo*. The resulting residue was dissolved in EtOAc (15 mL), washed with aq. citric acid (10% w/v, 3 × 20 mL), sat. aq. NaHCO₃ (3 × 20 mL), H₂O (20 mL) and brine (20 mL). The organic layer was passed through a hydrophobic frit and concentrated *in vacuo* to give **2.017b** (70 mg, 43%) as an off white solid; ¹H NMR (400 MHz, CDCl₃) δ ppm 7.93 (s, 1H), 7.38 (s, 1H), 3.64 (s, 3H), 3.27 (br.s, 6H); LCMS (formic acid), R_t = 0.70 min (100%), MH⁺ = 315.1, 317.1.

7-Bromo-N,5-dimethyl-4-oxo-4,5-dihydrothieno[3,2-c]pyridine-2-carboxamide (2.017c)

A mixture of **2.008** (150 mg, 0.52 mmol), DIPEA (0.18 mL, 1.04 mmol), HATU (238 mg, 0.63 mmol) and methylamine hydrochloride (46 mg, 0.68 mmol) in DMF (3.5 mL) was left to stir at rt for 18 h. The volatile components were removed *in vacuo*. The resulting residue was dissolved in EtOAc (10 mL) and washed with aq. citric acid (10% w/v, 10 mL) causing precipitation of a solid. The solid was filtered under reduced pressure, rinsed with H₂O (15 mL), collected and dried under vacuum at 40 °C to give **2.017c** (66 mg, 42%) as an off white solid; ¹H NMR (400 MHz, DMSO-d₆)

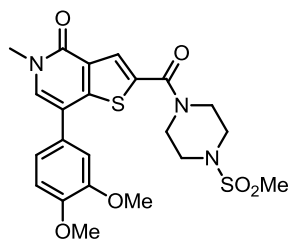
δ ppm 8.81-8.76 (m, 1H), 8.30 (s, 1H), 8.07 (s, 1H), 3.52 (s, 3H), 2.79 (d, $J = 4.7$, 3H); LCMS (formic acid), $R_t = 0.67$ min (82%), $MH^+ = 301.1, 303.1$.

7-Bromo-5-methyl-4-oxo-4,5-dihydrothieno[3,2-c]pyridine-2-carboxamide (2.017d)



A mixture of **2.008** (150 mg, 0.52 mmol), DIPEA (0.2 mL, 1.04 mmol), EDC (120 mg, 0.63 mmol) and 1-hydroxybenzotriazole ammonium salt (119 mg, 0.78 mmol) in DMF (3.0 mL) was left to stir at rt for 35 h. The volatile components were removed *in vacuo* and the resulting solid was suspended in H₂O (10 mL) and filtered under reduced pressure. The solid was washed with aq. citric acid (10% w/v, 10 mL), sat. aq. NaHCO₃ (10 mL) and H₂O (10 mL), collected and dried under vacuum at 40 °C to yield **2.017d** (97 mg, 65%) as an off white solid; ¹H NMR (400 MHz, DMSO-d₆) δ ppm 8.36 (s, 1H), 8.26 (br.s, 1H), 8.07 (s, 1H), 7.67 (br.s, 1H), 3.52 (s, 3H); LCMS (formic acid): $R_t = 0.62$ min (100%), $MH^+ 287.0, 289.0$.

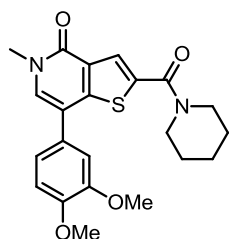
7-(3,4-Dimethoxyphenyl)-5-methyl-2-(4-(methylsulfonyl)piperazine-1-carbonyl)thieno[3,2-c]pyridin-4(5H)-one (2.005)



A mixture of **2.016** (140 mg, 0.32 mmol), (3,4-dimethoxyphenyl)boronic acid (72 mg, 0.40 mmol), K₂CO₃ (135 mg, 0.98 mmol) and Pd(PPh₃)₂Cl₂ (21 mg, 0.03 mmol) in H₂O (1.2 mL) and DME (7 mL) was heated at 120 °C in a microwave reactor for 0.5 h. The mixture was allowed to cool to rt and partitioned between EtOAc (20 mL) and H₂O (20 mL). The organic layer was filtered through Celite[®], passed through a hydrophobic frit and concentrated *in vacuo*. The resulting residue was purified by silica gel chromatography (0–5% MeOH in EtOAc). The resulting residue was purified by MDAP (formic acid). The appropriate fractions were combined and solvent evaporated *in vacuo* to give **2.005** (70 mg, 44%) as a white solid; m.p. 244–245 °C; ν_{max} (thin film)/cm⁻¹: 1650 (C=O), 1517 (aromatic C=C), 1256 (S=O); ¹H NMR (400 MHz, CDCl₃) δ ppm 7.87 (s, 1H), 7.26 (s, 1H), 7.12 (dd, $J = 8.2, 2.1$, 1H), 7.08 (d, $J = 2.1$, 1H), 6.99 (d, $J = 8.2$, 1H), 3.97 (s, 3H), 3.96 (s, 3H), 3.95–3.92 (m, 4H), 3.72 (s, 3H), 3.36–3.33 (m, 4H), 2.85 (s, 3H); ¹³C NMR (101 MHz, CDCl₃) δ ppm 163.1, 158.7, 150.0, 149.4, 149.3, 135.4, 132.4, 129.6, 128.2, 126.7, 120.0, 117.0, 111.7, 110.7, 56.1, 56.0, 45.9, 37.1, 34.9; N.B. one carbon missing from spectrum; HRMS (M + H)⁺ calculated for C₂₂H₂₆N₃O₆S₂, 492.1238; found 492.1258; LCMS

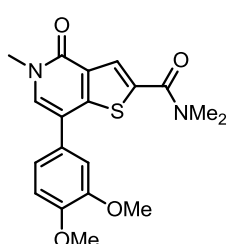
(formic acid), $R_t = 0.79$ min (99%), $MH^+ = 492.3$.

7-(3,4-Dimethoxyphenyl)-5-methyl-2-(piperidine-1-carbonyl)thieno[3,2-c]pyridin-4(5H)-one (2.018a)



A mixture of **2.017a** (230 mg, 0.65 mmol), 3,4-dimethoxyphenylboronic acid (147 mg, 0.81 mmol), K_2CO_3 (268 mg, 1.94 mmol) and $Pd(PPh_3)_2Cl_2$ (45 mg, 0.07 mmol) in H_2O (1.25 mL) and DME (7.5 mL) was heated at 120 °C in a microwave reactor for 0.5 h. The reaction mixture was allowed to cool to rt and diluted with EtOAc (20 mL). The solution was filtered through Celite[®], passed through a hydrophobic frit and concentrated *in vacuo*. The resulting residue was purified by silica gel chromatography (0-5% MeOH in DCM). The appropriate fractions were combined and solvent evaporated *in vacuo*. The resulting residue was purified by MDAP (formic acid). The appropriate fractions were combined and the solvent was evaporated *in vacuo* to give **2.018a** (121 mg, 45%) as an off white solid; m.p. 169–171 °C; ν_{max} (thin film)/ cm^{-1} : 2937, 1646 (C=O), 1594 (C=O), 1252, 726; 1H NMR (400 MHz, $CDCl_3$) δ ppm 7.82 (s, 1H), 7.22 (s, 1H), 7.14–7.08 (m, 2H), 6.97 (d, $J = 7.8$, 1H), 3.95 (s, 6H), 3.75–3.71 (m, 4H), 3.70 (s, 3H), 1.76–1.61 (m, 6H); ^{13}C NMR (101 MHz, $CDCl_3$) δ ppm 173.1, 158.8, 149.4, 149.2, 148.9, 137.1, 131.8, 129.6, 128.5, 125.7, 124.2, 120.0, 117.0, 111.7, 110.8, 56.1, 56.0, 37.0, 26.2, 24.5; HRMS ($M + H$)⁺ calculated for $C_{22}H_{25}N_2O_4S$, 413.1530; found 413.1534; LCMS (formic acid), $R_t = 0.93$ min (100%), $MH^+ = 413.3$.

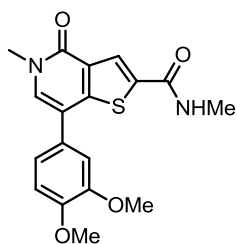
7-(3,4-Dimethoxyphenyl)-N,N,5-trimethyl-4-oxo-4,5-dihydrothieno[3,2-c]pyridine-2-carboxamide (2.018b)



A mixture of **2.017b** (70 mg, 0.22 mmol), (3,4-dimethoxyphenyl)boronic acid (49 mg, 0.27 mmol), K_2CO_3 (92 mg, 0.67 mmol) and $Pd(PPh_3)_2Cl_2$ (14 mg, 0.02 mmol) in H_2O (0.4 mL) and DME (1.7 mL) was heated at 120 °C in a microwave reactor for 0.5 h. The mixture was allowed to cool to rt and diluted with EtOAc (20 mL). The solution was filtered through Celite[®], passed through a hydrophobic frit and concentrated *in vacuo*. The resulting residue was purified by MDAP (formic acid). The appropriate fractions were combined and solvent evaporated *in vacuo* to give **2.018b** (47 mg, 57%) as a white solid; m.p. 127–128 °C; ν_{max} (thin film)/ cm^{-1} : 1635 (C=O), 1607 (C=O), 1515, 1256, 734; 1H NMR (400 MHz, $CDCl_3$) δ ppm 7.93 (s, 1H), 7.23 (s, 1H), 7.13 (dd, $J = 8.2, 2.2$,

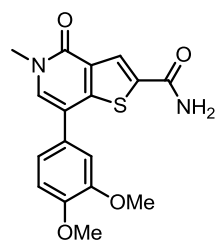
1H), 7.10 (d, $J = 2.2$, 1H), 6.98 (d, $J = 8.2$, 1H), 3.96 (s, 3H), 3.95 (s, 3H), 3.71 (s, 3H), 3.26 (br.s, 6H); ^{13}C NMR (101 MHz, CDCl_3) δ ppm 163.5, 158.8, 149.6, 149.4, 149.2, 137.6, 132.0, 129.9, 128.4, 126.6, 120.1, 117.0, 111.7, 110.8, 56.1, 56.0, 37.0; HRMS ($\text{M} + \text{H}$) $^+$ calculated for $\text{C}_{19}\text{H}_{21}\text{N}_2\text{O}_4\text{S}$, 373.1217; found 373.1226; LCMS (formic acid), $R_t = 0.78$ min (100%), $\text{MH}^+ = 373.2$.

7-(3,4-Dimethoxyphenyl)-N,5-dimethyl-4-oxo-4,5-dihydrothieno[3,2-c]pyridine-2-carboxamide (2.018c)



A mixture of **2.017c** (66 mg, 0.22 mmol), (3,4-dimethoxyphenyl)boronic acid (44 mg, 0.24 mmol), K_2CO_3 (91 mg, 0.66 mmol) and $\text{Pd}(\text{PPh}_3)_2\text{Cl}_2$ (14 mg, 0.02 mmol) in H_2O (0.25 mL) and DME (1.5 mL) was heated at 120 °C in a microwave reactor for 0.5 h. The reaction mixture was allowed to cool to rt and diluted with EtOAc (15 mL). The solution was filtered through Celite[®], passed through a hydrophobic frit and concentrated *in vacuo*. The resulting residue was purified by MDAP (formic acid). The appropriate fractions were combined and the solvent evaporated *in vacuo* to give **2.018c** (19 mg, 24%) as a white solid; ^1H NMR (400 MHz, CDCl_3) δ ppm 8.12 (s, 1H), 7.24 (s, 1H), 7.14–7.11 (m, 1H), 7.10–7.08 (m, 1H), 6.98 (d, $J = 8.1$, 1H), 6.57–6.50 (m, 1H), 3.96 (s, 6H), 3.71 (s, 3H), 3.06 (d, $J = 4.6$, 3H); LCMS (formic acid), $R_t = 0.74$ min (98%), $\text{MH}^+ = 359.2$.

7-(3,4-Dimethoxyphenyl)-5-methyl-4-oxo-4,5-dihydrothieno[3,2-c]pyridine-2-carboxamide (2.018d)



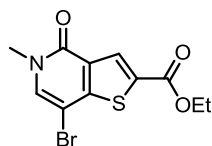
Method A:

A mixture of **2.017d** (90 mg, 0.31 mmol), (3,4-dimethoxyphenyl)boronic acid (68 mg, 0.37 mmol), K_2CO_3 (130 mg, 0.94 mmol) and $\text{Pd}(\text{PPh}_3)_2\text{Cl}_2$ (20 mg, 0.03 mmol) in DME (1.5 mL) and H_2O (0.25 mL) was heated to 120 °C for 0.5 h in a microwave reactor. The solution was allowed to cool to rt and diluted with EtOAc (15 mL). The solution was filtered through Celite[®], passed through a hydrophobic frit and concentrated *in vacuo*. The resulting residue was purified by MDAP (formic acid). The appropriate fractions were combined and the solvent evaporated *in vacuo* to give **2.018d** (5 mg, 5%) as a white solid.

Method B:

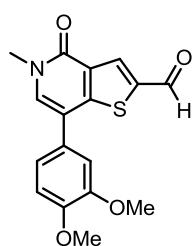
A solution of **2.021** (300 mg, 0.87 mmol), 1-hydroxybenzotriazole ammonium salt (199 mg, 1.30 mmol), EDC (200 mg, 1.04 mmol) and DIPEA (0.30 mL, 1.73 mmol) in DMF (4 mL) was left to stir at rt for 20 h. The reaction mixture was heated at 40 °C for 6 h and then 50 °C for 18 h. The volatile components were removed *in vacuo*. The resulting solid was suspended in EtOAc (30 mL), filtered under reduced pressure, rinsed with water H₂O (40 mL), collected and dried under vacuum at 40 °C to give **2.018d** (268 mg, 90%) as an off white solid; ¹H NMR (400 MHz, DMSO-d₆) δ ppm 8.31 (s, 1H), 8.23 (br.s, 1H), 7.81 (s, 1H), 7.58 (br.s, 1H), 7.21–7.17 (m, 2H), 7.09 (d, *J* = 8.8, 1H), 3.83 (s, 3H), 3.82 (s, 3H), 3.59 (s, 3H); LCMS (formic acid): R_t = 0.70 min (100%), MH⁺ = 345.2.

Ethyl 7-bromo-5-methyl-4-oxo-4,5-dihydrothieno[3,2-c]pyridine-2-carboxylate (2.019)



Iodoethane (0.03 mL, 0.35 mmol) was added to a solution of **2.008** (20 mg, 0.07 mmol) and NaHCO₃ (11 mg, 0.13 mmol) in DMF (0.4 mL) and the reaction mixture was left to stir at rt for 18 h. The mixture was concentrated *in vacuo* and the resulting residue was dissolved in EtOAc (15 mL) and washed with H₂O (2 × 20 mL) and brine (20 mL). The organic layer was passed through a hydrophobic frit and concentrated *in vacuo* to give **2.019** (77 mg, 77%) as a brown solid; ¹H NMR (400 MHz, CDCl₃) δ ppm 8.39 (s, 1H), 7.41 (s, 1H), 4.41 (q, *J* = 7.2, 2H), 3.63 (s, 3H), 1.42 (t, *J* = 7.2, 3H); LCMS (formic acid): R_t = 0.99 min (88%), MH⁺ = 316.1, 318.1.

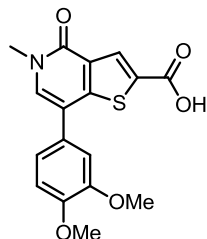
7-(3,4-Dimethoxyphenyl)-5-methyl-4-oxo-4,5-dihydrothieno[3,2-c]pyridine-2-carbaldehyde (2.022)



A mixture of **2.009** (1.00 g, 3.67 mmol), (3,4-dimethoxyphenyl)boronic acid (0.77 g, 4.23 mmol), K₂CO₃ (1.37 g, 9.92 mmol) and Pd(PPh₃)₂Cl₂ (0.23 g, 0.33 mmol) in DME (12 mL) and H₂O (2 mL) was heated at 120 °C in a microwave reactor for 0.5 h. The mixture was allowed to cool to rt, diluted with EtOAc (25 mL) and H₂O (5 mL) and filtered through Celite[®]. The filtrate was concentrated *in vacuo*. The resulting solid was suspended in EtOAc (50 mL), filtered under reduced pressure, rinsed with EtOAc (50 mL), collected and dissolved in DMSO (10 mL). The resulting solution was blown down under a stream of nitrogen at 40 °C to give **2.022** (750 mg, 62%) as a yellow solid; ¹H NMR (400 MHz, DMSO-d₆) δ ppm 10.04 (s,

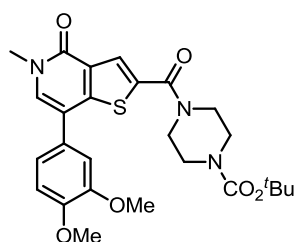
1H), 8.51 (s, 1H), 7.96 (s, 1H), 7.21–7.17 (m, 2H), 7.11 (d, $J = 8.8$, 1H), 3.83 (s, 3H), 3.82 (s, 3H), 3.62 (s, 3H); LCMS (formic acid), $R_t = 0.83$ min (95%), $MH^+ = 320.2$.

7-(3,4-Dimethoxyphenyl)-5-methyl-4-oxo-4,5-dihydrothieno[3,2-c]pyridine-2-carboxylic acid (2.021)



To a solution of **2.022** (750 mg, 2.27 mmol) in H_2O (10 mL) and DMSO (10 mL), sodium chlorite (1.44 g, 15.94 mmol), sodium dihydrogen phosphate (1.91 g, 15.94 mmol) and hydrogen peroxide (35% weight in H_2O , 0.49 mL, 15.94 mmol) were added. The mixture was left to stir at rt for 48 h. The mixture was acidified to pH 1 with glacial AcOH (15 mL) and concentrated *in vacuo* (DMSO remained). Addition of H_2O (20 mL) caused precipitation of a solid, which was filtered under reduced pressure, rinsed with H_2O (10 mL), collected and dried under vacuum at 40 °C to give **2.021** (562 mg, 72%) as a light orange solid; m.p. 241–243 °C (decomp.); ν_{max} (solid)/ cm^{-1} : 3002 (O-H), 1704 (C=O), 1635 (C=O), 1251, 744; 1H NMR (400 MHz, DMSO- d_6) δ ppm 13.42 (br.s, 1H), 8.02 (s, 1H), 7.87 (s, 1H), 7.22–7.16 (m, 2H), 7.10 (d, $J = 8.8$, 1H), 3.83 (s, 3H), 3.82 (s, 3H), 3.59 (s, 3H); ^{13}C NMR (101 MHz, DMSO- d_6) δ ppm 162.7, 157.6, 150.4, 149.1, 148.7, 134.9, 133.0, 130.0, 129.1, 127.9, 119.4, 114.9, 112.2, 111.2, 55.7, 55.6, 36.3; HRMS ($M + H$) $^+$ calculated for $C_{17}H_{16}NO_5S$, 346.0744; found 346.0753; LCMS (formic acid), $R_t = 0.75$ min (100%), $MH^+ = 346.2$.

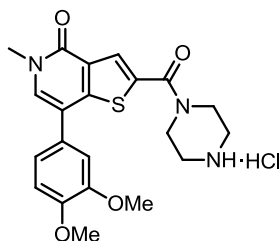
tert-Butyl 4-(7-(3,4-dimethoxyphenyl)-5-methyl-4-oxo-4,5-dihydrothieno[3,2-c]pyridine-2-carbonyl)piperazine-1-carboxylate (2.023)



A solution of **2.021** (70 mg, 0.20 mmol), *tert*-butyl piperazine-1-carboxylate (45 mg, 0.24 mmol), HATU (100 mg, 0.26 mmol) and DIPEA (0.07 mL, 0.41 mmol) in DMF (3 mL) was stirred at rt for 18 h. The volatile components were removed *in vacuo* and the resulting residue was dissolved in EtOAc (40 mL), washed with aq. citric acid (10% w/v, 3 × 30 mL), sat. aq. $NaHCO_3$ (3 × 30 mL), H_2O (30 mL) and brine (30 mL). The organic layer was passed through a hydrophobic frit and concentrated *in vacuo*. This residue was dissolved in DCM (1 mL) and a solid precipitated upon addition of cyclohexane (5 mL). The solid was filtered under reduced pressure, collected and dried under vacuum at 40 °C to give **2.023** (76 mg, 73%) as a white solid; 1H NMR (400 MHz, $CDCl_3$) δ ppm 7.85 (s, 1H), 7.24 (s, 1H),

7.12 (dd, $J = 8.2, 2.0$, 1H), 7.09 (d, $J = 2.0$, 1H), 6.98 (d, $J = 8.2$, 1H), 3.96 (s, 6H), 3.81–3.77 (m, 4H), 3.71 (s, 3H), 3.56–3.52 (m, 4H), 1.51 (s, 9H); LCMS (formic acid): $R_t = 1.01$ min (100%), MH^+ 514.3.

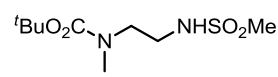
7-(3,4-Dimethoxyphenyl)-5-methyl-2-(piperidine-4-carbonyl)thieno[3,2-c]pyridin-4(5H)-one hydrochloride (2.025)



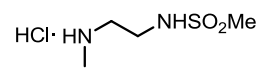
2.023 (30 mg, 0.06 mmol) was dissolved in 4 M HCl in 1,4-dioxane (3 mL) and left to stir at rt for 48 h. The volatile components were removed *in vacuo* and the resulting residue was dissolved in DCM (1.5 mL). Addition of Et₂O (5 mL) caused precipitation of a solid, which was filtered under reduced pressure, rinsed with Et₂O (20 mL) and

collected to give **2.025** (20 mg, 76%) as an off white solid; ¹H NMR (400 MHz, CDCl₃) δ ppm 10.07 (br.s, 2H), 7.89 (s, 1H), 7.25 (s, 1H), 7.12–7.07 (m, 1H), 7.07–7.04 (m, 1H), 6.97 (d, $J = 8.3$, 1H), 4.26–4.15 (m, 4H), 3.95 (s, 3H), 3.94 (s, 3H), 3.69 (s, 3H), 3.47–3.32 (m, 4H); LCMS (formic acid): $R_t = 0.60$ min (100%), MH^+ 414.2.

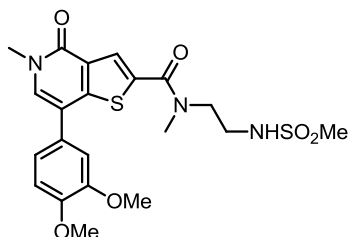
tert-Butyl methyl(2-(methylsulfonamido)ethyl)carbamate (2.027)

 To a solution of **2.026** (0.2 mL, 1.15 mmol) and triethylamine (0.32 mL, 2.30 mmol) in DCM (4.5 mL), methanesulfonyl chloride (0.1 mL, 1.26 mmol) was added at 0 °C. The mixture was allowed to warm to rt and left to stir for 22 h. The reaction mixture was diluted with DCM (20 mL) and washed with 0.5 M aq. HCl (2 × 25 mL), sat. aq. NaHCO₃ (2 × 25 mL) and brine (30 mL). The organic layer was passed through a hydrophobic frit and concentrated *in vacuo* to give **2.027** (239 mg, 83%) as a colourless oil; ¹H NMR (400 MHz, CDCl₃) δ ppm 5.06 (br.s, 1H), 3.44 (t, $J = 5.7$, 2H), 3.32 (t, $J = 5.7$, 2H), 2.93 (s, 3H), 2.92 (s, 3H), 1.49 (s, 9H).

N-(2-(Methylamino)ethyl)methanesulfonamide hydrochloride (2.028)

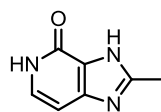
 **2.027** (239 mg, 0.95 mmol) was dissolved in 4 M HCl in 1,4-dioxane (3 mL) and the reaction mixture was left to stir at rt for 18 h. The volatile components were removed *in vacuo* to give **2.028** (178 mg, quant.) as a white solid; ¹H NMR (400 MHz, CDCl₃) δ ppm 3.42 (t, $J = 5.6$, 2H), 3.32 (t, $J = 5.6$, 2H), 3.02 (s, 3H), 2.75 (s, 3H).

7-(3,4-Dimethoxyphenyl)-N,5-dimethyl-N-(2-(methylsulfonamido)ethyl)-4-oxo-4,5-dihydrothieno[3,2-c]pyridine-2-carboxamide (2.024)



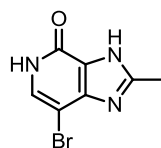
A mixture of **2.021** (100 mg, 0.29 mmol), **2.028** (53 mg, 0.35 mmol), HATU (143 mg, 0.38 mmol) and DIPEA (0.1 mL, 0.58 mmol) in DMF (3 mL) was left to stir at rt for 18 h. The volatile components were removed *in vacuo* and the resulting residue was dissolved in EtOAc (50 mL) and washed with aq. citric acid (10% w/v, 3 × 30 mL), sat. aq. NaHCO₃ (3 × 30 mL), H₂O (30 mL) and brine (30 mL). The organic layer was passed through a hydrophobic frit and concentrated *in vacuo*. The resulting residue was purified by MDAP (formic acid). The appropriate fractions were combined and the solvent evaporated *in vacuo* to give **2.024** (38 mg, 27%) as a pale yellow oil; ¹H NMR (400 MHz, CDCl₃) δ ppm 7.92 (s, 1H), 7.20 (s, 1H), 7.07–7.04 (m, 1H), 7.03 (d, *J* = 1.7, 1H), 6.93 (d, *J* = 8.3, 1H), 5.92 (br.s, 1H), 3.93 (s, 3H), 3.91 (s, 3H), 3.80–3.74 (m, 2H), 3.65 (s, 3H), 3.51–3.43 (m, 3H), 3.43–3.34 (m, 2H), 2.97 (s, 3H); LCMS (formic acid): R_t = 0.74 min (100%), MH⁺ 480.2.

2-Methyl-3H-imidazo[4,5-c]pyridin-4(5H)-one (2.039)



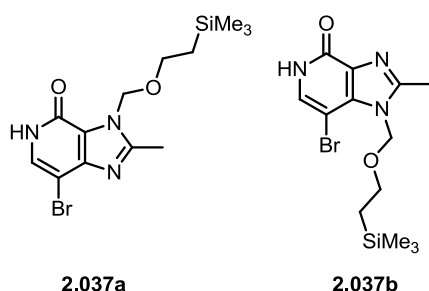
A suspension of **2.040** (2.00 g, 13.90 mmol) in AcOH (16 mL, 279.00 mmol) was heated at 160 °C in a microwave reactor for 3 h. Addition of MeCN (10 mL) caused precipitation of a solid, which was filtered under reduced pressure, rinsed with MeCN (50 mL), collected and dried under vacuum at 40 °C to give **2.039** (2.20 g, quant.) as an off white solid; ¹H NMR (400 MHz, CD₃OD) δ ppm 7.49 (d, *J* = 7.1, 1H), 6.74 (d, *J* = 7.1, 1H), 2.80 (s, 3H); LCMS (formic acid) R_t = 0.19 min (100%), MH⁺ 149.9.

7-Bromo-2-methyl-3H-imidazo[4,5-c]pyridin-4(5H)-one (2.038)



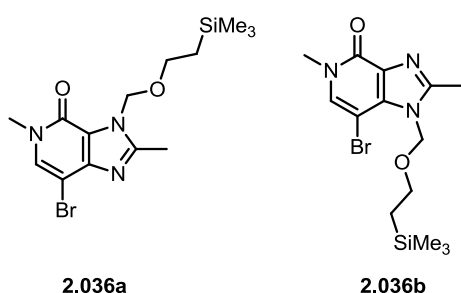
A suspension of **2.039** (1.50 g, 10.00 mmol) and NBS (2.70 g, 15.09 mmol) in DMF (60 mL) was heated at 65 °C for 6 h. The volatile components were removed *in vacuo* and the resulting solid was suspended in Et₂O (30 mL). The suspension was filtered under reduced pressure, rinsed with Et₂O (50 mL), collected and dried under vacuum at 40 °C. The resulting solid was purified by silica gel chromatography (0–10% 2 M NH₃ in MeOH in DCM). The appropriate fractions were combined and the solvent evaporated *in vacuo* to give **2.038** (733 mg, 32%) as a grey solid; ¹H NMR (400 MHz, CDCl₃) δ ppm 7.72 (s, 1H), 2.84 (s, 3H); LCMS (formic acid) R_t = 0.36 min (100%), MH⁺ 228.0, 230.0.

7-Bromo-2-methyl-3-((2-(trimethylsilyl)ethoxy)methyl)-3H-imidazo[4,5-c]pyridin-4(5H)-one (2.037a) and 7-bromo-2-methyl-1-((2-(trimethylsilyl)ethoxy)methyl)-1H-imidazo[4,5-c]pyridin-4(5H)-one (2.037b)



To a solution of **2.038** (733 mg, 3.21 mmol), in DMF (25 mL), SEMCl (0.9 mL, 4.82 mmol) was added drop-wise and the reaction mixture was left to stir at rt for 18 h. The solution was diluted with EtOAc (50 mL) and the organic layer was washed with sat. aq. NaHCO₃ (50 mL), passed through a hydrophobic frit and concentrated *in vacuo*. The resulting residue was purified by silica gel chromatography (0–10% 2 M NH₃ in MeOH in DCM). The appropriate fractions were combined and solvent evaporated *in vacuo* to give **2.037a** (major) and **2.037b** (minor) (768 mg, 67%) as a yellow oil and a 5:1 mixture of regioisomers; Major isomer: ¹H NMR (400 MHz, CDCl₃) δ ppm 7.34 (s, 1H), 5.92 (s, 2H), 3.69–3.60 (m, 2H), 2.68 (s, 3H), 0.94–0.88 (m, 2H), –0.03 (s, 9H), LCMS (formic acid) R_t = 0.97 min (88%), MH⁺ 358.1, 360.1; Minor isomer: ¹H NMR (400 MHz, CDCl₃) δ ppm 7.24 (s, 1H), 5.89 (s, 2H), 3.69–3.60 (m, 2H), 2.67 (s, 3H), 0.94–0.88 (m, 2H), –0.05 (s, 9H); LCMS (formic acid) R_t = 0.96 min (11%), MH⁺ 358.1, 360.1.

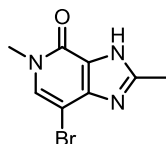
7-Bromo-2,5-dimethyl-3-((2-(trimethylsilyl)ethoxy)methyl)-3H-imidazo[4,5-c]pyridin-4(5H)-one (2.036a) and 7-Bromo-2,5-dimethyl-1-((2-(trimethylsilyl)ethoxy)methyl)-1H-imidazo[4,5-c]pyridin-4(5H)-one (2.036b)



To a solution of **2.037a** and **2.037b** (768 mg, 2.14 mmol) in DMF (16.5 mL), NaH (60% weight in mineral oil, 103 mg, 2.57 mmol) and MeI (0.2 mL, 2.36 mmol) were added at 0 °C. The reaction mixture was allowed to warm to rt and left to stir for 6 h. MeI (0.1 mL, 1.1 mmol) was added and the reaction mixture was left to stir for a further 18 h. The solution was diluted with EtOAc (50 mL), washed with sat. aq. NH₄Cl (60 mL) and brine (60 mL), passed through a hydrophobic frit and concentrated *in vacuo* to give **2.036a** (major) and **2.036b** (minor) (784 mg, 98%) as a yellow solid and 5:1 ratio of regioisomers; Major isomer: ¹H NMR (400 MHz, CDCl₃) δ ppm 7.32 (s, 1H), 5.96–5.94 (m, 2H), 3.68–3.62 (m, 5H), 2.68–2.67 (m, 3H), 0.94–0.89 (m, 2H), –0.01 (s, 9H); LCMS (formic acid) R_t = 1.10 min (79%), MH⁺ 372.0, 374.0; Minor isomer:

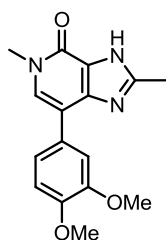
^1H NMR (400 MHz, CDCl_3) δ ppm 7.22 (s, 1H), 5.96–5.94 (m, 2H), 3.68–3.62 (m, 5H), 2.68–2.67 (m, 3H), 0.94–0.89 (m, 2H), -0.01 (s, 9H); LCMS (formic acid) $R_t = 1.09$ min (14%), MH^+ 372.0, 374.0.

7-Bromo-2,5-dimethyl-3H-imidazo[4,5-c]pyridin-4(5H)-one (2.035)

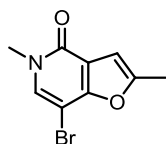


To a solution of **2.036a** and **2.036b** (794 mg, 2.13 mmol) in DCM (30 mL), TFA (3.3 mL, 42.7 mmol) was added. The reaction mixture was left to stir at rt for 24 h. The volatile components were removed *in vacuo* and the resulting residue was suspended in Et_2O (50 mL), filtered under reduced pressure, rinsed with Et_2O (50 mL), collected and dried under vacuum at 40 °C to give **2.035** (422 mg, 82%) as a white solid; m.p. 274–276 °C; ν_{max} (solid)/ cm^{-1} : 3016 (N-H), 1647 (C=O), 1546, 1143, 699; ^1H NMR (400 MHz, CD_3OD) δ ppm 7.81 (s, 1H), 3.66 (s, 3H), 2.67 (s, 3H); ^{13}C NMR (101 MHz, CD_3OD) δ ppm 155.8, 153.9, 142.7, 135.9, 124.4, 89.5, 37.3, 13.5; HRMS ($\text{M} + \text{H}$) $^+$ calculated for $\text{C}_8\text{H}_9\text{BrN}_3\text{O}$, 241.9924; found 241.9926; LCMS (formic acid) $R_t = 0.42$ min (90%), MH^+ 242.0, 244.0.

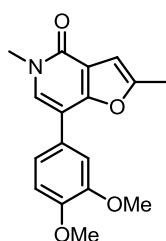
7-(3,4-Dimethoxyphenyl)-2,5-dimethyl-3H-imidazo[4,5-c]pyridin-4(5H)-one (2.032)



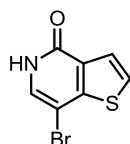
A mixture of **2.035** (50 mg, 0.21 mmol), (3,4-dimethoxyphenyl)boronic acid (45 mg, 0.25 mmol), PEPPSI-*i*Pr (13 mg, 0.02 mmol) and K_2CO_3 (63 mg, 0.46 mmol) in IPA (3 mL) and H_2O (1 mL) was heated at 120 °C in a microwave reactor for 0.5 h. The solution was allowed to cool to rt and diluted with EtOAc (50 mL). The solution was filtered through Celite[®], passed through a hydrophobic frit and concentrated *in vacuo*. The resulting residue was purified by MDAP (high pH). The appropriate fractions were combined and concentrated *in vacuo* to give **2.032** (20 mg, 32%) as a white solid; m.p. 249–250 °C; ν_{max} (thin film)/ cm^{-1} : 1652 (C=O), 1509, 1233, 1136, 1027, 813; ^1H NMR (400 MHz, CD_3OD) δ ppm 7.48 (s, 1H), 7.30–7.27 (m, 1H), 7.23 (dd, $J = 8.2, 2.0$, 1H), 7.07 (d, $J = 8.2$, 1H), 3.93 (s, 3H), 3.90 (s, 3H), 3.72 (s, 3H), 2.57 (s, 3H); ^{13}C NMR (101 MHz, CD_3OD) δ ppm 156.0, 153.8, 150.7, 150.4, 131.8, 128.9, 121.9, 113.4, 113.4, 56.6, 56.6, 37.0, 14.1, N.B. 3 carbon signals not visible in spectrum; HRMS ($\text{M} + \text{H}$) $^+$ calculated for $\text{C}_{16}\text{H}_{18}\text{N}_3\text{O}_3$, 300.1343; found 300.1342; LCMS (formic acid) $R_t = 0.57$ min (100%), MH^+ 300.2.

7-Bromo-2,5-dimethylfuro[3,2-c]pyridin-4(5H)-one (2.042)

Triethylsilane (0.4 mL, 2.34 mmol) was added in a single portion to solution of **2.041** (150 mg, 0.59 mmol) in TFA (5 mL, 0.59 mmol). The reaction mixture was heated at 40 °C and left to stir for 18 h. The volatile components were removed *in vacuo* and the resulting residue was purified by silica gel chromatography (0–100% EtOAc in cyclohexane). The appropriate fractions were combined and solvent evaporated *in vacuo* to give **2.042** (140 mg, 99%) as an off white solid; ¹H NMR (400 MHz, CD₃OD) δ ppm 7.32 (s, 1H), 6.67 (s, 1H), 3.63 (s, 3H), 2.48 (s, 3H); LCMS (formic acid) R_t = 0.77 min (84%), MH⁺ 242.0, 244.0.

7-(3,4-Dimethoxyphenyl)-2,5-dimethylfuro[3,2-c]pyridin-4(5H)-one (2.034)

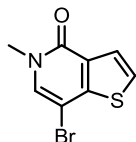
A mixture of **2.042** (140 mg, 0.59 mmol), (3,4-dimethoxyphenyl)boronic acid (126 mg, 0.69 mmol), PEPPSI-Pr (35 mg, 0.05 mmol) and K₂CO₃ (192 mg, 1.39 mmol) in IPA (1.5 mL) and H₂O (0.5 mL) was heated at 120 °C in a microwave reactor for 0.5 h. The reaction mixture was allowed to stand at rt for 48 h and then diluted with EtOAc (30 mL). The solution was filtered through Celite[®], passed through a hydrophobic frit and concentrated *in vacuo*. The resulting residue was purified by MDAP (formic acid). The appropriate fractions were combined and concentrated *in vacuo* to give **2.034** (62 mg, 36%) as a white solid; m.p. 84–85 °C; ν_{max} (solid)/cm⁻¹ 1513 (C=O), 1254, 1233, 808, 762; ¹H NMR (400 MHz, DMSO-d₆) 7.84 (s, 1H), 7.30 (dd, *J* = 8.3, 2.0, 1H), 7.27 (d, *J* = 2.0, 1H), 7.06 (d, *J* = 8.3, 1H), 6.63 (d, *J* = 1.1, 1H), 3.83 (s, 3H), 3.80 (s, 3H), 3.57 (s, 3H), 2.43 (d, *J* = 1.1, 3H); ¹³C NMR (101 MHz, DMSO-d₆) 157.6, 156.0, 153.8, 148.9, 148.3, 132.4, 125.2, 119.6, 116.0, 112.1, 110.9, 108.7, 102.9, 55.64, 55.57, 36.1, 13.4; HRMS (M + H)⁺ calculated for C₁₇H₁₈NO₄ 300.1235; found 300.1230; LCMS (formic acid) R_t = 0.89 min (100%), MH⁺ 300.2.

7-Bromothieno[3,2-c]pyridin-4(5H)-one (2.051)

To a solution of **2.050** in DMF (8.5 mL), NBS (224 mg, 1.26 mmol.) was added in a single portion. The reaction mixture was left to stir at rt for 20 h. The volatile components were removed *in vacuo* and the resulting residue was partitioned between DCM (30 mL) and H₂O (30 mL). The organic phase was separated and the aqueous extracted with DCM (3 × 30 mL). The combined organic layers were passed through a hydrophobic frit and

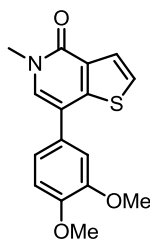
concentrated *in vacuo* to give **2.051** (257 mg, 84%) as a brown solid; $^1\text{H NMR}$ (400 MHz, CDCl_3) δ ppm 8.58 (br.s, 1H), 8.04 (s, 1H), 7.78 (d, $J = 5.4$, 1H), 7.45 (d, $J = 5.4$, 1H); LCMS (formic acid): $R_t = 0.71$ min (62%), MH^+ 130.2, 132.2.

7-Bromo-5-methylthieno[3,2-c]pyridin-4(5H)-one (2.052)



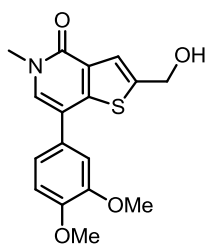
To a solution of **2.051** (257 mg, 1.12 mmol) and Cs_2CO_3 (1.1 g, 3.35 mmol) in THF (7 mL), MeI (0.14 mL, 2.23 mmol) was added. The reaction mixture was left to stir at rt for 20 h. The volatile components were removed *in vacuo* followed by the addition of H_2O (40 mL). The suspension was left to stir for 10 minutes before being filtered under reduced pressure, collected and dried under vacuum at 40 °C to give **2.052** (56 mg, 59%) as a brown solid; $^1\text{H NMR}$ (400 MHz, CDCl_3) δ ppm 7.77 (d, $J = 5.3$, 1H), 7.39 (d, $J = 5.3$, 1H), 7.33 (s, 1H), 3.64 (s, 3H); LCMS (formic acid): $R_t = 0.79$ min (88%), MH^+ 244.1, 246.1.

7-(3,4-Dimethoxyphenyl)-5-methylthieno[3,2-c]pyridin-4(5H)-one (2.043)



A mixture of **2.052** (160 mg, 0.65 mmol), (3,4-dimethoxyphenyl)boronic acid (143 mg, 0.79 mmol), K_2CO_3 (217 mg, 1.57 mmol) and PEPPSI-*i*Pr (40 mg, 0.06 mmol) in IPA (2.1 mL) and H_2O (0.7 mL) was heated to 120 °C in a microwave reactor for 0.5 h. The mixture was allowed to cool to rt and diluted with EtOAc (100 mL). The solution was filtered through Celite[®], passed through a hydrophobic frit and concentrated *in vacuo*. The resulting residue was purified by silica gel chromatography (0–5% MeOH in DCM). The appropriate fractions were combined and concentrated *in vacuo*. The resulting residue was purified by MDAP (formic acid). The appropriate fractions were combined and the solvent evaporated *in vacuo* to give **2.043** (64 mg, 32%) as a pale yellow solid; m.p. 177–178 °C; ν_{max} (solid)/ cm^{-1} : 1652 (C=O), 1511, 1256, 1027, 714; $^1\text{H NMR}$ (400 MHz, DMSO-d_6) δ ppm 7.70 (s, 1H), 7.64 (d, $J = 5.4$, 1H), 7.58 (d, $J = 5.4$, 1H), 7.20–7.18 (m, 1H), 7.16 (d, $J = 2.2$, 1H), 7.08 (d, $J = 8.1$, 1H), 3.83 (s, 3H), 3.81 (s, 3H), 3.59 (s, 3H); $^{13}\text{C NMR}$ (101 MHz, DMSO-d_6) 157.7, 149.0, 148.5, 147.0, 132.0, 129.5, 128.6, 125.6, 124.9, 119.4, 115.1, 112.2, 111.2, 55.6, 36.1; HRMS ($\text{M} + \text{H}$)⁺ calculated for $\text{C}_{16}\text{H}_{16}\text{NO}_3\text{S}$, 302.0851; found 302.0845; LCMS (formic acid): $R_t = 0.85$ min (100%), MH^+ 302.2.

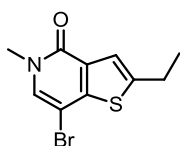
7-(3,4-Dimethoxyphenyl)-2-(hydroxymethyl)-5-methylthieno[3,2-c]pyridin-4(5H)-one (2.047)



To a solution of **2.022** (200 mg, 0.61 mmol) in EtOH (2 mL), NaBH₄ (115 mg, 3.04 mmol) was added and the reaction mixture was left to stir at rt for 18 h. The solution was quenched with 2 M aq. HCl (3 mL) and left to stir for 3 h and then concentrated *in vacuo*. The resulting residue was purified by MDAP (formic acid).

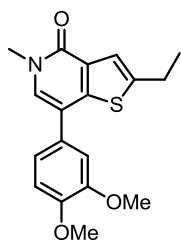
The appropriate fractions were combined and solvent evaporated *in vacuo* to give **2.047** (10 mg, 5%) as a white solid; ¹H NMR (400 MHz, CD₃OD) δ ppm 7.54 (s, 1H), 7.53–7.52 (m, 1H), 7.22–7.19 (m, 2H), 7.09 (d, *J* = 8.3, 1H), 4.83–4.82 (m, 2H), 3.91 (s, 3H), 3.91 (s, 3H), 3.71 (s, 3H); LCMS (formic acid): *R*_t = 0.72 min (100%), MH⁺ 332.1.

7-Bromo-2-ethyl-5-methylthieno[3,2-c]pyridin-4(5H)-one (2.054)

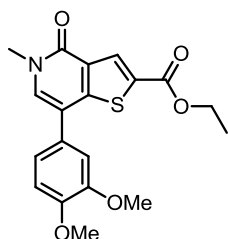


To a solution of **2.009** (250 mg, 0.92 mmol) in THF (3 mL), 1 M MeMgBr in Bt₂O (1.4 mL, 1.40 mmol) was added at –78 °C. The reaction mixture was allowed to warm to rt and left to stir for 18 h.

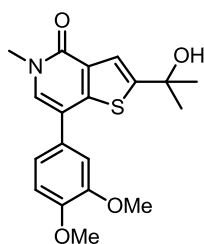
The solution was diluted with H₂O (30 mL) and extracted into EtOAc (3 × 30 mL). The combined organic layers were washed with sat. aq. NH₄Cl (60 mL), passed through a hydrophobic frit and concentrated *in vacuo*. The resulting solid was purified by silica gel chromatography (0–4% MeOH in DCM). The appropriate fractions were combined and the solvent evaporated *in vacuo* to give **2.053** (71 mg, 27%), which was used in the next step without further purification. To a solution of **2.053** in TFA (2 mL), triethylsilane (0.16 mL, 0.97 mmol) was added and the reaction mixture was heated at 40 °C for 18 h. Triethylsilane (0.08 mL, 0.49 mmol) was added and the reaction mixture was stirred for a further 20 h at 40 °C. The solution was allowed to cool to rt and diluted with H₂O (30 mL). The aqueous phase was extracted with EtOAc (3 × 30 mL) and the combined organic layers were washed with sat. aq. NaHCO₃ (3 × 50 mL), passed through a hydrophobic frit and concentrated *in vacuo*. The resulting residue was purified by silica gel chromatography (0–4% MeOH in DCM). The appropriate fractions were combined and solvent evaporated *in vacuo* to give **2.054** (45 mg, 18% over two steps) as a pale yellow solid; ¹H NMR (400 MHz, CDCl₃) δ ppm 7.45–7.43 (m, 1H), 7.29–7.26 (m, 1H), 3.61 (s, 3H), 2.92 (q, *J* = 7.6, 2H), 1.37 (t, *J* = 7.6, 3H); LCMS (formic acid) *R*_t = 1.01 min (52%), MH⁺ 272.0, 274.0.

7-(3,4-Dimethoxyphenyl)-2-ethyl-5-methylthieno[3,2-c]pyridin-4(5H)-one (2.044)

A mixture of **2.054** (45 mg, 0.17 mmol), (3,4-dimethoxyphenyl)boronic acid (36 mg, 0.12 mmol), K_2CO_3 (50 mg, 0.36 mmol) and PEPPSI-Pr (10 mg, 0.02 mmol) in IPA (1.5 mL) and H_2O (0.5 mL) was heated at 120 °C in a microwave reactor for 0.5 h. The solution was allowed to cool to rt and diluted with EtOAc (50 mL). The solution was filtered through Celite[®], passed through a hydrophobic frit and concentrated *in vacuo*. The resulting residue was purified by MDAP (formic acid). The appropriate fractions were combined and concentrated *in vacuo* to give **2.044** (15 mg, 29%) as a pale yellow solid; 1H NMR (400 MHz, $CDCl_3$) δ ppm 7.44–7.43 (m, 1H), 7.13–7.09 (m, 3H), 6.97 (d, $J = 7.8$, 1H), 3.96 (s, 6H), 3.69 (s, 3H), 2.91 (q, $J = 7.6$, 2H), 1.37 (t, $J = 7.6$, 3H); LCMS (formic acid) $R_t = 1.01$ min (97%), MH^+ 330.0.

Ethyl 7-(3,4-dimethoxyphenyl)-5-methyl-4-oxo-4,5-dihydrothieno[3,2-c]pyridine-2-carboxylate (2.020)

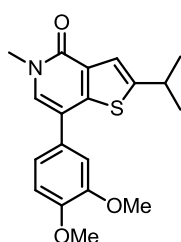
To a solution of **2.021** (250 mg, 0.72 mmol) and $NaHCO_3$ (122 mg, 1.45 mmol) in DMF (3.5 mL), EtI (0.3 mL, 3.62 mmol) was added. The reaction mixture was left to stir for 18 h at rt. EtI (0.1 mL, 1.45 mmol) and $NaHCO_3$ (61 mg, 0.7 mmol) were added and the reaction was left to stir for 2 h at rt, then at 50 °C for 18 h. The volatile components were removed *in vacuo* and the resulting residue was dissolved in EtOAc (50 mL). The organic layer was washed with H_2O (3 x 50 mL) and brine (50 mL), passed through a hydrophobic frit and concentrated *in vacuo* to give **2.020** (238 mg, 88%) as a grey solid; 1H NMR (400 MHz, $CDCl_3$) δ ppm 8.40 (s, 1H), 7.26 (s, 1H), 7.12 (dd, $J = 8.2, 2.0$, 1H), 7.07 (d, $J = 2.0$, 1H), 6.99 (d, $J = 8.2$, 1H), 4.40 (q, $J = 7.1$, 2H), 3.97 (s, 6H), 3.70 (s, 3H), 1.41 (t, $J = 7.1$, 3H); LCMS (formic acid) $R_t = 1.00$ min (98%), MH^+ 374.1.

7-(3,4-Dimethoxyphenyl)-2-(2-hydroxypropan-2-yl)-5-methylthieno[3,2-c]pyridin-4(5H)-one (2.049)

To a solution of **2.020** (211 mg, 0.57 mmol) in THF (3.5 mL), 3 M MeMgBr in Et_2O (0.5 mL, 1.41 mmol) was added drop-wise at 0 °C. The reaction mixture was allowed to warm to rt and was left to stir for 3 h. 3 M MeMgBr in Et_2O (0.2 mL, 0.60 mmol) was added and the reaction mixture was left to stir for a further 0.5 h.

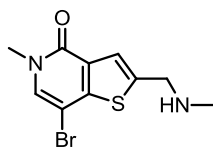
The solution was quenched with sat. aq. NH_4Cl (30 mL) and left to stand overnight. The aqueous phase was extracted into EtOAc (5 × 50 mL) and the combined organic layers were passed through a hydrophobic frit and concentrated *in vacuo* to give **2.049** (191 mg, 94%) as an orange solid; ^1H NMR (400 MHz, CDCl_3) δ ppm 7.52 (s, 1H), 7.12–7.09 (m, 2H), 7.05 (d, $J = 2.0$, 1H), 6.96 (d, $J = 8.3$, 1H), 3.95 (s, 3H), 3.93 (s, 3H), 3.67 (s, 3H), 1.72 (s, 6H); LCMS (formic acid) $R_t = 0.81$ min (98%), MH^+ 360.2.

7-(3,4-Dimethoxyphenyl)-2-isopropyl-5-methylthieno[3,2-c]pyridin-4(5H)-one (2.045)



To a solution of **2.049** (161 mg, 0.45 mmol) in TFA (3.5 mL), triethylsilane (0.36 mL, 2.24 mmol) was added drop-wise. The reaction mixture was heated at 40 °C for 5 h. The solution was allowed to cool to rt and diluted with H_2O (50 mL). The aqueous phase was extracted with EtOAc (4 × 50 mL) and the combined organic layers were washed with sat. aq. NaHCO_3 (3 × 50 mL), passed through a hydrophobic frit and concentrated *in vacuo*. The resultant residue was purified by MDAP (formic acid). The appropriate fractions were combined and solvent evaporated *in vacuo* to give **2.045** (45 mg, 29%) as an orange oil; m.p. 152–153 °C; ν_{max} (solid)/ cm^{-1} : 1649 (C=O), 1513, 1252, 1237, 766; ^1H NMR (400 MHz, DMSO-d_6) δ ppm 7.64 (s, 1H), 7.29 (d, $J = 1.0$, 1H), 7.17–7.13 (m, 2H), 7.09–7.05 (m, 1H), 3.82 (s, 3H), 3.81 (s, 3H), 3.57 (s, 3H), 3.26–3.17 (m, 1H), 1.13 (d, $J = 6.8$, 6H); ^{13}C NMR (101 MHz, DMSO-d_6) δ ppm 157.1, 151.6, 148.7, 148.3, 145.0, 131.3, 129.1, 128.4, 119.3, 119.2, 114.9, 111.9, 111.1, 55.5, 55.4, 35.9, 29.2, 24.0; HRMS ($\text{M} + \text{H}$) $^+$ calculated for $\text{C}_{19}\text{H}_{22}\text{NO}_3\text{S}$ 344.1319; found 344.1315; LCMS (formic acid) $R_t = 1.07$ min (96%), MH^+ 344.1.

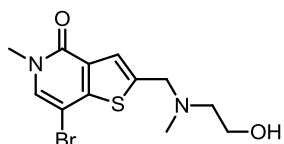
7-Bromo-5-methyl-2-((methylamino)methyl)thieno[3,2-c]pyridin-4(5H)-one (2.056a)



A mixture of **2.009** (250 mg, 0.92 mmol) and 2 M methylamine in MeOH (1.4 mL, 2.76 mmol) in MeOH (3.5 mL) and AcOH (0.35 mL) was heated to 50 °C for 4 h. Picoline borane complex (108 mg, 1.01 mmol) was added and the solution was left to stir for 20 h. The volatile components were removed *in vacuo* and the resulting residue was diluted with sat. aq. NaHCO_3 (40 mL). The aqueous phase was extracted with DCM (3 × 40 mL) and the combined organic layers were passed through a hydrophobic frit and

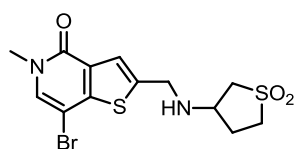
concentrated *in vacuo*. The resulting residue was purified by silica gel chromatography (0–7% 2 M NH₃ in MeOH in DCM). The appropriate fractions were combined and solvent evaporated *in vacuo* to give **2.056a** (126 mg, 48%) as a yellow solid; ¹H NMR (400 MHz, CDCl₃) δ ppm 7.54 (s, 1H), 7.27 (s, 1H), 4.01–3.98 (m, 2H), 3.61 (s, 3H), 2.50 (s, 3H); LCMS (formic acid): R_t = 0.45 min (98%), MH⁺ 287.0, 289.0.

7-Bromo-2-(((2-hydroxyethyl)(methyl)amino)methyl)-5-methylthieno[3,2-c]pyridin-4(5H)-one (2.056b)



A mixture of **2.009** (250 mg, 0.92 mmol), 2-(methylamino)ethanol (0.15 mL, 1.84 mmol) in AcOH (0.35 mL) and MeOH (3.5 mL) was left to stir at rt for 20 minutes. Picoline borane complex (108 mg, 1.01 mmol) was added and the solution was heated at 50 °C for 18 h. The volatile components were removed *in vacuo* and the resulting residue was diluted with sat. aq. NaHCO₃ (30 mL). The aqueous phase was extracted with DCM (3 × 30 mL) and the combined organic layers were passed through a hydrophobic frit and concentrated *in vacuo*. The resulting residue was purified by silica gel chromatography (0–4% MeOH in DCM). The appropriate fractions were combined and concentrated *in vacuo* to give **2.056b** (66 mg, 22%) as a colourless oil; m.p. 134–135 °C; ν_{\max} (solid)/cm⁻¹: 3342 (O-H), 2801, 1635 (C=O), 1578, 1037, 765; ¹H NMR (400 MHz, CDCl₃) δ ppm 7.54 (s, 1H), 7.28 (s, 1H), 3.84 (s, 2H), 3.67 (t, *J* = 5.4, 2H), 3.61 (s, 3H), 2.67 (t, *J* = 5.4, 2H), 2.33 (s, 3H); ¹³C NMR (101 MHz, CDCl₃) δ ppm 158.1, 149.1, 143.8, 132.4, 129.9, 123.9, 93.6, 58.6, 58.3, 57.0, 41.6, 36.9; HRMS (M + H)⁺ calculated for C₁₂H₁₆BrN₂O₂S 331.0110; found 331.0123; LCMS (formic acid): R_t = 0.45 min (100%), MH⁺ 331.1, 333.1.

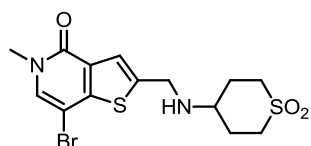
7-Bromo-2-(((1,1-dioxidotetrahydrothiophen-3-yl)amino)methyl)-5-methylthieno[3,2-c]pyridin-4(5H)-one (2.056c)



A mixture of **2.009** (250 mg, 0.92 mmol), 3-aminotetrahydrothiophene-1,1-dioxide (199 mg, 1.47 mmol) in MeOH (3.5 mL) and AcOH (0.35 mL) was left to stir for 3 h at 50 °C. Picoline borane complex (108 mg, 1.01 mmol) was added and the reaction mixture was left to stir for 4 h at 50 °C. The volatile components were removed *in vacuo* and the resulting residue was diluted with sat. aq. NaHCO₃ (40 mL). The aqueous phase was extracted with DCM (3 × 40 mL) and

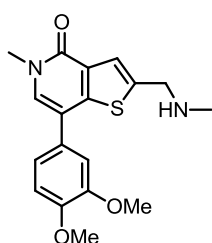
the combined organic layers were passed through a hydrophobic frit and concentrated *in vacuo*. The resulting residue was purified by silica gel chromatography (0–4% MeOH in DCM). The appropriate fractions were combined and evaporated *in vacuo* to give **2.056c** (340 mg, 95%) as a pale yellow solid; ¹H NMR (400 MHz, CDCl₃) δ ppm 7.57 (s, 1H), 7.28 (s, 1H), 4.13–4.06 (m, 2H), 3.74–3.67 (m, 1H), 3.63 (s, 3H), 3.37–3.29 (m, 2H), 3.12–3.04 (m, 1H), 2.99–2.93 (m, 1H), 2.53–2.43 (m, 1H), 2.20–2.10 (m, 1H); LCMS (formic acid): R_t = 0.50 min (100%), MH⁺ 391.1, 393.1.

7-Bromo-2-(((1,1-dioxidotetrahydro-2H-thiopyran-4-yl)amino)methyl)-5-methylthieno[3,2-c]pyridin-4(5H)-one (2.056d)



A mixture of **2.009** (250 mg, 0.92 mmol) and 4-aminotetrahydro-2H-thiopyran-1,1-dioxide hydrochloride (200 mg, 1.47 mmol) in MeOH (3.5 mL) and AcOH (0.35 mL) was left to stir at 50 °C for 4 h. Picoline borane complex (108 mg, 1.01 mmol) was added and the reaction mixture was left to stir at 50 °C for 20 h. The volatile components were removed *in vacuo* and the resulting residue was diluted with sat. aq. NaHCO₃ (40 mL). The aqueous phase was extracted with DCM (3 × 40 mL) and the combined organic layers were passed through a hydrophobic frit and concentrated *in vacuo*. The resulting residue was purified by silica gel chromatography (0–4% MeOH in DCM). The appropriate fractions were combined and solvent evaporated *in vacuo* to give **2.056d** (210 mg, 56%) as a pale yellow solid; ¹H NMR (400 MHz, CDCl₃) δ ppm 7.56 (s, 1H), 7.31 (s, 1H), 4.08–4.07 (m, 2H), 3.63 (s, 3H), 3.37–3.28 (m, 2H), 3.04–2.98 (m, 1H), 2.95–2.87 (m, 2H), 2.36–2.27 (m, 2H), 2.16–2.07 (m, 2H); LCMS (formic acid): R_t = 0.47 min (100%), MH⁺ 405.0, 407.0.

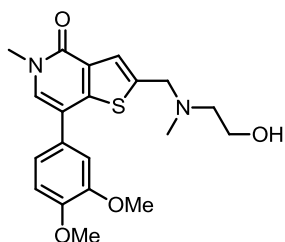
7-(3,4-Dimethoxyphenyl)-5-methyl-2-((methylamino)methyl)thieno[3,2-c]pyridin-4(5H)-one (2.055a)



A mixture of **2.056a** (126 mg, 0.44 mmol), (3,4-dimethoxyphenyl)boronic acid (96 mg, 0.53 mmol), PEPPSI-Pr (27 mg, 0.04 mmol) and K₂CO₃ (133 mg, 0.97 mmol) in H₂O (1 mL) and IPA (3 mL) was heated at 120 °C in a microwave reactor for 0.5 h. The reaction mixture was allowed to cool to rt and diluted with EtOAc (30 mL). The solution was filtered through Celite[®], passed through a hydrophobic frit and concentrated *in vacuo*. The resultant residue was

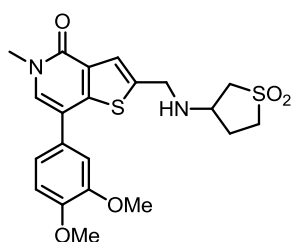
dissolved in MeOH (15 mL) and passed through a preconditioned (MeOH, 10 mL) aminopropyl column (10 g). The appropriate fractions were collected and concentrated *in vacuo*. The resulting residue purified by MDAP (high pH) The appropriate fractions were combined and concentrated *in vacuo* to give **2.055a** (66 mg, 44%) as a pale yellow oil; $^1\text{H NMR}$ (400 MHz, CDCl_3) δ ppm 7.54 (s, 1H), 7.15–7.10 (m, 2H), 7.09–7.07 (m, 1H), 6.95 (d, $J = 7.6$, 1H), 4.03–3.98 (m, 2H), 3.95 (s, 6H), 3.68 (s, 3H), 2.63–2.62 (m, 1H), 2.49 (s, 3H); LCMS (formic acid): $R_t = 0.58$ min (100%), MH^+ 345.2.

7-(3,4-Dimethoxyphenyl)-2-(((2-hydroxyethyl)(methyl)amino)methyl)-5-methylthieno[3,2-c]pyridin-4(5H)-one (2.055b)



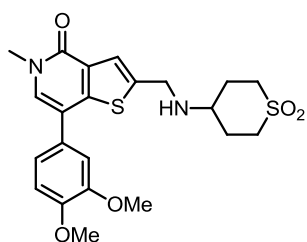
A mixture of **2.056b** (60 mg, 0.18 mmol), (3,4-dimethoxyphenyl)boronic acid (40 mg, 0.22 mmol), K_2CO_3 (55 mg, 0.40 mmol) and PEPPSI-*t*Pr (12 mg, 0.02 mmol) in H_2O (0.5 mL) and IPA (1.5 mL) was heated at 120 °C in a microwave for 0.5 h. The reaction mixture was allowed to cool to rt and diluted with EtOAc (50 mL). The solution was filtered through Celite[®], passed through a hydrophobic frit and concentrated *in vacuo*. The resulting residue was purified by MDAP (formic acid). The appropriate fractions were combined and concentrated *in vacuo*. The resulting residue was dissolved in MeOH (4 mL) and passed through a preconditioned (MeOH, 10 mL) amino propyl column (10 g). The appropriate fractions were combined and concentrated *in vacuo* to give **2.055b** (62 mg, 88%) as a colourless oil; ν_{max} (thin film)/ cm^{-1} : 3398 (O-H), 1637 (C=O), 1513, 1253, 1024, 726; $^1\text{H NMR}$ (400 MHz, DMSO-d_6) δ ppm 7.53 (s, 1H), 7.13 (s, 1H), 7.10 (dd, $J = 8.3, 2.0$, 1H), 7.06 (d, $J = 2.0$, 1H), 6.95 (d, $J = 8.3$, 1H), 3.93 (s, 6H), 3.82 (s, 2H), 3.67 (s, 3H), 3.62 (t, $J = 5.4$, 2H), 2.63 (t, $J = 5.4$, 2H), 2.31 (s, 3H); $^{13}\text{C NMR}$ (101 MHz, DMSO-d_6) δ ppm 158.2, 149.0, 148.7, 147.8, 142.2, 130.0, 129.7, 128.6, 123.3, 119.7, 117.0, 111.3, 110.7, 58.2, 57.7, 56.7, 55.7, 55.6, 41.2, 36.6; HRMS ($\text{M} + \text{H}$)⁺ calculated for $\text{C}_{20}\text{H}_{25}\text{N}_2\text{O}_4\text{S}$ 389.1530; found 389.1539; LCMS (high pH): $R_t = 0.79$ min (100%), MH^+ 389.21.

7-(3,4-Dimethoxyphenyl)-2-(((1,1-dioxidotetrahydrothiophen-3-yl)amino)methyl)-5-methylthieno[3,2-c]pyridin-4(5H)-one (2.055c)



A solution of **2.056c** (233 mg, 0.60 mmol), (3,4-dimethoxyphenyl)boronic acid (130 mg, 0.72 mmol), K_2CO_3 (181 mg, 1.31 mmol) and PEPPSI-*i*Pr (37 mg, 0.05 mmol) in H_2O (2 mL) and IPA (6 mL) was heated at 120 °C for 0.5 h in a microwave reactor. The reaction was allowed to cool to rt and diluted with EtOAc (50 mL). The solution was filtered through Celite[®], passed through a hydrophobic frit and concentrated *in vacuo*. The resulting residue was purified by MDAP (high pH). The appropriate fractions were combined and concentrated *in vacuo* to give **2.055c** (156 mg, 58%) as a pale orange solid; m.p. 171–172 °C; ν_{max} (solid)/ cm^{-1} : 1639 (C=O), 1515, 1253, 1109 (S=O), 768; 1H NMR (400 MHz, DMSO- d_6) δ ppm 7.65 (s, 1H), 7.45 (s, 1H), 7.18–7.14 (m, 2H), 7.07 (d, J = 9.0, 1H), 4.00–3.94 (m, 2H), 3.82 (s, 3H), 3.81 (s, 3H), 3.57 (s, 3H), 3.51–3.43 (m, 1H), 3.37–3.31 (m, 1H), 3.25–3.16 (m, 1H), 3.07–2.98 (m, 1H), 2.91–2.85 (m, 1H), 2.31–2.20 (m, 1H), 2.03–1.93 (m, 1H); ^{13}C NMR (101 MHz, DMSO- d_6) δ ppm 157.4, 149.0, 148.5, 146.3, 144.4, 131.7, 129.2, 128.6, 121.9, 119.4, 115.2, 112.1, 111.3, 56.3, 55.6, 55.5, 53.8, 50.4, 45.4, 36.1, 28.8; HRMS ($M + H$)⁺ calculated for $C_{21}H_{25}N_2O_5S_2$ 449.1199; found 449.1201; LCMS (high pH): R_t = 0.78 min (100%), MH^+ 449.2.

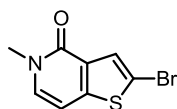
7-(3,4-Dimethoxyphenyl)-2-(((1,1-dioxidotetrahydro-2H-thiopyran-4-yl)amino)methyl)-5-methylthieno[3,2-c]pyridin-4(5H)-one (2.055d)



A solution of **2.056d** (204 mg, 0.50 mmol), (3,4-dimethoxyphenyl)boronic acid (110 mg, 0.60 mmol), PEPPSI-*i*Pr (31 mg, 0.05 mmol) and K_2CO_3 (153 mg, 1.11 mmol) in IPA (6 mL) and H_2O (2 mL) was heated at 120 °C in a microwave reactor for 0.5 h. The solution was allowed to cool to rt and diluted with EtOAc (50 mL). The solution was filtered through Celite[®], passed through a hydrophobic frit and concentrated *in vacuo*. The resulting residue was purified by MDAP (high pH). The appropriate fractions were combined and concentrated *in vacuo* to give **2.055d** (118 mg, 51%) as an off white solid; m.p. 190–191 °C; ν_{max} (solid)/ cm^{-1} : 1645 (C=O), 1515, 1253, 1126 (S=O); 1H NMR (400 MHz, DMSO- d_6) δ ppm 7.65 (s, 1H), 7.43 (s, 1H), 7.19–7.13 (m, 2H), 7.09–7.06 (m, 1H), 3.96 (s, 2H), 3.82 (s, 3H), 3.81 (s, 3H), 3.57 (s, 3H), 3.14–3.05 (m, 2H), 3.03–2.95 (m, 2H), 2.82–2.75 (m, 1H), 2.11–2.01 (m, 2H), 1.94–1.81 (m,

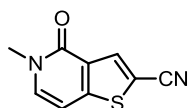
2H); ^{13}C NMR (101 MHz, DMSO- d_6) δ ppm 157.4, 149.0, 148.5, 146.1, 145.5, 131.6, 129.3, 128.6, 121.4, 119.4, 115.2, 112.1, 111.3, 55.6, 55.6, 49.9, 47.8, 44.8, 36.1, 28.9; HRMS (M + H) $^+$ calculated for $\text{C}_{22}\text{H}_{27}\text{N}_2\text{O}_5\text{S}_2$ 463.1362; found 463.1356; LCMS (formic acid): R_t = 0.60 min (95%), MH^+ 463.0.

2-Bromo-5-methylthieno[3,2-c]pyridin-4(5H)-one (2.060)



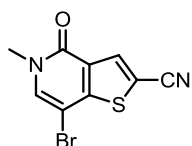
To a stirred suspension of **2.012** (10.00 g, 43.50 mmol) in THF (500 mL), Cs_2CO_3 (42.50 g, 130.00 mmol) was added. The mixture was left to stir at rt for 1 h. MeI (5.4 mL, 87.00 mmol) was added and the reaction mixture was left to stir for a further 18 h. The volatile components were removed *in vacuo*. The resulting solid was suspended in H_2O (200 mL), filtered under reduced pressure, washed with H_2O (100 mL), collected and dried under vacuum at 40 °C to give **2.060** (9.65 g, quant.) as a brown solid; ^1H NMR (400 MHz, CDCl_3) δ ppm 7.64 (s, 1H), 7.16 (d, J = 7.1, 1H), 6.57 (d, J = 7.1, 1H), 3.62 (s, 3H); LCMS (formic acid) R_t = 0.81 min (100%), MH^+ = 243.9, 245.9.

5-Methyl-4-oxo-4,5-dihydrothieno[3,2-c]pyridine-2-carbonitrile (2.061)



A mixture of **2.060** (1.50 g, 6.10 mmol.), zinc cyanide (1.44 g, 12.30 mmol) and $\text{Pd}(\text{PPh}_3)_4$ (640 mg, 0.50 mmol) in DMF (10 mL) was heated at 115 °C for 4.5 h in a microwave reactor. This process was repeated to provide a further 4 identical batches. The 5 batches were allowed to cool to rt, combined, diluted with EtOAc (50 mL), filtered through Celite[®] and concentrated *in vacuo*. The resulting residue was purified by silica gel chromatography (0–5% MeOH in DCM). The appropriate fractions were combined and solvent evaporated *in vacuo* to give **2.061** (4.45 g, 68%) as a pale yellow solid; ^1H NMR (400 MHz, CDCl_3) δ ppm 8.16 (s, 1H), 7.34 (d, J = 7.1, 1H), 6.66 (d, J = 7.1, 1H), 3.64 (s, 3H); LCMS (formic acid) R_t = 0.63 min (95%), MH^+ = 191.1.

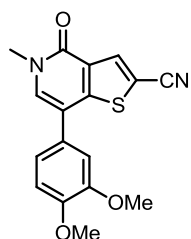
7-Bromo-5-methyl-4-oxo-4,5-dihydrothieno[3,2-c]pyridine-2-carbonitrile (2.062)



A solution of **2.061** (1.57 g, 7.80 mmol.) in THF (30 mL) was treated with NBS (2.09 g, 11.80 mmol.) and the reaction mixture was stirred at rt for 72 h. The volatile components were removed *in vacuo* and the resulting solid was suspended in Et_2O (50 mL), filtered under reduced pressure, washed with Et_2O (50 mL), collected and dried under vacuum at 40 °C to give **2.062** (1.81 g, 86%) as an off white solid; m.p. 274–276 °C; ν_{max} (solid)/ cm^{-1} : 2123 (C \equiv N), 1653 (C=O), 1583, 764; ^1H NMR (400 MHz, CDCl_3) δ ppm 8.24 (s, 1H), 7.50 (s, 1H), 3.65 (s, 3H); ^{13}C NMR (101 MHz, CDCl_3) δ ppm 157.4, 152.7, 136.8,

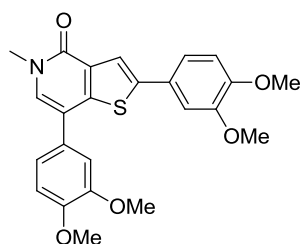
136.3, 129.1, 113.3, 109.0, 91.8, 37.2; HRMS (M + H)⁺ calculated for C₉H₆BrN₃OS 268.9379; found 268.9381; LCMS (formic acid) R_t = 0.83 min (95%), MH⁺ = 268.9, 270.9.

7-(3,4-Dimethoxyphenyl)-5-methyl-4-oxo-4,5-dihydrothieno[3,2-c]pyridine-2-carbonitrile (2.059)



A solution of **2.062** (654 mg, 1.70 mmol), (3,4-dimethoxyphenyl)boronic acid (418 mg, 2.30 mmol), K₂CO₃ (552 mg, 4.00 mmol) and PEPPSI-*i*-Pr (173 mg, 0.26 mmol) in IPA (9 mL) and H₂O (3 mL) was heated at 120 °C in a microwave reactor for 0.5 h. The reaction mixture was allowed to cool to rt, diluted with EtOAc (50 mL), filtered through Celite[®] and concentrated *in vacuo*. The resulting residue was purified by silica gel chromatography (0–10% MeOH in DCM). The appropriate fractions were combined and solvent evaporated *in vacuo*. The resulting residue was purified by silica gel chromatography (0–2% MeOH in DCM). The appropriate fractions were combined and solvent evaporated *in vacuo*. The resulting residue was purified by MDAP (formic acid). The appropriate fractions were combined and concentrated *in vacuo* to give **2.059** (125 mg, 23%) as a yellow solid; ¹H NMR (400 MHz, CDCl₃) δ ppm 8.20 (s, 1H), 7.34 (s, 1H), 7.08 (dd, *J* = 8.1, 2.0, 1H), 7.01 (d, *J* = 2.0, 1H), 6.99 (d, *J* = 8.1, 1H), 3.96 (s, 3H), 3.95 (s, 3H), 3.70 (s, 3H); LCMS (formic acid) R_t = 0.91 min (100%), MH⁺ = 327.1.

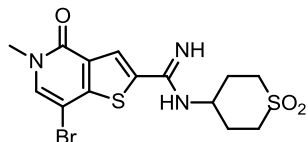
2,7-Bis(3,4-dimethoxyphenyl)-5-methylthieno[3,2-c]pyridin-4(5H)-one (2.063)



A solution of **2.062** (654 mg, 1.70 mmol), (3,4-dimethoxyphenyl)boronic acid (418 mg, 2.30 mmol), K₂CO₃ (552 mg, 4.00 mmol) and PEPPSI-*i*-Pr (173 mg, 0.26 mmol) in IPA (9 mL) and H₂O (3 mL) was heated at 120 °C in a microwave reactor for 0.5 h. The reaction mixture was allowed to cool to rt, diluted with EtOAc (50 mL), filtered through Celite[®] and concentrated *in vacuo*. The resulting residue was purified by silica gel chromatography (0–10% MeOH in DCM). The appropriate fractions were combined and solvent evaporated *in vacuo*. The resulting residue was purified by silica gel chromatography (0–2% MeOH in DCM). The appropriate fractions were combined and solvent evaporated *in vacuo* to give **2.063** (no yield obtained). **2.063** (10 mg) taken for structure elucidation; ¹H NMR (400 MHz, CDCl₃) δ ppm 7.84 (s, 1H), 7.21 (dd, *J* = 8.3, 2.2, 1H), 7.18 (d, *J* = 2.2, 1H), 7.15 (s, 1H), 7.13–7.14 (m, 1H), 7.11 (d,

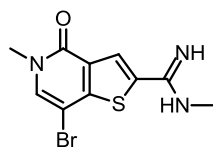
$J = 2.0$, 1H), 6.99 (d, $J = 8.3$, 1H), 6.89 (d, $J = 8.3$, 1H), 3.95 (s, 6H), 3.95 (s, 3H), 3.92 (s, 3H), 3.70 (s, 3H); LCMS (formic acid) $R_t = 1.04$ min (97%), $MH^+ = 438.1$.

7-Bromo-*N*-(1,1-dioxidotetrahydro-2H-thiopyran-4-yl)-5-methyl-4-oxo-4,5-dihydrothieno[3,2-*c*]pyridine-2-carboximidamide (2.064)



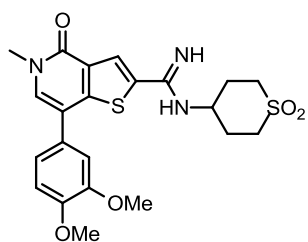
To a suspension of **2.062** (2.00 g, 7.43 mmol) in MeOH (30 mL), NaOMe solution in MeOH (25% by weight, 1.7 mL, 7.43 mmol) was added. The reaction mixture was heated at 75 °C for 3 h. 4-aminotetrahydro-2H-thiopyran-1,1-dioxide hydrochloride (1.66 g, 8.94 mmol) was added at 75 °C and the reaction mixture was stirred for a further 72 h. The volatile components were removed *in vacuo* and the resulting solid was suspended in MeOH (50 mL), filtered under reduced pressure, washed with MeOH (20 mL), collected and dried under vacuum at 40 °C to give **2.064** (2.69 g, 87%) as a white solid; 1H NMR (400 MHz, DMSO- d_6) δ ppm 8.17 (s, 1H), 7.99 (s, 1H), 6.79 (br.s, 2H), 3.67–3.59 (m, 1H), 3.51 (s, 3H), 3.27–3.17 (m, 2H), 3.10–3.01 (m, 2H), 2.08–1.99 (m, 2H), 1.98–1.88 (m, 2H); LCMS (formic acid) $R_t = 0.48$ min (96%), $MH^+ = 418.0$, 420.0.

7-Bromo-*N*,5-dimethyl-4-oxo-4,5-dihydrothieno[3,2-*c*]pyridine-2-carboximidamide (2.065)



A solution of **2.062** (50 mg, 0.19 mmol) and NaOMe solution in MeOH (25% by weight, 0.05 mL, 0.20 mmol) in MeOH (4 mL) was heated at 75 °C for 16 h. Methylamine hydrochloride (38 mg, 0.56 mmol) was added and the solution was left to stir for a further 3 h. The reaction mixture was allowed to cool to rt. The volatile components were removed *in vacuo* to give **2.065** (107 mg, quant.) as a pale yellow solid; 1H NMR (400 MHz, CD $_3$ OD) δ ppm 8.36 (s, 1H), 8.01 (s, 1H), 3.67 (s, 3H), 3.13 (s, 3H); LCMS (formic acid) $R_t = 0.45$ min (81%), $MH^+ = 300.0$, 302.0.

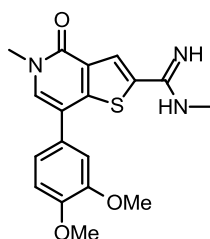
7-(3,4-Dimethoxyphenyl)-*N*-(1,1-dioxidotetrahydro-2H-thiopyran-4-yl)-5-methyl-4-oxo-4,5-dihydrothieno[3,2-*c*]pyridine-2-carboximidamide (2.057)



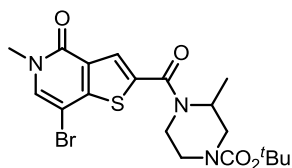
A mixture of **2.064** (128 mg, 0.18 mmol), (3,4-dimethoxyphenyl)boronic acid (43 mg, 0.24 mmol), K $_2$ CO $_3$ (64 mg, 0.46 mmol) and PEPPSI-*i*Pr (19 mg, 0.03 mmol) in H $_2$ O (0.5 mL) and IPA (1.5 mL) was heated at 120 °C for 0.5 h in a microwave reactor. The reaction mixture was allowed to cool to rt and diluted with EtOAc (50 mL). The solution was filtered

through Celite[®], passed through a hydrophobic frit and concentrated *in vacuo*. The resulting residue was purified by MDAP (formic acid). The appropriate fractions were combined and concentrated *in vacuo*. The resulting residue was dissolved in MeOH (10 mL) and passed through a preconditioned (MeOH, 20 mL) amino propyl column (10 g). The appropriate fractions were combined and concentrated *in vacuo* to give **2.057** (37 mg, 42%) as a white solid; m.p. 178–180 °C; ν_{\max} (solid)/ cm^{-1} : 1638 (C=N), 1583, 1520, 1257, 1118 (S=O); ^1H NMR (400 MHz, DMSO- d_6) δ ppm 8.11 (s, 1H), 7.72 (s, 1H), 7.19 (dd, J = 8.1, 2.1, 1H), 7.16 (d, J = 2.1, 1H), 7.10 (d, J = 8.1, 1H), 6.74 (br.s, 2H), 3.83 (s, 3H), 3.82 (s, 3H), 3.64–3.56 (m, 4H), 3.23–3.18 (m, 2H), 3.09–2.99 (m, 2H), 2.06–1.97 (m, 2H), 1.95–1.87 (m, 2H); ^{13}C NMR (101 MHz, DMSO- d_6) δ ppm 157.7, 149.3, 149.0, 148.6, 148.1, 142.4, 141.7, 133.1, 129.5, 128.4, 122.5, 119.5, 112.2, 111.5, 55.6, 55.5, 49.1, 48.4, 36.2, 30.1; HRMS ($M + H$)⁺ calculated for $\text{C}_{22}\text{H}_{26}\text{N}_3\text{O}_5\text{S}_2$ 476.1308; found 476.1303; LCMS (formic acid), R_t = 0.61 min (100%), MH^+ = 476.2.

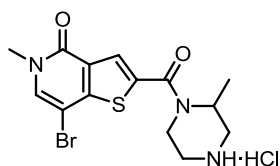
7-(3,4-Dimethoxyphenyl)-*N*,5-dimethyl-4-oxo-4,5-dihydrothieno[3,2-*c*]pyridine-2-carboximidamide (2.058)



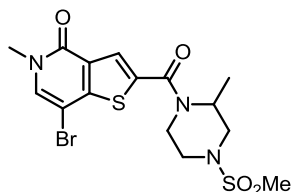
A mixture of **2.065** (107 mg, 0.21 mmol), (3,4-dimethoxyphenyl)boronic acid (47 mg, 0.26 mmol), K_2CO_3 (71 mg, 0.51 mmol) and PEPPSI-*i*-Pr (13 mg, 0.02 mmol) in IPA (1.5 mL) and H_2O (0.5 mL) was heated at 120 °C for 0.5 h in a microwave reactor. The reaction mixture was allowed to cool to rt and diluted with EtOAc (30 mL) and MeOH (20 mL). The solution was filtered through Celite[®], passed through a hydrophobic frit and concentrated *in vacuo*. The resulting residue was purified by MDAP (formic acid). The appropriate fractions were combined and concentrated *in vacuo*. The resulting residue was dissolved in MeOH (5 mL) and passed through a preconditioned (MeOH, 20 mL) amino propyl column (10 g). The appropriate fractions were combined and concentrated *in vacuo*. The resultant solid was purified by MDAP (high pH). The appropriate fractions were combined and concentrated *in vacuo* to give **2.058** (5 mg, 7%) as a white solid; ^1H NMR (400 MHz, CD_3OD) δ ppm 8.04 (s, 1H), 7.64 (s, 1H), 7.23–7.17 (m, 2H), 7.08 (d, J = 8.1, 1H), 3.92 (s, 3H), 3.90 (s, 3H), 3.72 (s, 3H), 2.96 (s, 3H); LCMS (formic acid), R_t = 0.58 min (100%), MH^+ = 358.2.

tert-Butyl 4-(7-bromo-5-methyl-4-oxo-4,5-dihydrothieno[3,2-c]pyridine-2-carbonyl)-3-methylpiperazine-1-carboxylate (2.076)

A mixture of **2.008** (1.50 g, 4.43 mmol), *tert*-butyl 3-methylpiperazine-1-carboxylate (1.2 mL, 5.75 mmol), HATU (2.00 g, 5.31 mmol) and DIPEA (1.5 mL, 8.85 mmol) in DMF (30 mL) was left to stir at rt for 20 h. The volatile components were removed *in vacuo* and the resulting residue was dissolved in EtOAc (50 mL) and washed with sat. aq. NaHCO₃ (50 mL). The organic layer was separated, passed through a hydrophobic frit and concentrated *in vacuo* to give **2.076** (1.95 g, quant.) as a brown oil; ¹H NMR (400 MHz, CDCl₃) δ ppm 7.83 (s, 1H), 7.38 (s, 1H), 4.74–4.62 (m, 1H), 4.29–4.20 (m, 1H), 3.79–3.70 (m, 1H), 3.64 (s, 3H), 3.42–3.29 (m, 1H), 3.24–3.16 (m, 2H), 3.15–3.07 (m, 1H), 1.50 (br.s, 9H), 1.35 (d, *J* = 6.7, 3H); LCMS (formic acid), R_t = 1.03 min (73%), MH⁺ = 470.1, 472.1.

7-Bromo-5-methyl-2-(2-methylpiperazine-1-carbonyl)thieno[3,2-c]pyridin-4(5H)-one hydrochloride (2.077)

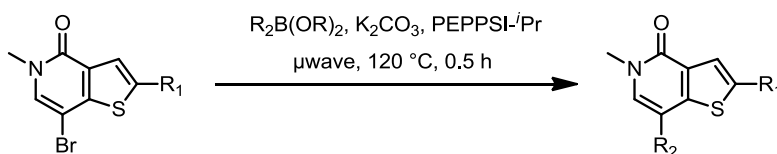
A suspension of **2.076** (1.95 g, 4.15 mmol) in 4 M HCl in 1,4-dioxane (10 mL, 329.00 mmol) was left to stir at rt for 18 h. The volatile components were removed *in vacuo* and the resulting residue was suspended in Et₂O (30 mL), filtered under reduced pressure, rinsed with Et₂O (50 mL) and collected to give **2.077** (2.24 g, quant.) as a brown solid; ¹H NMR (400 MHz, CD₃OD) δ ppm 7.98 (s, 1H), 7.91 (s, 1H), 4.53–4.45 (m, 1H), 3.68–3.54 (m, 6H), 3.51–3.39 (m, 3H), 1.52 (d, *J* = 7.1, 3H); LCMS (formic acid), R_t = 0.53 min (94%), MH⁺ = 370.1, 372.1.

7-Bromo-5-methyl-2-(2-methyl-4-(methylsulfonyl)piperazine-1-carbonyl)thieno[3,2-c]pyridin-4(5H)-one (2.078)

To a solution of **2.077** (2.24 g, 5.51 mmol) and triethylamine (3 mL, 22.03 mmol) in DCM (22 mL) at 0 °C, methanesulfonyl chloride (0.5 mL, 6.06 mmol) was added drop-wise. The reaction mixture was allowed to warm to rt and left to stir for 3 h. The reaction mixture was diluted with DCM (50 mL) and washed with 1 M aq. HCl (50 mL), sat. aq. NaHCO₃ (50 mL), H₂O (50 mL) and brine (50 mL). The organic layer was passed through a hydrophobic frit and concentrated *in vacuo* to give **2.078** (1.40 g, 57%) as a light brown solid; ¹H NMR (400 MHz, CD₃OD) δ ppm 7.85 (s, 1H), 7.40 (s, 1H), 4.88–4.78 (m, 1H), 4.48–4.37 (m, 1H),

3.88–3.79 (m, 1H), 3.68–3.59 (m, 5H), 3.01–2.93 (m, 1H), 2.87–2.78 (m, 4H), 1.49 (d, $J = 6.9$, 3H); LCMS (formic acid), $R_t = 0.78$ min (86%), $MH^+ = 470.4$, 472.3.

General Procedure 1: Synthesis of square array compounds



A mixture of the desired bromide (0.15 mmol, 1.0 eq.), boronic acid/ester (0.18 mmol, 1.2 eq.), K_2CO_3 (50 mg, 0.36 mmol, 2.4 eq.) and PEPPSI-*i*Pr (9 mg, 0.014 mmol, 0.09 eq.) in H_2O (0.3 mL) and IPA (0.9 mL) was heated at 120 °C in a microwave reactor for 0.5 h. The reaction mixture was allowed to cool to rt and diluted with EtOAc (3 mL). The solution was passed through a preconditioned (EtOAc, 10 mL) C-18 column (1 g) and washed with EtOAc (3 mL) and MeOH (2 mL). The filtrate was collected and blown down under nitrogen at 40 °C.

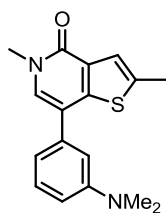
Purification procedure 1:

The resulting residue was purified by MDAP (formic acid). The solvent was evaporated under a stream of nitrogen at 40 °C to give the required product.

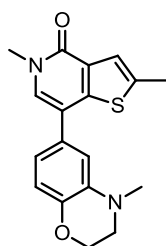
Purification procedure 2:

The resulting residue was purified by MDAP (high pH). The solvent was evaporated under a stream of nitrogen at 40 °C to give the required product.

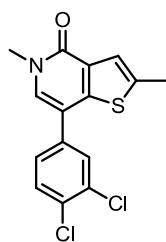
7-(3-(Dimethylamino)phenyl)-2,5-dimethylthieno[3,2-c]pyridin-4(5H)-one (2.068a)



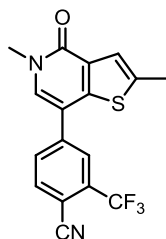
Following General Procedure 1 using **2.074** (39 mg, 0.15 mmol) and (3-(dimethylamino)phenyl)boronic acid (30 mg, 0.18 mmol) gave, following purification using procedure 1, **2.068a** (24 mg, 54%) as a white solid; m.p. 136–137 °C; ν_{max} (solid)/ cm^{-1} : 1645 (C=O), 1589, 769, 692; 1H NMR (400 MHz, $DMSO-d_6$) δ ppm 7.65 (s, 1H), 7.28–7.25 (m, 2H), 6.91–6.86 (m, 2H), 6.76 (dd, $J = 8.3$, 2.0, 1H), 3.57 (s, 3H), 2.96 (s, 6H), 2.52 (d, $J = 1.0$, 3H); ^{13}C NMR (101 MHz, $DMSO-d_6$) δ ppm 157.0, 150.5, 145.5, 138.8, 136.4, 131.3, 128.5, 129.2, 122.3, 115.7, 114.6, 111.5, 110.7, 35.9, 14.9; HRMS ($M + H$) $^+$ calculated for $C_{17}H_{19}N_2O_5S$ 299.1213; found 299.1213; LCMS (formic acid): $R_t = 1.13$ min (100%), $MH^+ = 299.2$.

2,5-Dimethyl-7-(4-methyl-3,4-dihydro-2H-benzo[b][1,4]oxazin-6-yl)thieno[3,2-c]pyridin-4(5H)-one (2.068b)

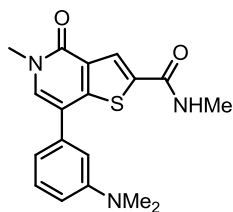
Following General Procedure 1 using **2.074** (30 mg, 0.15 mmol) and 4-methyl-2,3-dihydrobenzo-1,4-oxazine-6-boronic acid, pinacol ester (50 mg, 0.18 mmol) gave, following purification using procedure 1, **2.068b** (22 mg, 45%) as a white solid; $^1\text{H NMR}$ (400 MHz, CD_3OD) δ ppm 7.40 (s, 1H), 7.30 (s, 1H), 6.91–6.86 (m, 1H), 6.83–6.78 (m, 1H), 6.76 (d, $J = 8.1$, 1H), 4.31 (t, $J = 4.3$, 2H), 3.68 (s, 3H), 3.32–3.29 (m, 2H), 2.93 (s, 3H), 2.56 (s, 3H); LCMS (formic acid): $R_t = 1.04$ min (100%), $\text{MH}^+ = 327.1$.

7-(3,4-Dichlorophenyl)-2,5-dimethylthieno[3,2-c]pyridin-4(5H)-one (2.068c)

Following General Procedure 1 using **2.074** (39 mg, 0.15 mmol) and (3,4-dichlorophenyl)boronic acid (34 mg, 0.18 mmol) gave, following purification using procedure 1, **2.068c** (3 mg, 6%) as a white solid; $^1\text{H NMR}$ (400 MHz, DMSO-d_6) δ ppm 7.89–7.88 (m, 1H), 7.83 (s, 1H), 7.78 (d, $J = 8.3$, 1H), 7.65 (dd, $J = 8.3, 1.7$, 1H), 7.32–7.30 (d, $J = 1.7$, 1H), 3.57 (s, 3H), 2.54 (s, 3H); LCMS (formic acid): $R_t = 1.27$ min (100%), $\text{MH}^+ = 326.0$.

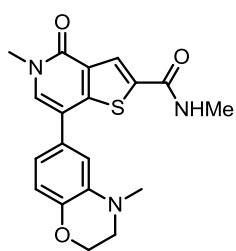
4-(2,5-Dimethyl-4-oxo-4,5-dihydrothieno[3,2-c]pyridin-7-yl)-2-(trifluoromethyl)benzonitrile (2.068d)

Following General Procedure 1 using **2.074** (39 mg, 0.15 mmol) and (4-cyano-3-(trifluoromethyl)phenyl)boronic acid (39 mg, 0.18 mmol) gave, following purification using procedure 1, **2.068d** (3 mg, 6%) as a white solid; $^1\text{H NMR}$ (400 MHz, CD_3OD) δ ppm 8.20 (br.s, 1H), 8.14–8.12 (m, 2H), 7.81 (s, 1H), 7.39–7.37 (m, 1H), 3.73 (s, 3H), 2.60 (d, $J = 1.22$, 3H); LCMS (formic acid): $R_t = 1.13$ min (100%), $\text{MH}^+ = 349.3$.

7-(3-(Dimethylamino)phenyl)-N,5-dimethyl-4-oxo-4,5-dihydrothieno[3,2-c]pyridine-2-carboxamide (2.069a)

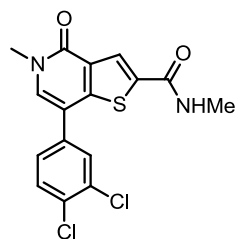
Following General Procedure 1 using **2.017c** (45 mg, 0.15 mmol) and (3-(dimethylamino)phenyl)boronic acid (30 mg, 0.18 mmol) gave, following purification using procedure 1, **2.069a** (14 mg, 27%) as a white solid; $^1\text{H NMR}$ (400 MHz, DMSO-d_6) δ ppm 8.75–8.70 (m, 1H), 8.25 (s, 1H), 7.82 (s, 1H), 7.31 (m, 1H), 6.93–6.88 (m, 2H), 6.79 (dd, $J = 8.3, 2.3$, 1H), 3.60 (s, 3H), 2.97 (s, 6H), 2.78 (d, $J = 4.6$, 3H); LCMS (formic acid): $R_t = 0.72$ min (100%), $\text{MH}^+ = 342.2$.

N,5-Dimethyl-7-(4-methyl-3,4-dihydro-2H-benzo[b][1,4]oxazin-6-yl)-4-oxo-4,5-dihydrothieno[3,2-c]pyridine-2-carboxamide (2.069b)



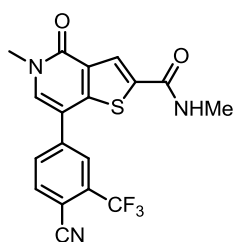
Following General Procedure 1 using **2.017c** (45 mg, 0.15 mmol) and 4-methyl-2,3-dihydrobenzo-1,4-oxazine-6-boronic acid, pinacol ester (50 mg, 0.18 mmol) gave, following purification using procedure 1, **2.069b** (22 mg, 40%) as a white solid; m.p. 200–203 °C; ν_{\max} (solid)/ cm^{-1} : 1643 (C=O), 1590 (C=O), 1511, 1313, 1230; $^1\text{H NMR}$ (400 MHz, DMSO- d_6) δ ppm 8.75–8.69 (m, 1H), 8.23 (s, 1H), 7.72 (s, 1H), 6.87 (d, $J = 2.0$, 1H), 6.84–6.75 (m, 2H), 4.30–4.24 (m, 2H), 3.58 (s, 3H), 3.30–3.27 (m, 2H), 2.89 (s, 3H), 2.78 (d, $J = 4.6$, 3H); $^{13}\text{CNMR}$ (101 MHz, DMSO- d_6) δ ppm 161.2, 157.8, 149.0, 143.7, 138.2, 137.0, 133.6, 129.5, 128.5, 125.1, 116.3, 115.6, 111.2, 64.5, 48.2, 38.2, 36.2, 26.2 (2 signals overlap); HRMS ($M + H$) $^+$ calculated for $\text{C}_{19}\text{H}_{20}\text{N}_3\text{O}_3\text{S}$ 370.1220; found 370.1221; LCMS (formic acid): $R_t = 0.86$ min (100%), $\text{MH}^+ = 370.15$.

7-(3,4-dichlorophenyl)-N,5-dimethyl-4-oxo-4,5-dihydrothieno[3,2-c]pyridine-2-carboxamide (2.069c)



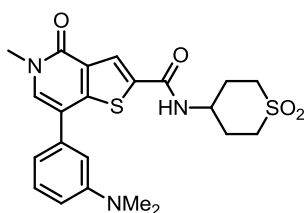
A mixture of **2.017c** (100 mg, 0.33 mmol), (3,4-dichlorophenyl)boronic acid (76 mg, 0.40 mmol), K_2CO_3 (110 mg, 0.80 mmol) and PEPPSI- i -Pr (20 mg, 0.03 mmol) in IPA (1.5 mL) and H_2O (0.5 mL) was heated at 120 °C in a microwave reactor for 0.5 h. The reaction mixture was allowed to cool to rt and diluted with EtOAc (20 mL). The solution was filtered through Celite[®] and concentrated *in vacuo*. The resulting residue was purified by MDAP (formic acid). The appropriate fractions were combined and concentrated *in vacuo* to give **2.069c** (5 mg, 4%) as a white solid; $^1\text{H NMR}$ (400 MHz, DMSO- d_6) 8.78 (m, 1H), 8.27 (s, 1H), 8.00 (s, 1H), 7.91 (d, $J = 2.1$, 1H), 7.81 (d, $J = 8.3$, 1H), 7.69 (dd, $J = 8.3$, 2.1, 1H), 3.60 (s, 3H), 2.79 (d, $J = 4.7$, 3H); LCMS (formic acid): $R_t = 1.03$ min (100%), $\text{MH}^+ = 367.1$.

7-(4-Cyano-3-(trifluoromethyl)phenyl)-*N*,5-dimethyl-4-oxo-4,5-dihydrothieno[3,2-*c*]pyridine-2-carboxamide (2.069d)



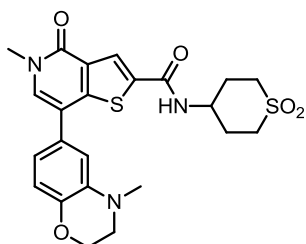
Following General Procedure 1 using **2.017c** (45 mg, 0.15 mmol) and (4-cyano-3-(trifluoromethyl)phenyl)boronic acid (39 mg, 0.18 mmol) gave, following purification using procedure 1, **2.069d** (2 mg, 3%) as a white solid; ^1H NMR (400 MHz, CD_3OD) δ ppm 8.22 (s, 1H), 8.17–8.16 (m, 3H), 7.96 (s, 1H), 3.74 (s, 3H), 2.94 (s, 3H); LCMS (formic acid): R_t = 0.93 min (100%), MH^- = 390.4.

7-(3-(Dimethylamino)phenyl)-*N*-(1,1-dioxidotetrahydro-2H-thiopyran-4-yl)-5-methyl-4-oxo-4,5-dihydrothieno[3,2-*c*]pyridine-2-carboxamide (2.070a)



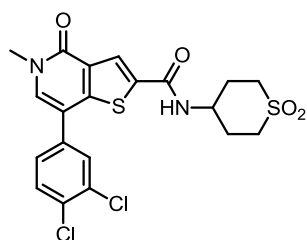
Following General Procedure 1 using **2.075** (63 mg, 0.15 mmol) and (3-(dimethylamino)phenyl)boronic acid (30 mg, 0.18 mmol) gave, following purification using procedure 1, **2.070a** (23 mg, 33%) as a white solid; m.p. 206–208 °C; ν_{max} (solid)/ cm^{-1} : 1628 (C=O), 1586 (C=O), 1291, 1124 (S=O), 844; ^1H NMR (400 MHz, $\text{DMSO}-d_6$) δ ppm 8.70 (d, J = 7.8, 1H), 8.40 (s, 1H), 7.82 (s, 1H), 7.34–7.26 (m, 1H), 6.92–6.86 (m, 2H), 6.79 (dd, J = 8.5, 2.1, 1H), 4.22–4.11 (m, 1H), 3.60 (s, 3H), 3.29–3.24 (m, 2H), 3.19–3.11 (m, 2H), 2.96 (s, 6H), 2.18–2.02 (m, 4H); ^{13}C NMR (101 MHz, $\text{DMSO}-d_6$) δ ppm 160.2, 159.5, 157.9, 150.8, 148.9, 137.8, 136.2, 134.3, 129.5, 125.8, 115.8, 114.8, 112.0, 111.0, 48.5, 44.6, 40.0, 36.3, 29.2; HRMS ($\text{M} + \text{H}$) $^+$ calculated for $\text{C}_{22}\text{H}_{26}\text{N}_3\text{O}_4\text{S}_2$ 460.1359; found 460.1370; LCMS (formic acid): R_t = 0.75 min (100%), MH^+ = 460.2.

***N*-(1,1-Dioxidotetrahydro-2H-thiopyran-4-yl)-5-methyl-7-(4-methyl-3,4-dihydro-2H-benzo[*b*][1,4]oxazin-6-yl)-4-oxo-4,5-dihydrothieno[3,2-*c*]pyridine-2-carboxamide (2.070b)**



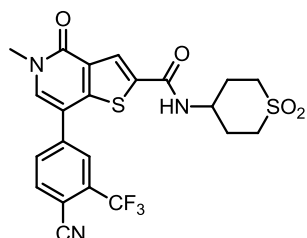
Following General Procedure 1 using **2.075** (63 mg, 0.15 mmol) and 4-methyl-2,3-dihydrobenzo-1,4-oxazine-6-boronic acid, pinacol ester (50 mg, 0.18 mmol) gave, following purification using procedure 1, **2.070b** (24 mg, 33%) as a white solid; ^1H NMR (400 MHz, $\text{DMSO}-d_6$) δ ppm 8.70 (d, J = 7.8, 1H), 8.40 (s, 1H), 7.75 (s, 1H), 6.88 (d, J = 2.0, 1H), 6.83 (dd, J = 8.1, 2.0, 1H), 6.79 (d, J = 8.1, 1H), 4.28 (t, J = 4.4, 2H), 4.22–4.12 (m, 1H), 3.59 (s, 3H), 3.32–3.24 (m, 4H), 3.20–3.12 (m, 2H), 2.90 (s, 3H), 2.19–2.03 (m, 4H); LCMS (formic acid): R_t = 0.84 min (100%), MH^+ = 488.3.

7-(3,4-Dichlorophenyl)-N-(1,1-dioxidotetrahydro-2H-thiopyran-4-yl)-5-methyl-4-oxo-4,5-dihydrothieno[3,2-c]pyridine-2-carboxamide (2.070c)



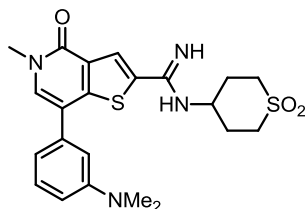
Following General Procedure 1 using **2.075** (63 mg, 0.15 mmol) and (3,4-dichlorophenyl)boronic acid (34 mg, 0.18 mmol) gave, following purification using procedure 1, **2.070c** (7 mg, 10%) as a white solid; ^1H NMR (400 MHz, DMSO- d_6) δ ppm 8.75 (d, $J = 8.1$, 1H), 8.44 (s, 1H), 8.01 (s, 1H), 7.92 (d, $J = 2.2$, 1H), 7.81 (d, $J = 8.3$, 1H), 7.69 (dd, $J = 8.3, 2.2$, 1H), 4.23–4.14 (m, 1H), 3.60 (s, 3H), 3.29–3.25 (m, 2H), 3.19–3.12 (m, 2H), 2.19–2.05 (m, 4H); LCMS (formic acid): $R_t = 1.00$ min (100%), $\text{MH}^+ = 486.3$.

7-(4-Cyano-3-(trifluoromethyl)phenyl)-N-(1,1-dioxidotetrahydro-2H-thiopyran-4-yl)-5-methyl-4-oxo-4,5-dihydrothieno[3,2-c]pyridine-2-carboxamide (2.070d)



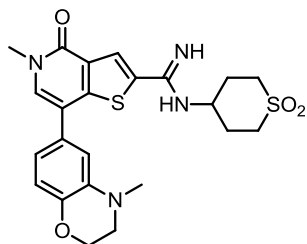
A mixture of **2.075** (100 mg, 0.24 mmol), (4-cyano-3-(trifluoromethyl)phenyl)boronic acid (62 mg, 0.29 mmol), K_2CO_3 (79 mg, 0.57 mmol) and PEPPSI- i Pr (15 mg, 0.02 mmol) in IPA (1.5 mL) and H_2O (0.5 mL) was heated at 120 °C in a microwave reactor for 0.5 h. The reaction mixture was allowed to cool to rt and diluted with EtOAc (50 mL). The solution was filtered through Celite[®] and concentrated *in vacuo*. The resulting residue was purified by MDAP (formic acid). The appropriate fractions were combined and concentrated *in vacuo* to give **2.070d** (11 mg, 9%) as a white solid; ^1H NMR (400 MHz, DMSO- d_6) δ ppm 8.78 (d, $J = 8.0$, 1H), 8.46 (s, 1H), 8.34 (d, $J = 8.0$, 1H), 8.27–8.20 (m, 3H), 4.25–4.15 (m, 1H), 3.63 (s, 3H), 3.30–3.25 (m, 2H), 3.19–3.11 (m, 2H), 2.21–2.04 (m, 4H); LCMS (formic acid): $R_t = 0.94$ min (100%), $\text{MH}^- = 508.5$

7-(3-(Dimethylamino)phenyl)-N-(1,1-dioxidotetrahydro-2H-thiopyran-4-yl)-5-methyl-4-oxo-4,5-dihydrothieno[3,2-c]pyridine-2-carboximidamide (2.071a)



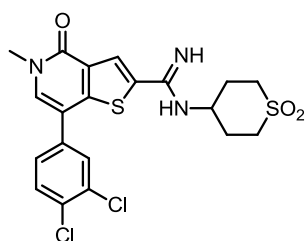
Following General Procedure 1 using **2.064** (63 mg, 0.15 mmol) and (3-(dimethylamino)phenyl)boronic acid (30 mg, 0.18 mmol) gave, following purification using procedure 2, **2.071a** (3 mg, 4%) as a white solid; ^1H NMR (400 MHz, CD_3OD) δ ppm 7.98 (s, 1H), 7.62 (s, 1H), 7.33 (m, 1H), 7.01–6.98 (m, 1H), 6.94 (d, $J = 8.2$, 1H), 6.85 (dd, $J = 8.2, 2.6$, 1H), 3.78–3.74 (m, 1H), 3.72 (s, 3H), 3.31–3.25 (m, 2H), 3.16–3.08 (m, 2H), 3.02 (s, 6H), 2.28–2.13 (m, 4H); LCMS (formic acid): $R_t = 0.91$ min (100%), $\text{MH}^+ = 459.4$.

***N*-(1,1-Dioxidotetrahydro-2H-thiopyran-4-yl)-5-methyl-7-(4-methyl-3,4-dihydro-2H-benzo[*b*][1,4]oxazin-6-yl)-4-oxo-4,5-dihydrothieno[3,2-*c*]pyridine-2-carboximidamide (2.071b)**



Following General Procedure 1 using **2.064** (63 mg, 0.15 mmol) and 4-methyl-2,3-dihydrobenzo-1,4-oxazine-6-boronic acid, pinacol ester (50 mg, 0.18 mmol) gave, following purification using procedure 2, **2.071b** (5 mg, 7%) as a white solid; $^1\text{H NMR}$ (400 MHz, CD_3OD) δ ppm 7.97 (s, 1H), 7.55 (s, 1H), 6.93 (d, $J = 2.0$, 1H), 6.85 (dd, $J = 8.2, 2.0$, 1H), 6.80 (d, $J = 8.2$, 1H), 4.33 (t, $J = 4.4$, 2H), 3.78–3.72 (m, 1H), 3.71 (s, 3H), 3.31–3.25 (m, 4H), 3.18–3.09 (m, 2H), 2.95 (s, 3H), 2.29–2.14 (m, 4H); LCMS (formic acid): $R_t = 0.66$ min (100%), $\text{MH}^+ = 487.2$.

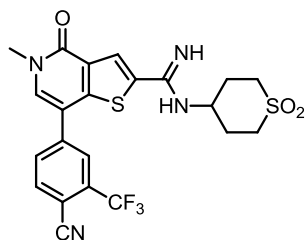
7-(3,4-Dichlorophenyl)-*N*-(1,1-dioxidotetrahydro-2H-thiopyran-4-yl)-5-methyl-4-oxo-4,5-dihydrothieno[3,2-*c*]pyridine-2-carboximidamide (2.071c)



A mixture of **2.064** (100 mg, 0.24 mmol), (3,4-dichlorophenyl)boronic acid (65 mg, 0.34 mmol), $\text{Pd}(\text{PPh}_3)_4$ (14 mg, 0.01 mmol) and K_2CO_3 (79 mg, 0.57 mmol) in H_2O (1 mL) and IPA (3 mL) was heated at 120 °C in a microwave reactor for 0.5 h. The reaction mixture was allowed to cool to rt and diluted with EtOAc (40 mL). The solution was filtered through Celite[®] and concentrated *in vacuo*. The resulting residue was purified by MDAP (formic acid). The appropriate fractions were combined and concentrated *in vacuo*. The resulting residue was dissolved in MeOH (5 mL) and passed through a preconditioned (MeOH, 20 mL) amino propyl column (10 g). The appropriate fractions were combined and concentrated *in vacuo*. The resulting solid was suspended in Et_2O (10 mL), filtered under reduced pressure, rinsed with Et_2O (20 mL), collected and dried under vacuum at 40 °C to give **2.071c** (16 mg, 14%) as a white solid; $^1\text{H NMR}$ (400 MHz, DMSO-d_6) δ ppm 8.14 (s, 1H), 7.89 (s, 1H), 7.88 (d, $J = 2.2$, 1H), 7.80 (d, $J = 8.4$, 1H), 7.68 (dd, $J = 8.2, 2.2$, 1H), 6.76 (br.s, 2H), 3.62–3.57 (m, 4H), 3.21–3.12 (m, 2H), 3.10–3.01 (m, 2H), 2.06–1.96 (m, 2H), 1.95–1.86 (m, 2H); LCMS (formic acid): $R_t = 0.80$ min (100%), $\text{MH}^+ = 484.0$.

7-(4-Cyano-3-(trifluoromethyl)phenyl)-N-(1,1-dioxidotetrahydro-2H-thiopyran-4-yl)-5-methyl-4-oxo-4,5-dihydrothieno[3,2-c]pyridine-2-carboximidamide

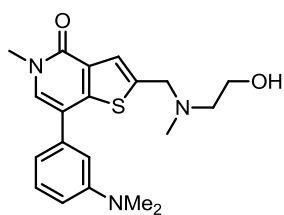
(2.071d)



A mixture of **2.064** (500 mg, 0.72 mmol), (4-cyano-3-(trifluoromethyl)phenyl)boronic acid (185 mg, 0.86 mmol), PEPPSI-*i*-Pr (44 mg, 0.07 mmol) and K_2CO_3 (238 mg, 1.72 mmol) in H_2O (1 mL) and IPA (3 mL) was heated to 120 °C in a microwave reactor for 0.5 h. The reaction mixture was allowed to cool to rt, diluted with EtOAc (40 mL), filtered through Celite[®] and concentrated *in vacuo*. The resulting residue was purified by MDAP (formic acid). The appropriate fractions were combined and concentrated *in vacuo*. The resulting residue was dissolved in MeOH (5 mL) and passed through a preconditioned (MeOH, 30 mL) amino propyl column (50 g). The appropriate fractions were combined and concentrated *in vacuo*. The resulting solid was suspended in Et_2O (20 mL), filtered under reduced pressure, rinsed with Et_2O (20 mL), collected and dried under vacuum at 40 °C to give **2.071d** (123 mg, 34%) as a white solid; 1H NMR (400 MHz, $DMSO-d_6$) δ ppm 8.33 (d, $J = 7.8$, 1H), 8.25–8.21 (m, 2H), 8.17 (s, 1H), 8.11 (s, 1H), 6.81 (br.s, 2H), 3.64–3.57 (m, 4H), 3.22–3.12 (m, 2H), 3.10–3.01 (m, 2H), 2.07–1.98 (m, 2H), 1.96–1.86 (m, 2H); LCMS (formic acid): $R_t = 0.93$ min (100%), $MH^+ = 509.3$.

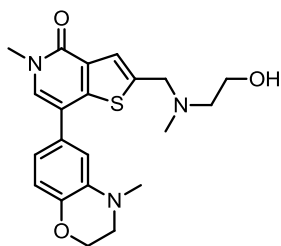
N.B. The synthesis of **2.071d** was originally carried out as part of the square array.

7-(3-(Dimethylamino)phenyl)-2-(((2-hydroxyethyl)(methyl)amino)methyl)-5-methylthieno[3,2-c]pyridin-4(5H)-one (2.072a)



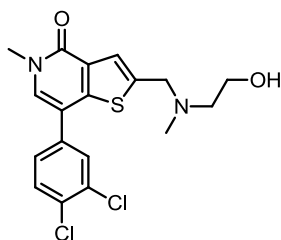
Following General Procedure 1 using **2.056b** (50 mg, 0.15 mmol) and (3-(dimethylamino)phenyl)boronic acid (30 mg, 0.18 mmol) gave, following purification using procedure 2, **2.072a** (5 mg, 9%) as a white solid; 1H NMR (400 MHz, CD_3OD) δ ppm 7.53–7.48 (m, 2H), 7.31 (s, 1H), 6.99–6.96 (m, 1H), 6.91 (d, $J = 7.6$, 1H), 6.85–6.80 (m, 1H), 3.88–3.85 (m, 2H), 3.71–3.66 (m, 5H), 3.00 (s, 6H), 2.62 (t, $J = 6.1$, 2H), 2.34 (s, 3H); LCMS (formic acid): $R_t = 0.93$ min (100%), $MH^+ = 372.4$.

2-(((2-Hydroxyethyl)(methyl)amino)methyl)-5-methyl-7-(4-methyl-3,4-dihydro-2H-benzo[b][1,4]oxazin-6-yl)thieno[3,2-c]pyridin-4(5H)-one (2.072b)



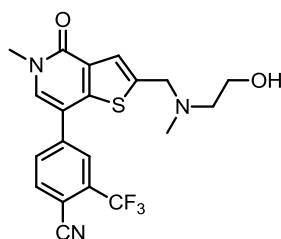
Following General Procedure 1 using **2.056b** (50 mg, 0.15 mmol) and 4-methyl-2,3-dihydrobenzo-1,4-oxazine-6-boronic acid, pinacol ester (50 mg, 0.18 mmol) gave, following purification using procedure 2, **2.072b** (35 mg, 58%) as a white solid; ¹H NMR (400 MHz, CD₃OD) δ ppm 7.48 (s, 1H), 7.44–7.41 (m, 1H), 6.91–6.88 (m, 1H), 6.84–6.74 (m, 2H), 4.33–4.28 (m, 2H), 3.87–3.84 (m, 2H), 3.70–3.65 (m, 5H), 3.31–3.28 (m, 2H), 2.92 (s, 3H), 2.61 (t, *J* = 6.0, 2H), 2.33 (s, 3H); LCMS (formic acid): *R*_t = 0.63 min (99%), *MH*⁺ = 400.3.

7-(3,4-Dichlorophenyl)-2-(((2-hydroxyethyl)(methyl)amino)methyl)-5-methylthieno[3,2-c]pyridin-4(5H)-one (2.072c)



Following General Procedure 1 using **2.056b** (50 mg, 0.15 mmol) and (3,4-dichlorophenyl)boronic acid (34 mg, 0.18 mmol) gave, following purification using procedure 2, **2.072c** (11 mg, 18%) as a white solid; ¹H NMR (400 MHz, CD₃OD) δ ppm 7.83–7.80 (m, 1H), 7.67–7.63 (m, 2H), 7.61–7.57 (m, 1H), 7.53–7.50 (m, 1H), 3.89–3.87 (m, 2H), 3.72–3.66 (m, 5H), 2.62 (t, *J* = 6.0, 2H), 2.35 (s, 3H); LCMS (high pH): *R*_t = 1.07 min (100%), *MH*⁺ = 397.3.

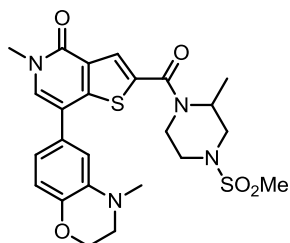
4-(2-(((2-Hydroxyethyl)(methyl)amino)methyl)-5-methyl-4-oxo-4,5-dihydrothieno[3,2-c]pyridin-7-yl)-2-(trifluoromethyl)benzonitrile (2.072d)



A mixture of **2.056b** (80 mg, 0.24 mmol), (4-cyano-3-(trifluoromethyl)phenyl)boronic acid (62 mg, 0.29 mmol), K₂CO₃ (80 mg, 0.58 mmol) and PEPPSI-*i*Pr (15 mg, 0.022 mmol) in IPA (1.5 mL) and H₂O (0.5 mL) was heated at 120 °C in a microwave reactor for 0.5 h. The reaction mixture was allowed to cool to rt and diluted with EtOAc (20 mL). The solution was filtered through Celite[®], passed through a hydrophobic frit and concentrated *in vacuo*. The resulting residue was purified by MDAP (formic acid). The resulting residue was dissolved in MeOH (5 mL) and passed through a preconditioned (MeOH, 20 mL) amino propyl column (10 g). The appropriate fractions were combined and solvent evaporated *in vacuo* to give **2.072d** (53 mg, 52%) as a pale yellow solid; ¹H NMR (400 MHz, CD₃OD) 8.21 (br.s, 1H), 8.17–8.12 (m, 2H), 7.85 (s,

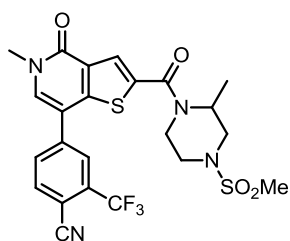
1H), 7.56–7.54 (m, 1H), 3.92–3.89 (m, 2H), 3.74 (s, 3H), 3.69 (t, $J = 6.0$, 2H), 2.63 (t, $J = 6.0$, 2H), 2.36 (s, 3H); LCMS (high pH): $R_t = 0.95$ min (100%), $MH^+ = 422.4$.

5-Methyl-7-(4-methyl-3,4-dihydro-2H-benzo[b][1,4]oxazin-6-yl)-2-(2-methyl-4-(methylsulfonyl)piperazine-1-carbonyl)thieno[3,2-c]pyridin-4(5H)-one (2.073b)



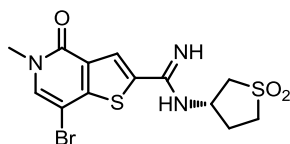
Following General Procedure 1 using **2.078** (67 mg, 0.15 mmol) and 4-methyl-2,3-dihydrobenzo-1,4-oxazine-6-boronic acid, pinacol ester (30 mg, 0.18 mmol) gave, following purification using procedure 1, **2.073b** (11 mg, 14%) as a white solid; 1H NMR (400 MHz, CD_3OD) δ ppm 7.89 (s, 1H), 7.61 (s, 1H), 6.93 (d, $J = 1.8$, 1H), 6.85 (dd, $J = 8.2, 1.8$, 1H), 6.80 (d, $J = 8.2$, 1H), 4.42–4.36 (m, 1H), 4.33 (t, $J = 4.4$, 2H), 3.78–3.73 (m, 1H), 3.72 (s, 3H), 3.61–3.56 (m, 1H), 3.55–3.46 (m, 1H), 3.09–3.03 (m, 1H), 2.98–2.85 (m, 8H) 1.46 (d, $J = 6.9$, 3H) N.B. 2H signal hidden under solvent peak; LCMS (formic acid): $R_t = 0.90$ min (100%), $MH^+ = 517.3$.

4-(5-Methyl-2-(2-methyl-4-(methylsulfonyl)piperazine-1-carbonyl)-4-oxo-4,5-dihydrothieno[3,2-c]pyridin-7-yl)-2-(trifluoromethyl)benzonitrile (2.073d)



Following General Procedure 1 using **2.078** (67 mg, 0.15 mmol) and (4-cyano-3-(trifluoromethyl)phenyl)boronic acid (39 mg, 0.18 mmol) gave, following purification using procedure 1, **2.073d** (16 mg, 20%) as a white solid; 1H NMR (400 MHz, CD_3OD) δ ppm 8.23–8.21 (m, 1H), 8.16–8.14 (m, 2H), 7.98 (s, 1H), 7.92 (s, 1H), 4.42–4.35 (m, 1H), 3.79–3.72 (m, 4H), 3.61–3.56 (m, 1H), 3.54–3.47 (m, 1H), 3.10–3.04 (m, 1H), 2.97–2.92 (m, 1H), 2.98–2.90 (m, 1H), 2.89 (s, 3H), 1.46 (d, $J = 6.9$, 3H); LCMS (formic acid): $R_t = 1.00$ min (100%), $MH^+ = 539.1$.

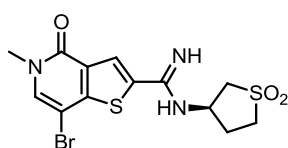
(S)-7-Bromo-N-(1,1-dioxidotetrahydrothiophen-3-yl)-5-methyl-4-oxo-4,5-dihydrothieno[3,2-c]pyridine-2-carboximidamide (2.080a)



To a suspension of **2.062** (100 mg, 0.37 mmol) in MeOH (20 mL), NaOMe (25% solution in MeOH) (0.1 mL, 0.37 mmol) was added. The reaction mixture was left to stir at 75 °C for 0.5 h. (S)-3-aminotetrahydrothiophene-1,1-dioxide hydrochloride (96 mg, 0.56 mmol) was added and the mixture was left to stir for 18 h at 75 °C. (S)-3-aminotetrahydrothiophene-1,1-dioxide hydrochloride (96 mg, 0.56 mmol) was added and the reaction mixture was stirred for a further 5 h at 75 °C. The volatile

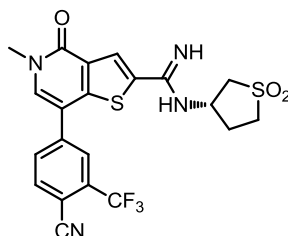
components were removed *in vacuo* and the resulting solid was suspended in MeOH (50 mL), filtered under reduced pressure, washed with MeOH (50 mL), collected and dried under vacuum at 40 °C to give **2.080a** (98 mg, 65%) as a white solid; ¹H NMR (400 MHz, DMSO-d₆) δ ppm 8.19 (s, 1H), 7.99 (s, 1H), 6.90 (br.s, 2H), 4.30–4.23 (m, 1H), 3.51 (s, 3H), 3.48–3.40 (m, 1H), 3.30–3.25 (m, 1H), 3.10–3.01 (m, 1H), 2.83–2.75 (m, 1H), 2.40–2.32 (m, 1H), 2.04–1.94 (m, 1H); LCMS (formic acid): R_t = 0.46 min (81%), MH⁺ = 404.0, 406.0.

(R)-7-Bromo-N-(1,1-dioxidotetrahydrothiophen-3-yl)-5-methyl-4-oxo-4,5-dihydrothieno[3,2-c]pyridine-2-carboximidamide (2.080b)



To a suspension of **2.062** (100 mg, 0.37 mmol) in MeOH (20 mL), NaOMe (25% solution in MeOH) (0.1 mL, 0.37 mmol) was added. The reaction mixture was left to stir at 75 °C for 0.5 h. (*R*)-3-aminotetrahydrothiophene-1,1-dioxide hydrochloride (191 mg, 1.12 mmol) was added and the mixture was left to stir for a 18 h at 75 °C. (*R*)-3-aminotetrahydrothiophene-1,1-dioxide hydrochloride (191 mg, 1.12 mmol) was added and the reaction mixture was stirred for a further 48 h at 75 °C. The volatile components were removed *in vacuo* and the resulting solid was suspended in MeOH (50 mL), filtered under reduced pressure and washed with MeOH (50 mL). The resulting filtrate was concentrated *in vacuo*. The resulting solid was suspended in DCM (50 mL), filtered under reduced pressure, washed with DCM (50 mL), collected and dried to give **2.080b** (126 mg, 71%) as a pale yellow solid; ¹H NMR (400 MHz, DMSO-d₆) δ ppm 8.19 (s, 1H), 7.99 (s, 1H), 6.90 (br.s, 2H), 4.30–4.23 (m, 1H), 3.51 (s, 3H), 3.48–3.40 (m, 1H), 3.30–3.25 (m, 1H), 3.10–3.01 (m, 1H), 2.83–2.75 (m, 1H), 2.40–2.32 (m, 1H), 2.04–1.94 (m, 1H); LCMS (formic acid): R_t = 0.45 min (92%), MH⁺ = 404.0, 406.0.

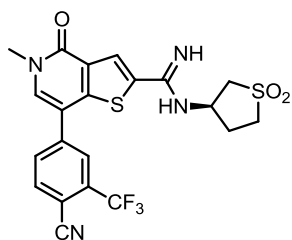
(S)-7-(4-Cyano-3-(trifluoromethyl)phenyl)-N-(1,1-dioxidotetrahydrothiophen-3-yl)-5-methyl-4-oxo-4,5-dihydrothieno[3,2-c]pyridine-2-carboximidamide (2.079a)



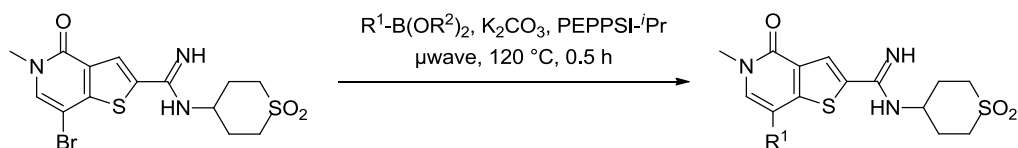
A mixture of **2.080a** (98 mg, 0.24 mmol), (4-cyano-3-(trifluoromethyl)phenyl)boronic acid (63 mg, 0.29 mmol), PEPPSI-*i*-Pr (15 mg, 0.02 mmol) and K₂CO₃ (80 mg, 0.58 mmol) in H₂O (1 mL) and IPA (3 mL) was heated at 120 °C in a microwave reactor for 0.5 h. The reaction mixture was allowed to cool to rt and diluted with EtOAc (40 mL). The solution was

filtered through Celite[®] and concentrated *in vacuo*. The resulting residue was purified by MDAP (formic acid). The appropriate fractions were combined and concentrated *in vacuo*. The resulting residue was dissolved in MeOH (5 mL) and passed through a preconditioned (MeOH, 20 mL) amino propyl column (10 g). The appropriate fractions were combined and concentrated *in vacuo* to give **2.079a** (17 mg, 14%) as a white solid; ¹H NMR (400 MHz, DMSO-d₆) δ ppm 8.33 (d, *J* = 7.8, 1H), 8.24–8.21 (m, 2H), 8.20 (s, 1H), 8.11 (s, 1H), 6.91 (br.s, 2H), 4.29–4.20 (m, 1H), 3.61 (s, 3H), 3.49–3.42 (m, 1H), 3.29–3.22 (m, 1H), 3.08–2.99 (m, 1H), 2.80–2.71 (m, 1H), 2.40–2.31 (m, 1H), 2.01–1.88 (m, 1H); LCMS (formic acid): R_t = 0.72 min (100%), MH⁺ = 495.1.

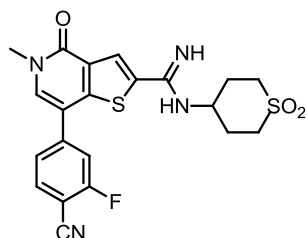
(R)-7-(4-Cyano-3-(trifluoromethyl)phenyl)-N-(1,1-dioxidotetrahydrothiophen-3-yl)-5-methyl-4-oxo-4,5-dihydrothieno[3,2-c]pyridine-2-carboximidamide (2.079b)



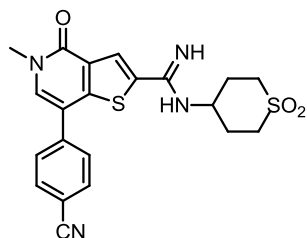
A mixture of **2.080b** (126 mg, 0.27 mmol), (4-cyano-3-(trifluoromethyl)phenyl)boronic acid (68 mg, 0.32 mmol), PEPPSI-*i*-Pr (16 mg, 0.02 mmol) and K₂CO₃ (88 mg, 0.64 mmol) in H₂O (1 mL) and IPA (3 mL) was heated at 120 °C in a microwave reactor for 0.5 h. The reaction mixture was allowed to cool to rt, diluted with EtOAc (40 mL), filtered through Celite[®] and concentrated *in vacuo*. The resulting residue was purified by MDAP (formic acid). The appropriate fractions were combined and concentrated *in vacuo*. The resulting residue was dissolved in MeOH (5 mL) and passed through a preconditioned (MeOH, 20 mL) amino propyl column (10 g). The appropriate fractions were combined and concentrated *in vacuo* to give **2.079b** (10 mg, 8%) as a white solid; ¹H NMR (400 MHz, DMSO-d₆) δ ppm 8.33 (d, *J* = 7.8, 1H), 8.24–8.21 (m, 2H), 8.20 (s, 1H), 8.11 (s, 1H), 6.91 (br.s, 2H), 4.29–4.20 (m, 1H), 3.61 (s, 3H), 3.49–3.42 (m, 1H), 3.29–3.22 (m, 1H), 3.08–2.99 (m, 1H), 2.80–2.71 (m, 1H), 2.40–2.31 (m, 1H), 2.01–1.88 (m, 1H); LCMS (formic acid): R_t = 0.71 min (100%), MH⁺ = 495.1.

General Procedure 2: Synthesis of amidine array compounds

A mixture of **2.064** (63 mg, 0.15 mmol, 1.0 eq.), boronic acid/ester (0.18 mmol, 1.2 eq.), K_2CO_3 (50 mg, 0.36 mmol, 2.4 eq.) and PEPPSI- ᵀPr (9 mg, 0.01 mmol, 0.09 eq.) in H_2O (0.3 mL) and IPA (0.9 mL) was heated at 120 °C in a microwave reactor for 0.5 h. The reaction mixture was allowed to cool to rt and diluted with EtOAc (3 mL). The solution was passed through a preconditioned (EtOAc, 5 mL) C-18 column (1 g) and rinsed with EtOAc (3 mL) and MeOH (2 mL). The filtrate was collected and blown down under nitrogen at 40 °C. The resulting residue was purified by MDAP (formic acid). The solvent was evaporated under a stream of nitrogen at 40 °C. The resulting residue was dissolved in MeOH (5 mL) and passed through a preconditioned (MeOH, 20 mL) amino propyl column (10 g). The appropriate fractions were combined and solvent evaporated *in vacuo* to give the required product.

7-(4-Cyano-3-fluorophenyl)-N-(1,1-dioxidotetrahydro-2H-thiopyran-4-yl)-5-methyl-4-oxo-4,5-dihydrothieno[3,2-c]pyridine-2-carboximidamide (2.081a)


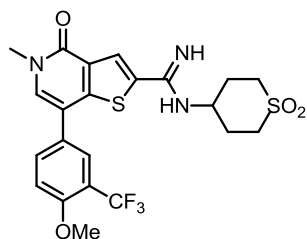
Following General Procedure 2 using 4-cyano-3-fluorophenylboronic acid (30 mg, 0.18 mmol), gave **2.081a** (10 mg, 14%) as an off white solid; 1H NMR (400 MHz, $DMSO-d_6$) δ ppm 8.17 (s, 1H), 8.12–8.07 (m, 1H), 8.04 (s, 1H), 7.83 (d, $J = 9.6$, 1H), 7.75 (dd, $J = 9.6, 1.6$, 1H), 6.80 (br.s, 2H), 3.63–3.57 (m, 4H), 3.22–3.13 (m, 2H), 3.12–3.03 (m, 2H), 2.06–1.97 (m, 2H), 1.96–1.86 (m, 2H); LCMS (formic acid): $R_t = 0.63$ min (100%), $MH^+ = 459.1$.

7-(4-Cyanophenyl)-N-(1,1-dioxidotetrahydro-2H-thiopyran-4-yl)-5-methyl-4-oxo-4,5-dihydrothieno[3,2-c]pyridine-2-carboximidamide (2.081b)


Following General Procedure 2 using 4-cyanophenylboronic acid (26 mg, 0.18 mmol), gave **2.081b** (18 mg, 26%) as an off white solid; 1H NMR (400 MHz, $DMSO-d_6$) δ ppm 8.16 (s, 1H), 8.00 (d, $J = 8.5$, 2H), 7.94 (s, 1H), 7.86 (d, $J = 8.5$, 2H), 6.77 (br.s, 2H), 3.63–3.58 (m,

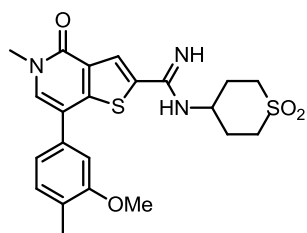
4H), 3.21–3.13 (m, 2H), 3.10–3.01 (m, 2H), 2.05–1.97 (m, 2H), 1.96–1.86 (m, 2H); LCMS (formic acid): $R_t = 0.59$ min (100%), $MH^+ = 474.3$.

***N*-(1,1-Dioxidotetrahydro-2H-thiopyran-4-yl)-7-(4-methoxy-3-(trifluoromethyl)phenyl)-5-methyl-4-oxo-4,5-dihydrothieno[3,2-*c*]pyridine-2-carboximidamide (2.081c)**



Following General Procedure 2 using (4-methoxy-3-trifluoromethylphenyl)boronic acid (40 mg, 0.18 mmol) gave, **2.081c** (32 mg, 40%) as a white solid; 1H NMR (400 MHz, DMSO- d_6) δ ppm 8.14 (s, 1H), 7.93 (dd, $J = 8.6, 2.3, 1H$), 7.80 (s, 1H), 7.79 (d, $J = 2.3, 1H$), 7.44 (d, $J = 8.6, 1H$), 6.75 (br.s, 2H), 3.97 (s, 3H), 3.64–3.57 (m, 4H), 3.21–3.12 (m, 2H), 3.10–3.01 (m, 2H), 2.06–1.97 (m, 2H), 1.96–1.87 (m, 2H); LCMS (formic acid): $R_t = 0.77$ min (100%), $MH^+ = 514.2$.

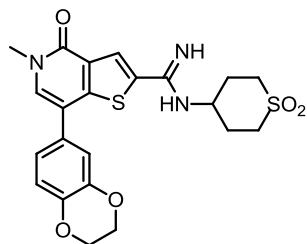
***N*-(1,1-Dioxidotetrahydro-2H-thiopyran-4-yl)-7-(3-methoxy-4-methylphenyl)-5-methyl-4-oxo-4,5-dihydrothieno[3,2-*c*]pyridine-2-carboximidamide (2.081d)**



Following General Procedure 2 using (3-methoxy-4-methylphenyl)boronic acid gave (30 mg, 0.18 mmol), **2.081d** (35 mg, 48%) as a white solid; m.p. 185–186 °C; ν_{max} (solid)/ cm^{-1} : 1637 (C=O), 1592 (C=N), 1251, 1119 (S=O); 1H NMR (400 MHz, DMSO- d_6) δ ppm 8.12 (s, 1H), 7.75 (s, 1H), 7.27 (d, $J = 7.8, 1H$), 7.15–7.09 (m, 2H), 6.73 (br.s, 2H), 3.85 (s, 3H), 3.65–3.56 (m, 4H), 3.23–3.15 (m, 2H), 3.07–2.97 (m, 2H), 2.20 (s, 3H), 2.06–1.96 (m, 2H), 1.95–1.86 (m, 2H); ^{13}C NMR (101 MHz, DMSO- d_6) δ ppm 157.7, 157.6, 149.2, 148.0, 141.8, 134.7, 133.3, 130.7, 129.6, 125.3, 122.4, 118.9, 115.3, 109.6, 55.3, 49.0, 48.4, 36.2, 30.1, 15.7; HRMS ($M + H$) $^+$ calculated for $C_{22}H_{26}N_3O_4S_2$ 460.1359; found 460.1346; LCMS (formic acid): $R_t = 0.71$ min (99%), $MH^+ = 460.2$.

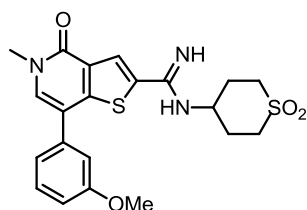
7-(2,3-Dihydrobenzo[b][1,4]dioxin-6-yl)-N-(1,1-dioxidotetrahydro-2H-thiopyran-4-yl)-5-methyl-4-oxo-4,5-dihydrothieno[3,2-c]pyridine-2-carboximidamide

(2.081e)



Following General Procedure 2 using 1,4-benzodioxane-6-boronic acid (32 mg, 0.18 mmol) gave, **2.081e** (32 mg, 43%) as a white solid; m.p. 237–240 °C; ν_{\max} (solid)/ cm^{-1} : 1636 (C=O), 1592 (C=N), 1254, 1124 (S=O), 1065, 854; ^1H NMR (400 MHz, DMSO-d_6) δ ppm 8.12 (s, 1H), 7.67 (s, 1H), 7.11–7.06 (m, 2H), 7.00 (d, $J = 8.1$, 1H), 6.72 (br.s, 2H), 4.31 (s, 4H), 3.64–3.58 (m, 1H), 3.57 (s, 3H), 3.22–3.13 (m, 2H), 3.10–3.01 (m, 2H), 2.07–1.97 (m, 2H), 1.96–1.87 (m, 2H); ^{13}C NMR (101 MHz, DMSO-d_6) δ ppm 157.6, 149.3, 147.9, 143.6, 143.2, 141.6, 133.2, 129.5, 128.9, 122.5, 120.3, 117.5, 115.9, 114.7, 64.1, 49.5, 48.6, 40.4, 36.2, 30.1; HRMS ($\text{M} + \text{H}$) $^+$ calculated for $\text{C}_{22}\text{H}_{23}\text{N}_3\text{O}_5\text{S}_2$ 474.1152; found 474.1160; LCMS (formic acid): $R_t = 0.61$ min (95%), $\text{MH}^+ = 474.20$.

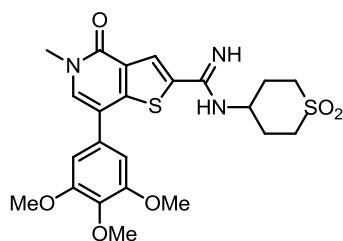
N-(1,1-Dioxidotetrahydro-2H-thiopyran-4-yl)-7-(3-methoxyphenyl)-5-methyl-4-oxo-4,5-dihydrothieno[3,2-c]pyridine-2-carboximidamide (2.081f)



Following General Procedure 2 using (3-methoxyphenyl)boronic acid (27 mg, 0.18 mmol) gave, **2.081f** (5 mg, 7%) as a white solid; ^1H NMR (400 MHz, DMSO-d_6) δ ppm 8.13 (s, 1H), 7.79 (s, 1H), 7.47–7.42 (m, 1H), 7.24–7.20 (m, 1H), 7.17–7.15 (m, 1H), 7.00 (dd, $J = 8.3, 2.3$, 1H), 6.74 (br.s, 2H), 3.83 (s, 3H), 3.64–3.57 (m, 4H), 3.22–3.13 (m, 2H), 3.09–3.00 (m, 2H), 2.06–1.96 (m, 2H), 1.96–1.86 (m, 2H); LCMS (formic acid): $R_t = 0.63$ min (98%), $\text{MH}^+ = 446.3$.

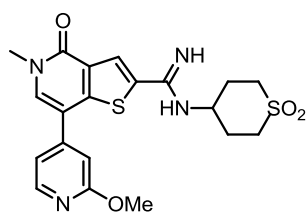
N-(1,1-Dioxidotetrahydro-2H-thiopyran-4-yl)-5-methyl-4-oxo-7-(3,4,5-trimethoxyphenyl)-4,5-dihydrothieno[3,2-c]pyridine-2-carboximidamide (2.081g)

(2.081g)



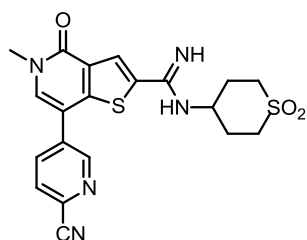
Following General Procedure 2 using (3,4,5-trimethoxyphenyl)boronic acid (38 mg, 0.18 mmol) gave, **2.081g** (15 mg, 19%) as a white solid; ^1H NMR (400 MHz, DMSO-d_6) δ ppm 8.12 (s, 1H), 7.78 (s, 1H), 6.92 (s, 2H), 6.75 (br.s, 2H), 3.84 (s, 6H), 3.73 (s, 3H), 3.67–3.61 (m, 1H), 3.59 (s, 3H), 3.26–3.17 (m, 2H), 3.07–2.98 (m, 2H), 2.06–1.97 (m, 2H), 1.96–1.88 (m, 2H); LCMS (formic acid): $R_t = 0.61$ min (95%), $\text{MH}^+ = 506.3$.

***N*-(1,1-Dioxidotetrahydro-2H-thiopyran-4-yl)-7-(2-methoxypyridin-4-yl)-5-methyl-4-oxo-4,5-dihydrothieno[3,2-*c*]pyridine-2-carboximidamide (2.081h)**



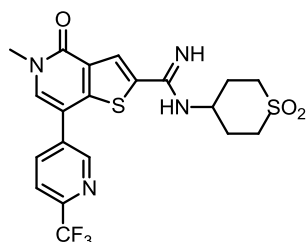
Following General Procedure 2 using 2-methoxypyridine-4-boronic acid (28 g, 0.18 mmol) gave, **2.081h** (20 mg, 28%) as a white solid; m.p. 186–188 °C; ν_{\max} (solid)/ cm^{-1} : 1641 (C=N), 1590, 1397, 1266, 1108 (S=O); ^1H NMR (400 MHz, DMSO- d_6) δ ppm 8.29 (d, J = 5.5, 1H), 8.15 (s, 1H), 8.00 (s, 1H), 7.29 (dd, J = 5.5, 1.3, 1H), 7.07 (d, J = 1.3, 1H), 6.77 (br.s, 2H), 3.92 (s, 3H), 3.64–3.57 (m, 4H), 3.21–3.13 (m, 2H), 3.11–3.02 (m, 2H), 2.08–1.98 (m, 2H), 1.97–1.90 (m, 2H); ^{13}C NMR (101 MHz, DMSO- d_6) δ ppm 164.3, 157.7, 149.2, 147.7, 146.4, 146.3, 141.8, 135.2, 129.9, 122.4, 115.4, 112.3, 107.9, 53.3, 49.5, 48.6, 36.4, 30.1; HRMS ($M + H$) $^+$ calculated for $\text{C}_{20}\text{H}_{22}\text{N}_4\text{O}_4\text{S}_2$ 447.1155; found 447.1153; LCMS (formic acid): R_t = 0.56 min (100%), MH^+ 447.2.

***N*-(1,1-Dioxidotetrahydro-2H-thiopyran-4-yl)-5-methyl-4-oxo-4,5-dihydrothieno[3,2-*c*]pyridine-2-carboximidamide (2.081i)**

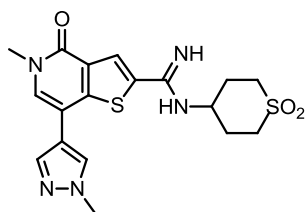


Following General Procedure 2 using 2-cyanopyridine-5-boronic acid (41 mg, 0.18 mmol) gave, **2.081i** (10 mg, 14%) as an off white solid; ^1H NMR (400 MHz, DMSO- d_6) δ ppm 9.04 (d, J = 2.0, 1H), 8.36 (dd, J = 8.2, 2.0, 1H), 8.19 (d, J = 8.2, 1H), 8.17 (s, 1H), 8.07 (s, 1H), 6.79 (br.s, 2H), 3.63–3.58 (m, 4H), 3.22–3.13 (m, 2H), 3.10–3.01 (m, 2H), 2.06–1.97 (m, 2H), 1.97–1.86 (m, 2H); LCMS (formic acid): R_t = 0.51 min (100%), MH^+ = 442.1.

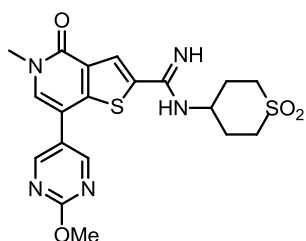
***N*-(1,1-Dioxidotetrahydro-2H-thiopyran-4-yl)-5-methyl-4-oxo-7-(6-(trifluoromethyl)pyridin-3-yl)-4,5-dihydrothieno[3,2-*c*]pyridine-2-carboximidamide (2.081j)**



Following General Procedure 2 using 2-(trifluoromethyl)pyridine-5-boronic acid (34 mg, 0.18 mmol) gave, **2.081j** (15 mg, 19%) as an off white solid; ^1H NMR (400 MHz, DMSO- d_6) δ ppm 9.03 (d, J = 1.8, 1H), 8.39 (dd, J = 8.1, 1.8, 1H), 8.18 (s, 1H), 8.08 (d, J = 8.1, 1H), 8.04 (s, 1H), 6.80 (br.s, 2H), 3.63–3.55 (m, 4H), 3.22–3.13 (m, 2H), 3.09–3.01 (m, 2H), 2.05–1.96 (m, 2H), 1.95–1.84 (m, 2H); LCMS (formic acid): R_t = 0.61 min (100%), MH^+ = 485.2.

***N*-(1,1-Dioxidotetrahydro-2H-thiopyran-4-yl)-5-methyl-7-(1-methyl-1H-pyrazol-4-yl)-4-oxo-4,5-dihydrothieno[3,2-*c*]pyridine-2-carboximidamide (2.081k)**

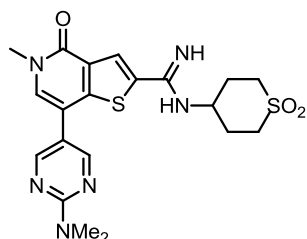
Following General Procedure 2 using 1-methylpyrazole-4-boronic acid pinacol ester (37 mg, 0.18 mmol) gave, **2.081k** (11 mg, 17%) as a white solid; $^1\text{H NMR}$ (400 MHz, DMSO-d_6) δ ppm 8.13 (s, 1H), 8.09 (s, 1H), 7.82 (s, 1H), 7.78 (s, 1H), 6.75 (br.s, 2H), 3.93 (s, 3H), 3.65–3.57 (m, 1H), 3.56 (s, 3H), 3.24–3.15 (m, 2H), 3.12–3.03 (m, 2H), 2.07–1.98 (m, 2H), 1.98–1.88 (m, 2H); LCMS (formic acid): $R_t = 0.44$ min (100%), $\text{MH}^+ = 420.3$.

***N*-(1,1-Dioxidotetrahydro-2H-thiopyran-4-yl)-7-(2-methoxypyrimidin-5-yl)-5-methyl-4-oxo-4,5-dihydrothieno[3,2-*c*]pyridine-2-carboximidamide (2.081l)**

A mixture of **2.064** (100 mg, 0.24 mmol), (2-methoxypyrimidin-5-yl)boronic acid (45 mg, 0.29 mmol), K_2CO_3 (79 mg, 0.57 mmol) and PEPPSI-Pr (15 mg, 0.09 mmol) in H_2O (0.5 mL) and IPA (1.5 mL) was heated to 120 °C in a microwave reactor for 0.5 h. The reaction mixture was allowed to cool to rt, diluted with EtOAc (20 mL), filtered through Celite[®] and concentrated *in vacuo*. The resulting residue was purified by MDAP (formic acid). The appropriate fractions were combined and solvent evaporated *in vacuo*. The resulting residue was dissolved in MeOH (5 mL) and passed through a preconditioned (MeOH, 20 mL) amino propyl column (10 g). The appropriate fractions were combined and solvent evaporated *in vacuo* to give **2.081l** (36 mg, 34%) as a white solid; m.p. 297–299 °C (decomp.); ν_{max} (solid)/ cm^{-1} : 1644 (C=N), 1602, 1473, 1409, 1114 (S=O); $^1\text{H NMR}$ (400 MHz, DMSO-d_6) δ ppm 8.86 (s, 2H), 8.15 (s, 1H), 7.86 (s, 1H), 6.77 (br.s, 2H) 4.00 (s, 3H), 3.64–3.58 (m, 4H), 3.23–3.14 (m, 2H), 3.08–2.99 (m, 2H), 2.06–1.97 (m, 2H), 1.95–1.87 (m, 2H); $^{13}\text{C NMR}$ (101 MHz, DMSO-d_6) δ ppm 164.6, 158.1, 157.7, 149.1, 147.8, 142.0, 134.3, 129.6, 123.8, 122.5, 108.5, 54.8, 49.3, 48.5, 36.3, 30.1; HRMS ($\text{M} + \text{H}^+$) calculated for $\text{C}_{19}\text{H}_{22}\text{N}_5\text{O}_4\text{S}_2$ 448.1108; found 448.1105; LCMS (formic acid): $R_t = 0.49$ min (100%), $\text{MH}^+ = 448.2$.

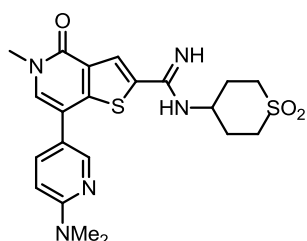
7-(2-(Dimethylamino)pyrimidin-5-yl)-N-(1,1-dioxidotetrahydro-2H-thiopyran-4-yl)-5-methyl-4-oxo-4,5-dihydrothieno[3,2-c]pyridine-2-carboximidamide

(2.081m)



A mixture of **2.064** (100 mg, 0.24 mmol), (2-(dimethylamino)pyrimidin-5-yl)boronic acid (48 mg, 0.29 mmol), K_2CO_3 (79 mg, 0.57 mmol) and PEPPSI-Pr (15 mg, 0.09 mmol) in H_2O (0.5 mL) and IPA (1.5 mL) was heated to 120 °C in a microwave reactor for 0.5 h. The reaction mixture was allowed to cool to rt, diluted with EtOAc (20 mL), filtered through Celite® and concentrated *in vacuo*. The resulting residue was purified by MDAP (formic acid). The appropriate fractions were combined and solvent evaporated *in vacuo*. The resulting residue was dissolved in MeOH (5 mL) and passed through a preconditioned (MeOH, 20 mL) amino propyl column (10 g). The appropriate fractions were combined and solvent evaporated *in vacuo* to give **2.081m** (26 mg, 0.06 mmol, 24%) as a white solid; 1H NMR (400 MHz, $DMSO-d_6$) δ ppm 8.57 (s, 2H), 8.13 (s, 1H), 7.72 (s, 1H), 6.75 (br.s, 2H), 3.64–3.58 (m, 1H), 3.56 (s, 3H), 3.23–3.14 (m, 8H), 3.08–3.00 (m, 2H), 2.05–1.97 (m, 2H), 1.95–1.87 (m, 2H); LCMS (formic acid): R_t = 0.56 min (100%), MH^+ = 461.2.

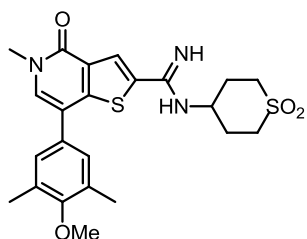
7-(6-(Dimethylamino)pyridin-3-yl)-N-(1,1-dioxidotetrahydro-2H-thiopyran-4-yl)-5-methyl-4-oxo-4,5-dihydrothieno[3,2-c]pyridine-2-carboximidamide (2.081n)



A mixture of **2.064** (100 mg, 0.24 mmol), (6-(dimethylamino)pyridin-3-yl)boronic acid (48 mg, 0.29 mmol), PEPPSI-Pr (15 mg, 0.02 mmol) and K_2CO_3 (79 mg, 0.57 mmol) in H_2O (1 mL) and IPA (3 mL) was heated to 120 °C in a microwave reactor for 0.5 h. The reaction mixture was allowed to cool to rt, diluted with EtOAc (40 mL), filtered through Celite® and concentrated *in vacuo*. The resulting residue was purified by MDAP (formic acid). The appropriate fractions were combined and concentrated *in vacuo*. The resulting residue was dissolved in MeOH (5 mL) and passed through a preconditioned (MeOH, 20 mL) amino propyl column (10 g). The appropriate fractions were combined and concentrated *in vacuo* to give **2.081n** (50 mg, 46%) as a white solid; 1H NMR (400 MHz, $DMSO-d_6$) δ ppm 8.30 (d, J = 2.4, 1H), 8.12 (s, 1H), 7.74 (dd, J = 8.8, 2.4, 1H), 7.66 (s, 1H), 6.77 (d, J = 8.8, 1H), 6.74 (br.s, 2H), 3.64–3.58 (m, 1H), 3.57 (s, 3H), 3.22–3.13 (m, 2H), 3.08 (s, 6H), 3.06–2.99 (m, 2H), 2.05–1.96 (m, 2H), 1.95–1.84 (m, 2H); LCMS (formic acid): R_t = 0.40 min (100%),

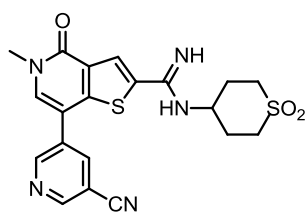
MH⁺ = 460.2.

***N*-(1,1-Dioxidotetrahydro-2H-thiopyran-4-yl)-7-(4-methoxy-3,5-dimethylphenyl)-5-methyl-4-oxo-4,5-dihydrothieno[3,2-*c*]pyridine-2-carboximidamide (2.081o)**



A mixture of **2.064** (100 mg, 0.24 mmol), (4-methoxy-3,5-dimethylphenyl)boronic acid (52 mg, 0.29 mmol), PEPPSI-*i*Pr (15 mg, 0.02 mmol) and K₂CO₃ (79 mg, 0.57 mmol) in H₂O (0.5 mL) and IPA (1.5 mL) was heated at 120 °C in a microwave reactor for 0.5 h. The reaction mixture was allowed to cool to rt, diluted with EtOAc (20 mL), filtered through Celite[®] and concentrated *in vacuo*. The resulting residue was purified by MDAP (formic acid). The appropriate fractions were combined and solvent evaporated *in vacuo*. The resulting residue was dissolved in MeOH (5 mL) and passed through a preconditioned (MeOH, 20 mL) amino propyl column (10 g). The appropriate fractions were combined and solvent evaporated *in vacuo* to give **2.081o** (52 mg, 46%) as a white solid; m.p. 267–269 °C; ν_{\max} (solid)/cm⁻¹: 1641 (C=N), 1286, 1118 (S=O), 850; ¹H NMR (400 MHz, DMSO-*d*₆) δ ppm 8.12 (s, 1H), 7.67 (s, 1H), 7.27 (s, 2H), 6.72 (br.s, 2H), 3.71 (s, 3H), 3.62–3.55 (m, 4H), 3.20–3.13 (m, 2H), 3.11–3.01 (m, 2H), 2.30 (s, 6H), 2.06–1.96 (m, 2H), 1.96–1.85 (m, 2H); ¹³C NMR (101 MHz, DMSO-*d*₆) δ ppm 157.7, 156.4, 149.3, 147.9, 141.6, 133.3, 131.2, 130.9, 129.5, 127.8, 122.5, 115.0, 59.3, 49.7, 48.7, 36.2, 30.2, 15.9; HRMS (M + H)⁺ calculated for C₂₃H₂₈F₃N₃O₄S₂ 474.1516; found 474.1516; LCMS (formic acid): R_t = 0.74 min (100%), MH⁺ = 474.2;

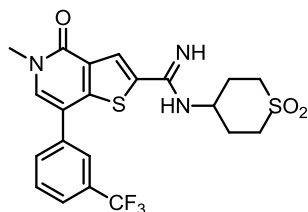
7-(5-Cyanopyridin-3-yl)-*N*-(1,1-dioxidotetrahydro-2H-thiopyran-4-yl)-5-methyl-4-oxo-4,5-dihydrothieno[3,2-*c*]pyridine-2-carboximidamide (2.081p)



A mixture of **2.064** (100 mg, 0.24 mmol), (5-cyanopyridin-3-yl)boronic acid (43 mg, 0.29 mmol), PEPPSI-*i*Pr (15 mg, 0.02 mmol) and K₂CO₃ (79 mg, 0.57 mmol) in H₂O (0.5 mL) and IPA (1.5 mL) was heated at 120 °C in a microwave reactor for 0.5 h. The reaction mixture was allowed to cool to rt, diluted with EtOAc (20 mL), filtered through Celite[®] and concentrated *in vacuo*. The resulting residue was purified by MDAP (formic acid). The appropriate fractions were combined and solvent evaporated *in vacuo*. The resulting residue was dissolved in MeOH (5 mL) and passed through a preconditioned (MeOH, 20 mL) amino propyl column (10 g). The appropriate

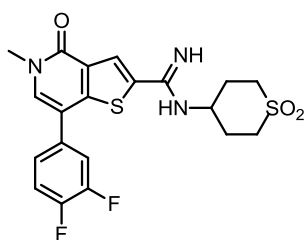
fractions were combined and solvent evaporated *in vacuo* to give **2.081p** (6 mg, 0.014 mmol, 6%) as a white solid; $^1\text{H NMR}$ (400 MHz, DMSO-d_6) δ ppm 9.15 (d, $J = 2.0$, 1H), 9.07 (d, $J = 2.0$, 1H), 8.62–8.59 (m, 1H), 8.17 (s, 1H), 7.99 (s, 1H), 6.79 (br.s, 2H), 3.63–3.58 (m, 4H), 3.21–3.13 (m, 2H), 3.10–3.01 (m, 2H), 2.06–1.97 (m, 2H) 1.97–1.87 (m, 2H); LCMS (formic acid): $R_t = 0.50$ min (97%), $\text{MH}^+ = 442.1$.

***N*-(1,1-Dioxidotetrahydro-2H-thiopyran-4-yl)-5-methyl-4-oxo-7-(3-(trifluoromethyl)phenyl)-4,5-dihydrothieno[3,2-*c*]pyridine-2-carboximidamide (2.081q)**



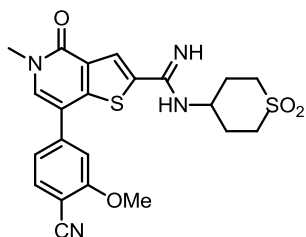
A mixture of **2.064** (100 mg, 0.24 mmol), (3-(trifluoromethyl)phenyl)boronic acid (54 mg, 0.29 mmol), PEPPSI-*t*Pr (15 mg, 0.02 mmol) and K_2CO_3 (79 mg, 0.57 mmol) in H_2O (0.5 mL) and IPA (1.5 mL) was heated at 120 °C in a microwave reactor for 0.5 h. The reaction mixture was allowed to cool to rt, diluted with EtOAc (40 mL), filtered through Celite[®] and concentrated *in vacuo*. The resulting residue was purified by MDAP (formic acid). The appropriate fractions were combined and concentrated *in vacuo*. The resulting residue was dissolved in MeOH (5 mL) and passed through a preconditioned (MeOH, 20 mL) amino propyl column (10 g). The appropriate fractions were combined and concentrated *in vacuo* to give **2.081q** (60 mg, 52%) as a white solid; m.p. 266–268 °C; ν_{max} (solid)/ cm^{-1} : 1634 (C=N), 1612, 1296 (C-F), 1115 (S=O); $^1\text{H NMR}$ (400 MHz, DMSO-d_6) δ ppm 8.16 (s, 1H), 8.02–7.98 (m, 1H), 7.94 (bs, 1H), 7.91 (s, 1H), 7.81–7.77 (m, 2H), 6.77 (br.s, 2H), 3.65–3.56 (m, 4H), 3.21–3.12 (m, 2H) 3.08–3.00 (m, 2H), 2.07–1.96 (m, 2H), 1.95–1.85 (m, 2H); $^{13}\text{C NMR}$ (101 MHz, DMSO-d_6) δ ppm 158.2, 149.7, 147.8, 142.2, 137.5, 135.2, 131.8, 130.7, 130.2, 130.3 (q, $J_{\text{C-F}} = 31.4$), 125.0 (q, $J_{\text{C-F}} = 3.7$), 124.54 (q, $J_{\text{C-F}} = 3.7$), 124.53 (q, $J_{\text{C-F}} = 272.5$), 123.0, 114.0, 50.0, 49.0, 36.8, 30.6; $^{19}\text{F NMR}$ (DMSO-d_6) δ ppm -61.1; HRMS ($\text{M} + \text{H}$)⁺ calculated for $\text{C}_{21}\text{H}_{21}\text{F}_3\text{N}_3\text{O}_3\text{S}_2$ 484.0971; found 484.0961. LCMS (formic acid) $R_t = 0.77$ min (100%), $\text{MH}^+ = 484.1$.

7-(3,4-Difluorophenyl)-N-(1,1-dioxidotetrahydro-2H-thiopyran-4-yl)-5-methyl-4-oxo-4,5-dihydrothieno[3,2-c]pyridine-2-carboximidamide (2.081r)



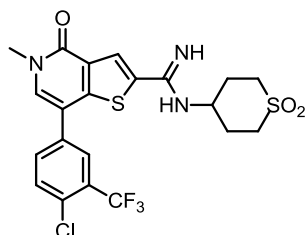
A mixture of **2.064** (100 mg, 0.24 mmol), (3,4-difluorophenyl)boronic acid (45 mg, 0.29 mmol), PEPPSI-Pr (15 mg, 0.02 mmol) and K_2CO_3 (79 mg, 0.57 mmol) in H_2O (0.5 mL) and IPA (1.5 mL) was heated at 120 °C in a microwave reactor for 0.5 h. The reaction mixture was allowed to cool to rt, diluted with EtOAc (20 mL), filtered through Celite® and concentrated *in vacuo*. The resulting residue was purified by MDAP (formic acid). The appropriate fractions were combined and solvent evaporated *in vacuo*. The resulting residue was dissolved in MeOH (5 mL) and passed through a preconditioned (MeOH, 20 mL) amino propyl column (10 g). The appropriate fractions were combined and solvent evaporated *in vacuo* to give **2.081r** (46 mg, 43%) as a white solid; 1H NMR (400 MHz, $DMSO-d_6$) δ ppm 8.15 (s, 1H) 7.82 (s, 1H), 7.71 (ddd, $J = 11.7, 7.8, 2.2, 1H,$), 7.65–7.57 (m, 1H), 7.55–7.50 (m, 1H), 6.77 (br.s, 2H), 3.64–3.55 (m, 4H), 3.22–3.13 (m, 2H), 3.11–3.01 (m, 2H) 2.06–1.96 (m, 2H), 1.96–1.85 (m, 2H); LCMS (formic acid): $R_t = 0.68$ min (100%), $MH^+ = 452.1$.

7-(4-Cyano-3-methoxyphenyl)-N-(1,1-dioxidotetrahydro-2H-thiopyran-4-yl)-5-methyl-4-oxo-4,5-dihydrothieno[3,2-c]pyridine-2-carboximidamide (2.081s)



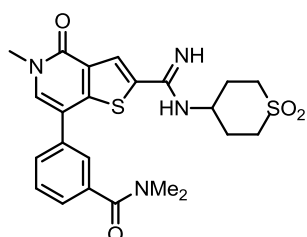
A mixture of **2.064** (100 mg, 0.24 mmol), (4-cyano-3-methoxyphenyl)boronic acid (51 mg, 0.29 mmol), PEPPSI-Pr (15 mg, 0.02 mmol) and K_2CO_3 (79 mg, 0.57 mmol) in H_2O (0.5 mL) and IPA (1.5 mL) was heated at 120 °C in a microwave reactor for 0.5 h. The reaction mixture was allowed to cool to rt, diluted with EtOAc (20 mL), filtered through Celite® and concentrated *in vacuo*. The resulting residue was purified by MDAP (formic acid). The appropriate fractions were combined and solvent evaporated *in vacuo*. The resulting residue was dissolved in MeOH (5 mL) and passed through a preconditioned (MeOH, 20 mL) amino propyl column (10 g). The appropriate fractions were combined and solvent evaporated *in vacuo* to give **2.081s** (24 mg, 21%) as a white solid; 1H NMR (400 MHz, $DMSO-d_6$) δ ppm 8.15 (s, 1H), 7.97 (s, 1H), 7.88 (d, $J = 8.0, 1H,$), 7.45 (d, $J = 1.4, 1H,$), 7.42 (dd, $J = 8.0, 1.4, 1H,$), 6.77 (br.s, 2H), 4.01 (s, 3H), 3.64–3.59 (m, 4H), 3.24–3.14 (m, 2H), 3.10–3.00 (m, 2H), 2.06–1.97 (m, 2H), 1.96–1.86 (m, 2H); LCMS (formic acid): $R_t = 0.65$ min (100%), $MH^+ = 471.2$.

7-(4-Chloro-3-(trifluoromethyl)phenyl)-N-(1,1-dioxidotetrahydro-2H-thiopyran-4-yl)-5-methyl-4-oxo-4,5-dihydrothieno[3,2-c]pyridine-2-carboximidamide (2.081t)



A mixture of **2.064** (100 mg, 0.24 mmol), (4-chloro-3-(trifluoromethyl)phenyl)boronic acid (65 mg, 0.29 mmol), Pd(PPh₃)₄ (14 mg, 0.01 mmol) and K₂CO₃ (79 mg, 0.57 mmol) in H₂O (1 mL) and IPA (3 mL) was heated at 120 °C in a microwave reactor for 0.5 h. The reaction mixture was allowed to cool to rt, diluted with EtOAc (40 mL), filtered through Celite[®] and concentrated *in vacuo*. The resulting residue was purified by MDAP (formic acid). The appropriate fractions were combined and evaporated *in vacuo*. The resulting residue was dissolved in MeOH (5 mL) and passed through a preconditioned (MeOH, 20 mL) amino propyl column (10 g). The appropriate fractions were combined and concentrated *in vacuo* to give **2.081t** (44 mg, 36%) as a white solid; ¹H NMR (400 MHz, DMSO-d₆) δ ppm 8.16 (s, 1H), 8.05–8.04 (m, 1H), 8.03–7.99 (m, 1H), 7.95 (s, 1H), 7.90 (d, *J* = 8.3, 1H), 6.77 (br.s, 2H), 3.64–3.57 (m, 4H), 3.21–3.12 (m, 2H), 3.09–3.01 (m, 2H), 2.06–1.96 (m, 2H), 1.96–1.85 (m, 2H); LCMS (formic acid): R_t = 0.82 min (100%), MH⁺ = 518.1.

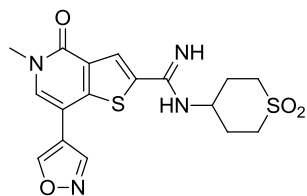
3-(2-(N-(1,1-Dioxidotetrahydro-2H-thiopyran-4-yl)carbamimidoyl)-5-methyl-4-oxo-4,5-dihydrothieno[3,2-c]pyridin-7-yl)-N,N-dimethylbenzamide (2.081u)



A mixture of **2.064** (100 mg, 0.24 mmol), (3-(dimethylcarbamoyl)phenyl)boronic acid (55 mg, 0.29 mmol), PEPPSI-Pr (15 mg, 0.02 mmol) and K₂CO₃ (79 mg, 0.57 mmol) in H₂O (0.5 mL) and IPA (1.5 mL) was heated at 120 °C in a microwave reactor for 0.5 h. The reaction mixture was allowed to cool to rt, diluted with EtOAc (20 mL), filtered through Celite[®] and concentrated *in vacuo*. The resulting residue was purified by MDAP (formic acid). The appropriate fractions were combined and solvent evaporated *in vacuo*. The resulting residue was dissolved in MeOH (5 mL) and passed through a preconditioned (MeOH, 20 mL) amino propyl column (10 g). The appropriate fractions were combined and solvent evaporated *in vacuo* to give **2.081u** (40 mg, 0.10 mmol, 41%) as a white solid; ¹H NMR (400 MHz, DMSO-d₆) δ ppm 8.14 (s, 1H), 7.83 (s, 1H), 7.73–7.69 (m, 1H), 7.64–7.57 (m, 2H), 7.46–7.42 (m, 1H), 6.76 (br.s, 2H), 3.65–3.58 (m, 4H), 3.22–3.13 (m, 2H), 3.08–3.02 (m, 2H),

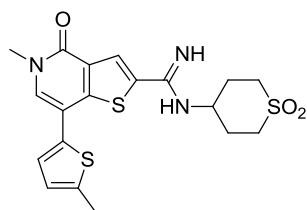
2.05–1.96 (m, 2H), 1.95–1.85 (m, 2H); LCMS (formic acid): $R_t = 0.55$ min (100%), $MH^+ = 487.2$.

***N*-(1,1-Dioxidotetrahydro-2H-thiopyran-4-yl)-7-(isoxazol-4-yl)-5-methyl-4-oxo-4,5-dihydrothieno[3,2-*c*]pyridine-2-carboximidamide (2.081v)**



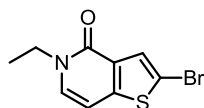
Following General Procedure 2 using 4-(4,4,5,5-tetramethyl-1,3,2-dioxaborolan-2-yl)isoxazole (35 mg, 0.18 mmol) gave a complex mixture of products as judged by LCMS analysis. Protodehalogenation of compound **2.064** was observed as the major product; LCMS (formic acid): $R_t = 0.39$ min (32%), $MH^+ = 340.2$.

***N*-(1,1-Dioxidotetrahydro-2H-thiopyran-4-yl)-5-methyl-7-(5-methylthiophen-2-yl)-4-oxo-4,5-dihydrothieno[3,2-*c*]pyridine-2-carboximidamide (2.081w)**

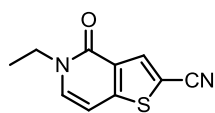


Following General Procedure 2 using (5-methylthiophen-2-yl)boronic acid (26 mg, 0.18 mmol) gave a complex mixture of products as judged by LCMS analysis. Protodehalogenation of compound **2.064** was observed as the major product; LCMS (formic acid): $R_t = 0.37$ min (39%), $MH^+ = 340.2$.

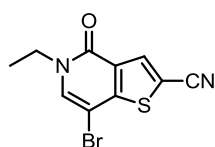
2-Bromo-5-ethylthieno[3,2-*c*]pyridin-4(5H)-one (2.084a)



A single portion of ethyl iodide (1.40 mL, 17.39 mmol) was added to a solution of **2.012** (2.00 g, 8.69 mmol) and CS_2CO_3 (8.50 g, 26.10 mmol) in THF (35 mL) at rt. The reaction mixture was heated at 60 °C for 18 h, then allowed to cool to rt and diluted with EtOAc (50 mL) and H_2O (50 mL). The separated aqueous phase was extracted with EtOAc (3 × 50 mL) and the combined organic layers were passed through a hydrophobic frit and concentrated *in vacuo* to give **2.084a** (2.30 g, quant.) as a light brown solid. 50 mg of **2.084a** was taken forward for purification by MDAP (formic acid), providing suitably pure material (44 mg, 0.17 mmol) for full characterisation; m.p. 124–125 °C; ν_{max} (solid)/ cm^{-1} : 1632 (C=O), 1577, 1082, 846, 761; 1H NMR (500 MHz, DMSO- d_6) δ ppm 7.62 (s, 1H), 7.56 (d, $J = 7.2$, 1H), 6.89 (d, $J = 7.2$, 1H), 3.99 (q, $J = 7.2$, 2H), 1.24 (t, $J = 7.2$, 3H); ^{13}C NMR (125 MHz, DMSO- d_6) δ ppm 156.4, 148.3, 133.8, 130.2, 127.0, 111.7, 100.8, 43.3, 14.6; HRMS ($M + H$) $^+$ calculated for C_9H_9BrNOS 257.9583; found 257.9585. LCMS (formic acid), $R_t = 0.89$ min (100%), $MH^+ = 258.0$, 260.0.

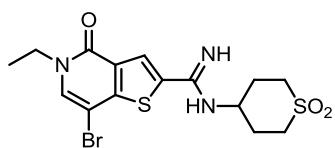
5-Ethyl-4-oxo-4,5-dihydrothieno[3,2-c]pyridine-2-carbonitrile (2.085a)

A mixture of **2.084a** (1.10 g, 4.26 mmol), zinc cyanide (1.00 g, 8.52 mmol), and Pd(PPh₃)₄ (0.44 g, 0.3 mmol) in DMF (10 mL) was heated to 115 °C in a microwave reactor for 3.5 h. This process was repeated to provide a second identical batch. The two batches were allowed to cool to room temperature, diluted with EtOAc (50 mL each) and combined. The solution was filtered through Celite[®] and concentrated *in vacuo*. The resulting residue was purified by silica gel chromatography (0–3% MeOH in DCM). The appropriate fractions were combined and concentrated *in vacuo* to give **2.085a** (1.70 g, 67%) as a light brown solid. 50 mg of **2.085a** was taken forward for purification by MDAP (formic acid), providing suitably pure material (33 mg, 0.16 mmol) for full characterisation; m.p. 157–158 °C; ν_{\max} (solid)/cm⁻¹: 2211 (C≡N), 1637 (C=O), 1595, 1247, 1078, 879, 780, 769; ¹H NMR (400 MHz, DMSO-d₆) δ ppm 8.32 (s, 1H), 7.82 (d, *J* = 7.2, 1H), 7.03 (d, *J* = 7.2, 1H), 4.00 (q, *J* = 7.2, 2H), 1.25 (t, *J* = 7.2, 3H); ¹³C NMR (101 MHz, DMSO-d₆) δ ppm 157.1, 151.1, 137.1, 136.7, 128.9, 114.2, 106.4, 100.9, 43.4, 14.5; HRMS (M + H)⁺ calculated for C₁₀H₉N₂OS 205.0430; found 205.0429. LCMS (formic acid), R_t = 0.76 min (98%), MH⁺ = 205.0.

7-Bromo-5-ethyl-4-oxo-4,5-dihydrothieno[3,2-c]pyridine-2-carbonitrile (2.086a)

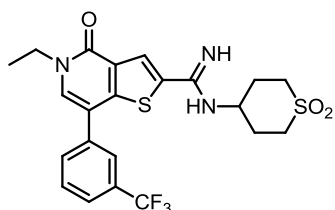
To a solution of **2.085a** (1.17 g, 5.73 mmol) in THF (20 mL), NBS (1.53 g, 8.59 mmol) was added portion-wise. The reaction mixture was left to stir at rt for 48 h. The volatile components were removed *in vacuo*. The resulting solid was suspended in Et₂O (50 mL), filtered under reduced pressure, washed with Et₂O (50 mL), collected and dried under vacuum at 40 °C to give **2.086a** (1.69 g, quant.) as an off white solid; m.p. 197–198 °C; ν_{\max} (solid)/cm⁻¹: 3041, 2220 (C≡N), 1654 (C=O), 1584, 1250, 1090, 766; ¹H NMR (500 MHz, DMSO-d₆) δ ppm 8.50 (s, 1H), 8.26 (s, 1H), 4.02 (q, *J* = 7.2, 2H), 1.26 (t, *J* = 7.2, 3H); ¹³C NMR (125 MHz, DMSO-d₆) δ ppm 156.1, 152.3, 138.2, 137.6, 128.3, 113.7, 107.0, 90.4, 43.9, 14.4; HRMS (M + H)⁺ calculated for C₁₀H₈BrN₂OS 282.9535; found 282.9534. LCMS (formic acid), R_t = 0.93 min (99%), MH⁺ = 283.0, 285.0.

7-Bromo-*N*-(1,1-dioxidotetrahydro-2H-thiopyran-4-yl)-5-ethyl-4-oxo-4,5-dihydrothieno[3,2-*c*]pyridine-2-carboximidamide (2.087a)



To a suspension of **2.086a** (1.00 g, 3.53 mmol) in MeOH (30 mL) at rt, sodium methoxide (25% weight in MeOH, 0.81 mL, 3.53 mmol) was added in a single portion. The reaction mixture was heated at 75 °C for 5 h. 4-Aminotetrahydro-2H-thiopyran-1,1-dioxide hydrochloride (1.98 g, 10.60 mmol) was added and the solution was heated for a further 18 h. The volatile components were removed *in vacuo* and the resulting solid was suspended in Et₂O (50 mL), filtered under reduced pressure, washed with Et₂O (50 mL) collected and dried under vacuum at 40 °C to give **2.087a** (1.55 g, quant.) as a white solid. 50 mg of **2.087a** was taken forward for purification by MDAP (high pH), providing suitably pure material (25 mg, 0.06 mmol) for full characterisation; m.p. 284–285 °C; ν_{\max} (solid)/cm⁻¹: 1646 (C=N), 1578, 1284, 1124 (S=O), 853, 769; ¹H NMR (500 MHz, DMSO-d₆) δ ppm 8.18 (s, 1H), 8.01 (s, 1H), 6.80 (br.s, 2H), 4.01 (q, *J* = 7.2, 2H), 3.68–3.61 (m, 1H), 3.27–3.20 (m, 2H), 3.10–3.03 (m, 2H), 2.09–2.00 (m, 2H), 1.99–1.90 (m, 2H), 1.26 (t, *J* = 7.2, 3H); ¹³C NMR (125 MHz, DMSO-d₆) δ ppm 156.9, 149.5, 134.6, 129.7, 123.2, 109.7, 92.0, 48.6, 43.7, 30.2, 14.8; HRMS (M + H)⁺ calculated for C₁₅H₁₉BrN₃O₃S₂ 432.0046; found 432.0046. LCMS (formic acid) R_t = 0.53 min (100%), MH⁺ = 432.1, 434.1.

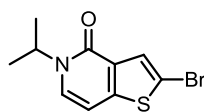
***N*-(1,1-Dioxidotetrahydro-2H-thiopyran-4-yl)-5-ethyl-4-oxo-7-(3-(trifluoromethyl)phenyl)-4,5-dihydrothieno[3,2-*c*]pyridine-2-carboximidamide (2.082)**



A mixture of **2.087a** (150 mg, 0.35 mmol), (3-(trifluoromethyl)phenyl)boronic acid (79 mg, 0.42 mmol), PEPPSI-*i*-Pr (21 mg, 0.03 mmol) and K₂CO₃ (115 mg, 0.83 mmol) in H₂O (1 mL) and IPA (3 mL) was heated at 120 °C in a microwave reactor for 0.5 h. The reaction mixture was allowed to cool to rt, diluted with EtOAc (40 mL), filtered through Celite[®] and concentrated *in vacuo*. The resulting residue was purified by MDAP (formic acid). The appropriate fractions were combined and concentrated *in vacuo*. The resulting residue was dissolved in MeOH (5 mL) and passed through a preconditioned (MeOH, 20mL) amino propyl column (10 g). The appropriate fractions were combined and concentrated *in vacuo* to give **2.082** (50 mg, 29%) as a white solid; m.p. 228–229 °C; ν_{\max} (solid)/cm⁻¹: 1640 (C=N), 1587, 1340, 1303 (C-F),

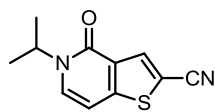
1117 (S=O); ^1H NMR (500 MHz, DMSO- d_6) δ ppm 8.15 (s, 1H), 8.03–7.98 (m, 1H), 7.98–7.94 (m, 1H), 7.91 (s, 1H), 7.82–7.76 (m, 2H), 6.77 (br.s, 2H), 4.10 (q, $J = 7.0$, 2H), 3.64–3.57 (m, 1H), 3.21–3.12 (m, 2H), 3.10–3.00 (m, 2H), 2.06–1.96 (m, 2H), 1.96–1.85 (m, 2H), 1.32 (t, $J = 7.0$, 3H); ^{13}C NMR (125 MHz, DMSO- d_6) δ ppm 157.6, 149.7, 147.7, 142.2, 137.5, 134.1, 131.9, 130.7, 130.5, 130.3 (q, $J_{\text{C-F}} = 31.7$), 125.0 (q, $J_{\text{C-F}} = 3.7$), 124.60 (q, $J_{\text{C-F}} = 3.7$), 124.59 (q, $J_{\text{C-F}} = 272.6$), 123.1, 114.4, 49.9, 49.0, 44.0, 30.6, 15.2; ^{19}F NMR (376 MHz, DMSO- d_6) δ ppm -61.0; HRMS ($\text{M} + \text{H}^+$) calculated for $\text{C}_{22}\text{H}_{23}\text{F}_3\text{N}_3\text{O}_3\text{S}_2$ 498.1128; found 498.1110. LCMS (formic acid) $R_t = 0.81$ min (100%), $\text{MH}^+ = 498.1$.

2-Bromo-5-isopropylthieno[3,2-c]pyridin-4(5H)-one (2.084b)



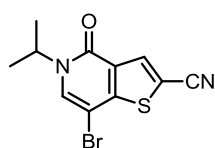
2-Iodopropane (1.3 mL, 13.04 mmol) was added in a single portion to a stirred suspension of **2.012** (1.50 g, 6.52 mmol) and K_2CO_3 (1.26 g, 9.13 mmol) in 1,4-dioxane (10 mL) at rt. The vial was sealed and heated at 150 °C in a microwave reactor for 5 h. The reaction mixture was allowed to cool to rt, diluted with EtOAc (30 mL) and H_2O (30 mL). The separated aqueous phase was extracted with EtOAc (3 x 30 mL) and the combined organic layers were passed through a hydrophobic frit and concentrated *in vacuo*. The resulting residue was purified by silica gel chromatography (gradient: 0–20% EtOAc in cyclohexane). The appropriate fractions were combined and solvent evaporated *in vacuo* to give **2.084b** (1.37 g, 77%) as a pale yellow solid; ^1H NMR (400 MHz, CDCl_3) δ ppm 7.62 (s, 1H), 7.20 (d, $J = 7.5$, 1H), 6.61 (d, $J = 7.5$, 1H), 5.25–5.48 (m, 1H), 1.40 (d, $J = 6.9$, 6H); LCMS (formic acid) $R_t = 0.99$ min (100%), $\text{MH}^+ = 271.9$, 273.9.

5-Isopropyl-4-oxo-4,5-dihydrothieno[3,2-c]pyridine-2-carbonitrile (2.085b)



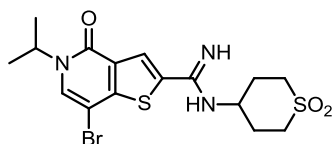
A mixture of **2.084b** (1.37 g, 5.02 mmol), zinc cyanide (1.18 g, 10.05 mmol) and $\text{Pd}(\text{PPh}_3)_4$ (0.52 g, 0.45 mmol) in DMF (12 mL) was heated at 115 °C in a microwave reactor for 5 h. The reaction mixture was allowed to cool to rt, diluted with EtOAc (30 mL), filtered through Celite[®] and concentrated *in vacuo*. The resulting residue was purified by silica gel chromatography (0–40% EtOAc in cyclohexane). The appropriate fractions were combined and solvent evaporated *in vacuo* to give **2.085b** (998 mg, 77%) as an off white solid; ^1H NMR (400 MHz, CDCl_3) δ ppm 8.17 (s, 1H), 7.39 (d, $J = 7.5$, 1H), 6.71 (d, $J = 7.5$, 1H), 5.40–5.32 (m, 1H), 1.42 (d, $J = 6.9$, 6H); LCMS (formic acid) $R_t = 0.82$ min (85%), $\text{MH}^+ = 219.0$.

7-Bromo-5-isopropyl-4-oxo-4,5-dihydrothieno[3,2-c]pyridine-2-carbonitrile (2.086b)



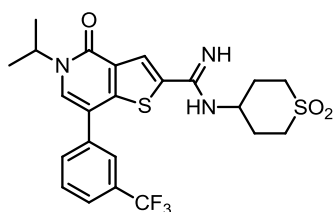
To a stirred solution of **2.085b** (998 mg, 4.57 mmol) in THF (15 mL), NBS (1.22 g, 6.86 mmol) was added in a single portion. The reaction mixture was left to stir at rt for 3 h. The volatile components were removed *in vacuo* and the resulting solid was suspended in Et₂O (50 mL), filtered under reduced pressure, rinsed with Et₂O (50 mL), collected and dried under vacuum at 40 °C to give **2.086b** (1.15 g, 85%) as a white solid; ¹H NMR (400 MHz, CDCl₃) δ ppm 8.25 (s, 1H), 7.48 (s, 1H), 5.38–5.28 (m, 1H), 1.43 (d, *J* = 6.9, 6H); LCMS (formic acid) *R*_t = 1.03 min (97%), *MH*⁺ = 296.9, 298.9.

7-Bromo-N-(1,1-dioxidotetrahydro-2H-thiopyran-4-yl)-5-isopropyl-4-oxo-4,5-dihydrothieno[3,2-c]pyridine-2-carboximidamide (2.087b)



To a suspension of **2.086b** (1.00 g, 3.37 mmol) in MeOH (30 mL), NaOMe (25% weight in MeOH, 0.8 mL, 3.37 mmol) was added in a single portion. The reaction mixture was heated at 75 °C for 0.5 h. 4-Aminotetrahydro-2H-thiopyran-1,1-dioxide hydrochloride (1.87 g, 10.10 mmol) was added and the solution was heated at 75 °C for a further 18 h. The volatile components were removed *in vacuo*. The resulting solid was suspended in MeOH (50 mL), filtered under reduced pressure, rinsed with MeOH (50 mL) collected and dried under vacuum at 40 °C to give **2.087b** (1.55 g, 93%) as a white solid; ¹H NMR (400 MHz, DMSO-*d*₆) δ ppm 8.21 (s, 1H), 7.95 (s, 1H), 5.19–5.10 (m, 1H), 3.75–3.66 (m, 1H), 3.41–3.05 (m, 4H), 2.31–2.21 (m, 2H), 2.10–1.95 (m, 2H), 1.35 (d, *J* = 6.9, 6H); LCMS (formic acid) *R*_t = 0.59 min (100%), *MH*⁺ = 446.0, 448.0.

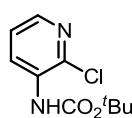
N-(1,1-Dioxidotetrahydro-2H-thiopyran-4-yl)-5-isopropyl-4-oxo-7-(3-(trifluoromethyl)phenyl)-4,5-dihydrothieno[3,2-c]pyridine-2-carboximidamide (2.083)



A mixture of **2.087b** (100 mg, 0.22 mmol), 3-(trifluoromethyl)phenylboronic acid (51 mg, 0.27 mmol), PEPPSI-*i*-Pr (15 mg, 0.02 mmol) and K₂CO₃ (74 mg, 0.54 mmol) in H₂O (1 mL) and IPA (3 mL) was heated at 120 °C in a microwave reactor for 0.5 h. The reaction mixture was allowed to cool to rt, diluted with EtOAc (40 mL), filtered through Celite[®] and concentrated *in vacuo*. The resulting residue was purified by mass directed

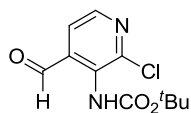
autopreparation (formic acid). The appropriate fractions were combined and concentrated *in vacuo*. The resulting residue was dissolved in MeOH (20 mL) and passed through a preconditioned (MeOH, 20 mL) amino propyl column (10 g). The appropriate fractions were combined and concentrated *in vacuo* to give **2.083** (35 mg, 31%) as a white solid; m.p. 159–160 °C; ν_{\max} (solid)/ cm^{-1} : 1637 (C=N), 1342, 1120 (S=O), 703; $^1\text{H NMR}$ (400 MHz, DMSO- d_6) δ ppm 8.15 (s, 1H), 8.02–7.93 (m, 2H), 7.82–7.74 (m, 3H), 6.76 (br.s, 2H), 5.27–5.18 (m, 1H), 3.65–3.56 (m, 1H), 3.21–3.10 (m, 2H), 3.10–2.98 (m, 2H), 2.06–1.95 (m, 2H), 1.95–1.86 (m, 2H), 1.42 (d, $J = 6.8$, 6H); HRMS ($M + H$) $^+$ calculated for $\text{C}_{22}\text{H}_{25}\text{F}_3\text{N}_3\text{O}_3\text{S}_2$ 512.1284; found 512.1286; LCMS (formic acid) $R_t = 0.86$ min (100%), ($M + H$) $^+ = 512.1$.

***tert*-Butyl (2-chloropyridin-3-yl)carbamate (3.006)**



A solution of **3.005** (50 g, 389.00 mmol) in THF (100 mL) was added drop-wise to a 1.0 M solution of NaHMDS in THF (570 mL, 856.00 mmol) over 0.5 h at -10 °C. The reaction mixture turned from a brown solution to a dense suspension so THF (100 mL) was added and the mixture was stirred for 0.5 h. Boc-anhydride (99 mL, 428.00 mmol) in THF (210 mL) was added drop-wise over 0.5 h at -10 °C. The reaction mixture was left to stir at this temperature for 3 h. 2 M HCl (450 mL) was added and the mixture was diluted with EtOAc (500 mL). The organic layer was separated and the aqueous extracted into EtOAc (3 × 300 mL). The combined organic layers were washed with water (1000 mL) and brine (1000 mL). The organic layer was separated, passed through a hydrophobic frit and concentrated *in vacuo*. The resulting residue was purified by silica gel chromatography (0–50% EtOAc in cyclohexane). The appropriate fractions were combined and solvent evaporated *in vacuo* to give **3.006** (81.08 g, 355.00 mmol, 91%) as a white solid; $^1\text{H NMR}$ (400 MHz, CDCl_3) δ ppm 8.52 (dd, $J = 8.3, 1.5$, 1H), 8.04 (dd, $J = 4.7, 1.5$, 1H), 7.23 (dd, $J = 8.3, 4.7$, 1H), 7.02 (br.s, 1H), 1.56 (s, 9H); LCMS (formic acid): $R_t = 1.06$ min (100%), $MH^+ = 229.0$. These data are in good agreement with literature values.^{105,220}

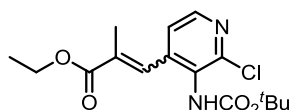
***tert*-Butyl (2-chloro-4-formylpyridin-3-yl)carbamate (3.007)**



A solution of **3.006** (20 g, 87.00 mmol) and TMEDA (29 mL, 192.00 mmol) in THF (400 mL) was cooled to -78 °C under nitrogen. $^n\text{BuLi}$ (1.6 M solution in hexanes) (120 mL, 192.00 mmol) was added drop-wise over 0.5 h. The reaction mixture was stirred at -78 °C for 1.5 h and then warmed to -20 °C and was left to stir for 20 minutes. The mixture was

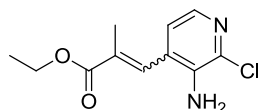
cooled to -78 °C and DMF (13.54 mL, 175.00 mmol) was added drop-wise over 15 minutes. The reaction mixture was stirred at -78 °C for 2 h and then warmed to -20 °C. The solution was quenched with sat. aq. NH₄Cl (300 mL) and diluted with EtOAc (300 mL). The organic layer was separated and washed with brine (300 mL). The organic layer was passed through a hydrophobic frit and concentrated *in vacuo*. The resulting residue was purified by silica gel chromatography (0–40% EtOAc in cyclohexane). The appropriate fractions were combined and solvent evaporated *in vacuo* to give **3.007** (14.62 g, 57.00 mmol, 65%) as a yellow solid; ¹H NMR (400 MHz, CDCl₃) δ ppm 9.99 (s, 1H), 8.37 (d, *J* = 4.9, 1H), 7.68 (d, *J* = 4.9, 1H), 6.93 (br.s, 1H), 1.54 (s, 9H); LCMS (formic acid): R_t = 0.96 min (61%), MH⁺ = 257.0. These data are in good agreement with literature values.¹⁰⁵

Ethyl 3-(3-((*tert*-butoxycarbonyl)amino)-2-chloropyridin-4-yl)-2-methylacrylate (3.009)



NaH [60% weight in mineral oil (5.26 g, 131.00 mmol)] was added portion-wise to a solution of **3.008** (28 mL, 131.00 mmol) in DMF (45 mL) at 0 °C. The reaction mixture was left to stir at this temperature for 0.5 h. A solution of **3.007** (22.5 g, 88.00 mmol) in DMF (45 mL) was added drop-wise over 0.5 h at 0 °C. The reaction mixture was left to stir at this temperature for 2 h and then quenched with sat. aq. NH₄Cl (200 mL) and EtOAc (200 mL). The organic layer was separated and the aqueous extracted with EtOAc (2 × 200 mL). The combined organic layers were passed through a hydrophobic frit and concentrated *in vacuo*. The resulting residue was purified by silica gel chromatography (0–60% EtOAc in cyclohexane). The appropriate fractions were combined and solvent evaporated *in vacuo* to give **3.009** (21.09 g, 61.90 mmol, 71%) as a yellow oil; ¹H NMR (400 MHz, CDCl₃) δ ppm 8.25 (d, *J* = 4.9, 1H), 7.54 (s, 1H), 7.18 (d, *J* = 4.9, 1H), 6.42 (br.s, 1H), 4.26 (q, *J* = 7.2, 2H), 1.97 (d, *J* = 1.5, 3H), 1.46 (s, 9H), 1.33 (t, *J* = 7.2, 3H); LCMS (formic acid): R_t = 1.11 min (81%), MH⁺ = 341.0. These data are in good agreement with literature values.¹⁰⁵

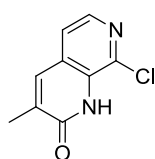
Ethyl 3-(3-amino-2-chloropyridin-4-yl)-2-methylacrylate (3.010)



HCl (4 M in 1,4-dioxane) (111 mL, 444.00 mmol) was added drop-wise to a solution of **3.009** (21.1 g, 61.90 mmol) in 1,4-dioxane (50 mL) at 0 °C. A precipitate appeared so 1,4-Dioxane (50 mL) was added. The reaction mixture was allowed to warm to rt and

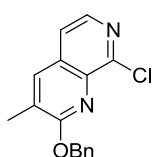
was stirred for 20 h. The reaction mixture was concentrated *in vacuo* and the resulting residue was diluted with DCM (200 mL) and washed with sat. aq. NaHCO₃ (200 mL) and brine (200 mL). The organic phase was passed through a hydrophobic frit and concentrated *in vacuo*. The resulting residue was purified by silica gel chromatography (0–50% EtOAc in cyclohexane). The appropriate fractions were combined and solvent evaporated *in vacuo* to give **3.010** (14.52 g, 60.30 mmol, 97%) as a pale yellow solid; ¹H NMR (400 MHz, CDCl₃) δ ppm 7.82 (d, *J* = 4.6, 1H), 7.45 (s, 1H), 6.95 (d, *J* = 4.6, 1H), 4.31 (q, *J* = 7.2, 2H), 4.19 (br.s, 2H), 1.99 (d, *J* = 1.5, 3H), 1.38 (t, *J* = 7.2, 3H); LCMS (formic acid): R_t = 0.96 min (95%), MH⁺ = 241.0. These data are in good agreement with literature values.¹⁰⁵

8-Chloro-3-methyl-1,7-naphthyridin-2(1H)-one (3.011)



A mixture of **3.010** (14.52 g, 60.30 mmol) and DBU (36.4 mL, 241.00 mmol) in Toluene (65 mL) was heated at 115 °C for 24 h. The reaction mixture was allowed to cool to rt and diluted with H₂O (120 mL). The aqueous layer was separated and washed with Et₂O (120 mL). The resulting organic layer was washed with H₂O (100 mL). NH₄Cl (39 g) in H₂O (150 mL) was added to the combined aqueous layers causing precipitation of a solid. This was left to stand for 0.5 h, filtered under reduced pressure, washed with H₂O (100 mL) and Et₂O (100 mL) and dried under vacuum at 40 °C for 18 h to give **3.011** (10.55 g, 54.20 mmol, 90%) as an off white solid; m.p. 225–227 °C; ν_{max} (solid)/cm⁻¹: 2979, 1727, 1178 (C=O), 1109, 877; ¹H NMR (400 MHz, DMSO-d₆) δ ppm 11.41 (br.s, 1H), 8.13 (d, *J* = 5.1, 1H), 7.86 (d, *J* = 1.2, 1H), 7.66 (d, *J* = 5.1, 1H), 2.16 (d, *J* = 1.2, 3H); ¹³C NMR (125 MHz, DMSO-d₆) 162.2, 140.6, 137.1, 136.1, 130.6, 134.4, 126.5, 120.3, 16.8; HRMS (M + H)⁺ calculated for C₉H₈ClN₂O 195.0320; found 195.0320. LCMS (formic acid): R_t = 0.61 min (100%), MH⁺ = 195.0. These data are in good agreement with literature values.¹⁰⁵

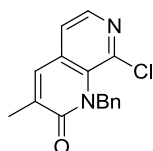
2-(Benzyloxy)-8-chloro-3-methyl-1,7-naphthyridine (3.012)



A mixture of **3.011** (4.38 g, 22.51 mmol) and K₂CO₃ (3.73 g, 27.00 mmol) in DMF (40 mL) was left to stir at rt for 10 minutes. Benzyl bromide (2.94 mL, 24.76 mmol) was added in a single portion and the reaction mixture was stirred for a further 48 h at rt, then quenched with H₂O (50 mL) and EtOAc (50 mL). The resulting suspension was filtered under reduced pressure to give **3.012** (4.46 g, 15.66 mmol, 70%) as a white solid. The filtrate was diluted with EtOAc (20 mL), separated and the aqueous extracted with

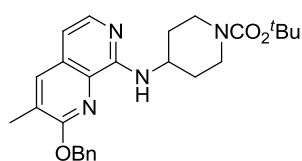
EtOAc (3 × 50 mL). The combined organic layers were passed through a hydrophobic frit and concentrated *in vacuo*. The resulting residue was purified by silica gel chromatography (0–40% EtOAc in cyclohexane). The appropriate fractions were combined and solvent evaporated *in vacuo* to give **3.012** (821 mg, 2.88 mmol, 13%) as a white solid; m.p. 161–162 °C; ν_{\max} (solid)/ cm^{-1} : 1453, 1414, 1236, 1142, 953, 755, 682; ^1H NMR (400 MHz, DMSO- d_6) δ ppm 8.25 (d, $J = 5.4$, 1H), 8.22 (d, $J = 1.0$, 1H), 7.78 (d, $J = 5.4$, 1H), 7.61 (d, $J = 7.1$, 2H), 7.44–7.38 (m, 2H), 7.37–7.31 (m, 1H), 5.62 (s, 2H), 2.38 (d, $J = 1.0$, 3H); ^{13}C NMR (101 MHz, DMSO- d_6) 161.5, 148.5, 140.6, 136.6, 136.6, 136.5, 130.7, 128.7, 128.3, 128.3, 128.0, 120.1, 67.8, 16.2; HRMS (M + H) $^+$ calculated for $\text{C}_{16}\text{H}_{14}\text{ClN}_2\text{O}$ 285.0789; found 285.0786. LCMS (formic acid): $R_t = 1.39$ min (100%), $\text{MH}^+ = 285.0$. These data are in good agreement with literature values.¹⁰⁵

1-Benzyl-8-chloro-3-methyl-1,7-naphthyridin-2(1H)-one (3.013)



A mixture of **3.011** (4.38 g, 22.51 mmol) and K_2CO_3 (3.73 g, 27.0 mmol) in DMF (40 mL) was left to stir at rt for 10 minutes. Benzyl bromide (2.94 mL, 24.76 mmol) was added in a single portion and the reaction mixture was stirred for a further 48 h, then quenched with water (50 mL) and EtOAc (50 mL). The resulting suspension was filtered under reduced and the filtrate was diluted with EtOAc (20 mL). The phases were separated and the aqueous extracted with EtOAc (3 × 50 mL). The combined organic layers were passed through a hydrophobic frit and concentrated *in vacuo*. The resulting residue was purified by silica gel chromatography (0–40% EtOAc in cyclohexane). The appropriate fractions were combined and solvent evaporated *in vacuo* to give **3.013** (386 mg, 1.36 mmol, 6%) as a white solid; ^1H NMR (400 MHz, DMSO- d_6) δ ppm 8.20 (d, $J = 4.8$, 1H), 7.97 (br.s, 1H), 7.68 (d, $J = 4.8$, 1H), 7.32–7.26 (m, 2H), 7.24–7.18 (m, 1H), 7.06 (d, $J = 7.1$, 2H), 5.85 (s, 2H), 2.21 (s, 3H); ^{13}C NMR (100 MHz, DMSO- d_6) 162.9, 141.3, 138.3, 135.5, 135.2, 134.6, 132.6, 129.7, 128.2, 126.4, 125.6, 121.5, 48.9, 17.4; LCMS (formic acid): $R_t = 1.09$ min (97%), $\text{MH}^+ = 285.0$.

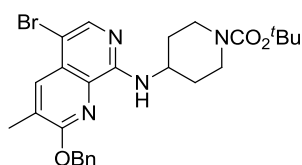
tert-Butyl 4-((2-(benzyloxy)-3-methyl-1,7-naphthyridin-8-yl)amino)piperidine-1-carboxylate (3.014)



tert-Butyl 4-aminopiperidine-1-carboxylate (3.35 g, 16.71 mmol) was added to a mixture of **3.012** (3.17 g, 11.14 mmol), $\text{Pd}_2(\text{dba})_3$ (0.82 g, 0.89 mmol), Brettphos (0.60 g, 1.11 mmol) and NaO^tBu (4.28 g, 44.6 mmol) THF

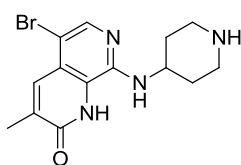
(50 mL). The reaction mixture was heated at 60 °C for 4 h. The reaction mixture was concentrated *in vacuo* and the resulting residue was diluted with DCM (100 mL) and washed with H₂O (100 mL). The separated organic layer was passed through a hydrophobic frit and concentrated *in vacuo*. The resulting residue was purified by silica gel chromatography (0–60% EtOAc in cyclohexane). The appropriate fractions were combined and solvent evaporated *in vacuo* to give **3.014** (7.99 g, 17.81 mmol, 96%) as an orange solid; ¹H NMR (400 MHz, DMSO-d₆) δ ppm 7.89 (d, *J* = 1.0, 1H), 7.79 (d, *J* = 5.6, 1H), 7.54 (d, *J* = 7.3, 2H), 7.42–7.35 (m, 2H), 7.34–7.28 (m, 1H), 6.78 (d, *J* = 5.6, 1H), 6.63 (d, *J* = 8.3, 1H), 5.59 (s, 2H), 4.27–4.14 (m, 1H), 4.04–3.91 (m, 2H), 3.04–2.84 (m, 2H), 2.32 (d, *J* = 1.0, 3H), 1.99–1.88 (m, 2H), 1.59–1.46 (m, 2H), 1.43 (s, 9H); LCMS (formic acid): R_t = 0.99 min (100%), MH⁺ = 449.2.

tert-Butyl 4-((2-(benzyloxy)-5-bromo-3-methyl-1,7-naphthyridin-8-yl)amino)piperidine-1-carboxylate (3.015)



To a solution of **3.014** (7.99 g, 17.81 mmol) in CHCl₃ (200 mL), NBS (3.49 g, 19.59 mmol) was added. The reaction mixture was left to stir for 18 h at rt and then diluted with H₂O (100 mL). The organic phase was separated, passed through a hydrophobic frit and concentrated *in vacuo*. The resulting solid was purified by silica gel chromatography (0–50% EtOAc in cyclohexane). The appropriate fractions were combined and solvent evaporated *in vacuo* to give **3.015** (8.17 g, 15.49 mmol, 87%) as an orange solid; ¹H NMR (400 MHz, CDCl₃) δ ppm 8.01 (s, 1H), 7.96 (d, *J* = 1.0, 1H), 7.51–7.47 (m, 2H), 7.44–7.38 (m, 2H), 7.37–7.31 (m, 1H), 6.19 (d, *J* = 8.1, 1H), 5.51 (s, 2H), 4.24–4.14 (m, 1H), 4.14–4.00 (m, 2H), 3.10–3.00 (m, 2H), 2.45 (d, *J* = 1.0, 3H), 2.17–2.09 (m, 2H), 1.53–1.50 (m, 11H); LCMS (formic acid): R_t = 1.67 min (95%), MH⁺ = 527.2, 529.2.

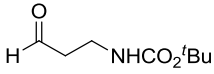
5-Bromo-3-methyl-8-(piperidin-4-ylamino)-1,7-naphthyridin-2(1H)-one (3.016)



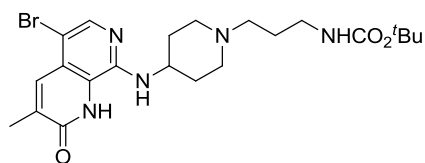
3.015 (2 g, 3.79 mmol) was dissolved in TFA (15 mL, 195.00 mmol) and left to stir at 80 °C for 3 h. The volatile components were removed *in vacuo*. Toluene (5 mL) was added and the solvent evaporated *in vacuo* (× 3). The resulting residue was dissolved in MeOH (20 mL) and passed through a preconditioned (MeOH, 100 mL) amino propyl column (70 g). The column was washed with MeOH (30 mL). The appropriate fractions were combined and solvent evaporated *in vacuo*

to give **3.016** (1.14 g, 3.38 mmol, 89%) as a yellow solid; ^1H NMR (400 MHz, DMSO- d_6) δ ppm 7.90 (s, 1H), 7.80 (d, $J = 1.2$, 1H), 6.87 (d, $J = 6.8$, 1H), 5.16 (br.s, 1H), 4.10–3.98 (m, 1H), 3.13–3.07 (m, 2H), 2.78–2.69 (m, 2H), 2.18 (d, $J = 1.2$, 3H), 2.05–1.94 (m, 2H), 1.59–1.39 (m, 2H); LCMS (formic acid): $R_t = 0.57$ min (94%), $\text{MH}^+ = 337.0, 339.0$.

***tert*-Butyl (3-oxopropyl)carbamate (3.017)**

 Dess Martin periodinane (944 mg, 2.23 mmol) was added to a solution of *tert*-butyl (3-hydroxypropyl)carbamate (0.29 mL, 1.71 mmol) in DCM (9 mL) at 0 °C. The reaction mixture was allowed to warm to rt and stirred for 18 h. The reaction mixture was quenched with 20% aq. $\text{Na}_2\text{S}_2\text{O}_3$ (20 mL) and sat. aq. NaHCO_3 (20 mL) and diluted with Et_2O (30 mL). The organic layer was separated and washed with 20% aq. $\text{Na}_2\text{S}_2\text{O}_3$ (20 mL), sat. aq. NaHCO_3 (20 mL) and brine (20 mL). The organic layer was passed through a hydrophobic frit and concentrated *in vacuo* to give **3.017** (316 mg, 1.82 mmol, quant.) as a colourless oil; ^1H NMR (400 MHz, CDCl_3) δ ppm 9.82 (s, 1H), 4.92 (1H, br. s), 3.47–3.40 (m, 2H) 2.12 (t, $J = 5.7$, 2H), 1.44 (s, 9H). These data are in good agreement with literature values.²²⁶

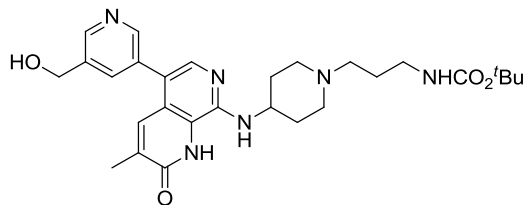
***tert*-Butyl (3-(4-((5-bromo-3-methyl-2-oxo-1,2-dihydro-1,7-naphthyridin-8-yl)amino)piperidin-1-yl)propyl)carbamate (3.018)**



A mixture of **3.016** (474 mg, 2.74 mmol) and **3.017** (1.11 g, 3.28 mmol) in MeOH (6 mL) and AcOH (0.6 mL) was heated at 50 °C for 3 h. Picoline borane complex (254 mg, 2.74 mmol) was added and the reaction mixture was heated at 50 °C for a further 18 h. The reaction mixture was concentrated *in vacuo* and the resulting residue diluted with sat. aq. NaHCO_3 (20 mL) and DCM (20 mL). The organic layer was separated and the aqueous extracted with DCM (3 × 20 mL). The combined organic layers were passed through a hydrophobic frit and concentrated *in vacuo*. The resulting residue was purified by silica gel chromatography (0–100% EtOH in EtOAc). The appropriate fractions were combined and solvent evaporated *in vacuo* to give **3.018** (850 mg, 1.72 mmol, 63%) as a yellow solid; ^1H NMR (400 MHz, DMSO- d_6) δ ppm 11.60 (br.s, 1H), 7.91 (s, 1H), 7.80 (d, $J = 1.0$, 1H), 6.85–6.75 (m, 2H), 3.93–3.82 (m, 1H), 2.95 (q, $J = 6.7$, 2H), 2.89–2.80 (m, 2H), 2.32–2.24 (m, 2H), 2.18 (d,

$J = 1.0$, 3H), 2.05–1.92 (m, 4H), 1.58–1.48 (m, 4H), 1.38 (s, 9H); LCMS (formic acid): $R_t = 0.75$ min (100%), $MH^+ = 494.1$, 496.1.

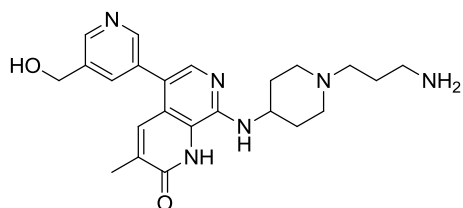
***tert*-Butyl (3-(4-((5-(5-(hydroxymethyl)pyridin-3-yl)-3-methyl-2-oxo-1,2-dihydro-1,7-naphthyridin-8-yl)amino)piperidin-1-yl)propyl)carbamate (3.019b)**



A mixture of **3.018** (500 mg, 1.01 mmol), 5-(hydroxymethyl)pyridin-3-yl)boronic acid (309 mg, 2.02 mmol), $Pd(OAc)_2$ (34 mg, 0.15 mmol), Catacxiium A (54 mg, 0.15 mmol) and K_2CO_3 (335 mg,

2.43 mmol) in 1,4-dioxane (3 mL) and H_2O (1.5 mL) was heated at 100 °C in a microwave reactor for 1 h. The reaction mixture was allowed to cool to rt, diluted with EtOAc (20 mL), filtered through Celite® and concentrated *in vacuo*. The resulting residue was purified by silica gel chromatography (0–100% EtOH in EtOAc). The appropriate fractions were combined and solvent evaporated *in vacuo* to give **3.019b** (576 mg, 1.10 mmol, quant.) as a yellow solid; 1H NMR (400 MHz, DMSO- d_6) δ ppm 11.54 (br.s, 1H), 8.56 (d, $J = 2.1$, 1H), 8.45 (d, $J = 2.1$, 1H), 7.75–7.69 (m, 2H), 7.51 (d, $J = 1.2$, 1H), 6.91 (d, $J = 6.6$, 1H), 6.83–6.76 (m, 1H), 4.62 (s, 2H), 4.05–3.92 (m, 1H), 2.95 (q, $J = 6.9$, 2H), 2.89–2.80 (m, 2H), 2.28 (t, $J = 6.9$, 2H), 2.08 (d, $J = 1.0$, 3H), 2.06–1.96 (m, 4H), 1.58–1.47 (m, 4H), 1.38 (s, 9H); LCMS (formic acid): $R_t = 0.46$ min (100%), $MH^+ = 523.3$.

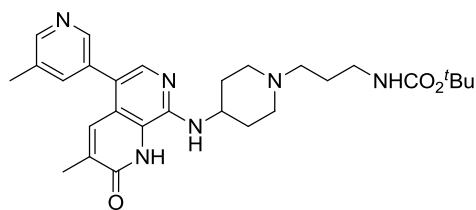
8-((1-(3-Aminopropyl)piperidin-4-yl)amino)-5-(5-(hydroxymethyl)pyridin-3-yl)-3-methyl-1,7-naphthyridin-2(1H)-one (3.002b)



A mixture of **3.019b** (170 mg, 0.33 mmol) in 4 M HCl in 1,4-dioxane (3 mL) was stirred for 18 h at rt. The reaction mixture was concentrated *in vacuo* and the resulting solid suspended in Et_2O (10 mL), filtered under

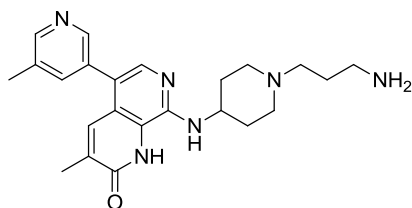
reduced pressure, washed with Et_2O (10 mL) and collected. The resulting solid was purified by MDAP (high pH). The appropriate fractions were combined and solvent evaporated *in vacuo* to give **3.002b** (65 mg, 0.15 mmol, 47%) as a yellow solid; 1H NMR (400 MHz, DMSO- d_6) δ ppm 8.57 (d, $J = 1.0$, 1H), 8.49 (d, $J = 1.7$, 1H), 7.83 (s, 1H), 7.63 (s, 1H), 7.58 (s, 1H), 4.77 (s, 2H), 4.10–4.01 (m, 1H), 3.08–2.99 (m, 2H), 2.79 (t, $J = 7.2$, 2H), 2.50 (t, $J = 7.2$, 2H), 2.30–2.13 (m, 7H), 1.82–1.63 (m, 4H); LCMS (high pH): $R_t = 0.60$ min (92%), $MH^+ = 423.4$.

tert-Butyl (3-(4-((3-methyl-5-(5-methylpyridin-3-yl)-2-oxo-1,2-dihydro-1,7-naphthyridin-8-yl)amino)piperidin-1-yl)propyl)carbamate (3.019c)

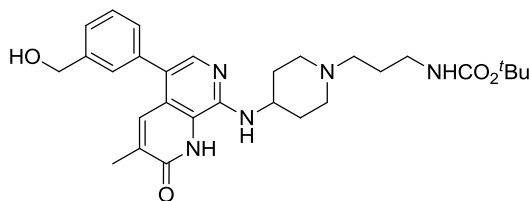


A mixture of **3.018** (120 mg, 0.24 mmol), (5-methylpyridin-3-yl)boronic acid (67 mg, 0.49 mmol), Pd(OAc)₂ (8 mg, 0.04 mmol), Catacxium A (13 mg, 0.04 mmol) and K₂CO₃ (81 mg, 0.58 mmol) in 1,4-Dioxane (2 mL) and H₂O (1 mL) was heated at 100 °C in a microwave reactor for 1 h. The reaction mixture was allowed to cool to rt, diluted with EtOAc (20 mL), filtered through Celite[®] and concentrated *in vacuo*. The resulting residue was purified by silica gel chromatography (0–100% EtOH in EtOAc). The appropriate fractions were combined and solvent evaporated *in vacuo* to give **3.019c** (70 mg, 0.14 mmol, 57%) as a yellow solid; ¹H NMR (400 MHz, CD₃OD) δ ppm 8.45 (s, 1H), 8.37 (d, *J* = 1.7, 1H), 7.73 (s, 2H), 7.62 (s, 1H), 4.14–4.04 (m, 1H), 3.11 (t, *J* = 6.7, 2H), 3.08–3.01 (m, 2H), 2.51–2.45 (m, 5H), 2.29–2.14 (m, 7H), 1.79–1.65 (m, 4H), 1.46 (s, 9H); LCMS (formic acid): R_t = 0.51 min (100%), MH⁺ = 507.3.

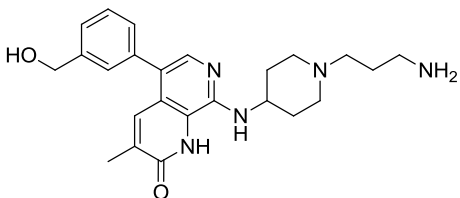
8-((1-(3-Aminopropyl)piperidin-4-yl)amino)-3-methyl-5-(5-methylpyridin-3-yl)-1,7-naphthyridin-2(1H)-one (3.002c)



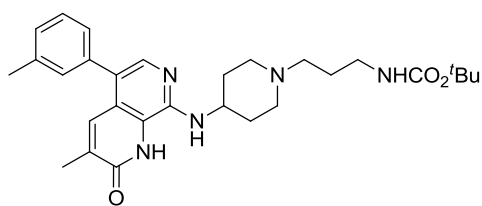
3.019c (70 mg, 0.14 mmol) was stirred in 4 M HCl in 1,4-dioxane (5 mL, 20.00 mmol) for 18 h. The reaction mixture was concentrated *in vacuo* and the resulting solid suspended in Et₂O (10 mL), filtered under reduced pressure, washed with Et₂O (10 mL) and collected. The resulting solid purified by MDAP (high pH). The appropriate fractions were combined and evaporated *in vacuo* to give **3.002c** (43 mg, 0.11 mmol, 77%) as a yellow solid; ¹H NMR (400 MHz, DMSO-d₆) δ ppm 8.44 (d, *J* = 1.7, 1H), 8.37 (d, *J* = 2.0, 1H), 7.67 (s, 1H), 7.62 (s, 1H), 7.49 (s, 1H), 6.85 (d, *J* = 6.6, 1H), 4.02–3.94 (m, 1H), 2.90–2.84 (m, 2H), 2.61–2.54 (m, 2H), 2.38 (s, 3H), 2.35–2.30 (m, 2H), 2.07 (d, *J* = 1.0, 3H), 2.05–1.97 (m, 4H), 1.56–1.47 (m, 4H); LCMS (high pH): R_t = 0.79 min (98%), MH⁺ = 407.5.

tert-Butyl (3-(4-((5-(3-(hydroxymethyl)phenyl)-3-methyl-2-oxo-1,2-dihydro-1,7-naphthyridin-8-yl)amino)piperidin-1-yl)propyl)carbamate (3.019g)

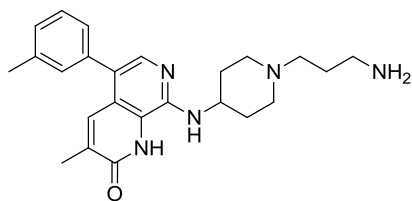
A mixture of **3.018** (300 mg, 0.61 mmol), (3-(hydroxymethyl)phenyl)boronic acid (184 mg, 1.21 mmol), Pd(OAc)₂ (20 mg, 0.09 mmol), Catacxium A (32 mg, 0.09 mmol) and K₂CO₃ (201 mg, 1.46 mmol) in 1,4-Dioxane (3 mL) and H₂O (1.5 mL) was heated at 100 °C in a microwave reactor for 1 h. The reaction mixture was allowed to cool to rt, diluted with EtOAc (20 mL), filtered through Celite[®] and concentrated *in vacuo*. The resulting residue was purified by silica gel chromatography (0–100% EtOH in EtOAc). The appropriate fractions were combined and solvent evaporated *in vacuo* to give **3.019g** (305 mg, 0.59 mmol, 96%) as a yellow solid; ¹H NMR (400 MHz, CD₃OD) δ ppm 7.73 (s, 1H), 7.71 (s, 1H), 7.50–7.26 (m, 4H), 4.70 (s, 2H), 4.15–4.03 (m, 1H), 3.15–3.07 (m, 4H), 2.59–2.50 (m, 2H), 2.42–2.31 (m, 2H), 2.23–2.14 (m, 5H), 1.81–1.68 (m, 4H), 1.46 (s, 9H); LCMS (formic acid): R_t = 0.61 min (96%), MH⁺ = 522.1.

8-((1-(3-Aminopropyl)piperidin-4-yl)amino)-5-(3-(hydroxymethyl)phenyl)-3-methyl-1,7-naphthyridin-2(1H)-one (3.002g)

3.019g (50 mg, 0.10 mmol) was stirred in 4 M HCl in 1,4-dioxane (2 mL, 8.00 mmol) for 18 h at rt. The reaction mixture was concentrated *in vacuo* and the resulting solid suspended in Et₂O (10 mL). The solvent was removed using a pipette and the remaining solid concentrated *in vacuo*. The resulting solid was purified by MDAP (formic acid). The appropriate fractions were combined and solvent evaporated *in vacuo*. The resulting residue was dissolved in MeOH (10 mL) and passed through a preconditioned (MeOH, 10 mL) amino propyl column (5 g), which was then washed with MeOH (20 mL). The filtrate was concentrated *in vacuo* to give **3.002g** (9 mg, 0.02 mmol, 22%) as a yellow solid; ¹H NMR (400 MHz, CD₃OD) δ ppm 7.68 (s, 1H), 7.65 (s, 1H), 7.50–7.45 (m, 2H), 7.43–7.38 (m, 2H), 7.30 (d, *J* = 7.6, 1H), 4.70 (s, 2H), 4.09–3.98 (m, 1H), 3.09–3.00 (m, 2H), 2.76 (t, *J* = 7.1, 2H), 2.53–2.47 (m, 2H), 2.30–2.13 (m, 7H), 1.80–1.63 (m, 4H); LCMS (formic acid): R_t = 0.37 min (100%), MH⁺ = 422.2.

tert-Butyl (3-(4-((3-methyl-2-oxo-5-(m-tolyl)-1,2-dihydro-1,7-naphthyridin-8-yl)amino)piperidin-1-yl)propyl)carbamate (3.019h)

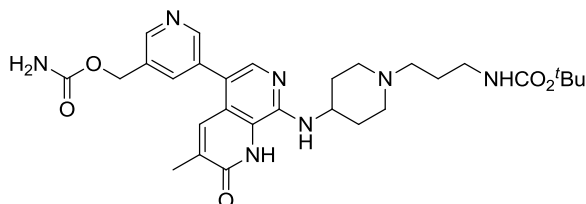
A mixture of **3.018** (300 mg, 0.61 mmol), (3-(hydroxymethyl)phenyl)boronic acid (184 mg, 1.21 mmol), Pd(OAc)₂ (20 mg, 0.09 mmol), Catacixium A (33 mg, 0.09 mmol) and K₂CO₃ (201 mg, 1.46 mmol) in 1,4-dioxane (3 mL) and H₂O (1.5 mL) was heated at 100 °C in a microwave reactor for 1 h. The reaction mixture was allowed to cool to rt, diluted with EtOAc (20 mL), filtered through Celite[®] and concentrated *in vacuo*. The resulting residue was purified by silica gel chromatography (0–100% EtOH in EtOAc). The appropriate fractions were combined and solvent evaporated *in vacuo* to give **3.019h** (69 mg, 0.14 mmol, 68%) as a yellow solid; ¹H NMR (400 MHz, CD₃OD) δ ppm 7.71–7.68 (m, 2H), 7.40–7.34 (m, 1H), 7.25 (d, *J* = 7.6, 1H), 7.19 (s, 1H), 7.15 (d, *J* = 7.6, 1H), 4.10–4.01 (m, 1H), 3.15–3.02 (m, 4H), 2.51–2.45 (m, 2H), 2.43 (s, 3H), 2.34–2.21 (m, 2H), 2.20–2.13 (m, 5H), 1.79–1.60 (m, 4H), 1.46 (s, 9H); LCMS (formic acid): R_t = 0.82 min (100%), MH⁺ = 506.3.

8-((1-(3-Aminopropyl)piperidin-4-yl)amino)-3-methyl-5-(m-tolyl)-1,7-naphthyridin-2(1H)-one (3.002h)

3.019h (69 mg, 0.14 mmol) was stirred in 4 M HCl in 1,4-dioxane (3 mL, 12.00 mmol) for 18 h at rt. The reaction mixture was concentrated *in vacuo* and the resulting solid suspended in Et₂O (10 mL), and concentrated *in vacuo*. The resulting solid was purified by MDAP (formic acid). The appropriate fractions were combined and solvent evaporated *in vacuo*. The resulting solid was dissolved in MeOH (10 mL) and passed through a preconditioned (MeOH, 10 mL) amino propyl column (10 g), which was then washed with MeOH (20 mL). The filtrate was concentrated *in vacuo* to give **3.002h** (30 mg, 0.07 mmol, 54%) as a yellow solid; m.p. 125–126 °C; *v*_{max} (solid)/cm⁻¹: 2922 (N-H), 1662 (C=O), 1594, 1444, 791; ¹H NMR (400 MHz, DMSO-d₆) δ ppm 7.66 (s, 1H), 7.53 (d, *J* = 1.2, 1H), 7.38–7.33 (m, 1H), 7.20 (d, *J* = 7.6, 1H), 7.17–7.11 (m, 2H), 6.80 (d, *J* = 6.6, 1H), 4.02–3.92 (m, 2H), 2.73–2.60 (m, 2H), 2.37 (s, 3H), 2.32 (t, *J* = 7.1, 2H), 2.06 (d, *J* = 1.2, 3H), 2.05–2.03 (m, 1H), 2.02–1.95 (m, 4H), 1.59–1.43 (m, 4H); ¹³C NMR (101 MHz, DMSO-d₆) δ ppm 162.1, 145.5, 138.4, 137.7, 136.6, 133.6, 133.1, 130.3, 128.4, 127.7, 126.9, 121.5, 120.9,

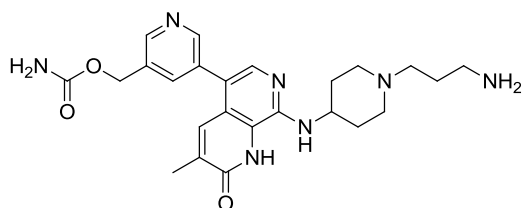
120.7, 55.7, 52.3, 47.9, 31.8, 21.0, 16.8; N. B. 2C signals hidden under solvent peak; HRMS (M + H)⁺ calculated for C₂₄H₃₂N₅O 406.2601; found 406.2605; LCMS (formic acid): R_t = 0.54 min (98%), MH⁺ = 406.1.

tert-Butyl (3-(4-((5-(5-((carbamoyloxy)methyl)pyridin-3-yl)-3-methyl-2-oxo-1,2-dihydro-1,7-naphthyridin-8-yl)amino)piperidin-1-yl)propyl)carbamate (3.019e)



To a mixture of **3.019b** (548 mg, 1.05 mmol) and pyridine (0.2 mL, 2.10 mmol) in DCM (8 mL), phenyl chloroformate (0.17 mL, 1.36 mmol) was added at 0 °C. The reaction mixture was left to stir at this temperature for 2 h. Phenyl chloroformate (0.17 mL, 1.36 mmol) was added and the reaction mixture was stirred for a further 1 h at 0 °C. The reaction mixture was diluted with sat. aq. NH₄Cl (20 mL) and DCM (10 mL). The organic layer was separated, passed through a hydrophobic frit and concentrated *in vacuo*. The resulting solution was diluted with DCM (5 mL), DMF (5 mL) and NH₄OH (0.12 mL, 1.05 mmol). The reaction mixture was left to stir at rt for 18 h. NH₄OH (0.12 mL, 1.05 mmol) was added and the solution was stirred for a further 24 h. The reaction mixture was diluted with DCM (10 mL) and H₂O (10 mL), and the organic layer separated. The aqueous layer was extracted into DCM (2 × 30 mL). The combined organic layers were passed through a hydrophobic frit and concentrated *in vacuo*. The resulting residue was purified by silica gel chromatography (10–100% EtOH in EtOAc). The appropriate fractions were combined and solvent evaporated *in vacuo* to give **3.019e** (364 mg, 0.64 mmol, 61%) as a yellow oil; ¹H NMR (400 MHz, CD₃OD) δ ppm 8.64–8.62 (m, 1H), 8.55–8.52 (m, 1H), 7.93–7.89 (m, 1H), 7.77 (s, 1H), 7.65–7.62 (m, 1H), 5.23 (s, 2H), 3.66–3.58 (m, 1H), 3.14–3.03 (m, 4H), 2.52–2.46 (m, 2H), 2.32–2.23 (m, 2H), 2.22–2.15 (m, 5H), 1.79–1.67 (m, 4H), 1.46 (s, 9H); LCMS (high pH): R_t = 0.85 min (76%), MH⁺ = 566.6.

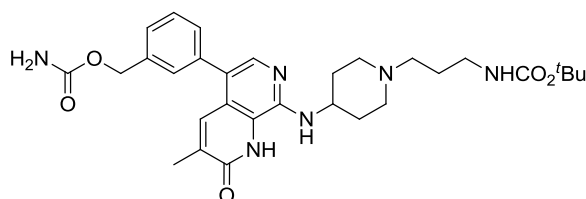
(5-(8-((1-(3-Aminopropyl)piperidin-4-yl)amino)-3-methyl-2-oxo-1,2-dihydro-1,7-naphthyridin-5-yl)pyridin-3-yl)methyl carbamate (3.002a)



3.019e (364 mg, 0.64 mmol) was stirred in 4 M HCl in 1,4-dioxane (5 mL, 20.00 mmol) for 18 h at rt. The reaction mixture was concentrated *in vacuo* and the resulting solid suspended in Et₂O

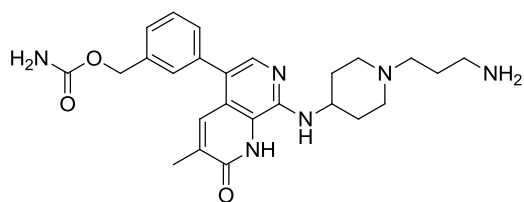
(10 mL), filtered under reduced pressure, washed with Et₂O (10 mL) and collected. The resulting solid was purified by MDAP (high pH). The appropriate fractions were combined and solvent evaporated *in vacuo* to give **3.002a** (170 mg, 0.37 mmol, 57%) as a pale yellow solid; m.p. 289–292 °C (decomp.); ν_{\max} (solid)/cm⁻¹: 3397 (N-H), 1737 (C=O), 1655 (C=O), 1594, 1336, 1088, 871, 669; ¹H NMR (400 MHz, DMSO-d₆) δ ppm 8.59 (d, *J* = 2.0, 1H), 8.53 (d, *J* = 2.0, 1H), 7.78–7.75 (m, 1H), 7.71 (s, 1H), 7.50 (d, *J* = 1.2, 1H), 6.88 (d, *J* = 6.8, 1H), 6.68 (br.s, 2H), 5.11 (s, 2H), 4.04–3.93 (m, 1H), 2.91–2.84 (m, 2H), 2.58 (t, *J* = 6.5, 2H), 2.33 (t, *J* = 7.2, 2H), 2.08 (d, *J* = 1.2, 3H), 2.06–1.98 (m, 4H), 1.56–1.47 (m, 4H); ¹³C NMR (125 MHz, DMSO-d₆) 162.4, 156.4, 149.2, 147.4, 146.3, 138.8, 136.5, 134.2, 132.8, 132.5, 132.5, 132.2, 120.7, 117.5, 62.5, 55.8, 52.3, 48.0, 31.8, 16.9; N.B. 2C signals hidden under solvent peak; HRMS (M + H)⁺ calculated for C₂₄H₃₂N₇O₃ 466.2555; found 466.2561. LCMS (high pH): R_t = 0.63 min (96%), MH⁺ = 466.5.

tert-Butyl (3-(4-((5-(3-((carbamoyloxy)methyl)phenyl)-3-methyl-2-oxo-1,2-dihydro-1,7-naphthyridin-8-yl)amino)piperidin-1-yl)propyl)carbamate (3.019i)



CDI (168 mg, 1.04 mmol) was added to a solution of **3.019g** (360 mg, 0.52 mmol) in THF (3 mL) and the reaction mixture was stirred at rt for 3 h. NH₄OH (0.12 mL, 1.04 mmol) was added and the mixture stirred for a further 18 h. The reaction mixture was diluted with H₂O (20 mL) and EtOAc (20 mL). The organic phase was separated and the aqueous was extracted with EtOAc (2 × 20 mL). The combined organic layers were passed through a hydrophobic frit and concentrated *in vacuo*. The resulting residue was purified by silica gel chromatography (0–100% EtOH in EtOAc). The appropriate fractions were combined and solvent evaporated *in vacuo* to give **3.019i** (241 mg, 0.43 mmol, 82%) as a yellow oil; ¹H NMR (400 MHz, CD₃OD) δ ppm 7.69–7.66 (m, 2H), 7.65–7.63 (m, 1H), 7.47–7.34 (m, 3H), 5.10 (s, 2H), 4.09–3.96 (m, 1H), 3.07–3.02 (m, 2H), 2.50–2.42 (m, 2H), 2.31–2.21 (m, 2H), 2.17–2.10 (m, 6H), 1.73–1.59 (m, 5H), 1.46–1.38 (m, 9H); LCMS (formic acid): R_t = 0.63 min (98%), MH⁺ = 565.3.

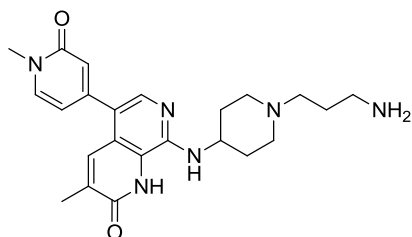
3-(8-((1-(3-Aminopropyl)piperidin-4-yl)amino)-3-methyl-2-oxo-1,2-dihydro-1,7-naphthyridin-5-yl)benzyl carbamate (3.002f)



3.019i (241 mg, 0.43 mmol) was stirred in 4 M HCl in 1,4-dioxane (3 mL, 12.00 mmol) for 18 h at rt. The reaction mixture was concentrated *in vacuo* and the resulting solid suspended in Et₂O

(10 mL), and concentrated *in vacuo*. The resulting solid was purified by MDAP (formic acid). The appropriate fractions were combined and concentrated *in vacuo*. The resulting solid was dissolved in MeOH (10 mL) and passed through a preconditioned (MeOH, 10 mL) amino propyl column (10 g) and washed with MeOH (20 mL). The filtrate was concentrated *in vacuo* to give **3.002f** (60 mg, 0.13 mmol, 30%) as a yellow solid; ¹H NMR (400 MHz, CD₃OD) δ ppm 7.68–7.65 (m, 2H), 7.51–7.46 (m, 1H), 7.44–7.39 (m, 2H), 7.35–7.32 (m, 1H), 5.16 (s, 2H), 4.08–4.00 (m, 1H), 3.08–3.00 (m, 2H), 2.77 (t, *J* = 7.1, 2H), 2.53–2.45 (m, 2H), 2.29–2.21 (m, 2H), 2.20–2.14 (m, 5H), 1.81–1.63 (m, 4H); LCMS (formic acid): *R*_t = 0.44 min (100%), *MH*⁺ = 465.2.

8-((1-(3-Aminopropyl)piperidin-4-yl)amino)-3-methyl-5-(1-methyl-2-oxo-1,2-dihydropyridin-4-yl)-1,7-naphthyridin-2(1H)-one (3.002d)



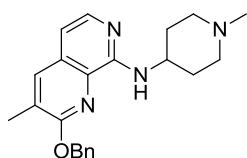
A mixture of **3.018** (150 mg, 0.30 mmol), 1-methyl-4-(4,4,5,5-tetramethyl-1,3,2-dioxaborolan-2-yl)pyridin-2(1H)-one (143 mg, 0.61 mmol), Pd(OAc)₂ (7 mg, 0.03 mmol), Catacixium A (11 mg, 0.03 mmol) and K₂CO₃

(84 mg, 0.61 mmol) in 1,4-dioxane (3 mL) and H₂O (1.5 mL) was heated at 100 °C in a microwave reactor for 1 h. The reaction mixture was allowed to cool to rt, diluted with EtOAc (50 mL) and DCM (50 mL), filtered through Celite[®] and concentrated *in vacuo*. The resulting residue was purified by silica gel chromatography (0–100% EtOH in EtOAc). The appropriate fractions were combined and solvent evaporated *in vacuo* to give **3.019d** (140 mg, 0.21 mmol, 71%) as a yellow oil; LCMS (formic acid): *R*_t = 0.53 min (62%), *MH*⁺ = 523.2.

3.019d (140 mg, 0.21 mmol) was immediately added to 4 M HCl in 1,4-dioxane (4 mL, 16.00 mmol) and the reaction mixture was left to stir at rt for 1 h. The volatile components were removed *in vacuo*. The resulting solid was purified by MDAP (high pH). The appropriate fractions were combined and concentrated *in vacuo* to give

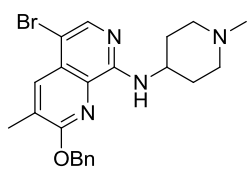
3.002d (34 mg, 0.08 mmol, 30%) as yellow solid; m.p. 210–212 °C; v_{\max} (solid)/ cm^{-1} : 3395 (N-H), 2936, 1647 (C=O), 1570, 1491, 1418, 1043, 864; ^1H NMR (400 MHz, DMSO- d_6) δ ppm 7.74 (d, J = 6.8, 1H), 7.71 (s, 1H), 7.64 (d, J = 1.2, 1H), 6.93 (d, J = 6.8, 1H), 6.33 (d, J = 2.0, 1H), 6.24 (dd, J = 6.8, 2.0, 1H), 5.10 (br.s, 2H), 4.02–3.91 (m, 1H), 3.47 (s, 3H), 2.91–2.78 (m, 2H), 2.59 (t, J = 6.7, 2H), 2.32 (t, J = 7.1, 2H), 2.10 (s, 3H), 2.05–1.92 (m, 4H), 1.57–1.41 (m, 4H); LCMS (high pH): R_t = 0.57 min (100%), MH^+ = 423.2; ^{13}C NMR (101 MHz, DMSO- d_6) δ ppm 162.6, 161.7, 148.6, 146.8, 139.2, 137.8, 133.8, 132.5, 121.6, 120.0, 118.5, 117.9, 107.2, 55.7, 52.2, 47.9, 36.4, 31.7, 16.9; N.B. 2C signals hidden under solvent peak; HRMS ($\text{M} + \text{H}$) $^+$ calculated for $\text{C}_{23}\text{H}_{31}\text{N}_6\text{O}_2$ 423.2503; found 423.2501; LCMS (high pH): R_t = 0.57 min (100%), MH^+ = 423.4.

2-(Benzyloxy)-3-methyl-N-(1-methylpiperidin-4-yl)-1,7-naphthyridin-8-amine (3.021a)



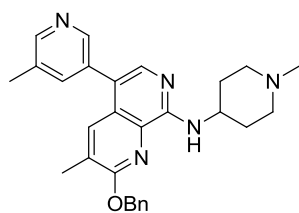
1-methylpiperidin-4-amine (0.40 mL, 3.16 mmol) was added to a mixture of **3.012** (600 mg, 2.11 mmol), $\text{Pd}_2(\text{dba})_3$ (154 mg, 0.17 mmol), Brettphos (113 mg, 0.21 mmol), and NaO^tBu (810 mg, 8.43 mmol) in THF (10 mL). The reaction mixture was heated at 60 °C for 4 h. The reaction mixture was concentrated *in vacuo* and the resulting residue was diluted with DCM (100 mL) and washed with H_2O (100 mL). The separated organic layer was passed through a hydrophobic frit and concentrated *in vacuo*. The resulting residue was purified by silica gel chromatography (0–60% EtOAc in cyclohexane). The appropriate fractions were combined and solvent evaporated *in vacuo* to give **3.021a** (688 mg, 1.90 mmol, 90%) as a orange oil; v_{\max} (thin film)/ cm^{-1} : 1500, 1310, 1250, 742; ^1H NMR (400 MHz, CD_3OD) δ ppm 7.77–7.74 (m, 1H), 7.69 (d, J = 5.9, 1H), 7.52–7.47 (m, 2H), 7.41–7.35 (m, 2H), 7.33–7.27 (m, 1H), 6.77 (d, J = 5.9, 1H), 5.53 (s, 2H), 4.02–3.92 (m, 1H), 2.98–2.86 (m, 2H), 2.38–2.24 (m, 8H), 2.15–2.03 (m, 2H), 1.74–1.62 (m, 2H); ^{13}C NMR (101 MHz, CD_3OD) δ ppm 161.4, 155.3, 140.2, 139.1, 137.6, 131.0, 129.7, 129.6, 128.9, 128.7, 128.6, 109.4, 69.4, 55.6, 48.0, 46.3, 32.9, 16.7; HRMS ($\text{M} + \text{H}$) $^+$ calculated for $\text{C}_{22}\text{H}_{27}\text{N}_4\text{O}$ 363.2179; found 363.2190; LCMS (formic acid): R_t = 0.56 min (100%), MH^+ = 363.2.

2-(Benzyloxy)-5-bromo-3-methyl-N-(1-methylpiperidin-4-yl)-1,7-naphthyridin-8-amine (3.022a)

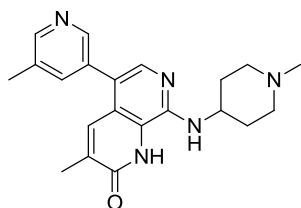


NBS (194 mg, 1.10 mmol) was added to a solution of **3.021a** (395 mg, 1.10 mmol) in THF (5 mL) and the mixture was stirred at rt for 4 h. The reaction mixture was concentrated *in vacuo*. The resulting residue was dissolved in DCM (30 mL) and washed with H₂O (50 mL). The organic phase was separated and the aqueous washed with DCM (3 × 50 mL). The combined organic layers were passed through a hydrophobic frit and concentrated *in vacuo*. The resulting residue was purified by silica gel chromatography (0–100% EtOH and EtOAc). The appropriate fractions were combined and solvent evaporated *in vacuo* to give **3.022a** (234 mg, 0.53 mmol, 49%) as an orange oil. ¹H NMR (400 MHz, CDCl₃) δ ppm 7.99 (s, 1H), 7.95 (d, *J* = 1.0, 1H), 7.52–7.48 (m, 2H), 7.46–7.39 (m, 2H), 7.37–7.31 (m, 1H), 6.20 (d, *J* = 8.1, 1H), 5.52 (s, 2H), 4.19–4.07 (m, 1H), 3.20–3.09 (m, 2H), 2.54–2.47 (m, 5H), 2.44 (d, *J* = 1.0, 3H), 2.24–2.17 (m, 2H), 1.93–1.83 (m, 2H); LCMS (formic acid): R_t = 0.90 min (98%), MH⁺ = 441.1, 443.1.

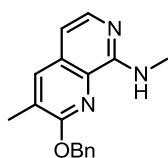
2-(Benzyloxy)-3-methyl-N-(1-methylpiperidin-4-yl)-5-(5-methylpyridin-3-yl)-1,7-naphthyridin-8-amine (3.023a)



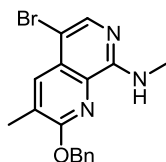
A mixture of **3.022a** (234 mg, 0.53 mmol), (5-methylpyridin-3-yl)boronic acid (145 mg, 1.06 mmol), Pd(OAc)₂ (12 mg, 0.05 mmol), Catacxiium A (19 mg, 0.05 mmol) and K₂CO₃ (147 mg, 1.06 mmol) in 1,4-dioxane (3 mL) and H₂O (1.5 mL) was heated at 100 °C in a microwave reactor for 1 h. The reaction mixture was allowed to cool to rt, diluted with EtOAc (20 mL), filtered through Celite[®] and concentrated *in vacuo*. The resulting residue was purified by silica gel chromatography (0–100% EtOH and EtOAc). The appropriate fractions were combined and solvent evaporated *in vacuo* to give **3.023a** (116 mg, 0.26 mmol, 48%) as a yellow solid; ¹H NMR (400 MHz, CD₃OD) δ ppm 8.41 (s, 1H), 8.37 (s, 1H), 7.73–7.69 (m, 2H), 7.68–7.65 (m, 1H), 7.53–7.48 (m, 2H), 7.42–7.34 (m, 2H), 7.33–7.27 (m, 1H), 5.57 (s, 2H), 4.07–3.95 (m, 1H), 2.96–2.88 (m, 2H), 2.44 (s, 3H), 2.36–2.23 (m, 8H), 2.16–2.08 (m, 2H), 1.79–1.66 (m, 2H); LCMS (formic acid): R_t = 0.62 min (96%), MH⁺ = 454.2.

3-Methyl-8-((1-methylpiperidin-4-yl)amino)-5-(5-methylpyridin-3-yl)-1,7-naphthyridin-2(1H)-one (3.020a)

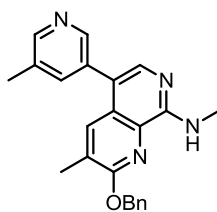
3.023a (116 mg, 0.26 mmol) was dissolved in TFA (3 mL, 38.90 mmol) and left to stir at 80 °C for 3 h. The volatile components were removed *in vacuo*. Toluene (5 mL) was added and the solvent evaporated *in vacuo* (x 3). The resulting residue was dissolved in MeOH (10 mL) and passed through a preconditioned (MeOH, 10 mL) amino propyl column (5 g). The appropriate fractions were combined and solvent evaporated *in vacuo*. The resulting residue was purified by MDAP (high pH). The appropriate fractions were combined and solvent evaporated *in vacuo* to give **3.020a** (65 mg, 0.18 mmol, 70%) as a yellow solid; m.p. 262–265 °C (decomp.); ν_{\max} (solid)/ cm^{-1} : 3392, 2926, 1660 (C=O), 1695, 1445, 860, 723; ^1H NMR (400 MHz, DMSO- d_6) δ ppm 11.47 (br.s, 1H), 8.44 (d, $J = 1.7$, 1H), 8.36 (d, $J = 1.7$, 1H), 7.71 (s, 1H), 7.62 (s, 1H), 7.51 (d, $J = 1.2$, 1H), 6.84 (d, $J = 6.6$, 1H), 4.00–3.91 (m, 1H), 2.80–2.74 (m, 2H), 2.37 (s, 3H), 2.18 (s, 3H), 2.07 (s, 3H), 2.05–1.94 (m, 4H), 1.59–1.44 (m, 2H); ^{13}C NMR (101 MHz, DMSO- d_6) 161.1, 148.7, 147.3, 139.3, 137.7, 133.0, 132.9, 132.0, 121.1, 120.6, 118.1, 54.5, 47.6, 46.2, 31.8, 18.0, 16.9; N.B. 2C signals not visible in spectrum; HRMS ($M + \text{H}^+$) calculated for $\text{C}_{21}\text{H}_{26}\text{N}_5\text{O}$ 364.2138; found 364.2132; LCMS (formic acid): $R_t = 0.35$ min (100%), $\text{MH}^+ = 364.1$.

2-(Benzyloxy)-N,3-dimethyl-1,7-naphthyridin-8-amine (3.021b)

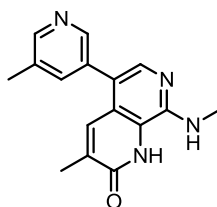
A 2 M solution of methanamine in THF, (1.58 mL, 3.16 mmol) was added to a mixture of **3.012** (600 mg, 2.107 mmol), $\text{Pd}_2(\text{dba})_3$ (154 mg, 0.17 mmol), Brettphos (113 mg, 0.21 mmol), and NaO^tBu (810 mg, 8.43 mmol) in THF (10 mL). The reaction mixture was heated at 60 °C for 4 h. The reaction mixture was concentrated *in vacuo* and the resulting residue was diluted with DCM (100 mL) and washed with H_2O (100 mL). The separated organic layer was passed through a hydrophobic frit and concentrated *in vacuo*. The resulting residue was purified by silica gel chromatography (0–60% EtOAc in cyclohexane). The appropriate fractions were combined and solvent evaporated *in vacuo* to give **3.021b** (273 mg, 0.98 mmol, 46%) as an orange oil; ^1H NMR (400 MHz, CD_3OD) δ ppm 7.63 (d, $J = 5.9$, 1H), 7.55 (s, 1H), 7.46–7.40 (m, 2H), 7.35–7.27 (m, 2H), 7.26–7.21 (m, 1H), 6.61 (d, $J = 5.9$, 1H), 5.41 (s, 2H), 3.02 (s, 3H), 2.22 (s, 3H); LCMS (formic acid): $R_t = 0.73$ min (99%), $\text{MH}^+ = 280.1$

2-(Benzyloxy)-5-bromo-N, 3-dimethyl-1,7-naphthyridin-8-amine (3.022b)

NBS (174 mg, 0.98 mmol) was added to a solution of **3.021b** (273 mg, 0.98 mmol) in THF (5 mL). The reaction mixture was stirred at rt for 3 h. The reaction mixture was concentrated *in vacuo*. The resulting residue was dissolved in DCM (30 mL) and washed with H₂O (50 mL). The organic phase was separated and the aqueous washed with DCM (3 × 50 mL). The combined organic layers were passed through a hydrophobic frit and concentrated *in vacuo* to give **3.022b** (350 mg, 0.98 mmol, quant.) as a brown solid; ¹H NMR (400 MHz, DMSO-d₆) δ ppm 8.00–7.97 (m, 2H), 7.56–7.52 (m, 2H), 7.44–7.39 (m, 2H), 7.37–7.32 (m, 1H), 5.64 (s, 2H), 3.00 (d, *J* = 4.6, 3H), 2.38 (s, 3H); LCMS (formic acid): R_t = 1.03 min (99%), MH⁺ = 357.9, 359.9.

2-(Benzyloxy)-N,3-dimethyl-5-(5-methylpyridin-3-yl)-1,7-naphthyridin-8-amine (3.023b)

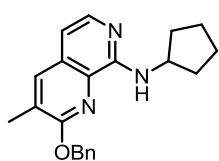
A mixture of **3.022b** (350 mg, 0.98 mmol), (5-methylpyridin-3-yl)boronic acid (268 mg, 1.95 mmol), Pd(OAc)₂ (22 mg, 0.10 mmol), Catacxiium A (35 mg, 0.10 mmol) and K₂CO₃ (270 mg, 1.9 mmol) in 1,4-dioxane (3 mL) and H₂O (1.5 mL) was heated at 100 °C in a microwave reactor for 1 h. The reaction mixture was allowed to cool to rt, diluted with EtOAc (20 mL), filtered through Celite[®] and concentrated *in vacuo*. The resulting residue was purified by silica gel chromatography (0–100% EtOAc in cyclohexane). The appropriate fractions were combined and solvent evaporated *in vacuo* to give **3.023b** (195 mg, 0.53 mmol, 54%) as a yellow solid; ¹H NMR (400 MHz, CD₃OD) δ ppm 8.41–8.39 (m, 1H), 8.37–8.35 (m, 1H), 7.70–7.68 (m, 2H), 7.67 (s, 1H), 7.52–7.48 (m, 2H), 7.40–7.35 (m, 2H), 7.33–7.28 (m, 1H), 5.54 (s, 2H), 3.13 (s, 3H), 2.43 (s, 3H), 2.28 (s, 3H); LCMS (formic acid): R_t = 0.73 min (97%), MH⁺ = 371.1.

3-Methyl-8-(methylamino)-5-(5-methylpyridin-3-yl)-1,7-naphthyridin-2(1H)-one (3.020b)

3.023b (195 mg, 0.53 mmol) was dissolved in TFA (3 mL, 38.90 mmol) and left to stir at 80 °C for 3 h. The volatile components were removed *in vacuo*. Toluene (5 mL) was added and the solvent evaporated *in vacuo* (× 3). The resulting residue was dissolved in MeOH (10 mL) and passed through a preconditioned (MeOH, 10 mL) amino propyl column (5 g). The appropriate fractions

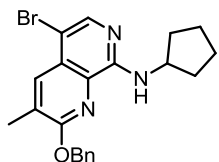
were combined and solvent evaporated *in vacuo*. The resulting residue was purified by MDAP (high pH). The appropriate fractions were combined and solvent evaporated *in vacuo* to give **3.020b** (31 mg, 0.11 mmol, 21%) as a yellow solid; m.p. >300 °C; ν_{\max} (solid)/ cm^{-1} : 3393 (N-H), 1697 (C=O), 1457, 836, 730; ^1H NMR (400 MHz, DMSO- d_6) δ ppm 11.35 (br. s, 1H), 8.45 (d, J = 1.6, 1H), 8.38 (d, J = 1.6, 1H), 7.74 (s, 1H), 7.66–7.61 (m, 1H), 7.56–7.50 (m, 1H), 7.09–7.00 (m, 1H), 3.33 (s, 3H), 2.97 (d, J = 4.4, 3H), 2.38 (s, 3H); ^{13}C NMR (101 MHz, DMSO- d_6) δ ppm 161.8, 148.5, 147.1, 145.8, 139.1, 137.4, 134.1, 132.8, 132.7, 131.9, 120.7, 120.5, 117.9, 28.1, 17.8, 16.7; HRMS ($M + H$) $^+$ calculated for $\text{C}_{16}\text{H}_{17}\text{N}_4\text{O}$ 281.1397; found 281.1405; LCMS (formic acid): R_t = 0.36 min (100%), MH^+ = 281.0.

2-(Benzyloxy)-*N*-cyclopentyl-3-methyl-1,7-naphthyridin-8-amine (3.021c)



Cyclopentanamine (0.18 mL, 1.84 mmol) was added to a mixture of **3.012** (350 mg, 1.23 mmol), $\text{Pd}_2(\text{dba})_3$ (90 mg, 0.10 mmol), Brettphos (66 mg, 0.12 mmol), and NaO^tBu (473 mg, 4.92 mmol) in THF (10 mL). The reaction mixture was heated at 60 °C for 18 h. The reaction mixture was concentrated *in vacuo* and the resulting residue was diluted with DCM (100 mL) and washed with H_2O (100 mL). The separated organic layer was passed through a hydrophobic frit and concentrated *in vacuo*. The resulting residue was purified by silica gel chromatography (0–100% EtOAc in cyclohexane). The appropriate fractions were combined and solvent evaporated *in vacuo* to give **3.021c** (403 mg, 1.20 mmol, 98%) as an orange solid; ^1H NMR (400 MHz, CDCl_3) δ ppm 7.89 (d, J = 5.6, 1H), 7.62 (d, J = 1.0, 1H), 7.52–7.47 (m, 2H), 7.42–7.36 (m, 2H), 7.35–7.30 (m, 1H), 6.68 (d, J = 5.6, 1H), 6.25 (d, J = 7.6, 1H), 5.49 (s, 2H), 4.54–4.44 (m, 1H), 2.36 (d, J = 1.0, 3H), 2.21–2.10 (m, 2H), 1.84–1.67 (m, 4H), 1.61–1.52 (m, 2H); LCMS (formic acid): R_t = 0.88 min (93%), MH^+ = 334.0.

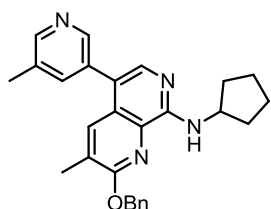
2-(Benzyloxy)-5-bromo-*N*-cyclopentyl-3-methyl-1,7-naphthyridin-8-amine (3.022c)



NBS (215 mg, 1.21 mmol) was added to a solution of **3.021c** (403 mg, 1.21 mmol) in THF (3 mL) and the mixture was stirred at rt for 4 h. The reaction mixture was concentrated *in vacuo*. The resulting residue was dissolved in DCM (50 mL) and washed with H_2O (50 mL). The organic phase was separated and the aqueous washed with DCM (3 × 50 mL). The combined organic layers were passed through a hydrophobic frit

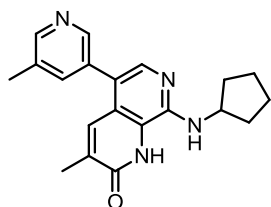
and concentrated *in vacuo*. The resulting residue was purified by silica gel chromatography (0–50% EtOAc in cyclohexane). The appropriate fractions were combined and solvent evaporated *in vacuo* to give **3.022c** (448 mg, 1.09 mmol, 90%) as an off white solid; $^1\text{H NMR}$ (400 MHz, CDCl_3) δ ppm 8.02 (s, 1H), 7.95 (d, $J = 1.0$, 1H), 7.52–7.47 (m, 2H), 7.43–7.37 (m, 2H), 7.36–7.31 (m, 1H), 6.26 (d, $J = 7.3$, 1H), 5.50 (s, 2H), 4.48–4.38 (m, 1H), 2.43 (d, $J = 1.0$, 3H), 2.20–2.11 (m, 2H), 1.84–1.67 (m, 4H), 1.66–1.51 (m, 2H); LCMS (formic acid): $R_t = 1.41$ min (100%), $\text{MH}^+ = 412.0$, 414.0.

2-(Benzyloxy)-N-cyclopentyl-3-methyl-5-(5-methylpyridin-3-yl)-1,7-naphthyridin-8-amine (3.023c)



A mixture of **3.022c** (440 mg, 1.07 mmol), (5-methylpyridin-3-yl)boronic acid (219 mg, 1.60 mmol), $\text{Pd}(\text{OAc})_2$ (24 mg, 0.11 mmol), Catacixium A (38 mg, 0.11 mol) and K_2CO_3 (295 mg, 2.13 mmol) in 1,4-dioxane (3 mL) and H_2O (1.5 mL) was heated at 100 °C in a microwave reactor for 2 h. The reaction mixture was allowed to cool to rt, diluted with EtOAc (20 mL), filtered through Celite[®] and concentrated *in vacuo*. The resulting residue was purified by silica gel chromatography (0–100% EtOAc in Cyclohexane). The appropriate fractions were combined and solvent evaporated *in vacuo* to give **3.023c** (259 mg, 0.61 mmol, 57%) as a yellow solid; $^1\text{H NMR}$ (400 MHz, CDCl_3) δ ppm 8.49 (d, $J = 1.7$, 1H), 8.46 (d, $J = 1.7$, 1H), 7.85 (s, 1H), 7.71 (d, $J = 1.0$, 1H), 7.55–7.48 (m, 3H), 7.43–7.37 (m, 2H), 7.36–7.31 (m, 1H), 6.39 (d, $J = 7.6$, 1H), 5.53 (s, 2H), 4.59–4.47 (m, 1H), 2.42 (s, 3H), 2.34 (d, $J = 1.0$, 3H), 2.24–2.15 (m, 2H), 1.86–1.69 (m, 4H), 1.66–1.56 (m, 2H); LCMS (formic acid): $R_t = 0.91$ min (75%), $\text{MH}^+ = 425.1$.

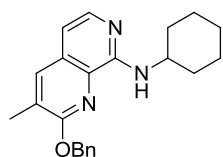
8-(Cyclopentylamino)-3-methyl-5-(5-methylpyridin-3-yl)-1,7-naphthyridin-2(1H)-one (3.020c)



3.023c (259 mg, 0.61 mmol) was dissolved in TFA (3 mL, 38.90 mmol) and left to stir at 80 °C for 4 h. The volatile components were removed *in vacuo*. Toluene (5 mL) was added and the solvent evaporated *in vacuo* ($\times 3$). The resulting residue was dissolved in MeOH (20 mL) and passed through a preconditioned (MeOH, 20 mL) amino propyl column (10 g). The column was rinsed with MeOH (50 mL) and the filtrate concentrated *in vacuo*. The resulting residue was suspended in MeOH (10 mL), filtered under reduced pressure,

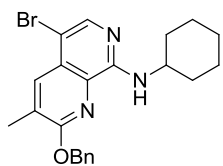
collected and dried at 40 °C under vacuum for 3 h to give **3.020c** (135 mg, 0.40 mmol, 66%) as a pale yellow solid; ¹H NMR (400 MHz, DMSO-d₆) δ ppm 11.49 (s, 1H), 8.45 (d, *J* = 1.6, 1H), 8.38 (d, *J* = 1.6, 1H), 7.72 (s, 1H), 7.64–7.62 (m, 1H), 7.51 (s, 1H), 6.94 (d, *J* = 5.9, 1H), 4.44–4.37 (m, 1H), 2.38 (s, 3H), 2.08 (s, 3H), 2.04–1.95 (m, 2H), 1.78–1.70 (m, 2H), 1.65–1.51 (m, 4H); LCMS (formic acid): *R*_t = 0.53 min (100%), *MH*⁺ = 335.0.

2-(Benzyloxy)-*N*-cyclohexyl-3-methyl-1,7-naphthyridin-8-amine (3.021d)



Cyclohexanamine (0.30 mL, 2.63 mmol) was added to a mixture of **3.012** (500 mg, 1.76 mmol), Pd₂(dba)₃ (129 mg, 0.14 mmol), Brettphos (94 mg, 0.18 mmol), and NaO^tBu (675 mg, 7.02 mmol) in THF (10 mL). The reaction mixture was heated at 60 °C for 4 h. The reaction mixture was concentrated *in vacuo* and the resulting residue was diluted with DCM (100 mL) and washed with H₂O (100 mL). The separated organic layer was passed through a hydrophobic frit and concentrated *in vacuo*. The resulting residue was purified by silica gel chromatography (0–60% EtOAc in cyclohexane). The appropriate fractions were combined and solvent evaporated *in vacuo* to give **3.021d** (555 mg, 1.60 mmol, 91%) as a yellow oil; ¹H NMR (400 MHz, CDCl₃) δ ppm 7.87 (d, *J* = 5.7, 1H), 7.61 (d, *J* = 1.0, 1H), 7.50 (d, *J* = 7.3, 2H), 7.42–7.35 (m, 2H), 7.35–7.29 (m, 1H), 6.66 (d, *J* = 5.7, 1H), 6.24 (d, *J* = 8.3, 1H), 5.53 (s, 2H), 4.14–4.03 (m, 1H), 2.37 (s, 3H), 2.18–2.07 (m, 2H), 1.83 (m, 2H), 1.73–1.66 (m, 2H), 1.56–1.48 (m, 2H), 1.39–1.31 (m, 2H); LCMS (formic acid): *R*_t = 0.93 min (95%), *MH*⁺ = 348.1.

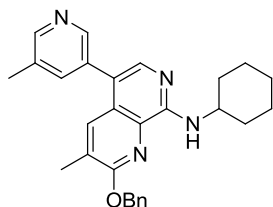
2-(Benzyloxy)-5-bromo-*N*-cyclohexyl-3-methyl-1,7-naphthyridin-8-amine (3.022d)



NBS (313 mg, 1.76 mmol) was added to a solution of **3.021d** (555 mg, 1.60 mmol) in THF (5 mL). The reaction mixture was stirred at rt for 1 h, then concentrated *in vacuo*. The resulting residue was dissolved in DCM (30 mL) and washed with H₂O (50 mL). The organic phase was separated and the aqueous washed with DCM (3 × 50 mL). The combined organic layers were passed through a hydrophobic frit and concentrated *in vacuo*. The resulting residue was purified by silica gel chromatography (0–50% EtOAc in cyclohexane). The appropriate fractions were combined and solvent evaporated *in vacuo* to give **3.022d** (457 mg, 1.07 mmol, 67%) as a yellow solid; ¹H NMR (400 MHz, CDCl₃) δ ppm 8.01 (s, 1H), 7.94 (d,

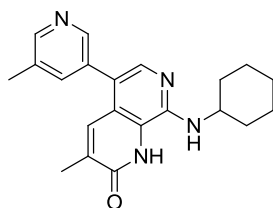
$J = 1.0$, 1H), 7.52–7.48 (m, 2H), 7.43–7.38 (m, 2H), 7.37–7.31 (m, 1H), 6.24 (d, $J = 8.1$, 1H), 5.51 (s, 2H), 4.08–3.96 (m, 1H), 2.43 (d, $J = 1.0$, 3H), 2.16–2.07 (m, 2H), 1.83–1.74 (m, 2H), 1.74–1.66 (m, 1H), 1.53–1.46 (m, 2H), 1.40–1.27 (m, 3H); LCMS (formic acid): $R_t = 1.54$ min (100%), $MH^+ = 426.0$, 428.0.

2-(Benzyloxy)-*N*-cyclohexyl-3-methyl-5-(5-methylpyridin-3-yl)-1,7-naphthyridin-8-amine (3.023d)



A mixture of **3.022d** (555 mg, 1.30 mmol), (5-methylpyridin-3-yl)boronic acid (357 mg, 2.60 mmol), $Pd(OAc)_2$ (29 mg, 0.13 mmol), Catacxiium A (47 mg, 0.13 mmol) and K_2CO_3 (360 mg, 2.60 mmol) in 1,4-dioxane (3 mL) and H_2O (1.5 mL) was heated at 100 °C in a microwave reactor for 1 h. The reaction mixture was allowed to cool to rt, diluted with EtOAc (20 mL), filtered through Celite® and concentrated *in vacuo*. The resulting residue was purified by silica gel chromatography (0–100% EtOAc in cyclohexane). The appropriate fractions were combined and solvent evaporated *in vacuo* to give **3.023d** (349 mg, 0.80 mmol, 61%) as a yellow solid; 1H NMR (400 MHz, CD_3OD) δ ppm 8.43 (s, 1H), 8.39 (s, 1H), 7.77–7.73 (m, 2H), 7.67 (s, 1H), 7.56–7.49 (m, 2H), 7.42–7.36 (m, 2H), 7.34–7.29 (m, 1H), 5.59 (s, 2H), 4.04–3.97 (m, 1H), 2.47 (s, 3H), 2.37 (s, 3H), 2.15–2.06 (m, 2H), 1.87–1.80 (m, 2H), 1.75–1.68 (m, 1H), 1.60–1.35 (m, 5H); LCMS (high pH): $R_t = 1.67$ min (100%), $MH^+ = 439.5$.

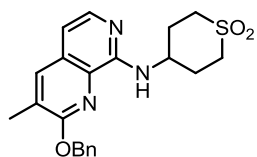
8-(Cyclohexylamino)-3-methyl-5-(5-methylpyridin-3-yl)-1,7-naphthyridin-2(1H)-one (3.020d)



3.023d (349 mg, 0.80 mmol) was dissolved in TFA (3 mL, 38.90 mmol) and left to stir at 80 °C for 3 h. The volatile components were removed *in vacuo*. Toluene (5 mL) was added and the solvent evaporated *in vacuo* (x3). The resulting residue was dissolved in MeOH (10 mL) and passed through a preconditioned (MeOH, 10 mL) amino propyl column (5 g). The appropriate fractions were combined and solvent evaporated *in vacuo*. The resulting residue was purified by MDAP (high pH). The appropriate fractions were combined and solvent evaporated *in vacuo* to give **3.020d** (19 mg, 0.06 mmol, 7%) as a pale yellow solid; m.p. 269–271 °C; v_{max} (solid)/ cm^{-1} : 2954, 1622 (C=O), 1593, 1452, 756; 1H NMR (400 MHz, $DMSO-d_6$) δ ppm 11.49 (br.s, 1H), 8.44 (d, $J = 1.8$, 1H), 8.37 (d, $J = 1.8$, 1H), 7.68 (s, 1H), 7.61 (s, 1H), 7.53–7.44 (m, 1H), 6.83 (d, $J = 6.8$, 1H),

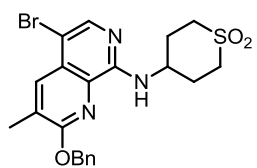
4.06–3.96 (m, 1H), 2.38 (s, 3H), 2.07 (s, 3H), 2.05–1.97 (m, 2H), 1.81–1.73 (m, 2H), 1.66–1.58 (m, 1H), 1.43–1.20 (m, 5H); ^{13}C NMR (101 MHz, DMSO- d_6) δ ppm 161.9, 148.4, 147.1, 139.1, 137.4, 132.8, 132.7, 131.9, 120.8, 117.7, 49.2, 32.5, 25.5, 24.7, 17.8, 16.7; N.B. 3C signals not visible in spectrum; HRMS ($M + H$) $^+$ calculated for $\text{C}_{21}\text{H}_{25}\text{N}_4\text{O}$ 349.2023; found 349.2026; LCMS (high pH): $R_t = 0.61$ min (100%), $\text{MH}^+ = 349.1$.

4-((2-(Benzyloxy)-3-methyl-1,7-naphthyridin-8-yl)amino)tetrahydro-2H-thiopyran 1,1-dioxide (3.021e)



4-Aminotetrahydro-2H-thiopyran 1,1-dioxide hydrochloride (342 mg, 1.84 mmol) was added to a mixture of **3.012** (350 mg, 1.23 mmol), $\text{Pd}_2(\text{dba})_3$ (90 mg, 0.10 mmol), Brettphos (66 mg, 0.12 mmol), and NaO^tBu (473 mg, 4.92 mmol) in THF (10 mL). The reaction mixture was heated at 60 °C for 18 h and then at 70 °C for 4 h. The reaction mixture was concentrated *in vacuo* and the resulting residue was diluted with DCM (100 mL) and washed with H_2O (100 mL). The separated organic layer was passed through a hydrophobic frit and concentrated *in vacuo*. The resulting residue was purified by silica gel chromatography (0–50% EtOH in EtOAc). The appropriate fractions were combined and solvent evaporated *in vacuo* to give **3.021e** (151 mg, 0.38 mmol, 31%) as a brown solid; ^1H NMR (400 MHz, CDCl_3) δ ppm 7.86 (d, $J = 5.9$, 1H), 7.68–7.65 (m, 1H), 7.51–7.46 (m, 2H), 7.44–7.38 (m, 2H), 7.37–7.31 (m, 1H), 6.78 (d, $J = 5.9$, 1H), 6.17 (d, $J = 7.8$, 1H), 5.50 (s, 2H), 4.43–4.32 (m, 1H), 3.27–3.11 (m, 4H), 2.55–2.47 (m, 2H), 2.42–2.38 (m, 3H), 2.36–2.23 (m, 2H); LCMS (formic acid): $R_t = 0.77$ min (98%), $\text{MH}^+ = 398.0$.

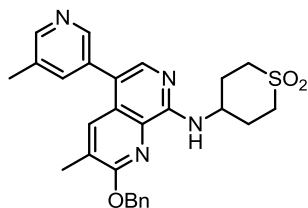
((2-(Benzyloxy)-5-bromo-3-methyl-1,7-naphthyridin-8-yl)amino)tetrahydro-2H-thiopyran 1,1-dioxide (3.022e)



NBS (68 mg, 0.38 mmol) was added to a solution of **3.021e** (151 mg, 0.38 mmol) in THF (3 mL) and the mixture was stirred at rt for 48 h. The reaction mixture was concentrated *in vacuo*. The resulting residue was dissolved in DCM (50 mL) and washed with H_2O (50 mL). The organic phase was separated and the aqueous washed with DCM (3 \times 50 mL). The combined organic layers were passed through a hydrophobic frit and concentrated *in vacuo*. The resulting residue was purified by silica gel chromatography (0–50% EtOAc in cyclohexane). The appropriate fractions were combined and solvent evaporated *in vacuo* to give **3.022e** (132 mg,

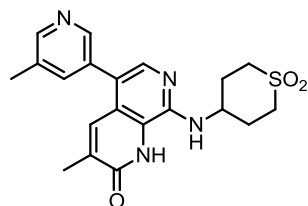
0.28 mmol, 73%) as an off white solid; $^1\text{H NMR}$ (400 MHz, DMSO-d_6) δ ppm 8.01–7.97 (m, 2H), 7.59–7.52 (m, 2H), 7.43–7.38 (m, 2H), 7.35–7.30 (m, 1H), 7.10 (d, $J = 8.6$, 1H), 5.66 (s, 2H), 4.47–4.35 (m, 1H), 3.45–3.35 (m, 2H), 3.14–3.07 (m, 2H), 2.40–2.37 (m, 3H), 2.31–2.20 (m, 4H); LCMS (formic acid): $R_t = 1.36$ min (100%), $\text{MH}^+ = 476.0, 478.0$.

4-((2-(Benzyloxy)-3-methyl-5-(5-methylpyridin-3-yl)-1,7-naphthyridin-8-yl)amino)tetrahydro-2H-thiopyran 1,1-dioxide (3.023e)



A mixture of **3.022e** (125 mg, 0.26 mmol), (5-methylpyridin-3-yl)boronic acid (72 mg, 0.53 mmol), $\text{Pd}(\text{OAc})_2$ (6 mg, 0.03 mmol), Catacixium A (9 mg, 0.03 mmol) and K_2CO_3 (73 mg, 0.53 mmol) in 1,4-dioxane (3 mL) and H_2O (1.5 mL) was heated at 100°C in a microwave reactor for 2 h. (5-Methylpyridin-3-yl)boronic acid (72 mg, 0.53 mmol) was added and the reaction mixture was heated at 100°C in a microwave reactor for a further 1 h. The reaction mixture was allowed to cool to rt, diluted with EtOAc (20 mL), filtered through Celite[®] and concentrated *in vacuo*. The resulting residue was purified by silica gel chromatography (0–50% EtOH in EtOAc). The appropriate fractions were combined and solvent evaporated *in vacuo* to give **3.023e** (91 mg, 0.19 mmol, 71%) as an off white solid; $^1\text{H NMR}$ (400 MHz, CDCl_3) δ ppm 8.50–8.45 (m, 2H), 7.81 (s, 1H), 7.73–7.70 (m, 1H), 7.54–7.46 (m, 3H), 7.45–7.39 (m, 2H), 7.37–7.32 (m, 1H), 6.28 (d, $J = 7.8$, 1H), 5.53 (s, 2H), 4.48–4.37 (m, 1H), 3.28–3.12 (m, 4H), 3.58–2.50 (m, 2H), 2.42 (s, 3H), 2.36 (s, 3H), 2.35–2.27 (m, 2H); LCMS (formic acid): $R_t = 0.85$ min (77%), $\text{MH}^+ = 489.2$.

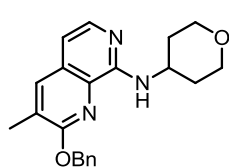
8-((1,1-Dioxidotetrahydro-2H-thiopyran-4-yl)amino)-3-methyl-5-(5-methylpyridin-3-yl)-1,7-naphthyridin-2(1H)-one (3.020e)



3.023e (91 mg, 0.19 mmol) was dissolved in TFA (3 mL, 38.90 mmol) and left to stir at 80°C for 4 h. The volatile components were removed *in vacuo*. Toluene (5 mL) was added and the solvent evaporated *in vacuo* ($\times 3$). The resulting residue was dissolved in MeOH (20 mL) and passed through a preconditioned (MeOH, 20 mL) amino propyl column (10 g). The column was rinsed with MeOH (30 mL) and the filtrate concentrated *in vacuo*. The resulting residue was suspended in MeOH (10 mL), filtered under reduced pressure, collected and dried at 40°C under vacuum for 3 h to give **3.020e** (11 mg,

0.03 mmol, 15%) as a pale yellow solid. ^1H NMR (400 MHz, DMSO- d_6) δ ppm 11.44 (s, 1H), 8.46 (d, $J = 1.6$, 1H), 8.38 (d, $J = 1.6$, 1H), 7.74 (s, 1H), 7.66–7.60 (m, 1H), 7.55–7.50 (m, 1H), 6.88 (d, $J = 6.4$, 1H), 4.48–4.37 (m, 1H), 3.30–3.19 (m, 4H), 2.38 (s, 3H), 2.34–2.38 (m, 2H), 2.16–2.05 (m, 5H); LCMS (formic acid): $R_t = 0.49$ min (100%), $\text{MH}^+ = 399.0$.

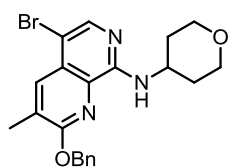
2-(Benzyloxy)-3-methyl-N-(tetrahydro-2H-pyran-4-yl)-1,7-naphthyridin-8-amine (3.021f)



Tetrahydro-2H-pyran-4-amine hydrochloride (254 mg, 1.84 mmol) was added to a mixture of **3.012** (350 mg, 1.23 mmol), $\text{Pd}_2(\text{dba})_3$ (90 mg, 0.10 mmol), Brettphos (66 mg, 0.12 mmol), and NaO^tBu (473 mg, 4.92 mmol) in THF (10 mL).

The reaction mixture was heated at 60 °C for 18 h. The reaction mixture was concentrated *in vacuo* and the resulting residue was diluted with DCM (100 mL) and washed with H_2O (100 mL). The separated organic layer was passed through a hydrophobic frit and concentrated *in vacuo*. The resulting residue was purified by silica gel chromatography (0–50% EtOH in EtOAc). The appropriate fractions were combined and solvent evaporated *in vacuo* to give **3.021f** (245 mg, 0.70 mmol, 57%) as a brown oil; ^1H NMR (400 MHz, CDCl_3) δ ppm 7.87 (d, $J = 5.7$, 1H), 7.63 (s, 1H), 7.52–7.47 (m, 2H), 7.42–7.36 (m, 2H), 7.36–7.30 (m, 1H), 6.71 (d, $J = 5.7$, 1H), 6.20 (d, $J = 8.1$, 1H), 5.50 (s, 2H), 4.36–4.25 (m, 1H), 4.06–3.99 (m, 2H), 3.67–3.59 (m, 2H), 2.37 (s, 3H), 2.17–2.09 (m, 2H), 1.70–1.57 (m, 2H); LCMS (formic acid): $R_t = 0.80$ min (95%), $\text{MH}^+ = 350.0$.

2-(Benzyloxy)-5-bromo-3-methyl-N-(tetrahydro-2H-pyran-4-yl)-1,7-naphthyridin-8-amine (3.022f)

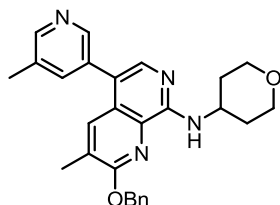


NBS (125 mg, 0.70 mmol) was added to a solution of **3.021f** (245 mg, 0.70 mmol) in THF (5 mL) and the mixture was stirred at rt for 1 h. The reaction mixture was concentrated *in vacuo*. The resulting residue was dissolved in DCM (50 mL) and

washed with H_2O (50 mL). The organic phase was separated and the aqueous washed with DCM (3 x 50 mL). The combined organic layers were passed through a hydrophobic frit and concentrated *in vacuo*. The resulting residue was purified by silica gel chromatography (0–50% EtOAc in cyclohexane). The appropriate fractions were combined and solvent evaporated *in vacuo* to give **3.022f** (266 mg, 0.62 mmol, 89%) as a yellow solid; ^1H NMR (400 MHz, CDCl_3) δ ppm 7.99 (s, 1H), 7.95–7.92

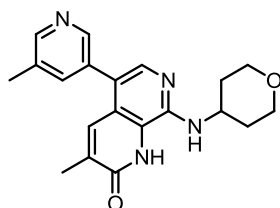
(m, 1H), 7.56–7.45 (m, 2H), 7.43–7.37 (m, 2H), 7.35–7.30 (m, 1H), 6.18 (d, $J = 8.1$, 1H), 5.50 (s, 2H), 4.30–4.19 (m, 1H), 4.06–3.99 (m, 2H), 3.65–3.60 (m, 2H), 2.43–2.40 (m, 3H), 2.16–2.07 (m, 2H), 1.68–1.56 (m, 2H); LCMS (formic acid): $R_t = 1.42$ min (97%), $MH^+ = 428.3, 430.3$.

2-(Benzyloxy)-3-methyl-5-(5-methylpyridin-3-yl)-N-(tetrahydro-2H-pyran-4-yl)-1,7-naphthyridin-8-amine (3.023f)



A mixture of **3.022f** (266 mg, 0.62 mmol), (5-methylpyridin-3-yl)boronic acid (170 mg, 1.24 mmol), $Pd(OAc)_2$ (14 mg, 0.06 mmol), Catacxiom A (22 mg, 0.06 mmol) and K_2CO_3 (172 mg, 1.24 mmol) in 1,4-dioxane (3 mL) and H_2O (1.5 mL) was heated at 100 °C in a microwave reactor for 1 h. The reaction mixture was allowed to cool to rt, diluted with EtOAc (20 mL), filtered through Celite[®] and concentrated *in vacuo*. The resulting residue was purified by silica gel chromatography (0–50% EtOH in EtOAc). The appropriate fractions were combined and solvent evaporated *in vacuo* to give **3.023f** (137 mg, 0.31 mmol, 50%) as a yellow solid; 1H NMR (400 MHz, $CDCl_3$) δ ppm 8.49–8.45 (m, 2H), 7.82 (s, 1H), 7.72–7.70 (m, 1H), 7.54–7.48 (m, 3H), 7.43–7.38 (m, 2H), 7.36–7.31 (m, 1H), 6.33 (d, $J = 8.3$, 1H), 5.54 (s, 2H), 4.40–4.29 (m, 1H), 4.10–4.02 (m, 2H), 3.69–3.62 (m, 2H), 2.43 (s, 3H), 2.35 (s, 3H), 2.20–2.12 (m, 2H), 1.72–1.59 (m, 2H); LCMS (formic acid): $R_t = 0.81$ min (93%), $MH^+ = 441.1$.

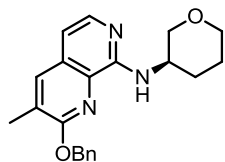
3-Methyl-5-(5-methylpyridin-3-yl)-8-((tetrahydro-2H-pyran-4-yl)amino)-1,7-naphthyridin-2(1H)-one (3.020f)



3.023f (137 mg, 0.31 mmol) was dissolved in TFA (3 mL, 38.90 mmol) and left to stir at 80 °C for 4 h. The volatile components were removed *in vacuo*. Toluene (5 mL) was added and the solvent evaporated *in vacuo* ($\times 3$). The resulting residue was dissolved in MeOH (20 mL) and passed through a preconditioned (MeOH, 30 mL) amino propyl column (10 g). The column was rinsed with MeOH (50 mL) and the filtrate concentrated *in vacuo*. The resulting residue was suspended in DMSO (3 mL) and MeOH (3 mL), filtered under reduced pressure, collected and dried at 40 °C under vacuum for 3 h to give **3.020f** (48 mg, 0.14 mmol, 44%) as a pale yellow solid; 1H NMR (400 MHz, $DMSO-d_6$) δ ppm 11.48 (br.s, 1H), 8.45 (d, $J = 1.6$, 1H), 8.37 (d, $J = 1.6$, 1H), 7.72 (s, 1H), 7.64–7.60 (m, 1H), 7.52 (s, 1H), 6.92 (d, $J = 6.1$, 1H), 4.29–4.17 (m, 1H), 3.96–3.87

(m, 2H), 3.49–3.42 (m, 2H), 2.38 (s, 3H), 2.08 (s, 3H), 2.03–1.94 (m, 2H), 1.58–1.45 (m, 2H); LCMS (formic acid): $R_t = 0.48$ min (100%), $MH^+ = 351.0$.

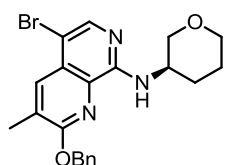
(R)-2-(Benzyloxy)-3-methyl-N-(tetrahydro-2H-pyran-3-yl)-1,7-naphthyridin-8-amine (3.021g)



(R)-tetrahydro-2H-pyran-3-amine hydrochloride (217 mg, 1.58 mmol) was added to a mixture of **3.012** (300 mg, 1.05 mmol), $Pd_2(dba)_3$ (77 mg, 0.08 mmol), Brettphos (57 mg, 0.11 mmol), and NaO^tBu (405 mg, 4.21 mmol) in THF (10 mL).

The reaction mixture was heated at 60 °C for 18 h and then at 70 °C for 3 h. The reaction mixture was concentrated *in vacuo* and the resulting residue was diluted with DCM (100 mL) and washed with H_2O (100 mL). The separated organic layer was passed through a hydrophobic frit and concentrated *in vacuo*. The resulting residue was purified by silica gel chromatography (0–100% EtOAc in cyclohexane). The appropriate fractions were combined and solvent evaporated *in vacuo* to give **3.021g** (147 mg, 0.42 mmol, 40%) as a yellow solid; 1H NMR (400 MHz, $CDCl_3$) δ ppm 7.86 (d, $J = 5.7$, 1H), 7.65–7.61 (m, 1H), 7.54–7.49 (m, 2H), 7.42–7.36 (m, 2H), 7.34–7.28 (m, 1H), 6.70 (d, $J = 5.7$, 1H), 6.53 (d, $J = 8.3$, 1H), 5.57–5.46 (m, 2H), 4.35–4.26 (m, 1H), 4.01 (dd, $J = 11.0, 2.9$, 1H), 3.77–3.72 (m, 2H), 3.63–3.56 (m, 1H), 2.37 (s, 3H), 2.09–1.99 (m, 1H), 1.89–1.76 (m, 2H), 1.71–1.61 (m, 1H); LCMS (formic acid): $R_t = 0.79$ min (91%), $MH^+ = 350.0$.

(R)-2-(Benzyloxy)-5-bromo-3-methyl-N-(tetrahydro-2H-pyran-3-yl)-1,7-naphthyridin-8-amine (3.022g)

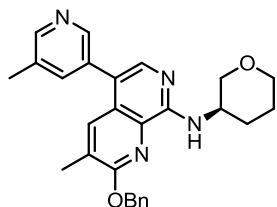


NBS (75 mg, 0.42 mmol) was added to a solution of **3.021g** (147 mg, 0.42 mmol) in THF (3 mL) and the mixture was stirred at rt for 4 h. The reaction mixture was concentrated *in vacuo*. The resulting residue was dissolved in DCM (50 mL) and washed with

H_2O (50 mL). The organic phase was separated and the aqueous washed with DCM (3 x 50 mL). The combined organic layers were passed through a hydrophobic frit and concentrated *in vacuo*. The resulting residue was purified by silica gel chromatography (0–50% EtOAc in cyclohexane). The appropriate fractions were combined and solvent evaporated *in vacuo* to give **3.022g** (115 mg, 0.27 mmol, 64%) as a yellow solid; 1H NMR (400 MHz, $CDCl_3$) δ ppm 7.99 (s, 1H), 7.94 (d, $J = 1.0$, 1H), 7.55–7.47 (m, 2H), 7.42–7.37 (m, 2H), 7.35–7.30 (m, 1H), 6.55 (d, $J = 8.3$, 1H), 5.60–5.46 (m, 2H), 4.30–4.20 (m, 1H), 3.98 (dd, $J = 11.1, 3.1$, 1H),

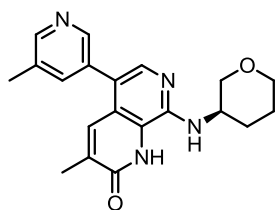
3.78–3.71 (m, 2H), 3.63–3.56 (m, 1H), 2.43 (d, $J = 1.0$, 3H), 2.05–1.97 (m, 1H), 1.88–1.77 (m, 2H), 1.70–1.62 (m, 1H); LCMS (formic acid): $R_t = 1.43$ min (100%), $MH^+ = 428.0, 430.0$.

(R)-2-(Benzyloxy)-3-methyl-5-(5-methylpyridin-3-yl)-N-(tetrahydro-2H-pyran-3-yl)-1,7-naphthyridin-8-amine (3.023g)



A mixture of **3.022g** (115 mg, 0.27 mmol), (5-methylpyridin-3-yl)boronic acid (74 mg, 0.54 mmol), $Pd(OAc)_2$ (6 mg, 0.03 mmol), Catacxiom A (10 mg, 0.03 mmol) and K_2CO_3 (74 mg, 0.54 mmol) in 1,4-dioxane (3 mL) and H_2O (1.5 mL) was heated at 100 °C in a microwave reactor for 2 h. The reaction mixture was allowed to cool to rt, diluted with EtOAc (20 mL), filtered through Celite® and concentrated *in vacuo*. The resulting residue was purified by silica gel chromatography (0–100% EtOAc in cyclohexane). The appropriate fractions were combined and solvent evaporated *in vacuo* to give **3.023g** (44 mg, 0.10 mmol, 37%) as a yellow oil; 1H NMR (400 MHz, $CDCl_3$) δ ppm 8.48 (d, $J = 1.8$, 1H), 8.46 (d, $J = 1.8$, 1H), 7.82 (s, 1H), 7.70 (d, $J = 1.1$, 1H), 7.55–7.51 (m, 3H), 7.42–7.37 (m, 2H), 7.35–7.30 (m, 1H), 6.68 (d, $J = 8.3$, 1H), 5.61–5.49 (m, 2H), 4.39–4.30 (m, 1H), 4.02 (dd, $J = 11.1, 3.1$, 1H), 3.79–3.74 (m, 2H), 3.67–3.60 (m, 1H), 2.42 (s, 3H), 2.34 (d, $J = 1.1$, 3H), 2.09–2.04 (m, 1H), 1.89–1.82 (m, 2H), 1.73–1.64 (m, 1H), LCMS (formic acid): $R_t = 0.84$ min (100%), $MH^+ = 441.1$.

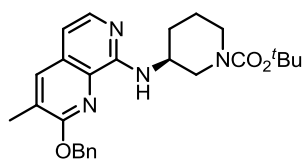
(R)-3-Methyl-5-(5-methylpyridin-3-yl)-8-((tetrahydro-2H-pyran-3-yl)amino)-1,7-naphthyridin-2(1H)-one (3.020g)



3.023g (44 mg, 0.10 mmol) was dissolved in TFA (3 mL, 38.9 mmol) and left to stir at 80 °C for 4 h. The volatile components were removed *in vacuo*. Toluene (5 mL) was added and the solvent evaporated *in vacuo* ($\times 3$). The resulting residue was dissolved in MeOH (20 mL) and passed through a preconditioned (MeOH, 20 mL) amino propyl column (10 g). The column was rinsed with MeOH (50 mL) and the filtrate concentrated *in vacuo*. The resulting residue was purified by MDAP (high pH). The appropriate fractions were combined and solvent evaporated *in vacuo* to give **3.020g** (10 mg, 0.03 mmol, 29%) as a pale yellow solid; 1H NMR (400 MHz, $DMSO-d_6$) δ ppm 11.53 (br.s, 1H), 8.45 (d, $J = 1.7$, 1H), 8.37 (d, $J = 1.7$, 1H), 7.71 (s, 1H), 7.65–7.66 (m, 1H), 7.51 (s, 1H), 6.88 (d, $J = 6.8$, 1H), 4.20–4.11 (m, 1H), 3.97 (dd, $J = 10.8, 2.9$, 1H), 3.79–3.71 (m,

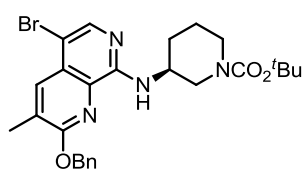
1H), 3.49–3.38 (m, 1H), 3.25–3.18 (m, 1H), 2.38 (s, 3H), 2.11–2.02 (m, 4H), 1.83–1.75 (m, 1H), 1.67–1.57 (m, 2H); LCMS (formic acid): $R_t = 0.51$ min (100%), $MH^+ = 351.0$.

(S)-tert-Butyl 3-((2-(benzyloxy)-3-methyl-1,7-naphthyridin-8-yl)amino)piperidine-1-carboxylate (3.021h)



(S)-tert-butyl 3-aminopiperidine-1-carboxylate (0.41 mL, 2.11 mmol) was added to a mixture of **3.012** (400 mg, 1.41 mmol), $Pd_2(dba)_3$ (103 mg, 0.11 mmol), Brettphos (75 mg, 0.14 mmol), and NaO^tBu (540 mg, 5.62 mmol) in THF (10 mL). The reaction mixture was heated at 60 °C for 4 h. The reaction mixture was concentrated *in vacuo* and the resulting residue was diluted with DCM (100 mL) and washed with H_2O (100 mL). The separated organic layer was passed through a hydrophobic frit and concentrated *in vacuo*. The resulting residue was purified by silica gel chromatography (0–100% EtOAc in cyclohexane). The appropriate fractions were combined and solvent evaporated *in vacuo* to give **3.021h** (538 mg, 1.20 mmol, 85%) as an orange oil; 1H NMR (400 MHz, $CDCl_3$) δ ppm 7.88 (d, $J = 5.6$, 1H), 7.64 (s, 1H), 7.52–7.46 (m, 2H), 7.42–7.36 (m, 2H), 7.35–7.29 (m, 1H), 6.72 (d, $J = 5.6$, 1H), 6.36 (d, $J = 7.3$, 1H), 5.54–5.42 (m, 2H), 4.30–4.20 (m, 1H), 3.89–3.75 (m, 1H), 3.54–3.37 (m, 2H), 2.37 (s, 3H), 2.08–2.00 (m, 1H), 1.81–1.71 (m, 2H), 1.68–1.60 (m, 1H), 1.42–1.21 (m, 10H); LCMS (formic acid): $R_t = 0.99$ min (98%), $MH^+ = 449.2$.

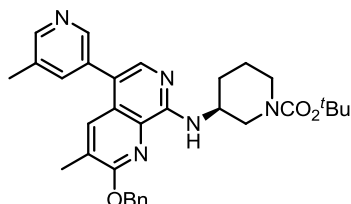
(S)-tert-Butyl 3-((2-(benzyloxy)-5-bromo-3-methyl-1,7-naphthyridin-8-yl)amino)piperidine-1-carboxylate (3.022h)



NBS (213 mg, 1.20 mmol) was added to a solution of **3.021h** (538 mg, 1.20 mmol) in THF (5 mL) and the mixture was stirred at rt for 48 h. The reaction mixture was concentrated *in vacuo*. The resulting residue was dissolved in DCM (50 mL) and washed with H_2O (50 mL). The organic phase was separated and the aqueous washed with DCM (3 x 50 mL). The combined organic layers were passed through a hydrophobic frit and concentrated *in vacuo*. The resulting residue was purified by silica gel chromatography (0–50% EtOAc in cyclohexane). The appropriate fractions were combined and solvent evaporated *in vacuo* to give **3.022h** (503 mg, 0.95 mmol, 80%) as an orange solid; 1H NMR (400 MHz, $CDCl_3$) δ ppm 8.01 (s, 1H), 7.95 (s, 1H), 7.51–7.45 (m, 2H), 7.42–7.37 (m, 2H), 7.36–7.30

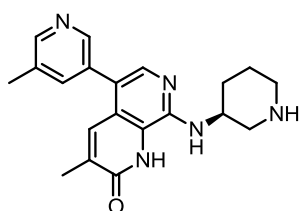
(m, 1H), 6.43–6.30 (m, 1H), 5.56–5.43 (m, 2H), 4.22–4.13 (m, 1H), 3.84–3.77 (m, 1H), 3.54–3.47 (m, 1H), 3.45–3.36 (m, 2H), 2.42 (s, 3H), 2.06–1.96 (m, 1H), 1.79–1.70 (m, 2H), 1.66–1.61 (m, 1H), 1.34 (br.s, 9H); LCMS (formic acid): $R_t = 1.69$ min (96%), $MH^+ = 527.2, 529.2$.

(S)-tert-Butyl 3-((2-(benzyloxy)-3-methyl-5-(5-methylpyridin-3-yl)-1,7-naphthyridin-8-yl)amino)piperidine-1-carboxylate (3.023h)



A mixture of **3.022h** (500 mg, 0.95 mmol), (5-methylpyridin-3-yl)boronic acid (260 mg, 1.90 mmol), $Pd(OAc)_2$ (21 mg, 0.1 mmol), Catacxiium A (34 mg, 0.1 mmol) and K_2CO_3 (262 mg, 1.90 mmol) in 1,4-dioxane (3 mL) and H_2O (1.5 mL) was heated at 100 °C in a microwave reactor for 1 h. The reaction mixture was allowed to cool to rt, diluted with EtOAc (20 mL), filtered through Celite[®] and concentrated *in vacuo*. The resulting residue was purified by silica gel chromatography (0–50% EtOAc in cyclohexane). The appropriate fractions were combined and solvent evaporated *in vacuo* to give **3.023h** (275 mg, 0.51 mmol, 54%) as a yellow oil; 1H NMR (400 MHz, $CDCl_3$) δ ppm 8.48 (d, $J = 1.8$, 1H), 8.46 (d, $J = 1.8$, 1H), 7.84 (s, 1H), 7.71 (s, 1H), 7.54–7.48 (m, 3H), 7.42–7.37 (m, 2H), 7.35–7.29 (m, 1H), 6.50 (d, $J = 7.3$, 1H), 5.58–5.45 (m, 2H), 4.32–4.25 (m, 1H), 3.90–3.78 (m, 1H), 3.55–3.42 (m, 3H), 2.41 (s, 3H), 2.34 (s, 3H), 2.10–2.01 (m, 1H), 1.84–1.73 (m, 2H), 1.72–1.61 (m, 1H), 1.35 (br.s, 9H); LCMS (formic acid): $R_t = 1.09$ min (100%), $MH^+ = 540.3$.

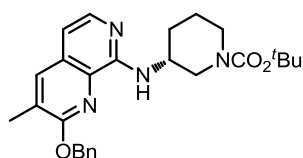
(S)-3-Methyl-5-(5-methylpyridin-3-yl)-8-(piperidin-3-ylamino)-1,7-naphthyridin-2(1H)-one (3.020h)



3.023h (116 mg, 0.22 mmol) was dissolved in TFA (3 mL, 38.90 mmol) and left to stir at 80 °C for 3 h. The volatile components were removed *in vacuo*. Toluene (5 mL) was added and the solvent evaporated *in vacuo* ($\times 3$). The resulting residue was dissolved in MeOH (10 mL) and passed through a preconditioned (MeOH, 10 mL) amino propyl column (10 g). The appropriate fractions were combined and solvent evaporated *in vacuo*. The resulting residue was purified by MDAP (high pH). The appropriate fractions were combined and solvent evaporated *in vacuo* to give **3.020h** (65 mg, 0.19 mmol, 87%) as a yellow solid; 1H NMR (400 MHz, $DMSO-d_6$) δ ppm 8.45 (d, $J = 1.8$, 1H), 8.37 (d, $J = 1.8$, 1H), 7.70 (s, 1H), 7.63 (s, 1H), 7.52 (d, $J = 1.1$, 1H), 6.83 (d, $J = 6.8$, 1H),

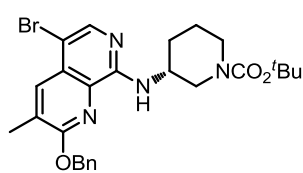
4.11–4.00 (m, 1H), 3.21–3.13 (m, 1H), 2.86–2.79 (m, 1H), 2.45–2.40 (m, 1H), 2.38 (s, 3H), 2.08 (d, $J = 1.1$, 3H), 2.04–1.96 (m, 1H), 1.74–1.64 (m, 1H), 1.54–1.41 (m, 2H); N.B. 1H hidden under solvent peak; LCMS (high pH): $R_t = 0.76$ min (97%), $MH^+ = 350.3$.

(*R*)-tert-Butyl 3-((2-(benzyloxy)-3-methyl-1,7-naphthyridin-8-yl)amino)piperidine-1-carboxylate (3.021i)



(*R*)-tert-butyl 3-aminopiperidine-1-carboxylate (0.36 mL, 1.84 mmol) was added to a mixture of **3.012** (350 mg, 1.23 mmol), $Pd_2(dba)_3$ (90 mg, 0.10 mmol), Brettphos (66 mg, 0.12 mmol), and NaO^tBu (473 mg, 4.92 mmol) in THF (10 mL). The reaction mixture was heated at 60 °C for 18 h. The reaction mixture was concentrated *in vacuo* and the resulting residue was diluted with DCM (100 mL) and washed with H_2O (100 mL). The separated organic layer was passed through a hydrophobic frit and concentrated *in vacuo*. The resulting residue was purified by silica gel chromatography (0–60% EtOAc in cyclohexane). The appropriate fractions were combined and solvent evaporated *in vacuo* to give **3.021i** (502 mg, 1.12 mmol, 91%) as an orange oil; 1H NMR (400 MHz, $CDCl_3$) δ ppm 7.88 (d, $J = 5.8$, 1H), 7.64 (s, 1H), 7.52–7.46 (m, 2H), 7.42–7.37 (m, 2H), 7.35–7.30 (m, 1H), 6.72 (d, $J = 5.8$, 1H), 6.36 (d, $J = 7.3$, 1H), 5.55–5.42 (m, 2H), 4.29–4.20 (m, 1H), 3.91–3.70 (m, 1H), 3.46–3.36 (m, 2H), 2.37 (s, 3H), 2.08–1.99 (m, 1H), 1.82–1.57 (m, 4H), 1.41 (br.s, 9H); LCMS (high pH): $R_t = 0.99$ min (100%), $MH^+ = 449.2$.

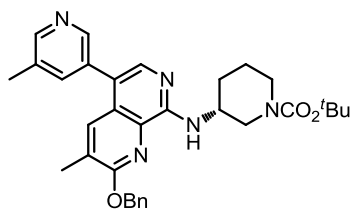
(*R*)-tert-Butyl 3-((2-(benzyloxy)-5-bromo-3-methyl-1,7-naphthyridin-8-yl)amino)piperidine-1-carboxylate (3.022i)



NBS (198 mg, 1.115 mmol) was added to a solution of **3.021i** (500 mg, 1.12 mmol) in THF (5 mL) and the mixture was stirred at rt for 1 h. The reaction mixture was concentrated *in vacuo*. The resulting residue was dissolved in DCM (50 mL) and washed with H_2O (50 mL). The organic phase was separated and the aqueous washed with DCM (3 x 50 mL). The combined organic layers were passed through a hydrophobic frit and concentrated *in vacuo*. The resulting residue was purified by silica gel chromatography (0–50% EtOAc in cyclohexane). The appropriate fractions were combined and solvent evaporated *in vacuo* to give **3.022i** (516 mg, 0.98 mmol, 88%) as a yellow solid; 1H NMR (400 MHz, $CDCl_3$) δ ppm 8.01 (s, 1H), 7.97–7.93 (m, 1H), 7.50–7.45 (m, 2H), 7.42–7.36 (m, 2H), 7.35–7.30 (m,

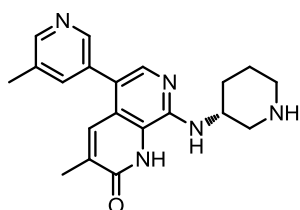
1H), 6.43–6.31 (m, 1H), 5.54–5.43 (m, 2H), 4.24–4.13 (m, 1H), 3.85–3.76 (m, 1H), 3.55–3.47 (m, 1H), 3.46–3.35 (m, 2H), 2.45–2.40 (m, 3H), 2.07–1.99 (m, 1H), 1.80–1.70 (m, 2H), 1.68–1.60 (m, 1H), 1.32 (br.s, 9H); LCMS (formic acid): $R_t = 1.69$ min (100%), $MH^+ = 527.2, 529.2$.

(R)-tert-Butyl 3-((2-(benzyloxy)-3-methyl-5-(5-methylpyridin-3-yl)-1,7-naphthyridin-8-yl)amino)piperidine-1-carboxylate (3.023i)



A mixture of **3.022i** (510 mg, 0.97 mmol), (5-methylpyridin-3-yl)boronic acid (265 mg, 1.93 mmol), $Pd(OAc)_2$ (22 mg, 0.10 mmol), Catacixium A (35 mg, 0.10 mmol) and K_2CO_3 (267 mg, 1.93 mmol) in 1,4-dioxane (3 mL) and H_2O (1.5 mL) was heated at 100 °C in a microwave reactor for 1 h. The reaction mixture was allowed to cool to rt, diluted with EtOAc (20 mL), filtered through Celite[®] and concentrated *in vacuo*. The resulting residue was purified by silica gel chromatography (0–50% EtOAc in cyclohexane). The appropriate fractions were combined and solvent evaporated *in vacuo* to give **3.023i** (339 mg, 0.63 mmol, 65%) as a yellow solid; ¹H NMR (400 MHz, $CDCl_3$) δ ppm 8.49–8.46 (m, 2H), 7.83 (s, 1H), 7.75–7.68 (m, 1H), 7.53–7.46 (m, 3H), 7.44–7.36 (m, 2H), 7.35–7.31 (m, 1H), 6.49 (d, $J = 6.8$, 1H), 5.58–5.43 (m, 2H), 4.34–4.22 (m, 1H), 3.92–3.78 (m, 1H), 3.57–3.39 (m, 3H), 2.41 (s, 3H), 2.34 (s, 3H), 2.12–2.01 (m, 1H), 1.83–1.73 (m, 2H), 1.69–1.65 (m, 1H), 1.34 (br.s, 9H); LCMS (formic acid): $R_t = 1.10$ min (100%), $MH^+ = 540.3$.

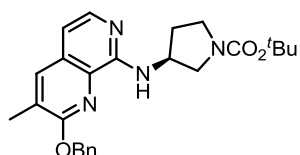
(R)-3-Methyl-5-(5-methylpyridin-3-yl)-8-(piperidin-3-ylamino)-1,7-naphthyridin-2(1H)-one (3.020i)



3.023i (339 mg, 0.63 mmol) was dissolved in TFA (3 mL, 38.90 mmol) and left to stir at 80 °C for 4 h. The volatile components were removed *in vacuo*. Toluene (5 mL) was added and the solvent evaporated *in vacuo* ($\times 3$). The resulting residue was dissolved in MeOH (10 mL) and passed through a preconditioned (MeOH, 10 mL) amino propyl column (10 g). The appropriate fractions were combined and solvent evaporated *in vacuo*. The resulting residue was purified by MDAP (high pH). The appropriate fractions were combined and solvent evaporated *in vacuo* to give **3.020i** (85 mg, 0.24 mmol, 39%) as a yellow solid; ¹H NMR (400 MHz, $DMSO-d_6$) δ ppm 8.45 (d, $J = 1.6$, 1H), 8.37 (d, $J = 1.6$, 1H), 7.70 (s, 1H), 7.65–7.60 (m, 1H), 7.52 (d, $J = 1.2$, 1H), 6.83 (d, $J = 7.1$,

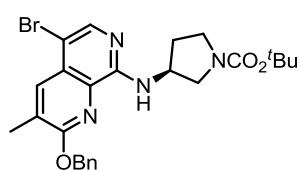
1H), 4.09–3.99 (m, 1H), 3.21–3.14 (m, 1H), 2.86–2.77 (m, 1H), 2.44–2.35 (m, 4H), 2.11–2.04 (m, 3H), 2.03–1.97 (m, 1H), 1.74–1.64 (m, 1H), 1.54–1.50 (m, 2H); N.B. 1H signal hidden under solvent peak; LCMS (formic acid): $R_t = 0.38$ min (100%), $MH^+ = 350.1$.

(S)-tert-Butyl 3-((2-(benzyloxy)-3-methyl-1,7-naphthyridin-8-yl)amino)pyrrolidine-1-carboxylate (3.021j)



(S)-tert-butyl 3-aminopyrrolidine-1-carboxylate (0.58 mL, 3.16 mmol) was added to a mixture of **3.012** (600 mg, 2.11 mmol), $Pd_2(dba)_3$ (154 mg, 0.17 mmol), Brettphos (113 mg, 0.21 mmol), and NaO^tBu (810 mg, 8.43 mmol) in THF (10 mL). The reaction mixture was heated at 60 °C for 2 h. The reaction mixture was concentrated *in vacuo* and the resulting residue was diluted with DCM (100 mL) and washed with H_2O (100 mL). The separated organic layer was passed through a hydrophobic frit and concentrated *in vacuo*. The resulting residue was purified by silica gel chromatography (0–40% EtOAc in cyclohexane). The appropriate fractions were combined and solvent evaporated *in vacuo* to give **3.021j** (872 mg, 2.00 mmol, 95%) as an orange oil; 1H NMR (400 MHz, CD_3OD) δ ppm 7.73–7.71 (m, 1H), 7.69 (d, $J = 5.9$, 1H), 7.46–7.42 (m, 2H), 7.36–7.31 (m, 2H), 7.28–7.22 (m, 1H), 6.77 (d, $J = 5.9$, 1H), 5.48 (s, 2H), 4.58–4.51 (m, 1H), 3.75–3.68 (m, 1H), 3.55–3.43 (m, 2H), 3.36–3.33 (m, 1H), 2.32 (d, $J = 1.0$, 3H), 2.30–2.20 (m, 1H), 2.06–1.96 (m, 1H), 1.43 (s, 9H); LCMS (formic acid): $R_t = 0.94$ min (99%), $MH^+ = 435.2$.

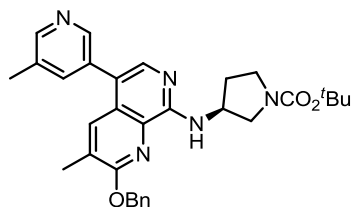
(S)-tert-Butyl 3-((2-(benzyloxy)-5-bromo-3-methyl-1,7-naphthyridin-8-yl)amino)pyrrolidine-1-carboxylate (3.022j)



NBS (357 mg, 2.01 mmol) was added to a solution of **3.021j** (872 mg, 2.01 mmol) in THF (5 mL) and the mixture was stirred rt for 2 h. The reaction mixture was concentrated *in vacuo*. The resulting residue was dissolved in DCM (50 mL) and washed with H_2O (50 mL). The organic phase was separated and the aqueous washed with DCM (3 × 50 mL). The combined organic layers were passed through a hydrophobic frit and concentrated *in vacuo* to give **3.022j** (1.05 g, 2.05 mmol, quant.) as a yellow solid; 1H NMR (400 MHz, $DMSO-d_6$) δ ppm 8.02–7.99 (m, 2H), 7.58–7.52 (m, 2H), 7.43–7.37 (m, 2H), 7.34–7.29 (m, 1H), 6.99–6.93 (m, 1H), 5.64 (s, 2H), 4.67–4.56 (m, 1H), 3.68–3.61 (m, 1H), 3.53–3.45 (m, 1H),

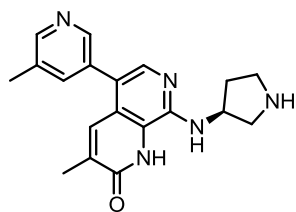
2.41–2.37 (m, 3H), 2.28–2.18 (m, 1H), 2.12–2.00 (m, 1H), 1.42 (s, 9H); N.B. 2H signal hidden under water peak; LCMS (formic acid): $R_t = 1.66$ min (100%), $MH^+ = 513.2, 514.2$.

(S)-tert-Butyl 3-((2-(benzyloxy)-3-methyl-5-(5-methylpyridin-3-yl)-1,7-naphthyridin-8-yl)amino)pyrrolidine-1-carboxylate (3.023j)



A mixture of **3.022j** (1.05 g, 2.05 mmol), (5-methylpyridin-3-yl)boronic acid (0.56 g, 4.09 mmol), $Pd(OAc)_2$ (0.05 g, 0.21 mmol), Catacxiium A (0.07 g, 0.21 mmol) and K_2CO_3 (0.57 g, 4.09 mmol) in 1,4-dioxane (7 mL) and H_2O (3.5 mL) was heated at 100 °C in a microwave reactor for 1 h. The reaction mixture was allowed to cool to rt, diluted with EtOAc (20 mL), filtered through Celite[®] and concentrated *in vacuo*. The resulting residue was purified by silica gel chromatography (0–100% EtOAc in cyclohexane). The appropriate fractions were combined and solvent evaporated *in vacuo* to give **3.023j** (389 mg, 0.74 mmol, 36%) as an orange oil; ¹H NMR (400 MHz, $CDCl_3$) δ ppm 8.50–8.45 (m, 2H), 7.84 (s, 1H), 7.72 (s, 1H), 7.53 (s, 1H), 7.51–7.46 (m, 2H), 7.45–7.38 (m, 2H), 7.36–7.31 (m, 1H), 6.40 (d, $J = 7.3$, 1H), 5.52 (s, 2H), 4.86–4.75 (m, 1H), 3.91–3.83 (m, 1H), 3.66–3.42 (m, 2H), 3.39–3.28 (m, 1H), 2.43 (s, 3H), 2.36 (s, 3H), 2.08–1.95 (m, 1H), 1.81–1.71 (m, 1H), 1.56 (br.s, 9H); LCMS (formic acid): $R_t = 1.07$ min (99%), $MH^+ = 526.3$.

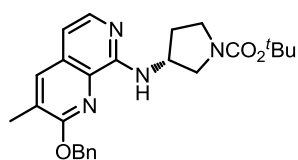
(S)-3-Methyl-5-(5-methylpyridin-3-yl)-8-(pyrrolidin-3-ylamino)-1,7-naphthyridin-2(1H)-one (3.020j)



3.023j (389 mg, 0.74 mmol) was dissolved in TFA (3 mL, 38.90 mmol) and left to stir at 80 °C for 3 h. The volatile components were removed *in vacuo*. Toluene (5 mL) was added and the solvent evaporated *in vacuo* ($\times 3$). The resulting residue was dissolved in MeOH (10 mL) and passed through a preconditioned (MeOH, 10 mL) amino propyl column (5 g). The appropriate fractions were combined and solvent evaporated *in vacuo*. The resulting residue was purified by MDAP (high pH). The appropriate fractions were combined and solvent evaporated *in vacuo* to give **3.020j** (177 mg, 0.53 mmol, 71%) as a yellow solid; ¹H NMR (400 MHz, $DMSO-d_6$) δ ppm 8.45 (d, $J = 1.6$, 1H), 8.38 (d, $J = 1.6$, 1H), 7.72 (s, 1H), 7.63 (s, 1H), 7.52 (d, $J = 1.2$, 1H), 7.20 (d, $J = 5.6$, 1H), 4.56–4.47 (m, 1H), 3.11–3.02 (m, 1H), 2.98–2.90 (m, 1H), 2.87–2.79 (m, 1H), 2.38

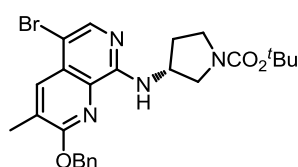
(s, 3H), 2.16–2.09 (m, 1H), 2.08 (d, $J = 1.2$, 3H), 1.85–1.72 (m, 2H); LCMS (formic acid): $R_t = 0.35$ min (100%), $MH^+ = 336.1$.

(*R*)-tert-Butyl 3-((2-(benzyloxy)-3-methyl-1,7-naphthyridin-8-yl)amino)pyrrolidine-1-carboxylate (3.021k)



(*R*)-tert-butyl 3-aminopyrrolidine-1-carboxylate (0.54 mL, 3.16 mmol) was added to a mixture of **3.012** (600 mg, 2.11 mmol), $Pd_2(dba)_3$ (154 mg, 0.17 mmol), Brettphos (113 mg, 0.21 mmol), and NaO^tBu (810 mg, 8.43 mmol) in THF (10 mL). The reaction mixture was heated at 60 °C for 2 h. The reaction mixture was concentrated *in vacuo* and the resulting residue was diluted with DCM (100 mL) and washed with H_2O (100 mL). The separated organic layer was passed through a hydrophobic frit and concentrated *in vacuo*. The resulting residue was purified by silica gel chromatography (0–50% EtOAc in cyclohexane). The appropriate fractions were combined and solvent evaporated *in vacuo* to give **3.021k** (950 mg, 2.19 mmol, quant.) as a orange solid; 1H NMR (400 MHz, $CDCl_3$) δ ppm 7.89 (d, $J = 5.3$, 1H), 7.64 (s, 1H), 7.52–7.46 (m, 2H), 7.43–7.37 (m, 2H), 7.36–7.29 (m, 1H), 6.75 (d, $J = 5.3$, 1H), 6.28 (d, $J = 7.3$, 1H), 5.49 (s, 2H), 4.81–4.70 (m, 1H), 3.88–3.81 (m, 1H), 3.62–3.49 (m, 2H), 3.35–3.27 (m, 1H), 2.38 (s, 3H), 2.35–2.27 (m, 1H), 2.05–1.94 (m, 1H), 1.48 (s, 9H); LCMS (formic acid): $R_t = 0.94$ min (95%), $MH^+ = 435.1$.

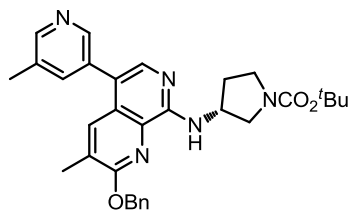
(*R*)-tert-Butyl 3-((2-(benzyloxy)-5-bromo-3-methyl-1,7-naphthyridin-8-yl)amino)pyrrolidine-1-carboxylate (3.022k)



NBS (389 mg, 2.19 mmol) was added to a solution of **3.021k** (950 mg, 2.19 mmol) in THF (5 mL) and the mixture was stirred at rt for 2 h. The reaction mixture was concentrated *in vacuo*. The resulting residue was dissolved in DCM (50 mL) and washed with H_2O (50 mL). The organic phase was separated and the aqueous washed with DCM (3 x 50 mL). The combined organic layers were passed through a hydrophobic frit and concentrated *in vacuo*. The resulting residue was purified by silica gel chromatography (0–50% EtOAc in cyclohexane). The appropriate fractions were combined and solvent evaporated *in vacuo* to give **3.022k** (965 mg, 1.88 mmol, 86%) as a pale yellow solid; 1H NMR (400 MHz, $DMSO-d_6$) δ ppm 8.07–7.99 (m, 2H), 7.56–7.52 (m, 2H), 7.44–7.37 (m, 2H), 7.35–7.29 (m, 1H), 7.00–6.91 (m, 1H), 5.64 (s, 2H), 4.68–4.56 (m, 1H), 3.69–3.61 (m,

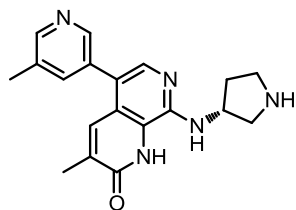
1H), 3.53–3.45 (m, 1H), 3.40–3.32 (m, 2H), 2.39 (s, 3H), 2.27–2.16 (m, 1H), 2.12–1.97 (m, 1H), 1.14 (br.s, 9H); LCMS (formic acid): $R_t = 1.60$ min (99%), $MH^+ = 513.2, 515.2$.

(R)-tert-Butyl 3-((2-(benzyloxy)-3-methyl-5-(5-methylpyridin-3-yl)-1,7-naphthyridin-8-yl)amino)pyrrolidine-1-carboxylate (3.023k)



A mixture of **3.022k** (850 mg, 1.66 mmol), (5-methylpyridin-3-yl)boronic acid (453 mg, 3.31 mmol), $Pd(OAc)_2$ (37 mg, 0.17 mmol), Catacxiium A (59 mg, 0.17 mmol) and K_2CO_3 (458 mg, 3.31 mmol) in 1,4-dioxane (7 mL) and H_2O (3.5 mL) was heated at $100\text{ }^\circ\text{C}$ in a microwave reactor for 1 h. The reaction mixture was allowed to cool to rt, diluted with EtOAc (20 mL), filtered through Celite[®] and concentrated *in vacuo*. The resulting residue was purified by silica gel chromatography (0–100% EtOAc in cyclohexane). The appropriate fractions were combined and solvent evaporated *in vacuo* to give **3.023k** (482 mg, 0.92 mmol, 55%) as an orange oil; 1H NMR (400 MHz, CD_3OD) δ ppm 8.39–8.36 (m, 1H), 8.34–8.31 (m, 1H), 7.69–7.64 (m, 3H), 7.47–7.42 (m, 2H), 7.37–7.30 (m, 2H), 7.28–7.22 (m, 1H), 5.53–5.50 (m, 2H), 4.65–4.57 (m, 1H), 3.78–3.70 (m, 1H), 3.56–3.43 (m, 2H), 3.41–3.33 (m, 1H), 2.39 (s, 3H), 2.34–2.21 (m, 4H), 2.11–2.01 (m, 1H), 1.42 (s, 9H); LCMS (formic acid): $R_t = 1.06$ min (100%), $MH^+ = 526.3$.

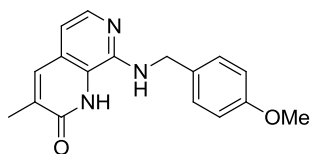
(R)-3-Methyl-5-(5-methylpyridin-3-yl)-8-(pyrrolidin-3-ylamino)-1,7-naphthyridin-2(1H)-one (3.020k)



3.023k (482 mg, 0.92 mmol) was dissolved in TFA (3 mL, 38.90 mmol) and left to stir at $80\text{ }^\circ\text{C}$ for 3 h. The volatile components were removed *in vacuo*. Toluene (5 mL) was added and the solvent evaporated *in vacuo* ($\times 3$). The resulting residue was dissolved in MeOH (10 mL) and passed through a preconditioned (MeOH, 10 mL) amino propyl column (10 g). The appropriate fractions were combined and solvent evaporated *in vacuo*. The resulting residue was purified by MDAP (high pH). The appropriate fractions were combined and solvent evaporated *in vacuo* to give **3.020k** (233 mg, 0.70 mmol, 76%) as a yellow solid; 1H NMR (400 MHz, $DMSO-d_6$) δ ppm 8.45 (d, $J = 1.6$, 1H), 8.38 (d, $J = 1.6$, 1H), 7.73 (s, 1H), 7.65–7.62 (m, 1H), 7.52 (d, $J = 1.1$, 1H), 7.30–7.24 (m, 1H), 4.56–4.49 (m, 1H), 3.23–3.14 (m, 1H), 3.12–3.04 (m, 1H), 3.00–2.91 (m, 1H),

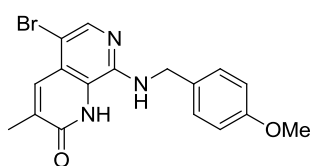
2.90–2.82 (m, 1H), 2.38 (s, 3H), 2.16–2.09 (m, 1H), 2.05 (d, $J = 1.1$, 3H), 1.88–1.76 (m, 1H); LCMS (formic acid): $R_t = 0.35$ min (100%), $MH^+ = 336.1$.

8-((4-Methoxybenzyl)amino)-3-methyl-1,7-naphthyridin-2(1H)-one (3.026)

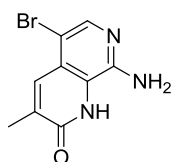


A mixture of **3.011** (900 mg, 4.62 mmol) and (4-methoxyphenyl)methanamine (8 mL, 61.20 mmol) was split into 2 × 5 mL microwave vials and heated at 150 °C for 4 h, then at 160 °C for 1 h. The resulting suspensions were combined, with DCM (30 mL) and filtered under reduced pressure. LCMS indicated a mixture of product and (4-methoxyphenyl)methanamine in both solid and filtrate. The solid and filtrate were combined and the suspension concentrated *in vacuo*. The resulting solid was suspended in MeOH (30 mL) and filtered under reduced pressure. The solid was collected to give **3.026** (1.14 g, 3.96 mmol, 83%) as an off white solid; 1H NMR (400 MHz, DMSO- d_6) δ ppm 11.28 (br.s, 1H), 7.75 (d, $J = 5.1$, 1H), 7.70–7.66 (m, 1H), 7.30 (d, $J = 8.6$, 2H), 7.20–7.12 (m, 1H), 6.95 (d, $J = 8.6$, 2H), 6.74 (d, $J = 5.4$, 1H), 4.56 (d, $J = 5.1$, 2H), 3.32 (s, 3H), 2.10 (s, 3H); LCMS (formic acid): $R_t = 0.57$ min (100%), $MH^+ = 296.0$.

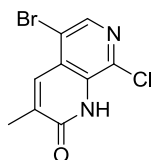
5-Bromo-8-((4-methoxybenzyl)amino)-3-methyl-1,7-naphthyridin-2(1H)-one (3.027)



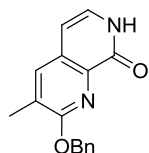
NBS (0.66 g, 3.72 mmol) was added to a solution of **3.026** (1.00 g, 3.39 mmol) in THF (20 mL). The reaction mixture was stirred at rt for 3 h. The volatile components were removed *in vacuo* and the resulting residue was dissolved in DCM (50 mL) and washed with H₂O (50 mL). The aqueous phase was extracted in to DCM (3 × 50 mL) and the combined organic layers were passed through a hydrophobic frit and concentrated *in vacuo*. The resulting solid was suspended in MeOH (30 mL), filtered under reduced pressure and collected to give **3.027** (478 mg, 1.28 mmol, 38%) as a brown solid; 1H NMR (400 MHz, CDCl₃) δ ppm 13.47 (br.s, 1H), 8.06 (s, 1H), 7.92–7.80 (m, 1H), 7.37 (d, $J = 8.3$, 2H), 7.10–6.99 (m, 1H), 6.92–6.79 (m, 2H), 4.78–4.61 (m, 2H), 3.77 (s, 3H), 1.88 (s, 3H); LCMS (formic acid): $R_t = 1.12$ min (93%), $MH^+ = 373.9$, 375.9.

8-Amino-5-bromo-3-methyl-1,7-naphthyridin-2(1H)-one (3.028)

3.027 (478 mg, 1.28 mmol) was dissolved in TFA (6 mL, 78.00 mmol) was heated at 80 °C for 18 h. The volatile components were removed *in vacuo*. Toluene (5 mL) was added and the solvent evaporated *in vacuo* (× 3). The resulting residue was dissolved in MeOH (20 mL) and passed through a preconditioned (MeOH, 40 mL) amino propyl column (20 g). The column was washed with MeOH (100 mL). The appropriate fractions were combined and solvent evaporated *in vacuo*. The resulting solid was suspended in Et₂O (10 mL), filtered under reduced pressure, washed with Et₂O (20 mL) and collected to give **3.028** (73 mg, 0.29 mmol, 22%) as a pale orange solid; ¹H NMR (400 MHz, DMSO-d₆) δ ppm 11.48 (br.s, 1H), 7.81 (s, 1H), 7.79–7.76 (m, 1H), 2.19 (s, 3H); LCMS (formic acid): R_t = 0.58 min (100%), MH⁺ = 253.9, 255.9.

5-Bromo-8-chloro-3-methyl-1,7-naphthyridin-2(1H)-one (3.029)

To a mixture of **3.028** (73 mg, 0.29 mmol) in conc. HCl (3 mL, 99.00 mmol), sodium nitrite (396 mg, 5.75 mmol) was added at 0 °C. The reaction mixture was stirred for 10 minutes, then CuCl (32 mg, 0.323 mmol) was added. The mixture was allowed to warm to rt and stirred for 18 h. The reaction mixture was diluted with sat. aq. NaHCO₃ (30 mL) and EtOAc (30 mL). The organic phase was separated and the aqueous extracted with EtOAc (3 × 40 mL). The combined organic phases were passed through a hydrophobic frit and concentrated *in vacuo* to give **3.029** (19 mg, 0.07 mmol, 24%) as an off white solid. ¹H NMR (400 MHz, DMSO-d₆) δ ppm 11.64 (br.s, 1H), 8.36 (s, 1H), 7.93 (s, 1H), 2.21 (s, 3H); LCMS (formic acid): R_t = 0.88 min (100%), MH⁺ = 272.8, 274.8.

2-(Benzyloxy)-3-methyl-1,7-naphthyridin-8(7H)-one (3.034)**Method A:**

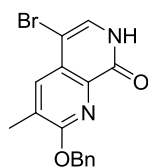
A mixture of **3.012** (350 mg, 1.23 mmol), Pd₂(dba)₃ (113 mg, 0.12 mmol), CsOH (61 mg, 3.69 mmol) and Bippyphos (62 mg, 0.12 mmol) in 1,4-dioxane (10 mL) was heated at 100 °C for 1 h in a microwave reactor. The reaction mixture was allowed to cool to rt, diluted with EtOAc (30 mL), filtered through Celite[®] and concentrated *in vacuo*. The resulting residue was purified by silica gel chromatography (0–100% EtOAc in cyclohexane).

The appropriate fractions were combined and solvent evaporated *in vacuo* to give **3.034** (109 mg, 0.41 mmol, 33%) as a pale yellow solid.

Method B:

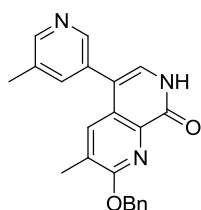
H₂O (0.25 mL, 14.05 mmol) was added to a mixture of **3.012** (2.00 g, 7.02 mmol), Pd₂(dba)₃ (0.32 g, 0.35 mmol), Brettphos (0.19 g, 0.35 mmol), and NaO^tBu (2.70 g, 28.10 mmol) in THF (30 mL). The reaction mixture was stirred at 70 °C for 2 h. The reaction mixture was concentrated *in vacuo* and the resulting residue was dissolved in DCM (50 mL) and washed with H₂O (50 mL). The aqueous phase was extracted with DCM (3 × 50 mL) and the combined organic layers were passed through a hydrophobic frit and concentrated *in vacuo*. The resulting residue was purified by silica gel chromatography (0–50% EtOH in EtOAc). The appropriate fractions were combined and solvent evaporated *in vacuo* to give **3.034** (1.71 g, 6.42 mmol, 91%) as a yellow solid; ¹H NMR (400 MHz, DMSO-d₆) δ ppm 11.39 (br.s, 1H), 7.89–7.85 (m, 1H), 7.57–7.52 (m, 2H), 7.42–7.36 (m, 2H), 7.35–7.30 (m, 1H), 7.14–7.09 (m, 1H), 6.44 (d, *J* = 6.9, 1H), 5.50 (s, 2H), 2.31–2.28 (m, 3H); LCMS (formic acid): R_t = 0.96 min (99%), MH⁺ = 267.0.

2-(Benzyloxy)-5-bromo-3-methyl-1,7-naphthyridin-8(7H)-one (3.033)



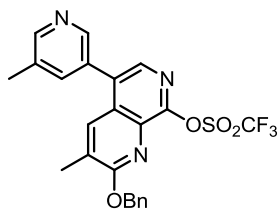
NBS (2.74 g, 15.38 mmol) was added to a mixture of **3.034** (4.10 g, 15.38 mmol) in THF (80 mL). The reaction mixture was left to stir at rt for 0.5 h. The reaction mixture was concentrated *in vacuo* and the resulting solid was suspended in DCM (20 mL), filtered under reduced pressure, washed with DCM (20 mL) and collected to give **3.033** (2.95 g, 8.55 mmol, 56%) as an off white solid; m.p. 255–258 °C (decomp.); ν_{\max} (solid)/cm⁻¹: 3208 (N-H), 1664 (C=O), 1410, 1080, 728; ¹H NMR (400 MHz, DMSO-d₆) δ ppm 11.73 (br.s., 1H) 7.91 (d, *J* = 1.0, 1H) 7.55 (d, *J* = 7.1, 2H) 7.48 (s, 1H) 7.36–7.42 (m, 2H) 7.30–7.36 (m, 1H) 5.52 (s, 2H) 2.35 (s, 3H); ¹³C NMR (101 MHz, DMSO-d₆) δ ppm 160.5, 159.2, 137.5, 136.9, 135.9, 128.8, 128.7, 128.3, 128.0, 127.9, 127.8, 95.2, 67.5, 15.9; HRMS (M + H)⁺ calculated for C₁₆H₁₄BrN₂O₂ 345.0233; found 345.0244; LCMS (formic acid): R_t = 1.13 min (100%), MH⁺ = 344.9, 346.9.

2-(Benzyloxy)-3-methyl-5-(5-methylpyridin-3-yl)-1,7-naphthyridin-8(7H)-one (3.032)



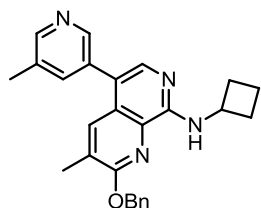
A mixture of **3.033** (1.50 g, 4.35 mmol), (5-methylpyridin-3-yl)boronic acid (1.19 g, 8.69 mmol), Pd(OAc)₂ (0.10 g, 0.44 mmol), Catacixium A (0.16 g, 0.44 mmol) and K₂CO₃ (1.20 g, 8.69 mmol) in 1,4-Dioxane (8 mL) and H₂O (4 mL) was heated at 100 °C in a microwave reactor for 1 h. The reaction mixture was allowed to cool to rt, diluted with EtOAc (50 mL) and DCM (50 mL), filtered through Celite® and concentrated *in vacuo*. The resulting residue was purified by silica gel chromatography (0–50% EtOH in EtOAc). The appropriate fractions were combined and solvent evaporated *in vacuo* to give **3.032** (1.32 g, 3.69 mmol, 85%) as a white solid; ¹H NMR (400 MHz, DMSO-d₆) δ ppm 11.72 (d, *J* = 4.4, 1H), 8.46 (d, *J* = 4.4, 1H), 8.41 (d, *J* = 1.6, 1H), 7.68–7.66 (m, 1H), 7.65–7.62 (m, 1H), 7.58–7.55 (m, 2H), 7.43–7.37 (m, 2H), 7.36–7.31 (m, 1H), 7.16–7.12 (m, 1H), 5.55 (s, 2H), 2.38 (s, 3H), 2.27 (s, 3H); LCMS (formic acid): R_t = 0.78 min (100%), MH⁺ = 358.0.

2-(Benzyloxy)-3-methyl-5-(5-methylpyridin-3-yl)-1,7-naphthyridin-8-yl trifluoromethanesulfonate (3.031)



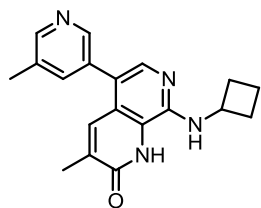
To a mixture of **3.032** (1.32 g, 3.69 mmol) in DCM (25 mL), pyridine (0.60 mL, 7.39 mmol) was added at 0 °C. The reaction mixture was left to stir for 0.5 h. Triflicanhydride (1.25 mL, 7.39 mmol) was added drop-wise and the reaction mixture was stirred at 0 °C for 1 h. The reaction mixture was diluted with DCM (50 mL) and washed with H₂O (50 mL) and brine (50 mL). The organic layer was separated, passed through a hydrophobic frit and concentrated *in vacuo* to give **3.031** (1.81 g, 3.70 mmol, quant.) as a pale yellow solid; m.p. 132–133 °C; *v*_{max} (solid)/cm⁻¹: 1424, 1204, 1139 (S=O), 871, 831, 693; ¹H NMR (400 MHz, CDCl₃) δ ppm 8.69 (s, 1H), 8.61 (s, 1H), 8.13 (s, 1H), 7.83–7.80 (m, 1H), 7.79–7.77 (m, 1H), 7.59–7.55 (m, 2H), 7.45–7.39 (m, 2H), 7.39–7.33 (m, 1H), 5.69 (s, 2H), 2.56 (s, 3H), 2.42 (d, *J* = 1.2, 3H); ¹³C NMR (101 MHz, CDCl₃) δ ppm 162.6, 150.9, 150.2, 147.2, 138.4, 137.8, 136.4, 133.7, 133.4, 132.6, 131.3, 131.0, 130.7, 128.5, 128.3, 128.2, 118.7 (q, *J*_{C-F} = 320.0), 69.1, 18.5, 17.1; ¹⁹F NMR (376 MHz, DMSO-d₆) δ ppm -74.1; HRMS (M + H)⁺ calculated for C₂₂H₁₉F₃N₃O₅S₂ 490.1043; found 490.1027; LCMS (formic acid): R_t = 1.48 min (100%), MH⁺ = 490.1.

2-(Benzyloxy)-N-cyclobutyl-3-methyl-5-(5-methylpyridin-3-yl)-1,7-naphthyridin-8-amine (3.023I)



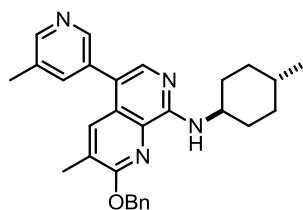
A mixture of **3.031** (200 mg, 0.41 mmol) and cyclobutanamine (0.10 mL, 1.23 mmol) and DIPEA (0.2 mL, 1.23 mmol) in MeCN (2.0 mL) was stirred in a microwave reactor at 140 °C for 1 h. The reaction mixture was concentrated *in vacuo* and the resulting residue was purified by silica gel chromatography (0–100% EtOAc in cyclohexane). The appropriate fractions were combined and solvent evaporated *in vacuo* to give **3.023I** (113 mg, 0.28 mmol, 67%) as a yellow oil; ¹H NMR (400 MHz, CDCl₃) δ ppm 8.47 (d, *J* = 1.7, 1H), 8.45 (d, *J* = 1.7, 1H), 7.83 (s, 1H), 7.69 (d, *J* = 1.0, 1H), 7.56–7.50 (m, 3H), 7.43–7.38 (m, 2H), 7.36–7.31 (m, 1H), 6.53 (d, *J* = 7.8, 1H), 5.55 (s, 2H), 4.79–4.67 (m, 1H), 2.60–2.56 (m, 2H), 2.41 (s, 3H), 2.33 (d, *J* = 1.0, 3H), 2.08–1.95 (m, 2H), 1.90–1.79 (m, 2H); LCMS (formic acid): *R*_t = 0.87 min (93%), *MH*⁺ = 411.1.

8-(Cyclobutylamino)-3-methyl-5-(5-methylpyridin-3-yl)-1,7-naphthyridin-2(1H)-one (3.020I)



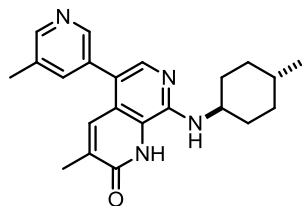
3.023I (110 mg, 0.27 mmol) was dissolved in TFA (3 mL, 38.90 mmol) and left to stir at 80 °C for 4 h. The volatile components were removed *in vacuo*. Toluene (5 mL) was added and the solvent evaporated *in vacuo* (× 3). The resulting residue was dissolved in MeOH (20 mL) and passed through a preconditioned (MeOH, 20 mL) amino propyl column (10 g). The column was rinsed with MeOH (50 mL) and the filtrate concentrated *in vacuo*. The resulting solid was suspended in DMSO (3 mL), filtered under reduced pressure, washed with MeOH (5 mL), collected and dried under vacuum at 40 °C for 4 h to give **3.020I** (26 mg, 0.08 mmol, 30%) as a yellow solid; m.p. 292–295 °C (decomp.); *v*_{max} (solid)/cm⁻¹: 3391, 2979, 1694 (C=O), 1659, 1443, 721; ¹H NMR (400 MHz, DMSO-*d*₆) δ ppm 11.39 (br.s, 1H), 8.44 (d, *J* = 1.6, 1H), 8.37 (d, *J* = 1.6, 1H), 7.70 (s, 1H), 7.63–7.60 (m, 1H), 7.51 (s, 1H), 7.22 (d, *J* = 5.9, 1H), 4.59–4.48 (m, 1H), 2.41–2.32 (m, 5H), 2.12–2.05 (m, 3H), 2.00–1.91 (m, 2H), 1.83–1.68 (m, 2H); ¹³C NMR (125 MHz, DMSO-*d*₆) δ ppm 161.9, 148.5, 147.1, 145.3, 139.2, 137.5, 134.5, 132.8, 131.8, 120.8, 120.0, 118.2, 46.4, 30.5, 17.9, 16.8, 15.0; N.B. 1C signal not visible in spectrum; HRMS (*M* + *H*)⁺ calculated for C₁₉H₂₁N₄O 321.1710; found 321.1713; LCMS (formic acid): *R*_t = 0.50 min (100%), *MH*⁺ = 321.0

2-(Benzyloxy)-3-methyl-N-((1*r*,4*r*)-4-methylcyclohexyl)-5-(5-methylpyridin-3-yl)-1,7-naphthyridin-8-amine (3.023m)

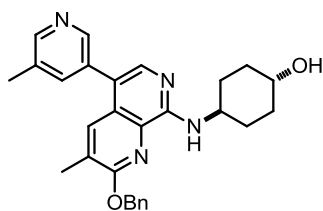


A mixture of **3.031** (150 mg, 0.31 mmol) and (1*r*,4*r*)-4-methylcyclohexanamine hydrochloride (138 mg, 0.92 mmol) and DIPEA (0.16 mL, 0.92 mmol) in MeCN (1.5 mL) was stirred in a microwave reactor at 140 °C for 1 h. The reaction mixture was concentrated *in vacuo* and the resulting residue was purified by silica gel chromatography (0–80% EtOAc in cyclohexane). The appropriate fractions were combined and solvent evaporated *in vacuo* to give **3.023m** (70 mg, 0.16 mmol, 51%) as a yellow oil; ¹H NMR (400 MHz, CDCl₃) δ ppm 8.44 (d, *J* = 1.8, 1H), 8.42 (d, *J* = 1.8, 1H), 7.80 (s, 1H), 7.68 (d, *J* = 1.0, 1H), 7.56–7.48 (m, 3H), 7.42–7.36 (m, 2H), 7.36–7.30 (m, 1H), 7.30 (d, *J* = 8.3, 1H), 5.52 (s, 2H), 4.09–3.95 (m, 1H), 2.42 (s, 3H), 2.33 (d, *J* = 1.0, 3H), 2.24–2.17 (m, 2H), 1.85–1.75 (m, 2H), 1.52–1.41 (m, 1H), 1.38–1.16 (m, 4H), 0.97–0.95 (m, 3H); LCMS (formic acid): R_t = 1.03 min (83%), MH⁺ = 453.1.

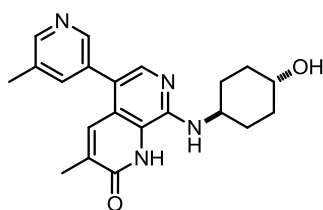
3-Methyl-8-(((1*r*,4*r*)-4-methylcyclohexyl)amino)-5-(5-methylpyridin-3-yl)-1,7-naphthyridin-2(1H)-one (3.020m)



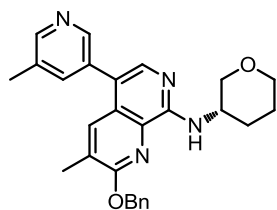
3.023m (65 mg, 0.14 mmol) was dissolved in TFA (3 mL, 38.90 mmol) and left to stir at 80 °C for 4 h. The volatile components were removed *in vacuo*. Toluene (5 mL) was added and the solvent evaporated *in vacuo*. The resulting residue was dissolved in MeOH (5 mL) and passed through a preconditioned (MeOH, 5 mL) amino propyl column (2 g). The column was rinsed with MeOH (5 mL) and the filtrate concentrated *in vacuo*. The resulting residue was purified by MDAP (high pH). The appropriate fractions were combined and solvent evaporated to give **3.020m** (6 mg, 0.02 mmol, 11%) as a yellow solid; ¹H NMR (400 MHz, DMSO-d₆) δ ppm 8.44 (d, *J* = 1.8, 1H), 8.36 (d, *J* = 1.8, 1H), 7.67 (s, 1H), 7.61 (s, 1H), 7.49 (s, 1H), 6.81 (d, *J* = 6.8, 1H), 4.00–3.88 (m, 1H), 2.38 (s, 3H), 2.10–2.02 (m, 5H), 1.78–1.68 (m, 2H), 1.34–1.19 (m, 2H), 1.13–0.99 (m, 2H), 0.91 (d, *J* = 6.4, 3H); N.B. 1H signal hidden under solvent peak; LCMS (high pH): R_t = 1.18 min (100%), MH⁺ = 363.3.

(1*r*,4*r*)-4-((2-(Benzyloxy)-3-methyl-5-(5-methylpyridin-3-yl)-1,7-naphthyridin-8-yl)amino)cyclohexanol (3.023n)

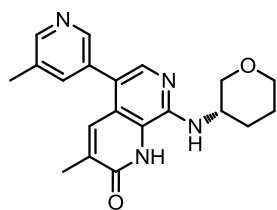
A mixture of **3.031** (150 mg, 0.31 mmol) and (1*r*,4*r*)-4-aminocyclohexanol (106 mg, 0.912 mmol) and DIPEA (0.16 mL, 0.92 mmol) in MeCN (1.5 mL) was stirred in a microwave reactor at 140 °C for 1 h. The reaction mixture was concentrated *in vacuo* and the resulting residue was purified by silica gel chromatography (0–80% EtOH in EtOAc). The appropriate fractions were combined and solvent evaporated *in vacuo* to give **3.023n** as a yellow oil; ¹H NMR (400 MHz, CDCl₃) δ ppm 8.47 (d, *J* = 1.8, 1H), 8.45 (d, *J* = 1.8, 1H), 7.83 (s, 1H), 7.70 (d, *J* = 1.0, 1H), 7.56–7.46 (m, 3H), 7.42–7.30 (m, 2H), 7.35–7.30 (m, 1H), 6.24 (d, *J* = 8.3, 1H), 5.52 (s, 2H), 4.17–4.06 (m, 1H), 3.57–3.52 (m, 1H), 2.42 (s, 3H), 2.33 (d, *J* = 1.0, 3H), 2.11–2.05 (m, 2H), 2.00–1.92 (m, 4H), 1.61–1.54 (m, 3H); LCMS (formic acid): R_t = 0.77 min (72%), MH⁺ = 455.4.

8-(((1*r*,4*r*)-4-Hydroxycyclohexyl)amino)-3-methyl-5-(5-methylpyridin-3-yl)-1,7-naphthyridin-2(1H)-one (3.020n)

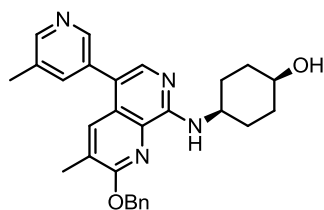
3.023n (81 mg, 0.18 mmol) was dissolved in TFA (3 mL, 38.90 mmol) and left to stir at 80 °C for 4 h. The volatile components were removed *in vacuo*. Toluene (5 mL) was added and the solvent evaporated *in vacuo* (× 3). The resulting residue was dissolved in MeOH (20 mL) and passed through a preconditioned (MeOH, 20 mL) amino propyl column (10 g). The column was rinsed with MeOH (50 mL) and the filtrate concentrated *in vacuo*. The resulting residue was purified by MDAP (high pH). The appropriate fractions were combined and solvent evaporated *in vacuo* to give **3.020n** (6 mg, 0.02 mmol, 9%) as a pale yellow solid; ¹H NMR (400 MHz, DMSO-*d*₆) δ ppm 11.43 (1H, s), 8.44 (d, *J* = 1.5, 1H), 8.37 (d, *J* = 1.5, 1H), 7.71 (s, 1H), 7.63–7.61 (m, 1H), 7.52–7.50 (m, 1H), 6.80 (d, *J* = 6.9, 1H), 4.54 (d, *J* = 4.4, 1H), 3.98–3.87 (m, 1H), 3.52–3.42 (m, 1H), 2.38 (s, 3H), 2.10–2.02 (m, 5H), 1.91–1.83 (m, 2H), 1.34–1.25 (m, 4H); LCMS (formic acid): R_t = 0.43 min (100%), MH⁺ = 365.0.

(S)-2-(Benzyloxy)-3-methyl-5-(5-methylpyridin-3-yl)-N-(tetrahydro-2H-pyran-3-yl)-1,7-naphthyridin-8-amine (3.023o)

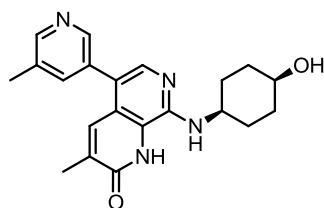
A mixture of **3.031** (200 mg, 0.41 mmol), and (S)-tetrahydro-2H-pyran-3-amine hydrochloride (169 mg, 1.23 mmol) and DIPEA (0.21 mL, 1.23 mmol) in MeCN (2.0 mL) was stirred in a microwave reactor at 140 °C for 2 h. The reaction mixture was concentrated *in vacuo* and the resulting residue was purified by silica gel chromatography (0–100% EtOAc in cyclohexane). The appropriate fractions were combined and solvent evaporated *in vacuo* to give **3.023o** (64 mg, 0.15 mmol, 36%) as a yellow oil; ¹H NMR (400 MHz, CDCl₃) δ ppm 8.48 (d, *J* = 1.6, 1H), 8.47 (d, *J* = 1.6, 1H), 7.83 (s, 1H), 7.71 (d, *J* = 1.0, 1H), 7.56–7.52 (m, 3H), 7.43–7.38 (m, 2H), 7.37–7.32 (m, 1H), 6.68 (d, *J* = 8.3, 1H), 5.64–5.49 (m, 2H), 4.40–4.32 (m, 1H), 4.06–4.00 (m, 1H), 3.80–3.74 (m, 2H), 3.68–3.60 (m, 1H), 2.43 (s, 3H), 2.35 (d, *J* = 1.0, 3H), 1.92–1.81 (m, 2H), 1.75–1.63 (m, 2H); LCMS (formic acid): R_t = 0.85 min (80%), MH⁺ = 441.1.

(S)-3-methyl-5-(5-methylpyridin-3-yl)-8-((tetrahydro-2H-pyran-3-yl)amino)-1,7-naphthyridin-2(1H)-one (3.020o)

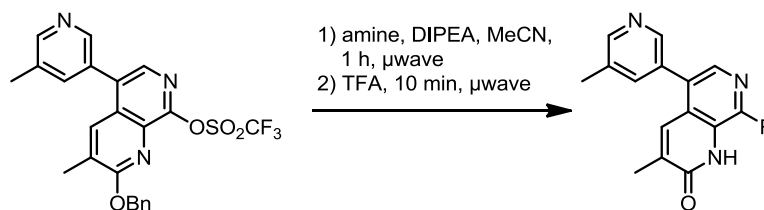
3.023o (110 mg, 0.25 mmol) was dissolved in TFA (3 mL, 38.90 mmol) and left to stir at 80 °C for 4 h. The volatile components were removed *in vacuo*. Toluene (5 mL) was added and the solvent evaporated *in vacuo* (× 3). The resulting residue was dissolved in MeOH (20 mL) and passed through a preconditioned (MeOH, 20 mL) amino propyl column (10 g). The column was rinsed with MeOH (50 mL) and the filtrate concentrated *in vacuo*. The resulting residue was purified by MDAP (high pH). The appropriate fractions were combined and solvent evaporated *in vacuo* to give **3.020o** (16 mg, 0.05 mmol, 18%) as a yellow solid; ¹H NMR (400 MHz, DMSO-d₆) δ ppm 11.54 (br.s, 1H), 8.45 (d, *J* = 1.8, 1H), 8.37 (d, *J* = 1.8, 1H), 7.70 (s, 1H), 7.64–7.61 (m, 1H), 7.51 (d, *J* = 1.0, 1H), 6.88 (d, *J* = 6.8, 1H), 4.20–4.12 (m, 1H), 3.97 (dd, *J* = 10.7, 2.9, 1H), 3.79–3.70 (m, 1H), 3.46–3.38 (m, 1H), 3.21 (dd, *J* = 10.7, 8.4, 1H), 2.38 (s, 3H), 2.08 (d, *J* = 1.0, 3H), 2.06–2.02 (m, 1H), 1.83–1.74 (m, 1H), 1.67–1.58 (m, 2H); LCMS (formic acid): R_t = 0.51 min (100%), MH⁺ = 351.1.

(1s,4s)-4-((2-(Benzyloxy)-3-methyl-5-(5-methylpyridin-3-yl)-1,7-naphthyridin-8-yl)amino)cyclohexanol (3.023p)

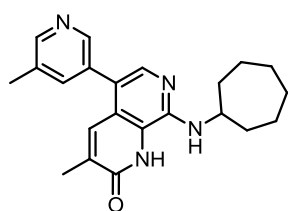
A mixture of **3.031** (200 mg, 0.41 mmol), and (1s,4s)-4-aminocyclohexanol (141 mg, 1.23 mmol) and DIPEA (0.21 mL, 1.23 mmol) in MeCN (2.0 mL) was stirred in a microwave reactor at 140 °C for 1 h. The reaction mixture was concentrated *in vacuo* and the resulting residue was purified by silica gel chromatography (0–100% EtOAc in cyclohexane, then 0–50% EtOH in EtOAc). The appropriate fractions were combined and solvent evaporated *in vacuo* to give **3.023p** (136 mg, 0.30 mmol, 73%) as a yellow oil; ¹H NMR (400 MHz, CDCl₃) δ ppm 8.48 (d, *J* = 1.8, 1H), 8.46 (d, *J* = 1.8, 1H), 7.82 (s, 1H), 7.71 (d, *J* = 1.1, 1H), 7.55–7.48 (m, 3H), 7.44–7.38 (m, 2H), 7.36–7.31 (m, 1H), 6.51 (d, *J* = 8.1, 1H), 5.55 (s, 2H), 4.28–4.20 (m, 1H), 4.04–3.96 (m, 1H), 2.43 (s, 3H), 2.35 (d, *J* = 1.1, 3H), 1.95–1.72 (m, 8H); LCMS (formic acid): *R*_t = 0.74 min (83%), *MH*⁺ = 455.2.

8-(((1s,4s)-4-hydroxycyclohexyl)amino)-3-methyl-5-(5-methylpyridin-3-yl)-1,7-naphthyridin-2(1H)-one (3.020p)

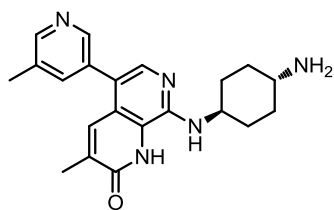
3.023p (136 mg, 0.30 mmol) was dissolved in TFA (3 mL, 38.90 mmol) and left to stir at 80 °C for 4 h. The volatile components were removed *in vacuo*. Toluene (5 mL) was added and the solvent evaporated *in vacuo* (× 3). The resulting residue was dissolved in MeOH (20 mL) and passed through a preconditioned (MeOH, 20 mL) amino propyl column (10 g). The column was rinsed with MeOH (50 mL) and the filtrate concentrated *in vacuo*. The resulting residue was purified by MDAP (high pH). The appropriate fractions were combined and solvent evaporated *in vacuo* to give **3.020p** (26 mg, 0.07 mmol, 24%) as a yellow solid; m.p. <300 °C; *v*_{max} (solid)/cm⁻¹: 3385 (O-H), 2919 (N-H), 1656 (C=O), 1526, 1370, 972, 717; ¹H NMR (400 MHz, DMSO-*d*₆) δ ppm 11.57 (br.s, 1H), 8.44 (d, *J* = 1.5, 1H), 8.37 (d, *J* = 1.5, 1H), 7.70 (s, 1H), 7.64–7.59 (m, 1H), 7.51 (s, 1H), 6.81 (d, *J* = 6.8, 1H), 4.41 (d, *J* = 2.8, 1H), 4.13–4.03 (m, 1H), 3.77–3.70 (m, 1H), 2.38 (s, 3H), 2.10–2.06 (m, 3H), 1.79–1.65 (m, 6H), 1.60–1.51 (m, 2H); ¹³C NMR (101 MHz, DMSO-*d*₆) δ ppm 161.7, 148.4, 147.1, 146.5, 139.0, 137.4, 134.1, 132.8, 132.7, 131.9, 120.9, 120.8, 117.7, 64.8, 47.8, 31.1, 27.0, 17.8, 16.7; HRMS (*M* + *H*)⁺ calculated for C₂₁H₂₅N₄O₂ 365.1972; found 365.1971; LCMS (high pH): *R*_t = 0.80 min (100%), *MH*⁺ = 365.3.

General Procedure 3A: Synthesis of 8-position array compounds

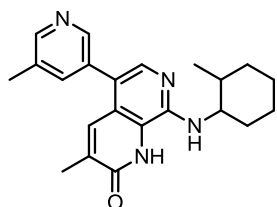
A mixture of **3.031** (150 mg, 0.31 mmol) and amine (0.92 mmol, 3 eq.) and DIPEA (0.16 mL, 0.92 mmol, 3 eq.) in MeCN (1.5 mL) was stirred in a microwave reactor at 140 °C for 1 h. The reaction mixture was concentrated *in vacuo* and the resulting residue was dissolved in TFA (1.5 mL, 19.47 mmol, 64 eq.) and heated at 100 °C in the microwave reactor for 10 minutes. The reaction mixture was allowed to cool to rt and concentrated *in vacuo*. The resulting residue was dissolved in MeOH (5 mL) and passed through a preconditioned (MeOH, 5 mL) amino propyl column (2 g). The column was washed with MeOH (10 mL). The filtrate was concentrated *in vacuo* and the resulting solid was purified by MDAP (high pH). The appropriate fractions were combined and solvent evaporated *in vacuo* to give the desired product.

8-(Cycloheptylamino)-3-methyl-5-(5-methylpyridin-3-yl)-1,7-naphthyridin-2(1H)-one (3.020q)

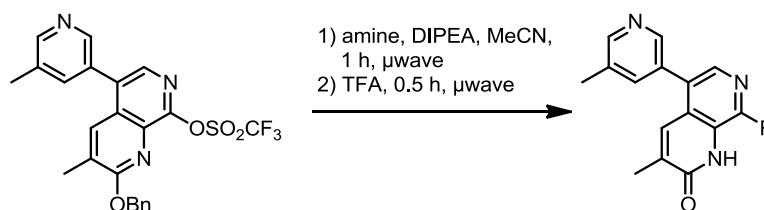
Following General Procedure 3A using cycloheptanamine (0.12 mL, 0.92 mmol), gave **3.020q** (27 mg, 0.07 mmol, 24%) as a yellow solid; m.p. 216–218 °C (decomp.); ν_{\max} (solid)/ cm^{-1} : 3399, 2919, 1661 (C=O), 1596, 1437, 878, 723; ^1H NMR (400 MHz, DMSO- d_6) δ ppm 11.50 (br.s, 1H), 8.44 (d, $J = 1.7$, 1H), 8.37 (d, $J = 1.7$, 1H), 7.70 (s, 1H), 7.62 (s, 1H), 7.50 (d, $J = 1.0$, 1H), 6.86 (d, $J = 7.1$, 1H), 4.30–4.18 (m, 1H), 2.38 (s, 3H), 2.07 (s, 3H), 2.04–1.95 (m, 2H), 1.70–1.45 (m, 10H); ^{13}C NMR (101 MHz, DMSO- d_6) δ ppm 162.2, 148.4, 147.1, 145.8, 138.9, 137.4, 133.9, 132.7, 132.6, 132.0, 120.7, 117.6, 51.0, 34.1, 28.1, 23.7, 17.8, 16.8; HRMS ($M + H$) $^+$ calculated for $\text{C}_{22}\text{H}_{27}\text{N}_4\text{O}$ 363.2179; found 363.2183; LCMS (high pH): $R_t = 1.19$ min (100%), $MH^+ = 363.3$.

8-(((1*r*,4*r*)-4-Aminocyclohexyl)amino)-3-methyl-5-(5-methylpyridin-3-yl)-1,7-naphthyridin-2(1H)-one (3.020r)

Following General Procedure 3A using ((1*r*,4*r*)-4-aminocyclohexyl)carbamate (197 mg, 0.92 mmol), gave **3.020r** (16 mg, 0.04 mmol, 14%) as a yellow solid; ¹H NMR (400 MHz, DMSO-*d*₆) δ ppm 8.44 (d, *J* = 1.7, 1H), 8.36 (d, *J* = 1.7, 1H), 7.67 (s, 1H), 7.64–7.59 (m, 1H), 7.49 (s, 1H), 6.81 (d, *J* = 6.8, 1H), 3.99–3.86 (m, 1H), 2.67–2.56 (m, 1H), 2.38 (s, 3H), 2.10–2.00 (m, 5H), 1.87–1.78 (m, 2H), 1.36–1.24 (m, 2H), 1.23–1.10 (m, 2H); LCMS (high pH): *R*_t = 0.70 min (94%), *MH*⁺ = 364.3.

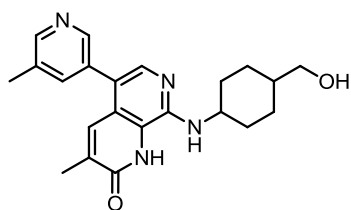
3-Methyl-8-((2-methylcyclohexyl)amino)-5-(5-methylpyridin-3-yl)-1,7-naphthyridin-2(1H)-one (3.020s)

Following General Procedure 3A using 2-methylcyclohexylamine (0.12 mL, 0.92 mmol), gave **3.020s** (4 mg, 10.50 μmol, 3%) as a yellow solid; ¹H NMR (400 MHz, CD₃OD) δ ppm 8.45 (s, 1H), 8.38 (s, 1H), 7.76–7.73 (m, 1H), 7.66 (s, 1H), 7.64–7.62 (m, 1H), 3.85–3.73 (m, 1H), 2.46 (s, 3H), 2.21 (s, 3H), 2.19–2.08 (m, 1H), 1.92–1.72 (m, 3H), 1.68–1.55 (m, 1H), 1.51–1.16 (m, 4H), 1.01 (d, *J* = 6.6, 3H); LCMS (high pH): *R*_t = 1.16 min (98%), *MH*⁺ = 363.4.

General Procedure 3B: Synthesis of 8-position array compounds

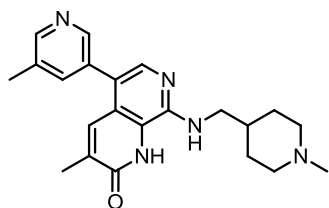
A mixture of **3.031** (100 mg, 0.20 mmol), amine (0.60 mmol, 3 eq.) and DIPEA (0.07 mL, 0.40 mmol, 2 eq.) in MeCN (1.5 mL) was heated at 140 °C for 1 h. The reaction mixture was allowed to cool to rt and concentrated *in vacuo*. The resulting residue was dissolved in TFA (2 mL, 128 eq.) and heated at 100 °C for 0.5 h. The reaction mixture was concentrated *in vacuo* and the resulting residue was dissolved in MeOH (5 mL) and passed through a preconditioned (MeOH, 5 mL) amino propyl column (2 g). The filtrate was concentrated *in vacuo* and the resulting residue was purified by MDAP (high pH). The appropriate fractions were combined and solvent evaporated *in vacuo* to the desired product.

8-((4-(Hydroxymethyl)cyclohexyl)amino)-3-methyl-5-(5-methylpyridin-3-yl)-1,7-naphthyridin-2(1H)-one (3.020t)



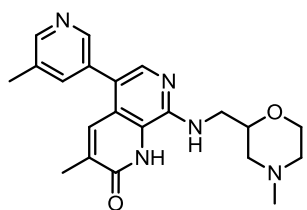
Following General Procedure 3B using (4-aminocyclohexyl)methanol (79 mg, 0.60 mmol), gave **3.020t** (27 mg, 0.07 mmol, 35%) as a pale yellow solid; m.p. 273–275 °C; ν_{\max} (solid)/ cm^{-1} : 3388 (O-H), 2903 (N-H), 1657 (C=O), 1594, 848, 716; ^1H NMR (400 MHz, DMSO- d_6) δ ppm 11.42 (br.s, 1H), 8.44 (d, $J = 1.6$, 1H), 8.37 (d, $J = 1.6$, 1H), 7.70 (s, 1H), 7.62 (s, 1H), 7.50 (s, 1H), 6.85 (d, $J = 6.4$, 1H), 4.41–4.35 (m, 1H), 3.99–3.89 (m, 1H), 3.27–3.24 (m, 2H), 2.38 (s, 3H), 2.14–2.02 (m, 5H), 1.85–1.78 (m, 2H), 1.45–1.32 (m, 1H), 1.32–1.19 (m, 2H), 1.10–0.96 (m, 2H); ^{13}C NMR (101 MHz, DMSO- d_6) δ ppm 161.9, 148.4, 147.0, 139.0, 137.5, 134.0, 132.8, 132.7, 131.9, 131.8, 120.8, 120.7, 117.6, 66.3, 49.9, 32.1, 28.3, 17.8, 16.7; N.B. 1C signal hidden under solvent peak; HRMS ($M + H$) $^+$ calculated for $\text{C}_{22}\text{H}_{27}\text{N}_4\text{O}_2$ 379.2129; found 379.2137; LCMS (high pH): $R_t = 0.82$ min (98%), $\text{MH}^+ = 379.2$.

3-Methyl-8-(((1-methylpiperidin-4-yl)methyl)amino)-5-(5-methylpyridin-3-yl)-1,7-naphthyridin-2(1H)-one (3.020u)



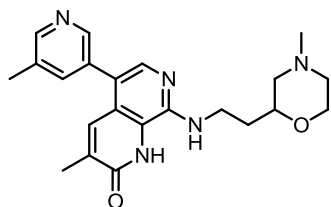
Following General Procedure 3B using (1-methylpiperidin-4-yl)methanamine (0.09 mL, 0.60 mmol), gave **3.020u** (23 mg, 0.06 mmol, 30%) as a yellow solid; m.p. 250–252 °C (decomp.); ν_{\max} (solid)/ cm^{-1} : 3388, 2910, 1653 (C=O), 1591, 1441, 860, 722, 675; ^1H NMR (400 MHz, DMSO- d_6) δ ppm 11.17 (br.s, 1H), 8.44 (d, $J = 1.7$, 1H), 8.37 (d, $J = 1.7$, 1H), 7.70 (s, 1H), 7.64–7.60 (m, 1H), 7.51 (d, $J = 1.2$, 1H), 6.95 (t, $J = 5.0$, 1H), 3.38–3.32 (m, 2H), 2.80–2.72 (m, 2H), 2.39 (s, 3H), 2.14 (s, 3H), 2.08 (d, $J = 1.0$, 3H), 1.88–1.79 (m, 2H), 1.78–1.71 (m, 2H), 1.66–1.54 (m, 1H), 1.30–1.18 (m, 2H); ^{13}C NMR (101 MHz, DMSO- d_6) δ ppm 161.9, 148.5, 147.1, 146.5, 139.0, 137.4, 134.2, 132.8, 131.9, 127.3, 120.8, 120.5, 117.9, 55.2, 46.9, 46.2, 34.5, 29.9, 17.8, 16.7; HRMS ($M + H$) $^+$ calculated for $\text{C}_{22}\text{H}_{28}\text{N}_5\text{O}$ 378.2288; found 378.2294; LCMS (high pH): $R_t = 0.80$ min (98%), $\text{MH}^+ = 378.4$.

3-Methyl-8-(((4-methylmorpholin-2-yl)methyl)amino)-5-(5-methylpyridin-3-yl)-1,7-naphthyridin-2(1H)-one (3.020v)



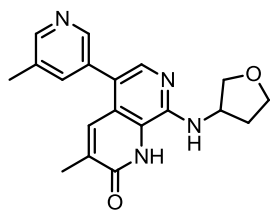
Following General Procedure 3B using (4-methylmorpholin-2-yl)methanamine (0.08 mL, 0.60 mmol), gave **3.020v** (8 mg, 0.02 mmol, 10%) as a yellow solid; ^1H NMR (400 MHz, CD_3OD) δ ppm 8.44 (d, $J = 1.8$, 1H), 8.36 (d, $J = 1.8$, 1H), 7.74–7.70 (m, 2H), 7.61 (d, $J = 1.5$, 1H), 3.96–3.89 (m, 1H), 3.89–3.81 (m, 1H), 3.72–3.62 (m, 2H), 3.60–3.52 (m, 1H), 2.94–2.86 (m, 1H), 2.74–2.68 (m, 1H), 2.46 (s, 3H), 2.30 (s, 3H), 2.22–2.15 (m, 4H), 2.02–1.94 (m, 1H); LCMS (high pH): $R_t = 0.78$ min (91%), $\text{MH}^+ = 337.3$.

3-Methyl-8-((2-(4-methylmorpholin-2-yl)ethyl)amino)-5-(5-methylpyridin-3-yl)-1,7-naphthyridin-2(1H)-one (3.020w)



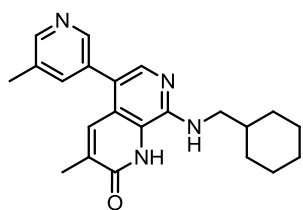
Following General Procedure 3B using 2-(4-methylmorpholin-2-yl)ethanamine (88 mg, 0.60 mmol), gave **3.020w** (8 mg, 0.02 mmol, 10%) as a yellow solid; ^1H NMR (400 MHz, DMSO-d_6) δ ppm 11.40 (br.s, 1H), 8.45 (s, 1H), 8.41–8.34 (m, 1H), 7.72 (s, 1H), 7.63 (s, 1H), 7.53 (s, 1H), 7.01–6.93 (m, 1H), 3.85–3.79 (m, 1H), 3.66–3.44 (m, 4H), 3.29 (s, 3H), 2.87–2.64 (m, 2H), 2.39 (s, 3H), 2.30–2.21 (m, 2H), 2.08 (s, 3H), 1.78–1.69 (m, 2H); LCMS (high pH): $R_t = 0.80$ min (96%), $\text{MH}^+ = 394.3$.

3-Methyl-5-(5-methylpyridin-3-yl)-8-((tetrahydrofuran-3-yl)amino)-1,7-naphthyridin-2(1H)-one (3.020x)



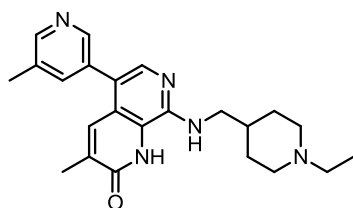
Following General Procedure 3B using tetrahydrofuran-3-amine (0.05 mL, 0.60 mmol), gave **3.020x** (12 mg, 0.04 mmol, 17%) as a yellow solid; ^1H NMR (400 MHz, DMSO-d_6) δ ppm 11.45 (br.s, 1H), 8.45 (d, $J = 1.8$, 1H), 8.37 (d, $J = 1.8$, 1H), 7.71 (s, 1H), 7.66–7.60 (m, 1H), 7.53–7.47 (m, 1H), 7.12 (d, $J = 5.6$, 1H), 4.66–4.56 (m, 1H), 3.96–3.86 (m, 2H), 3.80–3.73 (m, 1H), 3.64 (dd, $J = 9.0, 3.4$, 1H), 2.38 (s, 3H), 2.30–2.20 (m, 1H), 2.08 (d, $J = 1.0$, 3H), 1.98–1.88 (m, 1H); LCMS (high pH): $R_t = 0.78$ min (98%), $\text{MH}^+ = 337.3$.

8-((Cyclohexylmethyl)amino)-3-methyl-5-(5-methylpyridin-3-yl)-1,7-naphthyridin-2(1H)-one (3.042a)



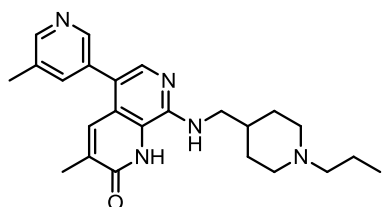
Following General Procedure 3B using cyclohexylmethanamine (0.08 mL, 0.60 mmol), gave **3.042a** (43 mg, 0.12 mmol, 58%) as a yellow solid; m.p. 216–218 °C (decomp.); ν_{\max} (solid)/ cm^{-1} : 3393 (N-H), 2923, 1655 (C=O), 1593, 1268, 680; ^1H NMR (400 MHz, DMSO-d_6) δ ppm 11.62 (br.s, 1H), 8.57 (s, 1H), 8.51 (s, 1H), 7.86 (s, 1H), 7.71 (s, 1H), 7.57 (s, 1H), 7.43–7.10 (m, 1H), 3.40–3.31 (m, 2H), 2.43 (s, 3H), 2.11 (s, 3H), 1.88–1.79 (m, 2H), 1.77–1.61 (m, 4H), 1.31–1.15 (m, 3H), 1.09–0.94 (m, 2H); ^{13}C NMR (101 MHz, DMSO-d_6) δ ppm 161.9, 148.5, 147.1, 146.5, 139.1, 137.4, 134.1, 132.8, 132.7, 132.1, 120.8, 120.7, 117.3, 47.7, 36.6, 30.5, 26.0, 25.4, 17.8, 16.7; HRMS ($\text{M} + \text{H}^+$) calculated for $\text{C}_{22}\text{H}_{27}\text{N}_4\text{O}$ 363.2179; found 363.2189; LCMS (formic acid): R_t = 0.69 min (100%), MH^+ = 363.2.

8-(((1-Ethylpiperidin-4-yl)methyl)amino)-3-methyl-5-(5-methylpyridin-3-yl)-1,7-naphthyridin-2(1H)-one (3.042b)



Following General Procedure 3B using (1-ethylpiperidin-4-yl)methanamine (87 mg, 0.61 mmol), gave **3.042b** (14 mg, 0.04 mmol, 18%) as a white solid; ^1H NMR (400 MHz, DMSO-d_6) δ ppm 11.48 (br.s, 1H), 8.44 (d, J = 1.8, 1H), 8.37 (d, J = 1.8, 1H), 7.70 (s, 1H), 7.62 (s, 1H), 7.51 (d, J = 1.2, 1H), 6.95 (t, J = 5.0, 1H), 3.38–3.32 (m, 2H), 2.92–2.83 (m, 2H), 2.38 (s, 3H), 2.30 (q, J = 7.1, 2H), 2.08 (s, 3H), 1.88–1.73 (m, 4H), 1.70–1.58 (m, 1H), 1.28–1.17 (m, 2H), 0.99 (t, J = 7.1, 3H); LCMS (formic acid): R_t = 0.35 min (100%), MH^+ = 392.2.

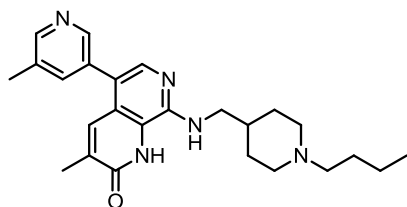
3-Methyl-5-(5-methylpyridin-3-yl)-8-(((1-propylpiperidin-4-yl)methyl)amino)-1,7-naphthyridin-2(1H)-one (3.042c)



Following General Procedure 3B using (1-propylpiperidin-4-yl)methanamine (96 mg, 0.60 mmol), gave **3.042c** (26 mg, 0.06 mmol, 31%) as an off white solid; ^1H NMR (400 MHz, DMSO-d_6) δ ppm 11.48 (br.s, 1H), 8.44 (d, J = 1.8, 1H), 8.37 (d, J = 1.8, 1H), 7.70 (s, 1H), 7.62 (s, 1H), 7.51 (d, J = 1.2, 1H), 6.95 (t, J = 4.9, 1H), 3.38–3.31 (m, 2H), 2.89–2.81 (m, 2H), 2.38 (s, 3H), 2.23–2.16 (m, 2H), 2.08 (d,

$J = 1.2$, 3H), 1.87–1.79 (m, 2H), 1.79–1.71 (m, 2H), 1.69–1.58 (m, 1H), 1.48–1.36 (m, 2H), 1.29–1.16 (m, 2H), 0.84 (t, $J = 7.3$, 3H); LCMS (high pH): $R_t = 0.92$ min (100%), $MH^+ = 406.4$.

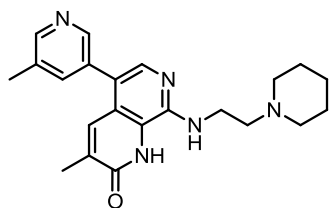
8-(((1-Butylpiperidin-4-yl)methyl)amino)-3-methyl-5-(5-methylpyridin-3-yl)-1,7-naphthyridin-2(1H)-one (3.042d)



Following General Procedure 3B using (1-butylpiperidin-4-yl)methanamine (104 mg, 0.60 mmol), gave **3.042d** (3 mg, 7.20 μ mol, 4%) as a yellow solid; 1H NMR (400 MHz, CD_3OD) δ ppm 8.50–8.44 (m, 1H), 8.42–8.36 (m, 1H), 7.77–7.66

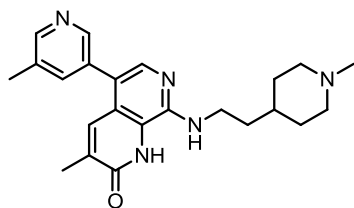
(m, 2H), 7.60 (s, 1H), 3.47 (d, $J = 6.6$, 2H), 3.12–3.03 (m, 2H), 2.50–2.43 (m, 5H), 2.21–2.08 (m, 5H), 1.97–1.78 (m, 3H), 1.60–1.50 (m, 2H), 1.46–1.30 (m, 4H), 0.95 (t, $J = 7.3$, 3H); LCMS (formic acid): $R_t = 0.42$ min (96%), $MH^+ = 420.3$.

3-Methyl-5-(5-methylpyridin-3-yl)-8-((2-(piperidin-1-yl)ethyl)amino)-1,7-naphthyridin-2(1H)-one (3.042e)

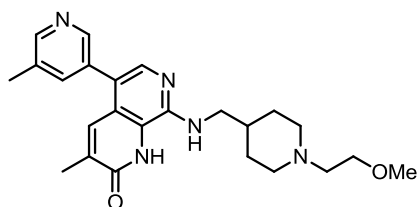


Following General Procedure 3B using 2-(piperidin-1-yl)ethanamine (79 mg, 0.60 mmol), gave **3.042e** (39 mg, 0.10 mmol, 51%) as a yellow solid; m.p. 240–242 $^{\circ}C$ (decomp.); ν_{max} (solid)/ cm^{-1} : 3396 (N-H), 2931, 1658 (C=O), 1595, 1451, 720; 1H NMR (400 MHz, CD_3OD)

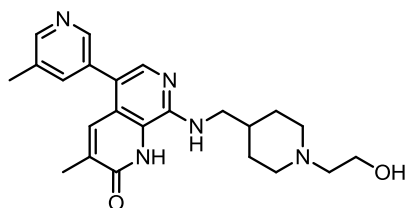
δ ppm 8.44 (d, $J = 1.6$, 1H), 8.36 (d, $J = 1.6$, 1H), 7.74–7.71 (m, 2H), 7.60 (d, $J = 1.0$, 1H), 3.72 (t, $J = 6.5$, 2H), 2.76 (t, $J = 6.5$, 2H), 2.63–2.56 (m, 4H), 2.46 (s, 3H), 2.19 (d, $J = 1.0$, 3H), 1.73–1.65 (m, 4H), 1.56–1.50 (m, 2H); ^{13}C NMR (101 MHz, $DMSO-d_6$) δ ppm 161.9, 148.5, 147.1, 146.5, 139.1, 137.4, 134.1, 132.8, 131.9, 120.9, 117.9, 57.5, 54.1, 38.6, 25.5, 24.0, 17.8, 16.7; HRMS ($M + H$) $^+$ calculated for $C_{22}H_{28}N_5O$ 378.2288; found 378.2298; LCMS (high pH): $R_t = 0.90$ min (100%), $MH^+ = 378.3$.

3-Methyl-8-((2-(1-methylpiperidin-4-yl)ethyl)amino)-5-(5-methylpyridin-3-yl)-1,7-naphthyridin-2(1H)-one (3.042f)

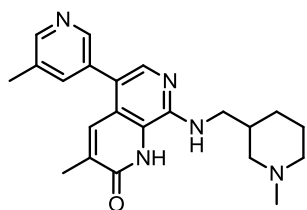
Following General Procedure 3B using 2-(1-methylpiperidin-4-yl)ethanamine (87 mg, 0.613 mmol), gave **3.042f** (29 mg, 0.07 mmol, 36%) as a yellow solid; ^1H NMR (400 MHz, DMSO- d_6) δ ppm 11.38 (br.s, 1H), 8.45 (d, $J = 1.8$, 1H), 8.37 (d, $J = 1.8$, 1H), 7.71 (s, 1H), 7.64–7.60 (m, 1H), 7.52 (d, $J = 1.2$, 1H), 6.92 (t, $J = 4.8$, 1H), 3.53–3.46 (m, 2H), 3.08–2.98 (m, 2H), 2.45–2.36 (m, 6H), 2.35–2.22 (m, 2H), 2.08 (d, $J = 1.2$, 3H), 1.83–1.74 (m, 2H), 1.63–1.55 (m, 2H), 1.53–1.44 (m, 1H), 1.36–1.20 (m, 2H); LCMS (high pH): $R_t = 0.85$ min (100%), $\text{MH}^+ = 392.3$.

8-(((1-(2-Methoxyethyl)piperidin-4-yl)methyl)amino)-3-methyl-5-(5-methylpyridin-3-yl)-1,7-naphthyridin-2(1H)-one (3.042g)

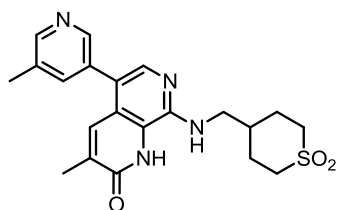
Following General Procedure 3B using (1-(2-methoxyethyl)piperidin-4-yl)methanamine (106 mg, 0.60 mmol), gave **3.042g** (12 mg, 0.03 mmol, 14%) as an orange solid; ^1H NMR (400 MHz, CD_3OD) δ ppm 8.46–8.43 (m, 1H), 8.35 (d, $J = 1.7$, 1H), 7.74 (s, 1H), 7.72–7.69 (m, 1H), 7.62 (d, $J = 1.2$, 1H), 3.68 (t, $J = 5.1$, 2H), 3.56–3.45 (m, 4H), 3.40 (s, 3H), 3.21–3.14 (m, 2H), 2.93–2.78 (m, 2H), 2.46 (s, 3H), 2.21–2.16 (m, 3H), 2.10–2.00 (m, 3H), 1.64–1.52 (m, 2H); LCMS (high pH): $R_t = 0.85$ min (96%), $\text{MH}^+ = 422.3$.

8-(((1-(2-Hydroxyethyl)piperidin-4-yl)methyl)amino)-3-methyl-5-(5-methylpyridin-3-yl)-1,7-naphthyridin-2(1H)-one (3.042h)

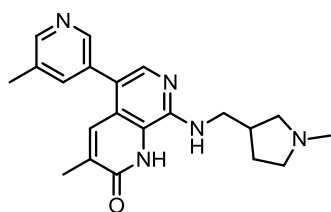
Following General Procedure 3B using 2-(4-(aminomethyl)piperidin-1-yl)ethanol (97 mg, 0.60 mmol), gave **3.042h** (8 mg, 0.02 mmol, 10%) as a pale yellow solid; ^1H NMR (400 MHz, DMSO- d_6) δ ppm 11.50 (br.s, 1H), 8.44 (d, $J = 1.6$, 1H), 8.37 (d, $J = 1.6$, 1H), 7.67 (s, 1H), 7.63–7.60 (m, 1H), 7.49 (d, $J = 1.0$, 1H), 6.95 (t, $J = 5.0$, 1H), 4.34–4.24 (m, 1H), 3.52–3.45 (m, 2H), 3.34 (t, $J = 5.9$, 2H), 2.91–2.84 (m, 2H), 2.40–2.33 (m, 5H), 2.07 (s, 3H), 1.97–1.88 (m, 2H), 1.78–1.70 (m, 2H), 1.68–1.58 (m, 1H), 1.30–1.17 (m, 2H); LCMS (high pH): $R_t = 0.75$ min (98%), $\text{MH}^+ = 408.3$.

3-Methyl-8-(((1-methylpiperidin-3-yl)methyl)amino)-5-(5-methylpyridin-3-yl)-1,7-naphthyridin-2(1H)-one (3.042i)

Following General Procedure 3B using (1-methylpiperidin-3-yl)methanamine (0.09 mL, 0.60 mmol), gave **3.042i** (20 mg, 0.05 mmol, 26%) as a yellow solid; ^1H NMR (400 MHz, DMSO- d_6) δ ppm 11.43 (br.s, 1H), 8.45 (d, $J = 1.8$, 1H), 8.37 (d, $J = 1.8$, 1H), 7.71 (s, 1H), 7.64–7.60 (m, 1H), 7.52 (d, $J = 1.2$, 1H), 6.97 (t, $J = 4.9$, 1H), 3.41–3.32 (m, 2H), 2.85–2.80 (m, 1H), 2.67–2.60 (m, 1H), 2.38 (s, 3H), 2.16 (s, 3H), 2.09 (d, $J = 1.0$, 3H), 1.97–1.83 (m, 2H), 1.79–1.61 (m, 4H), 1.52–1.40 (m, 1H), 1.05–0.92 (m, 1H); LCMS (high pH): $R_t = 0.86$ min (100%), $\text{MH}^+ = 378.3$.

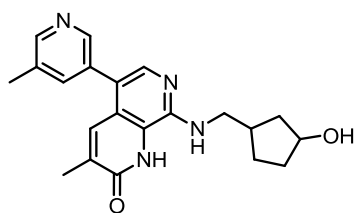
8-(((1,1-Dioxidotetrahydro-2H-thiopyran-4-yl)methyl)amino)-3-methyl-5-(5-methylpyridin-3-yl)-1,7-naphthyridin-2(1H)-one (3.042j)

Following General Procedure 3B using 4-(aminomethyl)tetrahydro-2H-thiopyran 1,1-dioxide hydrochloride (122 mg, 0.60 mmol), gave **3.042j** (6 mg, 0.02 mmol, 7%) as a pale yellow solid; ^1H NMR (400 MHz, DMSO- d_6) δ ppm 11.44 (br.s, 1H), 8.37 (d, $J = 1.7$, 1H), 7.75–7.71 (d, $J = 1.7$, 1H), 7.64–7.61 (m, 1H), 7.51 (s, 1H), 7.11–7.03 (m, 1H), 3.48–3.40 (m, 2H), 3.20–3.01 (m, 4H), 2.38 (s, 3H), 2.18–2.11 (m, 2H), 2.08 (s, 3H), 2.05–1.93 (m, 1H), 1.76–1.64 (m, 2H); LCMS (high pH): $R_t = 0.77$ min (92%), $\text{MH}^+ = 413.3$.

3-Methyl-5-(5-methylpyridin-3-yl)-8-(((1-methylpyrrolidin-3-yl)methyl)amino)-1,7-naphthyridin-2(1H)-one (3.042k)

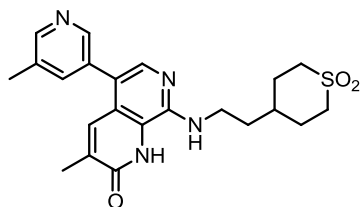
Following General Procedure 3B using (1-methylpyrrolidin-3-yl)methanamine (70 mg, 0.60 mmol), gave **3.042k** (11 mg, 0.03 mmol, 15%) as a yellow solid; ^1H NMR (400 MHz, CD_3OD) δ ppm 8.45–8.41 (m, 1H), 8.37–8.34 (m, 1H), 7.73–7.69 (m, 2H), 7.61–7.59 (m, 1H), 3.56 (d, $J = 7.3$, 2H), 2.92–2.85 (m, 1H), 2.76–2.66 (m, 3H), 2.54–2.47 (m, 1H), 2.45 (s, 3H), 2.43 (s, 3H), 2.18 (s, 3H), 2.17–2.10 (m, 1H), 1.75–1.64 (m, 1H); LCMS (high pH): $R_t = 0.83$ min (95%), $\text{MH}^+ = 364.3$.

8-(((3-Hydroxycyclopentyl)methyl)amino)-3-methyl-5-(5-methylpyridin-3-yl)-1,7-naphthyridin-2(1H)-one (3.042l)



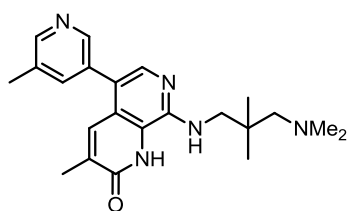
Following General Procedure 3B using 3-(aminomethyl)cyclopentanol (71 mg, 0.60 mmol), gave **3.042l** (29 mg, 0.08 mmol, 39%) as a pale yellow solid and mixture of diastereomers; ^1H NMR (400 MHz, DMSO- d_6) δ ppm 11.49 (br.s, 1H), 8.44 (d, $J = 1.8$, 1H), 8.37 (d, $J = 1.8$, 1H), 7.70 (s, 1H), 7.64–7.60 (m, 1H), 7.55–7.46 (m, 1H), 7.00–6.94 (m, 1H), 4.49–4.45 (m, 1H), 4.40–4.34 (m, 1H), 4.22–4.08 (m, 1H), 3.45 (dd, $J = 7.0, 5.3$, 1H), 3.40–3.35 (m, 1H), 2.38 (s, 3H), 2.27–2.16 (m, 1H), 2.11–2.06 (m, 3H), 2.05–1.96 (m, 1H), 1.95–1.79 (m, 1H), 1.77–1.64 (m, 1H), 1.57–1.40 (m, 1H), 1.29–1.21 (m, 1H); LCMS (high pH): $R_t = 0.78$ min (100%), $\text{MH}^+ = 365.4$.

8-((2-(1,1-Dioxidotetrahydro-2H-thiopyran-4-yl)ethyl)amino)-3-methyl-5-(5-methylpyridin-3-yl)-1,7-naphthyridin-2(1H)-one (3.042m)



Following General Procedure 3B using 4-(2-aminoethyl)tetrahydro-2H-thiopyran 1,1-dioxide (109 mg, 0.60 mmol), gave **3.042m** (5 mg, 0.01 mmol, 6%) as a yellow solid; ^1H NMR (400 MHz, DMSO- d_6) δ ppm 11.37 (br.s, 1H), 8.45 (d, $J = 1.7$, 1H), 7.72 (d, $J = 1.7$, 1H), 7.65–7.61 (m, 1H), 7.55–7.50 (m, 1H), 6.99–6.91 (m, 1H), 3.59–3.46 (m, 2H), 3.17–3.07 (m, 2H), 3.06–2.98 (m, 2H), 2.38 (s, 3H), 2.13–2.03 (m, 5H), 1.84–1.73 (m, 1H), 1.70–1.60 (m, 4H); LCMS (high pH): $R_t = 0.78$ min (100%), $\text{MH}^+ = 427.2$.

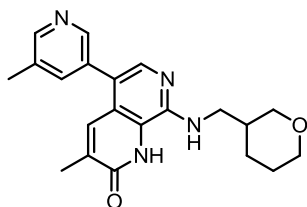
8-(((3-(Dimethylamino)-2,2-dimethylpropyl)amino)-3-methyl-5-(5-methylpyridin-3-yl)-1,7-naphthyridin-2(1H)-one (3.042n)



Following General Procedure 3B using *N,N,N',N'*-tetramethylpropane-1,3-diamine (0.10 mL, 0.60 mmol), gave **3.042n** (24 mg, 0.06 mmol, 31%); m.p. 179–181 °C; ν_{max} (solid)/ cm^{-1} : 3377, 2941, 1660 (C=O), 1596, 1425, 821, 723; ^1H NMR (400 MHz, DMSO- d_6) δ ppm 11.78 (br.s, 1H), 8.44 (d, $J = 1.5$, 1H), 8.37 (d, $J = 1.5$, 1H), 7.68 (s, 1H), 7.65–7.59 (m, 1H), 7.51 (s, 1H), 6.71–6.55 (m, 1H), 3.45–3.41 (m, 2H), 2.38 (s, 3H), 2.25 (s, 6H), 2.23–2.21 (m, 2H), 2.08 (s, 3H), 0.93 (s, 6H); ^{13}C NMR (101 MHz, DMSO- d_6) δ ppm 162.2, 148.4, 147.1, 138.7, 137.4, 132.8, 132.0, 120.9, 117.9,

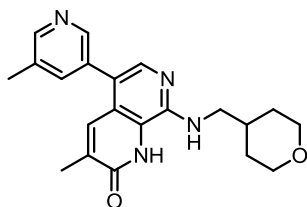
67.9, 49.5, 48.5, 36.9, 24.1, 17.8, 16.7; N.B. 3C signals not visible in spectrum; HRMS (M + H)⁺ calculated for C₂₂H₃₀N₅O 380.2445; found 380.2451; LCMS (high pH): R_t = 0.90 min (100%), MH⁺ = 380.4.

3-Methyl-5-(5-methylpyridin-3-yl)-8-(((tetrahydro-2H-pyran-3-yl)methyl)amino)-1,7-naphthyridin-2(1H)-one (3.042o)



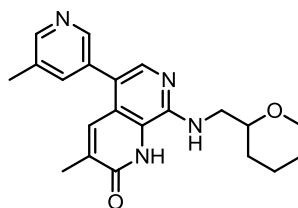
Following General Procedure 3B using (tetrahydro-2H-pyran-3-yl)methanamine (71 mg, 0.60 mmol), gave **3.042o** (32 mg, 0.07 mmol, 32%); m.p. 247–249 °C (decomp.); ν_{\max} (solid)/cm⁻¹: 3387 (N-H), 2922, 1656 (C=O), 1592, 1090; ¹H NMR (400 MHz, DMSO-d₆) δ ppm 11.44 (br.s, 1H), 8.45 (d, *J* = 1.6, 1H), 8.38 (d, *J* = 1.6, 1H), 7.71 (s, 1H), 7.63 (s, 1H), 7.52 (d, *J* = 1.2, 1H), 6.96 (t, *J* = 5.0, 1H), 3.90 (dd, *J* = 10.9, 2.3, 1H), 3.75 (dt, *J* = 11.1, 3.6, 1H), 3.41–3.32 (m, 3H), 2.23–3.15 (m, 1H), 2.38 (s, 3H), 2.08 (d, *J* = 1.0, 3H), 1.99–1.84 (m, 2H), 1.66–1.58 (m, 1H), 1.55–1.44 (m, 1H), 1.38–1.26 (m, 1H); ¹³C NMR (101 MHz, DMSO-d₆) δ ppm 161.9, 148.5, 147.1, 146.4, 139.0, 137.4, 134.2, 132.8, 131.8, 120.8, 120.6, 118.0, 70.7, 67.5, 43.3, 35.2, 27.2, 24.8, 17.8, 16.7; N.B. 1C signal not visible in spectrum; HRMS (M + H)⁺ calculated for C₂₁H₂₅N₄O₂ 365.1985; found 365.1972; LCMS (high pH): R_t = 0.88 min (98%), MH⁺ = 365.3.

3-Methyl-5-(5-methylpyridin-3-yl)-8-(((tetrahydro-2H-pyran-4-yl)methyl)amino)-1,7-naphthyridin-2(1H)-one (3.042p)



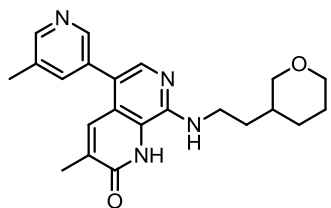
Following General Procedure 3B using (tetrahydro-2H-pyran-4-yl)methanamine (0.09 mL, 0.60 mmol) gave **3.042p** (81 mg, 0.22 mmol, 91%) as a pale yellow solid; m.p. 288–289 °C (decomp.); ν_{\max} (solid)/cm⁻¹: 3356 (N-H), 2923, 1663 (C=O), 1595, 1089, 722; ¹H NMR (400 MHz, DMSO-d₆) δ ppm 11.47 (br.s, 1H), 8.45 (d, *J* = 1.8, 1H), 8.37 (d, *J* = 1.8, 1H), 7.71 (s, 1H), 7.65–7.60 (m, 1H), 7.52 (d, *J* = 1.5, 1H), 6.98 (t, *J* = 5.1, 1H), 3.88 (dd, *J* = 11.2, 2.7, 2H), 3.40–3.34 (m, 2H), 2.38 (s, 3H), 2.08 (s, 3H), 1.97–1.84 (m, 1H), 1.75–1.66 (m, 2H), 1.34–1.20 (m, 2H). N.B. 2H hidden under water peak; ¹³C NMR (101 MHz, DMSO-d₆) δ ppm 161.9, 148.5, 147.1, 146.5, 139.0, 137.4, 132.8, 132.7, 131.9, 120.8, 120.7, 117.9, 66.8, 47.0, 34.1, 30.6, 17.8, 16.7; N.B. 1C signal not visible in spectrum; HRMS (M + H)⁺ calculated for C₂₁H₂₅N₄O₂ 365.1972; found 365.1975; LCMS (formic acid): R_t = 0.48 min (100%), MH⁺ = 365.2.

3-Methyl-5-(5-methylpyridin-3-yl)-8-(((tetrahydro-2H-pyran-2-yl)methyl)amino)-1,7-naphthyridin-2(1H)-one (3.042q)



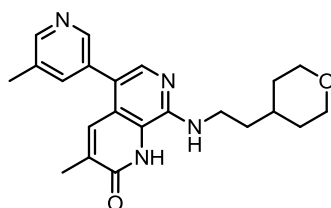
Following General Procedure 3B using (tetrahydro-2H-pyran-2-yl)methanamine (0.04 mL, 0.60 mmol), gave **3.042q** (19 mg, 0.05 mmol, 26%) as a yellow solid; ^1H NMR (400 MHz, DMSO- d_6) δ ppm 11.55 (br.s, 1H), 8.45 (d, $J = 1.5$, 1H), 8.41–8.36 (m, 1H), 7.71 (s, 1H), 7.65–7.62 (m, 1H), 7.51 (br.s, 1H), 7.17–7.11 (br.s, 1H), 3.95–3.87 (m, 1H), 3.57–3.49 (m, 2H), 3.48–3.41 (m, 1H), 3.40–3.34 (m, 1H), 2.38 (s, 3H), 2.08 (s, 3H), 1.85–1.74 (m, 1H), 1.72–1.64 (m, 1H), 1.53–1.44 (m, 3H), 1.33–1.19 (m, 1H); LCMS (high pH): $R_t = 0.93$ min (99%), $\text{MH}^+ = 365.2$.

3-Methyl-5-(5-methylpyridin-3-yl)-8-((2-(tetrahydro-2H-pyran-3-yl)ethyl)amino)-1,7-naphthyridin-2(1H)-one (3.042r)



Following General Procedure 3B using 2-(tetrahydro-2H-pyran-3-yl)ethanamine (0.09 mL, 0.60 mmol), gave **3.042r** (17 mg, 0.05 mmol, 22%) as a yellow solid; m.p. 290–291 °C (decomp.); ν_{max} (solid)/ cm^{-1} : 3397 (N-H), 2950, 1659 (C=O), 1595, 1092, 719; ^1H NMR (400 MHz, DMSO- d_6) δ ppm 11.42 (br.s, 1H), 8.44 (d, $J = 1.8$, 1H), 8.37 (d, $J = 1.8$, 1H), 7.71 (s, 1H), 7.64–7.60 (m, 1H), 7.53–7.50 (m, 1H), 6.92 (t, $J = 4.6$, 1H), 3.86–3.69 (m, 2H), 3.53–3.41 (m, 2H), 3.08–3.00 (m, 1H), 2.38 (s, 3H), 2.10–2.06 (m, 3H), 1.91–1.82 (m, 1H), 1.76–1.63 (m, 1H), 1.58–1.42 (m, 4H), 1.24–1.13 (m, 1H). NB. 1H signal hidden under water peak; ^{13}C NMR (101 MHz, DMSO- d_6) δ ppm 162.1, 148.5, 147.1, 146.2, 139.0, 137.4, 134.5, 132.8, 131.9, 120.7, 119.8, 117.9, 72.3, 67.4, 38.4, 33.2, 31.3, 29.3, 25.3, 17.8, 16.7; N.B. 1C signal not visible in spectrum; HRMS ($\text{M} + \text{H}$) $^+$ calculated for $\text{C}_{22}\text{H}_{27}\text{N}_4\text{O}_2$ 379.2143; found 379.2129; LCMS (high pH): $R_t = 0.92$ min (97%), $\text{MH}^+ = 379.4$.

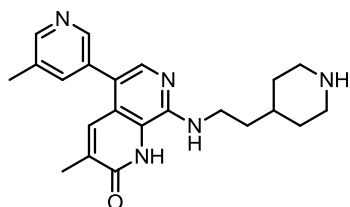
3-Methyl-5-(5-methylpyridin-3-yl)-8-((2-(tetrahydro-2H-pyran-4-yl)ethyl)amino)-1,7-naphthyridin-2(1H)-one (3.042s)



Following General Procedure 3B using 2-(tetrahydro-2H-pyran-4-yl)ethanamine (79 mg, 0.60 mmol), gave **3.042s** (16 mg, 0.04 mmol, 21%) as a yellow solid; ^1H NMR (400 MHz, DMSO- d_6) δ ppm 11.41 (br.s, 1H), 8.45 (br.s, 1H), 8.38 (br.s, 1H), 7.71 (s, 1H), 7.63 (s, 1H), 7.52 (s,

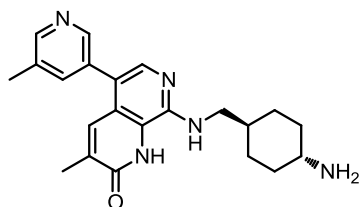
1H), 6.97–6.84 (m, 1H), 3.89–3.80 (m, 2H), 3.53–3.47 (m, 2H), 2.38 (s, 3H), 2.08 (s, 3H), 1.70–1.53 (m, 6H), 1.28–1.15 (m, 2H); N. B. 1H signal hidden under water peak; LCMS (high pH): $R_t = 0.90$ min (100%), $MH^+ = 379.2$.

3-Methyl-5-(5-methylpyridin-3-yl)-8-((2-(piperidin-4-yl)ethyl)amino)-1,7-naphthyridin-2(1H)-one (3.042t)



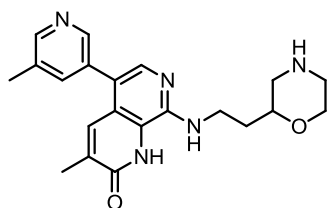
Following General Procedure 3B using *tert*-butyl 4-(2-aminoethyl)piperidine-1-carboxylate (0.14 mL, 0.60 mmol), gave **3.042t** (13 mg, 0.03 mmol, 17%) as a pale yellow solid; m.p. 278–280 °C (decomp.); ν_{\max} (solid)/ cm^{-1} : 3397 (N-H), 2919 (N-H), 1658 (C=O), 1594, 939, 794; ^1H NMR (400 MHz, DMSO- d_6) δ ppm 8.44 (d, $J = 1.6$, 1H), 8.37 (d, $J = 1.6$, 1H), 7.70 (s, 1H), 7.63–7.59 (m, 1H), 7.51 (d, $J = 1.1$, 1H), 6.90 (t, $J = 4.8$, 1H), 3.53–3.42 (m, 2H), 2.95–2.88 (m, 2H), 2.48–2.40 (m, 2H), 2.38 (s, 3H), 2.08 (d, $J = 1.1$, 3H), 1.66–1.61 (m, 2H), 1.58–1.49 (m, 3H), 1.10–0.98 (m, 2H); ^{13}C NMR (101 MHz, DMSO- d_6) δ ppm 162.1, 148.4, 147.1, 146.6, 138.9, 137.4, 134.1, 132.8, 132.7, 120.9, 120.7, 117.8, 46.1, 38.4, 36.1, 33.6, 33.1, 17.8, 16.8; HRMS ($M + H$) $^+$ calculated for $\text{C}_{22}\text{H}_{28}\text{N}_5\text{O}$ 378.2288; found 378.2292; LCMS (formic acid): $R_t = 0.34$ min (100%), $MH^+ = 378.3$.

8-(((1*r*,4*r*)-4-Aminocyclohexyl)methyl)amino)-3-methyl-5-(5-methylpyridin-3-yl)-1,7-naphthyridin-2(1H)-one (3.042u)



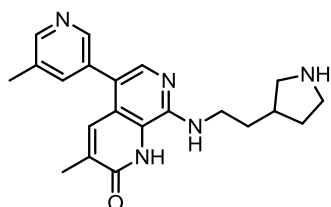
Following General Procedure 3B using ((1*r*,4*r*)-4-(aminomethyl)cyclohexyl)carbamate (140 mg, 0.60 mmol), gave **3.042u** (20 mg, 0.05 mmol, 26%) as a yellow solid; ^1H NMR (400 MHz, DMSO- d_6) δ ppm 8.44 (d, $J = 1.8$, 1H), 8.37 (d, $J = 1.8$, 1H), 7.67 (s, 1H), 7.63–7.59 (m, 1H), 7.50 (d, $J = 1.2$, 1H), 6.94 (t, $J = 5.1$, 1H), 3.37–3.24 (m, 3H), 2.38 (s, 3H), 2.07 (d, $J = 1.2$, 3H), 1.86–1.74 (m, 4H), 1.62–1.50 (m, 1H), 1.07–0.95 (m, 4H); LCMS (high pH): $R_t = 0.77$ min (100%), $MH^+ = 378.3$.

3-Methyl-5-(5-methylpyridin-3-yl)-8-((2-(morpholin-2-yl)ethyl)amino)-1,7-naphthyridin-2(1H)-one (3.042v)



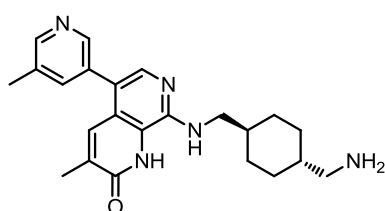
Following General Procedure 3B using *tert*-butyl 2-(2-aminoethyl)morpholine-4-carboxylate (141 mg, 0.60 mmol), gave **3.042v** (10 mg, 0.03 mmol, 13%) as a yellow solid; ¹H NMR (400 MHz, CD₃OD) δ ppm 8.46–8.41 (m, 1H), 8.35 (d, *J* = 1.7, 1H), 7.73–7.68 (m, 2H), 7.61 (d, *J* = 1.2, 1H), 3.94–3.86 (m, 1H), 3.71–3.60 (m, 4H), 2.98–2.91 (m, 1H), 2.90–2.83 (m, 2H), 2.65–2.58 (m, 1H), 2.46 (s, 3H), 2.21–2.15 (m, 3H), 1.93–1.75 (m, 2H); LCMS (high pH): R_t = 0.72 min (92%), MH⁺ = 380.3.

3-Methyl-5-(5-methylpyridin-3-yl)-8-((2-(pyrrolidin-3-yl)ethyl)amino)-1,7-naphthyridin-2(1H)-one (3.042w)



Following General Procedure 3B using *tert*-butyl 3-(2-aminoethyl)pyrrolidine-1-carboxylate (0.13 mL, 0.610 mmol), gave **3.042w** (9 mg, 0.03 mmol, 12%) as a yellow solid; ¹H NMR (400 MHz, CD₃OD) δ ppm 8.43–8.39 (m, 1H), 8.35 (d, *J* = 2.0, 1H), 7.72–7.69 (m, 1H), 7.60 (s, 1H), 7.56–7.52 (m, 1H), 3.61–3.55 (m, 2H), 3.29–3.22 (m, 1H), 3.13–3.05 (m, 1H), 3.05–2.96 (m, 1H), 2.68–2.60 (m, 1H), 2.45 (s, 3H), 2.36–2.26 (m, 1H), 2.19 (s, 3H), 2.16–2.07 (m, 1H), 1.89–1.79 (m, 2H), 1.61–1.50 (m, 1H); LCMS (formic acid): R_t = 0.33 min (100%), MH⁺ = 364.2.

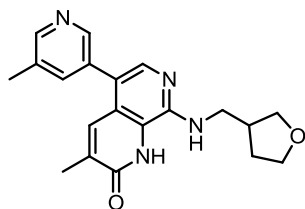
8-(((1*r*,4*r*)-4-(Aminomethyl)cyclohexyl)methyl)amino)-3-methyl-5-(5-methylpyridin-3-yl)-1,7-naphthyridin-2(1H)-one (3.042x)



Following General Procedure 3B using *tert*-butyl (((1*r*,4*r*)-4-(aminomethyl)cyclohexyl)methyl)carbamate (149 mg, 0.60 mmol), gave **3.042x** (40 mg, 0.10 mmol, 50%) as a yellow solid; m.p. 247–249 °C; ν_{max} (solid)/cm⁻¹: 3409 (N-H), 2910 (N-H), 1666 (C=O), 1423, 826, 721; ¹H NMR (400 MHz, DMSO-d₆) δ ppm 8.44 (d, *J* = 1.6, 1H), 8.37 (d, *J* = 1.6, 1H), 7.69 (s, 1H), 7.64–7.60 (m, 1H), 7.51 (d, *J* = 1.2, 1H), 6.96 (t, *J* = 4.9, 1H), 3.38–2.28 (m, 2H), 2.43–2.36 (m, 5H), 2.08 (s, 3H), 1.94–1.76 (m, 4H), 1.66–1.54 (m, 1H), 1.28–1.14 (m, 1H), 1.03–0.83 (m, 4H); ¹³C NMR (101 MHz, DMSO-d₆) δ ppm 162.1, 148.4, 147.1, 146.7, 138.9, 137.4, 134.0, 132.8, 132.7, 132.0, 120.8, 120.7, 117.8, 48.0, 47.6, 40.5, 37.1, 30.4, 29.9, 17.8, 16.8; HRMS

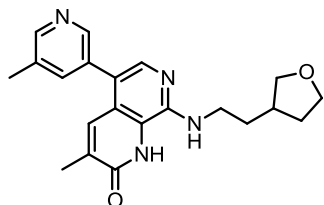
(M + H)⁺ calculated for C₂₃H₃₀N₅O 392.2445; found 392.2450; LCMS (high pH): R_t = 0.79 min (94%), MH⁺ = 392.4.

3-Methyl-5-(5-methylpyridin-3-yl)-8-(((tetrahydrofuran-3-yl)methyl)amino)-1,7-naphthyridin-2(1H)-one (3.042y)



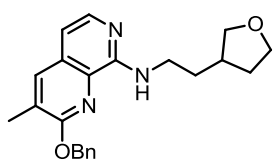
Following General Procedure 3B using (tetrahydrofuran-3-yl)methanamine (0.06 mL, 0.60 mmol), gave **3.042y** (17 mg, 0.05 mmol, 24%) as a yellow solid; m.p. 265–268 °C (decomp.); ν_{\max} (solid)/cm⁻¹: 3378 (N-H), 2865, 1659 (C=O), 1596, 1435, 722; ¹H NMR (400 MHz, DMSO-d₆) δ ppm 11.42 (br.s, 1H), 8.45 (d, *J* = 1.6, 1H), 8.37 (d, *J* = 1.6, 1H), 7.71 (s, 1H), 7.65–7.60 (m, 1H), 7.52 (d, *J* = 1.0, 1H), 7.05 (t, *J* = 4.9, 1H), 3.83–3.74 (m, 2H), 3.70–3.62 (m, 1H), 3.54–3.42 (m, 3H), 2.64–2.55 (m, 1H), 2.38 (s, 3H), 2.08 (d, *J* = 1.0, 3H), 2.06–1.99 (m, 1H), 1.70–1.58 (m, 1H); ¹³C NMR (101 MHz, DMSO-d₆) δ ppm 161.9, 148.5, 147.1, 146.4, 139.0, 137.4, 134.3, 132.8, 131.8, 120.8, 120.7, 118.2, 70.8, 66.8, 44.0, 38.2, 29.9, 17.8, 16.7; N.B. 1C signal not visible in spectrum; HRMS (M + H)⁺ calculated for C₂₀H₂₃N₄O₂ 351.1818; found 351.1816; LCMS (high pH): R_t = 0.79 min (96%), MH⁺ = 351.3.

3-Methyl-5-(5-methylpyridin-3-yl)-8-((2-(tetrahydrofuran-3-yl)ethyl)amino)-1,7-naphthyridin-2(1H)-one (3.042z)



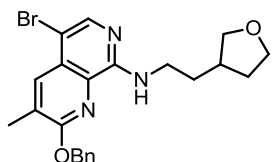
Following General Procedure 3B using 2-(tetrahydrofuran-3-yl)ethanamine (0.07 mL, 0.60 mmol), gave **3.042z** (26 mg, 0.07 mmol, 35%) as a pale yellow solid; m.p. 284–287 °C (decomp.); ν_{\max} (solid)/cm⁻¹: 3395 (N-H), 2922, 1659 (C=O), 1595, 1455, 1065, 720; ¹H NMR (400 MHz, DMSO-d₆) δ ppm 11.40 (br.s, 1H), 8.45 (d, *J* = 1.8, 1H), 8.38 (d, *J* = 1.8, 1H), 7.72 (s, 3H), 7.64–7.62 (m, 1H), 7.52 (d, *J* = 1.2, 1H), 6.98 (t, *J* = 4.5, 1H), 3.87–3.81 (m, 1H), 3.78–3.71 (m, 1H), 3.68–3.60 (m, 1H), 3.52–3.45 (m, 2H), 2.38 (s, 3H), 2.34–2.25 (m, 1H), 2.10–2.00 (m, 5H), 1.74–1.66 (m, 2H), 1.57–1.46 (m, 1H); ¹³C NMR (101 MHz, DMSO-d₆) δ ppm 161.9, 148.5, 147.0, 146.5, 139.1, 137.4, 134.1, 132.8, 132.7, 131.9, 120.8, 120.1, 118.0, 72.4, 66.9, 36.5, 32.3, 31.8, 17.8, 16.7; N.B. 1C signal hidden under solvent peak; HRMS (M + H)⁺ calculated for C₂₁H₂₅N₄O₂ 365.1972; found 365.1969; LCMS (high pH): R_t = 0.84 min (100%), MH⁺ = 365.2.

2-(Benzyloxy)-3-methyl-N-(2-(tetrahydrofuran-3-yl)ethyl)-1,7-naphthyridin-8-amine (3.044)



2-(tetrahydrofuran-3-yl)ethanamine (1.5 mL, 12.33 mmol) was added to a mixture of **3.012** (2.70 g, 9.48 mmol), Pd₂(dba)₃ (0.70 g, 0.76 mmol), Brettphos (0.51 g, 0.95 mmol), and NaO^tBu (3.65 g, 37.90 mmol) in THF (30 mL). The reaction mixture was heated at 70 °C for 18 h. The reaction mixture was allowed to cool to rt and concentrated *in vacuo*. The resulting residue was dissolved in DCM (50 mL) and washed with H₂O (40 mL). The aqueous layer was extracted with DCM (3 × 30 mL) and the combined organic layers were concentrated *in vacuo*. The resulting residue was purified by silica gel chromatography (0–100% EtOAc in cyclohexane). The appropriate fractions were combined and solvent evaporated *in vacuo* to give **3.044** (3.20 g, 8.80 mmol, 93%) as an orange oil; ¹H NMR (400 MHz, CDCl₃) δ ppm 7.90 (d, *J* = 5.8, 1H), 7.65 (d, *J* = 1.0, 1H), 7.52–7.48 (m, 2H), 7.43–7.38 (m, 2H), 7.37–7.31 (m, 1H), 6.72 (d, *J* = 5.8, 1H), 6.27 (t, *J* = 5.4, 1H), 5.51 (s, 2H), 4.01–3.96 (m, 1H), 3.92–3.85 (m, 1H), 3.81–3.73 (m, 1H), 3.70–3.58 (m, 2H), 3.47–3.42 (m, 1H), 2.38 (d, *J* = 1.0, 3H), 2.37–2.30 (m, 1H), 2.19–2.07 (m, 1H), 1.88–1.80 (m, 2H), 1.69–1.57 (m, 1H); LCMS (formic acid): R_t = 0.78 min (100%), MH⁺ = 364.2.

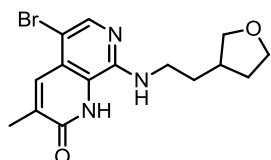
2-(Benzyloxy)-5-bromo-3-methyl-N-(2-(tetrahydrofuran-3-yl)ethyl)-1,7-naphthyridin-8-amine (3.045)



NBS (1.57 g, 8.80 mmol) was added to a mixture of **3.044** (3.20 g, 8.80 mmol) in THF (40 mL). The reaction mixture was left to stir at rt for 0.5 h. The reaction mixture was concentrated *in vacuo*. The resulting solid was dissolved in DCM (50 mL) and washed with H₂O (40 mL). The aqueous layer was extracted with DCM (3 × 30 mL) and the combined organic layers were concentrated *in vacuo*. The resulting residue was purified by silica gel chromatography (0–70% EtOAc in cyclohexane). The appropriate fractions were combined and solvent evaporated *in vacuo* to give **3.045** (3.55 g, 8.00 mmol, 91%) as an orange solid; m.p. 80–82 °C; ν_{max} (solid)/cm⁻¹: 1531, 1418, 1250, 730, 694; ¹H NMR (400 MHz, CDCl₃) δ ppm 8.03 (s, 1H), 7.96 (d, *J* = 1.0, 1H), 7.51–7.47 (m, 2H), 7.43–7.38 (m, 2H), 7.37–7.32 (m, 1H), 6.28 (t, *J* = 5.5, 1H), 5.51 (s, 2H), 4.00–3.94 (m, 1H), 3.92–3.85 (m, 1H), 3.81–3.73 (m, 1H), 3.64–3.55 (m, 2H), 3.47–3.41 (m, 1H), 2.43 (d, *J* = 1.0, 3H), 2.38–2.27 (m, 1H), 2.18–2.05 (m, 1H), 1.86–1.78 (m, 2H), 1.65–1.56 (m, 1H); ¹³C

NMR (101 MHz, DMSO- d_6) 160.4, 154.1, 141.4, 137.1, 135.9, 130.2, 128.6, 128.0, 127.7, 127.4, 127.1, 103.0, 73.4, 68.3, 67.9, 40.2, 37.3, 33.4, 32.5, 16.6; HRMS ($M + H$)⁺ calculated for $C_{22}H_{25}BrN_3O_2$ 442.1125; found 442.1122; LCMS (formic acid): R_t = 1.26 min (100%), MH^+ = 442.1, 444.1.

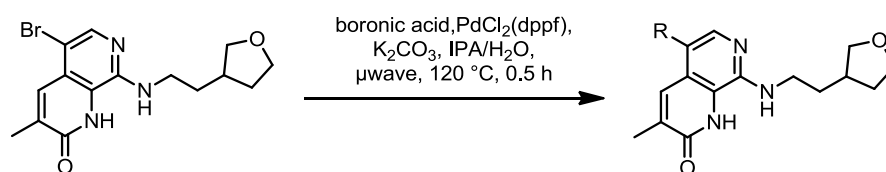
5-Bromo-3-methyl-8-((2-(tetrahydrofuran-3-yl)ethyl)amino)-1,7-naphthyridin-2(1H)-one (3.046)



A mixture of **3.045** (3.50 g, 7.91 mmol) in TFA (8 mL, 104.00 mmol) was stirred at 70 °C for 8 h. The reaction mixture was allowed to cool to rt and concentrated *in vacuo*.

The resulting residue was dissolved in MeOH (20 mL) and passed through a preconditioned (MeOH, 30 mL) amino propyl (20 g) column. The filtrate was concentrated *in vacuo*. The resulting residue was suspended in EtOAc (30 mL), filtered under reduced pressure, washed with EtOAc (30 mL) and collected to give **3.046** (2.10 g, 5.96 mmol, 75%) as a yellow solid; m.p. 80–82 °C; ν_{max} (solid)/ cm^{-1} : 1530, 1417, 1250, 730; 1H NMR (400 MHz, DMSO- d_6) δ ppm 11.49 (br.s, 1H), 7.91 (s, 1H), 7.80 (s, 1H), 3.85–3.78 (m, 2H), 3.76–3.69 (m, 1H), 3.66–3.59 (m, 1H), 3.29–3.23 (m, 1H), 2.29–2.20 (m, 2H), 2.18 (s, 3H), 2.06–1.98 (m, 1H), 1.71–1.63 (m, 2H), 1.55–1.43 (m, 1H); ^{13}C NMR (101 MHz, DMSO- d_6) δ ppm 161.9, 148.5, 147.0, 139.0, 137.4, 135.4, 134.3, 132.8, 132.7, 131.8, 121.0, 120.8, 117.9, 72.4, 66.9, 36.5, 32.3, 31.8, 17.8, 16.7; N.B. 1C signal hidden under solvent peak; HRMS ($M + H$)⁺ calculated for $C_{21}H_{25}N_4O_2$ 365.1972; found 365.1969; LCMS (formic acid): R_t = 0.92 min (100%), MH^+ = 352.1, 354.1.

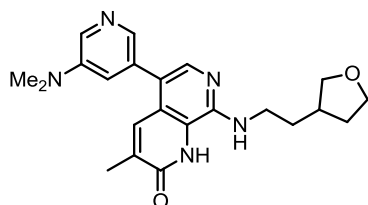
General Procedure 4A: Synthesis of 5-position array compounds



3.046 (42 mg, 0.12 mmol) was added to the appropriate boronic acid/ester (0.24 mmol, 2 eq.) followed by IPA (1 mL). A solution of K_2CO_3 (50 mg, 0.36 mmol, 3 eq.) in H_2O was added, followed by $PdCl_2(dppf)$ (9 mg, 0.012 mmol, 0.1 eq.). The reaction was sealed and heated in Anton Parr at 120 °C for 0.5 h. The reaction mixture was allowed to cool to rt, diluted with MeCN (3 mL) and loaded onto a preconditioned (MeCN, 5 mL) C18 SPE column (1 g). The column was washed with MeOH (3 mL). The solvent was evaporated under a stream of nitrogen at 40 °C and

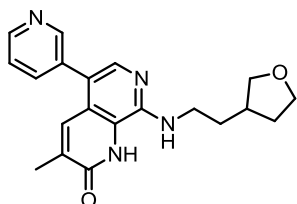
the resulting residue was purified by MDAP (high pH). The appropriate fractions were combined and solvent evaporated under a stream of nitrogen at 40 °C to give the desired product.

5-(5-(Dimethylamino)pyridin-3-yl)-3-methyl-8-((2-(tetrahydrofuran-3-yl)ethyl)amino)-1,7-naphthyridin-2(1H)-one (3.043a)



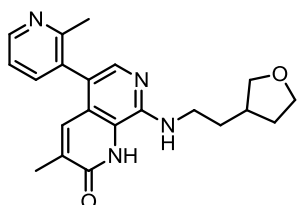
Following General Procedure 4A using (5-(dimethylamino)pyridin-3-yl)boronic acid (40 mg, 0.24 mmol), gave **3.043a** (3 mg, 8.13 μ mol, 6%) as a yellow solid; ^1H NMR (400 MHz, DMSO- d_6) δ ppm 8.14 (d, J = 2.8, 1H), 7.86 (d, J = 1.5, 1H), 7.71 (s, 1H), 7.55 (d, J = 1.5, 1H), 7.07–7.00 (m, 2H), 3.87–3.81 (m, 1H), 3.77–3.70 (m, 1H), 3.68–3.60 (m, 1H), 3.52–3.45 (m, 2H), 2.98 (s, 6H), 2.34–2.21 (m, 1H), 2.08 (d, J = 1.2, 3H), 2.07–2.00 (m, 1H), 1.75–1.65 (m, 2H), 1.56–1.47 (m, 1H); N.B. 1H signal hidden under water peak. LCMS (formic acid): R_t = 0.44 min (98%), MH^+ = 394.0.

3-Methyl-5-(pyridin-3-yl)-8-((2-(tetrahydrofuran-3-yl)ethyl)amino)-1,7-naphthyridin-2(1H)-one (3.043b)



Following General Procedure 4A using pyridin-3-ylboronic acid (30 mg, 0.24 mmol), gave **3.043b** (11 mg, 0.03 mmol, 22%) as a yellow solid; ^1H NMR (400 MHz, DMSO- d_6) δ ppm 11.41 (br.s, 1H), 8.63–8.57 (m, 2H), 7.84–7.79 (m, 1H), 7.74 (s, 1H), 7.54–7.48 (m, 2H), 7.01 (t, J = 4.8, 1H), 3.87–3.82 (m, 1H), 3.77–3.70 (m, 1H), 3.67–3.60 (m, 1H), 3.53–3.45 (m, 2H), 2.33–2.23 (m, 1H), 2.12–2.01 (m, 5H), 1.75–1.65 (m, 2H), 1.58–1.46 (m, 1H); N.B. 1H signal hidden under water peak. LCMS (formic acid): R_t = 0.46 min (93%), MH^+ = 351.0.

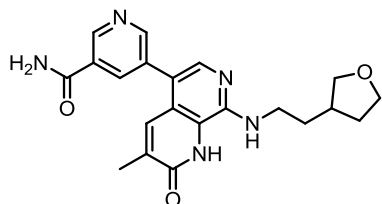
3-Methyl-5-(2-methylpyridin-3-yl)-8-((2-(tetrahydrofuran-3-yl)ethyl)amino)-1,7-naphthyridin-2(1H)-one (3.043c)



Following General Procedure 4A using (2-methylpyridin-3-yl)boronic acid (33 mg, 0.24 mmol), gave **3.043c** (12 mg, 0.03 mmol, 24%) as a yellow solid; ^1H NMR (400 MHz, DMSO- d_6) δ ppm 8.52 (dd, J = 4.9, 1.6, 1H), 7.62 (s, 1H), 7.56 (dd, J = 7.6, 1.8, 1H), 7.34–7.29 (m, 1H), 7.07 (d, J = 1.3, 1H), 6.99 (t, J = 4.8, 1H), 3.87–3.82 (m, 1H), 3.78–3.71 (m, 1H), 3.68–3.60

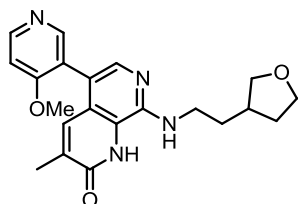
(m, 1H), 3.56–3.42 (m, 2H), 3.33–3.26 (m, 1H), 2.35–2.26 (m, 1H), 2.22 (s, 3H), 2.10–2.00 (m, 4H), 1.76–1.66 (m, 2H), 1.51–1.46 (m, 1H); LCMS (formic acid): $R_t = 0.42$ min (100%), $MH^+ = 365.2$.

5-(3-Methyl-2-oxo-8-((2-(tetrahydrofuran-3-yl)ethyl)amino)-1,2-dihydro-1,7-naphthyridin-5-yl)nicotinamide (3.043d)



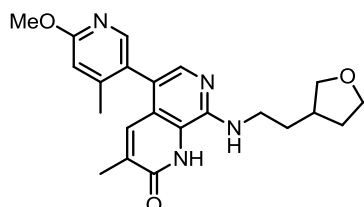
Following General Procedure 4A using 2-methyl-3-(4,4,5,5-tetramethyl-1,3,2-dioxaborolan-2-yl)pyridine (53 mg, 0.24 mmol), gave **3.043d** (11 mg, 0.03 mmol, 21%) as a yellow solid; 1H NMR (400 MHz, DMSO- d_6) δ ppm 11.46 (br.s, 1H), 9.04 (d, $J = 2.0$, 1H), 8.71 (d, $J = 2.0$, 1H), 8.24–8.17 (m, 2H), 7.76 (s, 1H), 7.62 (br.s, 1H), 7.52 (d, $J = 1.1$, 1H), 7.05 (t, $J = 4.9$, 1H), 3.88–3.81 (m, 1H), 3.77–3.70 (m, 1H), 3.68–3.60 (m, 1H), 3.55–3.45 (m, 2H), 2.33–2.23 (m, 1H), 2.09 (d, $J = 1.1$, 3H), 2.06–2.00 (m, 1H), 1.74–1.67 (m, 2H), 1.59–1.46 (m, 1H); N.B. 1H signal hidden under water peak; LCMS (formic acid): $R_t = 0.45$ min (100%), $MH^+ = 394.0$.

5-(4-Methoxypyridin-3-yl)-3-methyl-8-((2-(tetrahydrofuran-3-yl)ethyl)amino)-1,7-naphthyridin-2(1H)-one (3.043e)



Following General Procedure 4A using (4-methoxypyridin-3-yl)boronic acid (37 mg, 0.24 mmol), gave **3.043e** (6 mg, 0.02 mmol, 12%) as a yellow solid; 1H NMR (400 MHz, DMSO- d_6) δ ppm 8.52 (d, $J = 5.7$, 1H) 8.26 (s, 1H) 7.62 (s, 1H) 7.18 (d, $J = 5.7$, 1H) 7.14 (d, $J = 1.3$, 1H) 7.01 (t, $J = 4.9$, 1H) 3.87–3.82 (m, 1H), 3.78 (s, 3H), 3.71–3.75 (m, 1H) 3.67–3.60 (m, 1H) 3.40–3.51 (m, 2H) 3.32–3.26 (m, 1H) 2.33–2.24 (m, 1H) 2.00–2.11 (m, 4H) 1.75–1.66 (m, 2H) 1.59–1.46 (m, 1H); LCMS (formic acid): $R_t = 0.38$ min (100%), $MH^+ = 381.0$.

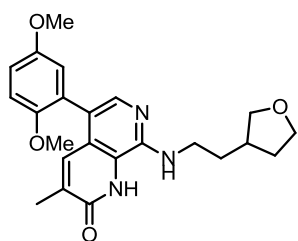
5-(6-Methoxy-4-methylpyridin-3-yl)-3-methyl-8-((2-(tetrahydrofuran-3-yl)ethyl)amino)-1,7-naphthyridin-2(1H)-one (3.043f)



Following General Procedure 4A using (6-methoxy-4-methylpyridin-3-yl)boronic acid (40 mg, 0.24 mmol), gave **3.043f** (11 mg, 0.03 mmol, 20%) as a yellow solid; 1H NMR (400 MHz, DMSO- d_6) δ ppm 7.91 (s, 1H) 7.59 (s, 1H) 7.10 (s, 1H) 6.96–6.92 (m, 1H) 6.82 (s, 1H) 3.88 (s, 3H) 3.82–3.86 (m, 1H) 3.77–3.71 (m, 1H) 3.66–3.61 (m, 1H) 3.45–

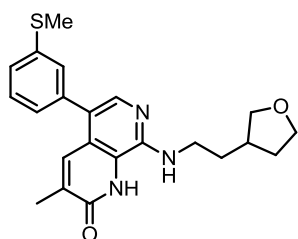
3.47 (m, 1H) 2.32–2.26 (m, 1H) 2.08–2.02 (m, 4H) 1.99 (s, 3H) 1.70–1.74 (m, 2H), 1.55–(m, 1H); N.B. 1H signal hidden under water peak; LCMS (formic acid): $R_t = 0.65$ min (99%), $MH^+ = 395.0$.

5-(2,5-Dimethoxyphenyl)-3-methyl-8-((2-(tetrahydrofuran-3-yl)ethyl)amino)-1,7-naphthyridin-2(1H)-one (3.043g)



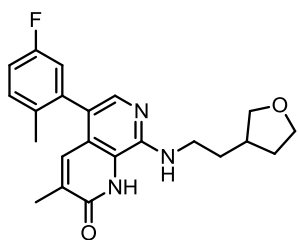
Following General Procedure 4A using (2,5-dimethoxyphenyl)boronic acid (44 mg, 0.24 mmol), gave **3.043g** (8 mg, 0.02 mmol, 14%) as a yellow solid; 1H NMR (400 MHz, DMSO- d_6) δ ppm 11.33 (br.s., 1H) 7.60 (s, 1H) 7.15 (s, 1H) 7.05 (d, $J = 9.0$, 1H) 6.97 (dd, $J = 9.0$, 3.2 1H) 6.88 (t, $J = 4.7$, 1H) 6.77 (d, $J = 3.2$, 1H) 3.87–3.81 (m, 1H) 3.71–3.76 (m, 4 H) 3.60–3.66 (m, 4 H) 3.43–3.49 (m, 2H) 2.25–2.32 (m, 1H) 2.00–2.07 (m, 4H) 1.65–1.74 (m, 2H) 1.55–1.48 (m, 1H); N.B. 1H signal hidden under water peak; LCMS (formic acid): $R_t = 0.69$ min (100%), $MH^+ = 410.0$.

3-Methyl-5-(3-(methylthio)phenyl)-8-((2-(tetrahydrofuran-3-yl)ethyl)amino)-1,7-naphthyridin-2(1H)-one (3.043h)



Following General Procedure 4A using (3-(methylthio)phenyl)boronic acid (40 mg, 0.24 mmol), gave **3.043h** (17 mg, 0.04 mmol, 33%) as a yellow solid; 1H NMR (400 MHz, DMSO- d_6) δ ppm 11.38 (br.s, 1H), 7.70 (s, 1H), 7.53 (s, 1H), 7.43–7.38 (m, 1H), 7.28 (d, $J = 7.7$, 1H), 7.21–7.19 (m, 1H), 7.12 (d, $J = 7.7$, 1H), 6.93 (t, $J = 4.3$, 1H), 3.85–3.81 (m, 1H), 3.75–3.70 (m, 1H), 3.66–3.60 (m, 1H), 3.50–3.44 (m, 2H), 2.31–2.24 (m, 1H), 2.07–2.00 (m, 4H), 1.73–1.67 (m, 2H), 1.53–1.47 (m, 1H); N.B. CH_3 and 1H signals hidden under DMSO and water peaks respectively; LCMS (formic acid): $R_t = 0.82$ min (99%), $MH^+ = 396.0$.

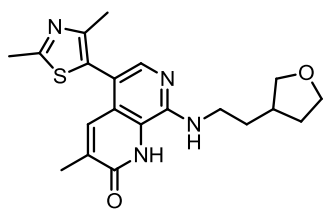
5-(5-Fluoro-2-methylphenyl)-3-methyl-8-((2-(tetrahydrofuran-3-yl)ethyl)amino)-1,7-naphthyridin-2(1H)-one (3.043i)



Following General Procedure 4A using (5-fluoro-2-methylphenyl)boronic acid (37 mg, 0.24 mmol), gave **3.043i** (15 mg, 0.04 mmol, 29%) as a yellow solid; m.p. 120–121 °C (decomp.); ν_{max} (solid)/ cm^{-1} : 3394 (N-H), 2921, 1659 (C=O), 1594, 1447, 703; 1H NMR (600 MHz, DMSO- d_6) δ ppm 11.42 (br.s, 1H) 7.59 (s, 1H) 7.33–7.41 (m, 1H) 7.17 (td, $J = 8.53$, 2.38, 1H)

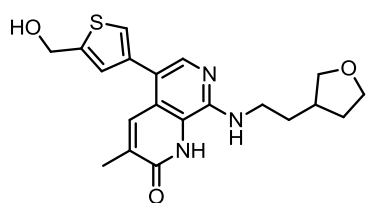
7.06 (s, 1H) 7.01 (dd, $J = 9.26, 2.11$, 1H) 6.93 (t, $J = 4.00$, 1H) 3.84 (t, $J = 7.34$, 1H) 3.71–3.78 (m, 1H) 3.68–3.61 (m, 1H) 3.39–3.55 (m, 2H) 3.27–3.31 (m, 1H) 2.34–2.25 (m, 1H) 2.03–2.06 (m, 1H) 2.01–2.05 (m, 3H) 1.98 (s, 3H) 1.63–1.77 (m, 2H) 1.47–1.57 (m, 1H); ^{13}C NMR (151 MHz, DMSO- d_6): δ ppm 161.9, 160.2 (d, $J_{\text{C-F}} = 242.4$), 146.1, 138.4, 138.0 (d, $J_{\text{C-F}} = 7.7$), 134.3, 133.0, 131.5 (d, $J_{\text{C-F}} = 8.3$), 121.1, 120.2, 119.7, 117.3 (d, $J_{\text{C-F}} = 20.7$), 114.4 (d, $J_{\text{C-F}} = 20.5$), 72.3, 66.9, 40.2, 36.5, 32.3, 31.8, 19.0, 16.6; HRMS ($\text{M} + \text{H}$) $^+$ calculated for $\text{C}_{22}\text{H}_{25}\text{FN}_3\text{O}_2$ 382.1925; found 382.1927; LCMS (formic acid): $R_t = 0.78$ min (99%), $\text{MH}^+ = 382.0$.

5-(2,4-Dimethylthiazol-5-yl)-3-methyl-8-((2-(tetrahydrofuran-3-yl)ethyl)amino)-1,7-naphthyridin-2(1H)-one (3.043j)



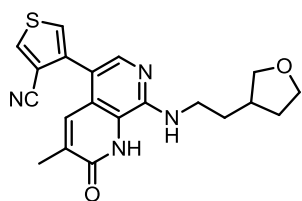
Following General Procedure 4A using 2,4-dimethyl-5-(4,4,5,5-tetramethyl-1,3,2-dioxaborolan-2-yl)thiazole (57 mg, 0.24 mmol), gave **3.043j** (12 mg, 0.03 mmol, 23%) as a yellow solid; ^1H NMR (600 MHz, DMSO- d_6) δ ppm 114.46 (br.s, 1H), 7.71 (s, 1H) 7.37 (s, 1H) 7.07 (t, $J = 4.7$, 1H) 3.85–3.81 (m, 1H) 3.75–3.70 (m, 1H) 3.66–3.59 (m, 1H) 3.42–3.49 (m, 2H) 2.65 (s, 3H) 2.31–2.23 (m, 1H) 2.10 (s, 3H) 2.08 (s, 3H) 2.00–2.05 (m, 1H) 1.65–1.72 (m, 2H) 1.54–1.46 (m, 1H); N.B. 1H signal hidden under water peak; LCMS (formic acid): $R_t = 0.65$ min (98%), $\text{MH}^+ = 385.0$.

5-(5-(Hydroxymethyl)thiophen-3-yl)-3-methyl-8-((2-(tetrahydrofuran-3-yl)ethyl)amino)-1,7-naphthyridin-2(1H)-one (3.043k)



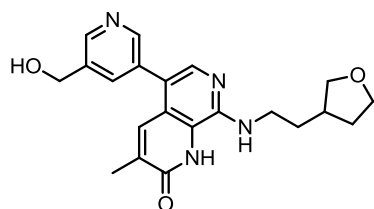
Following General Procedure 4A using (4-(4,4,5,5-tetramethyl-1,3,2-dioxaborolan-2-yl)thiophen-2-yl)methanol (58 mg, 0.24 mmol), gave **3.043k** (17 mg, 0.04 mmol, 33%) as a yellow solid; ^1H NMR (600 MHz, DMSO- d_6) δ ppm 11.35 (br.s, 1H), 7.74 (s, 1H), 7.70 (s, 1H), 7.39 (d, $J = 1.0$, 1H), 7.05 (s, 1H), 6.90 (t, $J = 4.7$, 1H), 5.50 (br.s, 1H), 4.68 (s, 2H), 3.85–3.81 (m, 1H), 3.76–3.71 (m, 1H), 3.65–3.61 (m, 1H), 3.49–3.41 (m, 1H), 2.32–2.22 (m, 1H), 2.11–2.08 (d, $J = 1.0$, 3H), 2.07–1.99 (m, 1H), 1.73–1.65 (m, 2H), 1.53–1.45 (m, 1H); N.B. 1H signal hidden under water peak; LCMS (formic acid): $R_t = 0.57$ min (95%), $\text{MH}^+ = 385.9$.

4-(3-Methyl-2-oxo-8-((2-(tetrahydrofuran-3-yl)ethyl)amino)-1,2-dihydro-1,7-naphthyridin-5-yl)thiophene-3-carbonitrile (3.043l)



Following General Procedure 4A using 4-(4,4,5,5-tetramethyl-1,3,2-dioxaborolan-2-yl)thiophene-3-carbonitrile (56 mg, 0.24 mmol), gave **3.043l** (7 mg, 0.02 mmol, 13%) as a yellow solid; ¹H NMR (600 MHz, DMSO-d₆) δ ppm 11.44 (br.s, 1H), 8.72 (d, *J* = 3.0, 1H), 7.78 (d, *J* = 3.0, 1H), 7.74 (s, 1H), 7.43 (s, 1H), 7.08 (t, *J* = 4.5, 1H), 3.86–3.81 (m, 1H), 3.77–3.72 (m, 1H), 3.66–3.60 (m, 1H), 3.51–3.45 (m, 2H), 2.31–2.25 (m, 1H), 2.09 (s, 3H), 2.07–2.01 (m, 1H), 1.74–1.66 (m, 2H), 1.55–1.48 (m, 1H); N.B. 1H signal hidden under water peak; LCMS (formic acid): *R*_t = 0.67 min (99%), *MH*⁺ = 380.9.

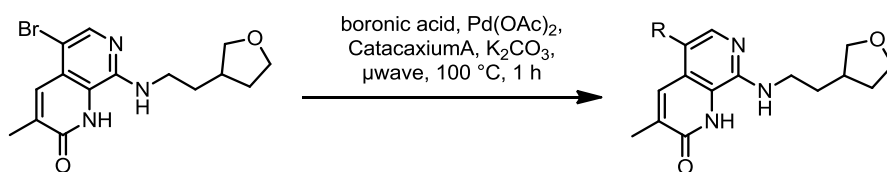
5-(5-(Hydroxymethyl)pyridin-3-yl)-3-methyl-8-((2-(tetrahydrofuran-3-yl)ethyl)amino)-1,7-naphthyridin-2(1H)-one (3.043m)



A mixture of **3.046** (150 mg, 0.43 mmol), (5-(hydroxymethyl)pyridin-3-yl)boronic acid (130 mg, 0.85 mmol), Pd(OAc)₂ (10 mg, 0.04 mmol), Catacixium A (15 mg, 0.04 mmol) and K₂CO₃ (118 mg, 0.85 mmol) in 1,4-dioxane (1 mL) and H₂O (0.5 mL) was heated at 100 °C in a microwave reactor for 2 h. The reaction mixture was allowed to cool to rt and Pd(OAc)₂ (10 mg, 0.04 mmol) and Catacixium A (15 mg, 0.04 mmol) were added. The mixture was heated for a further 1 h 100 °C in the microwave. The reaction mixture was allowed to cool to rt and (5-(hydroxymethyl)pyridin-3-yl)boronic acid (130 mg, 0.85 mmol) was added and the mixture was heated at 100 °C for 1 h in the microwave. The reaction mixture was allowed to cool to rt, diluted with EtOAc (5 mL) and DCM (5 mL), filtered through Celite[®] and concentrated *in vacuo*. The resulting residue was purified by silica gel chromatography (0–100% EtOH in EtOAc). The appropriate fractions were combined and solvent evaporated *in vacuo* to give **3.043m** (57 mg, 0.15 mmol, 35%) as a yellow solid. **3.043m** (17 mg, 0.04 mmol) was taken forward for further purification by MDAP (high pH). The fractions were combined and solvent evaporated *in vacuo* to give **3.043m** (3 mg, 6.60 μmol, 15%) as a yellow solid; ¹H NMR (400 MHz, CD₃OD) δ ppm 8.58 (d, *J* = 2.1, 1H), 8.48 (d, *J* = 2.1, 1H), 7.88–7.86 (m, 1H), 7.76 (s, 1H), 7.64 (d, *J* = 1.1, 1H), 4.76 (s, 2H), 3.99–3.93 (m, 1H), 3.91–3.84 (m, 1H), 3.80–3.73 (m, 1H), 3.63–3.56 (m, 2H), 3.46–3.40 (m, 1H), 2.42–

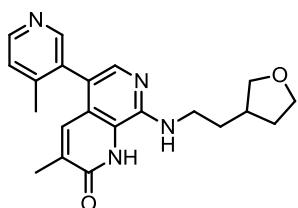
2.35 (m, 1H), 2.18 (d, $J = 1.1$, 3H), 2.16–2.11 (m, 1H), 1.88–1.77 (m, 2H), 1.68–1.59 (m, 1H); LCMS (formic acid): $R_t = 0.42$ min (97%), $MH^+ = 381.2$.

General Procedure 4B: Synthesis of 5-position array compounds



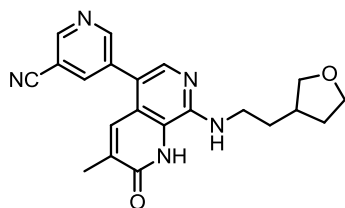
A mixture of **3.046** (50 mg, 0.14 mmol), appropriate boronic acid/ester (0.28 mmol, 2 eq.), $Pd(OAc)_2$ (3 mg, 0.01 mmol, 0.07 eq.), Catacaxium A (5 mg, 0.01 mmol, 0.07 eq.) and K_2CO_3 (39 mg, 0.28 mmol) in 1,4-Dioxane (1 mL) and H_2O (0.5 mL) was heated at 100 °C in a microwave reactor for 1 h. The reaction mixture was allowed to cool to rt, diluted with EtOAc (20 mL), filtered through Celite® and concentrated *in vacuo*. The resulting residue was purified by MDAP (high pH). The appropriate fractions were combined and solvent evaporated *in vacuo* to give the desired product.

3-Methyl-5-(4-methylpyridin-3-yl)-8-((2-(tetrahydrofuran-3-yl)ethyl)amino)-1,7-naphthyridin-2(1H)-one (3.043n)



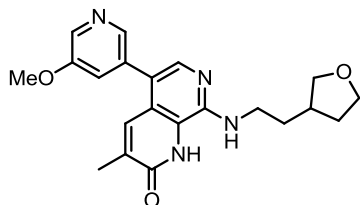
Following General Procedure 4B using (4-methylpyridin-3-yl)boronic acid (39 mg, 0.28 mmol) and heating for 4 h. The reaction mixture was allowed to cool to rt and $Pd(OAc)_2$ (3 mg, 0.01 mmol), Catacaxium A (5 mg, 0.01 mmol) and K_2CO_3 (39 mg, 0.28 mmol) were added and the reaction mixture was heated at 100 °C in a microwave reactor for 1 h. The reaction mixture was allowed to cool to rt and purified as described in General Procedure 4B, to give **3.043n** (3 mg, 3.90 μ mol, 5%) as a yellow solid; 1H NMR (400 MHz, CD_3OD) δ ppm 8.47 (d, $J = 5.3$, 1H), 8.32 (s, 1H), 7.65 (s, 1H), 7.44 (d, $J = 5.3$, 1H), 7.18 (d, $J = 1.1$, 1H), 4.00–3.94 (m, 1H), 3.92–3.85 (m, 1H), 3.81–3.73 (m, 1H), 3.65–3.54 (m, 2H), 3.47–3.40 (m, 1H), 2.46–2.34 (m, 1H), 2.24–2.17 (m, 1H), 2.15 (s, 3H), 2.14 (d, $J = 1.1$, 3H), 1.89–1.81 (m, 2H), 1.70–1.62 (m, 1H); LCMS (formic acid): $R_t = 0.43$ min (100%), $MH^+ = 365.2$.

5-(3-Methyl-2-oxo-8-((2-(tetrahydrofuran-3-yl)ethyl)amino)-1,7-naphthyridin-5-yl)nicotinonitrile (3.043o)



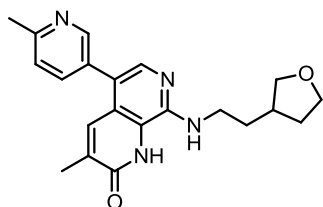
Following General Procedure 4B using (5-cyanopyridin-3-yl)boronic acid (42 mg, 0.28 mmol), gave **3.043o** (12 mg, 0.03 mmol, 23%) as a yellow solid; ^1H NMR (400 MHz, DMSO- d_6) δ ppm 11.43 (br.s, 1H), 9.04 (d, $J = 2.1$, 1H), 8.87 (d, $J = 2.1$, 1H), 8.40–8.35 (m, 1H), 7.78 (s, 1H), 7.58 (d, $J = 1.1$, 1H), 7.10 (t, $J = 4.9$, 1H), 3.87–3.83 (m, 1H), 3.77–3.70 (m, 1H), 3.68–3.60 (m, 1H), 3.53–3.45 (m, 2H), 2.32–2.24 (m, 1H), 2.10 (d, $J = 1.1$, 3H), 2.06–2.00 (m, 1H), 1.73–1.66 (m, 2H), 1.56–1.45 (m, 1H); N.B. 1H signal hidden under water peak; LCMS (formic acid): $R_t = 0.61$ min (100%), $\text{MH}^+ = 376.3$.

5-(5-Methoxy-3-yl)-3-methyl-8-((2-(tetrahydrofuran-3-yl)ethyl)amino)-1,7-naphthyridin-2(1H)-one (3.043p)



Following General Procedure 4B using 3-methoxy-5-(4,4,5,5-tetramethyl-1,3,2-dioxaborolan-2-yl)pyridine (67 mg, 0.28 mmol), gave **3.043p** (4 mg, 10.51 μmol , 7%) as a yellow solid; ^1H NMR (400 MHz, DMSO- d_6) δ ppm 8.33 (d, $J = 1.7$, 1H), 8.18 (d, $J = 1.7$, 1H), 7.76 (s, 1H), 7.57 (d, $J = 1.2$, 1H), 7.39 (dd, $J = 2.7$, 1.7, 1H), 7.02 (t, $J = 4.9$, 1H), 3.89 (s, 3H), 3.87–3.82 (m, 1H), 3.77–3.71 (m, 1H), 3.68–3.60 (m, 1H), 3.54–3.44 (m, 2H), 2.35–2.24 (m, 1H), 2.09 (d, $J = 1.2$, 3H), 2.07–2.00 (m, 1H), 1.75–1.66 (m, 2H), 1.56–1.44 (m, 1H); N.B. 1H signal hidden under water peak; LCMS (formic acid): $R_t = 0.56$ min (100%), $\text{MH}^+ = 381.3$.

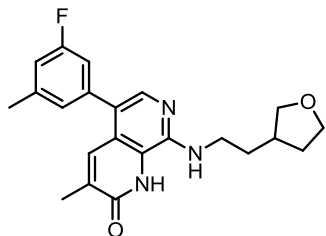
3-Methyl-5-(6-methylpyridin-3-yl)-8-((2-(tetrahydrofuran-3-yl)ethyl)amino)-1,7-naphthyridin-2(1H)-one (3.043q)



Following General Procedure 4B using (6-methylpyridin-3-yl)boronic acid (39 mg, 0.28 mmol), gave **3.043q** (14 mg, 0.04 mmol, 27%) as a yellow solid; ^1H NMR (400 MHz, DMSO- d_6) δ ppm 8.44 (d, $J = 2.0$, 1H), 7.72–7.68 (m, 2H), 7.52 (d, $J = 1.1$, 1H), 7.36 (d, $J = 8.1$, 1H), 7.00 (t, $J = 4.8$, 1H), 3.88–3.81 (m, 1H), 3.77–3.70 (m, 1H), 3.67–3.60 (m, 1H), 3.52–3.43 (m, 2H), 2.54 (s, 3H), 2.33–2.24 (m, 1H), 2.08 (d, $J = 1.1$, 3H), 2.06–1.99

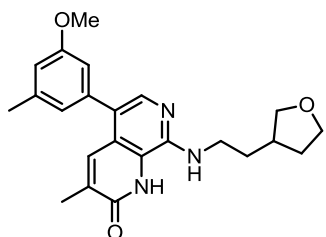
(m, 1H), 1.76–1.64 (m, 2H), 1.57–1.46 (m, 1H); N.B. 1H signal hidden under water peak; LCMS (formic acid): $R_t = 0.45$ min (100%), $MH^+ = 365.3$.

5-(3-Fluoro-5-methylphenyl)-3-methyl-8-((2-(tetrahydrofuran-3-yl)ethyl)amino)-1,7-naphthyridin-2(1H)-one (3.043r)



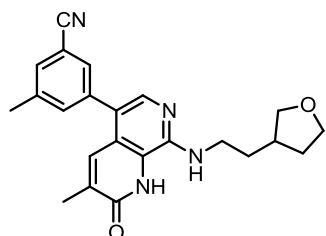
Following General Procedure 4B using (3-fluoro-5-methylphenyl)boronic acid (44 mg, 0.28 mmol), gave **3.043r** (2 mg, 3.93 μ mol, 3%) as a yellow solid; 1H NMR (400 MHz, CD_3OD) δ ppm 7.72 (s, 1H), 7.67 (s, 1H), 7.03–3.97 (m, 2H), 6.94–6.89 (m, 1H), 4.00–3.93 (m, 1H), 3.92–3.85 (m, 1H), 3.80–3.72 (m, 1H), 3.62–3.54 (m, 2H), 3.46–3.41 (m, 1H), 2.43 (s, 3H), 2.41–2.34 (m, 1H), 2.21–2.11 (m, 4H), 1.87–1.79 (m, 2H), 1.70–1.59 (m, 1H), LCMS (formic acid): $R_t = 0.83$ min (100%), $MH^+ = 382.2$.

5-(3-methoxy-5-methylphenyl)-3-methyl-8-((2-(tetrahydrofuran-3-yl)ethyl)amino)-1,7-naphthyridin-2(1H)-one (3.043s)



Following General Procedure 4B using 2-(3-methoxy-5-methylphenyl)-4,4,5,5-tetramethyl-1,3,2-dioxaborolane (88 mg, 0.28 mmol), gave **3.043s** (5 mg, 0.01 mmol, 9%) as a yellow solid; 1H NMR (400 MHz, $DMSO-d_6$) δ ppm 11.34 (br.s, 1H), 7.70 (s, 1H), 7.58 (s, 1H), 6.91–6.86 (m, 1H), 6.81–6.78 (m, 1H), 6.75–6.74 (m, 1H), 6.71–6.68 (m, 1H), 3.88–3.82 (m, 1H), 3.77 (s, 3H), 3.76–3.71 (m, 1H), 3.67–3.61 (m, 1H), 3.52–3.43 (m, 2H), 2.35 (s, 3H), 2.33–2.24 (m, 1H), 2.08 (s, 3H), 2.06–2.00 (m, 1H), 1.75–1.67 (m, 2H), 1.57–1.48 (m, 1H); N.B. 1H signal hidden under water peak; LCMS (high pH): $R_t = 1.12$ min (96%), $MH^+ = 394.4$.

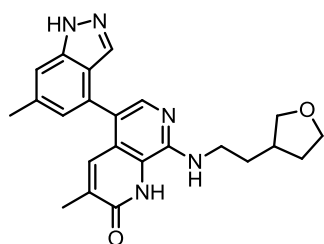
3-Methyl-5-(3-methyl-2-oxo-8-((2-(tetrahydrofuran-3-yl)ethyl)amino)-1,2-dihydro-1,7-naphthyridin-5-yl)benzonitrile (3.043t)



A mixture of **3.046** (60 mg, 0.17 mmol), 3-methyl-5-(4,4,5,5-tetramethyl-1,3,2-dioxaborolan-2-yl)benzonitrile (46 mg, 0.19 mmol), $Pd(OAc)_2$ (4 mg, 0.02 mmol), Catacxiium A (6 mg, 0.02 mmol) and K_2CO_3 (47 mg, 0.34 mmol) in 1,4-dioxane (1 mL) and H_2O (0.5 mL) was heated at 100 $^\circ C$ in a microwave reactor for 1 h. The reaction mixture was allowed to cool to rt, diluted with EtOAc (20 mL), filtered through Celite[®] and concentrated *in*

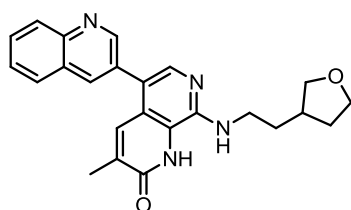
vacuo. The resulting residue was purified by MDAP (high pH). The appropriate fractions were combined and solvent *evaporated in vacuo* to give **3.043t** (3 mg, 7.72 μmol , 5%) as a yellow solid; $^1\text{H NMR}$ (400 MHz, CD_3OD) δ ppm 7.70 (s, 1H), 7.62–7.58 (m, 2H), 7.56–7.50 (m, 2H), 3.99–3.93 (m, 1H), 3.90–3.83 (m, 1H), 3.81–3.73 (m, 1H), 3.62–3.53 (m, 2H), 3.45–3.39 (m, 1H), 2.48 (s, 3H), 2.43–2.34 (m, 1H), 2.21–2.10 (m, 4H), 1.87–1.78 (m, 2H), 1.69–1.58 (m, 1H); LCMS (formic acid): $R_t = 0.78$ min (96%), $\text{MH}^+ = 389.5$.

3-Methyl-5-(6-methyl-1H-indazol-4-yl)-8-((2-(tetrahydrofuran-3-yl)ethyl)amino)-1,7-naphthyridin-2(1H)-one (3.043u)



A mixture of **3.046** (120 mg, 0.34 mmol), (1H-indazol-4-yl)boronic acid (83 mg, 0.51 mmol), $\text{Pd}(\text{OAc})_2$ (8 mg, 0.03 mmol), Catacxiium A (12 mg, 0.03 mmol) and K_2CO_3 (94 mg, 0.68 mmol) in 1,4-dioxane (2 mL) and H_2O (1 mL) was heated at 100 $^\circ\text{C}$ in a microwave reactor for 1 h. The reaction mixture was allowed to cool to rt, diluted with EtOAc (20 mL), filtered through Celite[®] and concentrated *in vacuo*. The resulting residue was dissolved purified by MDAP (formic acid). The appropriate fractions were combined and solvent evaporated *in vacuo*. The resulting residue was dissolved in MeOH (10 mL) and passed through a preconditioned (MeOH, 5 mL) amino propyl column (1 g). The filtrate was concentrated *in vacuo* to give **3.043u** (7 mg, 0.02 mmol, 6%) as a yellow solid; $^1\text{H NMR}$ (400 MHz, DMSO-d_6) δ ppm 13.21 (s, 1H), 11.43 (br.s, 1H), 7.80 (s, 1H), 7.72 (s, 1H), 7.48–7.42 (m, 1H), 7.38 (s, 1H), 7.07–7.03 (m, 1H), 6.98 (t, $J = 4.8$, 1H), 3.89–3.82 (m, 1H), 3.79–3.72 (m, 1H), 3.69–3.59 (m, 1H), 3.55–3.47 (m, 2H), 2.35–2.25 (m, 1H), 2.10–2.02 (m, 1H), 1.99 (s, 3H), 1.77–1.69 (m, 2H), 1.59–1.47 (m, 1H); N.B. 1H signal hidden under water peak; LCMS (high pH): $R_t = 0.86$ min (100%), $\text{MH}^+ = 390.3$.

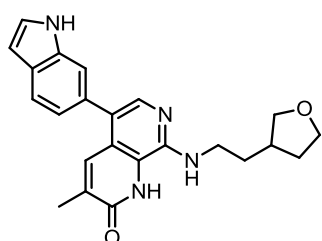
3-Methyl-5-(quinolin-3-yl)-8-((2-(tetrahydrofuran-3-yl)ethyl)amino)-1,7-naphthyridin-2(1H)-one (3.043v)



A mixture of **3.046** (70 mg, 0.20 mmol), quinolin-3-ylboronic acid (38 mg, 0.22 mmol), $\text{Pd}(\text{OAc})_2$ (4 mg, 0.02 mmol), Catacxiium A (7 mg, 0.02 mmol) and K_2CO_3 (55 mg, 0.40 mmol) in 1,4-dioxane (1 mL) and H_2O (0.5 mL) was heated at 100 $^\circ\text{C}$ in a microwave reactor for 1 h. The reaction mixture was allowed to cool to rt, diluted with EtOAc

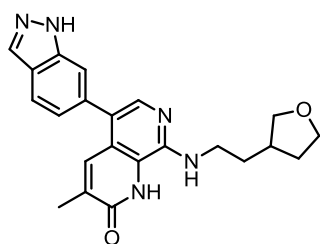
(20 mL), filtered through Celite[®] and concentrated *in vacuo*. The resulting residue was purified by MDAP (high pH). The appropriate fractions were combined and solvent evaporated *in vacuo* to give **3.043v** (15 mg, 0.04 mmol, 19%) as a yellow solid; ¹H NMR (400 MHz, DMSO-d₆) δ ppm 11.44 (br.s, 1H), 8.92 (d, *J* = 2.2, 1H), 8.38 (d, *J* = 2.2, 1H), 8.13–8.03 (m, 2H), 7.86 (s, 1H), 7.83–7.78 (m, 1H), 7.69–7.62 (m, 2H), 7.04 (t, *J* = 4.5, 1H), 3.89–3.83 (m, 1H), 3.78–3.71 (m, 1H), 3.68–3.60 (m, 1H), 3.56–3.47 (m, 2H), 2.34–2.24 (m, 1H), 2.12–2.01 (m, 4H), 1.77–1.68 (m, 2H), 1.59–1.48 (m, 1H); N.B. 1H signal hidden under water peak; LCMS (high pH): *R*_t = 0.96 min (100%), *MH*⁺ = 401.4.

5-(1H-Indol-6-yl)-3-methyl-8-((2-(tetrahydrofuran-3-yl)ethyl)amino)-1,7-naphthyridin-2(1H)-one (3.043w)



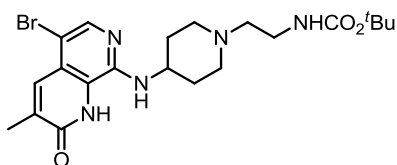
A mixture of **3.046** (70 mg, 0.20 mmol), 6-(4,4,5,5-tetramethyl-1,3,2-dioxaborolan-2-yl)-1H-indole (53 mg, 0.22 mmol), Pd(OAc)₂ (4 mg, 0.02 mmol), Catacixium A (7 mg, 0.02 mol) and K₂CO₃ (55 mg, 0.40 mmol) in 1,4-dioxane (1 mL) and H₂O (0.5 mL) was heated at 100 °C in a microwave reactor for 1 h. The reaction mixture was allowed to cool to rt, diluted with EtOAc (20 mL), filtered through Celite[®] and concentrated *in vacuo*. The resulting residue was dissolved purified by MDAP (formic acid). The appropriate fractions were combined and solvent evaporated *in vacuo*. The resulting residue was dissolved in MeOH (5 mL) and passed through a preconditioned (MeOH, 5 mL) amino propyl column (2 g). The filtrate was concentrated *in vacuo* to give **3.043w** (14 mg, 0.04 mmol, 18%) as a yellow solid; ¹H NMR (400 MHz, DMSO-d₆) δ ppm 11.36 (br.s, 1H), 11.22 (br.s, 1H), 7.77 (s, 1H), 7.44 (d, *J* = 8.3, 1H), 7.36 (d, *J* = 1.2, 1H), 7.35–7.33 (m, 1H), 7.22–7.16 (m, 1H), 6.92 (dd, *J* = 7.1, 1.0, 1H), 6.88 (t, *J* = 4.9, 1H), 6.06–6.03 (m, 1H), 3.89–3.83 (m, 1H), 3.79–3.71 (m, 1H), 3.68–3.61 (m, 1H), 3.55–3.45 (m, 2H), 2.38–2.27 (m, 1H), 2.11–2.02 (m, 1H), 1.97 (d, *J* = 1.0, 3H), 1.76–1.69 (m, 2H), 1.59–1.48 (m, 1H); N.B. 1H signal hidden under water peak; LCMS (high pH): *R*_t = 0.96 min (94%), *MH*⁺ = 389.4.

5-(1H-indazol-6-yl)-3-methyl-8-((2-(tetrahydrofuran-3-yl)ethyl)amino)-1,7-naphthyridin-2(1H)-one (3.043x)

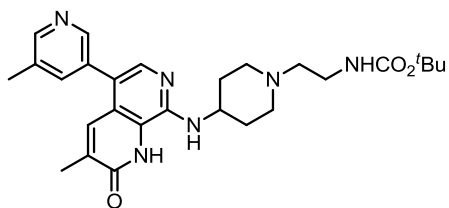


A mixture of **3.046** (70 mg, 0.20 mmol), (1H-indazol-6-yl)boronic acid (35 mg, 0.22 mmol), Pd(OAc)₂ (4 mg, 0.02 mmol), Catacixium A (7 mg, 0.02 mol) and K₂CO₃ (55 mg, 0.40 mmol) in 1,4-dioxane (1 mL) and H₂O (0.5 mL) was heated at 100 °C in a microwave reactor for 1 h. The reaction mixture was allowed to cool to rt, diluted with EtOAc (20 mL), filtered through Celite[®] and concentrated *in vacuo*. The resulting residue was purified by MDAP (high pH). The appropriate fractions were combined and solvent evaporated *in vacuo* to give **3.043x** (3 mg, 7.70 μmol, 4%) as a yellow solid; ¹H NMR (400 MHz, DMSO-d₆) δ ppm 13.09 (br.s, 1H), 11.37 (br.s, 1H), 8.12 (s, 1H), 7.84 (d, *J* = 8.1, 1H), 7.76 (s, 1H), 7.59 (s, 1H), 7.47 (s, 1H), 7.10 (dd, *J* = 8.1, 1.2, 1H), 6.92 (t, *J* = 4.8, 1H), 3.89–3.82 (m, 1H), 3.78–3.71 (m, 1H), 3.68–3.62 (m, 1H), 3.52–3.46 (m, 2H), 2.35–2.25 (m, 1H), 2.10–2.01 (m, 4H), 1.75–1.69 (m, 2H), 1.57–1.48 (m, 1H); N.B. 1H signal hidden under water peak; LCMS (high pH): R_t = 0.86 min (91%), MH⁺ = 390.4.

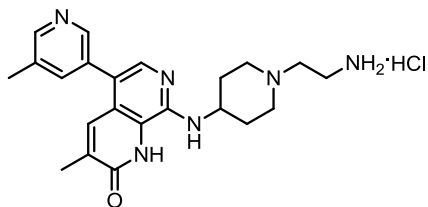
tert-Butyl (2-(4-((5-bromo-3-methyl-2-oxo-1,2-dihydro-1,7-naphthyridin-8-yl)amino)piperidin-1-yl)ethyl)carbamate (3.049)



A mixture of **3.016** (94 mg, 0.59 mmol) and **3.048** (219 mg, 0.65 mmol) in MeOH (5 mL) and AcOH (0.5 mL) was heated at 50 °C for 3 h. Picoline borane complex (55 mg, 0.59 mmol) was added and the reaction mixture was heated at 50 °C for a further 18 h. The reaction mixture was concentrated *in vacuo* and the resulting residue diluted with sat. aq. NaHCO₃ (20 mL) and DCM (20 mL). The organic layer was separated and the aqueous extracted with DCM (3 × 20 mL). The combined organic layers were passed through a hydrophobic frit and concentrated *in vacuo*. The resulting residue was purified by silica gel chromatography (0–50% EtOH in EtOAc). The appropriate fractions were combined and solvent evaporated *in vacuo* to give **3.049** (123 mg, 0.26 mmol, 43%) as a yellow solid; ¹H NMR (400 MHz, DMSO-d₆) δ ppm 11.59 (br.s, 1H), 7.90 (s, 1H), 7.79 (s, 1H), 6.86–6.79 (m, 1H), 6.65 (t, *J* = 5.1, 1H), 3.91–3.82 (m, 1H), 3.06–3.00 (m, 2H), 2.88–2.80 (m, 2H), 2.36–2.29 (m, 2H), 2.17 (s, 3H), 2.10–2.02 (m, 2H), 1.97–1.90 (m, 2H), 1.49–1.42 (m, 2H), 1.38 (s, 9H); LCMS (formic acid): R_t = 0.73 min (100%), MH⁺ = 480.2, 482.2.

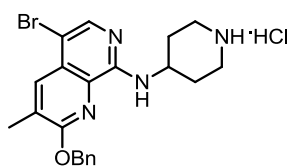
tert-Butyl (2-(4-((3-methyl-5-(5-methylpyridin-3-yl)-2-oxo-1,2-dihydro-1,7-naphthyridin-8-yl)amino)piperidin-1-yl)ethyl)carbamate (3.050)

A mixture of **3.049** (123 mg, 0.26 mmol), (5-methylpyridin-3-yl)boronic acid (70 mg, 0.51 mmol), Pd(OAc)₂ (6 mg, 0.03 mmol), Catacxiom A (9 mg, 0.03 mmol) and K₂CO₃ (71 mg, 0.51 mmol) in 1,4-dioxane (3 mL) and H₂O (1.5 mL) was heated at 100 °C in a microwave reactor for 1 h. The reaction mixture was allowed to cool to rt, diluted with EtOAc (20 mL), filtered through Celite[®] and concentrated *in vacuo*. The resulting residue was purified by silica gel chromatography (0–50% EtOH in EtOAc). The appropriate fractions were combined and solvent evaporated *in vacuo* to give **3.050** (88 mg, 0.18 mmol, 70%) as a yellow solid; ¹H NMR (400 MHz, CDCl₃) δ ppm 13.37 (br.s, 1H), 8.51 (d, *J* = 1.6, 1H), 8.47 (d, *J* = 1.6, 1H), 7.87 (s, 1H), 7.69 (d, *J* = 1.0, 1H), 7.54–7.50 (m, 1H), 6.75 (d, *J* = 6.1, 1H), 5.13–4.99 (m, 1H), 4.30–4.16 (m, 1H), 3.30–3.21 (m, 2H), 3.04–2.92 (m, 2H), 2.57–2.48 (m, 2H), 2.45 (s, 3H), 2.34 (s, 3H), 2.31–2.18 (m, 4H), 1.87–1.75 (m, 2H), 1.46 (s, 9H); LCMS (formic acid): R_t = 0.51 min (98%), MH⁺ = 493.3.

8-((1-(2-Aminoethyl)piperidin-4-yl)amino)-3-methyl-5-(5-methylpyridin-3-yl)-1,7-naphthyridin-2(1H)-one hydrochloride (3.047a)

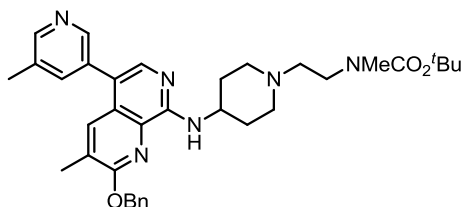
3.050 (116 mg, 0.24 mmol) was dissolved in 4 M HCl in 1,4-dioxane (3 mL, 12.00 mmol) and left to stir at rt for 18 h. The reaction mixture was concentrated *in vacuo* and the resulting residue was purified by MDAP (high pH). The appropriate fractions were combined and solvent evaporated *in vacuo* to give **3.047a** (36 mg, 0.09 mmol, 39%) as a yellow solid; ¹H NMR (400 MHz, DMSO-d₆) δ ppm 8.44 (d, *J* = 1.8, 1H), 8.37 (d, *J* = 1.8, 1H), 7.70 (s, 1H), 7.64–7.60 (m, 1H), 7.51 (d, *J* = 1.2, 1H), 6.88 (d, *J* = 6.8, 1H), 5.47 (br.s, 3H), 4.04–3.94 (m, 1H), 2.90–2.80 (m, 2H), 2.70–2.63 (m, 2H), 2.37 (s, 3H), 2.36–2.31 (m, 2H), 2.11–1.96 (m, 7H), 1.58–1.46 (m, 2H); LCMS (high pH): R_t = 0.77 min (92%), MH⁺ = 393.4.

2-(Benzyloxy)-5-bromo-3-methyl-N-(piperidin-4-yl)-1,7-naphthyridin-8-amine hydrochloride (3.051)



3.015 (1.21 g, 2.29 mmol) was stirred in 4 M HCl in 1,4-dioxane (10 mL, 40.00 mmol) for 18 h at rt. The volatile components were removed *in vacuo* and the resulting solid was suspended in Et₂O (30 mL), filtered under reduced pressure, washed with Et₂O (30 mL), collected and dried under vacuum at 40 °C for 3 h to give **3.051** (842 mg, 1.81 mmol, 79%) as a yellow solid; ¹H NMR (400 MHz, DMSO-d₆) δ ppm 8.09 (s, 1H), 7.96 (s, 1H), 7.58–7.53 (m, 2H), 7.45–7.39 (m, 2H), 7.37–7.31 (m, 1H), 5.71 (s, 2H), 5.21 (br.s, 2H), 4.34–4.26 (m, 1H), 3.42–3.35 (m, 2H), 2.12–3.00 (m, 2H), 2.42 (s, 3H), 2.18–2.10 (m, 2H), 2.04–1.90 (m, 2H); LCMS (formic acid): R_t = 0.87 min (93%), MH⁺ = 427.0, 429.0.

tert-Butyl (2-(4-((2-(benzyloxy)-3-methyl-5-(5-methylpyridin-3-yl)-1,7-naphthyridin-8-yl)amino)piperidin-1-yl)ethyl)(methyl)carbamate (3.054)

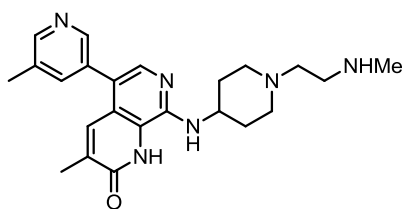


A mixture of **3.051** (0.16 mL, 0.95 mmol) and **3.052** (448 mg, 1.05 mmol) in MeOH (5 mL) and AcOH (0.5 mL) was heated at 50 °C for 3 h. Picoline borane complex (89 mg, 0.95 mmol) was added and the reaction mixture was heated at 50 °C for a further 48 h. **3.052** (0.16 mL, 0.95 mmol) and picoline borane complex (89 mg, 0.95 mmol) were added and the reaction mixture was stirred at 50 °C for 24 h. The reaction mixture was concentrated *in vacuo* and the resulting residue diluted with sat. aq. NaHCO₃ (20 mL) and DCM (20 mL). The organic layer was separated and the aqueous extracted with DCM (3 × 20 mL). The combined organic layers were passed through a hydrophobic frit and concentrated *in vacuo*. The resulting residue was purified by silica gel chromatography (0–100% EtOAc in cyclohexane). The appropriate fractions were combined and solvent evaporated *in vacuo* to give **3.053** (284 mg, 0.49 mmol, 31%) as a yellow oil, which was used directly in the next step.

A mixture of **3.053** (284 mg, 0.49 mmol), (5-methylpyridin-3-yl)boronic acid (133 mg, 0.97 mmol), Pd(OAc)₂ (11 mg, 0.05 mmol), Catacxium A (17 mg, 0.05 mmol) and K₂CO₃ (134 mg, 0.97 mmol) in 1,4-dioxane (3 mL) and H₂O (1.5 mL) was heated at 100 °C in a microwave reactor for 1 h. The reaction mixture was allowed to cool to rt, diluted with EtOAc (50 mL) and DCM (50 mL), filtered through Celite[®] and concentrated *in vacuo*. The resulting residue was purified by silica gel

chromatography (0–50% EtOH in EtOAc). The appropriate fractions were combined and solvent evaporated *in vacuo* to give **3.054** (123 mg, 0.21 mmol, 42%) as a yellow oil; $^1\text{H NMR}$ (400 MHz, CDCl_3) δ ppm 8.50–8.43 (m, 2H), 7.82 (s, 1H), 7.72–7.68 (m, 1H), 7.54–7.47 (m, 3H), 7.42–7.37 (m, 2H), 7.35–7.30 (m, 1H), 6.35 (d, $J = 8.3$, 1H), 5.52 (s, 2H), 4.20–4.10 (m, 1H), 3.44–3.32 (m, 2H), 2.97–2.88 (m, 5H), 2.57–2.48 (m, 2H), 2.42 (s, 3H), 2.34 (s, 3H), 2.21–2.14 (m, 2H), 2.04–1.98 (m, 2H), 1.71–1.63 (m, 2H), 1.47 (s, 9H); LCMS (high pH): $R_t = 0.75$ min (96%), $\text{MH}^+ = 597.2$.

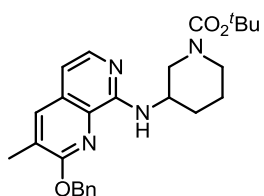
3-Methyl-8-((1-(2-(methylamino)ethyl)piperidin-4-yl)amino)-5-(5-methylpyridin-3-yl)-1,7-naphthyridin-2(1H)-one (3.047b)



3.054 (123 mg, 0.206 mmol) was dissolved in TFA (2 mL, 26.00 mmol) and heated in a microwave reactor for 0.5 h. The reaction mixture was allowed to cool to rt and concentrated *in vacuo*. Toluene (5 mL) was added and the mixture concentrated *in vacuo*.

The resulting residue was dissolved in MeOH (5 mL) and passed through a preconditioned (MeOH, 5 mL) amino propyl column (2 g). The appropriate fractions were combined and solvent evaporated *in vacuo*. The resulting residue was purified by MDAP (high pH). The appropriate fractions were combined and solvent evaporated *in vacuo* to give **3.047b** (10 mg, 0.03 mmol, 12%) as a yellow solid; $^1\text{H NMR}$ (400 MHz, CD_3OD) δ ppm 8.44–8.40 (m, 1H), 8.37–8.34 (m, 1H), 7.73–7.69 (m, 1H), 7.66 (s, 1H), 7.60–7.55 (m, 1H), 4.10–4.00 (m, 1H), 3.04–2.94 (m, 2H), 2.77 (t, $J = 6.7$, 2H), 2.57 (t, $J = 6.7$, 2H), 2.48–2.42 (m, 6H), 2.31–2.22 (m, 2H), 2.18 (s, 3H), 2.17–2.09 (m, 2H), 1.75–1.60 (m, 2H); LCMS (high pH): $R_t = 0.82$ min (98%), $\text{MH}^+ = 407.4$.

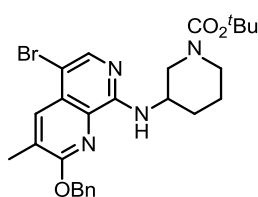
tert-Butyl 3-((2-(benzyloxy)-3-methyl-1,7-naphthyridin-8-yl)amino)piperidine-1-carboxylate (3.056)



3.055 (0.44 mL, 2.28 mmol) was added to a mixture of **3.012** (500 mg, 1.76 mmol), $\text{Pd}_2(\text{dba})_3$ (129 mg, 0.14 mmol), Brettphos (94 mg, 0.18 mmol), and NaO^tBu (675 mg, 7.02 mmol) in THF (10 mL). The reaction mixture was heated at 70 °C for 2 h. The reaction mixture was allowed to cool to rt and concentrated *in vacuo*. The resulting residue was dissolved in DCM (20 mL) and washed with H_2O (30 mL). The aqueous layer was extracted with DCM (3 × 20 mL) and the combined organic layers were concentrated *in vacuo*. The resulting residue was purified by

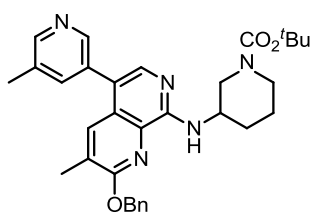
silica gel chromatography (0–50% EtOAc in cyclohexane). The appropriate fractions were combined and solvent evaporated *in vacuo* to give **3.056** (533 mg, 1.19 mmol, 68%) as an orange oil; $^1\text{H NMR}$ (400 MHz, CDCl_3) δ ppm 7.89 (d, $J = 5.7$, 1H), 7.65 (d, $J = 1.0$, 1H), 7.52–7.48 (m, 2H), 7.43–7.37 (m, 2H), 7.36–7.30 (m, 1H), 6.73 (d, $J = 5.7$, 1H), 6.37 (d, $J = 7.8$, 1H), 5.57–5.43 (m, 2H), 4.29–4.20 (m, 1H), 3.90–3.77 (m, 1H), 3.56–3.37 (m, 3H), 2.38 (d, $J = 1.0$, 3H), 2.09–2.00 (m, 1H), 1.80–1.71 (m, 2H), 1.68–1.60 (m, 1H), 1.32 (br.s, 9H); LCMS (formic acid): $R_t = 0.96$ min (100%), $\text{MH}^+ = 407.4$.

***tert*-Butyl 3-((2-(benzyloxy)-5-bromo-3-methyl-1,7-naphthyridin-8-yl)amino)piperidine-1-carboxylate (3.057)**



NBS (211 mg, 1.19 mmol) was added to a solution of **3.056** (533 mg, 1.19 mmol) THF (5 mL). The reaction mixture was left to stir at rt for 18 h. The reaction mixture was concentrated *in vacuo*. The resulting solid was dissolved in DCM (50 mL) and washed with H_2O (40 mL). The aqueous layer was extracted with DCM (3 \times 30 mL) and the combined organic layers were concentrated *in vacuo* to give **3.057** (612 mg, 1.16 mmol, 98%) as a yellow solid; $^1\text{H NMR}$ (400 MHz, CDCl_3) δ ppm 8.02 (s, 1H), 7.97 (d, $J = 1.0$, 1H), 7.51–7.46 (m, 2H), 7.43–7.38 (m, 2H), 7.36–7.31 (m, 1H), 5.56–5.44 (m, 2H), 4.29–4.16 (m, 1H), 3.84–3.74 (m, 1H), 3.50–3.40 (m, 3H), 2.44 (d, $J = 1.0$, 3H), 2.07–1.98 (m, 1H), 1.80–1.73 (m, 2H), 1.68–1.66 (m, 1H), 1.29 (br.s, 9H); LCMS (formic acid): $R_t = 1.66$ min (86%), $\text{MH}^+ = 527.1$, 529.1.

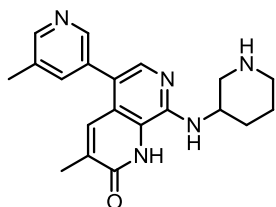
***tert*-Butyl 3-((2-(benzyloxy)-3-methyl-5-(5-methylpyridin-3-yl)-1,7-naphthyridin-8-yl)amino)piperidine-1-carboxylate (3.058)**



A mixture of **3.057** (200 mg, 0.38 mmol), (5-methylpyridin-3-yl)boronic acid (104 mg, 0.76 mmol), $\text{Pd}(\text{OAc})_2$ (9 mg, 0.04 mmol), Catacxiom A (14 mg, 0.04 mmol) and K_2CO_3 (105 mg, 0.76 mmol) in 1,4-dioxane (3 mL) and H_2O (1.5 mL) was heated at 100 $^\circ\text{C}$ in a microwave reactor for 1 h. The reaction mixture was allowed to cool to rt, diluted with EtOAc (20 mL), filtered through Celite[®] and concentrated *in vacuo*. The resulting residue was purified by silica gel chromatography (0–100% EtOAc in cyclohexane). The appropriate fractions were combined and solvent evaporated *in vacuo* to give **3.058** (159 mg, 0.30 mmol, 78%) as a white solid; $^1\text{H NMR}$ (400 MHz, CDCl_3) δ ppm 8.50–8.46 (m, 2H), 7.84 (s, 1H), 7.71 (d, $J = 1.0$, 1H), 7.54–7.48 (m, 3H), 7.43–7.37 (m,

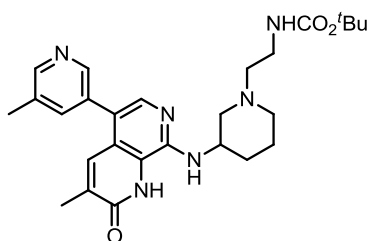
2H), 7.36–7.30 (m, 1H), 6.50 (d, $J = 7.6$, 1H), 5.59–5.46 (m, 2H), 4.33–4.25 (m, 1H), 3.90–3.81 (m, 1H), 3.57–3.41 (m, 3H), 2.43 (s, 3H), 2.34 (d, $J = 1.0$, 3H), 2.11–2.02 (m, 1H), 1.83–1.76 (m, 2H), 1.72–1.62 (m, 1H), 1.36 (br.s, 9H); LCMS (formic acid): $R_t = 1.08$ min (97%), $MH^+ = 540.4$.

3-Methyl-5-(5-methylpyridin-3-yl)-8-(piperidin-3-ylamino)-1,7-naphthyridin-2(1H)-one (3.059)



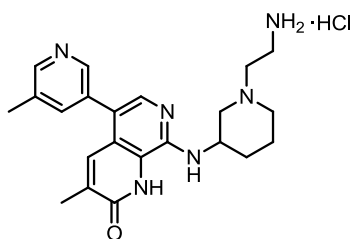
A mixture of **3.058** (159 mg, 0.30 mmol) in TFA (3 mL, 38.90 mmol) was heated at 80 °C for 18 h. The reaction mixture was diluted with toluene (10 mL) and concentrated *in vacuo*. The resulting residue was diluted with MeOH (10 mL) and passed through a preconditioned (MeOH, 10 mL) amino propyl column (2 g). The filtrate was concentrated *in vacuo* to give **3.059** (94 mg, 0.27 mmol, 91%) as an orange oil; 1H NMR (400 MHz, $CDCl_3$) δ ppm 8.55–8.35 (m, 2H), 7.72 (s, 1H), 7.58–7.46 (m, 2H), 4.64–4.61 (m, 1H), 3.38–3.30 (m, 1H), 3.25–3.19 (m, 1H), 3.16–3.06 (m, 1H), 2.43 (s, 3H), 2.33–2.23 (m, 1H), 2.18–2.05 (m, 5H), 1.89–1.77 (m, 2H); LCMS (high pH): $R_t = 0.71$ min (99%), $MH^+ = 350.3$.

tert-Butyl (2-(3-((3-methyl-5-(5-methylpyridin-3-yl)-2-oxo-1,2-dihydro-1,7-naphthyridin-8-yl)amino)piperidin-1-yl)ethyl)carbamate (3.061a)



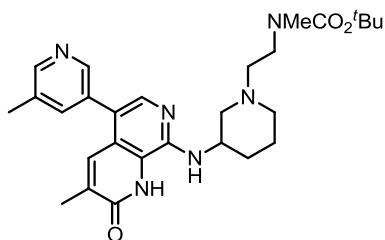
A mixture of **3.060a** (107 mg, 0.67 mmol) and **3.059** (94 mg, 0.27 mmol) in MeOH (3 mL) and AcOH (0.3 mL) was heated at 50 °C for 2 h. Picoline borane complex (25 mg, 0.27 mmol) was added and the reaction mixture was heated at 50 °C for a further 18 h. The reaction mixture was concentrated *in vacuo* and the resulting residue diluted with sat. aq. $NaHCO_3$ (20 mL) and DCM (20 mL). The organic layer was separated and the aqueous extracted with DCM (3 x 20 mL). The resulting residue was purified by silica gel chromatography (0–70% EtOH in EtOAc). The appropriate fractions were combined and solvent evaporated *in vacuo* to give **3.061a** (99 mg, 0.20 mmol, 75%) as a yellow oil; 1H NMR (400 MHz, CD_3OD) δ ppm 8.39 (d, $J = 1.5$, 1H), 8.31 (d, $J = 1.5$, 1H), 7.69 (s, 1H), 7.67–7.65 (m, 1H), 7.57 (d, $J = 1.1$, 1H), 4.32–4.23 (m, 1H), 3.21–3.14 (m, 2H), 3.13–3.07 (m, 2H), 2.50–2.44 (m, 2H), 2.41 (s, 3H), 2.14 (d, $J = 1.1$, 3H), 2.03–1.94 (m, 2H), 1.85–1.77 (m, 2H), 1.75–1.65 (m, 2H), 1.38 (s, 9H); LCMS (high pH): $R_t = 1.06$ min (98%), $MH^+ = 493.4$.

8-((1-(2-Aminoethyl)piperidin-3-yl)amino)-3-methyl-5-(5-methylpyridin-3-yl)-1,7-naphthyridin-2(1H)-one hydrochloride (3.047e)



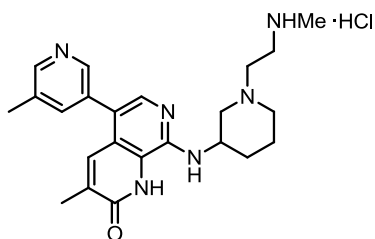
A mixture of **3.061a** (99 mg, 0.20 mmol) in 4 M HCl in 1,4-dioxane (3 mL, 99.00 mmol) was stirred at rt for 48 h. The reaction mixture was concentrated *in vacuo*. The resulting residue was suspended in Et₂O (10 mL), filtered under reduced pressure, washed with Et₂O (10 mL), collected and dried under vacuum at 40 °C for 3 h to give **3.047e** (85 mg, 0.20 mmol, 99%) as a light brown solid; ¹H NMR (400 MHz, CD₃OD) δ ppm 8.91–8.84 (m, 2H), 8.62 (s, 1H), 7.87–7.78 (m, 2H), 4.71–4.60 (m, 1H), 4.16–3.88 (m, 1H), 3.66–3.48 (m, 6H), 2.69 (s, 3H), 2.39–2.31 (m, 4H), 2.27–2.03 (m, 4H); LCMS (high pH): R_t = 0.73 min (100%), MH⁺ = 393.4.

tert-Butyl methyl(2-(3-((3-methyl-5-(5-methylpyridin-3-yl)-2-oxo-1,2-dihydro-1,7-naphthyridin-8-yl)amino)piperidin-1-yl)ethyl)carbamate (3.061b)



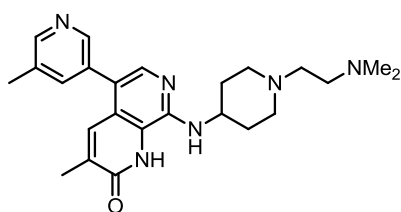
A mixture of **3.060b** (173 mg, 1.00 mmol) and **3.059** (140 mg, 0.40 mmol) in MeOH (3 mL) and AcOH (0.3 mL) was heated at 50 °C for 2 h. Picoline borane complex (37 mg, 0.40 mmol) was added and the reaction mixture was heated at 50 °C for a further 18 h. The reaction mixture was concentrated *in vacuo* and the resulting residue diluted with sat. aq. NaHCO₃ (20 mL) and DCM (20 mL). The organic layer was separated and the aqueous extracted with DCM (3 × 20 mL). The resulting residue was purified by silica gel chromatography (0–70% EtOH in EtOAc). The appropriate fractions were combined and solvent evaporated *in vacuo* to give **3.061b** (146 mg, 0.29 mmol, 72%) as a yellow solid; ¹H NMR (400 MHz, CD₃OD) δ ppm 8.42 (d, *J* = 1.6, 1H), 8.35 (d, *J* = 1.6, 1H), 7.73 (s, 1H), 7.72–7.69 (m, 1H), 7.61 (d, *J* = 1.2, 1H), 4.37–4.27 (m, 1H), 3.47–3.37 (m, 2H), 3.20–3.12 (m, 1H), 2.89 (s, 3H), 2.82–2.72 (m, 1H), 2.61–2.53 (m, 2H), 2.45 (s, 3H), 2.37–2.28 (m, 1H), 2.19 (s, 3H), 2.05–1.97 (m, 1H), 1.88–1.80 (m, 1H), 1.76–1.67 (m, 1H), 1.59–1.50 (m, 2H), 1.43 (s, 9H); LCMS (high pH): R_t = 1.17 min (97%), MH⁺ = 507.4.

3-Methyl-8-((1-(2-(methylamino)ethyl)piperidin-3-yl)amino)-5-(5-methylpyridin-3-yl)-1,7-naphthyridin-2(1H)-one hydrochloride (3.047f)



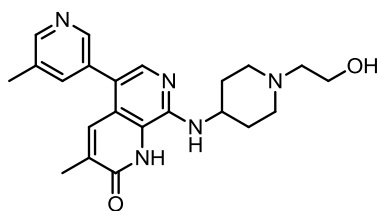
A mixture of **3.061b** (146 mg, 0.29 mmol) in 4 M HCl in 1,4-dioxane (3 mL, 99.00 mmol) was stirred at rt for 3 h. The reaction mixture was concentrated *in vacuo*. The resulting residue was suspended in Et₂O (10 mL), filtered under reduced pressure, washed with Et₂O (10 mL), collected and dried under vacuum at 40 °C for 3 h to give **3.047f** (131 mg, 0.30 mmol, quant.) as a yellow solid; ¹H NMR (400 MHz, DMSO-d₆) δ ppm 11.14 (br.s, 1H), 9.58–9.47 (m, 2H), 8.85–8.79 (m, 2H), 8.42 (s, 1H), 7.84 (s, 1H), 7.73–7.76 (m, 1H), 7.64 (s, 1H), 4.68–4.54 (m, 1H), 3.83–3.74 (m, 1H), 3.72–3.64 (m, 1H), 3.63–3.56 (m, 1H), 3.54–3.49 (m, 2H), 3.47–3.40 (m, 2H), 3.09–2.90 (m, 1H), 2.60–2.57 (m, 3H), 2.55 (s, 3H), 2.18–2.09 (m, 4H), 2.03–1.95 (m, 2H), 1.68–1.54 (m, 1H); LCMS (high pH): R_t = 0.79 min (94%), MH⁺ = 407.4.

8-((1-(2-(Dimethylamino)ethyl)piperidin-4-yl)amino)-3-methyl-5-(5-methylpyridin-3-yl)-1,7-naphthyridin-2(1H)-one (3.047c)



Following General Procedure 3B using 1-(2-(dimethylamino)ethyl)piperidin-4-amine (0.11 mL, 0.60 mmol), gave **3.047c** (5 mg, 0.01 mmol, 6%) as a yellow solid; ¹H NMR (400 MHz, CD₃OD) δ ppm 8.45–8.40 (m, 1H), 8.36 (d, *J* = 1.5, 1H), 7.73–7.70 (m, 1H), 7.66 (s, 1H), 7.59–7.55 (m, 1H), 4.10–3.99 (m, 1H), 3.06–2.97 (m, 2H), 2.60–2.52 (m, 4H), 2.45 (s, 3H), 2.32–2.25 (m, 8H), 2.19–2.10 (m, 5H), 1.74–1.61 (m, 2H); LCMS (high pH): R_t = 0.87 min (99%), MH⁺ = 421.4.

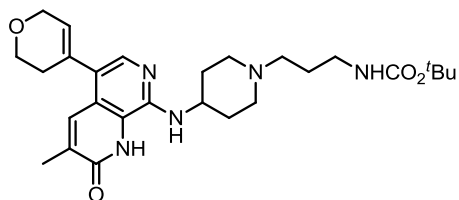
8-((1-(2-Hydroxyethyl)piperidin-4-yl)amino)-3-methyl-5-(5-methylpyridin-3-yl)-1,7-naphthyridin-2(1H)-one (3.047d)



Following General Procedure 3B using 2-(4-aminopiperidin-1-yl)ethanol (88mg, 0.60 mmol), gave **3.047d** (24 mg, 0.06 mmol, 30%) as a yellow solid; m.p. 217–220 °C (decomp.); ν_{max} (solid)/cm⁻¹: 3393 (N-H), 1659 (C=O), 1595, 1450, 720; ¹H NMR (400 MHz, DMSO-d₆) δ ppm 8.46–8.42 (m, 1H), 8.37 (d, *J* = 2.0, 1H), 7.70 (s, 1H), 7.64–7.60 (m, 1H), 7.50 (d, *J* = 1.2, 1H), 4.37–4.28 (m, 1H), 4.04–3.93 (m, 1H), 3.55–3.46 (m, 2H), 2.92–2.85 (m, 2H), 2.44–2.36 (m, 5H), 2.16–2.04 (m, 5H), 2.02–

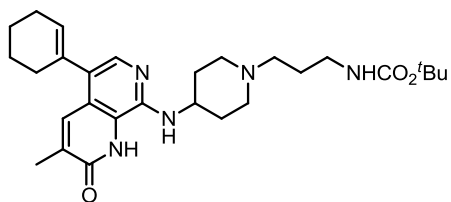
1.94 (m, 2H), 1.58-1.46 (m, 2H); ^{13}C NMR (101 MHz, DMSO- d_6) δ ppm 162.0, 148.5, 147.1, 145.8, 139.0, 137.4, 134.1, 132.9, 132.8, 131.9, 120.9, 120.6, 117.9, 60.3, 58.7, 52.7, 47.9, 31.7, 17.8, 16.7; HRMS (M + H) $^+$ calculated for $\text{C}_{22}\text{H}_{28}\text{N}_5\text{O}_2$ 394.2238; found 394.2247; LCMS (high pH): R_t = 0.75 min (87%), MH^+ = 394.2.

***tert*-Butyl (3-(4-((5-(3,6-dihydro-2H-pyran-4-yl)-3-methyl-2-oxo-1,2-dihydro-1,7-naphthyridin-8-yl)amino)piperidin-1-yl)propyl)carbamate (3.063a)**



A mixture of **3.018** (220 mg, 0.45 mmol), 2-(3,6-dihydro-2H-pyran-4-yl)-4,4,5,5-tetramethyl-1,3,2-dioxaborolane (122 mg, 0.58 mol), $\text{Pd}(\text{OAc})_2$ (10 mg, 0.04 mmol), Catacxiium A (16 mg, 0.04 mmol) and K_2CO_3 (123 mg, 0.89 mmol) in 1,4-dioxane (2 mL) and H_2O (1 mL) was heated at 100 °C in a microwave reactor for 1 h. The reaction mixture was allowed to cool to rt, diluted with EtOAc (20 mL), filtered through Celite[®] and concentrated *in vacuo*. The resulting solid was purified by silica gel chromatography (0–50% EtOH in EtOAc). The appropriate fractions were combined and solvent evaporated *in vacuo* to give **3.063a** (107 mg, 0.22 mmol, 48%) as a yellow solid; ^1H NMR (400 MHz, CD_3OD) δ ppm 7.81 (d, J = 1.0, 1H), 7.63 (s, 1H), 5.81–5.87 (m, 1H), 4.34–4.29 (m, 2H), 4.10–4.03 (m, 1H), 3.99–3.95 (m, 2H), 3.13–3.09 (m, 4H), 2.65–2.60 (m, 2H), 2.42–2.38 (m, 3H), 2.23 (d, J = 1.0, 3H), 2.23–2.21 (m, 3H), 1.80–1.72 (m, 4H), 1.45 (s, 9H); LCMS (formic acid): R_t = 0.58 min (81%), MH^+ = 498.3.

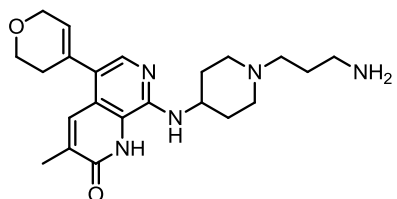
***tert*-Butyl (3-(4-((5-(cyclohex-1-en-1-yl)-3-methyl-2-oxo-1,2-dihydro-1,7-naphthyridin-8-yl)amino)piperidin-1-yl)propyl)carbamate (3.063c)**



A mixture of **3.018** (0.17 mL, 0.79 mmol), 2-(cyclohex-1-en-1-yl)-4,4,5,5-tetramethyl-1,3,2-dioxaborolane (0.17 mL, 0.80 mmol), $\text{Pd}(\text{OAc})_2$ (14 mg, 0.06 mmol), Catacxiium A (22 mg, 0.06 mmol) and K_2CO_3 (168 mg, 1.21 mmol) in 1,4-dioxane (2 mL) and H_2O (1 mL) was heated at 100 °C in a microwave reactor for 1 h. The reaction mixture was allowed to cool to rt, diluted with EtOAc (20 mL), filtered through Celite[®] and concentrated *in vacuo*. The resulting solid was suspended in DCM (20 mL), filtered under reduced pressure, rinsed with DCM (20 mL) and H_2O (20 mL). The solid was collected to give **3.063c** (185 mg, 0.37 mmol, 62%) as a yellow solid; ^1H NMR (400 MHz, DMSO- d_6) δ ppm 11.35

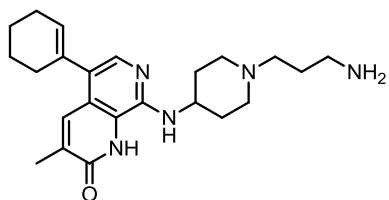
(br.s, 1H), 7.57 (s, 1H), 7.49 (s, 1H), 6.79–6.72 (m, 1H), 6.59 (d, $J = 6.6$, 1H), 3.95–3.84 (m, 1H), 2.98–2.90 (m, 2H), 2.85–2.78 (m, 2H), 2.29–2.23 (m, 2H), 2.21–2.14 (m, 4H), 2.11 (s, 3H), 2.04–1.91 (m, 4H), 1.77–1.63 (m, 4H), 1.57–1.49 (m, 2H), 1.48–1.42 (m, 2H), 1.38 (s, 9H); LCMS (formic acid): $R_t = 0.78$ min (95%), $MH^+ = 496.3$.

8-((1-(3-Aminopropyl)piperidin-4-yl)amino)-5-(3,6-dihydro-2H-pyran-4-yl)-3-methyl-1,7-naphthyridin-2(1H)-one (3.062a)



3.063a (30 mg, 0.060 mmol) was dissolved in 4 M HCl in 1,4-dioxane (3 mL, 12.00 mmol) and left to stir at rt for 2 h. The reaction mixture was concentrated *in vacuo* and the resulting solid was purified by MDAP (high pH). The appropriate fractions were combined and solvent evaporated *in vacuo* to give **3.062a** (13 mg, 0.03 mmol, 54%) as a yellow solid; m.p. 217–20 °C; ν_{max} (solid)/ cm^{-1} : 3387 (N-H), 2927, 1655 (C=O), 1583, 1450, 1121, 850; 1H NMR (400 MHz, DMSO- d_6) δ ppm 7.68 (d, $J = 1.0$, 1H), 7.59 (s, 1H), 6.66 (d, $J = 6.8$, 1H), 5.73–5.69 (m, 1H), 4.71 (br.s, 2H), 4.25–4.20 (m, 2H), 3.97–3.88 (m, 1H), 3.87–3.82 (m, 2H), 2.88–2.80 (m, 2H), 2.60–2.53 (m, 2H), 2.35–2.37 (m, 4H), 2.13 (d, $J = 1.0$, 3H), 2.04–1.92 (m, 4H), 1.56–1.40 (m, 4H); ^{13}C NMR (400 MHz, DMSO- d_6) δ ppm 162.2, 145.3, 136.9, 133.4, 133.2, 131.2, 126.5, 122.1, 120.8, 79.1, 64.8, 63.6, 55.8, 52.3, 47.8, 31.8, 30.4, 16.8; N.B. 1C signal hidden under solvent peak; HRMS ($M + H$) $^+$ calculated for $C_{22}H_{32}N_5O_2$ 398.2551; found 398.2563; LCMS (formic acid): $R_t = 0.35$ min (100%), $MH^+ = 398.3$.

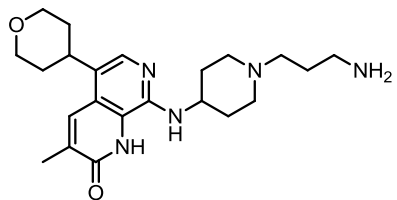
8-((1-(3-Aminopropyl)piperidin-4-yl)amino)-5-(cyclohex-1-en-1-yl)-3-methyl-1,7-naphthyridin-2(1H)-one (3.062c)



3.063c (40 mg, 0.08 mmol) was dissolved in 4 M HCl in 1,4-dioxane (3 mL, 12.00 mmol) and left to stir at rt for 18 h. The reaction mixture was concentrated *in vacuo* and the resulting solid was purified by MDAP (high pH). The appropriate fractions were combined and solvent evaporated *in vacuo* to give **3.062c** (12 mg, 0.03 mmol, 38%) as a yellow solid; 1H NMR (400 MHz, DMSO- d_6) δ ppm 7.61 (d, $J = 1.0$, 1H), 7.53 (s, 1H), 6.59 (d, $J = 6.6$, 1H), 5.63–5.59 (m, 1H), 4.99 (br.s, 2H), 3.97–3.84 (m, 1H), 2.88–2.80 (m, 2H), 2.60–2.55 (m, 2H), 2.35–2.28 (m, 2H), 2.22–

2.14 (m, 4H), 2.12 (d, $J = 1.0$, 3H), 2.03–1.93 (m, 4H), 1.78–1.63 (m, 4H), 1.55–1.41 (m, 4H); LCMS (high pH): $R_t = 1.10$ min (96%), $MH^+ = 396.4$.

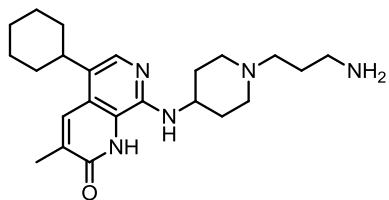
8-((1-(3-Aminopropyl)piperidin-4-yl)amino)-3-methyl-5-(tetrahydro-2H-pyran-4-yl)-1,7-naphthyridin-2(1H)-one (3.062b)



A solution of **3.063a** (77 mg, 0.16 mmol) in EtOH (20 mL) was hydrogenated in the H-Cube using a 10% Pd/C cat cart (50 °C, 40 barr pressure) for 3 h. The reaction mixture was concentrated *in vacuo* to give **3.064a** (60 mg, 0.12 mmol, 78%) as a yellow solid.

3.064a (60 mg, 0.12 mmol) was dissolved in 4 M HCl in 1,4-dioxane (3 mL, 12.00 mmol) and left to stir at rt for 2 h. The reaction mixture was concentrated *in vacuo* and the resulting solid was purified by MDAP (high pH). The appropriate fractions were combined and solvent evaporated *in vacuo* to give **3.062b** (18 mg, 0.05 mmol, 38%) as a yellow solid; 1H NMR (400 MHz, CD_3OD) δ ppm 7.97 (s, 1H), 7.62 (s, 1H), 4.08–4.02 (m, 2H), 4.00–3.90 (m, 1H), 3.70–3.61 (m, 2H), 3.25–3.15 (m, 1H), 3.02–2.96 (m, 2H), 2.76–2.68 (m, 2H), 2.48–2.42 (m, 2H), 2.27 (s, 3H), 2.24–2.16 (m, 2H), 2.14–2.07 (m, 2H), 1.85–1.77 (m, 4H), 1.76–1.69 (m, 2H), 1.66–1.59 (m, 2H); LCMS (high pH): $R_t = 0.71$ min (100%), $MH^+ = 400.4$.

8-((1-(3-Aminopropyl)piperidin-4-yl)amino)-5-cyclohexyl-3-methyl-1,7-naphthyridin-2(1H)-one (3.062d)



A solution of **3.063c** (145 mg, 0.29 mmol) in EtOH (20 mL) was hydrogenated in the H-Cube using a 10% Pd/C cat cart (50 °C, 40 barr pressure) for 3 h. The reaction mixture was concentrated *in vacuo* to give **3.064c** (60 mg, 0.12 mmol, 41%) as a pale yellow solid.

3.064c (60 mg, 0.12 mmol) was dissolved in 4 M HCl in 1,4-dioxane (3 mL, 12.00 mmol) and left to stir at rt for 2 h. The reaction mixture was concentrated *in vacuo* and the resulting solid was purified by MDAP (high pH). The appropriate fractions were combined and solvent evaporated *in vacuo* to give **3.062d** (13 mg, 0.03 mmol, 27%) as a yellow solid; 1H NMR (400 MHz, $DMSO-d_6$) δ ppm 7.88 (s, 1H), 7.64 (s, 1H), 6.49 (d, $J = 6.6$, 1H), 4.61 (br.s, 2H), 3.93–3.82 (m, 1H), 2.91–2.80 (m, 4H), 2.59–2.53 (m, 2H), 2.35–2.27 (m, 2H), 2.15 (s, 3H), 2.02–1.91 (m, 4H), 1.82–1.75 (m, 5H), 1.54–1.38 (m, 8H); LCMS (high pH): $R_t = 0.49$ min (98%), $MH^+ = 398.4$.

5 Appendix

5.1 TR-FRET assay protocol

Brd9 TR-FRET assay

Ligand preparation

A solution of Alexa Fluor 647 hydroxysuccinimide ester in DMF was added to a 1.5 fold excess of N-(5-aminopentyl)-2-((4S)-6-(4-chlorophenyl)-8-methoxy-1-methyl-4H-benzo[f][1,2,4]triazolo[4,3-a][1,4]diazepin-4-yl)acetamide, also in DMF, and when thoroughly mixed, the solution was basified by the addition of a 3 fold excess of diisopropylethylamine. Reaction progress was followed by electrospray LC/MS and when judged complete, the product was isolated and purified by reverse-phase C18 HPLC. The final compound was converted to the ammonium salt and characterised by mass spectroscopy and analytical reverse-phase HPLC.

Protocol for BRD9 ligand FRET assay

All assay components were dissolved in buffer composition of 50 mM HEPES pH 7.4, 50 mM NaCl, 5% Glycerol, 1 mM DTT and 1mM CHAPS. The final concentration of Brd9 protein was at 10 nM and the Alexa Fluor647 ligand was at K_d (~100 nM for Brd9). These components were premixed and 5 μ l of this reaction mixture was added to all wells containing 50 nl of various concentrations of test compound or DMSO vehicle (0.5% DMSO final) in Greiner 384 well black low volume microtitre plates and incubated in dark for 30 min at rt. Detection reagents were prepared in assay buffer by diluting Eu-W1024 Anti-6xHis Antibody (AD0111 PerkinElmer) to 1.5 nM FAC. 5 μ l of this solution was then added to all wells. The plates were read on the Envision reader and the donor and acceptor counts were determined. From this, the ratio of acceptor/donor was calculated ($\lambda_{ex} = 337$ nm, $\lambda_{em\ donor} = 615$ nm, $\lambda_{em\ acceptor} = 665$ nm) and used for data analysis. All data were normalized to the robust mean of 16 high and 16 low control wells on each plate. A four parameter curve fit of the following form was then applied.

$$y = \frac{a - d}{1 + \left(\frac{x}{c}\right)^b} + d$$

Where 'a' is the minimum, 'b' is the Hill slope, 'c' is the pIC_{50} and 'd' is the maximum.

All other TR-FRET assays were conducted in a similar manner with different ligands and concentrations.

5.2 Thermal shift analysis

Thermal shift analysis is a technique which quantifies the strength of ligand-protein binding without the need for displacement of a known binding partner. The temperature at which a protein melts is measured by the increase in fluorescence intensity of a dye that interacts with the hydrophobic core, exposed as the structure unfolds. The difference in the melting temperature in the presence and absence of a ligand is found to be proportional to the binding affinity of the small molecule (**Figure 1**).

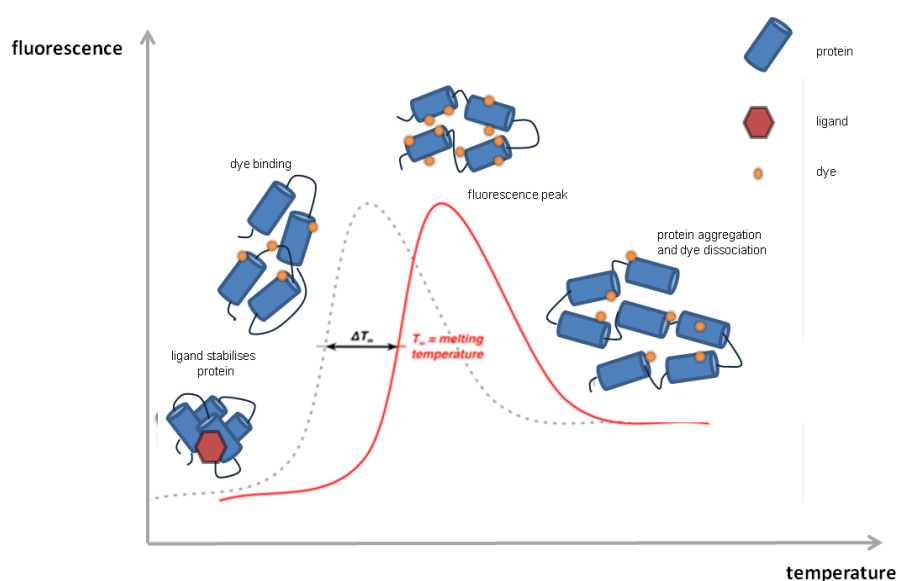


Figure 1: Thermal shift assay.

5.3 Isothermal titration calorimetry

ITC measures the heat energy change associated with protein-ligand binding. Typically, an experiment is conducted by the step-wise addition of ligand solution into a sample cell containing a known concentration of protein. The resulting reaction either absorbs or releases heat proportional to the amount of ligand-protein binding. As this technique relies on a heat compensation principle, the instrument responds by adjusting the temperature of the sample cell to maintain an identical temperature to the adjacent reference vessel. The heat change recorded upon addition of the ligand is plotted as the power required to maintain a constant temperature between the two cells (**Figure 2**).

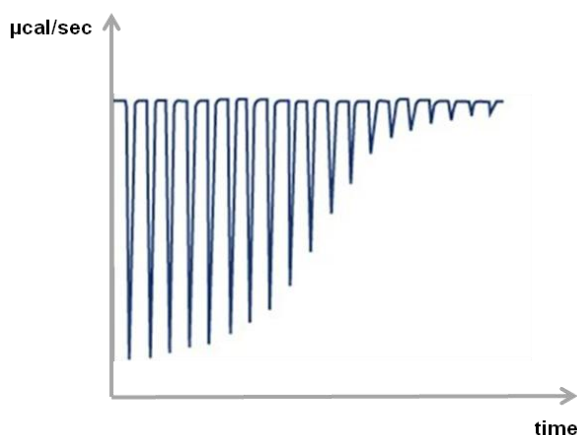


Figure 2: Example graph from an ITC experiment.

The data consists of a series of peaks, with each representing a single injection of ligand solution. As the amount of uncomplexed protein progressively decreases after each injection of ligand, the magnitude of the peaks becomes smaller until saturation is reached. The pattern of these heat effects as a function of the ligand/protein molar ratio can be analysed to give the thermodynamic parameters of the interaction. More specifically, a single experiment provides an evaluation of the Gibbs free energy change (ΔG) and its components: ΔH , the change in enthalpy; ΔS , the change in entropy; and K_d , the dissociation constant (**Equation 1**).

$$\Delta G = \Delta H - T\Delta S$$

$$\Delta G = -RT\ln K_d$$

Equation 1: Definition of Gibbs free energy (ΔG).

ΔH represents the net change in the number and/or strength of non-covalent bonds going from the free to bound state. Indeed, the formation of correctly positioned

interactions such as hydrogen-bonds, Van der Waals interactions and electrostatic contacts, provides favourable (that is negative) enthalpies. However, desolvation of polar groups upon binding leads to an enthalpic penalty.

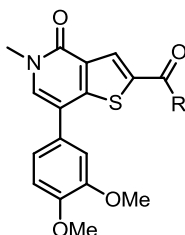
ΔS represents the change in entropy upon ligand binding. Improving entropic contributions can often be achieved by increasing the lipophilicity of the ligand. Lipophilic compounds desolvate more readily, resulting in a significant entropic reward. However, the extent of lipophilicity must be balanced in order to provide an optimal physico-chemical property profile. The entropy gain associated with liberation of solvent works against the entropic loss through constraining the ligand upon binding. The loss in translational, rotational and therefore conformational degrees of freedom leads to a loss in entropy. Therefore, in order to optimise this contribution, there must be very little conformational change of the free ligand compared to its bound state.

5.4 Brd9 Amide array

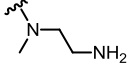
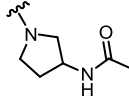
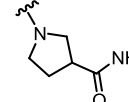
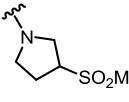
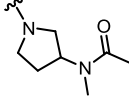
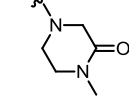
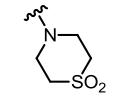
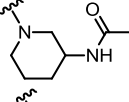
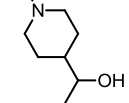
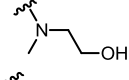
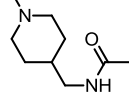
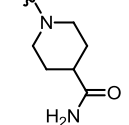
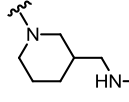
5.4.1 General experimental procedure

To a solution of **2.021** (52 mg, 0.15 mmol, 1.0 eq.), HATU (57 mg, 0.15 mmol, 1.0 eq.), and DIPEA (0.08 mL, 0.45 mmol, 3.0 eq.) in DMF (0.4 mL), the appropriate amine (0.12 mmol, 1.0 eq.) was added. The reaction mixture was left to stand for 18 h at rt. The mixture was diluted with DMF (1 mL) and purified MDAP (formic acid). The appropriate fractions were combined and the solvent evaporated under a stream of nitrogen at 40 °C to give the required product.

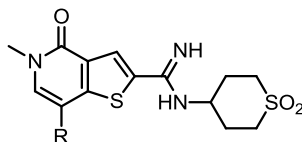
5.4.2 Amide array TR-FRET data



2.030	R =	Brd9 LE	Brd9 pIC ₅₀	Brd4 BD1 pIC ₅₀	Brd4 BD2 pIC ₅₀	Selectivity
a		0.36	7.9	7.3	7.0	x4
b		0.34	7.8	7.3	7.0	x3
c		0.31	7.1	6.7	6.5	x2.5
d		0.27	7.0	7.3	6.9	x<1
e		0.31	6.7	6.2	5.8	x4
f		0.31	6.6	6.4	6.5	x2
g		0.29	6.9	5.3	4.8	x40

2.030	R =	Brd9 LE	Brd9 pIC ₅₀	Brd4 BD1 pIC ₅₀	Brd4 BD2 pIC ₅₀	Selectivity
h		0.28	5.9	6.3	5.8	x4
i		0.25	5.9	5.1	4.9	x8
j		0.24	5.7	5.2	4.6	x5
k		0.24	5.8	5.3	4.6	x4
l		0.23	5.5	5.2	4.6	x2
m		0.25	5.5	5.1	4.5	x4
n		0.24	5.5	4.6	4.5	x8
o		0.23	5.5	5.0	4.7	x3
p		0.23	5.4	4.8	4.4	x5
q		0.26	5.4	5.0	4.5	x2.5
r		0.21	5.3	4.9	<4.3	x3
s ²⁵³		0.22	5.3	4.7	<4.3	x5
t		0.21	5.2	4.7	<4.3	x3

5.5 Brd9 Amidine array TR-FRET data



2.081	R =	Brd9 LE	Brd9 pIC ₅₀	Brd4 BD1 pIC ₅₀	Brd4 BD2 pIC ₅₀	Selectivity
a		0.31	7.1	5.4	<4.3	x50
b ²⁵⁴		0.33	7.3	5.7	4.7	x40
c		0.32	7.9	5.8	4.9	x126
d		0.36	8.1	6.1	5.2	x100
e		0.33	7.7	6.4	5.2	x20
f		0.36	7.9	6.1	5.0	x63
g		0.33	8.1	6.0	5.3	x200
h		0.35	7.7	6.0	5.1	x50
i ²⁵⁵		0.31	6.8	5.3	4.7	x32
j		0.31	7.1	5.3	4.5	x63
k		0.23	7.8	6.2	5.5	x40

2.081	R =	Brd9 LE	Brd9 pIC ₅₀	Brd4 BD1 pIC ₅₀	Brd4 BD2 pIC ₅₀	Selectivity
l ²⁵⁵		0.17	6.5	5.1	4.6	x25
m		0.31	7.1	5.9	5.1	x16
n		0.20	7.6	6.3	5.5	x20
o		0.35	8.1	6.1	5.1	x100
p		0.29	6.4	4.8	<4.3	x40
q		0.33	7.8	5.6	4.8	x158
r		0.34	7.4	5.6	4.6	x63
s ²⁵⁴		0.33	7.8	5.9	4.9	x79
t		0.32	7.7	5.5	4.7	x158
u		0.30	7.3	5.8	4.8	x32

5.6 BROMOscan bromodomain profiling

Bromodomain profiling was provided by DiscoverX Corp. (Fremont, CA, USA) on the basis of BROMOscan. This screen accounted for the determination of the K_d between I-BRD9 and each of the 34 DNA tagged bromodomains included in the assay, by binding competition against a reference immobilized ligand (<http://www.discoverx.com>).

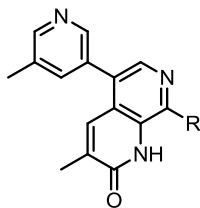
5.6.1 Full data for compound 2.081q

Gene Symbol	K _d (nM)	Gene Symbol	K _d (nM)
ATAD2A	> 30000	BRPF1	= 180
ATAD2B	> 30000	BRPF3	= 3200
BAZ2A	= 4100	CECR2	= 32
BAZ2B	> 30000	CREBBP	= 350
Brd1	= 1200	EP300	= 940
Brd2 BD1	= 570	FALZ	= 1600
Brd2 BD2	= 5100	GCN5L2	= 5500
Brd3 BD1	= 400	PBRM1 BD2	> 30000
Brd3 BD2	= 6100	PBRM1 BD5	> 30000
Brd4 BD1	= 340	PCAF	= 3600
Brd4 BD2	= 3100	SMARCA2	> 30000
Brd7	= 120	SMARCA4	> 30000
Brd8 BD1	= 2800	TAF1 BD2	= 1800
Brd8 BD2	> 30000	TAF1L BD2	= 5600
Brd9	= 0.66	TRIM24(PHD,Bromo.)	23000
BrdT BD1	= 630	TRIM33(PHD,Bromo.)	> 30000
BrdT BD2	= 3400	WDR9 BD2	> 30000

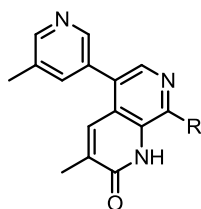
5.6.2 Full data for compound 2.082 (I-BRD9)

Gene Symbol	K _d (nM)	Gene Symbol	K _d (nM)
ATAD2A	> 30000	BRPF1	= 2100
ATAD2B	> 30000	BRPF3	> 30000
BAZ2A	> 30000	CECR2	= 140
BAZ2B	> 30000	CREBBP	= 740
Brd1	= 17000	EP300	= 770
Brd2 BD1	= 3200	FALZ	= 22000
Brd2 BD2	> 30000	GCN5L2	> 30000
Brd3 BD1	= 3000	PBRM1 BD2	> 30000
Brd3 BD2	= 16000	PBRM1 BD5	> 30000
Brd4 BD1	= 1400	PCAF	> 30000
Brd4 BD2	= 17000	SMARCA2	> 30000
Brd7	= 380	SMARCA4	> 30000
Brd8 BD1	= 13000	TAF1 BD2	= 7500
Brd8 BD2	> 30000	TAF1L BD2	= 12000
Brd9	= 1.9	TRIM24(PHD,Bromo.)	> 30000
BrdT BD1	= 1500	TRIM33(PHD,Bromo.)	> 30000
BrdT BD2	= 15000	WDR9 BD2	> 30000

5.7 TAF1 8-Position array 1

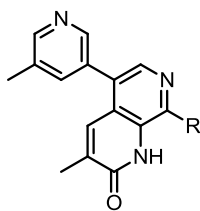


3.020	R =	TAF1 BD2 pIC ₅₀	Brd4 BD1 pIC ₅₀	Brd4 BD2 pIC ₅₀	Selectivity	CLND sol. (μg/mL)	AMP (nm/s)
a		6.5	5.7	4.6	x6	117	<3
b		5.5	<4.3	<4.3	x16	22	310
c		6.4	<4.3	5.3	x13	9	220
d ²⁴⁰		6.3	4.6	4.9	x25	6	420
e ²⁵⁶		5.9	5.5	4.4	x2.5	18	120
f		-	-	-	-	-	-
g		5.9	<4.3	4.8	x13	53	490
h		6.0	4.9	5.0	x10	129	14
i		5.8	5.1	<4.3	x5	142	34
j		6.3	5.0	4.7	x20	79	<10
k		6.2	5.3	4.6	x8	86	81
l		6.0	<4.3	<4.3	x50	3	260
m		5.8	5.1	5.1	x5	5	200

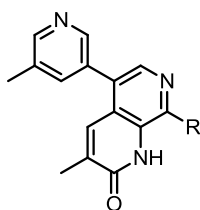


3.020	R =	TAF1 BD2 pIC ₅₀	Brd4 BD1 pIC ₅₀	Brd4 BD2 pIC ₅₀	Selectivity	CLND sol. (µg/mL)	AMP (nm/s)
n		6.4	4.8	5.4	x10	67	110
o ²⁵⁷		6.4	4.4	5.1	x20	39	560
p		6.1	5.1	4.9	x10	103	230
q ²⁵⁸		6.0	4.5	<4.3	x32	12	140
r		6.5	5.1	5.3	x16	146	<3
s ²⁵⁹		5.4	<4.3	<4.3	x13	9	230
t		6.3	4.8	5.4	x8	8	230
u		6.4	4.8	4.8	x40	179	<3
v		5.9	5.0	4.4	x8	212	210
w ²⁴¹		6.0	4.5	4.9	x13	155	180
x		6.2	<4.3	5.0	x16	25	370

5.8 TAF1 8-Position array 2

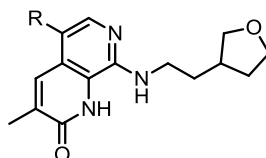


3.042	R =	TAF1 BD2 pIC ₅₀	Brd4 BD1 pIC ₅₀	Brd4 BD2 pIC ₅₀	Selectivity	CLND sol. (µg/mL)	AMP (nm/s)
a ²⁶⁰		5.9	4.9	<4.3	x10	7	250
b		-	-	-	-	-	-
c		6.3	4.5	4.7	x40	170	140
d		6.2	4.5	4.8	x25	166	220
e		5.5	<4.3	<4.3	x16	154	200
f		6.6	4.8	5.3	x20	-	-
g		6.1	4.4	4.6	x32	135	100
h		6.4	4.7	4.9	x32	146	<3
i		6.2	5.3	<4.3	x8	166	85
j		5.8	<4.3	<4.3	x32	28	180
k		6.6	5.2	5.0	x25	170	260
l		6.3	4.9	5.2	x13	29	200
m		-	-	-	-	-	-

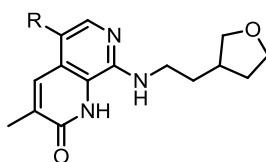


3.042	R =	TAF1 BD2 pIC ₅₀	Brd4 BD1 pIC ₅₀	Brd4 BD2 pIC ₅₀	Selectivity	CLND sol. (µg/mL)	AMP (nm/s)
n ²⁶¹		6.0	4.6	4.5	x25	67	200
o		6.2	<4.3	<4.3	x80	22	330
p		-	-	-	-	-	-
q		5.7	<4.3	<4.3	x25	24	280
r		-	-	-	-	-	-
s		-	-	-	-	-	-
t		-	-	-	-	-	-
u		6.6	4.9	5.4	x16	150	<3
v		6.2	4.6	4.9	x20	149	<10
w		6.7	4.9	5.4	x20	-	<10
x		-	-	-	-	-	-

5.9 TAF1 5-Position array



3.043	R =	TAF1 BD2 pIC ₅₀	Brd4 BD1 pIC ₅₀	Brd4 BD2 pIC ₅₀	Selectivity	CLND sol. (µg/mL)	AMP (nm/s)
a		6.5	4.9	5.1	x25	13	460
b		5.9	<4.3	5.2	x5	24	390
c		<5.0	<4.3	<4.3	x<1	52	330
d		6.4	<4.3	4.9	x32	15	<10
e ²⁶²		5.1	4.8	5.3	x<1	8	230
f ²⁶³		5.6	4.4	4.5	x8	13	540
g		<5.0	5.4	4.7	x<1	5	500
h		5.4	5.3	5.6	x<1	2	300
i ²⁶⁴		5.1	4.7	5.1	x1	7	460
j ²⁴⁶		5.1	<4.3	<4.3	x6	18	470
k		5.5	5.3	5.8	x<1	16	470
l ²⁶⁵		5.5	<4.3	6.1	x<1	7	350
m		5.9	<4.3	4.9	x10	23	37



3.043	R =	TAF1 BD2 pIC ₅₀	Brd4 BD1 pIC ₅₀	Brd4 BD2 pIC ₅₀	Selectivity	CLND sol. (µg/mL)	AMP (nm/s)
n		6.2	4.7	5.2	x10	186	350
o ²⁴⁵		5.7	<4.3	<4.3	x25	12	390
p		6.4	4.7	4.9	x32	16	410
q		6.4	5.2	5.3	x13	17	300
r		-	<4.3	<4.3	-	1	-
s ²⁶⁶		5.6	4.4	4.4	x16	6	560
t ²⁶⁷		<5.0	4.4	4.6	x<1	4	<3
u		7.2	6.1	6.3	x8	10	-
v		6.2	5.4	5.3	x6	7	830
w		<5.0	5.3	5.9	x<1	4	-
x		5.5	5.5	5.6	x1	2	380

6 References

- [1] Franklin, R. E.; Gosling, R. G. *Nature* **1953**, *171*, 740–741.
- [2] Wilson, M. H. F.; Stokes, A. R.; Wilson, H. R. *Nature* **1953**, *171*, 738–740.
- [3] Watson, J. D.; Crick, F. H. C. *Nature* **1953**, *171*, 737–738.
- [4] Watson, J. D.; Crick, F. H. C. *Nature* **1953**, *171*, 964–967.
- [5] Structure of DNA:
<http://www.goldiesroom.org/Note%20Packets/20%20Molecular%20Genetics/00%20Molecular%20Genetics--WHOLE.htm> (accessed 06/10/2015).
- [6] Berg, J. M.; Tymoczko, J. L.; Stryer, L. **2002**, *Biochemistry*, 5th edn., W. H. Freeman and Company, New York.
- [7] Crick, F. *Nature* **1970**, *227*, 561–563.
- [8] Furdas, S. D.; Carlino, L.; Sippl, W.; Jung, M. *MedChemComm.* **2012**, *3*, 123–134.
- [9] Hake, S. B.; Xiao, A.; Allis, C. D. *Brit. J. Cancer* **2004**, *90*, 761–769.
- [10] Holliday, R. *Science* **1987**, *238*, 163–170.
- [11] Arrowsmith, C. H.; Bountra, C.; Fish, P. V.; Lee, K.; Schapira, M. *Nat. Rev. Drug Discov.* **2012**, *11*, 384–400.
- [12] Strahl, B. D.; Allis, D. C. *Nature* **2000**, *403*, 41–45.
- [13] Jones, P. A.; Archer, T. K.; Baylin, S. B.; Beck, S.; Berger, S.; Bernstein, B. E.; Carpten, J. D.; Clark, S. J.; Costello, J. F.; Doerge, R. W.; Esteller, M.; Feinberg, A. P.; Gingeras, T. R.; Grealley, J. M.; Henikoff, S.; Herman, J. G.; Jackson-Grosby, L. J.; Jenuwein, T.; Jirtle, R. L.; Kim, Y. J.; Laird, P. W.; Lim, B.; Marteinsen, R.; Polyak, K.; Stunnenberg, H.; Tlsty, T. D.; Tycko, B.; Ushijima, T.; Zhu, J.; Pirrotta, V.; Allis, C. D.; Elgin, S. C.; Rine, J.; Wu, C. *Nature* **2008**, *454*, 711–715.
- [14] Sanchez, R.; Zhou, M. M.; *Curr. Opin. Drug Discov. Devel.* **2009**, *12*, 659–665.
- [15] Gardner, K. E.; Allis, C. D.; Strahl, B. D. *J. Mol. Biol.* **2011**, *409*, 36–46.
- [16] Grunstein, M. *Nature* **1997**, *389*, 349–352.
- [17] Hewings, D. S.; Rooney, T. P. C.; Jennings, L. E.; Hay, D. A.; Schofield, C. J.; Brennan, P. E.; Knapp, S.; Conway, S. J. *J. Med. Chem.* **2012**, *55*, 9393–9413.
- [18] Cole, P. A. *Nat. Chem. Biol.* **2008**, *4*, 590–597.
- [19] Duvic, M.; Vu, J. *Expert Opin. Investig. Drugs* **2007**, *16*, 1111–1120.

- [20] Bertino, E. M.; Otterson, G. A. *Expert Opin. Investig. Drugs* **2011**, *20*, 1151–1158.
- [21] Lau, O. D.; Kundu, T. K.; Soccio, R. E.; Ait-Si-Ali, S.; Khalil, E. M.; Vassilev, A.; Wolffe, A. P.; Nakatani, Y.; Roeder, R. G.; Cole, P. A. *Mol. Cell* **2000**, *5*, 589–595.
- [22] Bowers, E. M.; Yan, G.; Mukherjee, C.; Orry, A.; Wang, L.; Holbert, M. A.; Crump, N. T.; Hazzalin, C. A.; Liszczak, G.; Yuan, H.; Larocca, C.; Saldanha, A. S.; Abagyan, R.; Sun, Y.; Meyers, D. J.; Marmorstein, R.; Mahadevan, L. C.; Alani, R. M.; Cole, P. A. *Chem. Biol.* **2011**, *17*, 471–482.
- [23] Filippakopoulos, P.; Knapp, S. *FEBS Lett.* **2012**, *586*, 2692–2704.
- [24] Haynes, S. R.; Dollard, C.; Winston, F.; Beck, S.; Trowsdale, J.; Dawid, I. B. *Nucleic Acids Res.* **1992**, *20*, 2603.
- [25] Steiner, S.; Magno, A.; Huang, D.; Caflisch, A. *FEBS Lett.* **2013**, *587*, 2158–2163.
- [26] Filippakopoulos, P.; Picaud, S.; Mangos, M.; Keates, T.; Lambert, J. P.; Barsyte-Lovejoy, D.; Felletar, I.; Volkmer, R.; Muller, S.; Pawson, T.; Gingras, A. C.; Arrowsmith, C. H.; Knapp, S. *Cell* **2012**, *149*, 214–231.
- [27] Chung, C. W.; Witherington, J. *J. Biomol. Screening* **2011**, *16*, 1170–1185.
- [28] Dhalluin, C.; Carlson, J. E.; Zeng, L.; He, C.; Aggarwal, A. K.; Zhou, M. M. *Nature* **1999**, *399*, 491–496.
- [29] Mujtaba, S.; Zeng, L.; Zhou, M. M. *Oncogene* **2007**, *26*, 5521–5527.
- [30] Zeng, L.; Zhou, M. M. *FEBS Lett.* **2002**, *513*, 124–128.
- [31] Vidler, L. R.; Brown, N.; Knapp, S.; Hoelder, S.; Heightman, T. D. *Mol. Biosyst.* **2011**, *7*, 2899–2908.
- [32] Vollmuth, F.; Geyer, M. *Angew. Chem. Int. Ed. Engl.* **2010**, *49*, 6768–6772.
- [33] Flynn, M. E.; Huang, O. W.; Poy, F.; Oppikofer, M.; Bellon, S. F.; Tang, Y. *Cell* **2015**, *23*, 1801–1814.
- [34] Philpott, M.; Yang, J.; Tumber, T.; Federov, O.; Uttarkar, S.; Filippakopoulos, P.; Picaud, S.; Keates, T.; Felletar, I.; Ciulli, A.; Knapp, S.; Heightman, T. D. *Mol. Biosyst.* **2011**, *7*, 2899–2908.
- [35] Muller, S.; Filippakopoulos, P.; Knapp, S. *Expert Rev. Mol. Med.* **2011**, *13*, e29.
- [36] Chung, C. W.; Tough, D. F. *Drug Discov. Today Ther. Strategies* **2012**, *9*, 111–120.

- [37] Prinjha, R. K.; Witherington, J.; Lee, K. *Trends in Pharmacol. Sci.* **2012**, *33*, 146-153.
- [38] Chung, C. W. *Prog. Med. Chem.* **2012**, *51*, 1–55.
- [39] Zuber, J.; Shi, J.; Wang, E.; Rappaport, A. R.; Herrmann, H.; Sison, E. A.; Magoon, D.; Qi, J.; Blatt, K.; Wunderlich, M.; Taylor, M. J.; Johns, C.; Chica, A.; Mulloy, J. C.; Kogan, S. C.; Brown, P.; Valent, P.; Bradner, J. E.; Lowe, S. W.; Vakoc, C. R. *Nature* **2011**, *478*, 524–528.
- [40] Ciró, M.; Prosperini, E.; Quarto, M.; Grazini, U.; Walfridsson, J.; McBlane, F.; Nucifero, P.; Pacchiana, G.; Capra, M.; Christensen, J.; Helin, K. *Cancer Res.* **2009**, *69*, 8491–8498.
- [41] Tsai, W. W.; Wang, Z.; Yiu, T. T.; Akdemir, K. C.; Xia, W.; Winter, S.; Tsai, C. Y.; Shi, X.; Schwarzer, D.; Plunkett, W.; Aronow, B.; Gozani, O.; Fischle, W.; Hung, M. C.; Patel, D. J.; Barton, M. C. *Nature* **2010**, *468*, 927–932
- [42] Mullighan, C. G.; Zhang, J.; Kasper, L. H.; Lerach, S.; Payne-Tuner, D.; Phillips, L. A.; Heatley, S. L.; Holmfeldt, L.; Collins-Underwood, J. R.; Ma, J.; Beutow, K. H.; Pui, C. H.; Baker, S. D.; Brindle, P. K.; Downing, J. R. *Nature* **2011**, *471*, 235–239.
- [43] Xiao, X.; Li, B. X.; Mitton, B.; Ikeda, A.; Sakamoto, K. M. *Curr. Cancer Drug Targets* **2010**, *10*, 384–391.
- [44] Filippalopoulos, P.; Qi, J.; Picaud, S.; Shen, Y.; Smith, W. B.; Fedorov, O.; Morse, E. M.; Keates, T.; Hickman, T. T.; Felletar, I.; Philpott, M.; Munro, S.; McKeown, M. R.; Wang, Y.; Christie, A. L.; West, N.; Cameron, M. J.; Schwartz, B.; Heightman, T. D.; La Thangue, N.; French, C. A.; Wiest, O.; Kung, A. L.; Knapp, S.; Bradner, J. E. *Nature* **2010**, *468*, 1067–1073.
- [45] French, C. A. *Cancer Genet. Cytonet.* **2010**, *203*, 16–20.
- [46] Grayson, A. R.; Walsh, E. M.; Cameron, M. J.; Godec, J.; Ashworth, T.; Ambrose, J. M.; Aserlind, A. B.; Hang, H.; Evan, G. I.; Kluk, M. J.; Bradner, J. E.; Aster, J. C.; French, C. A. *Oncogene* **2013**, *33*, 1736–1742.
- [47] Nicodeme, E.; Jeffrey, K. L.; Schaefer, U.; Beinke, S.; Dewell, S.; Chung, C. W.; Chandwani, R.; Marazzi, I.; Wilson, P.; Coste, H.; White, J.; Kirilovsky, J.; Rice, C. M.; Lora, J. M.; Prinjha, R. K.; Lee, K.; Tarakovsky, A. *Nature* **2010**, *468*, 1119–1123.
- [48] Delmore, J. E.; Issa, G. C.; Lemieux, M. E.; Rahl, P. B.; Shi, J.; Jacobs, H. M.; Kastiris, E.; Gilpatrick, T.; Paranal, R. M.; Qi, J.; Chesi, M.; Schinzel, A. C.; McKeown, M. R.; Heffernan, T. P.; Vakoc, C. R.; Leif Bergsagel, P.;

- Ghobrial, I. M.; Richardson, P. G.; Young, R. A.; Hahn, W. C.; Anderson, K. C.; Kung, A. L.; Bradner, J. E.; Mitsiades, C. S. *Cell* **2011**, *146*, 904–917.
- [49] Kadoch, C.; Hargreaves, D. C.; Hodges, C.; Elias, L.; Ho, L.; Ranish, J.; Crabtree, G. R. *Nat. Genet.* **2013**, *45*, 592–601.
- [50] Scotto, L.; Narayan, G.; Nandula, S. V.; Subramaniam, S.; Kaufmann, A. M.; Wright, J. D.; Pothuri, B.; Mansukhani, M.; Schneider, A.; Arias-Pulido, H.; Murty, V. V. *Cancer* **2008**, *7*, 58–67.
- [51] Middeljans, E.; Wan, X.; Jansen, P. W.; Sharma, V.; Stunnenberg, H. G.; Logie, C. *PLoS ONE* **7**(3): e33834. DOI: 10.1371/journal.pone.0033834.
- [52] Severinsen, J. E.; Bjarkam, C. R.; Kiaer-Larsen, S.; Olsen, I. M.; Nielsen, M. M.; Blechingberg, J.; Nielsen, A. L.; Holm, I. E.; Foldager, L.; Young, B. D.; Muir, W. J.; Blackwood, D. H. R.; Corydon, T. J.; Mors, O.; Børghlum, A. D. *Mol. Psychiatry* **2006**, *11*, 1126–1138.
- [53] Koga, M.; Ishiguro, H.; Yazaki, S.; Horiuchi, Y.; Arai, M.; Niizato, K.; Iritani, S.; Itokawa, M.; Inada, T.; Iwata, N.; Ozaki, N.; Ujike, H.; Kunugi, H.; Sasaki, T.; Takahashi, M.; Watanabe, Y.; Someya, T.; Kakita, A.; Takahashi, H.; Nawa, H.; Muchardt, C.; Yaniv, M.; Arinami, T. *Hum. Mol. Genet.* **2009**, *18*, 248324–248394.
- [54] Urdinguio, R. G.; Sanchez-Mut, J. V.; Esteller, M. *Lancet Neurol.* **2009**, *8*, 1056–1072.
- [55] Roelfsema, J. H.; Peters, D. J. *Expert Rev. Mol. Med.* **2007**, *9*, 1–16.
- [56] Pal, D. K.; Evgrafov, O. V.; Tabares, P.; Zhang, F.; Durner, M.; Greenberg, D. A. *Am. J. Hum. Genet.* **2003**, *73*, 261–270.
- [57] Tang, W.; Basu, S.; Kong, X.; Pankow, J. S.; Aleksic, N.; Tan, A.; Cushman, M.; Boerwinkle, E.; Folsom, A. R. *Blood* **2010**, *116*, 5032–5036.
- [58] Chidambaram, M.; Radha, V.; Mohan, V. *Metabolism* **2010**, *59*, 1760–1766.
- [59] Aulchenko, Y. S.; Ripatti, S.; Lindqvist, I.; Boomsma, D.; Heid, I. M.; Pramstaller, P. P.; Penninx, B. W. J. H.; Janssens, A. C. J. W.; Wilson, J. F.; Spector, T.; Martin, N. G.; Pedersen, N. L.; Kyvik, K. O.; Kaprio, J.; Hofman, A.; Freimer, N. B.; Jarvelin, M.-R.; Gyllensten, U.; Campbell, H.; Rudan, I.; Johansson, A.; Marroni, F.; Hayward, C.; Vitart, V.; Jonasson, I.; Pattaro, C.; Wright, A.; Hastie, N.; Pichler, I.; Hicks, A. A.; Falchi, M.; Willemsen, G.; Hottenga, J.-J.; De Geus, E. J. C.; Montgomery, G. W.; Whitfield, J.; Magnusson, P.; Saharinen, J.; Perola, M.; Silander, K.; Isaacs, A.; Sijbrands, E. J. G.; Uitterlinden, A. G.; Witteman, J. C. M.; Oostra, B. A.; Elliott, P.;

- Ruukonen, A.; Sabatti, C.; Gieger, C.; Meitinger, T.; Kronenberg, F.; Döring, A.; Wichmann, H.-E.; Smit, J. H.; McCarthy, M. I.; Van Duijn, C. M.; Peltonen, L. *Nature Genet.* **2009**, *41*, 47–55.
- [60] Lu, Y.; Feskens, E. J. M.; Boer, J. M. A.; Imholz, S.; Verschuren, W. M. M.; Wijmenga, C.; Vaarhorst, A.; Slagboom, E.; Müller, M.; Dollé, M. E. T. *Atherosclerosis* **2010**, *213*, 200–205.
- [61] Pons, D.; Trompet, S.; De Craen, A. J. M.; Thijssen, P. E.; Quax, P. H. A.; De Vries, M. R.; Wierda, R. J.; Van den Elsen, P. J.; Monraats, P. S.; Ewing, M. M.; Heijmans, B. T.; Slagboom, P. E.; Zwinderman, A. H.; Doevendans, P. A. F. M.; Tio, R. A.; De Winter, R. J.; De Maat, M. P. M.; Iakoubova, O. A.; Sattar, N.; Shepherd, J.; Westendorp, R. G. J.; Jukema, J. W. *Heart* **2011**, *97*, 143–150.
- [62] Wang, F.; Blanton, W. P.; Bellkina, A.; Lebrasseur, N. K.; Dennis, G. V. *J. Biochem.* **2009**, *425*, 71–83.
- [63] Madhi, H.; Fisher, B. A.; Kallberg, H.; Plant, D.; Malmstrom, V.; Ronnelid, J.; Charles, P.; Ding, B.; Alfredsson, L.; Padyukov, L.; Symmons, D. P.; Venables, P. J.; Klareskog, L.; Lundberg, K. *Nat. Genet.* **2009**, *41*, 1319–1324.
- [64] Franke, A.; McGovern, D. P.; Barrett, J. C.; Wang, K.; Radford-Smith, G. L.; Ahmad, T.; Lees, C. W.; Balschun, T.; Lee, J.; Roberts, R.; Anderson, C. A.; Bis, J. C.; Bumpstead, S.; Ellinghaus, D.; Festen, E. M.; Georges, M.; Green, T.; Haritunians, T.; Jostins, L.; Latiano, A.; Mathew, C. G.; Montgomery, G. W.; Prescott, N. J.; Raychaudhuri, S.; Rotter, J. I.; Schumm, P.; Sharma, Y.; Simms, L. A.; Taylor, K. D.; Whiteman, D. *Nat. Genet.* **2010**, *42*, 1118–1125.
- [65] Rajenrasozhan, S.; Yao, H.; Rahman, I. *COPD* **2009**, *6*, 291–297.
- [66] Deng, W.-G.; Zhu, Y.; Wu, K. K. *Blood* **2004**, *103*, 2135–2142.
- [67] Chi, T. *Nat. Rev. Immunol.* **2004**, *4*, 965–977.
- [68] Greenwald, R. J.; Tumang, J. R.; Sinha, A.; Currier, N.; Cardiff, R. D.; Rothstein, T. L.; Faller, D. V.; Dennis, G. V. *Blood* **2004**, *103*, 1475–1484.
- [69] LPS is a component of the outer membrane of Gram negative bacteria. It induces a strong immune response in normal mammalian cells.
- [70] NFκB is a protein complex which controls the transcription of DNA. It is known to play a key role in regulating immune response to infection.
- [71] Chung, C. W.; Coste, H.; White, J. H.; Mirguet, O.; Wilde, J.; Gosmini, R. L.; Delves, C.; Magny, S. M.; Woodward, R.; Hughes, S. A.; Boursier, E. V.;

- Flynn, H.; Bouillot, A. M.; Bamborough, P.; Brusq, J. M. G.; Gellibert, F. J.; Jones, E. J.; Riou, A. M.; Homes, P.; Martin, S. L.; Uings, I. J.; Toum, J.; Clement, C. A.; Boullay, A. B.; Grimley, R. L.; Blandel, F. M.; Prinjha, R. K.; Lee, K.; Kirilovsky, J.; Nicodeme, E. *J. Med. Chem.* **2011**, *54*, 3827–3838.
- [72] Bailey, D.; Jahagirdar, R.; Gordon, A.; Hafiana, A.; Campbell, S.; Chatur, S.; Wagner, G. S.; Hansen, H. C.; Chiacchia, F. S.; Johansson, J.; Krimbou, L.; Wong, N. C. W. Genest, J. *J. Am. Coll. Cardiol.* **2010**, *55*, 2580–2589.
- [73] Picaud, S.; Wells, C.; Felletar, I.; Brotherton, D.; Martin, S.; Savitsky, P.; Diez-Dacal, B.; Philpott, M.; Bountra, C.; Lingard, H.; Fedorov, O.; Muller, S.; Brennan, P. E.; Knapp, S.; Filippakopoulos, P. *Proc. Natl. Acad. Sci. U.S.A.* **2013**, *49*, 19754–19759.
- [74] McLure, K. G.; Gesner, E. M.; Tsujikawa, L.; Kharenko, O. A.; Attwell, S.; Campeau, E.; Wasiak, S.; Stein, A.; White, A.; Fontano, E.; Suto, R. K.; Wong, N. C. W.; Wagner, G. S.; Hansen, H. C.; Young, P. R. *PLoS ONE* **8**(12): e83190. doi: 10.1371/journal.pone.0083190.
- [75] McBride, A. A.; McPhillips, M. G.; Oliveira, J. G. *Trends Microbiol.* **2004**, *12*, 527–529.
- [76] Mujtaba, S.; He, Y.; Zeng, L.; Farooq, A.; Carlson, J. E.; Ott, M.; Verdin, E.; Zhou, M. M. *Mol. Cell* **2002**, *9*, 575–586.
- [77] Bunnage, M. E.; Chekler, E. L. P.; Jones, L. H. *Nat. Chem. Biol.* **2013**, *9*, 195–199.
- [78] Frye, S. V. *Nat. Chem. Biol.* **2010**, *6*, 159–161.
- [79] Arrowsmith, C. H.; Audia, J. E.; Austin, C.; Baell, J.; Bennett, J.; Blagg, J.; Bountra, C.; Brennan, P. E.; Brown, P. J.; Bunnage, M. E.; Buser-Doepner, C.; Campbell, R. M.; Carter, A. J.; Cohen, P.; Copeland, R. A.; Cravatt, B.; Dahlin, J. L.; Dhanak, D.; Edwards, A. E.; Frye S. V.; Gray, N.; Grimshaw, C, E.; Hepworth, D.; Howe, T.; Huber, K. V. M.; Jin, J.; Knapp, S.; Kotz, J. D.; Krugar, R. G.; Lowe, D.; Mader, M. M.; Marsden, B.; Mueller-Fahrnow, A.; Müller, S.; O'Hagen, R. C.; Overington, J. P.; Owen, D. R.; Rosenberg, S. H.; Roth, B.; Ross, R.; Schapira, M.; Schreiber, S. L.; Shoichet, B.; Sundström, M.; Superti-Furga, G.; Taunton, J.; Toledo-Sherman, L.; Walpole, C.; Walters, M. A.; Willson, T. M.; Workman, P.; Young, R. N.; Zuercher, W. J. *Nat. Chem. Biol.* **2015**, *11*, 536–541.
- [80] Sweis, R. F. *ACS Med. Chem. Lett.* **2015**, *6*, 618–621.
- [81] Muller, S.; Brown, P. J. *Clin. Pharmacol. Ther.* **2012**, *92*, 689–693.

- [82] Jubb, H.; Higuieruelo, A. P.; Winter, A.; Blundell, T. L. *Trends Pharmacol. Sci.* **2012**, *33*, 241–248.
- [83] Valkov, E.; Sharpe, T.; Marsh, M.; Greive, S.; Hyvönen, M. *Top. Curr. Chem.* **2012**, *317*, 145–179.
- [84] Vidler, L. R.; Brown, N.; Knapp, S.; Hoelder, S. *J. Med. Chem.* **2012**, *55*, 7346–7359.
- [85] For reviews of BET bromodomain inhibitors and their therapeutic potential, see: (a) Hewings, D. S.; Rooney, T. P. C.; Jennings, L. E.; Hay, D. A.; Schofield, C. J.; Brennan, P. E.; Knapp, S.; Conway, S. J. *J. Med. Chem.* **2012**, *55*, 9393–9413; (b) Knapp, S.; Weinmann, H. *ChemMedChem* **2013**, *3*, 1885–1891; (c) Sweis, R. F.; Michaelides, M. R. *Annu. Rep. Med. Chem.* **2013**, *48*, 185–199; (d) Jennings, L. E.; Measures, A. R.; Wilson, B. G.; Conway, S. J. *Future Med. Chem.* **2014**, *6*, 179–204. (e) Garnier, J. M.; Sharp, P. P.; Burns, C. J. *Expert Opin. Ther. Patents* **2014**, *24*, 185–199; (f) Gallenkamp, D.; Gelato, K. A.; Haendler, B.; Weinmann, H. *ChemMedChem* **2014**, *9*, 438–464.
- [86] Miyoshi, S.; Ooike, S.; Iwata, K.; Hikawa, H.; Sugahara, K. Antitumour Agent. Int. Pat. Appl. WO 2009/084693, **2009**.
- [87] Hepatocytes are the chief functional cells of the liver.
- [88] Mirguet, O.; Gosmini, R.; Toum, J.; Clement, C. A.; Barnathan, M. Brusq, J. M.; Mordaunt, J. E.; Grimes, R. M.; Crowe, M.; Pineau, O.; Ajakane, M.; Daugan, A.; Jeffrey, P.; Cutler, L.; Haynes, A. C.; Smithers N. N.; Chung, C. W.; Bamborough, P.; Uings, I. J.; Lewis, A.; Witherington, J.; Parr, N.; Prinjha, R. K.; Nicodeme, E. *J. Med. Chem.* **2013**, *56*, 7501–7515.
- [89] Gosmini, R.; Nguyen, V. L.; Toum, J.; Simon, C.; Brusq, J.-M. G.; Krysa, G.; Mirguet, O.; Riou-Eymard, A. M.; Boursier, E. V.; Trottet, L.; Bamborough, P.; Clark, H.; Chung, C. W.; Cutler, L.; Demonet, E. H.; Kaur, R.; Lweis, A. J.; Schilling, M. B.; Soden, P. E.; Taylor, S.; Walker, A. L.; Walker, W. D.; Prinjha, R. K.; Nicodeme, E. *J. Med. Chem.* **2014**, *57*, 8111–8131
- [90] Zhang, G.; Plotnikov, A. N.; Rusinova, E.; Shen, T.; Morohasshi, K.; Joshua, J.; Zeng, L.; Mujtaba, S.; Ohlmeyer, M.; Zhou, M. M. *J. Med. Chem.* **2013**, *56*, 9251–9264.
- [91] Dawson, M. A.; Prinjha, R. K.; Dittmann, A.; Giotopoulos, G.; Bantscheff, M.; Chan, W. I.; Robertson, S.; Chun, C. W.; Hopf, C.; Savitski, M. M.; Huthmacher, C.; Gudgin, E.; Lugo, D.; Beinke, S.; Chapman, T. D.; Roberts,

- E. J.; Soden, P. E.; Auger, K. R.; Mirguet, O.; Doehner, K.; Delwel, R.; Burnett, A. K.; Jeffrey, P.; Drewes, G.; Lee, K.; Huntly, B. J. P.; Kouzarides, T. *Nature* **2011**, *478*, 529–533.
- [92] Bamborough, P.; Diallo, H.; Goodacre, J. D.; Gordon, L.; Lewis, A.; Seal, J. T.; Wilson, D. M.; Woodrow, M. D.; Chung, C. W. *J. Med. Chem.* **2012**, *55*, 587–596.
- [93] Hewings, D. S.; Wang, M.; Philpott, M.; Fedorov, O.; Uttarkar, S.; Filippakopoulos, P.; Picaud, S.; Vuppusetty, C.; Marsden, B.; Knapp, S.; Conway, S. J.; Heightman, T. D. *J. Med. Chem.* **2011**, *54*, 6761–6770.
- [94] Hewings, D. S.; Fedorov, O.; Filippakopoulos, P.; Martin, S.; Picaud, S.; Tumber, A.; Wells, C.; Olcina, M. M.; Freeman, K.; Gill, A.; Ritchie, A. J.; Sheppard, D. W.; Russell, A. J.; Hammond, E. M.; Knapp, S.; Brennan, P. E.; Conway, S. J. *J. Med. Chem.* **2013**, *56*, 3217–3227.
- [95] Hay, D.; Fedorov, O.; Filippakopoulos, P.; Martin, S.; Philpott, M.; Picaud, S.; Hewings, D. S.; Uttakar, S.; Heightman, T. D.; Conway, S. J.; Knapp, S.; Brennan, P. E. *MedChemComm.* **2013**, *4*, 140–144.
- [96] Mirguet, O.; Lamotte, Y.; Donche, F.; Toum, J.; Gellibert, F.; Bouillot, A.; Gosmini, R.; Nguyen, V. L.; Delannee, D.; Seal, J.; Blandel, F.; Boullay, A. B.; Boursier, E.; Martin, S.; Brusq, J. M.; Krysa, G.; Riou, A.; Tellier, R.; Costaz, A.; Huet, P.; Dudit, Y.; Trottet, L.; Kirilovsky, J.; Nicodeme, E. *Bioorg. Med. Chem. Lett.* **2012**, *22*, 2963–2967.
- [97] Seal, J.; Lamotte, Y.; Donche, F.; Bouillot, A.; Mirguet, O.; Gellibert, F.; Nicodeme, E.; Krysa, G.; Kirilovsky, J.; Beinke, S.; McCleary, S.; Rioja, I.; Bamborough, P.; Chung, C. W.; Gordon, L.; Lewis, T.; Walker, A. L.; Cutler, L.; Lugo, D.; Wilson, D. M.; Witherington, J.; Lee, K.; Prinjha, R. K. *Bioorg. Med. Chem. Lett.* **2012**, *22*, 2968–2972.
- [98] Zhao, L.; Cao, D.; Chen, T.; Wang, Y.; Miao, Z.; Xu, Y.; Chen, W.; Wang, X.; Li, Y.; Du, Z.; Xiong, B.; Li, J.; Xu, C.; Zhang, N.; He, J.; Shen, J. *J. Med. Chem.* **2013**, *56*, 3833–3851.
- [99] Fish, P. V.; Filippakopoulos, P.; Bish, G.; Brennan, P. E.; Bunnage, M. E.; Cook, A. S.; Fedorov, O.; Gerstenberger, B. S.; Jones, H.; Knapp, S.; Marsden, B.; Nocka, K.; Owen, D. R.; Philpott, M.; Picaud, S.; Primiano, M. J.; Ralph, M. J.; Sciammetta, N.; Trzuppek, J. D. *J. Med. Chem.* **2012**, *55*, 9831–9837.

- [100] Picaud, S.; Da Costa, D.; Thanasopoulou, A. *Cancer Res.* **2013**, *73*, 3336–3346.
- [101] Bromosporine: <http://www.thesgc.org/chemical-probes/bromosporine> (accessed 06/10/2015).
- [102] Fedorov, O.; Lingard, H.; Wells, C.; Monteiro, O. P.; Picaud, S.; Keates, T.; Yapp, C.; Philpott, M.; Martin, S. J.; Felletar, M. I.; Marsden, B.; Filippakopoulos, P.; Müller, S.; Knapp, S.; Brennan, P. E. *J. Med. Chem.* **2014**, *57*, 462–476.
- [103] Caron, C.; Lestrat, C.; Marsal, S.; Escoffier, E.; Curtet, S.; Virolle, V.; Barbry, P.; Debernardi, A.; Brambilla, C.; Brambilla, E.; Rousseaux, S.; Khochbin, S. *Oncogene* **2010**, *29*, 5171–5181.
- [104] Harner, M. J.; Chauder, B. A.; Phan, J.; Fesik, S. W. *J. Med. Chem.* **2014**, *57*, 9687–9692.
- [105] Demont, E. H.; Chung, C. W.; Furze, R. C.; Grandi, P.; Michon, A. M.; Wellaway C.; Barrett, N.; Bridges, A. M.; Craggs, P. D.; Diallo, H.; Dixon, D. P.; Douault, C.; Emmons, A. J.; Jones, E. J.; Karamshi, B. V.; Locke, K.; Mitchell, D. J.; Mouzon, B. H.; Prinjha, R. K.; Roberts, A. D.; Sheppard, R. J.; Watson, R. J.; Bamborough, P. *J. Med. Chem.* **2015**, *58*, 5649–5673.
- [106] Bamborough, P.; Chung, C. W.; Furze, R. C.; Grandi, P.; Michon, A. M.; Sheppard, R. J.; Barnett, H.; Diallo, H.; Dixon, D. J.; Douault, C.; Jones, E. J.; Karamshi, B.; Mitchell, D. J.; Prinjha, R. K.; Rau, C.; Watson, R. J.; Werner, T.; Demont, E. H. *J. Med. Chem.* **2015**, *58*, 6151–6178.
- [107] Ferguson, F. M.; Fedorov, O.; Chaikaud, A.; Philpott, M.; Muniz, J. R. C.; Felletar, I.; von Delft, F.; Heightman, T.; Knapp, S.; Abell, C.; Ciulli, A. *J. Med. Chem.* **2013**, *56*, 10183–10187
- [108] Chen, P.; Chaikuad, A.; Bamborough, P.; Bantscheff, M.; Bountra, C.; Chung, C. W.; Fedorov, O.; Grandi, P.; Jung, D.; Lesniak, R.; Lindon, M.; Müller, S.; Philpott, M.; Prinjha, R.; Rogers, C.; Selenski, C.; Tallant, C.; Werner, T.; Willson, T. M.; Knapp, S.; Drewry, D. H. *J. Med. Chem.* **2015**, DOI: 10.1021/acs.jmedchem.5b00209.
- [109] Drouin, L.; McGrath, S.; Vidler, L. R.; Chaikuad, A.; Monteiro, O.; Tallant, C.; Philpott, M.; Rogers, C.; Fedorov, O.; Liu, M.; Akhtar, W.; Hayes, A.; Raynaud, F.; Müller, S.; Knapp, S.; Hoelder, S. *J. Med. Chem.* **2015**, *5*, 2553–2559.

- [110] Guetzoyan, L.; Ingham, R. J.; Nikbin, N.; Rossignol, J.; Wolling, M.; Baumert, M.; Burgess-Brown, N. A.; Strain-Damerell, C. M.; Shrestha, L.; Brennan, P. E.; Fedorov, O.; Knapp, S.; Ley, S. V. *MedChemComm.* **2014**, *5*, 540–546.
- [111] Picaud, S.; Strocchia, M.; Terracciano, S.; Lauro, G.; Mendez, J.; Daniels, D. L.; Ricco, R.; Bifulco, G.; Bruno, I.; Fillipakopoulos, P. *J. Med. Chem.* **2015**, *58*, 2718–2736.
- [112] Machleidt, T.; Woodroffe, C. C.; Schwinn, M. K.; Méndez, J.; Robers, M. B.; Zimmerman, K.; Otto, P.; Daniels, D. L.; Kirkland, T. A.; Wood, K. V. *ACS Chem. Biol.* **2015**, *10*, 1797–1804.
- [113] Clark, P. G. K.; Vieira, L. C. C.; Tallant, C.; Fedorov, O.; Singleton, D. C.; Rogers, C. M.; Monteiro, O. P.; Bennett, J. M.; Baronio, R.; Müller, S.; Daniels, D. L.; Méndez, J.; Knapp, S.; Brennan, P. E.; Dixon, D. J. *Angew. Chem. Int. Ed. Engl.* **2015**, *127*, 1–6.
- [114] BI-9564: A chemical probe for BRD9 and BRD7. <http://www.thesgc.org/chemical-probes/BI-9564> (accessed 06/10/2015).
- [115] Hay, D. A.; Rogers, C. M.; Fedorov, O.; Tallant, C.; Martin, S.; Monteiro, O. P.; Müller, S.; Knapp, S.; Schofield, C. J.; Brennan, P. E. *MedChemComm.* **2015**, *6*, 1381–1386.
- [116] Ullah, M.; Pelletier, N.; Xiao, L.; Zhao, S. P.; Wang, K.; Degerny, C.; Tahmasebi, S.; Cayrou, C.; Doyon, Y.; Goh, S. L.; Champagne, N.; Cote, J.; Yang, X. *J. Mol. Cell. Biol.* **2008**, *28*, 6828–6843.
- [117] OF-1: A chemical probe for BRPF bromodomains. <http://www.thesgc.org/chemical-probes/OF-1> (accessed 06/10/2015).
- [118] NI-57: A chemical probe for BRPF bromodomains. <http://www.thesgc.org/node/9363> (accessed 06/10/2015).
- [119] PFI-4: a chemical probe for BRPF1B. <http://www.thesgc.org/node/9362> (accessed 06/10/2015).
- [120] Demont, E. H.; Bamborough, P.; Chung, C. W.; Craggs, P. D.; Fallon, D.; Gordon, L. J.; Grandi, P.; Hobbs, C. I.; Hussain, J.; Jones, E. J.; Le Gall, A.; Michon, A. M.; Mitchell, D. J.; Prinjha, R. K.; Roberts, A. D.; Sheppard, R. J.; Watson, R. *ACS Med. Chem. Lett.* **2014**, *11*, 1190–1195.
- [121] BROMOscan: <http://www.discoverx.com/services/drug-discovery-development-services/epigenetic-profiling/bromoscan> (accessed 06/10/2015).

- [122] Mujtaba, S.; He, Y.; Zeng, L.; Yan, S.; Plotnikova, O.; Sanchez, R.; Zeleznik-Le, N. J.; Ronai, Z.; Zhou, M. M. *Mol. Cell* **2004**, *13*, 251–263.
- [123] p53 is a tumour suppressor.
- [124] Borah, J. C.; Mujtaba, S.; Karakikes, I.; Zeng, L.; Muller, M.; Patel, J.; Moshkina, N.; Morohashi, K.; Zhang, W.; Gerona-Navarro, G.; Hajjar, R. J.; Zhou, M. M. *Chem. Biol.* **2011**, *18*, 531–541.
- [125] I-CBP112: A CREBBP/EP300-selective chemical probe. <http://www.thesgc.org/chemical-probes/ICBP112> (accessed 06/10/2015).
- [126] Hay, D. A.; Fedorov, O.; Martin, S.; Singleton, D. C.; Tallant, C.; Wells, C.; Picaud, S.; Philpott, M.; Monteiro, O. P.; Rogers, C. M.; Conway, S. J.; Rooney, T. P. C.; Tumber, A.; Yapp, C.; Filippakopoulos, P.; Bunnage, M. E.; Müller, S.; Knapp, S.; Schofield, C. J.; Brennan, P. E. *J. Am. Chem. Soc.* **2014**, *136*, 9308–9319.
- [127] Rooney, T. P. C.; Filippakopoulos, P.; Fedorov, O.; Picaud, S.; Cortopassi, W. A.; Hay, D. A.; Martin, S.; Tumber, A.; Rogers, C. M.; Philpott, M.; Wang, M.; Thompson, A. L.; Heightman, T. D.; Pryde, D. C.; Cook, A.; Paton, R. S.; Müller, S.; Knapp, S.; Brennan, P. E.; Conway, S. J. *Angew. Chem. Int. Ed.* **2014**, *53*, 6126–6130.
- [128] Unzue, A.; Xu, M.; Dong, J.; Wiedmer, L.; Spiliopoulos, D.; Caflisch, A.; Nevado, C. *J. Med. Chem.* **2015**, DOI:10.1021/acs.jmedchem.5b00172.
- [129] Zeng, L.; Li, J.; Muller, M.; Yan, S.; Mujtaba, S.; Pan, C.; Wang, Z.; Zhou, M. M. *J. Am. Chem. Soc.* **2005**, *127*, 2376–2377.
- [130] Mujtaba, S.; He, Y.; Zeng, L.; Farooq, A.; Carlson, J. E.; Ott, M.; Verdin, E.; Zhou, M. M. *Mol. Cell* **2002**, *9*, 575–586.
- [131] Medina, P. P.; Carretero, J.; Fraga, M. F.; Esteller, M.; Sidransky, D.; Sanchez-Cespedes, M. *Gene Chromosome Canc.* **2004**, *41*, 170–177.
- [132] PFI-3: Selective chemical probe for SMARCA domains. <http://www.thesgc.org/chemical-probes/PFI-3> (accessed 06/10/2015).
- [133] Vangamudi, B.; Paul, T. A.; Shah, P. K.; Kost-Alimova, M.; Nottebaum, L.; Shi, X.; Zhan, Y.; Leo, E.; Mahadeshwar, H. S.; Protopopov, A.; Futreal, A.; Tieu, T. N.; Peoples, M.; Heffernan, T. P.; Marszalek, J. P.; Toniatti, C.; Petrocchi, A.; Verhelle, D.; Owen, D. R.; Draetta, G.; Jones, P.; Palmer, W. S.; Sharma, S.; Andersen, J. N. *Cancer Res.* **2015**, *75*, 3965–3878.

- [134] McKeown, M. R.; Shaw, D. L.; Fu, H.; Liu, S.; Xu, X.; Marineau, J. J.; Huang, Y.; Zhang, X.; Buckley, D. L.; Kadam, A.; Zhang, Z.; Blacklow, S. C.; Qi, J.; Zhang, W.; Bradner, J. E. *J. Med. Chem.* **2014**, *57*, 9019–9027.
- [135] Bennett, J. M.; Fedorov, O.; Tallant, C.; Monteiro, O. P.; Meier, J.; Gamble, V.; Savitski, P.; Nunez-Alonso, G. A.; Haendler, B.; Rogers, C.; Brennan, P. E.; Müller, S.; Knapp, S. *J. Med. Chem.* **2015**, DOI: 10.1021/acs.jmedchem.5b00458.
- [136] Palmer, W. S.; Poncet-Montange, G.; Liu, G.; Petrocchi, A.; Reyna, N.; Subramanian, G.; Theroff, J.; Yau, A.; Kost-Alimova, M.; Bardenhagen, J. P.; Leo, E.; Shepard, H. E.; Tieu, T. N.; Shi, X.; Zhan, Y.; Zhao, S.; Draetta, G.; Toniatti, C.; Jones, P.; Do, M. G.; Anderson, J. N. *J. Med. Chem.* **2015**, DOI: 10.1021/acs.jmedchem.5b00405.
- [137] TP core identified by BD1 program team.
- [138] pIC₅₀: <4.3 on 1 of 7 test occasions Brd4 BD2; pIC₅₀: <4.3 on 1 of 4 test occasions Brd2 BD2.
- [139] Cellzome, **2013**, GSK unpublished work.
- [140] Cheng, Y.; Prusoff, W. H. *Biochem. Pharmacol.* **1973**, *22*, 3099–3108.
- [141] Humphreys, P. **2013**, GSK unpublished work.
- [142] pIC₅₀: <4.3 on 2 of 7 test occasions Brd4 BD1.
- [143] pIC₅₀: <4.3 on 1 of 6 test occasions Brd4 BD2.
- [144] Chung, C. W. **2013**, GSK unpublished work.
- [145] Freire, E. *Chem. Biol. Drug Des.* **2009**, *74*, 468–472.
- [146] Mortenson, P. N.; Murray, C. W. *J. Comput. Aided Mol. Des.* **2011**, *25*, 663–667.
- [147] Hopkins, A. L.; Keseru, G. M.; Leeson, P. D.; Rees, D. C.; Reynolds, C. H. *Nat. Rev. Drug Discov.* **2014**, *13*, 105–121.
- [148] Hopkins, A. L.; Groom, C. R.; Alex, A. *Drug Discov. Today* **2004**, *9*, 430–431.
- [149] Lipinski, C. A.; Lombardo, F.; Dominy, B. W.; Feeney, P. J. *Adv. Drug Del. Rev.* **2001**, *46*, 3–26.
- [150] Young, R. J.; Green, D. V. S.; Luscombe, C. N.; Hill, A. *Drug Discov. Today* **2011**, *16*, 822–830.
- [151] Hann, M. M.; Keseru, G. M. *Nature Rev. Drug Discov.* **2012**, *11*, 355–365.
- [152] Al-Horani, R. A.; Mehta, A. Y.; Desai, U. R. *Eur. J. Med. Chem.* **2012**, *54*, 771–783.

- [153] Nadin, A.; Hattotuwigama, C.; Churcher, I. *Angew. Chem. Int. Ed. Engl.* **2012**, *51*, 1114–1122.
- [154] Lovering, F.; Bikker, J.; Humblet, C. *J. Med. Chem.* **2009**, *52*, 6752–6756.
- [155] X-ray crystallography by Chung, C. W.
- [156] Gentile, G.; Bernasconi, G.; Pozzan, A.; Merlo, G.; Marzorati, P.; Bamborough, P.; Bax, B.; Bridges, A.; Brough, C.; Carter, P.; Cutler, G.; Neu, M.; Takada, M. *BioOrg. Med. Chem. Lett.* **2011**, *21*, 4823–4827.
- [157] Compounds synthesised by R. Watson and R. Bit **2012**, GSK unpublished work.
- [158] Bjork, M.; Grivas, S. J. *J. Heterocyclic Chem.* **2006**, *43*, 101–109.
- [159] Fujita, R.; Yoshisuji, T.; Wakayanagi, S.; Wakamatsu, H.; Matsuzak, H. *Chem. Pharm. Bull.* **2006**, *54*, 204–208.
- [160] Balkrishna, B. S.; Childers, W. E.; Pinnick, H. W. *Tetrahedron* **1981**, *37*, 2091–2096.
- [161] Han, S. Y.; Kim, Y. A. *Tetrahedron* **2004**, *60*, 2447–2467.
- [162] Groll, M.; Götz, M.; Kaiser, M.; Weyher, E.; Moroder, L. *Chem. Biol.* **2006**, *13*, 607–614.
- [163] Miyaura, N.; Suzuki, A. *Chem. Rev.* **1995**, *95*, 2457–2483.
- [164] Aoki, S.; Cao, L.; Matsui, K.; Rachmat, R.; Akiyama, S.; Kobayashi, M. *Tetrahedron* **2004**, *60*, 7053–7059.
- [165] Ghosh, A.; Luo, J.; Liu, C.; Weltrowska, G.; Lemieux, C.; Chung, N. N.; Lu, Y.; Schiller, P. W. *J. Med. Chem.* **2008**, *51*, 5866–5870.
- [166] Zhang, Q.; Ni, B.; Headley, A. D. *Tetrahedron* **2008**, *64*, 5091–5097.
- [167] pIC₅₀: <4.3 on 1 of 3 test occasions Brd4 BD2.
- [168] pIC₅₀: <4.3 on 1 of 2 test occasions Brd4 BD2.
- [169] pIC₅₀: <4.3 on 2 of 4 test occasions Brd4 BD2.
- [170] Compound synthesised by D. Mitchell **2013**, GSK unpublished work.
- [171] Compounds synthesised by M. Crane **2013**, GSK unpublished work.
- [172] Compounds synthesised by D. Barrios Antunez **2013**, GSK unpublished work.
- [173] Compounds synthesised by R. Bit **2012**, GSK unpublished work.
- [174] Tai, V. **2012**, GSK unpublished work.
- [175] Valente, C.; Calimsiz, S.; Hoi, K. H.; Mallik, D.; Sayah, M.; Organ, M. G. *Angew. Chem. Int. Ed. Engl.* **2012**, *51*, 3314–3332.

- [176] West, C. T.; Donnelly, S. J.; Kooistra, D. A.; Doyle, M. P. *J. Org. Chem.* **1973**, *38*, 2675–2681.
- [177] Abdel-Magid, A. F.; Carson, K. G.; Harris, B. D.; Maryanoff, C. A.; Shah, R. D. *J. Org. Chem.* **1996**, *61*, 3849–3862.
- [178] Sato, S.; Sakamoto, T.; Miyazawa, E.; Kikugawa, Y. *Tetrahedron* **2004**, *60*, 7899–7906.
- [179] Roger, R.; Neilson, D. G. *Chem. Rev.* **1961**, *61*, 179–211.
- [180] Borza, I.; Bozo, E.; Barta-Szalai, G.; Kiss, C.; Tarkanyi, G.; Demeter, A.; Gati, T.; Hada, V.; Kolok, S.; Gere, A.; Fodor, L.; Nagy, J.; Galgoczy, K.; Magdo, I.; Agai, B.; Fetter, J.; Bertha, F.; Keseru, G. M.; Horvath, C.; Farkas, S.; Greiner, I.; Domany, G. *J. Med. Chem.* **2007**, *50*, 901–914.
- [181] Altermann, M.; Hallberg, A. *J. Org. Chem.* **2000**, *35*, 7984–7989.
- [182] Goosen, L. J.; Collet, F.; Goossen, K. *Isr. J. Chem.* **2010**, *50*, 617–629.
- [183] Cornella, J.; Larossa, I. *Synthesis* **2012**, *44*, 653–676.
- [184] Dai, J. J.; Liu, J. H.; Luo, D. F.; Liu, L. *Chem. Commun.* **2011**, *47*, 677–679.
- [185] Wang, Y. F.; Zhu, X.; Chiba, S. *J. Am. Chem. Soc.* **2012**, *134*, 3679–3682.
- [186] Mathews, T. P.; Kennedy, A. J.; Kharel, Y.; Kennedy, P. C.; Nicorara, O.; Sunkara, M.; Morris, A. J.; Wamhoff, B. R.; Lynch, K. R.; Macdonald, T. L. *J. Med. Chem.* **2010**, *53*, 2766–2778.
- [187] Compounds synthesised by P. Humphreys **2013**, GSK unpublished work.
- [188] pIC₅₀: <4.3 on 2 of 6 test occasions Brd4 BD1.
- [189] Hongbin, S.; Jiangxin, L.; Jiahai, Z.; Weiqun, S.; Hongda, H.; Chao, X.; Haiming, D.; Jihui, W. *Biochem. Biophys. Res. Commun.* **2007**, *358*, 435–441.
- [190] Kubinyi, K. *Quant. Struct. Act. Relat.* **1988**, *7*, 121–133.
- [191] pIC₅₀: <4.3 on 3 of 6 test occasions Brd9; pIC₅₀: <4.3 on 1 of 2 test occasions Brd4 BD1; pIC₅₀: <4.3 on 4 of 6 test occasions Brd7.
- [192] pIC₅₀: <4.3 on 1 of 3 test occasions Brd9; pIC₅₀: <4.3 on 2 of 6 test occasions Brd7.
- [193] pIC₅₀: <4.3 on 2 of 3 test occasions Brd9.
- [194] pIC₅₀: <4.3 on 4 of 6 test occasions Brd9; pIC₅₀: <4.3 on 2 of 3 test occasions Brd4 BD1; pIC₅₀: <4.3 on 4 of 6 test occasions Brd7.
- [195] pIC₅₀: <4.3 on 2 of 4 test occasions Brd9; pIC₅₀: <4.0 on 3 of 5 test occasions BRPF1.
- [196] pIC₅₀: <4.3 on 4 of 7 test occasions Brd4 BD2.

- [197] pIC₅₀: <4.3 on 4 of 6 test occasions Brd7.
- [198] pIC₅₀: <4.3 on 1 of 3 test occasions Brd4 BD1.
- [199] pIC₅₀: <4.3 on 2 of 3 test occasions Brd4 BD1 and BD2.
- [200] BROMOscan assay principle: www.discoverx.com (accessed 06/10/2015).
- [201] All studies involving the use of animals were conducted after review by the GlaxoSmithKline (GSK) Institutional Animal Care and Use Committee and in accordance with the GSK Policy on the Care, Welfare and Treatment of Laboratory Animals.
- [202] Smith, D. A.; Di, L.; Kerns, E. H. *Nature Rev. Drug Discov.* **2010**, *9*, 929–939.
- [203] Theodoulou, N. H.; Bamborough, P.; Bannister, A. J.; Becher, I.; Bit, R. A.; Che, K. H.; Chung, C. W.; Dittmann, A.; Drewes, G.; Drewry, D. H.; Gordon, L.; Grandi, P.; Leveridge, M.; Lindon, M.; Michon, A. M.; Molnar, J.; Robson, S.I.C.; Tomkinson, N. C. O.; Kouzarides, T.; Prinjha, R. K.; Humphreys, P. G. *J. Med. Chem.* **2015**, DOI: 10.1021/acs.jmedchem.5b0025.
- [204] I-BRD9: A Chemical Probe for BRD9. <http://www.thesgc.org/chemical-probes/I-BRD9/teaser> (accessed 06/10/2015).
- [205] Burley, S. K.; Roeder, R. G. *Annu. Rev. Biochem.* **1996**, *65*, 769–799.
- [206] Demeny, M. A.; Soutoglou, E.; Nagy, Z.; Scheer, E.; Janoshazi, A.; Richardot, M.; Argentini, M.; Kessler, P.; Laszlo, T. *PLoS ONE*, **2007**, *3*, e316, DOI:10.1371/journal.pone.0000316.
- [207] Jacobson, R. H.; Ladurner, A. G.; King, D. S.; Tjian, R. *Science* **2000**, *288*, 1422–1425.
- [208] Tavassoli, P.; Wafa, L. A.; Cheng, H.; Zoubeydi, A.; Fazli, M. G.; Snoek, R.; Rennie, P. S. *Mol. Endocrinol.* **2010**, *24*, 696–708.
- [209] Centeno, F.; Ramirez-Salzar, E.; Garcia-Villa, E.; Gariglio, P. *Intervirology* **2008**, *51*, 137–143.
- [210] Makino, S.; Kaji, R.; Ando, S.; Tomizawa, M.; Yasuno, K.; Goto, S.; Matsumoto, S.; Tabuena, M.D.; Maranon, E.; Dantes, M.; Lee, L. V.; Ogasawara, K.; Tooyama, I.; Akatsu, H.; Nishimura, M.; Tamiya, G. *Am. J. Hum. Genet.* **2007**, *80*, 393–406.
- [211] Wasserman, D. A.; Sauer, F. *J. Cell Sci.* **2001**, *114*, 2895–2902.
- [212] Allende-Vega, N.; McKenzie, L.; Meek, D. *Mol. Cell Biochem.* **2008**, *316*, 99–106.

- [213] Wang, H.; Curran, E. C.; Hinds, T. R.; Wang, E. H.; Zheng, N. *Cell Res.* **2014**, *24*, 1433–1444.
- [214] Moriniere, J.; Rousseaux, S.; Steuerwald, U.; Soler-Lopez, M.; Curtet, S.; Vitte, A. L.; Govin, J.; Gaucher, J.; Sadoul, K.; Hart, D. J.; Krijgsveld, J.; Khochbin, S.; Muller, C. W.; Petpsa, C. *Nature* **2009**, *461*, 664–669.
- [215] Ritchie, T. J.; MacDonald, S. J. F. *Drug Discov. Today* **2009**, *14*, 1011–1020.
- [216] Delaney, J. S. *J. Chem. Inf. Comput. Sci.* **2004**, *44*, 1000–1005.
- [217] Lamanna, C.; Westerberg, G.; Maccari, L. *J. Med. Chem.* **2008**, *51*, 2891–2897.
- [218] Docking studies performed by P. Bamborough **2015**, GSK unpublished work.
- [219] Compounds synthesised by ATAD2 program team **2014**, GSK unpublished work.
- [220] Scott, J. P. *Synlett* **2006**, 2083–2086.
- [221] Fan, W.; Haxell, T. F. N.; Jenks, M. G.; Kawanishi, N.; Lee, S.; Liu, H.; Malaska, M. J.; Moore, J. A.; Ogino, Y.; Onozaki, Y.; Pandi, B. (Merck Sharp & Dohme Corp.), Int. PCT Pub. No. WO2010/104933 A1 **2010**.
- [222] Wadsworth, W. S.; Emmons, W. D. *J. Am. Chem. Soc.* **1961**, *83*, 1733–1738.
- [223] Guram, A. S.; Buchwald, S. L. *J. Am. Chem. Soc.* **1994**, *116*, 7901–7902.
- [224] Paul, F.; Patt, J.; Hartwig, J. F. *J. Am. Chem. Soc.* **1994**, *116*, 5969–5970.
- [225] Sato, S.; Sakamoto, T.; Miyazawa, E.; Kikugawa, Y. *Tetrahedron* **2004**, *60*, 7899–7906.
- [226] Skerlj, R. T.; Bridger, G. J.; Kaller, A.; McEachern, E. J.; Crawford, J. B.; Zhou, Y.; Atsma, B.; Langille, J.; Nan, S.; Veale, D.; Wilson, T.; Harwig, C.; Hatse, S.; Princen, K.; De Clercq, E. D.; Schols, D. *J. Med. Chem.* **2010**, *53*, 3376–3388.
- [227] Miyaura, N.; Suzuki, A. *Chem. Rev.* **1995**, *95*, 2457–2483.
- [228] pIC₅₀: <5.0 on 1 of 4 test occasions TAF1 BD2.
- [229] Castanet, S. A.; Colobert, F.; and Broutin, P. E. *Tetrahedron. Lett.* **2002**, *43*, 5047–5048.
- [230] Olah, G. A.; Wang, Q.; Sandford, G.; Surya Prakash, G. K. *J. Org. Chem.* **1993**, *58*, 3194–3195.
- [231] Lainchbury, M.; Matthews, T. P.; McHardy, T.; Boxall, K. J.; Walton, M. I.; Eve, P. D.; Hayes, A.; Valenti, M. R.; Brandon, A. K.; Box, G.; Wynne

- Aherne, G.; Reader, J. C.; Raynaud, F. I.; Eccles, S. A.; Garrett, M. D.; Collins, I. *J. Med. Chem.* **2012**, *55*, 10229–10240.
- [232] Carroll, F. I.; Lee, J. R.; Navarro, H. A.; Ma, W.; Brieady, L. E.; Abraham, P.; Damaj, M. I. Martin, B. R. *J. Med. Chem.* **2002**, *45*, 4755–4761.
- [233] Zhang, Z.; Liu, C.; Song, T.; Wu, Z.; Liang, X.; Zhao, Y.; Shen, X.; Chen, H. *Eur. J. Med. Chem.* **2013**, *60*, 410–420.
- [234] Wang, R.; Shen-Ci, L.; Zhang, Y. M.; Shi, Z. J.; Zhang, W. *Org. Biomol. Chem.* **2011**, *9*, 5802-5808.
- [235] Lavery, C. B.; Rotta-Loria, N. L.; McDonald, R. *Adv. Synth. Catal.* **2013**, *355*, 981–987.
- [236] Gowrisankar, S.; Sergeev, A. G.; Anbarasan, P.; Spannenberg, A.; Neumann, H.; Beller M. *J. Am. Chem. Soc.* **2010**, *132*, 11592–11598.
- [237] Anderson, K. W.; Ikawa, T.; Tundel, R. E.; Buchwald, S. L. *J. Am. Chem. Soc.* **2006**, *128*, 10694–10695.
- [238] Watson, R. **2012**, GSK unpublished work.
- [239] Cacchi, S.; Carangio, A.; Fabrizi, G.; Moro, L.; Pace, P. *Synlett.* **1997**, *12*, 1400–1402.
- [240] pIC₅₀: <4.3 on 2 of 3 test occasions Brd4 BD1; pIC₅₀: <5.0 on 3 of 4 test occasions TAF1 BD2.
- [241] 3.020v pIC₅₀: <4.3 on 1 of 2 test occasions Brd4 BD2; 3.020w pIC₅₀: <4.3 on 1 of 2 test occasions Brd4 BD1.
- [242] pIC₅₀: <4.3 on 1 of 2 test occasions Brd4 BD1.
- [243] pIC₅₀: <4.3 on 1 of 2 test occasions BRPF1.
- [244] Compounds synthesised by O'Sullivan, M. **2015**, GSK unpublished work.
- [245] pIC₅₀: <5.0 on 1 of 2 test occasions TAF1 BD2.
- [246] pIC₅₀: <5.0 on 3 of 4 test occasions TAF1 BD2.
- [247] pIC₅₀: <4.3 on 1 of 2 test occasions BRD4 BD1.
- [248] pIC₅₀: <4.3 on 1 of 2 test occasions BRD4 BD1.
- [249] pIC₅₀: <4.3 on 1 of 2 test occasions Brd4 BD1; pIC₅₀: <4.3 on 1 of 2 test occasions Brd4 BD2.
- [250] Data are n=1.
- [251] pIC₅₀: <4.0 on 1 of 2 test occasions PCAF.
- [252] Müller, K.; Faeh, C.; Diederich, F. *Science* **2007**, *317*, 1881–1886.
- [253] pIC₅₀: <4.3 on 1 of 2 test occasions Brd4 BD1.
- [254] pIC₅₀: <4.3 on 1 of 3 test occasions Brd4 BD2.

- [255] pIC₅₀: <4.3 on 1 of 2 test occasions Brd4 BD2.
- [256] pIC₅₀: <4.3 on 1 of 2 test occasions Brd4 BD2.
- [257] pIC₅₀: <4.3 on 1 of 2 test occasions BRD4 BD1.
- [258] pIC₅₀: <4.3 on 1 of 2 test occasions BRD4 BD1.
- [259] pIC₅₀: <5.0 on 1 of 2 test occasions TAF1 BD2.
- [260] pIC₅₀: <5.0 on 1 of 2 test occasions TAF1 BD2.
- [261] pIC₅₀: <4.3 on 1 of 2 test occasions BRD4 BD1.
- [262] pIC₅₀: <5.0 on 3 of 4 test occasions TAF1 BD2.
- [263] pIC₅₀: <4.3 on 1 of 2 test occasions BRD4 BD1; pIC₅₀: <4.3 on 1 of 2 test occasions BRD4 BD2.
- [264] pIC₅₀: <5.0 on 3 of 4 test occasions TAF1 BD2.
- [265] pIC₅₀: <5.0 on 2 of 4 test occasions TAF1 BD2.
- [266] pIC₅₀: <5.0 on 3 of 4 test occasions TAF1 BD2; pIC₅₀: <4.3 on 1 of 2 test occasions BRD4 BD1.
- [267] pIC₅₀: <4.3 on 1 of 2 test occasions BRD4 BD1; pIC₅₀: <4.3 on 1 of 2 test occasions BRD4 BD2.